Investigation into the role of long non-coding RNAs in neuroblastoma and glioma

Aikaterini Bountali

Thesis submitted for the title of Doctor of Philosophy in Cancer Sciences

March 2021

Keele University

Abstract

Long non-coding RNAs (lncRNAs) play key roles in several processes in healthy and cancer settings and the underpinning mechanisms of their action are thoroughly investigated. In line with this, this study investigates the role of the lncRNA myocardial infarction associated transcript (*MIAT*) and other novel lncRNAs in neuroblastoma and glioblastoma.

Silencing of *MIAT*, both siRNA- and GapmeR-mediated, led to decreased long-term survival, promoted apoptosis and attenuated migration in neuroblastoma and glioblastoma cells. RNA sequencing showed that reduced *MIAT* expression levels were associated with perturbed expression of genes involved in cancer-related processes, such as cell growth and survival, migration, reactive oxygen species (ROS) production and apoptosis. Further analysis confirmed that *MIAT* knockdown induces an increase in ROS levels in neuroblastoma cells and was associated with perturbed expression of genes involved in apoptosis, on mRNA and protein level. Notably, RNA sequencing also revealed that *MIAT* acts as *cis* and *trans* gene expression regulator and contributes to regulating alternative splicing.

Given the complex signalling networks of metformin action, short- and long-term exposure of neuroblastoma cells to metformin was used as a platform for an RNA sequencing approach, which revealed that hundreds of novel lncRNAs display aberrant expression and could, therefore, be potentially involved in the regulation of cell fate determination. Of these, the knockdown of *LINC00176* and *LOC648987* led to increased apoptosis and decreased migration. Furthermore, multiple novel pathways, in which the novel lncRNAs could be integrated, were discovered to be deregulated, including DNA replication and DNA damage response-related pathways.

Taken together, this study suggests that *MIAT* exerts a key role in neuroblastoma and glioblastoma cells, confirming its oncogenic role, while multiple novel lncRNAs could also be drivers of cell fate decisions in metformin response of neuroblastoma cells. Further research is essential to establish *MIAT* and other novel lncRNAs, such as *LINC00176* and *LOC648987*, as biomarkers and therapeutic targets.

.

Acknowledgements

First and foremost, I would like to thank my lead supervisor Dr Mirna Mourtada-Maarabouni for her endless practical and psychological support and guidance throughout these years. Without her patience, help, encouragement and advice, both scientific and personal, this work would not have been carried out, and for this, I am more than grateful.

Secondly, I would like to thank Professor Gwyn Williams, who, as my second supervisor, provided his help and expertise on a daily basis in the lab and most importantly tolerated me during my days of grumpiness. Equally, I would like to express my deepest gratitude to Dr Daniel Tonge, who kindly helped me complete the Bioinformatics part of the current work. Without his guidance and tuition, this would not have been possible.

Also, I owe a special 'thanks' to my friend Dr Florian Noulin (Keele University), without whom I would not have survived these tough years. His experience, guidance in the lab and, foremost, friendship, have been priceless and I am more than grateful to be considered his friend. Another special 'thanks' to all of my friends and family, who- despite the distance- have honoured me with their love, friendship, psychological, mental and practical support and have believed in me during times when I did not!

Finally, I would like to thank all our supportive staff, including our technicians, cleaners and our stars, Mrs Jayne Bromley and Mrs Chris Bain, for making my lab life smooth. Your support has been much appreciated!

Abbreviations

Annexin V/7-AAD	Annexin V/ 7-amino-actinomycin D
AO	Acridine orange
APAF1	Apoptotic Peptidase Activating Factor 1
BAD	BCL-2 Associated Agonist Of Cell Death
BAX	BCL-2 Associated X, apoptosis regulator
BCL-2	B-cell lymphoma 2
BID	BH3 Interacting Domain Death Agonist
BIK	BCL-2 Interacting Killer
BIRC	Baculoviral IAP Repeat Containing
CASC2	Cancer Susceptibility 2
CASP	Caspase
ceRNA	Competing endogenous RNA
c-Myc	V-Myc Avian Myelocytomatosis Viral Oncogene Homologue
DDR	DNA Damage Response
DE	Differentially Expressed
DGCR8	DiGeorge Syndrome Critical Region gene 8
DIABLO	Diablo IAP-binding mitochondrial protein
EGFR	Epidermal Growth Factor ReceptorFas Cell Surface Death Receptor
FAS	Growth Arrest and DNA Damage Inducible Alpha
GADD45A	Growth-Arrest Specific 5
GAS5	Glioblastoma
GBM	Host Gene
HG	Hypoxia-Inducible Factor
HIF	Hox transcript antisense intergenic RNA
HOTAIR	Long intergenic/intervening RNA
lincRNA	Long non-coding RNA
lncRNA	Locked Nucleic Acid GapmeR
LNA GapmeR	Metastasis Associated Lung Adenocarcinoma Transcript 1
MALAT1	Mitogen-activated protein kinase
MAPK	Myeloid Cell Leukemia 1
MCL1	

MIAT	Myocardial Infarction-Associated Transcript
miRNA	Micro RNA
MOMP	Mitochondrial Outer Membrane Permeabilisation
MYCN	V-Myc Avian Myelocytomatosis Viral Oncogene Neuroblastoma
NAT	Natural Antisense Transcript
NB	Neuroblastoma
NCYM/MYCNOS	MYCN Opposite Strand
NEAT1	Nuclear paraspeckle assembly transcript 1
NOXA	Phorbol-12-Myristate-13-Acetate-Induced Protein 1
NRF2	Nuclear Factor Erythroid 2-Related Factor 2
Oct1 (POU2F1)	Octamer-Binding Transcription Factor 1
PARVB	Parvin Beta
PI3K/Akt	Phosphatidylinositol-3-Kinase/ Akt Serine/Threonine Kinase
PBN	Alpha-phenyl-N-tert-butyl nitrone
PS	Phosphatidylserine
ROS	Reactive Oxygen Species
siRNA	Small interfering RNA
snoRNA	Small Nucleolar RNA
SF1	Splicing Factor 1
Sp	Specificity protein
TGF-beta	Transforming Growth Factor Beta
TP53	Tumour Protein 53
TP73	Tumour Protein 73
TSG	Tumour Suppressor Gene
XIAP	X-linked Inhibitor of Apoptosis
XIST	X-inactive Specific Transcript

Contents

List of Tables

List of Figures

Chapter 1: Introduction

1.1. Neuroblastoma

Neuroblastoma took its name owing to present cells being associated with fibrils in arrangements similar to neuroblasts (Wright, 1910). In contemporary oncology, the term neuroblastoma (NB) is used to describe a broad spectrum of neuroblastic tumours including neuroblastomas, which comprise the most common type, ganglioneuroblastomas and ganglioneuromas (Shohet and Foster, 2017). NB is the most common extracranial paediatric cancer that affects primarily infants and young children (Hara, 2012). The likelihood of NB appearance varies by age, with most cases being detected during the perinatal age and then decreasing with the increase of age over the first ten years of life. Adolescent or young adult cases are rare and tend to appear as an indolent disease rather than a fatal one (Shohet and Foster, 2017; Nakagawara *et al.*, 2018). NBs comprise ~7-10% of all tumours of childhood and they are the third most common paediatric tumours after leukaemias and tumours of the brain/CNS (Kamijo and Nakagawara, 2012; Pandey and Kanduri, 2015; Luksch *et al.*, 2016). They account for approximately 15% of all cancer-related deaths in childhood (Mullassery and Losty, 2016). For unknown reasons, they tend to be more prevalent in boys comparing to girls (Nakagawara *et al.*, 2018) and the incidence of the tumour is similar across the populations of industrialised countries. Since NB is a relatively rare disease, no environmental factor- tumour development associations have been established yet (Shohet and Foster, 2017). The median age of diagnosis is 18 months (Hara, 2012; Kamijo and Nakagawara, 2012). The vast majority of the cases arise as sporadic tumours with only ~1-2% of the patients having a family history of the disease, but when this is present it follows an autosomal dominant inheritance pattern (Shohet and Foster, 2017). Familial predisposition is also usually characterised by aberrant expression of ALK Receptor Tyrosine Kinase (*ALK)* and Paired Like Homeobox 2B *(PHOX2B)*, while less common cases have been reported with Neurofibromin 1 (*NF1),* Kinesin Family Member 1B *(KIF1B),* LIM domain only 1/3 *(LMO1/3)* and Polypeptide N-Acetylgalactosaminyltransferase 14 *(GALNT14)* mutations (Ahmed *et al.*, 2017).

1.1.1. Diagnosis

Around 37% of the NB cases are diagnosed as infants, 50% by the age of 2 and a rough 75-90% of all patients are younger than 5 years old at the time of diagnosis (Ratner *et al.*, 2016; Ahmed *et al.*, 2017). Similarly to other tumours, NB is diagnosed using a combination of means, including laboratory tests, radiography imaging techniques and pathology. Perinatal cases can be found as suprarenal masses, as diagnosed by ultrasound examination, during or just after pregnancy (Nakagawara *et al.*, 2018).

Given that NBs are metabolically active tumours, some of the secreted catecholamine metabolites can be used for diagnostic purposes. More specifically, dopamine (DA) vanillyl mandelic acid (VMA) and homovanillic acid (HVA) measured in urine samples have proved to be useful diagnostic tools of high sensitivity (66-100%), and in addition, HVA/VMA and DA/VMA ratios have been shown to be associated with prognosis. Moreover, lactate dehydrogenase (LDH) comprises a diagnostic, as well as prognostic, indicator linked with poor histology and prognosis. Finally, high levels of serum ferritin (>142 ng/ml) and neuron-specific enolase (NSE) (>100ng/ml) have been used as diagnostic means, as well as indicators of prognosis (Mullassery and Losty, 2016; Ahmed *et al.*, 2017).

In terms of imaging-based diagnostic tools, computed tomography (CT) and magnetic resonance imaging (MRI) comprise the commonly used means to diagnose the disease and determine the size of the tumour, the regional expansion, the involvement of lymph nodes, as well as distant spread-if any- to the neck, the thorax the abdominal area and/or the pelvis, while the use of sonography and endoscopy is limited (Ahmed *et al.*, 2017; Arora and Bandopadhyaya, 2018). In order to enhance the power of diagnosis, radioiodine-labelled meta-iodobenzylguanidine ($^{123/131}$I-MIBG), an analogue of norepinephrine that is selectively concentrated in the sympathetic nervous system, has been employed to detect not only primary NBs but also metastatic sites. In combination with MIBG, ^{18}F-fluorodeoxyglucose positron emission tomography (FDG-PET) is used to detect metastases in patients where MIBG is not efficient enough (Mullassery and Losty, 2016; Ahmed *et al.*,

2017). MIBG can also be combined with single-photon emission tomography (SPECT) to provide an even more accurate anatomical localisation of the tumour (Tolbert and Matthay, 2018). Finally, newer radiologic applications are being investigated to be used for NB diagnosis, including ^{18}F–fluoro-dihydroxyphenylalanine (18F-DOPA- PET/CT) and ^{68}Ga-1,4,7,10-tetraazacyclododecane-1,4,7,10-tetraacetic-acid-1-Nal3-octreotide (68Ga-DOTANOC- PET/CT) (Arora and Bandopadhyaya, 2018; Tolbert and Matthay, 2018).

In addition to the aforementioned ways to diagnose NBs and their metastases, tissue biopsy, either surgical or minimally invasive image-guided, and histological analysis can prove useful in confirming a diagnosis. Circulating tumour cells and tumour DNA in peripheral blood could also contribute to diagnosis via their "NB-specific" genetic and genomic pattern. Although they are not common in practice yet, they comprise a potent diagnostic tool, especially when used in conjunction with urine/serum catecholamine metabolite detection (Mullassery and Losty, 2016; Ahmed *et al.*, 2017).

1.1.2. Pathogenesis and Clinical Features

NB is a tumour of the sympathetic nervous system, thus arising in tissues of the sympathetic nervous system, the adrenal medulla and the paraspinal ganglia (Hara, 2012; Pandey and Kanduri, 2015). Neuroblastoma originates from the neuro-ectoderm, and specifically from embryonic neural crest cells, which normally give rise to the sympathetic nervous system, due to their improper development and differentiation (Kamijo and Nakagawara, 2012; Pandey and Kanduri, 2015; Mazzoccoli *et al.*, 2016). Normally, during the developmental period of the embryo, the neural crest cells develop to eventually differentiate into different lineages, including sympathetic neuronal cells, sensory cells, enteric cells and melanocytes. The majority of the cells will undergo programmed cell death, mostly apoptosis, while the remainder will differentiate terminally to give rise to mature neuronal cells like ganglion cells (Nakagawara *et al.*, 2018). The fetal adrenal medulla consists of a mix of chromaffin cells and mature ganglion cells and, therefore, NBs

have been postulated to arise from a pluripotent precursor cell or either of these cell types, but not from any lineage other than the sympathoadrenal, suggesting that the oncogenic events occur after the decision for the cells to differentiate into sympathetic neurons has been taken (Kamijo and Nakagawara, 2012; Nakagawara *et al.*, 2018). From a molecular perspective, it is becoming evident that components of the transcriptional machinery, such as V-Myc Avian Myelocytomatosis Viral Oncogene Neuroblastoma (*MYCN),* Achaete-Scute Family BHLH Transcription Factor 1 *(Mash1),* Inhibitor Of DNA Binding 2 *(Id2*), Heart And Neural Crest Derivatives Expressed 2 *(dHAND2),* Hypoxia Inducible Factor *(HIF)* and Paired Like Homeobox 2 (*PHOX2)*, are involved in the commitment to the sympathetic lineage fate and are, therefore, speculated to also play an important role in NB development (Nakagawara *et al*., 2018).

In ~70% of the patients NBs present as abdominal masses. In terms of primary sites of appearance, the adrenal gland comprises the most common one with ~40% of the cases arising there, followed by the abdominal area (~25%), the thorax (15%), the cervix (5%) and the pelvic sympathetic ganglia (5%) (Ahmed *et al.*, 2017). The clinical features of NBs are highly diverse and massively depend on the site of the primary lesion, age, as well as on the presence and the extent of metastases and paraneoplastic syndromes, ranging from asymptomatic cases to cases of severe pain. NBs of the neck/ upper chest (thoracic tumours) can be diagnosed as “incidentaloma” upon chest radiography, and cause Horner’s syndrome (ptosis, miosis, anhidrosis), while those across the spinal cord can expand and cause paralysis. Abdominal NBs are often accompanied by swelling and/or symptoms due to organ compression (constipation, urinary retention) (Kamijo and Nakagawara, 2012; Mullassery and Losty, 2016).

Nearly half of the NB patients have localised or regional disease at diagnosis, while 35% of the cases present with regional lymph node spread. At the same time, 50% of the diagnosed cases present with distant metastases at diagnosis, which occurs through the lymphatic and haematopoietic routes (Ahmed *et al.*, 2017; Shohet and Foster, 2017; Tolbert

and Matthay, 2018). High stage NBs also metastasise to lymph nodes and bone marrow, liver, skin, orbits and dura, while intracranial and pulmonary spread comprises an uncommon metastatic possibility (Kamijo and Nakagawara, 2012; Shohet and Foster, 2017), and when the metastases are severe the clinical state of the patient gets poorer. In these cases, some typical symptoms are the periorbital ecchymosis ("raccoon eyes") and proptosis, while some cases present with pallor, weight loss, pain, fever and visual impairment. A minority of cases present with diarrhoea in cases of secondary vasoactive intestinal peptide secreting tumours ("VIPomas"), flushing and massive sweating in catecholamine-secreting tumours and immune-mediated nystagmus/ "dancing eyes" with the cerebellar "opsoclonus-myoclonus" syndrome (Mullassery and Losty, 2016; Ahmed *et al.*, 2017).

1.1.3. Patient Classification

The clinical outcomes of NBs may vary widely, from spontaneous regression due to neuronal differentiation and/or apoptosis to malignant progression (Kamijo and Nakagawara, 2012; Nakagawara *et al.*, 2018). To evaluate and predict this, careful patient stratification is essential. To date, patients are stratified into very low, low, intermediate, high and ultra-high risk groups. This stratification is based primarily on histologic characteristics, age at diagnosis, stage and genetic/molecular profiles, with age at diagnosis being the most indicative prognostic factor (Hara, 2012; Pandey and Kanduri, 2015; Nakagawara *et al.*, 2018). Given the fact that NB is characterised by high heterogeneity, both inter- and intra- tumour, the need for accurate patient classification is more urgent than ever before (Aveic *et al.*, 2018). This high degree of heterogeneity is partly the consequence of the fact that NBs arise from tissues that are still differentiating during embryonal development, and, thus, the initiation of oncogenesis could occur at multiple time points (Shohet and Foster, 2017).

Historically, NB patients were stratified using the International Neuroblastoma Staging System (INSS), which was primarily based on the aggressiveness of the surgical approach employed. However, in order to standardise the staging regardless the surgical approach, the International Neuroblastoma Risk Group (INRG) was then adopted, incorporating image-defined risk factors (IDRFs) identified before surgery, including pathological and biological markers, such as tumour extension into a second body compartment, encasement of any large blood vessels, tracheal or large bronchial compression, involvement of major nerve roots (such as the brachial plexus), invasion of the spinal canal, or infiltration of the nearby kidneys, mesentery, pericardium, liver, diaphragm or pancreas. These are predictive of worse event-free and overall survival (Tolbert and Matthay, 2018) (Table 1.1). However, caution must be taken when using these two systems in tandem, since discrepancies can easily occur. (Ahmed *et al.*, 2017; Shohet and Foster, 2017). Another widely adopted staging system for NBs, the International Neuroblastoma Pathology Classification (INPC), inherent to its name classifies NBs based on their pathology and histology. In particular, the classifications are performed based on the relative abundance of neural-type cells (primitive neuroblasts, differentiating neuroblasts, maturing ganglion cells) versus Schwann-type cells (immature and mature Schwann cells), the extent of cell differentiation, the mitosis karyorrhexis index (MKI) and the age of the patient. In general, better prognosis is associated with differentiating cells, low to intermediate MKI and age <1.5 years (Mullassery and Losty, 2016; Ahmed *et al.*, 2017).

Table 1.1. Comparison of NB staging systems.

Tumor extent	INRG* staging system		INSS*	
Localized tumor	L1:	Localized tumor not involving vital structures as defined by the list of image-defined risk factors (IDRFs) and confined to one body compartment	Stage 1:	Localized tumor confined to the area of origin; complete gross excision with negative lymph nodes
	L2:	Locoregional tumor with presence of one or more IDRFs	Stage 2:	Localized tumor with incomplete gross excision or positive ipsilateral lymph node
			Stage 3:	Tumor extending across the midline or with bilateral lymph node involvement
Metastatic tumor	M:	Distant metastatic disease (except stage MS)	Stage 4:	Dissemination of tumor to distant lymph nodes, bone, bone marrow, liver or other organs (except stage 4S)
Metastatic tumor	MS:	Metastatic disease in children younger than 18 months with metastasis confined to skin, liver, and/or bone marrow (<10%)	Stage 4S:	Localized tumor with dissemination limited to liver, skin and bone marrow (<10%)

***INRG:** International Neuroblastoma Risk Group**; INSS:** International Neuroblastoma Staging System (adapted from Ahmed *et al.*, 2017).

Nevertheless, the molecular heterogeneity of NB added an extra layer of difficulty in choosing the most suitable therapeutic regiment for NB patients, and therefore, a tumour biology component has been added to the stratification strategy. Consequently, the latest patient stratification scheme includes the INRG staging, age, histologic category, grade of tumour differentiation, *MYCN* amplification, 11q aberration and ploidy, with some further molecular markers conferring even greater accuracy (see below) (Table 1.2). In general, according to this system poor or absent cell differentiation, *MYCN* amplification, and presence of 11q aberration and diploidy are regarded as unfavourable biological characteristics and are associated with poor outcome. Overall, very low risk is defined as >85% event-free survival, low risk 75-85%, intermediate risk 50-75% and high risk <50% (Nakagawara *et al.*, 2018; Tolbert and Matthay, 2018).

Table 1.2. The INRG staging system with incorporated genetic characteristics.

Risk group for treatment	INRG stage	IDRFs in primary tumor	Distant metastases	Age (month)	Histological category	Grade of differentiation	MYCN status	Genomic profile	Ploidy
Very-low	L1	Absent	Absent	Any	GNB nodular, NB	Any	–	Any	Any
	L1 or L2	Any	Absent	Any	GN, GNB intermixed	Any	–	Any	Any
	MS	Any	Present	<12	Any	Any	–	Favorable	Any
Low	L2	Present	Absent	<18	GNB nodular, NB	Any	–	Favorable	Any
	L2	Present	Absent	≧18	GNB nodular, NB	Differentiating	–	Favorable	Any
	M	Any	Present	<18	Any	Any	–	Any	Hyperdiploid
Intermediate	L2	Present	Absent	<18	GNB nodular, NB	Any	–	Unfavorable	Any
	L2	Present	Absent	≧18	GNB nodular, NB	Differentiating	–	Unfavorable	Any
	L2	Present	Absent	≧18	GNB nodular, NB	Poorly differentiated, undifferentiated	–	Any[a]	Any
	M	Any	Present	<12	Any	Any	–	Unfavorable and/or diploid	
	MS	Any	Present	12–18	Any	Any	–	Favorable	Any
	MS	Any	Present	<12	Any	Any	–	Unfavorable	Any
High	L1	Absent	Absent	Any	GNB nodular, NB	Any	+	Any	Any
	L2	Present	Absent	≧18	GNB nodular, NB	Poorly differentiated, undifferentiated	+	Any	Any
	M	Any	Absent	12–18	Any	Any	–	Unfavorable and/or diploid	
	M	Any	Present	<18	Any	Any	+	Any	Any
	M	Any	Present	≧18	Any	Any	Any	Any	Any
	MS	Any	Present	12–18	Any	Any	–	Unfavorable	Any
	MS	Any	Present	<18	Any	Any	+	Any	Any

[a]Some clinical trial groups consider unfavourable pathology with Stage L2, over 18 months of age.
GN: ganglioneuroma; **GNB**, ganglioneuroblastoma. Adapted from Nakagawara *et al*., 2018.

In very low risk NB patients, several tumours display spontaneous regression or even complete remission when short-term chemotherapy is provided. The **very low risk** group (~28% of all patients) is comprised by patients falling in the L1/L2 INSS stage, with ganglioneuroma maturing or ganglioneuroblastoma intermixed histology, L1 without *MYCN* amplification, and stage MS, younger than 18 months old and without 11q loss. **Low risk** NB patients (~50% of all patients) are INSS stage 1 or 2A/B but without *MYCN* amplification, and INSS stage 4S characterised by hyperdiploidy, younger than 1-year-old, favourable histology and have generally favourable clinical prognosis. **Intermediate risk** patients comprise a very heterogeneous group, with variable prognoses depending on the histological and molecular background. Generally, non-low risk cases without poor

prognostic factors fall within this group. As a result, this group includes INSS stage 3/ 4 patients, <1 year old without *MYCN* amplification, INSS stage 4 patients, 12-18 months old, with favourable histology but no *MYCN* amplification, INSS stage 4S patients, < 1-year-old (*MYCN* non-amplified, unfavourable histology and DNA index>1), and finally, patients in INSS stage 4S (*MYCN* non-amplified, favourable histology and DNA index=1) (Shohet and Foster, 2017; Nakagawara *et al.*, 2018).

On the other hand, **high risk** patients are characterised by amplified *MYCN*, which is a well-established oncogene, age older than 18 months and tumours that are highly aggressive and metastatic, little or no response to chemotherapy and generally, have poor clinical outcome with a five-year event-free survival percentage 30-50% (Hara, 2012; Pandey and Kanduri, 2015). Although the overall survival of NB patients has significantly improved over the past decades, high risk NBs still remain one of the toughest tumours to cure, despite the advances and combination regimes in treatment (Kamijo and Nakagawara, 2012; Nakagawara *et al.*, 2018). In line with this, high risk survivors very often develop second malignant neoplasms, importantly haematologic ones (Applebaum *et al.*, 2017). As a sub-category of high risk patients, there is a group that is described as **ultra-high risk.** Patients in this group are characterised by high levels of tyrosine hydroxylase (TH) and PHOX2B in the bloodstream, *MYCN* amplification and bone metastasis, with overall and event-free survival rates of 0% (Huang and Weiss, 2013; Nakagawara *et al.*, 2018).

1.1.4. Molecular Characteristics

The molecular and genetic profiling is of paramount importance for patient stratification and, therefore, for better prediction and prognostication. One of the most important and earliest identified genetic alterations in high-risk NB is the amplification of the *MYCN*-containing locus 2p24, which is observed in ~20-25% of the cases (Kamijo and Nakagawara, 2012; Pandey and Kanduri, 2015; Nakagawara *et al.*, 2018). Notably, *NCYM* (also known as

MYCNOS) which is a *de novo* evolved cis- antisense gene of *MYCN*, is also 100% co-amplified and co-expressed with *MYCN, and* its co-overexpression is also associated with unfavourable prognosis, as it acts by stabilizing N-Myc through the inhibition of the protein responsible for the degradation of N-Myc [Glycogen Synthase Kinase 3 Beta (GSK3β)] (Nakagawara *et al.*, 2018). Other genetic signatures include gains at chromosomes 1q, 2p and, significantly at 17q (especially unbalanced gains) and chromosomal losses at 1p (identified in 30-35% of all NBs), 3p and 11q (35-45% of primary NBs) (Domingo-Fernandez *et al.*, 2013; Youssef *et al.*, 2014; Pandey and Kanduri, 2015; Ahmed *et al.*, 2017). Finally, alterations of the total DNA content of the tumour cells are an indication of prediction and prognosis. In general terms, higher DNA content, in other words, hyperdiploid tumours with DNA index (DI)>1 respond better to therapy and have better prognosis compared to those with DI=1, i.e. diploid (Ahmed *et al.*, 2017).

In addition to these genomic aberrations, numerous studies have identified gene-specific risk-related mutations. A lot of these aberrations are to some extent N-Myc-related. For example, *ALK* activating mutations have been reported, especially in cases of hereditary NB, and have been associated with pre-malignant states (Kamijo and Nakagawara, 2012; Domingo-Fernandez *et al.*, 2013; Pandey and Kanduri, 2015). Due to its proximity to *MYCN* on chromosome 2, *ALK* is also co-amplified with *MYCN* and plays an oncogenic role by activating the PI3K and RAS/MAPK pathways (Nakagawara *et al.*, 2018). Aurora kinase A (*AURKA*), another N-Myc stabiliser is also frequently overexpressed in *MYCN*-amplified tumours (Nakagawara *et al.*, 2018). In addition, lin-28 homologue B (*LIN28B*) is overexpressed in high risk cases and is an indicator of poor prognosis (Nakagawara *et al.*, 2018). Of note are the perturbations of the tropomyosin-related kinase (Trk) family expression levels. For TrkA, overexpression is associated with low-risk NBs, while low expression with high-risk NBs with unfavourable prognosis. On the contrary, TrkB and its ligand brain-derived neurotrophic factor (BDNF) are highly expressed mainly in *MYCN*-amplified NBs and are indicators of poor prognosis. (Kamijo and Nakagawara, 2012;

Nakagawara *et al.*, 2018). Further, overexpressed Telomerase Reverse Transcriptase (*TERT*) and Alpha-thalassaemia/ mental retardation syndrome X-linked (*ATRX*) are found in 25% and ~11% of high risk NBs, respectively, and are indicators of poor outcome (Ahmed *et al.*, 2017; Nakagawara *et al.*, 2018). *LMO1/3* aberrations are linked to advanced disease and poor outcome (Nakagawara *et al.*, 2018), and Neuroblastoma Breakpoint Family Member 23 (*NBPF23),* BRCA1 Associated RING Domain 1 *(BARD1),* AT-Rich Interaction Domain 1A/1B *(ARID1A/ARID1B), Neuroblastoma RAS Viral (V-Ras) Oncogene Homolog (NRAS),* Leucine-Rich Repeat Neuronal 1 *(NLRR1)* and Chromodomain Helicase DNA Binding Protein 9 *(CHD9)* alterations have also been associated with aggressiveness and poor prognosis (Nakagawara *et al.*, 2018; Tolbert and Matthay, 2018).

Aberrant expression of tumour suppressor genes (TSGs) is also common in NBs. Loss of TP53, the most well-known TSG, has been found in relapsed, treatment-resistant NB cases (Singhal *et al.*, 2017; Nakagawara *et al.*, 2018). Moreover, loss of caspase 8 (CASP8) expression has been found in a generous percentage of NBs (25-35%), primarily in high-risk ones (Kamijo and Nakagawara, 2012; Huang and Weiss, 2013). Deletion or loss of function of KIF1Bβ is, as well, correlated with advanced disease stages, low expression of the Calmodulin-binding Transcription Activator 1 (CAMTA1) and Tumor Suppressor In Lung Cancer 1 (TSLC1) is associated with poor outcome, and the absence or very low levels of the Chromodomain Helicase DNA Binding Protein (CHD5) chromatin remodeller have been found in high risk NBs, resistant to therapy (Nakagawara *et al.*, 2018).

Apart from the genetic changes that confer poor prognosis and outcome for NB patients, the contribution of non-genetic aberrations, that is epigenetic changes and non-coding RNAs (see section 1.4.6.2.), should not be ignored. In fact, members of the suppressive polycomb group of proteins, have been associated with NB genesis and progression by suppressing multiple TSGs, such as Castor Zinc Finger 1 (*CASZ1),* Clusterin *(CLU*), RUNX Family Transcription Factor 3 *(RUNX3)* and Nerve Growth Factor Receptor *(NGFR)*. A member of the complex, Bmi-1 is highly expressed in nearly all primary NBs (~90%) and

contributes to tumourigenesis through the repression of the TSGs KIF1Bβ and TSLC1 (Nakagawara *et al.*, 2018).

1.1.5. Therapeutic approaches

Given the high heterogeneity of NBs, the therapeutic approaches employed for patient treatments should comply with the needs and stratification of the patient. Therefore, treatments differ massively, ranging from just observation and follow-up of the tumour for very low risk patients with spontaneous regression to aggressive, combination therapy for the high risk patient group (Tolbert and Matthay, 2018).

Briefly, the current treatment for low risk patients consists predominantly of surgical excision. This is often accompanied by chemotherapy when there is a residual tumour or the anatomical location of the tumour does not permit surgery. In other therapeutic regimens, surgery or relapse is followed by chemotherapy and irradiation is given when neurological symptoms arise (Nakagawara *et al.*, 2018). For intermediate risk patients, the therapeutic approaches are diverse, due to the high diversity of the patients' characteristics in this group, but usually include surgery, chemotherapy and/or radiotherapy (Mullassery and Losty, 2016; Nakagawara *et al.*, 2018; Tolbert and Matthay, 2018).

For high risk patients, treatment consists of combination therapy including surgical excision of the tumour, radiotherapy and chemotherapy, including induction, consolidation and maintenance phases, and autologous hematopoietic stem cell transplantation (AHSCT) (Mullassery *et al*.,2014; Mullassery and Losty, 2016; Nakagawara *et al.*, 2018). The most common induction therapy for high risk NBs includes the use of alkylators (temozolomide-TMZ, cyclophosphamide, ifophamide), anthracyclins, topoisomerase inhibitors (topotecan, irinotecan, etoposide, doxorubicin), platinum compounds (carboplatin) and vinca alkaloids, (Hara, 2012; Nakagawara *et al.*, 2018; Yavuz *et al.*, 2018) as well as ^{131}I-MIBG therapy (Ratner *et al.*, 2016; Nakagawara *et al.*, 2018). Despite the aggressiveness and the multi-modal nature of the therapeutic approaches, the prognosis of this group remains relatively poor, creating the necessity of new, smarter treatment strategies.

To address some of the problems caused by poor delivery of chemotherapeutic agents, the use of nanoparticles (liposomes, nanocrystals, viruses etc.) could prove to be really useful (Arora and Bandopadhyaya, 2018). Meanwhile, other alternative sorts of therapy are under intensive investigation. For instance, differentiation-inducing therapy using retinoids, such as 13-cis retinoic acid results in some improvement of the overall survival in some patients (Mullassery and Losty, 2016; Nakagawara *et al.*, 2018). Like in a diversity of other malignancies, immunotherapy is a promising approach for NBs. For high risk NBs, the use of a chimeric anti-GD2 monoclonal antibody, with or without the administration of interleukin 2 (IL-2) and granulocyte monocyte colony-stimulating factor (GM-CSF) is currently under thorough investigation (Mullassery and Losty, 2016). In addition, immune checkpoint inhibitors, such as the anti-PD-L1 inhibitors atezolizumab and pembrolizumab are already in clinical trial stage (Nakagawara *et al.*, 2018), and CAR-T therapy, as well as vaccines, are being investigated (Tolbert and Matthay, 2018). What is more, new lines of therapy include targeted therapy (Ratner *et al.*, 2016). Some appealing targets include *ALK, MYCN*, and the Phosphatidylinositol-3-Kinase/AKT Serine/Threonine Kinase /mammalian target of rapamycin (PI3K/AKT/mTOR) pathway. To this end, some very promising agents are being tested against these targets, such as small molecule ALK inhibitors, Aurora kinase A inhibitors, [e.g. TP-0903 (Aveic *et al.*, 2018)], and difluoromethylornithin (DFMO), and PI3K, Akt and mTOR inhibitors, respectively (Huang and Weiss, 2013; Nakagawara *et al.*, 2018). In addition, the multikinase inhibitor sorafenib, PLK1 (polo-like kinase 1) inhibitors and rapamycin, comprise agents that are already in clinical trials (Hara, 2012; Kamijo and Nakagawara, 2012; Nakagawara *et al.*, 2018). Finally, a number of other agents are currently in premature experimental stages but do present outstanding potential, such as HDAC inhibitors [e.g. romidepsin (Hegarty *et al.*, 2017)] N-acetyl aspartate (Mazzoccoli *et al.*, 2016), actinomycin D (Wang *et al.*, 2007), tetramethylpyrazine (Yan *et al.*, 2014), nitrofuran compounds (McNeil *et al.*, 2013), interferon-β (Dedoni *et al.*, 2010), and metformin (Costa *et al.*, 2014).

1.2. Glioma

Glioma is the most common malignant tumour of the Central Nervous System (CNS) in adults (Goodenberger and Jenkins, 2012; Y. F. Gao *et al.*, 2016) with 50% of the diagnosed brain tumours being gliomas (Boussiotis and Charest, 2018). Primary brain tumours are by far fewer, comparing to metastatic disseminated tumours to the CNS (Nikaki *et al.*, 2017; Boussiotis and Charest, 2018). The incidence is higher in industrialised countries, and especially in white populations and men, mainly during the sixth decade of life (Nikaki *et al.*, 2017). Gliomas are generally neuroectodermal tumours and based on their cellular origin they are classified according to WHO (World Health Organisation) into astrocytomas, oligodendrogliomas, mixed tumours, like oliogoastrocytomas, and ependymomas (Goodenberger and Jenkins, 2012; Zhang and Leung, 2014).

The current study focuses on the most malignant, yet most common, glioma: glioblastoma, also known as glioblastoma multiforme (GBM). GBMs account for approximately 15% of all primary brain and CNS tumours and 55% of all gliomas. GBMs are almost invariably fatal with overall survival of just one year (Zhang and Leung, 2014; André-Grégoire and Gavard, 2017; Nikaki *et al.*, 2017). In fact, patients with glioblastomas have a 5-year survival rate of only 5% (Goodenberger and Jenkins, 2012), while the median survival rate is ~1 year for patients treated with surgery, chemotherapy and radiotherapy (Ramos *et al.*, 2016; Capdevila *et al.*, 2017). Sadly, this poor survival rate has been improved only slightly, despite the multimodal therapy in use (Ferrer *et al.*, 2018). GBMs can be either primary or secondary depending on their clinical presentation, with the vast majority (~85%) being primary (Boussiotis and Charest, 2018).

Notably, there is a clear distinction between adult gliomas and their paediatric counterparts (Weller *et al.*, 2015). In general, paediatric tumours of the brain affect patients of ages 0-19, are characterised by high heterogeneity and differ significantly from the adult in terms of incidence, histological characteristics, sites of origin and responsiveness to treatment regimes. Nervous system tumours are the most common solid malignancy of childhood,

comprising the leading cause of cancer-related morbidity and mortality (Firme and Marra, 2014). The classification remains the same as in adult gliomas, based on the WHO histological criteria (see section 1.2.3) (Hargrave, 2009; Ryall *et al*., 2017). GBM, being one of the most severe and incurable malignancies across the lifespan, remains virtually incurable in children, as well, with only 10-30% of patients surpassing the 2-year survival. The majority of paediatric GBMs (pGBMs) arise *de novo* and unlike adult gliomas, low grade gliomas rarely transform into high grade ones. Potential cells of gliomagenesis origin are neural stem cells and more differentiated progenitor cells, such as oligodendrocyte precursor cells (Sturm *et al.*, 2014). The incidence, anatomic location, progression mode and histopathology of pGBM, as well as the molecular features, differ importantly from those of adult GBM, rendering current adult GBM treatments, such as temozolomide (TMZ), ineffective for pGBM (Fontebasso *et al.*, 2013; Ryall *et al.*, 2017), although some histological characteristics, especially in cases of diffuse tumours (explained in section 1.2.3) remain shared (Ryall *et al*., 2017).

1.2.1. Diagnosis

Typically, patients with primary gliomas remain asymptomatic until very bold manifestations of the tumour emerge. These include headaches, seizures, nausea/emesis, syncope, neurocognitive dysfunction, personality changes, sensory loss, gait imbalance, urinary incontinence, hemiplegia, aphasia, hemispatial neglect, and visual field impairment. At the same time, secondary GBMs, i.e. those arising from lower grade lesions, such as astrocytomas, display symptoms more than six months prior to diagnosis (Goodenberger and Jenkins, 2012; Boussiotis and Charest, 2018). Diagnosis can be performed using a plethora of diagnostic tests and means, including molecular tests and tumour imaging techniques.

MRI with gadolinium (Gd) enhancement is the golden standard for the detection of brain lesions, their response to therapy, as well as their recurrence. As an alternative to or in

combination with MRI, ^{18}F-FDG-PET has also been widely used to assess the same features of gliomas. Despite its established use as a diagnostic means, ^{18}F-FDG does not comprise the most appropriate radio-labelled trace to detect brain lesions. In line with this, a number of radio-labelled agents have been developed, including radio-labelled amino acids, hypoxia-related detection agents, proliferation markers, such as ^{18}F- Fluorothymidine (^{18}F-FLT), and membrane biosynthesis-disruption detectors, like ^{18}F-choline (Nikaki *et al.*, 2017). In current diagnostics, MRI and PET are used in a supplementary fashion to achieve optimal detection of the tumour burden and grade. As a rule, LGGs do not present Gd enhancement, ^{18}F-FLT uptake or alterations in cerebral blood volume (CBV), while HGGs have mild and high Gd enhancement and ^{18}F- FLT uptake for grade III and IV gliomas, respectively (Collet *et al.*, 2015; Nikaki *et al.*, 2017). However, both MRI and ^{18}F-FDG-PET, despite their almost ubiquitous use have their limitations. While MRI offers evidence of the morphology of gliomas, it offers very limited information on the biological traits of the lesion. Meanwhile, although ^{18}F-FDG-PET was initially suggested to distinguish among the tumour grades based on the positive association of tumour grade and glycolysis rate, its use has been hampered owing to the fact that normal brain areas also display high glucose metabolism (La Fougère *et al.*, 2011; André-Grégoire and Gavard, 2017; Nikaki *et al.*, 2017).

Unfortunately, to date there exist only a few reliable, established molecular markers of GBM that are used for diagnostic purposes, despite the massive molecular changes underpinning GBM genesis and development (also refer to section 1.2.4) (André-Grégoire and Gavard, 2017). Among them, the most widely used are the 6-O-methylguanine-DNA methyltransferase (*MGMT*) methylation status, the Endothelial Growth Factor (EGFRvIII) variant, the Isocitrate Dehydrogenase 1 (*IDH1*) and V-Raf Murine Sarcoma Viral Oncogene Homolog B (*BRAF*) mutations, and the 1p/19q co-deletion (Westphal and Lamszus, 2015; Saadeh *et al*., 2018). To overcome the diagnosis challenge, the detection of GBM-derived extracellular vesicles is a promising alternative, since they can be easily obtained with non-

invasive techniques, unlike intracranial tumour biopsies, and also, their molecular and cellular content reflects that of the mother GBM cells. Besides, the short half-life of the circulating vesicles suggests a rather accurate diagnosis time-wise and can reflect rapid changes of the tumour (André-Grégoire and Gavard, 2017; Azam *et al.*, 2019). Nevertheless, accurate diagnosis of gliomas, although of utmost importance, remains lagging.

1.2.2. Pathogenesis and Clinical Features

Gliomas are tumours that arise from glial cells, anywhere in the brain, usually in the cerebral hemispheres (Nikaki *et al.*, 2017; Saadeh *et al.*, 2018). However, the exact cellular origin of GBMs remains largely unknown. Although it has been suggested that GBMs arise from glial cells that undergo malignant transformation, it has been postulated and backed up with evidence that GBMs may also originate from neural stem cells (NSCs) residing in the ventricular-subventricular zone (V-SVZ) (Capdevila *et al.*, 2017). Despite the fact that, traditionally, it has been believed that postnatally the CNS does not generate new neurons, a population of NSCs persists and generates neurons, astrocytes, and oligodendrocytes in two forebrain proliferative niches, which can, in turn, give rise to GBMs (Ramos *et al.*, 2016).

Diffuse gliomas, including GBMs, are characterised by infiltrative growth through the CNS parenchyma, a feature that vastly contributes to the tumours' aggressiveness. Tumour cells invade either individually or as groups, to form a network throughout the neuropil. This results in the generation of secondary structures with neoplastic cells surrounding neurons (perineuronal satellitosis) and blood vessels (perivascular satellitosis), as well as myelinated fibres. These structures can also extend beyond the pial margin (subpial spread). (Ryall *et al.*, 2017; Ferrer *et al.*, 2018; Sampetrean and Saya, 2018).

Interestingly, surgically resected GBMs consist of neoplastic cells but also of rich non-neoplastic stromal cells, which surprisingly comprise about 30-40% of the tumour bulk. Non-neoplastic cells include non-transformed astrocytes and oligodendrocytes, endothelial

cells (ECs), pericytes and numerous, diverse immune cells, all of them orchestrating a very abnormal extracellular matrix and each one of them uniquely contributing to tumour progression (Boussiotis and Charest, 2018; Ferrer, Moura Neto and Mentlein, 2018). For example, astrocytes have been shown to protect the tumour from TMZ by preventing apoptosis (Chen *et al.*, 2015). Tractography imaging has also revealed a massive loss of white matter around GBMs, suggesting that there is a significant loss in the density of healthy neurons in and around the tumour, and therefore, a loss of oligodendrocytes, the supportive cells responsible for neuronal myelination (Boussiotis and Charest, 2018). In addition, the vasculature of the brain is comprised of ECs and pericytes, with ECs physically interacting with astrocytes to form the blood-brain barrier (BBB). In contrast with the normal brain, the GBM vasculature is highly proliferative allowing for abnormal blood vessel structures (e.g. with blunted ends) to be generated. This, in turn, leads to the generation of hypoxic regions, something critical for treatment failure, as well as to severe haemorrhage. In other cases, abnormal blood vessel permeability leads to severe oedemas, a typical feature of the clinical image of GBMs (Saito and Tominaga, 2017; Boussiotis and Charest, 2018; Ferrer *et al.*, 2018). Cerebral oedema may result in increased intracranial pressure and acute herniation syndromes which can cause permanent brain damage (Esquenazi *et al*., 2017).

A very important clinical feature of GBMs is their unique immune landscape since even in normal physiological conditions the brain's immunity differs from the rest of the body's. Within malignant gliomas, the immune repertoire consists of microglia, peripheral macrophages, myeloid-derived suppressor cells (MDSCs), natural killer (NK) cells, leukocytes, $CD4^+$ T helper cells, $CD8^+$ cytotoxic T cells and Tregs. A very large proportion of the total immune cells of a glioma are tumour associated macrophages (TAMs), which undergo a transition from a pro-inflammatory "M1" phenotype promoting inflammatory, anti-tumour responses, to a "M2" phenotype that is immunosuppressive, and therefore tumour cell-protective. Interestingly, this pattern is also observed in the tumour microglial cells.

TAMs hold the capacity to produce and secrete growth and angiogenic factors, as well as immunosuppressive cytokines, thus promoting glioma progression. High abundance of TAMs has been observed in higher grade tumours compared to lower, rendering the presence of TAMs a prognostic factor of poor outcome (Murray *et al.*, 2014; Boussiotis and Charest, 2018). Meanwhile, MDSCs act by suppressing the cytotoxic activity of NK cells, secreting immunosuppressive cytokines and activating Tregs (Marvel and Gabrilovich, 2015). NK cells that would normally target abnormal cells for cell lysis, do not recognise tumour cells as abnormal, since tumour cells, like normal self- cells, express MHC class I molecules on their surface that interact with the killer cell immunoglobulin-like receptor of NK cells to inhibit destruction. In addition, NK cell abundance is relatively low in GBM patients (Wiendl *et al.*, 2002; Fadul *et al.*, 2011). Tumour infiltrating leukocytes (TILs) are present in the tumour microenvironment, although in lower abundance and less potent to exert their cytotoxic role, as they are suppressed by TGF-β and IL-10 secreted by glioma and stromal cells. Importantly, there is accumulating evidence that GBMs overexpress PD-L1, which binds the inhibitory checkpoint molecule PD-1 and in turn inhibits $CD4^+$ and $CD8^+$ activation. Finally, the immunosuppressive phenotype is enhanced by the accumulation of DCs and Tregs in the tumour microenvironment, with intratumoural Tregs being linked to poor prognosis (Kmiecik *et al.*, 2013; Perng and Lim, 2015).

Some patients present with pseudo-recurrence or pseudo-regression about two months after treatment with TMZ or radiation therapy, adding an extra level of complexity in the follow-up (Nihashi, Dahabreh and Terasawa, 2013; Nikaki *et al.*, 2017). Although GBM is a highly infiltrative tumour diffusing through the CNS, it rarely metastasises outside of it, given the very short overall survival of the tumour. In fact, even within the CNS, extracranial metastases are rare, affecting 0.4-0.5% of the patients (da Cunha and Maldaun, 2019). When it does metastasise, the most common sites are the lungs, pleura and cervical lymph nodes, and there are also a few cases of skin metastasis (Lewis *et al.*, 2017).

1.2.3. Patient Classification

For CNS tumours the tumour grade is determined based on histopathological features, according to St Anne-Mayo grading system (Gupta and Dwivedi, 2017). The predominant characteristics that are assessed are the presence of nuclear pleomorphism (atypia), mitotic activity and cellularity, endothelial cell proliferation, and necrosis. The more increased all of these features are, the higher the grade of the tumour. In particular, tumours that do not meet any of the criteria are classified as grade I, tumours that meet one criterion are grade II, tumours that meet any two criteria are grade III, and finally, tumours that fulfil three or all four criteria are classified as grade IV (Goodenberger and Jenkins, 2012; Gupta and Dwivedi, 2017). Generally, grade I and II gliomas are considered as low grade gliomas (LGGs), and histopathologically they are either grade I (pilocytic) astrocytomas or grade II astrocytomas or oligodendrogliomas, which can progress to higher grade tumours. For LGGs the 5-year survival rate is approximately 50% (Goodenberger and Jenkins, 2012; Zhang and Leung, 2014). On the contrary, grade III and IV gliomas are considered as high grade gliomas (HGGs) and include grade III anaplastic astrocytomas, which usually progress to grade IV astrocytomas, also known as glioblastomas, and grade III oligodendrogliomas (Goodenberger and Jenkins, 2012; Gao *et al.*, 2016).

1.2.4. Molecular Characteristics

Despite being universally used, this classification was based primarily on histopathological features of the tumours examined microscopically, with different potential cells of origin and different differentiation levels, causing confusion in diagnosis and patient stratification. As a result, there was an urgent need to encompass molecular characteristics into the tumour classification in order to make the diagnosis, prediction and prognosis more accurate. This was achieved through the updated WHO 2016 classification of the CNS tumours, which incorporated some fundamental genetic and molecular characteristics of the tumours to re-classify them with greater accuracy and eliminate interlaboratory discrepancies. The main molecular and genetic aberrancies met in adult gliomas that have been introduced in the

classification criteria are the *IDH1* R132H mutation, the *IDH2* R172K mutation, the 1p/19q co-deletion, the MGMT methylation status, the *TERT* C228T and C250T mutations, the *ATRX* loss, the TP53 loss or loss of function and the H3K27M mutation (Table 1.3) (Louis *et al.*, 2016; Gupta and Dwivedi, 2017).

Table 1.3. WHO 2016 histological grading of tumours of the CNS, incorporating the molecular status.

	I	II	III	IV	Grade unknown
Diffuse astrocytic and oligodendroglial tumors		Diffuse astrocytoma IDH mutant IDH wild type Oligodendroglioma IDH mutant, and1p19q co-deleted	Anaplastic astrocytoma IDH mutant IDH wild type Anaplastic oligodendroglioma, IDH mutant, and1p19q co-deleted	Diffuse midline glioma, H3 K27M-mutant Glioblastoma, IDH wild type Glioblastoma, IDH mutant	
Other astrocytic tumors	Pilocytic astrocytoma Subependymal giant cell astrocytoma	Pleomorphic xanthoastrocytoma Pilomyxoid astrocytoma	Anaplastic pleomorphic xanthoastrocytoma		
Ependymal tumors	Subependymoma Myxopapillary ependymoma	Ependymoma Papillary Clear cell Tanycytic Ependymoma, RELA fusion positive	Anaplastic ependymoma		
Choroid plexus tumors	Choroid plexus papilloma	Atypical choroid plexus papilloma	Choroid plexus carcinoma		
Other gliomas	Angiocentric glioma	Chordoid glioma of the third ventricle	Astroblastoma		
Neuronal and mixed neuronal-glial tumors	Dysplastic gangliocytoma of cerebellum Desmoplastic infantile astrocytoma/ ganglioglioma Dysembryoplastic neuroepithelial tumor Gangliocytoma Ganglioglioma Papillary glioneuronal tumor Rosette-forming glioneuronal tumor of the fourth ventricle Paraganglioma	Central neurocytoma Extraventricular neurocytoma Cerebellar liponeurocytoma	Anaplastic ganglioglioma		Diffuse leptomeningeal glioneuronal tumor
Tumors of the pineal region	Pineocytoma	Pineal parenchymal tumor of intermediate differentiation Papillary tumor of the pineal region (could be Grade III also)		Pineoblastoma	
Tumors of cranial and paraspinal nerves	Schwannoma Perineurioma Hybrid nerve sheath tumors		MPNST Epithelioid MPNST MPNST with perineurial differentiation (could be I, II, IV)		
Meningiomas	Meningioma	Atypical	Anaplastic (malignant)		
Mesenchymal tumors	Solitary fibrous tumor/ hemangiopericytoma: Grade 1, 2, 3 Hemangioblastoma				
Tumors of the sellar region	Craniopharyngioma Granular cell tumor Pituicytoma Spindle cell oncocytoma				

IDH: Isocitrate dehydrogenase; **CNS**: Central nervous system; **NOS**: Not otherwise specified; **MPNST**: Malignant peripheral nerve sheath tumour; **AT/RT**: Atypical teratoid/rhabdoid tumour. (adapted from Gupta and Dwivedi, 2017).

In specific, IDH mutations are the most important distinguisher between glioma and gliosis and are present in oligodendrogliomas, astrocytomas and GBMs, especially the secondary ones arising from astrocytomas. They have generally been correlated with favourable prognosis (Gupta and Dwivedi, 2017; Kondo, 2017). In grade II/III gliomas, and, in a non-1p/19q co-deleted setting they contribute an intermediate clinical outcome (Goodenberger and Jenkins, 2012; Weller *et al.*, 2015; X. Q. Zhang *et al.*, 2015). In addition, the paired deletion of chromosome arms 1p and 19q is indicative of lower grade gliomas, such as oligodendrogliomas and mixed oligoastrocytomas, and has, as well, a favourable outcome (Goodenberger and Jenkins, 2012; Weller *et al.*, 2015). At the same time, it is a reliable predictive biomarker to assess response to chemotherapy and radiation therapy (Gupta and Dwivedi, 2017).

MGMT codes for a DNA repair protein that removes alkyl-groups from the O6 position of guanine residues. Alkylating agents, such as TMZ, act by causing DNA damage, which needs functional DNA repair enzymes, such as MGMT, in order to be repaired. Therefore, if MGMT is in an active state, the DNA damage is repaired, thus nullifying the effect of TMZ. Hypermethylation of the *MGMT* promoter inactivates MGMT, allowing TMZ to induce DNA damage which remains unrepaired. As a result, *MGMT* hypermethylation has been reported in all GBM subtypes, and when present is correlated with improved prognosis and good response to alkylating agents therapy, such as TMZ (Goodenberger and Jenkins, 2012; Gupta and Dwivedi, 2017).

TERT mutations are more prevalent in higher grade lesions, mainly oligdendrogliomas and GBMs and are linked to radiotherapy resistance and poor overall outcome (Wiestler *et al.*, 2013; K. Gao *et al.*, 2016). Loss of ATRX is an indicator of anaplastic tumours, including anaplastic astrocytomas (45%), anaplastic oligoastrocytomas (27%) and anaplastic oligdendrogliomas (10%), and is also frequent in paediatric astrocytomas (Wiestler *et al.*, 2013; Gupta and Dwivedi, 2017). Deletions and/or mutations in p53 are spread virtually

across all gliomas, mainly medulloblastomas, GBMs and IDH-mutant astrocytomas (Gupta and Dwivedi, 2017; Kondo, 2017).

The H3 K27M mutation is usually found in midline structures, including the brain stem, thalamus and spinal cord. H3K27 is a commonly methylated residue and is related to gene activation when monomethylated, but gene silencing when di-/trimethyated. Although the mutant H3 account for a small percentage (3.6-17.6%), the whole H3 pool is affected, with K27M leading to a global loss of H3K27me2/3. In brief, polycomb repressor complex 2 (PRC2), which is responsible for the epigenetic gene silencing maintenance via trimethylating H3K27, aberrantly interacts with the mutant histone. In fact, the enhancer of zeste homolog 2 (EZH2) catalytic subunit of PRC2 which establishes the H3K27me3 mark is not properly bound to H3. Consequently, PRC2 targets are no longer repressed, leading to gliomagenesis and, thus, conferring poor outcome (Jones and Baker, 2014; Sturm *et al.*, 2014; Wesseling and Capper, 2018).

Apart from the newly-incorporated in CNS tumour classification genetic and molecular marks, there are a plethora of other well-established markers that contribute to patient stratification. In terms of chromosomal aberrations, chromosome 7 gain and chromosome 10 loss are common in the classical GBM subgroup, while loss of heterozygosity (LOH) of 17p is a common feature of the proneural GBM subgroup. 9p21.3 deletions are extremely common both in GBMs and in lower grade malignancies. Mutations in *EGFR,* basic fibroblast growth factor *(bFGF)*, *PDGF* (platelet-derived growth factor), Phosphatase and Tensin homolog (*PTEN*), Retinoblastoma (*Rb*), *NF1* and E2F Transcription Factor 1 (*E2F-1*) are also frequently met in gliomas, and either alone or in combination with each other and with chromosomal aberrations, are predictive and prognostic markers (Goodenberger and Jenkins, 2012; Gao *et al.*, 2016). Pilocytic astrocytomas are virtually always marked with mutations in the MAPK pathway (Wesseling and Capper, 2018). However, epigenetic marks have also emerged and have been used in patient stratification. The most reliable one has been the methylation pattern of CpG islands. Hypermethylated CpG islands have

been reported in a subset of proneural GBMs and are associated with younger age of onset and favourable prognosis. This phenotype is also known as glioma CpG island methylator phenotype (G-CIMP) (Boussiotis and Charest, 2018). Finally, several non-coding RNA signatures are being tested for their potential use as biomarkers of the disease (see section 1.11.2).

High grade gliomas, both astrocytomas and mainly GBMs, comprise extremely heterogeneous entities, both at the cellular level and molecular/genetic make-up (Hempel *et al.*, 2018; Sampetrean and Saya, 2018). According to the new classification, and mainly based on the IDH mutational status, GBMs are divided into IDH-wildtype (~90% of the cases, de novo GBMs, usually in patients over 55 years old), IDH-mutant (~10% of the cases, mainly secondary GBMs, earlier onset), and GBM not otherwise specified (NOS), for those cases where the IDH status determination is not possible (Louis *et al.*, 2016; Wesseling and Capper, 2018). Based on their molecular repertoire, historically, GBMs used to be further categorised into four subtypes: the proneural- with most of the secondary GBMs belonging to this category-, the neural, the mesenchymal and the classical, based on their molecular and genetic profiles (Goodenberger and Jenkins, 2012). More recently, however, GBMs of the neural type have been recognised as tumours with excessive adjacent neural tissue, and have, therefore, been regarded as artefacts (Boussiotis and Charest, 2018). The proneural GBMs are divided into two subgroups: those characterised by Platelet-Derived Growth Factor Receptor Alpha (PDGFRα) overexpression and loss of p53, and those with IDH recurrent mutations. The latter group often has also a G-CIMP phenotype, and this combination offers better prognosis. The classical group harbours aberrant expression of wildtype or mutated EGFR, almost invariably have a homozygous deletion of the INK4a/ARF locus, and in a lot of cases have loss of PTEN. Finally, the driving and most characteristic aberration in mesenchymal GBMs is the loss of the tumour suppressor NF1 (Boussiotis and Charest, 2018).

1.2.5. Therapeutic approaches

Despite the development of multimodal treatments, some of which are quite aggressive, including surgical resection when possible, local radiotherapy and systemic chemotherapy (primarily with alkylators) in the past decades, patient outcomes remain unsatisfactory, rendering gliomas, and especially GBMs, one of the most morbid and mortal cancers across the lifespan (Zhang and Leung, 2014; Hu *et al.*, 2016). So far, despite our profound knowledge of the basic molecular mechanisms underpinning the genesis and progression of GBMs and the use of distinct biomarkers to stratify patients, personalized treatment according to molecular/ genetic profiling remains utopic. On the contrary, the golden standard of treatment is given to almost all patients, including surgical excision in cases where the tumour localisation is permissive, followed by concomitant fractionated 60Gy radiation with TMZ, and adjuvant TMZ afterwards. The administration of steroids, usually dexamethasone (Dex), is common practice after surgery for neurological symptomatic relief (Marlow *et al.*, 2017; Boussiotis and Charest, 2018). Furthermore, targeted therapy attempts have shown very limited success as part of GBM therapeutic regimens, as the examples of EGFR and BRAF/MEK inhibitors clearly illustrate, due to the extreme intra tumour heterogeneity, the clonal evolution of the tumour cells and the emergence of secondary mutations, as well as the pathway redundancy (Olson *et al.*, 2014; Prados *et al.*, 2015). Anti-angiogenic targeted therapies, such as the widely used anti-VEGF monoclonal antibody bevacizumab, a selective multi-targeted receptor tyrosine kinase inhibitor of VEGFR-1, VEGFR-2, VEGFR-3, PDGFR-α/β, and c-kit, pazopanib and sorafenib, two small molecular inhibitors of several tyrosine protein kinases such as VEGFR and PDGFR and *RAF* proto-oncogene serine/threonine-protein kinase (Raf) kinases, have also shown very limited success (Olson *et al.*, 2014; Ferrer *et al*., 2018).

Given the tumour biology of GBMs, the reasons for treatment therapy failure are multiple and diverse. One massively limiting factor is the poor drug delivery, due to the existence of the blood-brain barrier (BBB) (~2% of therapeutic agents can cross the BBB) (Saito and

Tominaga, 2017; Hua *et al.*, 2018). Another important contributing factor is the presence of glial stem cells (GSCs), which confer resistance to chemotherapy and radiotherapy due to their self-renewal properties and their ability to overuse their DNA repair system comparing to the non-stem cells (Marlow *et al.*, 2017; Boussiotis and Charest, 2018). Upregulating multidrug resistance genes, such as the Breast Cancer Resistance Protein (BCRP), DNA repair enzymes (e.g. MGMT), anti-apoptotic factors (e.g. survivin) and pro-survival pathways, including autophagy constitutes another means of rendering chemotherapy ineffective. The biophysical properties of the tumour's microenvironment, for instance, stromal stiffness, interstitial pressure and fluid flow can also be an obstacle for efficient drug delivery (Saito and Tominaga, 2017). The excessive adverse effects of potent chemotherapeutic agents is also a thus far unsolved problem in GBM treatment (Marlow *et al.*, 2017). Besides, the glucocorticoids administered to patients post-surgery to relieve treatment-related adverse effects compromise immune responses and in turn the patients' survival (Boussiotis and Charest, 2018).

To overcome the delivery barrier of the BBB, as well as the increased cytotoxicity of systemic therapy, a useful approach is the use of convention-enhanced delivery (CED), with which the BBB is circumvented by delivering the drug directly into the tumour via continuous positive-pressure infusion (Saito and Tominaga, 2017). So far, the only such strategy used in the clinic is Gliadel®, a carmustine wafer that gradually releases chloroethylnitrosourea (BCNU) into the resection cavity (Saito and Tominaga, 2017). Another way to facilitate and enhance drug delivery is the use of ultrasound (Saito and Tominaga, 2017). An alternative way is the use of receptor-mediated transcytosis (RMT), which relies on ligand-receptor interactions and aids the accumulation of the drug at a specific site, with or without the use of micro- or nanoparticles (Hua *et al.*, 2018; Shankar *et al.*, 2018).

Other promising therapeutic approaches include the use of unconventional genotoxic chemotherapeutics. For instance, the susceptibility of IDH1 mutant tumours to NAD^+

depletion could be exploited by inhibiting the nicotinamide phosphoribosyltransferase (NAMPT). The advantages of such an approach include the selective tumour cell killing without the requirement of DNA damage or active replication (Shankar *et al.*, 2018). Another clever strategy that is gaining popularity is targeting the deregulated epigenetic machineries. This includes inhibiting histone methyltransferases that are known to promote tumour progression, such as G9a and EZH2, and such effort has been made with the testing of BIX-01294, and DZNep and Tazemetostat, respectively. Histone demethylation mediated by histone demethylases (HDMs) is also associated with tumour progression, and as a result, inhibiting HDMs with selective inhibitors (e.g. KDM6A/B, GSKJ4) could be a promising treatment option. Histone acetylation is correlated with transcription activation and is controlled by histone acetyltransferases (HATs) and histone deacetylases (HDACs). Importantly, an oncogenic role in gliomas has been attributed to a number of HDACs (p300, PCAF and GCN5), making them potential targets for therapy. In line with that, several HDAC inhibitors have been developed, including those targeting zinc-dependent HDACis, such as vorinostat, panobinostat, trichostatin A (TSA) and valproic acid (VPA), and the NAD^+ -dependent Sirtuin HDACs. However, their efficacy and suitability remain to be proved. Finally, the efficacy of DNA Methyltransferase (DNMT) inhibitors also remains controversial (Shortt *et al.*, 2017; Chen *et al.*, 2018).

Given the immense importance of the immune landscape in GBMs, it comes as no surprise that a lot of effort is being put on reversing their ongoing immunosuppression to turn it into a functional, immune system-mediated anti tumour attack. To this end a plethora of immunotherapeutic approaches are being explored, some with very promising results. One such approach is the use of vaccines and is based on the uniqueness of glioma neo-antigens. The principle follows the one of normal vaccination: the patient is immunised with specific peptides derived from their own tumour conjugated to a carrier protein and develop an immune response against the tumour. Rindopepimut (Celldex) is an anti-EGFRvIII peptide vaccine in clinical trials against glioma (Paff *et al.*, 2014; Boussiotis and Charest,

2018). This immune response can be enhanced with the administration of the immune stimulatory IL-2. In addition to peptide vaccines, DNA vaccines and DC vaccines are being tested, following the same principles, with DC vaccines showing very promising results (Reardon and Mitchell, 2017). Oncolytic virotherapy is another concept being tested in the field of cancer immunotherapy and relies on the ability of viruses to highjack the cells replication machinery and use it for their own replication, ultimately leading to cell death. Numerous viruses have been used for in this effort including herpes simplex virus 1, adenovirus, poliovirus, parvovirus, reovirus, measles virus, Newcastle disease virus and Zika virus (Maxwell *et al.*, 2017). Furthermore, like in many other tumours, there are several lines of evidence suggesting that CAR-T therapy comprises an efficient therapeutic approach. For GBM, some of the specific antigens being tested include EGFRvIII, epidermal growth factor receptor 2 (HER2), IL-133α2 and ephrin type-A receptor 2 (Brown *et al.*, 2016). Finally, as in various other tumours, the most successful immunotherapeutic approach is the checkpoint inhibitors. Anti-CTLA-4 therapy has shown the first evidence of being an effective treatment, either as a monotherapy or even more in combination with anti-PD-1 or irradiation (Belcaid *et al.*, 2014). Anti-PD-1 and anti-PD-L1 therapies are thoroughly being tested at the moment, either as monotherapies or as part of combination therapy with other checkpoint inhibitors or other modalities. For instance, ongoing trials are testing anti-PD L1 with/without radiotherapy and bevacizumab, as well as anti-PD-1 with TMZ and radiotherapy (Boussiotis and Charest, 2018). Although some of the findings in the field are encouraging, whether or not immunotherapy will increase the GBM patients' overall survival rates remains to be uncovered.

1.3. Hallmarks of Cancer

Cancer is one of the leading causes of death worldwide and has, therefore, been thoroughly investigated for the past decades. It is characterised by multistep progression and involves deregulations of both the genome and the epigenome (Costa, 2005). Hanahan

and Weinberg (2000) described all the six major characteristics of cancer. A decade later, they published a revisited version of their initial review, now presenting almost twice as many recurring features of cancer cells (Hanahan and Weinberg, 2011). In order to deeply understand the modes of initiation and progression of NB and GBM, as well as to examine the key molecules mediating these processes, it is first of paramount importance to understand the complexity and abundance of cellular and molecular changes cancerous cells undergo. Therefore, the different hallmarks of cancer in a neuroblastoma and GBM context are outlined briefly below.

Sustaining proliferative signalling and evading growth suppressors

Cancer cells are capable of sustaining proliferative signalling. To achieve this, they employ a number of different mechanisms, including the induction of autocrine and paracrine signalling, the disruption of negative feedback loops, the maintenance of hyperactive receptors, and, importantly, the constant activation of crucial oncogenes in cancer-related pathways, such as *Ras, Raf* and *c-Myc* (Hanahan and Weinberg, 2011). *BRAF* mutations (Saadeh et al., 2018) and loss of *p53* (Gupta and Dwivedi, 2017) are among the most common mutations in GBM while *MYCN*, a MYC family member, amplifications confer poor prognosis in NB patients (Ahmed *et al.*, 2017; Nakagawara *et al.*, 2018). At the same time, they can evade the negative regulation normally performed by growth suppressors. These suppressors are the so-called tumour suppressor genes and include the well-studied *Rb* in cell cycle control, *p53* in DNA damage repair and apoptosis, the mTOR inhibitor PTEN and others (Hanahan and Weinberg, 2011). *Rb* and *PTEN* are commonly mutated in GBMs (Gao *et al.*, 2016).

Resisting cell death

Importantly, tumour cells have mechanisms that help them acquire resistance to programmed cell death, i.e. apoptosis. Apoptosis is vastly dependent on the sensor of DNA damage, p53, and therefore, when p53 is for some reason deregulated or depleted, as in cancer cells, the whole equilibrium is disturbed and the anti-apoptotic part is favoured, finally causing resistance to apoptosis (Hanahan and Weinberg, 2011). Notably, loss of *p53* is one of the most common molecular alterations in GBMs (Gupta and Dwivedi, 2017) and an indicative aberration of advanced NBs (Nakagawara *et al.*, 2018).

The two branches of apoptosis, the extrinsic and the intrinsic, are regulated by two groups of molecules: the regulators (e.g. receptors and some caspases) and the downstream effectors. In healthy cells there is a dynamic equilibrium between pro-apoptotic [e.g. BCL-2 Associated X, Apoptosis Regulator (Bax), BCL-2 Antagonist/Killer (Bak)] and anti-apoptotic [e.g. B-cell lymphoma 2/xL/w (BCL-2/BCL-xL/BCL-w), Myeloid Cell Leukemia 1 (Mcl1), BCL-2-Related Protein A1 (BFL1] molecules (Campbell and Tait, 2018). Essentially, in both pathways extracellular/intracellular stimuli or their absence trigger the initiation of intracellular signalling cascades and ultimately, at the end of the cascade, apoptotic cells are marked with “eat me” flags and are phagocytosed (Radogna *et al*. 2015; Pistritto *et al.*, 2016).

The extrinsic pathway, also known as the “Death Receptor” (DR) pathway, is triggered by ligand-induced activation of DRs belonging to the tumour necrosis factor receptor (TNFR) superfamily, such as Fas, and TNF-related apoptosis-inducing ligand (TRAIL) or TNFR1 (Radogna, Dicato and Diederich, 2015; Marín-Rubio *et al.*, 2019). The best-characterised signalling systems of death receptors-ligands include TNFR1-TNFα, FAS (CD95, APO-1)-FasL, TRAILR1 (DR4)-TRAIL, TRAILR2 (DR5)-TRAIL (Pistritto *et al.*, 2016). After the receptor trimerises, the assembly of the death-inducing signalling complex (DISC) is triggered, and in turn, recruits pro-caspase-8 and Fas-Associated Death Domain (FADD). The DISC forms due to homotypic interactions employing the death domain (DD) and death

effector domains (DED) of adaptor proteins, such as FADD or TRADD and the initiator caspases, procaspase-8 and -10. DISC assembly ensures procaspase-8/10 oligomerization and cleavage-mediated activation, leading to subsequent cleavage and release of the active initiator caspase. As a result, the active caspase-8 cleaves downstream effector caspases (caspases-3, -6 and -7), which, once activated, induce DNA fragmentation and subsequently apoptosis. In principle, however, the extrinsic pathway occurs without the involvement of the BCL-2 family. Nevertheless, in some cells and under specific circumstances, the intrinsic and extrinsic pathways overlap and caspase-8 cleavage mediates the activation of the BH3 Interacting Domain Death Agonist (Bid), a pro-apoptotic member of the Bcl-2 family, generating a truncated version of the protein (tBid) (Micheau *et al*, 2013; Radogna *et al*., 2015). Apart from this "canonical" apoptosis activation, mediated by either Fas or TRAILR, the DR pathway can also be triggered by perforin (da Fonseca *et al.*, 2010) and TNFR1-TNFα. In the latter case, binding of TNF-α to TNF-RI induces the formation of a membrane bound-complex (complex I), composed of Receptor Interacting Serine/Threonine Kinase 1 (RIPK1), TNF Receptor Associated Factor 2 (TRAF-2), TNFRSF1A Associated Via Death Domain (TRADD), Inhibitors Of Apoptosis (IAPs), the linear ubiquitin chain assembly complex (LUBAC) and Inhibitors Of Nuclear Factor Kappa B Kinase (IKKs) that mainly triggers NF-κB activation and promotes cell survival via the transcriptional regulation of the caspase-8 inhibitor c-FLIP. From complex I, a pro-apoptotic cytosolic complex (complex II) is formed, composed of caspase-8 and FADD. Complex II formation is partly regulated by LUBAC, which contains HOIL-1-Interacting Protein (HOIP), Heme-Oxidized IRP2 Ubiquitin Ligase 1 (HOIL-1) and Sharpin and its pro-apoptotic function is inhibited by c-FLIP (Cellular FLICE (FADD-like IL-1β-converting enzyme)-inhibitory protein). Given that the majority of cells are proficient for NF-kB activation, upon TNF-α stimulation, TNF-R1 usually fails to induce apoptosis (Micheau *et al*., 2013; Vasilikos *et al.*, 2017).

The intrinsic cell death pathway, also known as the “Mitochondrial pathway”, is triggered by intracellular death signals generated by some sort of cellular stress, such as DNA damage, growth factor starvation, oxidative stress, hypoxia, hyperthermia, endoplasmic reticulum stress from disruption of calcium stores or accumulation of unfolded proteins, and, microbial infection (Campisi *et al.*,2014; Radogna *et al.*, 2015; Pistritto *et al.*, 2016). The mitochondrial pathway is initiated when the outer mitochondrial membrane loses its potential (loss of Δψ). Upon disruption of the mitochondrial outer membrane (mitochondrial outer membrane permeability-MOMP), the proteins normally confined in the intermembrane space spread into the cytosol. The release of these apoptogenic factors, such as cytochrome c, apoptosis-inducing factor (AIF), second mitochondria-derived activator of caspase (Smac) / direct inhibitor of apoptosis proteins (IAP) Binding protein with Low PI (DIABLO) or Omi/high-temperature requirement protein A (HtrA2) from the mitochondrial intermembrane space into the cytosol leads to the formation of a large cytosolic complex, composed of cytochrome c and Apaf-1, called apoptosome. The central component of the apoptosome is Apaf-1, a caspase-activating protein that oligomerises upon binding Cyt-c and then binds procaspase-9 via interaction with its caspase recruitment domain (CARD). At the same time, Smac/DIABLO or Omi/HtrA2 enhance caspase activation by binding to IAPs, thereby disrupting the interaction of IAPs with caspase-3 or -9. In turn, the activated caspase-9 cleaves and activates the executioner caspases, thus initiating the caspase cascade, which ultimately leads to apoptosis (Fulda, 2009; Hassan *et al.*, 2014; Pistritto *et al.*, 2016).

As mentioned above, oxidative stress comprises one of the main sources of intracellular stress that triggers apoptosis. Oxidative stress is the direct result of the imbalance generated between the formation and elimination of oxidant species. When the formation outweighs the elimination, the accumulation of these species, including reactive oxygen species (ROS) and reactive nitrogen species (RNS), may result in the formation of oxidative modifications in biological macromolecules, including DNA, proteins and lipids. Such

excessive generation of free radicals may be the result of intracellular processes, such as metabolism or inflammation, or exogenous factors, like irradiation and smoking (Silva *et al.*, 2018; Lv *et al.*, 2019). ROS may activate or inhibit the NFκB pathway, depending on the cellular context, which can in turn, either enhance or inhibit apoptosis. At the same time, ROS have been found to promote tumourigenesis, angiogenesis and metastasis via interfering with the MAPK/ERK, PI3K/AKT/mTOR and protein kinase D (PKD) pathways (Kim and Jang, 2019; NavaneethaKrishnan *et al*., 2019). However, in higher levels, ROS induce apoptosis through both the extrinsic and intrinsic pathway, via various mechanisms (Mohammadi *et al.*, 2019; NavaneethaKrishnan *et al*., 2019). Triggering oxidative stress via augmenting the levels of ROS or eliminating their scavengers remains a traditional chemotherapeutical approach, especially in cases of non-resectable tumours and also as an irradiation sensitiser (Silva *et al*., 2018; Mohammadi *et al.*, 2019).

Meanwhile, two other mechanisms of programmed cell death that operate at basal levels in healthy cells, necro(pto)sis and autophagy, seem to be deregulated in cancer cells. Elevated necrosis causes inflammatory responses in the tumour cell microenvironment, attracting tumour-promoting molecules; increased autophagy, on the other hand, is protective for cells against cell death (White and DiPaola, 2009; Hanahan and Weinberg, 2011). There is accumulating evidence suggesting the diverse roles and types of necroptosis that are associated with cancer, mainly through the alternative bridging role of caspase-8 (Tummers and Green, 2017). The interplay among these complex programmed cell death processes and the major players are illustrated in Figure 1.1.

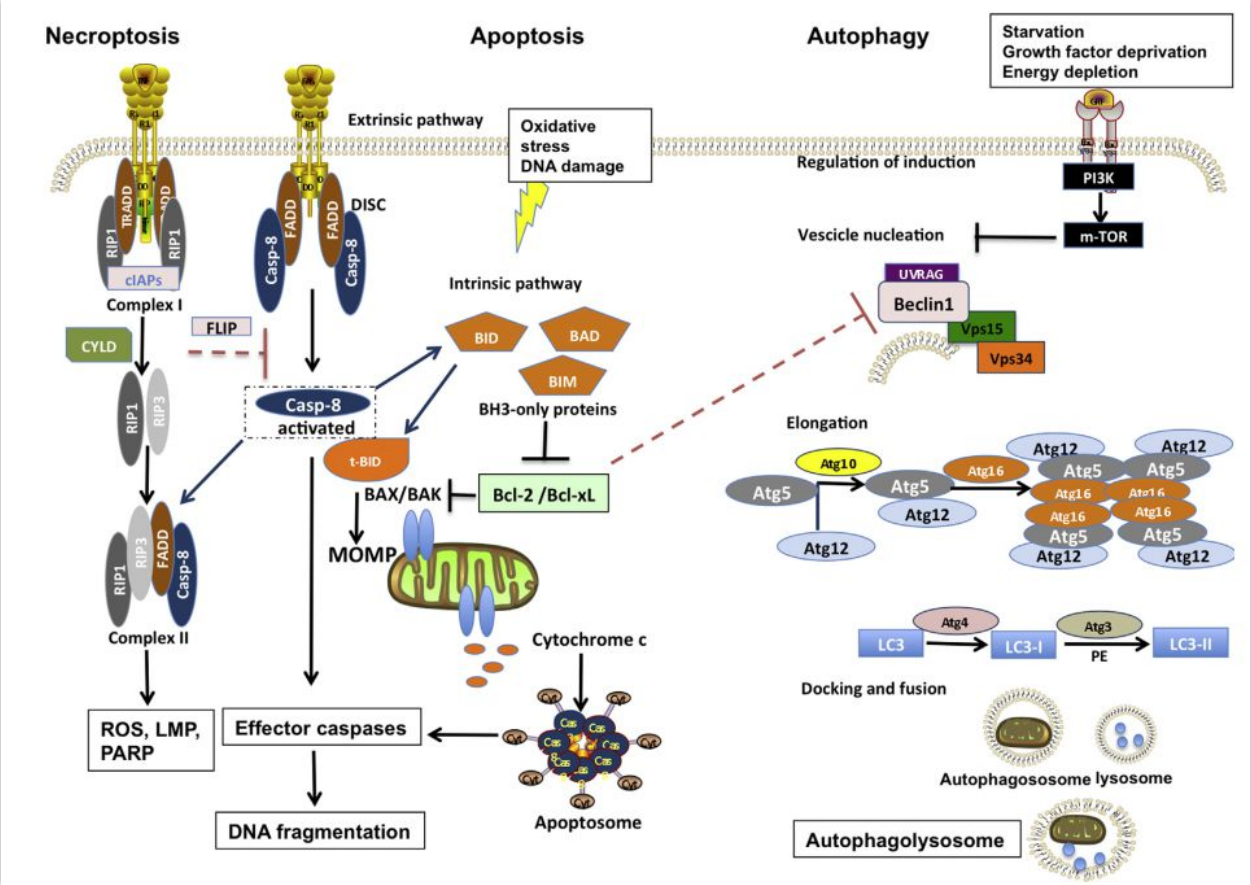

Figure 1.1. The basic network pathways of programmed cell death, including apoptosis, necrosis and autophagy. Two main pathways that result in the activation of caspases trigger apoptosis. The intrinsic apoptotic pathway, activated by oxidative stress and/or DNA damage, is regulated by BCL-2 family proteins and requires the permeabilisation of the outer mitochondrial membrane (MOMP). Pro-apoptotic Bax and Bak, through oligomerization, induce MOMP forming channels that allow the release of mitochondrial cytochrome c, which results in the assembly of a caspase-activating complex called the apoptosome. The anti-apoptotic BCL-2 family members BCL-2, BCL-xL and Mcl1 act against this pro-death function by inhibiting Bax/Bak oligomerization and MOMP. However, BH3-only proteins such as Bim or Bad promote MOMP via Bax/Bak channels by blocking antiapoptotic BCL-2 family members. The extrinsic pathway of apoptosis is mediated by death receptors such as Fas, tumour necrosis factor receptor 1 (TNFR1), or TNF-related apoptosis-inducing ligand (TRAIL). The execution of necroptosis involves reactive oxygen species (ROS), lysosomal membrane permeabilisation (LMP) and Poly (ADP-ribose) polymerase (PARP). Autophagy starts with the nucleation of an isolation membrane or phagophore, which sequesters cellular material in a double-membrane vesicle (autophagosome) for lysosomal hydrolase degradation after its fusion with a lysosome (autophagolysosome). Autophagy may also be a non-apoptotic form of programmed cell death and/or can intimately cross-link with apoptosis by a molecular crosstalk between the two pathways. The autophagy core process (induction, elongation and maturation steps) is regulated by autophagy-related proteins (ATGs) and BCL-2 anti-apoptotic members (Bcl-2/Bcl-xL). Conversely, pro-apoptotic BH3-only proteins induce autophagy by blocking Bcl-2-Beclin-1 interaction. mTOR: mammalian target of rapamycin; PI3K: phosphatidylinositol 3-kinase (adapted from Radogna et al., 2015).

Enabling replicative immortality

Along with these, cancer cells can also skip contact inhibition, i.e. the inhibition of cell proliferation because of the cell contact in dense populations. Some of the crucial players are cadherins and NF2 (Neurofibromin-2) (Hanahan and Weinberg, 2011). Also, in contrast to normal cells that undergo a limited number of divisions which are to a great extent controlled by the inactivation of telomerase (the DNA polymerase responsible for the maintenance of the telomeric ends of chromosomes), this is not the case for cancer cells. Telomerase is often reactivated in cancer cells, leading to indefinite divisions, resistance to senescence, and, therefore, cell immortalization (Hanahan and Weinberg, 2011). In line with this, *TERT* is often mutated in GBMs (Gao *et al*., 2016; Gupta and Dwivedi, 2017) and overexpressed in NBs (Ahmed *et al*., 2017), and in both cases, it is an indicator of poor outcome.

Inducing angiogenesis and activating invasion and metastasis

What is more, the normally quiescent vasculature is turned on by an 'angiogenic switch' during tumour progression. As a result, new vessels are constantly sprouting out providing oxygen and nutrients that help to sustain the expanding neoplasms. A number of molecules have been accused of promoting angiogenesis and primarily members of the VEGF family (Hanahan and Weinberg, 2011). In GBM, the vast deregulations of the VEGF family have turned it into an attractive therapeutic target for targeted therapy (Ferrer *et al*., 2018), while the evidence of the role of VEGF in NB remains conflicting (Weng *et al*., 2017). Another significant characteristic that tumours gradually acquire is the ability to locally invade tissues and metastasise, either to proximal or to distal organs/tissues. The alterations of cell-cell and cell-ECM (extra-cellular matrix) interactions promote the local tumour invasion and comprise the first step of a multi-step and time-consuming procedure (invasion-metastasis cascade). Tumour cells first acquire characteristics of mesenchymal cells (e.g.

N-cadherin expression, fibroblast-like shape etc.) through a procedure called 'EMT' (epithelial to mesenchymal transition). This is followed by their entry in neighbouring blood or lymphatic vessels (intravasation), their circulation in the bloodstream/ lymphatic system, their escape into the parenchyma of permissive distal tissues (extravasation and MET- mesenchymal to epithelial transition), the formation of micrometastatic nodules and finally the growth of these lesions to form macroscopic tumours (colonisation) (Hanahan and Weinberg, 2011). CXCR4, a chemokine receptor with a leading role in the tumour microenvironment, is overexpressed in aggressive NBs, ultimately leading to metastasis (Borriello *et al*., 2016), while in GBMs, MMPs (matrix metalloproteinases) are highly expressed and associated with poor survival (Thompson and Sontheimer, 2019).

Deregulating cellular energetics and avoiding immune destruction

The adoption of an alternative metabolic strategy has been attributed to cancer cells. This is known as the Warburg effect, according to which cancer cells vastly rely on glycolysis to produce energy, even in aerobic conditions (also termed aerobic glycolysis). This state has been associated with contexts in which oncogenes are hyperactive and tumour suppressors are down-regulated, and is also promoted by hypoxia (Hanahan and Weinberg, 2011). The high metabolic rate of tumour cells also results in the accumulation of ROS (Rodic and Vincent, 2018; NavaneethaKrishnan *et al*., 2019). In this context, high levels of *LYAR* (Ly1 Antibody Reactive) gene expression, an oxidative stress regulator, in human neuroblastoma tissues predicted poor event-free and overall survival in neuroblastoma patients (Sun *et al.*, 2017). In GBMs, knockdown of *HIF1A*, a master regulator transcription factor of hypoxia, in human and murine glioma cells impaired their migration in vitro and their invasion in vivo (Méndez *et al.*, 2010). Finally, tumours find ways to escape the recognition and destruction by the immune system. There is piling evidence suggesting that this is mediated both by the secretion of immune-suppressive factors by tumour cells that eliminate the action of T-cells and natural killer cells (NKs) and by the attraction of

regulatory T-cells that compromise the attempts of tumour destruction (Hanahan and Weinberg, 2011).

Tumour promoting inflammation and genome instability and mutation

All these traits comprise established characteristics of cancer cells. After intensive research, it has been proved that there exist some conditions that facilitate the emergence and establishment of these features. One of them is the inflammatory response in tumour sites. It affects the initiation stage of tumourigenesis and is caused primarily by the tumour associated macrophages (TAMs), which attract other pro-inflammatory elements of the immune system that, in turn, trigger oncogenic cascades, mainly via cytokine/chemokine secretion (Hanahan and Weinberg, 2011). TAMs promote neuroblastoma via STAT3 phosphorylation and up-regulation of c-Myc (Hadjidaniel *et al.*, 2017), while they comprise the dominant infiltrating immune cell population in GBMs, exerting different functions in distinct GBM subtypes (Chen and Hambardzumyan, 2018). The other one is the generalised genomic instability that tumours acquire during the course of the multi-step carcinogenesis. This can be triggered by mutations in a variety of combinations, but also by non-mutational changes that affect the gene regulation; in other words, epigenetic alterations (Hanahan and Weinberg, 2011).

1.4. Long non-coding RNAs (LncRNAs)

1.4.1. Discovery and definition

The advent of and the subsequent advances in Next Generation Sequencing have revolutionised our interpretation of the architecture, regulation and complexity of the eukaryotic genome. The data acquired from a number of consortia, such as ENCODE (ENCODE Project Consortium, 2004) and FANTOM (Bono *et al.*, 2003), have contributed vastly to the discovery, quantification and characterisation of this relatively newly

discovered class of RNAs (Qureshi and Mehler, 2012). The classification of RNAs as coding or non-coding has been challenging, however, the most widely accepted method of achieving it is analysing the open reading frames (ORFs) of a candidate transcript. Based on this criterion, RNAs that lack an apparent ORF are classified as non-coding (Cao, 2014; Mohanty *et al.*, 2015). ncRNAs can be further divided into two subcategories: small and long ncRNAs, based primarily on their length.

Small ncRNAs include ncRNAs with length <200nt and include a great variety of regulatory RNAs, such as the well-studied tRNAs, small nuclear RNAs (snRNAs), microRNAs (miRNAs), PIWI-interacting RNAs (piRNAs), small nucleolar RNAs (snoRNAs), promoter-associated small RNAs (PASRs) and small inhibitory RNAs (siRNAs) (Qureshi, Mattick and Mehler, 2010; Qureshi and Mehler, 2012; Schmitz, Grote and Herrmann, 2016), as well as some new categories including tiRNAs (transcription initiation RNAs)/spliRNAs deriving from the transcription start sites and borders of exons, respectively (Mattick, 2018). Of them, miRNAs are small cytoplasmic RNAs that are 20-23nt in length and have attracted a lot of interest due to their crucial role in gene expression regulation by means of inducing gene silencing. miRNAs are transcribed in the nucleus as precursor molecules and are then exported to the cytoplasm. They are then diced by the DICER complex into double-stranded molecules. One of the two strands takes part in the formation of RNA-induced silencing complexes in order to silence gene expression post-transcriptionally (Wang and Chang, 2011; Boon *et al.*, 2016). miRNAs have been intensively studied over the past decade and be involved in several diseases, including cancer (Qureshi and Mehler, 2012; Diederichs *et al.*, 2016).

Long ncRNAs (lncRNAs) are RNA molecules that are either longer than 2kb with a limited coding potential or RNA molecules of >200nt length with no protein-coding capacity (Cao, 2014; Clark and Blackshaw, 2014). However, this classification is not standardized, since the cut-off point of 200nt has been arbitrarily utilised, based on RNA purification protocols (Mercer *et al*., 2009; Hung and Chang, 2011; Boon *et al.*, 2016). Moreover, very large

regulatory RNAs have been identified to be spread along the human genome, such as the very long intergenic RNAs (vlincRNAs, transcripts of >50kb length) and the macroRNAs (Laurent *et al.*, 2012; Lazorthes *et al.*, 2015). The different subcategories of RNAs are schematically presented in Figure 1.2.

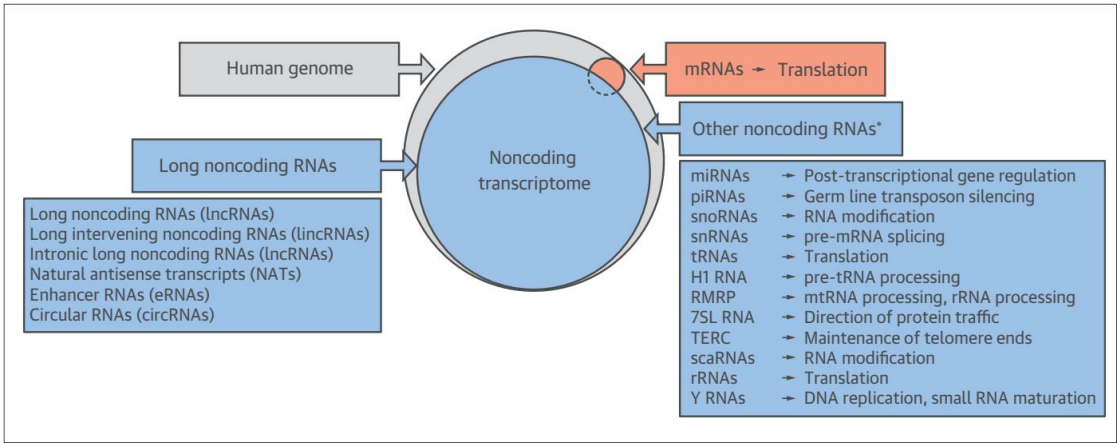

Figure 1.2. Non-coding RNAs of the human transcriptome. Most of the human genome is transcribed, but only a small percentage is translated into proteins, thus resulting in a vastly non-coding transcriptome with various ncRNA species. The classification does not rely on a strict 200nt cutoff. H1 RNA: RNA component of ribonuclease P; miRNAs: microRNAs; mRNA: messenger RNA; mtRNA: mitochondrial RNA; piRNAs: piwi-interacting RNAs; RMRP: RNA component of RNase MRP; rRNA: ribosomal RNA; scaRNAs: small Cajal body-specific RNAs; 7SL RNA: signal recognition particle RNA; snoRNAs: small nucleolar RNAs; snRNAs: small nuclear RNAs; TERC: telomerase RNA component; tRNAs: transfer RNAs; YRNAs: part of the RoRNP (adapted from Boon *et al.,* 2016).

1.4.2. Characteristics and classification

lncRNAs are among the most abundant classes of ncRNAs, with the numbers varying from at least 9640 to the recently reported 58648 in human (Bernstein *et al.*, 2012; Yang, Lu and Yuan, 2014; Iyer *et al.*, 2015), and their expression is significantly enriched in the brain (Qureshi *et al.*, 2010; Qureshi and Mehler, 2012). Their expression is elegantly regulated, following a spatiotemporal- and environmental stimulus-specific fashion (Amaral and Mattick, 2008; Cabili *et al.*, 2011). In fact, they have proved to be expressed in lower levels, but with higher tissue specificity, compared to protein-coding genes (Ning *et al.*, 2017; Pop *et al.*, 2018). This lineage/tissue specificity is a quite expectable feature if one takes into consideration the fact that positive selection acts more rapidly on regulatory elements

comparing to protein-coding ones and that these regulatory elements have different structure-function constraints and are subject to rapid turnover (Mattick, 2018).

Many lncRNAs resemble mRNAs, taking into account that they are, as well, transcribed by RNA polymerase II, they are often 5' capped and 3' polyadenylated. Also, they are often multi-exonic and most of them are subject to alternative splicing (the process via which exons are linked with each other in a number of different combinations to generate different isoforms of the same gene) (Qureshi *et al*., 2010; Schmitz *et al*., 2016; Ning *et al.*, 2017; Mattick, 2018). However, they possess more tandem repeat elements and retrotransposons, comparing to mRNAs (Clark and Blackshaw, 2014). Some of the lncRNAs are used as precursor molecules for shorter functional RNAs, such as snoRNAs and miRNAs (Mattick and Makunin, 2005; Wilusz *et al*., 2009; Qureshi *et al*., 2010). As new evidence is coming to light, the importance of lncRNAs is becoming more apparent, but at the same time, their distinction is becoming more blurred due to confounding factors, such as the fact that some of them can also possess protein-coding activity (Wilusz *et al.*, 2009; Banfai *et al*., 2012; Clark and Blackshaw, 2014; Fang and Fullwood, 2016). This is also supported by the fact that several lncRNAs are somehow associated with ribosomes, probably by having incorporated ORFs that bind to ribosomes to give rise to small polypeptides, but this remains a speculation that needs to be further investigated (Ingolia *et al*., 2011; van Heesch *et al.*, 2014; Yao *et al*., 2019).

Finally, the majority of lncRNAs display low levels of evolutionary conservation, although exceptions do exist, for example, lncRNAs transcribed from ultra-conserved elements (UCEs) (~3% of lncRNAs), which exhibit really high levels of conservation, as the name itself indicates (Clark and Blackshaw, 2014; Fang and Fullwood, 2016). Furthermore, there are fluctuations in the levels of conservation even between elements of the same lncRNA; exonic regions, for example, are more conserved than intronic (Clark and Blackshaw, 2014; Ning *et al.*, 2017; Mattick, 2018). What is noteworthy, however, is the fact that although the sequence conservation tends to be relatively low, equivalent lncRNAs have been found in

syntenic genomic regions across several species (Clark and Blackshaw, 2014; Fang and Fullwood, 2016; Schmitz *et al.*, 2016). This indicates that functional conservation does exist and also, that sequence conservation is less needed in lncRNAs to maintain their function (Pang *et al*., 2006; Laurent *et al.*, 2012; Boon *et al.*, 2016; Schmitz *et al*., 2016).

LncRNAs comprise a very heterogeneous class of molecules, making it even more challenging to consistently categorise them. So far, the most commonly applied criterion has been their genomic position relative to neighbouring protein-coding genes *(*Chen *et al.*, 2015; Schmitz *et al*., 2016). The basic categories are:

- **Long/large intergenic/intervening RNAs (lincRNAs)**: they usually possess signatures indicative of active transcription (e.g. H3K4me3/H3K36me3, polyadenylation, RNA pol II occupancy) (Guttman *et al.*, 2009; Marques *et al.*, 2013; Clark and Blackshaw, 2014; Pop *et al.*, 2018). lincRNAs can be transcribed from gene regulatory regions, like UTRs, promoters and enhancers (Qureshi and Mehler, 2012). They are located between but do not overlap with protein-coding genes, comprise the largest group of functional lncRNAs and are primarily involved in epigenetic regulation (Pop *et al.*, 2018).

- **Enhancer RNAs (eRNAs) and promoter upstream transcripts (PROMPTs)**: lncRNAs transcribed from enhancers (Schmitz *et al.*, 2016) and promoters, respectively. eRNAs are mostly bidirectionally transcribed, display certain chromatin marks (H3K4me1 and H3K27ac modifications) (Clark and Blackshaw, 2014) and should not be confused with the enhancer-associated lncRNAs (elncRNAs) that are mostly unidirectionally transcribed from low H3K4me3/H3K4me1 ratio promoters (Marques *et al*., 2013). PROMPTs have not yet been attributed a specific function; however, it is postulated that the process of transcription itself is of importance and not the lncRNA (Yao *et al.*, 2019).
- **Intronic lncRNAs**: lncRNAs expressed from intronic regions (Schmitz *et al.*, 2016).

- **Circular lncRNAs (circRNAs):** the result of the back-splicing from introns of mRNAs or lncRNAs, acquiring a stable circular configuration (Clark and Blackshaw, 2014; Boon *et al.*, 2016; Schmitz *et al.*, 2016; Yao *et al*., 2019).
- **Mitochondrial lncRNAs**: stem-loop lncRNAs produced in the mitochondria (SncmtRNA), as well as Anti-sense mitochondrial ncRNA (AsncmtRNA) (Chandra Gupta and Nandan Tripathi, 2017).
- Novel classes: **telomeric lncRNAs** (Azzalin *et al.*, 2007), together with the newly discovered **sno-lncRNAs**, flanked by snoRNAs (Geisler and Coller, 2013) and circular intronic (ciRNAs), deriving from excised introns. Of particular interest are the newly discovered **3'UTR-derived lncRNAs**, which are expressed separately from their associated mRNA, and also respond to different signals (Mattick, 2018).

LncRNAs can also be transcribed from the same promoter as a protein-coding gene (proximal promoter) divergently (pancRNAs) or from a different promoter acting convergently, i.e. transcribing the opposite strand of the protein-coding gene. Other lncRNAs can overlap with other transcripts in either a sense or antisense (natural antisense transcripts- NATs) manner, elegantly regulating their expression, especially in the case of NATs (Clark and Blackshaw, 2014; Schmitz *et al*., 2016) (Figure 1.3). Overlapping genes of lncRNA-protein-coding pairs could originate via a process called overprinting, during which new genes are created from pre-existing sequences, with lncRNAs being younger comparing to their pair protein-coding genes in most cases (Ning *et al*., 2017).

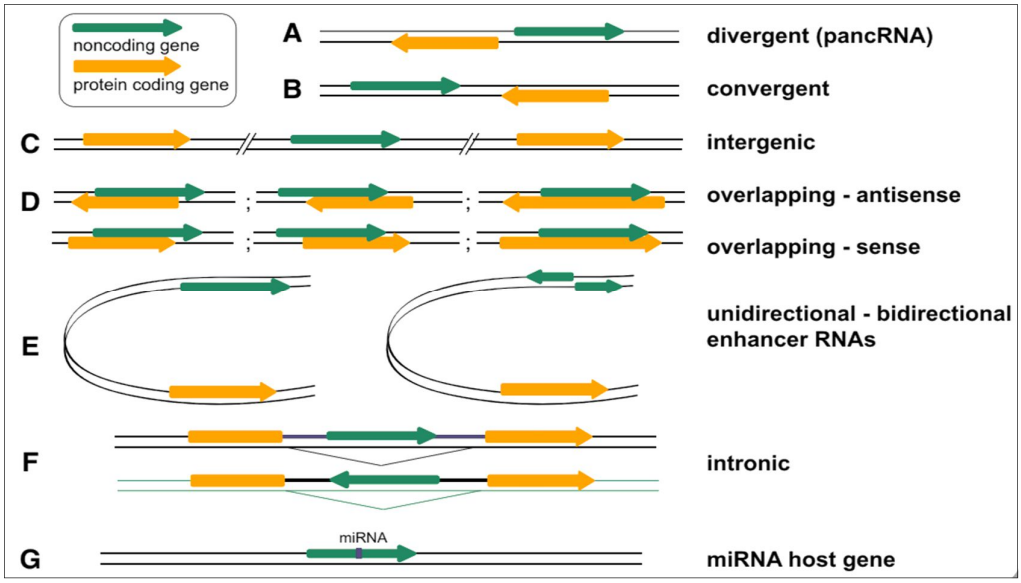

Figure 1.3. Classification of lncRNAs relative to neighbouring protein-coding gene(s). The most frequently used classification of lncRNAs is based on their location in the genome in relation to neighbouring, usually protein-coding genes. Divergently transcribed lncRNA originating from the opposite strand of the same promoter region as the adjacent gene (A); lncRNA and neighbouring gene convergently transcribed from opposite strands, facing each other (B); long intergenic/intervening lncRNA –lincRNA, usually distal (>10kb) to other genes (C); lncRNAs overlapping with neighbouring genes, either in opposite directions (antisense-upper case) or in the same direction (sense-lower case) (D); enhancer RNAs transcribed either uni-(left) or bi-(right) directionally (E); intronic lncRNAs transcribed from introns of genes (F); lncRNA hosting a microRNA (G). lncRNAs are painted in green, while protein-coding genes are painted in orange (adapted from Schmitz *et al.*,2016).

1.4.3. Localisation

The localisation of lncRNAs inside the cell can be a putative indicator of their function. lncRNAs are predominantly located in two cellular compartments: the nucleus and the cytoplasm (Banfai *et al.*, 2012; Schmitz *et al.,* 2016). Many studies reported that the enrichment of the nucleus in lncRNAs is significantly larger compared to the cytoplasm, implying the involvement of lncRNAs in epigenetic mechanisms. The main reason for this nuclear retention is the presence of C-rich sequences deriving from *Alu* elements, which interact with the nuclear matrix protein Heterogeneous Nuclear Ribonucleoprotein K (hnRNPK). In addition, some newly discovered lncRNAs with unconventional forms and biogenesis tend to remain in the nucleus (Figure 1.4) (Yao *et al.*, 2019). Moreover, recent studies have generated great controversy over the matter,

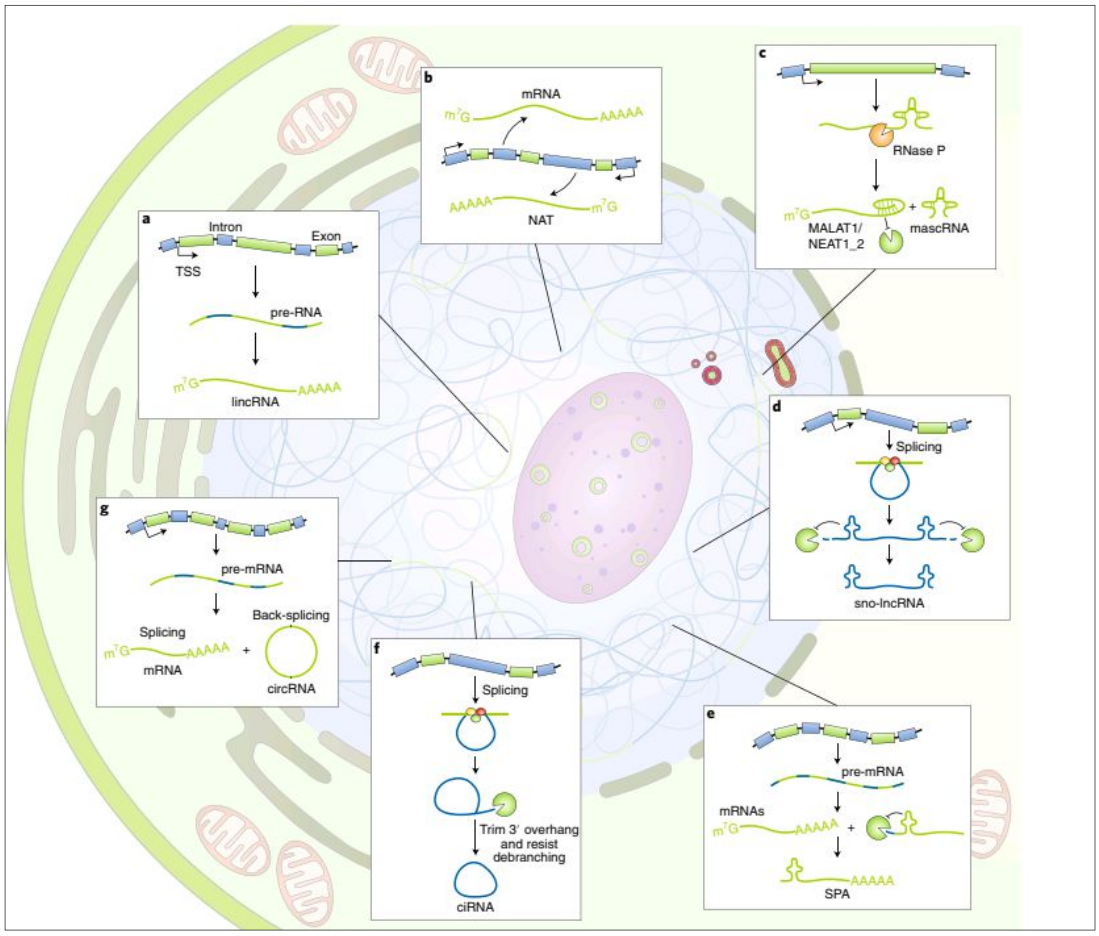

Figure 1.4. The diverse nuclear-retained lncRNAs. Large intervening/intergenic non-coding RNAs (lincRNAs), transcribed by Pol II from intergenic regions, are presumably capped, spliced and polyadenylated. (a); natural antisense transcripts (NATs) are transcribed from the opposite strands of protein-coding genes by Pol II and are presumably mRNA-like lncRNAs (b); MALAT1 and NEAT1_2 are processed by RNase P and stabilized by U-A-U triple helix structures at their 3' ends. Their 3'-end products are further processed to form MALAT1-associated small cytoplasmic RNA (mascRNAs), which are ~60 nt in length (c); snoRNA-ended lncRNAs (sno-lncRNAs) are derived from excised introns. During splicing, the formation of a snoRNP complex at each end protects the intronic sequences from degradation, leading to the accumulation of sno-lncRNAs flanked by snoRNAs but lacking a 5' m7G cap and 3' poly(A) tail (d); 5' snoRNA-ended and 3'-polyadenylated lncRNAs (SPAs) are derived from readthrough transcripts, and their 5' ends are protected by co-transcriptionally assembled snoRNPs (e); circular intronic RNAs (ciRNAs) are derived from excised introns and depend on consensus RNA sequences to avoid debranching of the lariat introns (f); circular RNA (circRNAs) are produced by back-splicing circularization of exons of pre-mRNAs. During splicing, pre-mRNAs can be spliced into mRNAs or back-spliced into circRNAs (g) (adapted from Yao *et al.,* 2019).

suggesting more generalised cytoplasmic localisation and novel roles for lncRNAs, such as the regulation of translation (Mattick, 2018).

LncRNAs have been also found in novel loci inside the cell nucleus (Cheng *et al.*, 2016). As part of regulatory machineries (described later), the positioning of lncRNAs, as well as chromatin, is not stochastic, but, on the contrary, finely regulated and associated with specific nuclear compartments (Cremer and Cremer, 2010; Cheng *et al.*, 2016). In line with that and taking into account that the eukaryotic nucleus is highly compartmentalised (Hirose and Nakagawa, 2012), RNA, as well as DNA and proteins, can form non-membranous, dynamic nuclear structures (Cheng *et al.*, 2016). In fact, more than ten such nuclear bodies have been discovered, placed in the interchromosomal space, serving as sites of multiple uses, such as the generation of molecular machineries (Mao *et al.*, 2011; Hirose and Nakagawa, 2012). This category includes the nucleolus, nuclear speckles (identical to the previously discovered interchromatin granules-ICGs-, 20-25/nucleus, irregularly shaped, 0.8-1.8 μm in diameter) accommodating crucial for the splicing machinery factors, promyelocytic leukaemia protein bodies (PML bodies), paraspeckles (average diameter of 0.36μm bodies in close proximity to nuclear speckles, 10-20/nucleus) and nuclear stress bodies (nSBs) (Hirose and Nakagawa, 2012). Importantly, several lncRNAs have been associated with a number of nuclear bodies. In these nuclear bodies, they can either be solely located, or also function structural components ("architectural RNAs") and functional elements, either as reservoirs of important molecules or actively. For example, nSBs are generated upon heat shock as a result of the transcription of Satellite III (SatIII) and the entrapment of multiple splicing factors by the same molecule (Yao *et al.,* 2019). *MALAT1* (metastasis-associated lung adenocarcinoma transcript 1), also known as *NEAT2* (nuclear enrichment abundant transcript 2), is enriched in nuclear speckles and is involved in alternative splicing. Furthermore, the lncRNA *NEAT1* (nuclear enrichment abundant transcript 1) is a structural and functional component of paraspeckles and finally, the lncRNA *MIAT* (myocardial infarction associated transcript) is localised in novel nuclear

bodies that do not co-localise with any known bodies, and functions similarly to *MALAT1* (see section 1.5.) (Hirose and Nakagawa, 2012; Laurent *et al*., 2012; Cheng *et al*., 2016; Yao *et al*., 2019).

1.4.4. Mechanisms of function

As the involvement of lncRNAs in a diversity of biological processes is becoming stably more significant, the need to provide further elucidation and insight concerning their acting mechanisms is becoming vital. Consequently, a lot of research groups have been working intensively towards this end and have provided a number of potential mechanistic models. As suggested by Wang and Chang (2011) and Fang and Fullwood (2016), a lncRNA can function as a signal, a decoy, a scaffold, a guide, an enhancer and a short peptide (Figures 1.5.-1.8). Virtually all of these functions involve, at least to some extent, chromatin remodelling, especially when they occur in the nucleus (Cheng *et al*., 2016). Further, the functions are not mutually exclusive, pointing towards the high plasticity and flexibility of lncRNAs (Wang and Chang, 2011).

To understand deeply these modes of function, one should keep in mind the versatility of RNA. Thus, lncRNAs can exert their functions in various ways. Firstly, through sequence-specific interactions, either RNA-RNA or RNA-DNA, a way that is very common when NATs are involved. Typical examples of such interactions involve *p15AS* (p15 antisense transcript) and the *CDKN1A* (cyclin-dependent kinase inhibitor 1A) antisense RNA for the former case, and the *DHFR* (dihydrofolate reductase) locus regulation by the non-coding *DHFR* for the latter case (Martianov *et al*., 2007; Hung and Chang, 2011). Secondly, interactions can be structure-mediated, because lncRNAs can form secondary and tertiary structures to bridge molecules that are distal to each other or exert their own function (Pop *et al*., 2018). *RepA* (repeat A) and *GAS5* (Growth Arrest-specific 5) are indicative examples of lncRNAs that fall within this category (Mourtada-Maarabouni *et al*., 2009; Hung and Chang, 2011). Finally, given that a rough 25% of all proteins contain nucleic acid binding

domains, it is likely that proteins form complexes with lncRNAs to reach their target, using them as adaptors (Hung and Chang, 2011).

Another significant feature of lncRNAs is that they can function *in cis* or *trans* (Clark and Blackshaw, 2014; Engreitz *et al.*, 2016). They function *in cis* when they regulate the function of neighbouring genes of the same genomic locus, meaning that their action is limited to a proximal area (e.g. *ANRIL*, also known as *CDKN2B-AS1*cyclin-dependent kinase inhibitor 2B antisense transcript 1). On the other hand, they can function *in trans* when their effect is exerted on distal loci, in the same or even a different chromosome (e.g. *HOTAIR*-Hox transcript antisense intergenic RNA) (Qureshi *et al*., 2010; Kornienko *et al*., 2013; Clark and Blackshaw, 2014; Boon *et al*., 2016). Intriguingly, some lncRNAs, such as the *DHFR* (Wilusz *et al*., 2009) and *CISTR-ACT* (*cis*- and *trans*- chromosomal interaction) lncRNA, can act in both ways (Maass *et al*., 2014). In cases where lncRNAs act in cis only, this might be the result of direct, local functions of the lncRNA locus, while in cases of dual-action, this might be the indirect, downstream result of the lncRNA acting somewhere else (Engreitz *et al.*, 2016). Taking all the above into consideration, it comes as no surprise that lncRNAs have so many different roles, which are analysed below.

1.4.4.1. LncRNAs as signals

Functioning as a **signal**, a lncRNA has the mission to regulate transcription as a response to a diversity of stimuli. This is convenient for the cell since their transcription occurs in a very tight spatial and temporal frame. In addition, having a lncRNA as a signal is time-saving, since it skips the time-consuming procedure of translation. For some lncRNAs, it is the final transcript that is essential for subsequent regulation (*cis*- and *trans*-acting lncRNAs), while for others it is the process of lncRNA transcription itself that mediates the signalling (*cis*-acting RNAs only) (Wang and Chang, 2011; Kornienko *et al.*, 2013). Examples of such function can be found in the process of establishing allele-specific expression of genes, either through imprinting-related lncRNA expression (e.g.

KCNQ1OT1- KCNQ1 opposite transcript 1 or long QT intronic transcript 1, and *Air*-antisense of *IGF2R* non-protein-coding RNA lncRNAs) or dosage-compensation-related lncRNA transcription, mainly during X chromosome inactivation (e.g. *Xist*-X-inactive specific transcript, *Tsix*) (Wang and Chang, 2011). In both cases, the expression of specific lncRNAs leads to active silencing, as discussed below. Following the same principles, a number of lncRNAs establish the controlled expression of genes during early development. For example, it has been found that there is a number of lncRNAs that are transcribed from the *HOX* clusters, during the development of the anterior-posterior axis (e.g. *HOTAIR, HOTTIP*) (Wang and Chang, 2011). Other lncRNAs are tightly bound to processes maintaining the pluripotent identity of the cell through the regulation of known pluripotency factors, such as Oct4, Sox2 and Nanog [e.g. *linc-RoR* and *MIAT* (Sheik Mohamed *et al.*, 2010). Another stimulus that can induce the expression of lncRNAs functioning as a signal is organismal stress, which could be, for example, DNA damage, as in the case of *linc-p21* (Huarte *et al.*, 2010) and *PANDA* (p21-associated ncRNA DNA damage-activated) (Hung *et al.*, 2011) - both located upstream of *CDKN1A*- or even cold, as in the case of the lncRNAs *COLDAIR* and *COOLAIR* in plants (Wang and Chang, 2011; Chen *et al*., 2015). Also, the expression level of a protein-coding gene often correlates with the expression level of an eRNA involved in its expression. In this case, the eRNAs acquire a more 'promoter-like' identity. Finally, lncRNAs are surprisingly involved in procedures mediating the mRNA degradation (e.g. *1/2 –sbsRNAs*- half-STAU1-binding site RNAs- in Staufen 1-mediated mRNA decay) (Wang and Chang, 2011).

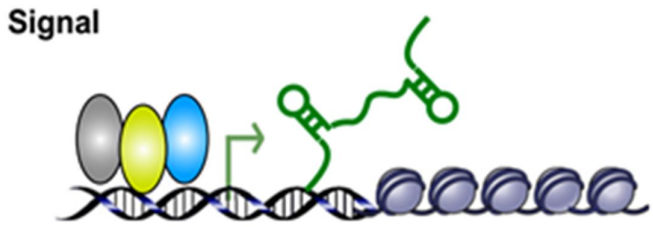

Figure 1.5. Schematic representation of lncRNAs functioning as signals: lncRNA expression can faithfully reflect the combinatorial actions of transcription factors (coloured ovals) or signalling pathways to indicate gene regulation in space and time (adapted from Wang and Chang, 2011).

1.4.4.2. LncRNAs as decoys

LncRNAs functioning as **molecular decoys** (also known as competing endogenous RNAs-ceRNAs) act primarily in a straightforward mechanism: once these lncRNAs are transcribed they bind to molecules that are important for expression regulation and titrate them away. These molecules can range from chromatin modifiers to transcription factors, co-activators and repressors, and from other ribonucleoprotein complexes to miRNAs (Wang and Chang, 2011). In essence, they act as baits to prevent these crucial molecules from reaching their target. A typical example in this group is the *DHFR*- associated lncRNA which binds TFIIB (transcription factor IIB) and thus prevents it from binding to the proximal promoter, further preventing the initiation of transcription (Martianov *et al.*, 2007). Similarly, *TERRA* (telomeric repeat-containing RNA) regulates the telomere formation and consequently the chromosomal end protection (Azzalin *et al.*, 2007), *PANDA* induces cell survival by inhibition of the apoptotic machinery through NF-YA binding (Hung *et al.*, 2011; Maass *et al.*, 2014; Mohanty *et al.*, 2015) and *GAS5* induces partial resistance to glucocorticoids via glucocorticoid receptor (GR) repression through the antagonistic occupation of the receptor (Mourtada-Maarabouni *et al.*, 2009). *MALAT 1* retains serine/arginine (SR) splicing factors in nuclear speckles preventing the correct alternative splicing (Tripathi *et al.*, 2010). Despite their low abundance and mainly nuclear localisation, which could deteriorate the ability of

lncRNAs to act as ceRNAs for miRNA sponging, a couple of other lncRNAs act as natural 'miRNA sponges' to prevent miRNA-mediated gene regulation in cancerous settings (Wilusz *et al*., 2009; Wang and Chang, 2011; Tay *et al*., 2014) [e.g. *CDR1AS* for the miRNA *let-7* (Schmitz *et al*., 2016; Yao *et al*., 2019), *lincMD1*-muscle differentiation 1- for miR-133 and 135 (Chen *et al.,* 2015), *IPS1*-induced by phosphate starvation 1- for miR-399 (Wilusz *et al*., 2009; Wang and Chang, 2011), *lincRoR* for miR-145 (Wang *et al*., 2013) and *TUG1*-taurine upregulated gene 1- for miR-26a (Li *et al*., 2016; Zhao *et al*., 2019)]. Finally, circRNAs comprise a relatively new class of potent ceRNAs, mainly due to their stability (Tay *et al*., 2014).

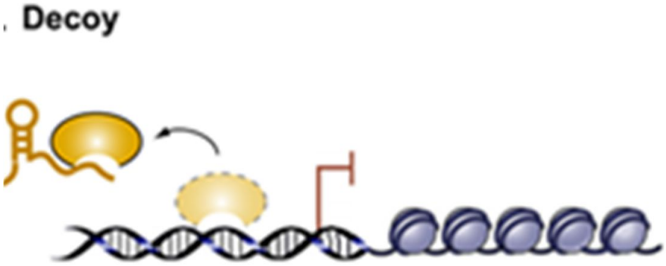

Figure 1.6. Schematic representation of lncRNAs functioning as molecular decoys: lncRNAs can titrate transcription factors and other proteins away from chromatin or titrate the protein factors into nuclear subdomains (adapted from Wang and Chang, 2011).

1.4.4.3. LncRNAs as scaffolds

LncRNAs can also act as **scaffolds**, a feature that had been attributed to proteins until recently (Wang and Chang, 2011; Fang and Fullwood, 2016). Scaffolds, either protein or lncRNA, serve as platforms that can orchestrate elegantly gene expression by bringing together at a given place and time a variety of effector molecules, which can act either synergistically or antagonistically (Spitale *et al*., 2011). Indicative examples of lncRNAs in this category are *TERC* (telomerase RNA), which brings together TERT (telomerase reverse transcriptase) and other accessory proteins for the maintenance of telomeres (Wang and Chang, 2011; Maass *et al*., 2014), pericentromeric heterochromatin-associated

lncRNAs, *ANRIL,* which is a scaffold for both PRC1 and PRC2 complexes facilitating gene silencing (Kotake *et al.*, 2011), and, again, the well-studied *HOTAIR. HOTAIR* is remarkable in the sense that it can bind simultaneously two complexes: PRC2 at the first 5' 300nt and LSD1/CoREST/REST at the 3' 700nt. The former complex mediates the H3K27 methylation leading to gene repression, while the latter demethylates H3K4, counteracting gene activation. Collectively, this leads to a synchronised effort of effector genes' repression (Tsai *et al.*, 2010). Similarly, other lncRNAs can bind both complexes with similar results (Khalil *et al.*, 2009). *Firre* can also act as a scaffold to alter interchromosomal interactions via the recruitment of hnRNPU (Heterogeneous Nuclear Ribonucleoprotein U), while CCAT1-L (Colorectal Cancer-Associated Transcript1- long isoform) can do so by interacting with CTCF (CCCTC-Binding Factor) to create enhancer-promoter loops (Yao *et al.*, 2019). The model of 'intelligent scaffolds' finely illustrates this mode of function: lncRNAs can interact with proteins and other RNAs, sometimes with relatively low affinities, resulting in the formation of micro-domains that can, in turn, regulate gene expression by letting key components go once they meet elements to which they can bind with higher affinity (Laurent *et al.*, 2012).

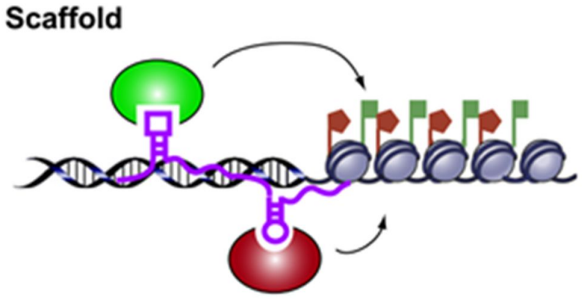

Figure 1.7. Schematic representation of lncRNAs functioning as scaffolds: lncRNAs can bring together multiple proteins to form ribonucleoprotein complexes. The lncRNA-RNP may act on chromatin as illustrated to affect histone modifications. In other instances, the lncRNA scaffold is structural and stabilizes nuclear structures or signalling complexes (adapted from Wang and Chang, 2011).

1.4.4.4. LncRNAs as guides

For the lncRNAs that act as **guides,** the task is exactly inherent to the name: to bind proteins and drive the localisation of the RNA/protein complex to a specific target(s), acting either *in cis* or *in trans*. To perform this task, active chromatin remodelling is necessary (Wang and Chang, 2011). These chromatin changes can occur co-transcriptionally *in cis,* involving RNA pol II. Alternatively, they can occur *in trans* as a target for other small regulatory RNAs, achieved by duplex or triplex formation (RNA: DNA or RNA:DNA: DNA) or by identification of chromatin marks (Hung and Chang, 2011; Wang and Chang, 2011; Pop *et al.*, 2018). Examples of *in cis*-regulation include lncRNAs such as *Xist, pRNA* (promoter-associated RNA, which is complementary to the ribosomal DNA promoter), and *HOTTIP,* while examples of regulation *in trans* include *HOTAIR, linc-p21* and *Jpx*. Significantly, both chromatin activating (e.g. MLL- mixed-lineage leukemia, TxG-trithorax group) and repressive (PRC- polycomb repressor complex-) machineries can participate in this type of regulation, as well as transcription factors themselves, adding an extra step of complexity to this acting mechanism. Regardless of the particular details, though, the mission remains the same: to convey regulatory information through epigenetic modifications, in order to finally control the gene of interest (Wang and Chang, 2011).

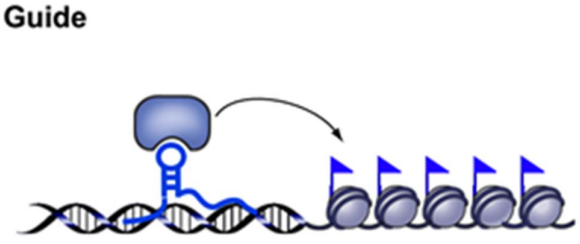

Figure 1.8. Schematic representation of lncRNAs functioning as guides: lncRNAs can recruit chromatin-modifying enzymes to target genes, either *in cis* (near the site of lncRNA production) or *in trans* to distant target genes (adapted from Wang and Chang, 2011).

1.4.4.5. LncRNAs as enhancers and short peptides

LncRNAs can also be produced by enhancers (**eRNAs**) to function by influencing the 3D DNA conformation, i.e. chromatin. Their role is not fully elucidated yet, but one model suggests that they function by remaining attached to the enhancer to bind proteins. These proteins, in turn, bind to distal promoters to enable RNA transcription, forming the so-called chromatin loops. In light of this, eRNAs are crucial for the establishment and maintenance of these loops (Kornienko *et al.*, 2013; Fang and Fullwood, 2016). Generally, the transcription of eRNAs has been associated with gene activation (Clark and Blackshaw, 2014), but some exceptions (e.g. *Haunt* lncRNA) have been reported (Schmitz *et al.*, 2016). Finally, some lncRNAs have been found to also encode **short peptides**, that are likely to exert some functions, but further research is needed to come to safe and generalised conclusions (Ingolia *et al*., 2011; Fang and Fullwood, 2016; Schmitz *et al*., 2016).

Impressively, a generous proportion of the aforementioned and other lncRNAs can have multiple functions, a fact that indicates their complexity and biological significance. For example, *HOTTIP* can function both as a signal and as a guide, while *HOTAIR* can function both as a signal and a scaffold. As Wang and Chang (2011) suggest, lncRNAs can acquire a 'stepwise complexity': they can start having a basic function, e.g. eRNAs, and gradually obtain new characteristics that help them 'climb the hierarchy' to become decoys, guides and scaffolds.

1.4.4.6. The effects of lncRNAs on transcriptional regulation

LncRNAs can exert any of these functions, or, as it often happens, a combination of them, to control gene expression both at the level of transcription, theoretically during any of its

stages (Kornienko *et al.*, 2013; Schmitz *et al.*, 2016), and at the post-transcriptional level (Mercer *et al*., 2009; Geisler and Coller, 2013) (Figure 1.9).

Given the exquisite mechanisms of actions and characteristics of lncRNAs, it is natural that they regulate transcription at so many levels and in so diverse ways. NATs and lincRNAs close to protein-coding genes can repress transcription, possibly via the mechanism of transcriptional collision: RNA polymerase II complexes moving along opposite strands cannot bypass each other and collide, leading to the cessation of RNA polymerase II and its removal by ubiquitination mediated proteolysis (Mohanty *et al.*, 2015; Fang and Fullwood, 2016). Other lncRNAs repress transcription through direct RNA: DNA interaction, as in the case of *DHFR*, where the non-coding *DHFR* (*ncDHFR*), which is produced by a minor promoter, binds to the major promoter further inhibiting its interaction with TFIIB (Mohanty *et al.*, 2015) and the case of *TERRA*, where DNA-RNA hybrids promote homologous recombination at the telomeres. The formation of R-loops, which bring together several components of the transcription machinery is another strategy: lncRNAs coordinate regulation via binding to other proteins that can be either transcription factors or activators/repressors, instead of binding to DNA itself. For example, *PANDA* -acting as a decoy- binds and sequesters the nuclear transcription factor NF-YA, resulting in cell survival promotion through repression of the apoptotic programme (Wang and Chang, 2011; Yao *et al*., 2019). Thus, they can act either as co-activators or co-repressors, to promote or repress gene transcription respectively (Chen and Carmichael, 2010; Wang and Chang, 2011; Mohanty *et al*., 2015).

Furthermore, gene regulation at the transcription level can even be mediated by direct interactions of lncRNAs with RNA polymerase II. Such examples include the lncRNA *NRON* (non-coding repressor of NFAT) that prevents the nuclear localisation of NFAT (nuclear factor of activated T-cells) by means of binding its accessory nuclear transporters like KPNB1 (Karyopherin subunit beta-1), CSE1L (Chromosome segregation 1-like protein), CUL4B (Cullin 4B), and *linc-p21* that changes the localisation of hnRNPK to repress p53-

regulated genes (Wilusz *et al.,* 2009; Mohanty *et al.*, 2015). A well-studied example of a lncRNA acting as a transcriptional co-activator is *Evf-2 (*DLX6 antisense RNA 1). The Dlx homeobox-containing family of genes are involved in neurodevelopment and neuronal patterning and are regulated by two enhancers in the Dlx5/6 locus. One of them gives rise to *Evf-2*, which binds to the protein Dlx2 to eventually activate Dlx5 and Dlx6 (Ponting *et al.*, 2009). Similarly, *HSR1* (heat shock RNA-1) binds to HSF1 (heat shock TF 1) in response to heat shock, to promote the expression of relative genes, and *SRA* (an isoform of steroid receptor RNA activator) acts a co-activator for steroid receptors (Wilusz *et al*., 2009; Chen and Carmichael, 2010). On the other hand, several transcriptional co-repressors have been discovered. For instance, a lncRNA is transcribed from the 5' regulatory region of Cyclin D1 *(CCND1)* upon ionizing radiation. It then binds to TLS (translocated in liposarcoma), allosterically modifies it and in turn, TLS inhibits the acetyltransferase activity of CBP (CREB binding protein) and p300, ultimately resulting in the inhibition of CCND1 transcription (Wang *et al.*, 2008; Chen and Carmichael, 2010). Finally, in terms of direct RNA polymerase II interactions, heat shock-induced short interspersed repeat elements (SINEs) produce *Alu* lncRNAs that bind RNA polymerase II to prevent the pre-initiation complex formation, and thus, the transcription from commencing (Chen and Carmichael, 2010; Chen *et al*., 2015; Yao *et al.*, 2019). Notably, lncRNA-mediated transcription interference can occur both during the initiation and elongation stages (Yao *et al*., 2019).

1.4.4.7. The effects of lncRNAs on post-transcriptional regulation

LncRNAs can efficiently regulate a broad variety of post-transcriptional processes, including mRNA editing and, especially, (alternative) splicing, transportation, stability and degradation, as well as translation (Mercer *et al.*, 2009; Wapinski and Chang, 2011; Ning *et al.*, 2017).

As regulators of the mRNA processing, lncRNAs have the flexibility to influence alternative splicing through various pathways (Romero-Barrios *et al.*, 2018). NATs can influence the

splicing patterns, once transcribed, directly by forming RNA: RNA inhibitory duplexes (e.g. *MYC* and *c-Erbα* in neuroblastoma) or indirectly, as in case of the case of *ZEB2* (Amaral and Mattick, 2008; Mercer *et al*., 2009; Boon *et al.*, 2016). Even more indirectly, lncRNAs acting as decoys can deprive splicing machinery of crucial elements, like SR-rich proteins which are sequestered in special nuclear domains by *MALAT1*, leading to incomplete or modulated alternative splicing (Geisler and Coller, 2013). The potential involvement of lncRNAs in RNA editing, e.g. adenosine to inosine (A-to-I) editing by ADAR (adenosine deaminase acting on RNA), has been implied and is a subject of investigation (Laurent *et al.*, 2012; Geisler and Coller, 2013). Finally, details on the potential role of lncRNAs in mRNA trafficking from the nucleus to the cytoplasm and/ or vice versa remain to be elucidated.

LncRNAs have been implicated to participate in the regulation of mRNA stability, decay and translation. A very representative example of a lncRNA acting to promote mRNA stability by rescuing it from the repressing activity of miRNAs is that of the *BACE1-AS* (beta-site-APP-cleaving enzyme antisense RNA). This is achieved via the RNA: RNA complex that is formed between *BACE1* mRNA and *BACE1-AS*, which prevents miR-485-5p from binding to the mRNA, consequently stabilizing it (Wapinski and Chang, 2011; Geisler and Coller, 2013). In contrast, target mRNAs can be destabilised by the activity of lncRNAs, as it happens in the case of 1/2 –sbsRNAs (Wang and Chang, 2011; Geisler and Coller, 2013; Yao *et al*., 2019). Finally, given the fact that miRNAs are crucial elements of post-transcription and post-translation regulation, ultimately leading to gene silencing, it should be stressed that several lncRNAs can eliminate their action by controlling their availability. As described above, this is achieved by lncRNAs that function as decoys-miRNA sponges. These lncRNAs can be either traditionally linear or can belong to the novel miRNA sponge class of circular lncRNAs that are even more stable and potent (e.g. circular *ANRIL, CDR1AS*- Cerebellar degeneration-related antigen 1 antisense- for miR-7) (Geisler and Coller, 2013; Mohanty *et al.*, 2015). Finally, in a similar fashion, lncRNAs can act as decoys

for elements involved in RNA decay. For instance, PUMILIO1/2 (PUM1/2) binds to a PUMILIO response element located on the 3' UTR of mRNAs and triggers their deadenylation and decapping, thereby destabilising them and preventing their translation. *NORAD* (non-coding RNA activated by DNA damage) sequesters PUM1/2, thereby promoting the downstream translation of mRNAs (Yao *et al*., 2019).

1.4.4.8. The effects of lncRNAs on translation and post-translational modifications (PTMs)

Many lncRNAs have been found to be associated with ribosomes. Given that only an extremely limited number of lncRNAs is translated to make short peptides, a more reasonable explanation of the phenomenon is that lncRNAs are somehow involved with the process of translation. For example, it could be hypothesised that some lncRNAs interfere with translation regulation by attaching to ribosomes and keeping them occupied until a proper signal is received to release them and make them available to form the translation machinery (van Heesch *et al.*, 2014). Research has revealed that *Uchl1AS* (ubiquitin carboxyl-terminal L1 antisense RNA) promotes the formation of active polysomes on Uchl1 mRNA and therefore its translation (Carrieri *et al.*, 2012; Boon *et al.*, 2016; Yao *et al*., 2019). Finally, *linc-p21* and *KCS1A*S (Nishizawa *et al.*, 2008) have been found to directly interfere with RNA translation, as well. LncRNAs also interfere with PTMs via masking sites bound by PTM enzymes or PTM sites. For example, *lnc-DC*, a lncRNA specifically expressed in DCs, binds to STAT3 and promotes its phosphorylation by inhibiting the phosphatase that would normally dephosphorylate it (SHp1). Another lncRNA, *NKILA* (NFκB interacting lncRNA), alters the phosphorylation pattern of IκB, ultimately leading to the activation of the pathway and the suppression of breast cancer metastasis (Yao *et al.*, 2019).

1.4.4.9. The effect of lncRNAs on chromatin remodelling

Taking all the aforementioned mechanisms and modes of function of lncRNAs, it is of pivotal importance to realise the strong link between lncRNAs and epigenetic modifications.

Epigenetics is defined as the study of heritable changes in gene expression that are not caused by changes or mutations in the DNA sequence (Maass *et al.*, 2014). Epigenetic modifications include primarily DNA methylation at cytosine residues, various histone modifications (e.g. phosphorylation, acetylation, methylation and ubiquitination) and ncRNA-mediated processes (Lennartsson and Ekwall, 2009; Yen *et al.*, 2016). Histone modifications are part of the epigenetic machinery: more than 60 have been discovered and they are part of the dynamic regulatory epigenetic network, capable of activating or repressing gene expression (Maass *et al*., 2014). As a result, the importance of the machineries that establish the histone signatures has been highlighted. In the context of lncRNA mediated regulation, it has to be noted that it is exactly the interaction with chromatin regulators that primarily makes this regulation feasible, especially at the level of transcriptional regulation. These interactions may be weak and occur between lncRNAs and chromatin modifiers that are highly expressed and possess high RNA-binding capacity, such as the MLL, G9, PRC1, and importantly, the PRC2 complex (Kornienko *et al.*, 2013; Clark and Blackshaw, 2014; Schmitz *et al*., 2016). This is supported by the finding that in a cohort of 3300 human lincRNAs study 20% of them were found to be bound by PRC2 (Khalil *et al.*, 2009; Chen and Carmichael, 2010; Fang and Fullwood, 2016; Pop *et al.*, 2018). For example, *HOTAIR* has been reported to suppress the expression of *HoxD* by directly recruiting the PRC2 complex to the locus (Yao, Wang and Chen, 2019). Precisely, a common mechanism is the recruitment of these complexes to specific loci, either *in cis* or *in trans* (Cheng *et al.*, 2016), to establish either repressive (e.g. Polycomb Group- PcG) or activating/transcription permissive (e.g. TxG) chromatin states (Wilusz *et al.*, 2009).

1.4.4.10. The role of lncRNAs in nuclear architecture

The transcription of lncRNAs can be involved in the formation of special nuclear domains, thereby regulating the gene expression indirectly (Maass *et al*., 2014). Several lncRNAs are associated with the formation and the functionality of such nuclear domains. For example,

TUG1 has been linked to repressive PcG bodies (Geisler and Coller, 2013), while *MALAT1* is enriched in nuclear bodies and regulates alternative splicing, and *NEAT1* is involved in the formation of paraspeckles and retaining A-to-I-modified mRNAs in the nucleus (Chen and Carmichael, 2010; Cheng *et al.*, 2016). In addition, upon cellular stress, a number of lncRNAs can be induced from ICGs to act as decoys for several proteins (e.g. VHL -Von Hippel-Lindau disease tumour suppressor-, Hsp70-heat shock protein 70-, MDM2/PML- E3 ubiquitin-protein ligase Mdm2/ Promyelocytic leukaemia protein-) to restrict them into the nucleolus in the detention centre (DC) (Cheng *et al.*, 2016). Finally, *MIAT* is located in special nuclear subunits and is speculated to be involved in alternative splicing, as detailed below (Sone *et al.*, 2007). Astonishingly, lncRNAs are involved in another, different aspect of nuclear architecture, this of the assembly and maintenance of the cytoskeleton itself, as well as the mitotic spindle. Although this has been studied in *Xenopus,* it is likely to apply for mammals, as well (Kloc *et al*., 2005; Wilusz *et al*., 2009). The basic roles of lncRNAs are schematically represented in Figure 1.9.

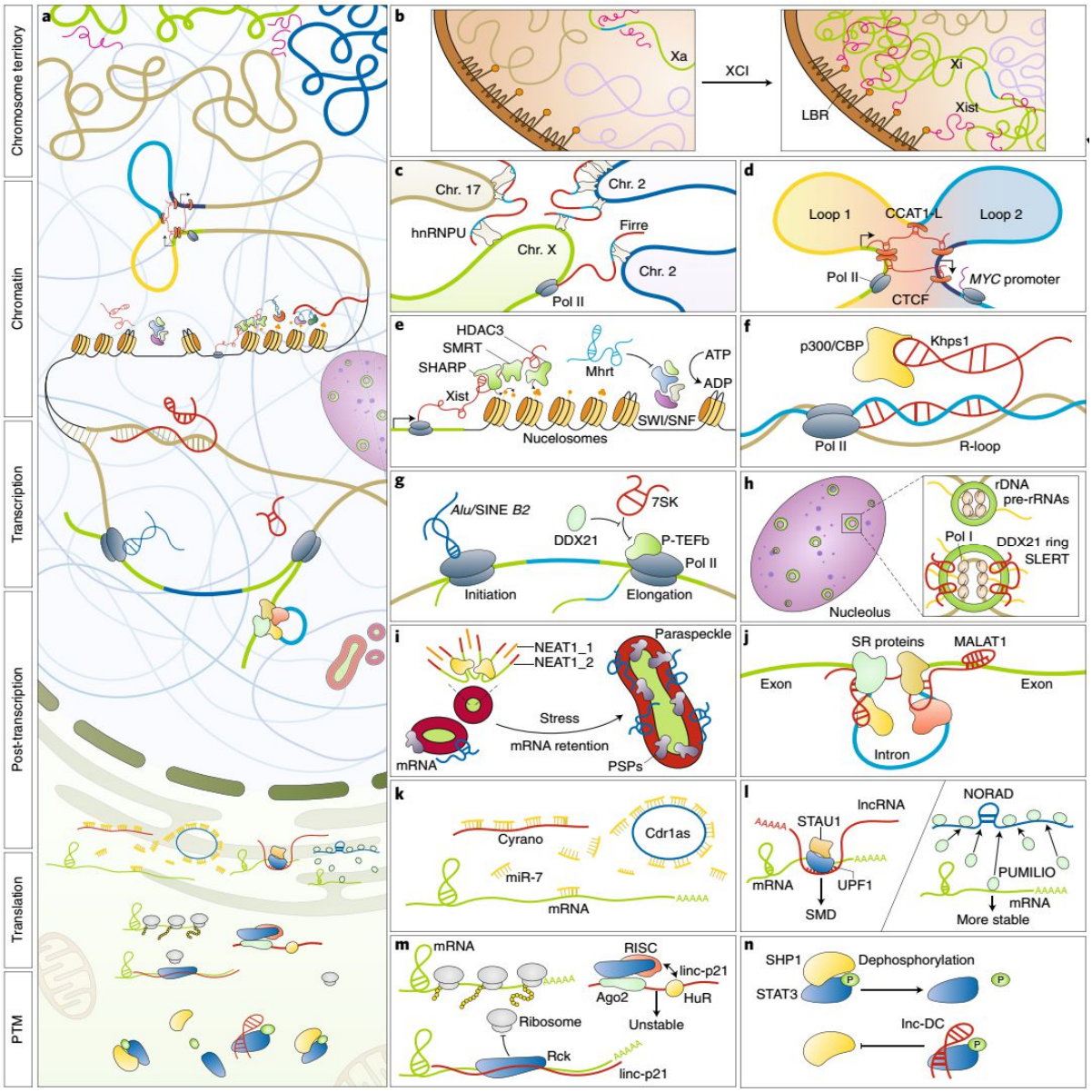

Figure 1.9. Schematic representation of the various roles and cellular functions of lncRNAs. A snapshot of cellular functions of lncRNAs with examples shown in b–n (a); *Xist* modulates inactive X chromosome (Xi) architecture during X chromosome inactivation (XCI) (b); *Firre* transcripts localise to their transcription site and five additional autosomal chromosomal loci in trans to affect interactions between distant genomic regions (c); CCAT1-L accumulates in cis to modulate chromatin loops between enhancers and the promoter of MYC (d); lncRNAs regulate chromatin accessibility. Left, *Xist* recruits HDAC1-associated repressor protein (SHARP),. Right, *Mhrt* prevents SWI/SNF binding to corresponding DNA loci (e); Khps1 enhances Pol II transcription by forming an R-loop (f); lncRNAs interfere with Pol II transcription machineries both at the initiation (left) and elongation (right) stages (g); *SLERT* promotes Pol I transcription by binding DDX21 to alter its conformation (h); *NEAT1* is an architectural lncRNA that nucleates paraspeckles. (i); *MALAT1* interacts with SR proteins and alters their phosphorylation to impact pre-mRNA splicing in splicing speckles (j); A regulatory network consisting of different types of ncRNAs. Cyrano, harbouring miR-7 binding sites, targets miR-7 for degradation and prevents miR-7 from repressing its target RNAs including the circRNA *Cdr1as* (k); lncRNAs modulate mRNA stability by associating with proteins involved in mRNA degradation. Left, double-stranded RNAs formed by Alu-containing lncRNAs with mRNA 3′ UTRs recruit STAU1 to induce STAU1-mediated mRNA decay (SMD). Right, *NORAD* stabilizes PUMILIO 1/2 (PUM1/2)-targeted mRNAs via sequestering PUM1/2 from mRNAs (l); lncRNAs regulate translation. Association of lincRNA-p21 (*linc-p21*) with HuR favours the recruitment of let-7/Ago2 (m); lncRNAs modulate post-translational modifications. *Lnc-DC* directly interacts with STAT3 to prevent its dephosphorylation by SHP1 (n) (adapted from Yao *et al*., 2019).

1.4.5. Physiological roles of lncRNAs

Together with the aforementioned roles of lncRNAs during gene expression regulating processes, lncRNAs are involved in numerous cellular processes and functions. These include cell cycle control, retrotransposon silencing, meiotic entry, cell differentiation and pluripotency, hematopoiesis, T-cell activation along with other significant epigenetic processes, for instance, imprinting of genomic loci and dosage compensation, either transcriptionally(Table 1.4a) or post-transcriptionally (Table 1.4b) (Costa, 2005; Wilusz *et al*., 2009; Geisler and Coller, 2013). For some of these roles, the mechanisms of lncRNA biogenesis may be of greater importance than the lncRNA itself (Furlan *et al.*, 2018; Mattick, 2018).

Table 1.4a. lncRNA-mediated gene regulation transcriptionally.

lncRNA	Stage of action	Role	Mechanism	Reference(s)
Xist	Transcriptionally	X-chromosome inactivation	Chromatin-mediated repression	(Geisler and Coller, 2013; Maass et al., 2014)
Tsix	Transcriptionally	X-chromosome inactivation	Xist repression via transcriptional interference	(Fenoglio *et al.*, 2013; Maass *et al.*, 2014)
KCNQ1OT1	Transcriptionally	Genomic imprinting	Chromatin-mediated repression of *KCNQ1*	(Wang and Chang, 2011; Geisler and Coller, 2013)
Air	Transcriptionally	Genomic imprinting	Chromatin-mediated repression of I*GFR2,* transcriptional interference	(Fenoglio *et al.*, 2013; Chen *et al.*, 2015)
HOTAIR	Transcriptionally	Development	Chromatin-mediated repression of the *HOXD* locus	(Wang and Chang, 2011; Fang and Fullwood, 2016)
HOTTIP	Transcriptionally	Development	Chromatin-mediated activation of the *HOXA* locus	(Wang *et al.*, 2011; Kornienko *et al.*, 2013; Fang and Fullwood, 2016)
Evf-2	Transcriptionally	Development	Chromatin-mediated activation of the *Dlx5/Dlx6* locus	(Wilusz *et al.*, 2009; Chen and Carmichael, 2010; Schmitz *et al.*, 2016)
ncDHFR	Transcriptionally	Nucleic acid synthesis	*DHFR* inhibition via inhibition of the pre-initiation complex formation	(Wang and Chang, 2011; Mohanty *et al.*, 2015)
Linc-RoR	Transcriptionally	Pluripotency/ Differentiation	Targeted by the key pluripotency factors Oct4, Sox2, and Nanog	(Guttman *et al.*, 2009; Wang and Chang, 2011; Clark and Blackshaw, 2014)
NRON	Transcriptionally	T-cell differentiation/ activation	Repression of *NFAT*-mediated transcription via prevention of its nuclear localisation	(Wilusz *et al.*, 2009; Qureshi, Mattick and Mehler, 2010; Mohanty *et al.*, 2015)
PANDA	Transcriptionally	Cell cycle control/apoptosis regulation	Limitation of pro-apoptotic genes and cell cycle arrest via NF-YA interactions	(Wang and Chang, 2011; Maass *et al.*, 2014; Chen *et al.*, 2015)
ANRIL	Transcriptionally	Cell cycle control/apoptosis regulation	Chromatin-mediated repression of the *INK4b-ARF-INK4a* locus	(Wang and Chang, 2011; Gutschner and Diederichs, 2012; Fang and Fullwood, 2016)
Linc-p21	Transcriptionally	Apoptosis regulation	Repression of p53-regulated genes by regulation of hnRNP-K localisation	(Huarte *et al.*, 2010; Wang and Chang, 2011)
GAS5	Transcriptionally	GR regulation	Repression of GR-mediated transcription via DNA mimicry	(Mourtada-Maarabouni *et al.*, 2009; Hung and Chang, 2011; Wang and Chang, 2011)

Table 1.4b. lncRNA-mediated gene regulation post-transcriptionally.

lncRNA	Stage of action	Role	Mechanism	Reference(s)
BACE1-AS	Post-transcriptionally	BACE-mediated amyloid precursor protein cleavage	BACE1 mRNA stabilisation via inhibition of miRNA-related repression	(Qureshi and Mehler, 2012; Fenoglio *et al.*, 2013; Clark and Blackshaw, 2014)
½-sbsRNA	Post-transcriptionally	Down-regulation of mRNAs	Staufen-mediated mRNA decay	(Wang and Chang, 2011; Geisler and Coller, 2013)
CDR1-AS	Post-transcriptionally	Down-regulation of miRNA-mediated repression	miRNA sequestration	(Geisler and Coller, 2013; Clark and Blackshaw, 2014; Mohanty *et al.*, 2015)
MALAT1	mRNA processing	Pre-mRNA splicing regulation	SR splicing factor regulation via scaffolding by nuclear speckles	(Moran *et al*., 2012; Geisler and Coller, 2013; Yoshimoto *et al.*, 2016)
MIAT	mRNA processing	Pre-mRNA splicing regulation	Splicing factor regulation via scaffolding by subnuclear bodies	(Cheng *et al.*, 2016; Sattari *et al.*, 2016)
NEAT1	mRNA processing	A-to-I modified mRNA retention in paraspeckles	Induction of paraspeckle formation	(Chen and Carmichael, 2010; Hirose and Nakagawa, 2012; Cheng *et al.*, 2016)

1.4.5.1. Dosage compensation and imprinting

X-chromosome inactivation and imprinting were the first mechanisms that were associated with lncRNAs. Dosage compensation or X-chromosome inactivation (XCI) refers to the mechanisms by which the difference in gene dosage for X-linked genes between female organisms (XX) and male organisms (XY) is silenced, by means of inactivation of a whole X chromosome (Xi), leaving only one active X chromosome (Xa) (Bernstein and Allis, 2005; Fenoglio *et al.*, 2013).

XCI is controlled by elements of a specific genomic locus, known as X inactivation centre (XIC). A lncRNA called *Xist* is highly expressed from Xi during the process, but not from Xa. *Xist* recruits PRC2 complexes, pulls up further X-chromosomal regions *in cis,* and spreads the inactivation via formation and spreading of repressive chromatin, i.e. H3K27 tri-methylated chromatin. This spreading depends also on *RepA,* a lncRNA transcribed from

the *Xist* locus. At the same time, the NAT of *Xist,* called *Tsix,* is expressed in Xa, preventing *RepA* from binding to PRC2 complexes, thus keeping the Xa active. On top of that, another lncRNA, Jpx, displaces the transcription factor CTCF (CCCTC-binding factor) that normally inhibits Xist, thus further transactivating *Xist.* These findings indicate that lncRNAs control XCI via an elegant, multi-level regulatory system (Fenoglio *et al.*, 2013; Maass *et al.*, 2014; Mohanty *et al.*, 2015). Finally, more recent lines of evidence have revealed that *Xist* may also reshape chromatin architecture by recruiting Xi to the nuclear lamina, given that it can associate with nuclear lamina via interaction with lamin B receptor (LBR) (Yao *et al.*, 2019).

Imprinting is the phenomenon of the monoallelic expression of a subset of genes, either from the paternal or the maternal allele in diploid organisms (Fenoglio *et al.*, 2013; Mohanty *et al.*, 2015). Similarly to XCI, imprinting is controlled by differentially methylated DNA regions called ICRs (imprinting control regions). In several imprinted clusters both protein-coding genes and lncRNAs can be found to be expressed, like *IGFR2 (insulin-like* growth factor 2*)/Air, Dlk1 (*Protein delta homolog 1*)/MEG3* (maternally expressed 3) and *Nesp (*Neuroendocrine secretory protein 55*)/Nespas (*Neuroendocrine secretory protein 55 antisense*)/Gnas* (Guanine nucleotide-binding protein G(s) subunit alpha isoforms short Gene) (Fenoglio *et al.*, 2013).

Among the best-studied imprinting-associated lncRNAs are the *Kcnq1ot1* and *Air*, both of which cause suppression of gene expression on the paternal allele. They both act by recruiting chromatin suppressive complexes such as PRC2 and G9a to induce the establishment of H3K27me3 and H3K9me3 marks to subsequently silence *KCNQ1* and *IGFR2*, respectively (Fenoglio *et al.*, 2013; Yao *et al.*, 2019).

1.4.5.2. Development and differentiation

The fact that lncRNAs are positively correlated with the developmental complexity of organisms implies their important involvement in the regulation of developmental, as well as differentiation, procedures. Notably, the proportion of mammalian genome devoted to cognitive function during development, suggests that a plethora of lncRNAs is of vital

importance for this process. In line with this, the predominance of lncRNA expression in the brain is aligning with this concept (Mattick, 2018). One such example is the imprinting-associated lncRNA *MEG3*. This imprinting-associated lncRNA exerts its effect *in cis*, by regulating genes important for development and survival. Its deletion leads to pre-and peri-natal lethality, underlining its importance (Zhou *et al.*, 2010; Schmitz *et al.*, 2016). Another important case is the Hox gene cluster. This homeodomain-containing TF cluster is essential for the anterior-posterior axis formation in bilateral organisms (Wang and Chang, 2011; Fenoglio *et al.*, 2013). Mammals have four such clusters, A-D. *HOTAIR* and *Frigidair* are lncRNAs transcribed from the *HoxC* locus. As previously described, *HOTAIR* acts *in trans,* both as a signal and a scaffold, primarily by recruiting PRC2 to spread H3K27me3 marks to repress the *HoxD* cluster (Bracken and Helin, 2009; Wang and Chang, 2011; Fang and Fullwood, 2016). On the other hand, *HOTTIP* and *Mistral* lncRNAs are transcribed from the *HoxA* locus (Fenoglio *et al.*, 2013). *HOTTIP* acts as a signal and an *in cis* guide via chromatin looping to drive histone methylation and gene transcription (Wang and Chang, 2011; Kornienko *et al.*, 2013). A set of other development-related lncRNAs have also been reported, including *Fendrr* (fetal-lethal non-coding developmental regulatory RNA) and *Playrr* that are involved in organ development, and *DEANR1* (Definitive Endoderm-associated long non-coding RNA 1) that is associated with mesoderm and endoderm development (Schmitz *et al.*, 2016).

Considering the importance of the cellular differentiation programmes, it is expected that lncRNAs play some role in this finely regulated tuning process. In fact, some lincRNAs were first discovered in murine embryonic stem cells; however, this field is still premature. Regardless, some lncRNAs have indeed been associated with the maintenance of pluripotency, such as the lncRNAs *RoR* and *MIAT* (Guttman *et al.*, 2009; Sheik Mohamed *et al.*, 2010; Clark and Blackshaw, 2014). Other lncRNAs have been associated with driving cells to undergo a specific lineage fate, such as *Bvht* (Braveheart) for the cardiovascular lineage, *TUG1* for retinal fate, *TUNA, Six3OS* and *Sox2dot* for neuronal fate, *linc-MD1* for

the muscular differentiation and *MIAT* for retinal and neuronal development (Fenoglio *et al.*, 2013; Clark and Blackshaw, 2014; Maass *et al*., 2014).

1.4.6. Roles of lncRNAs in pathological settings

Given the emerging roles that are constantly being attributed to lncRNAs, it is not surprising that their deregulation and malfunction is a significant part of the aetiology of numerous diseases.

1.4.6.1. Central Nervous System-related conditions

The human nervous system (CNS) comprises the most sophisticated, complex and highly evolved biological system. lncRNA expression is enriched in the CNS, in a spatiotemporal manner to promote the neuronal diversification and specification (Mercer *et al.*, 2008; Qureshi *et al.*, 2010; Clark and Blackshaw, 2014). LncRNAs expressed during neural and brain development include *Dali, Evf-2, ncRMS* (non-coding rhabdomyosarcoma), *MIAT* and *ANCR* (anti-differentiation ncRNA) (Schmitz *et al*., 2016). Notably, lncRNAs expressed in the CNS are preferentially located in close proximity of protein-coding genes involved in neurodevelopment and function primarily *in cis* (Dinger *et al*., 2008; Qureshi *et al.*, 2010). As a natural consequence of the overwhelming presence and influence of lncRNAs in every CNS-related aspect, such as brain patterning, neuro- and gliogenesis, synaptic and neural plasticity (Fenoglio *et al*., 2013), their involvement in CNS-related pathological settings is inevitable.

Several lncRNAs have been implicated in a wide spectrum of neurodevelopmental disorders. Some of them are associated with imprinting, such as the Prader-Willi Syndrome (PWS) and the Angelman Syndrome (AS). The *PWS-AS* locus is only maternally expressed and some studies have identified the lncRNA *Ube3a-AS* transcript as a potential regulator of the paternal allele repression (Costa, 2005; Qureshi, Mattick and Mehler, 2010; Fenoglio *et al.*, 2013). Besides, two FMR1 (Fragile X mental retardation protein)-dysregulation-related syndromes can be linked to lncRNAs: the fragile-X syndrome (FXS) and the fragile-X-associated tremor and ataxia syndrome (FXTAS). So far two lncRNAs have been

associated with these syndromes, named *ASFMR1* and *FMR4*. Moreover, spinocerebellar ataxia type 8 (SCA8), a dominant autosomal disease has a lncRNA-based (*ATXN8OS*-Ataxin 8 opposite strand) causation (Qureshi *et al.*, 2010; Fenoglio *et al.*, 2013). *DGCR5* is another lncRNA that has been implicated in disorders displaying brain malformations and cognitive and behavioural abnormalities, such as the DiGeorge Syndrome. Finally, *NRON* has been suspected to be part of Down's Syndrome (DS) pathophysiology (Qureshi *et al.*, 2010).

LncRNAs are also key players of the pathobiology of neurodegenerative disorders. The best-investigated case is this of *BACE1-AS* (β-site amyloid precursor protein-cleaving enzyme 1 antisense transcript) in the development of Alzheimer's disease (AD). AD is characterized by the accumulation of β-amyloid plaques in the brain. These plaques are formed by β- amyloid peptides, which are the result of BACE-mediated APP (amyloid precursor protein) cleavage. In AD patients *BACE1-AS* promotes the production of these plaques since its upregulation leads to extra stabilisation of *BACE1* mRNA and, therefore, more protein production. *BC200 (*brain cytoplasmic RNA 1)*,* another lncRNA has been also implicated in AD (Fenoglio *et al.*, 2013; Clark and Blackshaw, 2014). Other lncRNAs that belong to this category are the cyclin D1-related lncRNA found in FUS/TLS-mutated ALS (amyotrophic lateral sclerosis) patients and a number of REST-associated candidate lncRNAs in patients with Huntington's Disease (HD) (Qureshi *et al*., 2010).

LncRNAs have also been, at least partly, responsible for mediating immune responses of the CNS, as suggested by findings supporting their involvement in neuroimmunological disorders, like multiple sclerosis, which is characterised by abnormal $CD8^+$ T-cell activity. (Qureshi *et al.*, 2010) Restless Legs Syndrome (RLS) and epileptogenesis may also involve lncRNA-mediated regulation (Qureshi *et al.*, 2010). Finally, a wide range of psychiatric disorders, including schizophrenia (SZ), schizoaffective disorder, bipolar disorder, major depression and autistic spectrum disorders, have been suspected to be affected by the lncRNA *DISC2*-mediated regulation of *DISC1.* Recently another lncRNA,

MIAT, was found to be involved in SZ (Costa, 2005; Qureshi *et al.*, 2010; Fenoglio *et al.*, 2013).

1.4.6.2. Cancer

Numerous studies have confirmed that the involvement of lncRNAs in a diversity of cancers (Costa, 2005; Moran *et al.*, 2012) (Table 1.5). Prostate cancer has been associated with the deregulation of a couple of lncRNAs, including *PCA3 (*prostate cancer antigen 3*), PCAT1 (*prostate cancer-associated transcript 1*), CTBP1-AS1 (*C-terminal-binding protein 1 antisense RNA 1) and *PCGEM1 (*prostate-specific transcript non-protein-coding) (Costa, 2005; Maass *et al.*, 2014). Colorectal cancer, as well, has been correlated with a number of lncRNAs, such as *KCNQ1OT1* and *PCAT1* (Maass *et al.*, 2014). In addition, a set of lncRNAs have been associated with breast tumours (e.g. *SRA, BC200 and HOTAIR*) (Moran *et al.*, 2012; Maass *et al.*, 2014), with hepatocellular carcinomas, like *HULC (*highly up-regulated in liver cancer) and *HOTTIP*, with lung cancer (e.g. *MALAT1* in non-small cell lung carcinoma), as well as with melanoma and haematologic malignancies (e.g. *HOTTIP*) (Costa, 2005; Moran *et al.*, 2012; Maass *et al.*, 2014). Perturbations in the expression of a number of lncRNAs have been associated with CNS tumours like medulloblastomas, gliomas and meningiomas (e.g. *H19, TUG1* and *NOS2A-AS*- Nitric oxide synthase, inducible antisense) (Qureshi *et al.*, 2010), as well as with tumours of the sympathetic nervous system, such as neuroblastomas (Pandey and Kanduri, 2015).

LncRNAs can act as oncogenes, tumour suppressors, as well as drivers of metastasis (Cao, 2014; Chandra Gupta and Nandan Tripathi, 2017). They have been associated with multiple hallmarks of cancer and potentially the expanding knowledge of the field will associate them with the full spectrum of these known hallmarks (Gutschner and Diederichs, 2012; Rao *et al.*, 2017). Although the exact acting mechanisms have not yet been fully elucidated for all cancer-associated lncRNAs, the roles of some of them have been thoroughly studied (Table 1.5). On the grounds that perturbations in the cell cycle regulation

are tightly bound to tumour formation and progression, a number of cell cycle-related lncRNAs have been studied (Kitagawa *et al.*, 2013; Pop *et al.*, 2018). In addition, several cell death resistance-associated lncRNAs have been studied, primarily those associated with p53-mediated apoptosis. For example, a NAT called *Wrap53* (WD40-encoding RNA antisense to p53) stabilises p53 at the mRNA level, thus promoting its expression and its overexpression can sensitise tumour cells to apoptosis (Mahmoudi *et al.*, 2009). However, upon its overexpression in cancerous settings, it has been found to act as an oncogene, promoting cellular transformation (Mahmoudi *et al.*, 2011). Furthermore, upregulation of lncRNAs in various cancers, for instance, *linc-p21* (transcribed near the $p21^{Cip1}$ gene, another CDK inhibitor and p53 regulator) and *PANDA*, leads to suppression of apoptosis in response to DNA damage, thus promoting carcinogenesis (Hung *et al.*, 2011; Kitagawa *et al.*, 2013; Maass *et al.*, 2014). Another lncRNA, *BC200,* has been attributed oncogenic properties in breast cancer settings by binding to the tumour suppressor BCL-xS pre-mRNA and recruiting hnRNPA1/B2 to suppress its expression (Stevens and Oltean, 2019). In addition, snoRNA host gene expression has been attributed oncogenic properties, like in the case of *SNHG16* (Chi *et al.*, 2019; Yu *et al.*, 2019), *SNHG1* (Sahu *et al.*, 2016; N. Zhang *et al.*, 2019; Yang *et al.*, 2019) and *SNHG7* (Chi *et al.*, 2019). Finally, Cancer Susceptibility Candidate 15 (*CASC15* or *linc00340*), *CASC9* and *TUG1* recruit the chromatin remodeler EZH2 to suppress the expression of the tumour suppressor Programmed Cell Death 4 (PDCD4) in various cancers (Zhao *et al.*, 2019).

Depending on the tumour setting, the same lncRNA can behave as an oncogene or a tumour suppressor. Of particular interest is *ANRIL*, the antisense transcript of the CDK inhibitor $p15^{ink4b}$ that is transcribed from the *INK4* locus. *ANRIL* silences the transcription of the *INK4* locus via PRC1/PRC2 recruitment and consequent chromatin repression. Upon oncogenic processes, *ANRIL* can be either upregulated or downregulated, acting as an oncogene or a tumour suppressor, respectively (Kitagawa *et al.*, 2013; Fang and Fullwood, 2016).

Table 1.5. Deregulated lncRNAs in cancer.

lncRNA	Type of cancer	Expression	Cancer Hallmark	Reference(s)
PCAT-1	Prostate, colorectal	↑	Sustaining proliferation	(Gutschner and Diederichs, 2012; Zhang et al., 2016)
ANRIL	Prostate, leukaemia, oesophageal	↑	Evading growth suppressors	(Gutschner and Diederichs, 2012; Mohanty *et al.*, 2015; Fang and Fullwood, 2016)
GAS5	Colorectal, cervical, breast, leukaemia	↓	Evading growth suppressors	(Mourtada-Maarabouni *et al.*, 2009; Mohanty *et al.*, 2015; Zhang et al., 2016; Zhao *et al.*, 2019)
Linc-p21	Various tumour cell lines	↑	Evading growth suppressors	(Gutschner and Diederichs, 2012; Maass *et al.*, 2014)
TERC	Various tumour cell lines	↑	Enabling replicative immortality	(Gutschner and Diederichs, 2012)
TERRA	Various tumour cell lines	↓	Enabling replicative immortality	(Gutschner and Diederichs, 2012; Maass *et al.*, 2014; Mohanty *et al.*, 2015)
SRA	Breast	↑	Activating metastasis	(Yao *et al.*, 2010; Gutschner and Diederichs, 2012)
MALAT1	Lung, liver, colorectal, ovarian, pancreatic, endometrial, multiple myeloma, osteosarcoma, pancreas, breast, uterus, neuroblastoma, glioma	↑	Sustaining proliferation Activating metastasis	(Costa, 2005; Fang and Fullwood, 2016; Zhang et al., 2016)
HOTAIR	Gastric, colorectal. lung, endometrial, cervical, breast, glioma, liver, pancreatic	↑	Activating metastasis	(Maass *et al.*, 2014; Fang and Fullwood, 2016; Zhang *et al.*, 2016)
HULC	Liver, pancreatic	↑	Activating metastasis	(Gutschner and Diederichs, 2012; Maass *et al.*, 2014)
BC200	Breast, cervical, oesophagus, lung, ovarian, parotid, tongue,	↑	Activating metastasis	(Costa, 2005; Gutschner and Diederichs, 2012; Mohanty *et al.*, 2015)
PCGEM-1	prostate	↑	Resisting cell death	(Costa, 2005; Gutschner and Diederichs, 2012; Ling *et al.*, 2015)
H19	Liver, breast, stomach	↑	Sustaining proliferation	(Ling *et al.*, 2015; Mohanty *et al.*, 2015; Fang and Fullwood, 2016)
KNCQ1OT1	Colorectal, breast	↑	N/A	(Maass *et al.*, 2014; Mohanty *et al.*, 2015; Fang and Fullwood, 2016)
TUG1	Epithelial squamous cell, bladder, renal cell, glioma, cervical, endometrial, melanoma, gastric	↑ ↓	Sustaining proliferation Resisting cell death Activating metastasis	(Mohanty *et al.*, 2015; Z. Li *et al.*, 2016; Zhang et al., 2016; Zhou *et al.*, 2019)
NEAT1	Prostate, acute promyelocytic leukaemia, laryngeal squamous cell cancer, glioma	↑ ↓	Resisting cell death	(Almnaseer and Mourtada-Maarabouni, 2016; Lo *et al.*, 2016; Gao *et al.*, 2016)
MIAT	Glioma, chronic lymphocytic leukaemia, diffuse large B-cell lymphoma, neuroblastoma, breast	↑	Resisting cell death	(Zhang *et al.*, 2013; Mei-Yee Kiang *et al.*, 2015; Sattari *et al.*, 2016; Almnaseer and Mourtada-Maarabouni, 2018; Bountali *et al.*, 2019)

Moreover, *TUG1* can play oncogenic or tumour suppressor roles, depending on the type of tumour, but is predominantly addressed as an oncogenic lncRNA (Zhou *et al.*, 2019). As far as lncRNAs acting as tumour suppressors are concerned, *TERRA* has been implicated as a tumour suppressor, since its repression promotes cell immortalization (Gutschner and Diederichs, 2012). *GAS5* acts as a ceRNA that sponges miR-21 to liberate the pro-apoptotic PDCD4 and let it exert its tumour suppressor activity in cervical cancer. Similarly, *linc00472*, DiGeorge Syndrome Critical Region Gene 5 (*DGCR5*) and *TUG1* sponge miR-196a, miR-320a, and miR-21, respectively, to let PDCD4 act as a tumour suppressor in colorectal cancer, pancreatic ductal adenocarcinoma, and osteosarcoma, respectively (Zhao *et al.*, 2019).

Moreover, *MALAT1* has been found to be upregulated in numerous cancers, contributing to both the increase of cell proliferation, (Kitagawa *et al.*, 2013) and, primarily, to increased metastatic potential in various cancers [e.g. in lung (Costa, 2005; Fang and Fullwood, 2016), liver (Fang and Fullwood, 2016), colorectal (Fang and Fullwood, 2016), and ovarian (Cao, 2014)]. In tandem, upregulated *TUG1* in cancers has been associated with increased tumour size and distant metastasis (Zhou *et al.*, 2019).

Given their distinct differential expression in healthy cells versus cancerous cells, as well as their detection in biological fluids, including plasma, serum, urine and saliva, lncRNAs represent perfect biomarker candidates for tumour diagnosis and patient stratification towards better prediction and prognosis (Chandra Gupta and Nandan Tripathi, 2017; Pop *et al.*, 2018). A very indicative such case is *PCA3,* which is massively overexpressed in prostate cancer, but not in other cancers or healthy cells, and has, therefore, been approved for prostate cancer diagnosis. Numerous other lncRNAs have also been attributed predictive values for prostate cancer (*MALAT, FR0348383, AK024556, XLOC_007697, LOC100287482, XLOC_005327, XLOC_008559 and XLOC_009911*). Similarly, *UCA1* comprises a diagnostic test for transitional cell carcinoma and oral squamous cell carcinoma (OSCC), and *HOTAIR, NEAT1* and *MEG3* for OSCC (Chandra

Gupta and Nandan Tripathi, 2017). Meanwhile, *CCAT1/2* have been associated with prognosis for colon, hepatocellular (HCC) and oesophageal cancer. HCC prognostic lncRNAs include *SNHG3, PANDAR, hPVT1*, and *HOTAIR*. The *HOTAIR* expression could also be of prognostic value in gallbladder cancer (GBC) patients, acute myeloid leukaemia patients, small-cell lung cancer patients, colon cancer patients, breast cancer patients and oesophageal squamous cell carcinoma patients. Some other lncRNAs that are linked with cancer prognosis include *ANRIL* for GBC, *AFAP1-AS1*(Actin Filament Associated Protein 1 Anti-sense 1) for pancreatic cancer, *LINC00472, H19* and *KCNQ101T* for breast cancer, lncRNA-ATB for colorectal cancer, *SChLAP1* (SWI/SNF Complex Antagonist Associated With Prostate Cancer 1) for prostate cancer and *HIF1A-AS2* for TNBC91 (Chandra Gupta and Nandan Tripathi, 2017; Pop *et al.*, 2018). lncRNAs associated with tumours of the CNS, and specifically NB and GBMs are analysed separately below. lncRNAs are also potent biomarkers of tumour recurrence, especially for breast cancer (Liu *et al.*, 2016; Jiang *et al.*, 2016). Finally, SNPs (single nucleotide polymorphisms) are associated with cancer predisposition. In fact, ~90% of disease-related SNPs are found in non-coding areas and a number of them are found in lncRNAs loci (Ling *et al.*, 2015). Of these, some are strongly associated with various cancers, for instance, an SNP in *ANRIL* that is associated with glioma (Ling *et al.*, 2015) and a set of SNP variants, which are associated with poor NB prognosis (Pandey and Kanduri, 2015).

LncRNAs in Neuroblastoma

Given the inadequate means of patient stratification and the ineffective means of therapy, the search for novel biomarkers and therapeutic targets has been intensive. A number of lncRNAs have been identified to be associated with NB predisposition and/or associated with the tumour itself since their expression levels are perturbed. Like protein-coding genes, in a tumour setting, they can act as oncogenes to drive tumourigenesis and tumour progression, as tumour suppressors to inhibit oncogenic processes, and can be involved in virtually all hallmarks of cancer.

Many oncogenic lncRNAs have been identified and studied. Among them, some are co-deregulated with typical chromosomal aberrations, in particular chromosomal gains in the case of oncogenes (Rombaut *et al.*, 2019), as in the case of the overexpressed *ncRAN* (non-coding RNA expressed in aggressive neuroblastoma) in NBs with the 17q gain (Watters *et al.*, 2013; Pandey and Kanduri, 2015; Rombaut *et al.*, 2019). The deregulation of other lncRNAs is the result of focal amplifications. A typical such example is the co-amplification of *lncUSMycN* with *MYCN* in NBs (Pandey and Kanduri, 2015; Zhao *et al.*, 2018). lncRNA *CAI2* (*CDKN2A/ARF* Intron 2 lncRNA), whose overexpression is associated with high risk NBs, regardless of the *MYCN* amplification status, suggesting its tumourigenic properties (Barnhill *et al.*, 2014; Pandey and Kanduri, 2015) is another example. In addition, a number of lncRNAs are transcribed from ultra-conserved regions and are significantly associated with patient prognosis in the high-risk NB group (e.g. *T-UC 300A*) (Domingo-Fernandez *et al.*, 2013; Pandey and Kanduri, 2015). The expression of snoRNA host gene 16 (*SNHG16*) was revealed to be in line with the clinical staging of NB, and high *SNHG16* (as well as *SNHG1* and *SNHG7*) expression was positively associated with poor clinical outcome. *SNHG16* is a cell proliferation regulator in NB through transcriptional and translational pathways (Chi *et al.*, 2019; Yu *et al.*, 2019). Knockdown of linc01105 inhibited neuroblastoma cell proliferation, migration and invasion, and induced apoptosis. In addition, *LINC01105* affected the expression of p53 and BCL-2 family proteins

and activated the caspase cascade, promoted the expression of the miR-6769b-5p target gene *VEGFA* by acting as a sponge, leading to the conclusion it acts as an oncogene in NB (Ye *et al.*, 2019). *Xist* also displays oncogenic activity in NB via the recruitment of EZH2 to the tumour suppressor DKK1 (Dickkopf Wnt signalling pathway inhibitor 1), thus inactivating it (Zhang *et al.*, 2019). *MIAT* has recently been confirmed to be acting as an oncogene in NB cells by regulating apoptosis through the production of ROS, long term cell survival and migration (Bountali *et al*., 2019) (Appendix I).

In other cases, NB-related lncRNAs possessing anti-tumour properties are vastly deregulated, like in the case of the deleted tumour suppressor *NDM29* (neuroblastoma differentiation marker 29) in NBs with chromosome 11 loss (Nakagawara *et al.*, 2018; Zhao *et al.*, 2018). What is more, fluctuations in the levels of lncRNAs may be noticed for lncRNAs that are located in chromosomes which lack an apparently important role in NB formation and progression, as in the case of *NBAT1* (neuroblastoma associated transcript 1) and *CASC15* lncRNA on chromosome 6 (Russell *et al.*, 2015; Mondal and Kanduri, 2019). *NBAT1* normally acts as a tumour suppressor that inhibits cell proliferation and invasion through the silencing of REST (RE1 Silencing Transcription Factor). Its down-regulation has been linked with high risk NBs and is significantly related to poor clinical outcomes (Pandey *et al.*, 2014; Huarte, 2015; Nakagawara *et al.*, 2018; Mondal and Kanduri, 2019). *FOXD3-AS1* (Forkhead Box D3 Anti-sense RNA 1) induces neuronal differentiation and inhibits cell growth, invasion, and metastasis by binding to poly(ADP-ribose) polymerase 1 (PARP1) to inhibit the poly-ADP-ribosylation (PARylation) and activation of the epigenetic regulator CTCF, resulting in de-repressed expression of downstream tumor-suppressive genes (Zhao *et al.*, 2018). The expression of the tumour suppressor *MEG3* has also been found to be downregulated in NBs (Chi *et al.*, 2019).

The list of lncRNAs that are associated with NB is steadily growing (Batagov *et al.*, 2013) and now includes lncRNAs whose deregulation is clearly implicated in poor outcomes. *Paupar* (Pandey and Kanduri, 2015; Zhao *et al.*, 2018)*, linc-NeD125* (Bevilacqua *et al.*,

2015), as well as the metastasis-associated lncRNAs *MALAT1* (Pandey and Kanduri, 2015; Bi *et al.*, 2017), *HOXD-AS1* (Yarmishyn *et al.*, 2014; Li *et al.*, 2018), *LINC01296* (Jing Wang *et al.*, 2019), Ets-1 promoter-associated non-coding RNA (*pancEts-1*) (Li *et al.*, 2018) are included in this extensive list. Also, SNPs on lncRNAs could be of significant prognostic value, as in the cases of *NBAT1* and *CASC15* lncRNA (Pandey *et al.*, 2014; Chi *et al.*, 2019; Mondal and Kanduri, 2019). Finally, various attempts have been made to generate accurate lncRNA-based profiles and signatures, to easily, but at the same time reliably, classify patients and allocate them to a clinically relevant risk group (Sahu *et al.*, 2018; Rombaut *et al.*, 2019; Yerukala Sathipati *et al.*, 2019), as well as predict the chances of recurrence (Utnes *et al.*, 2019). These lncRNAs can be extremely useful biomarkers, and, at least some of them, promising therapeutic targets.

LncRNAs in Glioma

The lagging patient stratification for both children and adults with gliomas, together with the inefficiency of the therapeutic approaches for gliomas, have contributed to the generation of a shift to novel approaches. The differential expression patterns of lncRNAs between tumour cells and their normal counterparts render lncRNAs perfect candidates for glioma diagnosis and prognosis, as well as perfect therapeutic candidates since they have been postulated to be involved in glioma progression (Pop *et al.*, 2018). There is now mounting evidence that points towards the direction that lncRNAs regulate a number of oncogenic events and processes in gliomas and are also associated with tumour prognosis.

A plethora of GBM-associated lncRNAs possesses oncogenic properties. As aforementioned, lncRNAs are involved in DNA methylation and chromatin remodelling. In gliomas, such examples as the *linc-POU3F3* and the well-known *HOTAIR* have been reported to promote glioma pathogenesis. Besides, high expression of *HOTAIR* is associated with poorer prognosis (Guo *et al.*, 2015; Ramos *et al.*, 2016; Gao *et al.*, 2016; Pop *et al.*, 2018). Another well- studied lncRNA, *H19*, has also been implicated in glioma

progression and invasion and its upregulation is correlated with poor prognosis (Qureshi *et al*., 2010; Mei-Yee Kiang *et al.*, 2015; Gao *et al*., 2016; Pop *et al.*, 2018). The lncRNA *CRNDE* (colorectal neoplasia differentially expressed) also shows elevated expression in gliomas and is positively correlated with EGFR amplification. The effects of this alteration are clear mostly in GBMs, while they are less dramatic in other gliomas, and include increased cell growth and invasion (Mei-Yee Kiang *et al*., 2015; Ramos *et al*., 2016; Gao *et al.*, 2016). Its oncogenic activity is exerted by promoting cell growth, invasion and migration via different cancer-related pathways and, interestingly via being regulated by c-Myc (Pop *et al*., 2018). Among the genes which are well-established in glioma pathogenesis and progression, *MALAT1* and *NEAT1* have been reported to play key roles, with the former activating the ERK/MAPK oncogenic pathway, and the latter binding the tumour suppressor miR-449b-5p, leading to the increase of the c-Met oncogene (Gao *et al.*, 2016; Zhen *et al.*, 2016; Pop *et al.*, 2018). The expression of *MALAT1* is elevated comparing to normal tissues and, also, positively correlated with more malignant phenotypes and TMZ resistance (Mei-Yee Kiang *et al*., 2015; Pop *et al.*, 2018). *SOX2OT* (SOX2 Overlapping Transcript), *TUG1*, and *Xist* also promote cell proliferation, migration and invasion, and in parallel, inhibit apoptosis in GSCs and glioma cells, respectively (Mei-Yee Kiang *et al.,* 2015; Gao et al., 2016; Li et al., 2016; Shi *et al.*, 2017; Pop *et al.*, 2018). *MIAT* has recently been confirmed to act as an oncogene in GBM cells by regulating apoptosis, long term cell survival and migration (Bountali *et al.*, 2019). Finally, *LOC441204, HIF1A-AS2* and Zinc finger Anti-sense 1 (*ZFAS1*) are overexpressed in GBMs, contributing to tumour progression and poor prognosis (Lv *et al*., 2017; Pop *et al*., 2018).

By contrast, numerous lncRNAs tend to act as tumour suppressors in glioma settings. For instance, overexpression of *MEG3* has been reported in gliomas and has been associated with prolonged survival. *MEG3* acts as a tumour suppressor by both inhibiting cell proliferation and activating the p53-mediated apoptotic pathway (Liu *et al*., 2015; Mei-Yee Kiang *et al*., 2015). *ADAMTS9-AS2* (A disintegrin and metalloproteinase with

thrombospondin motifs 9 antisense RNA 2) is largely downregulated in gliomas and negatively correlated with tumour grade and prognosis. *linc-RoR*–although usually serving as an oncogene- and *lincRNA-p21* act as tumour suppressors in GBM context (Ramos *et al.*, 2016; Pop *et al.*, 2018). Finally, a novel lncRNA, *LINC00657* has been found to act as a tumour suppressor in GBM (Chu *et al.*, 2019).

As in the case of NB, the list of lncRNAs implicated in gliomas is rapidly growing, something that provides an opportunity window for more accurate patient stratification towards prognosis and more personalized treatment. A large number of novel lncRNAs are now validated players of the glioma pathogenesis [e.g. *HOXA11-AS* (Gao *et al.*, 2016)*, HULC* (Gao *et al.*, 2016)*, ASLNC22381* and *ASLNC20819* (Mei-Yee Kiang *et al.,* 2015; Gao *et al.*, 2016), *ATB* (Gao *et al.*, 2016), *AB073614* (Hu *et al.*, 2016; Gao *et al.*, 2016), *CASC2* (Wang *et al.*, 2015; Gao *et al.*, 2016; Palmieri *et al.*, 2017), *GAS5* (Mei-Yee Kiang *et al.*, 2015; Gao *et al.*, 2016)] (Figure 1.10). In addition, in line with the hypothesis that several lncRNA-coding pairs show opposite type of expression correlation in healthy versus cancerous cases (Chandra Gupta and Nandan Tripathi, 2017), an altered correlation status of SAM Domain, SH3 Domain And Nuclear Localization Signals 1 *(SAMSN1*) and its Anti-sense transcript 1 (*SAMSN1-AS1*) could prove to be a potential biomarker of GBM diagnosis and prognosis (Ning *et al.*, 2017). Finally, lncRNA profiling and signature sets are being generated to make the prognostication even easier and, mainly more accurate (Han *et al.*, 2012; Li *et al.*, 2014). In a first attempt, signature profiles were generated to distinguish between low and high grade gliomas (Zhang *et al.*, 2012). In subsequent approaches and as far as GBM is concerned, more intense research has led to the generation of GBM-specific lncRNA signatures, such as the six-lncRNA signature discovered by Zhang *et al*. (2013) and the four-lncRNA signature discovered by Chen *et al*., (2017), as well as the lncRNA molecular classification of different GBM subtypes (Reon *et al.*, 2016).

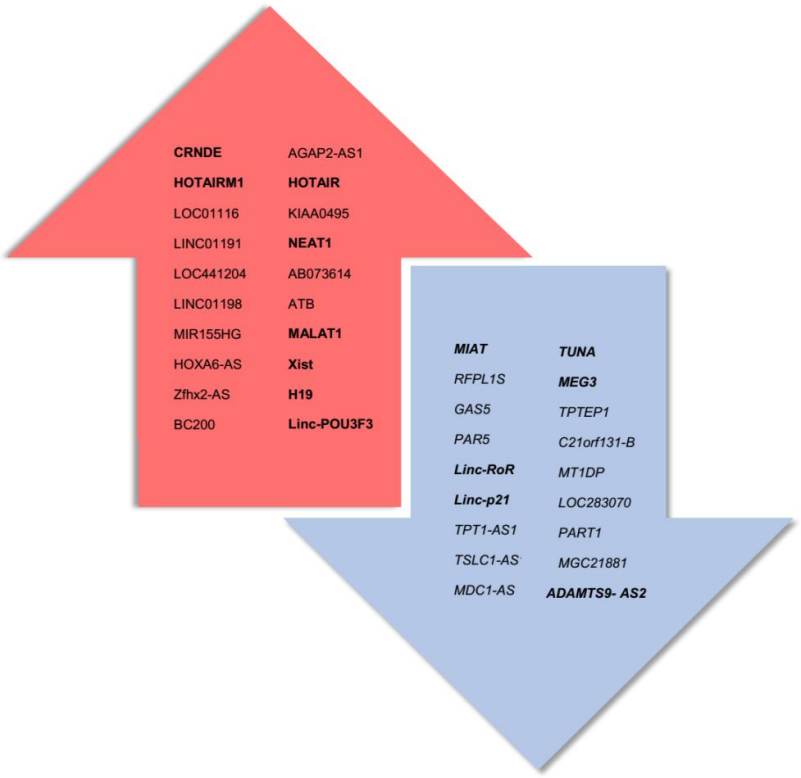

Figure 1.10. Graphical representation of differentially expressed lncRNAs in GBM compared to normal cells. The red arrow includes upregulated lncRNAs, while the blue arrow includes downregulated lncRNAs. lncRNAs in bold are also part of developmental processes.

1.5. Myocardial Infarction-Associated Transcript (*MIAT*)

Apart from the nuclear and cytoplasmic lncRNAs, a number of sub-nuclear bodies exist, which are associated with specific cellular processes. In line with this, a number of lncRNAs have been reported to be localised at such bodies. Some indicative such examples are the well-characterised *MALAT1* and *NEAT1*, as well as the relatively newly discovered and characterised *MIAT*. In spite of its relative youth in the field of lncRNAs, *MIAT* is steadily gaining researchers' attention, and in turn, there exists a rapidly growing body of evidence that suggests its importance in healthy and pathological settings, including cancer. Nevertheless, in order to elucidate its role in cancer, and in specific NB and GBM, it is essential to understand its molecular characteristics, mode of action, as well as its role in normal cells. An overview of these is briefly outlined in this section.

1.5.1. Characterisation

MIAT, also known as *Gomafu* and *RNCR2* (retinal non-coding RNA 2) is a lncRNA that is located in special sub-nuclear bodies. *MIAT* is a ~10kb long transcript transcribed from chromosome 22q12.1 (Figure 1.11), with the full-length transcript (isoform 1) accommodating 5 exons (Fakhr-Eldeen *et al.*, 2019). It is highly conserved in mammals, birds and amphibians (Sone *et al.*, 2007; Boon *et al.*, 2016; Cheng *et al.*, 2016). In contrast to *MALAT1* and *NEAT1*, which are ubiquitously expressed in numerous cells/ tissues, *MIAT* is mainly expressed in some cells of the fetal brain and the adult brain/CNS [including Müller glia, neurons and endothelial cells (Tsuiji *et al.*, 2011; Jiang *et al.*, 2016; Sha *et al.*, 2018)], especially in the retinal tissue. In fact, this suggests that its expression begins in differentiating progenitor cells and is maintained in particular types of post-mitotic neurons only (Sone *et al.*, 2007; Cheng *et al.*, 2016). Its involvement in the maintenance of pluripotency has been demonstrated in vivo in mouse embryonic stem cells, where it participates in a positive feedback loop with the stemness markers Oct4 and Nanog (Sheik Mohamed *et al.*, 2010).

MIAT is localised across the nucleoplasm in a spotted pattern (inherent to its Japanese name, *Gomafu,* which means spotted), but these 'spots' do not co-localise with any of the known sub-nuclear bodies, and this localisation is actively maintained (Sone *et al.*, 2007; Cheng *et al.*, 2016). In addition, *MIAT* is polyadenylated at the 3' end, has at least 4 alternatively spliced variants in human and 10 in mouse, and as analyses have shown, it is unlikely to serve as a miRNA precursor (Ishii *et al.*, 2006; Sone *et al.*, 2007). Although *MIAT* is a mRNA-like lincRNA, it escapes nuclear export and is invariably retained in the nucleus (Sone *et al.*, 2007; Tsuiji *et al.*, 2011).

Although the research on *MIAT* is still at premature stage, it is thought to participate in pre-mRNA splicing through its binding to SF1 (splicing factor 1), although this interaction is not essential for the localisation of *MIAT* (Cheng *et al.*, 2016). It has also been shown that it binds QK1 (quaking homolog, KH domain RNA binding protein), SRSF1 (serine/arginine-

rich splicing factor 1) and Celf3 (CUGBP Elav-Like Family Member 3) and that its deregulation generates abnormal splicing patterns (Ishizuka *et al.*, 2014; Cheng *et al.*, 2016; Sattari *et al.*, 2016). This is achieved through a UACUAAC repeat on *MIAT* which binds SF1 with greater affinity comparing to the mammalian branch point consensus sequence (Tsuiji *et al.*, 2011). In addition, it has been postulated that the knockdown of proteins associated with *MIAT*, such as Celf3 could modulate its expression and distribution (Ishizuka *et al.*, 2014). Taken together, these suggest a *MALAT1*-like mechanism of action for *MIAT* in pre-mRNA splicing regulation (Cheng *et al.*, 2016). Interestingly, *MIAT* also behaves as a miRNA sponge, especially in cancerous context (Fakhr-Eldeen *et al.*, 2019) (described in section 1.5.3).

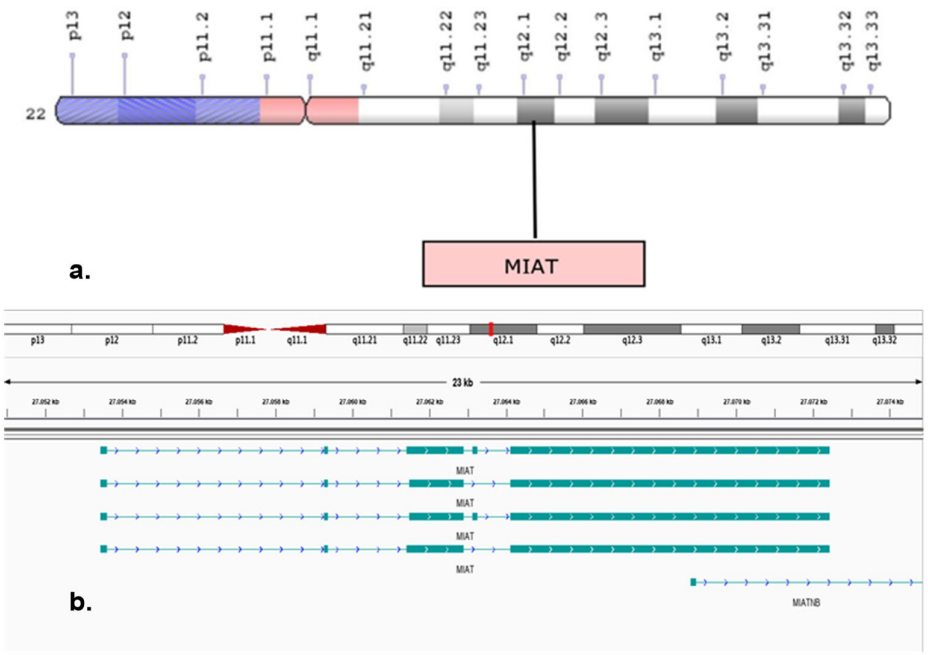

Figure 1.11. *MIAT* locus and variants. *MIAT* is a 10kb long transcript transcribed from chromosome 22q12.1 that produces four isoforms as a result of alternative splicing. *MIAT* lies within the cytogenetic band: 22q12.1 on chromosome 22 (base pairs 26,657,482 to 26,676,478) (by Ensembl) (a); the four different *MIAT* variants in human. Variant 1 (NR_003491.3) represents the longest transcript; variant 2 (NR_033319.2) lacks an alternate 5' exon compared to variant 1; variant 3 (NR_033320.2) uses an alternate splice site in the 5' end of the transcript compared to variant 1; variant 4 (NR_033321.2) uses an alternate splice site and lacks an alternate 5' exon compared to variant 1; browser view from RefSeq on the GRCh38.p13 primary assembly [Integrative Genomics Viewer (IGV)] (b).

1.5.2. *MIAT* in Diseases

MIAT was first discovered as a myocardial infraction associated lncRNA, inherent to the name (Ishii *et al.*, 2006). In this context, *MIAT* is indeed associated with a number of heart conditions, including myocardial infarction (MI) and coronary artery disease (CAD) and some SNPs have been linked to susceptibility for these disorders (Ishii *et al.*, 2006; Boon *et al.*, 2016; Liao *et al.*, 2016). In line with this, vasculature-related disorders have been linked with SNPs or increased expression of *MIAT* (Zhong *et al.*, 2018; Fakhr-Eldeen *et al.*, 2019; Hao *et al.*, 2019). Furthermore, *MIAT* is involved in the regulation of endothelial cell function (Boon *et al.*, 2016), as well as in the interplay of blood vessels and nerves, through VEGF regulation, especially under hypoxic conditions (Jiang *et al.*, 2016). *MIAT* is also involved in eye diseases, such as diabetic retinopathies and cataract (Jiang *et al.*, 2016; Shen *et al.*, 2016). *MIAT* is also responsible for pluripotency feedback loops maintenance and specific lineage commitment (neuronal and retinal) (Sheik Mohamed *et al.*, 2010; Liao *et al.*, 2016). Given its importance in the brain physiology, as well as its massive enrichment in the brain, it is a natural consequence that level fluctuations are related to CNS disorders, and in particular, brain disorders. Importantly, in these cases and in contrast to the rest of the disorders, the problem occurs due to the reduced expression of *MIAT* or, alternatively, due to the existence of specific SNPs, as in the cases of AD (Jiang *et al.*, 2016) and paranoid SZ and anxiety (Fenoglio *et al.*, 2013; Barry *et al.*, 2014; Liao *et al.*, 2016) (Table 1.6).

1.5.3. *MIAT* in Cancer

Finally, as expected, *MIAT* has been implicated in a diversity of cancers. Notably, as far as brain/CNS-related tumours are concerned, *MIAT* has been elucidated to be the most abundant lincRNA in NB, as well as a modulator of both *MYCN* and *PHOX2B* (Rombaut *et al.*, 2019). Moreover, several lines of evidence have already implicated *MIAT* in NB and glioma pathogenesis and progression (Zhang *et al.*, 2013; Mei-Yee Kiang *et al.*, 2015;

Bountali *et al.*, 2019). Interestingly, high *MIAT* expression has been associated with prolonged survival in GBM patients (Zhang *et al.*, 2013), while in other tumours *MIAT* is predominantly found to be upregulated and confer poorer outcome. So far, *MIAT* has been implicated in the genesis and progression of a plethora of malignancies, including CLL (chronic lymphocytic leukaemia), DLBL (diffuse large B-cell lymphoma) (Sattari *et al.*, 2016), breast cancer (Almnaseer and Mourtada-Maarabouni, 2018; Li *et al.*, 2018; Zhang *et al.*, 2019; Liu *et al.*, 2019), gastric cancer (Zhang *et al.*, 2013; Pop *et al.*, 2018), clear cell renal cell carcinoma (Qu *et al.*, 2018; Zhang *et al.*, 2019), osteosarcoma (Zhang *et al.*, 2019), lung cancer (Fu et al., 2018; Zhang et al., 2019), neuroendocrine prostate cancer (Crea et al., 2016), and papillary thyroid cancer (Liu et al., 2019) (Table 1.6). Importantly, in numerous cancer types, *MIAT* exerts its oncogenic activity by acting as a miRNA sponge, to either promote oncogenic pathways or inhibit tumour suppressive ones in a diversity of cancer-related processes. Such examples include lung cancer, where gefitinib resistance is achieved through epigenetic regulation of miR-34a by *MIAT* (Fu *et al.*, 2018), and invasion is also regulated by *MIAT* via regulating miR-150 in the ZEB1 pathway (Zhang *et al.*, 2017). Other pairs include *MIAT* with miR-155-5p in breast cancer progression (Luan *et al.*, 2017), *MIAT* and miR-214 in hepatocellular carcinoma (Huang *et al.*, 2018), *MIAT* and miR-29c in clear cell renal carcinoma (Qu *et al.*, 2018), *MIAT* and miR-141 in gastric cancer (Sha *et al.*, 2018) and many more. Nevertheless, further research is required to fully shed light to the actual acting mechanisms of *MIAT* in various cancer types and to validate its predictive and/or prognostic value.

Table 1.6. Diseases associated with aberrations of *MIAT*.

Disease		Expression/ Aberration	Reference(s)
Heart & Vasculature conditions	**Myocardial Infarction**	rs2301523 SNP	(Ishii *et al.*, 2006; Liao *et al.*, 2016)
	Coronary Artery Disease	rs2301523 SNP	(Ishii *et al.*, 2006; Liao *et al.*, 2016)
	Diabetic cardiomyopathy	rs2301523 SNP	(Zhou *et al.*, 2017; Hao *et al.*, 2019)
	β- thalassaemia	↑	(Fakhr-Eldeen, Toraih and Fawzy, 2019)
	Microvascular Dysfunction	↑	(Yan *et al.*, 2015; Liao *et al.*, 2016; Zhong *et al.*, 2018)
	Ischemic Stroke	↑	(Hao *et al.*, 2019)
	Atherosclerosis	↑	(Yan *et al.*, 2015; Zhong *et al.*, 2018)
CNS Disorders	***Alzheimer's Disease***	↓	(Fenoglio *et al.*, 2013; Liao *et al.*, 2016; Jiang *et al.*, 2016)
	Paranoid Schizophrenia & Anxiety	↓ / rs1894720 SNP	(Barry *et al.*, 2014; Rao *et al.*, 2014; Liao *et al.*, 2016; Zhong *et al.*, 2018)
Eye Disorders	**Cataract**	↑	(Shen *et al.*, 2016)
	Diabetic Retinopathy	↑	(Liao *et al.*, 2016; Jiang *et al.*, 2016; Fu *et al.*, 2018; Zhong *et al.*, 2018)
Other Disorders	***Age-related Hearing Loss***	rs1894720 SNP	(Hao *et al.*, 2019)
	Chronic Chagas Disease	↑	(Hao *et al.*, 2019)
Cancer	***Chronic Lymphocytic Leukaemia***	↑	(Sattari *et al.*, 2016; Hao *et al.*, 2019)
	B-cell acute lymphocytic leukaemia	↓	(Sattari *et al.*, 2016)
	Diffuse large B-cell lymphoma	↑	(Sattari *et al.*, 2016)
	Clear cell renal cell carcinoma	↑	(Qu *et al.*, 2018; Zhang *et al.*, 2019)
	Osteosarcoma	↑	(Zhang *et al.*, 2019)
	Breast cancer	↑	(Almnaseer and Mourtada-Maarabouni, 2018; Zhang *et al.*, 2019; Liu *et al.*, 2019)
	Lung cancer	↑	(Fu *et al.*, 2018; C. Zhang *et al.*, 2019)
	Neuroendocrine prostate cancer	↑	(Crea *et al.*, 2016)
	Papillary thyroid cancer	↑	(Wei Liu, Wang, *et al.*, 2019)
	Gastric cancer		(Li *et al.*, 2017; Sha *et al.*, 2018)
	GBM	↕	(Zhang *et al.*, 2013; Pop *et al.*, 2018)

1.6. Aims and Objectives

There is accumulating evidence that the adoption of lncRNAs as biomarkers for diagnosis, prediction and prognosis, as well as their use as therapeutic targets, is a promising alternative towards better patient stratification and more efficient treatment of many kinds of cancer (Gutschner and Diederichs, 2012). Given that lncRNA expression has been found to be enriched in the CNS in a spatiotemporal manner (Mercer *et al.*, 2008; Qureshi *et al.*, 2010; Clark and Blackshaw, 2014) and that a growing list of ncRNAs has been proved to be associated with neuroblastoma and glioma, especially GBM (Mei-Yee Kiang *et al.*, 2015; Pandey and Kanduri, 2015; Pop *et al.*, 2018), the discovery of new, potent and reliable target lncRNAs is of paramount importance.

To this end, the current study investigates the role of lncRNAs in glioma and neuroblastoma. The ultimate aims of the study are to unveil the underpinning role of *MIAT* in the regulation of glioma and neuroblastoma cell fate decision and identify novel lncRNAs with a potential role in the control of this process.

Chapter 2: Materials & Methods

2.1. Cell culture and passaging

Three cell lines were used to perform the studies reported herein: the human neuroblastoma SH-SY5Y cell line, purchased from the ATCC (ATCC® CRL-2266™), the human astrocytoma/GBM 1321N1 cell line and the human GBM T98G cell line, kindly donated by Dr N. Leslie, Heriot-Watt University. SH-SY5Y and 1321N1 were cultured using the HyClone™ DMEM/F12 1:1 growth media (GE Healthcare Life Sciences, Catalogue # SH30126.01,), supplemented with 10% heat-inactivated fetal bovine serum (Biosera, Catalogue # FB-1001S/500), 2μM L-Glutamine (Gibco, Catalogue # 25030081), 1μM Sodium Pyruvate (Sigma-Aldrich, Catalogue # S8636) and 10mg/ml gentamicin solution (Sigma-Aldrich, Catalogue # G1272). For T98G the same recipe was used, supplemented with an extra 10% FBS, 15% cell-conditioned growth media and 1% MEM non-essential amino acid solution (Sigma-Aldrich, Catalogue # 7145). All cells were incubated in a humidified incubator at 37°C and 5% CO_2 and upon reaching ~80% confluence, were washed twice with phosphate buffered saline (PBS), and harvested by trypsinisation. The trypsinisation occurred by adding 3ml of 0.25% Trypsin/EDTA solution (Sigma-Aldrich, Catalogue # T4049), followed by returning the flask to the incubator for 3 minutes to facilitate cell detachment from the plastic. An equal volume of media (3ml) was added to the flask to inactivate the trypsin and the content of the flask was transferred to a 15 ml centrifuge tube, was centrifuged (1500 rpm, 7 minutes), and finally, the cell pellet was resuspended in the appropriate volume of growth media to acquire an $8x10^4$ cells/ml cell density for SH-SY5Y, a $15x10^4$ cells/ml cell density for 1321N1 and T98G. Cell lines were replaced with fresh stocks after a maximum culture period of 2 months.

2.2. Cell freezing and recovery

Cells were occasionally stored at -140°C in liquid nitrogen for long term use. They were resuspended in 1ml of a special cryoprotectant media composed of 80% growth media, 9% FBS and 11% DMSO (dimethyl sulphoxide) (Sigma-Aldrich, Catalogue # D2650), left at -

80°C overnight and subsequently transferred to the liquid nitrogen. For their recovery, the cells were thawed in a 37°C water bath, resuspended in 5ml of fresh complete growth media, centrifuged at 1500 rpm for 7 minutes and finally resuspended in the appropriate volume of growth media and placed in a humidified incubator (37°C, 5% CO_2).

2.3. LncRNA knockdown

2.3.1. Transfection efficiency

The efficiency of nucleofection was determined using the Silencer™ siRNA Labeling Kit with Cy™3 dye (Ambion, Catalogue #1632). The dye was prepared according to the manufacturer's instructions. 18.3µl RNase free water, 5µl 10x labelling buffer, 19.2µl –ve siRNA (20µM) and 7.5µl Cy3 reagent were first added into a 1.5ml Eppendorf tube. The mix was covered with aluminium foil and was incubated on a heat block at 37°C for 1h, after which aliquots were stored in -80°C for long-term use or -20°C for short-term use. The cells were transfected with 20µM Cy3-labelled siRNA (4µl for nucleofection), were incubated in 6-well plates and were finally harvested after 48/72 h. Cell viability (~80% for SH-SY5Y, ~90% for 1321N1 and ~95% for T98G) was assessed using the MUSE® Cell Analyzer (Millipore) and transfection efficiency was determined using the EVOS FL Cell Imaging System (Life Technologies). Cells were first observed and counted under transmitted light, followed by fluorescent microscopy and scoring of the transfected (red) cells using overlay images. Transfections of at least 50% of positive cells were considered successful. The transfection efficiency of nucleofection was 61-86% for SH-SY5Y cells, 88-94% for nucleofection-transfected 1321N1 cells, and 89-97% for T98G cells (Figure 2.1).

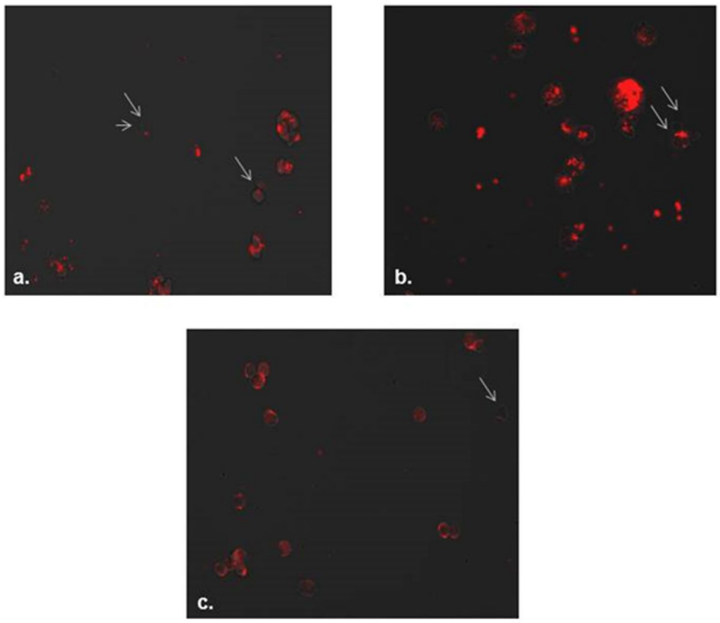

Figure 2.1. A representative image of nucleofection efficiency for all cell lines. Cells were transfected with 20μM Cy3-labelled siRNA (4μl for nucleofection) and were incubated for 48/72 h. The transfection efficiency was 61-86% for nucleofection of SH-SY5Y cells (a), 88-94% for nucleofection for 1321N1 cells (b) and 89-97% for T98G cells (c). Grey arrows indicate non-transfected cells. All images are overlays of equivalent light and fluorescent images, taken using the EVOS fluorescent microscope.

2.3.2. RNA interference

The experiments were performed using nucleofection as a method of transfection. The siRNAs used included the Silencer® Negative control siRNA (Ambion, Catalogue #4611) and three different *MIAT*-specific siRNAs: MIAT_1 siRNA, MIAT_2 siRNA and MIAT_3 siRNA (QIAGEN) targeting different sites of the fifth exon of the full-length MIAT transcript [NR_003491 (10193 bp)] at a final concentration of 500nM (Table 2.1 and Figure 2.2). The Amaxa™ Cell Line Nucleofector™ Kit V (LONZA) and the program A-023 were used for the SH-SY5Y cell line, and the Ingenio® kit (Mirus) and the programmes T-016 and X-001 were used for the 1321N1and T98G cell lines, respectively. $1.5x10^6$ (SH-SY5Y) and $1.2\ x10^6$ (1321N1 and T98G) cells were transfected according to the manufacturer's protocol, and

were incubated for 48 h and re-plated at $1x10^5$ and $0.5\ x10^5$ cells/ml (SH-SY5Y, and 1321N1/T98G, respectively) for subsequent assessment of cell survival, apoptosis and migration.

Table 2.1. The details of *MIAT*-specific siRNAs.

Cat #/ ID	Name/ Symbol	Target	Location	Sequence (5'→3')
AM4611	-ve	N/A		N/A
SI04287423	MIAT_1	*MIAT*	7284-7304	GGUCUAACAUUCCUCGUUATT
SI04314919	MIAT_2	*MIAT*	6488-6508	GCGGGUCUUUCCUACGCUATT
SI04344158	MIAT_3	*MIAT*	5109-5129	UGGUGUGAUUAACCUACUATT

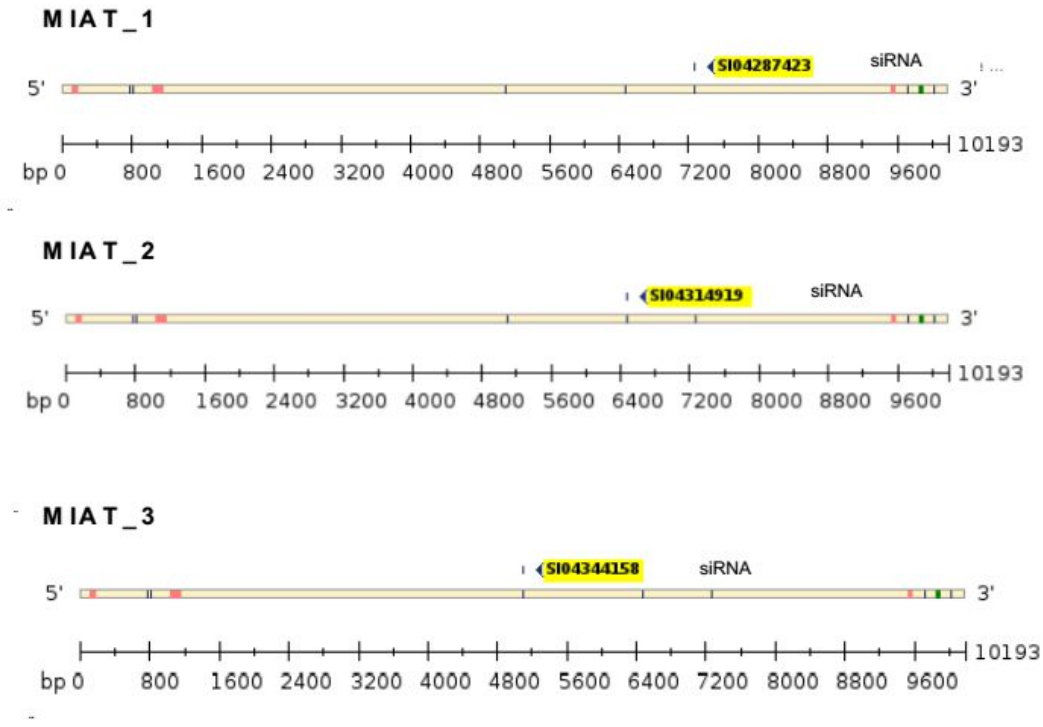

Figure 2.2. Schematic representation of the targeting sites of the MIAT-specific siRNAs. The targeting site of MIAT_1 is represented on the top, the equivalent of MIAT_2 in the middle, while the bottom schema represents the targeting site of MIAT_3.

2.3.3. LNA GapmeR –mediated knockdown

In addition to siRNAs, LNA GapmeRs (Locked Nucleic Acid GapmeRs) were used in a series of experiments to knockdown *MIAT*, *LINC00176* and *LOC648987*. Antisense LNA GapmeRs are highly potent, single-stranded antisense oligonucleotides (ASOs) for silencing of lncRNAs in cell cultures. These single-stranded, antisense oligonucleotides (ASOs) catalyse RNase H-dependent degradation of complementary RNA targets. They are 16 nucleotides long and are enriched with LNA (locked nucleic acid) in the flanking regions and DNA in a LNA-free central gap. The LNA-containing flanking regions increase target binding affinity, while also conferring nuclease resistance to the antisense oligo. When the GapmeR is hybridised to its target RNA, the central DNA gap activates RNase H cleavage of the opposing RNA strand. LNA GapmeRs have fully modified phosphorothioate (PS) backbones, which ensure exceptional resistance to enzymatic degradation (Grünweller *et al.*, 2003; Lundin *et al.*, 2013).

The GapmeRs that were used included the Negative control A Antisense LNA GapmeR (QIAGEN), three custom-designed GapmeRs (namely 1_1, 2_1, 2_2) targeting different sites of the fifth exon of the full length *MIAT* transcript [NR_003491 (10193 bp)], three custom-designed GapmeRs targeting different sites of the full length *LINC00176* (NC_000020.11) (namely LINC_1-targeting intron 4, LINC_2- targeting exon 3, LINC_3-targeting exon 3) and three custom-designed GapmeRs targeting different sites of the full length *LOC648987* (NC_000005.10) (namely LOC_1- targeting exon 3, LOC_2-targeting intron 4, LOC_3-targeting intron 5) (QIAGEN) (Table 2.2). The Amaxa™ Cell Line Nucleofector™ Kit V (LONZA) and the program A-023 were used for the SH-SY5Y cell line, and the Ingenio® kit (Mirus) and the programmes T-016 and X-001 were used for the 1321N1and T98G cell lines, respectively. $1.5x10^6$ (SH-SY5Y) and $1.2\ x10^6$ (1321N1 and T98G) cells were transfected according to the manufacturer's protocol, and were incubated for 48 h and re-plated at $1x10^5$ and $0.5\ x10^5$ cells/ml (SH-SY5Y, and 1321N1/T98G, respectively) for subsequent assessment of cell survival, apoptosis and migration. In this

case, the final concentration of the GapmeRs was 100nM for *MIAT* knockdown and 200nM for *LINC00176* and *LOC648987*.

Table 2.2. LNA GapmeR details.

Cat #/ ID	Name/ Symbol	Target	Location	Sequence (5'→3')
LG00000002	-ve	N/A	N/A	N/A
LG00188240	1_1	*MIAT*	5734-5749	ACGGGTTAGTAATCGA
LG00188250	2_1	*MIAT*	10165-10180	CAGCGTGAATTGATTT
LG00188251	2_2	*MIAT*	8275-8290	TACAATTGGTTAGCTC
LG00200609	LINC_1	*LINC00176*	4007-4022	GGATAAATCAGGAGAC
LG00200610	LINC_2	*LINC00176*	2254-2269	GGTCTTGGATTAACTT
LG00200611	LINC_3	*LINC00176*	1582-1597	TGTGATTAAATGCTGT
LG00200628	LOC_1	*LOC648987*	3411-3426	GAGAACCTCCGGAATA
LG00200629	LOC_2	*LOC648987*	28122-28137	AGCGACGCGAAACAAG
LG00200630	LOC_3	*LOC648987*	52101-52116	GCATTGGAGTGGTAGT

2.4. RNA extraction

Total RNA was extracted from cells using the Direct-zol™ RNA MiniPrep kit (ZYMO RESEARCH, Cat # R2050), according to the manufacturer's protocol. Spin column-based nucleic acid purification is a solid phase extraction method to quickly purify nucleic acids. This method relies on the fact that nucleic acid will bind to the solid phase of silica under certain conditions.

Cells were treated with TRIsure (BIOLINE, Catalogue # BIO-38032), left at room temperature for 5 minutes. TRIsure is a monophasic solution of phenol and guanidinium isothiocyanate that simultaneously solubilizes DNA and RNA and denatures proteins. Then an equal volume of 100% ethanol was added to facilitate RNA precipitation. The mixture was then transferred into a Zymo-Spin™ IIC Column in a Collection Tube and was centrifuged for 1 minute at 13000 RCF. Afterwards, the column was transferred into a new Collection Tube and the Collection Tube containing the flow-through was discarded. RNA samples were then in-column DNase treated for genomic DNA residues to be eliminated by

being washed with 400μl RNA Wash Buffer, followed by the addition of 80μl of a DNase 1 cocktail and incubation for 15 minutes at room temperature. Then, after being centrifuged (1 minute, 13000 RCF), 400μl Direct-zol™ RNA PreWash (binding solution) were added to the column followed by a centrifugation step (1 minute, 13000 RCF). The centrifuge forces the binding solution through a silica gel membrane that is inside the spin column so that the nucleic acids bind to the silica-gel membrane as the solution passes through. This step was repeated twice and then 700μl RNA Wash Buffer were added to the column, followed by centrifugation for 1 minute at 13000 RCF. An extra 2-minute centrifugation was also performed to ensure that all flow-through was discarded. The columns were transferred carefully into an RNase-free tube and the RNA was eluted with 20 μl of DNase/RNase-Free Water by being centrifuged at 16000 RCF for 1 minute. Finally, RNA samples were kept in -80°C.

2.4.1. Gel electrophoresis

The assessment of the quality and the quantity of RNA samples was performed by spectrophotometric analysis (NanoDrop™ 1000, ThermoFisher Scientific) and gel electrophoresis. Samples with NanoDrop 260nm/280nm absorbance ratio 1.8-2 were considered of high quality. The RNA integrity was also evaluated with gel electrophoresis via the examination of the 28S and 18S ribosomal RNA bands. In intact RNA samples, the upper ribosomal band (28S in eukaryotic cells) should be about twice the intensity of the lower band (18S in eukaryotic cells). The gel electrophoresis was performed using a standardised 1% agarose gel [1%w/v agarose in 1X TAE (Tris-acetate-EDTA) buffer] and Ethidium Bromide (EtBr) (Sigma-Aldrich) as a fluorescent tag (4μl EtBr/ 50ml TAE). The mix was prepared, microwaved for 2 minutes, left to cool down and afterwards, 5μl of EtBr were added. The mix was poured into a casting tray and left to solidify for 30 minutes. 1μg of total RNA was prepared in RNase-free water for each RNA sample, 2μl loading buffer were added (final volume= 7μl) and the samples were loaded to the gel. A Hyperladder marker

was used for the relative quantification of the samples (HyperLadder I, BIOLINE, Catalogue # BIO-33053). The samples were run at 100 Volt for 30 minutes and were finally photographed under UV light (White/UV)

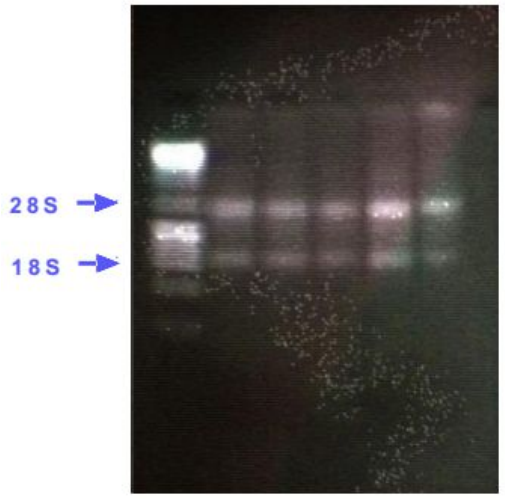

Figure 2.3. A representative image of RNA analysis by agarose gel electrophoresis. The figure shows a representative example of samples derived from SH-SY5Y cells, transfected with different siRNAs, together with their controls. A 2:1 intensity ratio between 28S and 18S rRNA, which is a feature of intact RNA, is observed for all the samples. The image was taken using a white/UV Transilluminator ImageStore 7500.

2.5. Real-time PCR (RT-qPCR)

2.5.1. Reverse transcription

RNA extracted from transfected cells was reverse transcribed into cDNA using the Omniscript® RT kit (QIAGEN, Catalogue # 205111), 10 μM random primers (Invitrogen, Catalogue # 48190-011) and 10 units/μl RNaseOUT recombinant ribonuclease inhibitor (Invitrogen, Catalogue # 10777019), following the manufacturer's instructions. The reverse transcription master mix was added to the samples as shown in Table 2.3, which were treated according to the manufacturer's manual in a TECHNE Prime thermal cycler (TECHNE) (Table 2.4).

Table 2.3. The reverse transcription mix.

Component	Volume/reaction
10x buffer RT	2 µl
dNTPmix (5mM each dNTP)	2 µl
Random primers (10µM)	2 µl
RNase inhibitor (RNAseOUT) (10units/µl)	1 µl
Omniscript Reverse Transcriptase	1 µl
RNase-free water	Variable
Template RNA (2µg)	Variable
Total Reaction Volume	**20µl**

Table 2.4. Cycling conditions for reverse transcription.

Method	Number of cycles	Duration	Temperature (°C)
Reverse transcription	1	5’	95
	1	60’	37

2.5.2. Real-time PCR

Real-time PCR was subsequently performed for the synthesized cDNA, using TaqMan probes SensiFAST™ Probe Hi-ROX mix (Bioline, Catalogue # BIO-82020) and gene-specific TaqMan Gene Expression Assays (Table 2.5). The housekeeping gene 18S rRNA was used as an endogenous control for normalisation (Hs99999901_s1 and eukaryotic 18S rRNA endogenous control-VIC™/MGB probe, Applied Biosystems, Catalogue # 4319413E), according to the manufacturer’s instructions. Each PCR reaction contained 12.5µl of SensiFAST™, 7.25µl of Nuclease-free H_2O, 1.25µl of gene-specific assay and 4µl of newly synthesized cDNA, to a total volume of 25µl and the cycling conditions are

described in Table 2.6. The ABI Prism 7000 (Applied Biosystems) was used for the measurement of real-time fluorescence and the ABI Prism 7000 SDS software was used to perform the data analysis. Expression comparisons were made relative to the negative (-ve) siRNA transfected cells, using the $2^{-\Delta\Delta Ct}$ method.

Table 2.5. TaqMan® gene expression assays' details.

Method	Catalogue #/ ID	Target	Exon boundary	Assay location
TaqMan®	Hs99999901_s1	*18S*	1-1	604
	4319413E	*18S*	1-1	604
	Hs00402814_m1	*MIAT*	5	1864
	Hs00153408_m1	*c-Myc*	2-3	1325
	Hs01552829_m1	*Oct1 (POU2F1)*	8-9	1013
	Hs00988121_s1	*LINC00176*	1-1	378
	Hs00987326_s1	*LOC648987*	1-1	2304

Table 2.6. Cycling conditions for RT-qPCR.

Method	Number of cycles	Duration	Temperature (°C)
RT-qPCR & RT² Profiler PCR Arrays	1	10'	95
	40	15" 1'	95 60

2.5.3. RT² Profiler PCR Arrays

RT² Profiler PCR Arrays provide a reliable way to analyse simultaneously the expression levels of a panel of genes involved in a specific molecular pathway using 96-well plates (QIAGEN). For these experiments, the samples used had already been measured for *MIAT* expression by RT-qPCR after siRNA-mediated knockdown, and the expression of *MIAT* had been confirmed to be silenced by ~90%. Two different Arrays were used: the RT² Profiler™ PCR Array Human Cell Death PathwayFinder (QIAGEN, Catalogue # PAHS-212Z) and the RT² Profiler™ PCR Array Human Apoptosis (QIAGEN, Catalogue # PAHS-

012Z), each one containing in total 84 genes (one/well) and 12 quality and endogenous controls. The Human Cell Death PathwayFinder includes genes associated both with apoptosis (e.g. *Casp2, BCL-2, Apaf1*), necrosis (e.g. *Kcnip1, Tnfrsf1a/11b*) and autophagy (e.g. *Atg3/12, Ulk1*), while the Human Apoptosis one assesses exclusively the expression of apoptosis-related genes, such as *XIAP, Mcl1, Bid* and *Fas*. The experiments were performed following the manufacturer's protocol using the RT^2 First Strand Kit (QIAGEN, Catalogue # 330401) and RT² SYBR Green ROX qPCR Mastermix (QIAGEN, Catalogue # 330520). The genomic DNA elimination mix was prepared, containing the RNA (0.5μg in 8μl RNase-free water) and buffer GE (2μl), and after an incubation of 5 minutes at 42°C and 1 minute on ice, the freshly-made reverse transcription mix was added to the samples (containing 4μl buffer BC3, 1μl control P2, 2μl RE3 reverse transcriptase mix and 3μl RNase-free water per reaction). Then 25μl of the PCR mix (1350μl RT² SYBR Green Mastermix, 102μl cDNA synthesis reaction mix, 1248μl RNase-free water per plate) was added to each one of the wells containing a dried assay. The plates were sealed tightly with 8-cap strips and were placed in an ABI Prism 7000 cycler and were run using the cycling steps described in Table 2.6. The RT^2 Profiler PCR Array analysis was performed using QIAGEN's Data Analysis web portal (geneglobe.qiagen.com/gb/analyze/).

2.6. Assessment of cell survival

2.6.1. Vital dye (trypan blue) exclusion assay

At specific time intervals after transfection (48/72 h), cell survival was assessed by at least two independent methods. First, both cell count and viability were determined using trypan blue solution 0.4% (Sigma-Aldrich, Catalogue # T8154) vital dye staining. The use of trypan blue is based on a straightforward principle: trypan blue is a cell membrane non-permeable azo dye and will only penetrate cells with compromised cell membrane, i.e. dead cells. Therefore, live cells with intact cell membranes remain transparent on the haemocytometer, while dead cells are stained blue.

2.6.2. MUSE® Cell Analyzer Flow Cytometry

Viable and total cell count, as well as the percentage of viability, were acquired by flow cytometry using the MUSE® Cell Analyzer (Millipore) and the MUSE® Count and Viability Kit (Millipore, Catalogue # MCH100102). The Muse® Cell Analyzer uses miniaturised fluorescence detection and microcapillary cytometry to deliver highly quantitative single-cell analysis. This laser-based fluorescence detection of each cell event can evaluate up to three cellular parameters (cell size and two colours). Both viable and non-viable cells are differentially stained based on their permeability to the DNA-binding dyes in the reagent. One of the dyes is membrane-permeant and stains the DNA in all viable nucleated cells. This parameter is used to discriminate nucleated cells from debris and non-nucleated cells. The Muse™ System counts the stained nucleated events and uses the cellular size properties to distinguish cellular debris from cells to ultimately determine a precise total cell count. The other dye specifically stains the nucleus of dead and dying cells that have lost their membrane integrity. This parameter is used to distinguish between live cells (which do not take up the dye) stained non-viable or dying cells (displayed on the Muse™ system as "VIABILITY") (Figure 2.4).

The experiments were performed according to adapted manufacturer's instructions: trypsinised cells were diluted with the reagent (50µl of cell suspension:150µl of Muse Count and Viability Reagent). Cells were allowed to stain for 5 minutes at room temperature and were counted. Gates were set according to the manufacturer's instructions and following optimisation experiments. The results were analysed using the MUSE 1.5 Analysis software (Millipore).

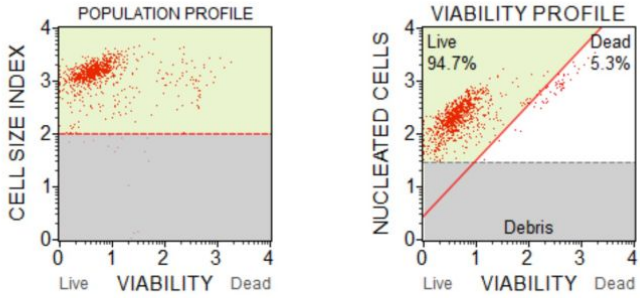

Viable Cells / mL :	8.31E+05
Viability % :	94.70 %
Total Cells / mL :	8.77E+05
Total Viable Cells in Original Sample :	8.31E+05
Total Cells in Original Sample :	8.77E+05
Dilution Factor :	4.00
Original Volume :	1.00 mL
Events Acquired :	1015

Figure 2.4. Representative image of the output of the Muse® Cell Analyzer displaying the results of the number of viable cells and viability. T98G parental cells were stained using the Muse Count and Viability Reagent and these results were obtained after completion of acquisition using the Muse™ Cell Count and Viability Software, which automatically performs calculations and displays data in two dot plots: the population profile distinguishing cells from debris (left panel) and the viability profile distinguishing alive from dead cells (right panel).

2.6.3. MTS assay

The evaluation of the effect of the drug used in this study, Metformin (Metformin hydrochloride, Sigma-Aldrich, Catalogue # PHR 1084) on SH-SY5Y viability, i.e. its cytotoxicity, as well as of the effect of the down-regulation of lncRNAs was performed by the MTS assay, using the CellTiter 96® Aqueous One Solution Cell Proliferation Assay (PROMEGA, Catalogue # G3580), which contains a tetrazolium compound [3-(4,5-dimethylthiazol-2-yl)-5-(3-carboxymethoxyphenyl)-2-(4-sulfophenyl)-2H-tetrazolium, inner salt; MTS] and an electron coupling reagent (phenazine ethosulfate; PES). PES has enhanced chemical stability, which allows it to be combined with MTS to form a stable solution. The MTS tetrazolium compound (Owen's reagent) is bioreduced by cells into a coloured formazan product that is soluble in tissue culture media. This conversion is

presumably accomplished by NADPH or NADH produced by dehydrogenase enzymes in metabolically active cells. The quantity of formazan product as measured by the amount of 490nm absorbance is directly proportional to the number of living cells in culture. For all MTS experiments, on the day of the measurement, 20µl of the CellTiter 96® Aqueous One Solution Cell Proliferation Assay was added, followed by a 3h incubation at 37°C and finally, measurements were taken at 490 nm using the Infinite M200 PRO plate reader (Tecan Life Sciences).

To acquire optimal results, an initial number of cells per well that produces an assay signal near the low end of the linear range of the assay must be chosen. To this end, a series of optimisation experiments were performed and revealed that among the different seeding cell densities tested (0.6/0.8/1/1.2/1.4 $x10^5$ cells/ml), the most appropriate cell density was $1x10^5$ cells/ml for SH-SY5Y and $0.8x10^5$ for 1321N1 and T98G cells. Another set of experiments tested the concentration of the drug (metformin) needed to acquire optimal cytotoxicity levels (10/ 20/ 50/ 100/ 200/ 500/ 1000µM and 2-50 mM) at 48/72 h after metformin was added to the culture. The growth inhibitory effect of metformin was calculated according to the following equation: **% inhibition of cell growth = 100- [OD490 of treated sample / OD490 of untreated sample (control)] x 100**

For the metformin cytotoxicity experiments, cells were seeded in 96-well plates (100µl/well), incubated for 24h and subsequently, treatment was added (drug diluted in growth media-100µl/well) and cells were incubated for 48 h/72 h.

For the lncRNA knockdown experiments, cells were nucleofected, re-plated at the densities mentioned above after 48 h, and then incubated for the desired time interval (48/72 h). For the experiments testing whether *LINC00176* and *LOC648987* down-regulation sensitises SH-SY5Y cells to metformin cells were treated with 20mM metformin at 24h after re-plating and were then incubated for an extra 48/72 h.

2.7. Assessment of apoptosis-mediated cell death

2.7.1 Flow cytometry

Flow cytometry comprises one of the most reliable and widely used methods to assess cell death, especially when it is apoptosis-mediated. The sample is placed on the flow cytometer and the fluidics system (the tubing, pumps, and valves) organises the initial sample suspension into a single-file stream of cells as they make their journey through the flow cytometer for analysis. The cells interact with laser light at a point called the interrogation point (laser intercept). When the laser light beam illuminates a single cell, some of the light will strike physical structures within the cell, causing the light to scatter. This light scatter can be measured and correlated with relative cell size and structures inside the cell. These measurements are termed forward angle scatter (FSC) and side angle scatter (SSC), depending on where the light is collected with regards to the path of the laser. Simultaneously, light from the laser will excite all fluorophores associated with the cell, which produces a fluorescence emission. All of this light is collected by the detector and processed through the electronics component of the flow cytometer (Adan *et al.*, 2017).

With regards to assessing cell death, a common means of flow cytometry is via the use of Annexin V. Annexin V (or Annexin A5) is a member of the annexin family of intracellular proteins that binds to phosphatidylserine (PS) in a calcium-dependent manner. PS is normally only found on the intracellular layer of the cell membrane in healthy cells, but during early apoptosis, membrane asymmetry is lost and as an indicative cellular feature, PS is flipped out to the external leaflet. Therefore, fluorochrome-labelled Annexin V can be used to specifically target and identify apoptotic cells. However, Annexin V binding alone cannot differentiate between apoptotic and necrotic cells. To this end, to distinguish between the necrotic and apoptotic cells, 7-amino-actinomycin D (7-AAD) is used. Early apoptotic cells will exclude 7-AAD, while late stage apoptotic cells will stain positively, due to the passage of these dyes into the nucleus where they bind to DNA. 7-AAD has a high DNA binding constant and as a result, is efficiently excluded by intact cells. When excited

by 488 laser light, 7-AAD fluorescence is detected in the far red range of the spectrum (650 nm long-pass filter) (Zimmermann and Meyer, 2011; Bundscherer *et al.*, 2013). The combination of these two components gives rise to 4 different populations, as described in Table 2.7 and Figure 2.4.

In this study, in order to evaluate the effect of the knockdown of the studied lncRNAs on the levels of cell death in neuroblastoma and glioblastoma cell lines, dual staining was performed using the FITC-Annexin V Apoptosis Detection Kit with 7-AAD (BioLegend, Catalogue # 640922), according to the manufacturer's instructions. The cells were nucleofected, re-plated after 48 h and assessed 48 h/72 h after re-plating. On the day of the assessment, cells were harvested, washed twice with cell staining buffer (BioLegend, Catalogue # 420201), and resuspended in 100µl of Annexin V Binding Buffer. Afterwards, 5µl of FITC Annexin V and 5µl of 7-AAD Viability Staining Solution were added to each sample, followed by a 15-minute incubation (room temperature, darkness) and finally 400µl of Annexin V Binding Buffer were added and samples were analysed with a 6-2L Guava® easyCyte Benchtop Flow Cytometer (Merck). The analysis was performed using the guavaSoft 3.3 software. The terms "apoptotic cells" and "apoptosis" throughout the current study refer to both early and late apoptotic cell populations.

Table 2.7. The different populations as appearing using the dual FITC-Annexin V and 7-AAD staining system. Annexin V distinguishes cells with externalised PS, an indicative sign of apoptosis, while 7-amino-actinomycin D (7-AAD) distinguishes cells with compromised membrane integrity, an indicator of cell death.

Population	FITC-Annexin V	7-AAD
Non-apoptotic	-ve	-ve
Early apoptotic	+ve	-ve
Late apoptotic/ necrotic	+ve	+ve
Dead/ cell debris	-ve	+ve

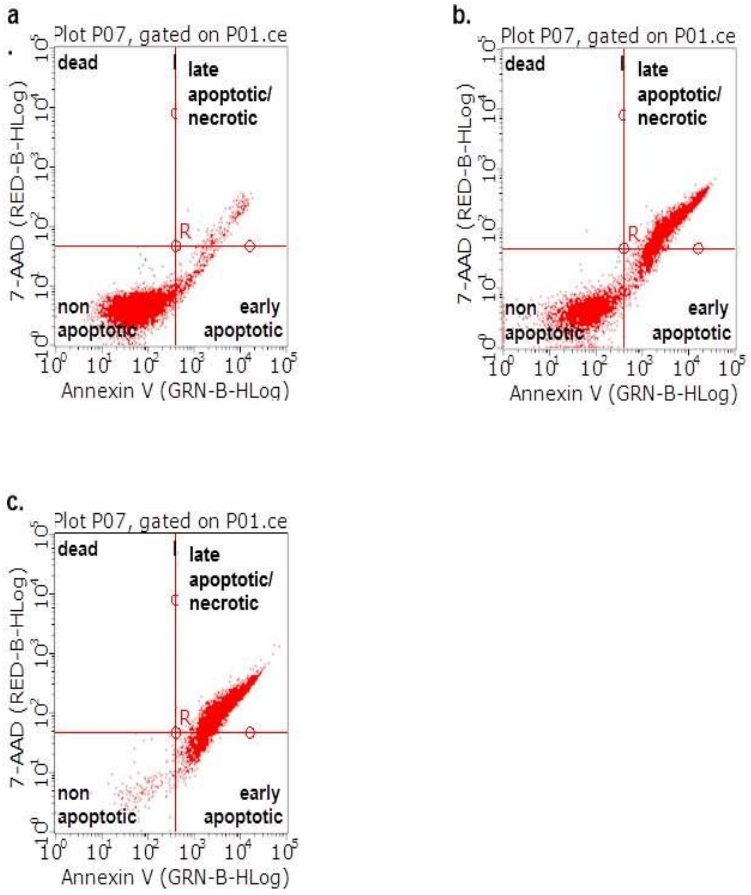

Figure 2.5. Representative image of the cell population distribution after dual FITC-Annexin V and 7-AAD staining. 1321N1 parental cells were stained using the FITC-Annexin V Apoptosis Detection Kit with 7-AAD (BioLegend), without any treatment (a), half population without any treatment and half after being heated at 60°C for 20 minutes (b) and after the whole population being heated at 60°C for 20 minutes (c).

2.7.2. Acridine orange

Acridine orange (AO) is a cell-permeable dye frequently used in fluorescent microscopy. It binds or intercalates to nucleic acids, both DNA and RNA, and due to its inherent physicochemical characteristics fluoresces green at 520 nm when bound to dsDNA, or red at 650nm when bound to ssDNA or RNA (Rijal, 2015). Therefore, it is a common means of assessing apoptosis-mediated cell death. In particular, AO fluoresces green in apoptotic cells displaying condensed chromatin and fragmented nuclei, two fundamental characteristics of cells undergoing apoptosis (Byvaltsev *et al.*, 2019). In this study, at

specific time intervals after transfection or re-plating (48 and 72 h) apoptosis was determined by the assessment of the nuclear morphology using fluorescence microscopy after staining with acridine orange (25µg/ml) (Sigma-Aldrich, Catalogue # 235474).

2.8. Assessment of long-term cell survival (Anchorage-dependent clonogenic assay)

The long term survival of the cells depends on their ability to form colonies. Therefore, siRNA or GapmeR transfected cells were re-plated 48/72 h post-transfection in 6-well plates at optimised densities and conditions after a series of optimisation experiments for all cell lines. For these experiments, parental cells were seeded at different densities (25/50/75/100/150/200/300/400/450/500/600/800 cells/ml), with different percentages of cell-conditioned media and were observed at different time points (2/3 weeks post-seeding). The optimal cell density was based on the ability of the cells to form single colonies (i.e. distinct colonies that do not merge) containing at least 50 cells (Franken *et al.*, 2006). The percentage of cell-conditioned media and incubation time needed were also based on the same criteria. The best seeding density for this assay was 500 cells/ml, 75 cells/ml and 100 cells/ml for SH-SY5Y, 1321N1 and T98G, respectively (Table 2.8). The colonies were stained with 1% w/v crystal violet (Sigma-Aldrich, Catalogue # C3886), air-dried and counted. Photos of the colonies were obtained using a GS-800 Calibrated Densitometer (Bio-rad).

Table 2.8. Colony forming assay optimal conditions for SH-SY5Y, 1321N1 and T98G cell lines.

Cell Line	Optimal cell density (cells/ml)	% Cell-conditioned growth media (15 vs 25)	Incubation time (2 vs 3 weeks)
SH-SY5Y	500	15	3
1321N1	75	15	2
T98G	100	25	2

2.9. Cell migration

The ability of cell migration was assessed by the wound healing assay. The wound healing assay is a standard *in vitro* technique for assessing collective cell migration in two dimensions. In this assay, a cell-free area is created in a confluent monolayer by physical exclusion or by removing the cells from the area through mechanical, thermal or chemical damage. Exposure to the cell-free area prompts the cells to migrate into the gap (Jonkman *et al.*, 2014). In this study, cells were re-plated in 12-well plates in triplicates at $2x10^5$ and $1x10^5$ cells/ml (SH-SY5Y, and 1321N1/T98G, respectively), were incubated until fully confluent (for 24 and 48 h for 1321N1/T98G and SH-SY5Y, respectively), and a small linear scratch was introduced to the cell monolayer using a 200µl pipette tip. The cells were then washed with PBS to ensure the removal of detached cells, and 3 ml of fresh media was added to the wells. The cells were observed under transmitted light using the EVOS FL Cell Imaging System (Life Technologies) and gap measurements were taken at 0/18/24h and 0/24/48 h for 1321N1/T98G and SH-SY5Y, respectively, and the gap closure was calculated using the formula **[(Pre-migration)area-(Migration)area/ (Pre-migration)area] x100** for 15 measurements per sample. Image analysis was performed using the ImageJ software.

2.10. RNA sequencing and Pathway analysis

Global gene expression changes in response to *MIAT* silencing and metformin treatment were determined by sequencing the whole transcriptome. This approach has key advantages over equivalent microarray analyses including identification and quantification of unknown transcripts and novel splice variants. Total RNA was extracted as detailed in section 2.4. Next-generation sequencing was conducted by the Earlham Institute (Norwich, UK); sequencing libraries were prepared using the NEXTflex directional RNA-Seq Library Kit, and following stringent quality control measures, sequenced to a depth of approximately 30 million reads per sample, 150bp PE read metric, on the HiSeq 4000 platform.

Raw sequencing data were trimmed of sequencing adapters and low quality reads using the Trimgalore package, a wrapper that incorporates CutAdapt and FastQC. Quality controlled reads were aligned to Human Genome build (hg19) using Tophat, a splice-junction aware mapping utility necessary for the successful mapping of any Intron-spanning (multi-exon) transcripts, transcripts were assembled using Cufflinks (with GTF support) and the number of reads mapping to each feature counted and expressed as FPKM using the CuffNorm package.

Differentially expressed mRNAs were condensed into gene networks representing biological and disease processes using iPathwayGuide (Advaita Bioinformatics, Ann Arbor, MI, USA), to elucidate key mechanisms responsible for mediating the phenotypic effects of gene knockdown. These data were analyzed in the context of pathways obtained from the Kyoto Encyclopedia of Genes and Genomes (KEGG) database, gene ontologies from the Gene Ontology Consortium database, miRNAs from the miRBase and TARGETSCAN databases, network of regulatory relations from BioGRID: Biological General Repository for Interaction Datasets v3.4.154., and diseases from the KEGG database. The RNA sequencing results were analysed using the iPathway Guide by Advaita Bioinformatics (advaitabio.com).

2.11. Assessment of Reactive Oxygen Species (ROS) production

2.11.1. Flow cytometry

The production of ROS as part of the apoptotic response upon the down-regulation of *MIAT* in 1321N1 and T98G cells was measured by flow cytometry using the CellROX® Green Reagent (Life Technologies, Catalogue # C10444). This cell-permeable reagent is non-fluorescent while in a reduced state, while they exhibit a strong fluorescent signal upon oxidation. For this series of experiments, 1321N1 cells and T98G cells (cultured in FBS-free growth media to avoid excessive autofluorescence), were nucleofected with either the

Negative control siRNA or MIAT_2 and subsequently, the levels of ROS production were assessed after 48 h and 72 h. The cells were harvested, the CellROX® Green Reagent was added to a final concentration of 2μM and the samples were incubated for 30 minutes at 37°C. The cells were then washed 3 times with PBS and were then analysed by the 6-2L Guava® easyCyte Benchtop Flow Cytometer (Merck). The analysis was performed using the guavaSoft 3.3 software.

2.11.2. Alpha-phenyl-N-tert-butyl nitrone (PBN) -mediated ROS scavenging

Due to the increased levels of autofluorescence observed when using the CellROX® Green Reagent in SH-SY5Y cells, an alternative strategy of ROS production evaluation was adopted. Alpha-phenyl-N-tert-butyl nitrone (PBN) is a widely used free radical scavenger with few side-effects when used in animal studies (Gao *et al.*, 2007; Munoz *et al.*, 2017). A series of optimisation experiments testing the scavenging capacity of different concentrations (500/600/700/800/900μM) of PBN and different administration methods (simultaneous administration versus sequential, with PBN being administrated first, before the addition of H_2O_2) against ROS produced upon *MIAT* knockdown, as well as against H_2O_2 30% w/w, a well-known ROS inducer, was carried out first. The most efficient scavenger proved to be the administration of 600μM PBN (diluted in 100% DMSO) in a sequential way. In particular, SH-SY5Y cells were nucleofected with either a Negative control siRNA or one of the *MIAT*- specific RNAs (MIAT_2 or MIAT_3) and re-plated at $1x10^5$ cells/ml. After 24h a DMSO vehicle was added to the control group of each sample, PBN alone in a second group, H_2O_2 alone in a third group and in a fourth group PBN was added first, followed by a 1-hour incubation and H_2O_2 was added at the end. Apoptosis was then assessed after 8, 24 or 48 h with acridine orange and cell viability was assessed after 48/72 h with MTS assay.

2.12. Western Blot

2.12.1. Cell lysis

In order for the total proteome to be extracted from cells, cell lysates were prepared. Cells were harvested, washed and cell numbers were adjusted to a total $6x10^5$ cells/ sample using a haemocytometer. The cells were then resuspended and lysed with 30µl RIPA (radioimmunoprecipitation assay) lysis and extraction buffer (25mM Tris-HCl pH 7.6, 150mM NaCl, 1% NP-40, 1% sodium deoxycholate, 0.1% SDS) (ThermoFisher Scientific, Catalogue # 89900) and were incubated on ice for 15 minutes. 1µl of protease inhibitor cocktail (Millipore, Catalogue # 535140) was added to eliminate the activity of proteases and protect the integrity of the proteins. The samples were then centrifuged for 10 minutes at 10000 rpm and the supernatant was transferred into a new tube. 20µl of Laemmli 2× Concentrate Buffer (Sigma-Aldrich, Catalogue # S3401) were added to 20µl of each sample and the mix was boiled at 90°C for 10 minutes on a Heat Block.

2.12.2. Western Blot preparation

The protein samples were loaded onto a 12% Mini-PROTEAN™ TGX® gel (Bio-rad, Catalogue # 456-1043) and run on a PowerPac™ HC (Bio-rad) machine for 45 minutes at 150V, 3A in running buffer [25mM Tris-Base (ICN Biomedicals, Catalogue # 819623), 190mM glycine (BDH, Catalogue # 444495D), 0.1% SDS (Sigma-Aldrich, Catalogue # L-5750) at pH= 8.3]. The gel was then removed from the running tank and placed into the transfer "sandwich", composed of the supporting grid, two sponge pads and two filter papers soaked in transfer buffer (one on each side of the grid) and the nitrocellulose membrane (GE Healthcare, Catalogue # 45-004-000). The wet transfer was performed for 1 hour and 30 minutes at 100V, 0.3A in a tank containing the transfer buffer (25mM Tris-Base (ICN Biomedicals, Catalogue # 819623), 190mM glycine (BDH, Catalogue # 444495D), 20% v/v Methanol at pH=8.3]. After the transfer, the blot was blocked for 1 hour in 5% w/v milk in TBS-T [20x TBS buffer (ThermoFisher Scientific, Catalogue # 28358) diluted to a

final volume of 1L, supplemented with 1% Tween], followed by three 5-minute washes in TBS. Subsequently, one of the primary mouse anti-human antibodies described in Table 2.9 was added to the blot and the blot was incubated overnight at 4°C on a roller, followed by three 5-minute washes in TBS. The secondary antibody (Polyclonal Goat Anti-Mouse Immunoglobulin-HRP, Dako, Catalogue # P0447) was then added (1:1000 dilution in 5% milk in TBS-T) and the blot was incubated for 1 hour at room temperature on a roller. Finally, the blot was washed 3 times for 5 minutes each and was developed using the ECL solution (Clarity™ Western ECL Substrate, Catalogue # 1705060) on a ChemiDoc™MP Imaging System (Bio-rad). When the stripping of the blot was essential, it was performed using the Restore™ PLUS Western Stripping Buffer (Bio-rad, Catalogue # 46430), according to the manufacturer's instructions. The blot was first washed three times for 5 minutes with TBS-T, was immersed in Restore™ PLUS Western Stripping Buffer for 10 minutes, washed again three times for 5 minutes with TBS-T, blocked for 30 minutes in 5% w/v milk in TBS-T, washed three times for 5 minutes with TBS-T and finally incubated overnight at 4°C on a roller in the desired primary antibody. The protein size was determined using the Precision Plus Protein™ Dual Color Standards protein ladder (Bio-rad, Catalogue # 161-0374) and image analysis was performed using the ImageJ software.

Table 2.9. Primary antibodies' details.

Target protein	Catalogue #/ ID	Clonality	Dilution
Mcl1	Transduction Laboratories, M54020	Mouse-monoclonal	1:1000
Caspase-8	Millipore, AM46	Mouse-monoclonal	1:500
XIAP	Santa Cruz, sc-55550	Mouse-monoclonal	1:500
BAD	Santa Cruz, sc-8044	Mouse-monoclonal	1:500
BID	Santa Cruz, sc-373939	Mouse-monoclonal	1:500
β- Actin	Sigma-Aldrich, A5441	Mouse-monoclonal	1:5000

2.13. Statistical analysis

Statistical analyses were performed using GraphPad Prism 6 (GraphPad Software). Data are presented as the mean ± SEM; the number of observations (n) refers to different transfected samples, each transfection being conducted on a separate culture of cells. Comparisons were made using an unpaired T-test or One-Way ANOVA with Bonferroni's multiple comparison test (MCT). Where multiple parameters were compared, Two-Way ANOVA with Sidak, Tukey or Dunnett multiple comparisons was used. Differences were considered as statistically significant when the *P-value* was <0.05 (95% confidence intervals).

Chapter 3: The role of *MIAT* in the cell fate determination of neuroblastoma and glioblastoma cells

3.1. Introduction

MIAT, also known as *Gomafu* and *RNCR2*, is a 10kb long nuclear lncRNA that is transcribed from chromosome 22q12.1 and is localised across the nucleoplasm in a spotted pattern (Blackshaw *et al.*, 2004; Sone *et al.*, 2007; Tsuiji *et al.*, 2011; Boon *et al.*, 2016; Cheng *et al.*, 2016). Several lines of evidence suggest that *MIAT* participates in pre-mRNA splicing through its binding to splicing factors (SF1, QK1, SRSF1 and Celf3) and that its deregulation generates abnormal splicing patterns (Ishizuka *et al.*, 2014; Cheng *et al.*, 2016; Sattari *et al.*, 2016). Apart from its physiological roles in a healthy setting, *MIAT* has been linked to various diseases and disorders (Ishii *et al.*, 2006; Fenoglio *et al.*, 2013; Boon *et al.*, 2016; Liao *et al.*, 2016), as well as various cancers.

Although *MIAT* has been implicated in the genesis and progression of a plethora of malignancies, including haematologic malignancies (Sattari *et al.*, 2016), breast cancer (Almnaseer and Mourtada-Maarabouni, 2018; Li *et al.*, 2018; Zhang *et al.*, 2019; Liu *et al.*, 2019), gastric cancer (Zhang *et al.*, 2013; Pop *et al.*, 2018), clear cell renal cell carcinoma (Qu *et al.*, 2018; Zhang *et al.*, 2019), osteosarcoma (Zhang *et al.*, 2019), lung cancer (Fu *et al.*, 2018; Zhang *et al.*, 2019), neuroendocrine prostate cancer (Crea *et al.*, 2016), papillary thyroid cancer (Liu *et al.,* 2019) and intrahepatic cholangiocarcinoma (Zhou *et al.*, 2019), its role in neuroblastoma has been largely understudied. As far as GBM is concerned, only a handful of studies have been dedicated to uncovering the link of *MIAT* with the tumour, and of these, the vast majority has investigated *MIAT*'s role in patient prognosis. High *MIAT* expression had been linked with better survival in GBM patients (Zhang *et al.*, 2013). Further, the expression of *MIAT* is upregulated after de-methylation treatment, a common therapeutic approach, in GBM patients (Zhang and Leung, 2014). Also, the prognostic value of *MIAT* has been established for GBM patient stratification together with 5 other lncRNAs, as part of a 6-lncRNA signature (Zhang *et al.*, 2013; Zhang and Leung, 2014; Mei-Yee Kiang *et al.*, 2015). Nevertheless, the knowledge of the mechanisms mediating these effects in both tumours, as well as of the eligibility of this molecule as a biomarker for

patient diagnosis and stratification, remains limited, as the precise modes of action of *MIAT* in these systems are far from being fully unveiled.

To this end, this chapter aims to shed light on the underpinning role of the subnuclear body-associated lncRNA *MIAT* in the determination of cell fate in neuroblastoma and glioblastoma cells. More specifically, the role of *MIAT* in the regulation of both short- and long-term cell survival, cell death and cell migration of neuroblastoma and glioma cells was investigated via transiently silencing the expression of *MIAT* in these cells.

3.2. Materials and Methods

3.2.1. Cell culture

The experiments incorporated in this chapter were conducted using the human neuroblastoma SH-SY5Y cell line and the human astrocytoma/ glioblastoma 1321N1 cell line, cultured using the HyClone™ DMEM/F12 1:1 growth media, supplemented with 10% heat-inactivated fetal bovine serum, 2 μM L-Glutamine, 1 μM Sodium Pyruvate and 10mg/ml gentamicin solution, as well as the human glioblastoma T98G cell line, cultured in the aforementioned growth media, supplemented with an extra 10% FBS, 15% cell-conditioned growth media and 1% MEM non-essential amino acid solution, as described in section 2.1.

3.2.2. RNA interference

In this series of experiments SH-SY5Y, 1321N1 and T98G cells were transfected with siRNAs using Nucleofection. The siRNAs used (500nM) included the Silencer® Negative control siRNA and three different *MIAT*-specific siRNAs: MIAT_1, MIAT_2 and MIAT_3 (details can be found in Table 2.1), targeting different sites of the fifth exon of the full-length *MIAT* transcript, as detailed in section 2.3.2.

In addition to siRNAs, LNA GapmeRs were used in this series of experiments to knockdown *MIAT,* to validate the observed effects. The GapmeRs that were used (100nM) included the Negative control A Antisense LNA GapmeR and three custom-designed GapmeRs (namely 1_1, 2_1, 2_2) (details can be found in Table 2.2) targeting different sites of the fifth exon of the full-length *MIAT* transcript, as described in section 2.3.3.

3.2.3. Real-time PCR (RT-qPCR)

Total RNA was extracted from cells using the Direct-zol™ RNA MiniPrep kit, according to the manufacturer's protocol and the quality was measured with NanoDrop (as detailed in sections 2.4 and 2.4.1).

RNA extracted from transfected cells was then reverse transcribed into cDNA using the Omniscript® RT kit, as described in section 2.5.1. Real-time PCR was subsequently performed for the synthesised cDNA. Specific primers were used against *MIAT,* while 18S rRNA was used as a housekeeping gene (Table 3.1), as described in section 2.5.2.

Table 3.1. TaqMan® gene expression assays' details.

Method	Catalogue #/ ID	Target	Exon boundary	Assay location
TaqMan®	**Hs99999901_s1**	*18S*	1-1	604
	4319413E	*18S*	1-1	604
	Hs00402814_m1	*MIAT*	5	1864

3.2.4. Functional analysis: determination of cell survival, apoptosis and cell migration

For the lncRNA knockdown experiments, after transfection, cells were harvested by trypsinisation and after 48 h were plated for 48 and 72 h. **Cell survival** was assessed using

trypan blue solution vital dye staining (explained in section 2.6.1), and by flow cytometry using the MUSE® Cell Analyzer and the MUSE® Count and Viability Kit, as detailed in section 2.6.2. The long term survival of the cells was assessed with the clonogenic assay. siRNA-transfected cells were incubated for 2-3 weeks (as detailed in Table 2.8), were stained with 1% w/v crystal violet and counted, as presented in section 2.8.

In order to evaluate the effect of the knockdown of *MIAT* on the levels of **apoptosis-mediated cell death** in all cell lines, the cells were stained with acridine orange (25μg/ml), and their morphology was observed with fluorescence microscopy at specific time intervals after plating (48 and 72 h), as described in section 2.7.2.

The **migratory ability** of the cells was assessed by the wound healing assay (detailed in section 2.9.). The gaps were measured using the EVOS FL Cell Imaging System at 0, 24 and 48 h and the gap closure was calculated using the formula **[(Pre-migration)area-(Migration)area/(Pre-migration)area] x100** for 15 measurements per sample. Image analysis was performed using the ImageJ software.

3.2.5. Statistical analysis

Statistical analyses were performed using GraphPad Prism 6 (GraphPad Software). Data are presented as the mean ± SEM; the number of observations (n) refers to different transfected samples, each transfection being conducted on a separate culture of cells. Comparisons were made using an unpaired T-test or One-Way ANOVA with Bonferroni's multiple comparison test (MCT). Where multiple parameters were compared, Two-Way ANOVA with Sidak, Tukey or Dunnett multiple comparisons was used. Statistical significance was set at the 0.05 level. Differences were considered as statistically significant when *P-value* was <0.05 (95% confidence intervals).

3.3. Results

3.3.1. The effects of *MIAT* knockdown on the survival of SH-SY5Y neuroblastoma cells

The first step encompassed in the investigation of how *MIAT* affects the determination of cell fate was to examine the effects of *MIAT* silencing on cell survival, including both short- and long-term, in the neuroblastoma cell line. For this, SH-SY5Y neuroblastoma cells were transfected via nucleofection with one of three different siRNAs which target different sites of *MIAT*. The short-term survival was measured with trypan blue vital dye exclusion and with flow cytometry using the MUSE® Cell Analyzer. All of the *MIAT*-specific siRNAs significantly silenced the expression of *MIAT* (~70% for MIAT_1 and MIAT_3, and 80% for MIAT_2), as validated with RT-qPCR (Figure 3.1a). However, although there was a tendency of reduced-short term survival, the reduction was not statistically significant for any of the three siRNAs, as measured by vital dye staining 48 h post-plating (Figure 3.1b) and 72 h post-plating (Figure 3.1d), or as measured by flow cytometry 48 h post-plating (Figure 3.1c) and 72 h post-plating (Figure 3.1e). In this instance, it has to be noted that the numbers of viable cells acquired by the trypan blue exclusion method are nearly double those acquired by the flow cytometry method. This could be attributed to the fact that SH-SY5Y cells are a highly clumping cell line, and therefore, cell clusters of high volume are excluded from the count when using the MUSE® Cell Analyzer.

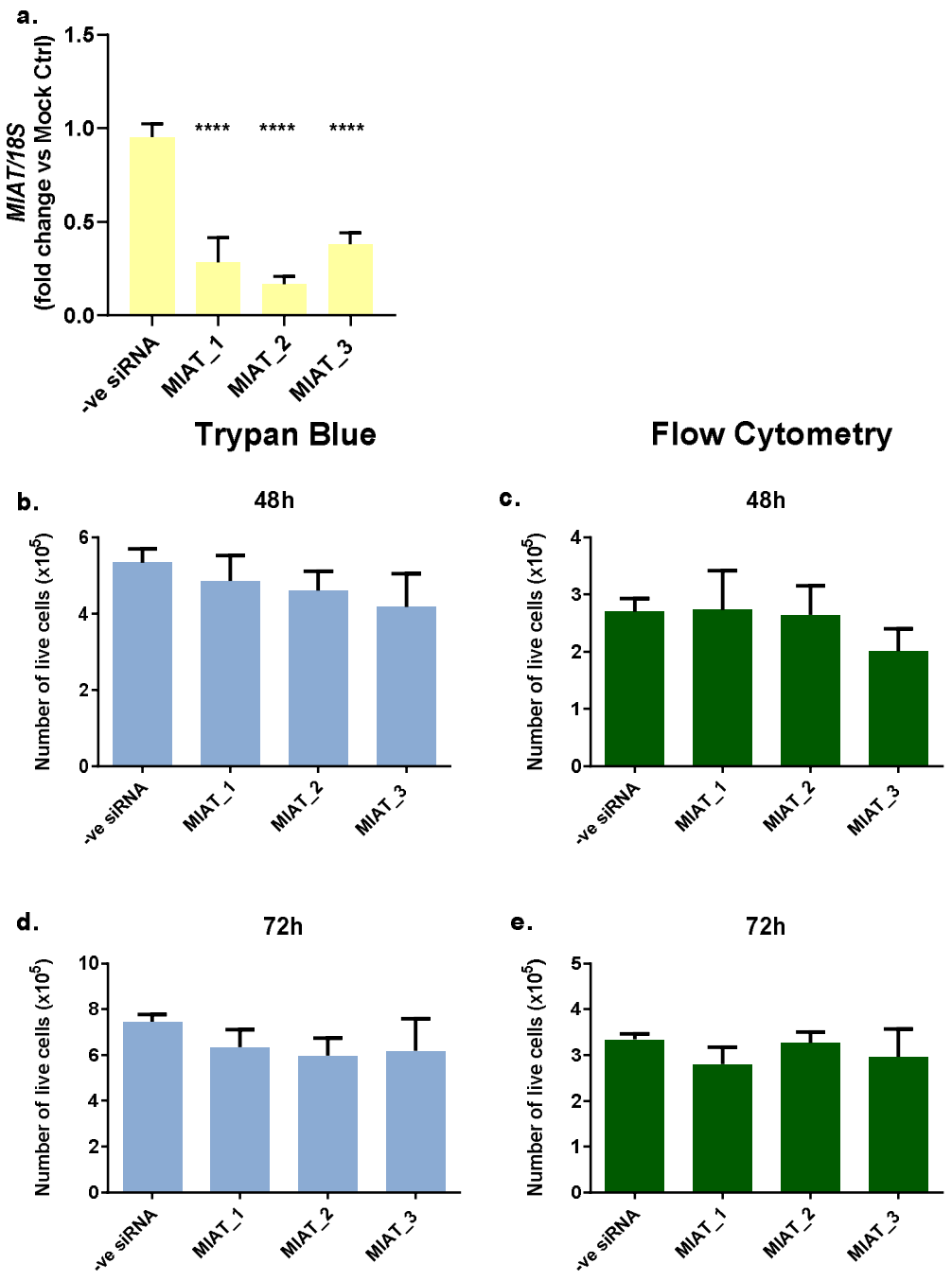

Figure 3.1. *MIAT*-specific down-regulation does not affect the short-term cell survival of SH-SY5Y cells. SH-SY5Y cells were transfected with the –ve siRNA or one of the three *MIAT*-specific siRNAs using nucleofection, incubated for 48 h, plated, incubated for another 48 and 72 h and assessed. The relative expression of *MIAT* was measured by Real-Time PCR 48 h post-transfection, and was significantly lower for all siRNAs (a); *MIAT* down-regulation does not lead to a statistically significant change in the number of viable cells as assessed with trypan blue exclusion (b, d) and flow cytometry (c, e) after 48 or 72 h, respectively **** indicate a *p-value*<0.001, as measured by One-way ANOVA tests with multiple comparisons (MCT). Data are represented as mean +/- SEM, n=4 experiments for MIAT_1, n=5 experiments for MIAT_2/3.

In addition to the effect of *MIAT*'s down-regulation on the short-term survival of the SH-SY5Y cells, we next evaluated the effect on the basal levels of apoptosis. Due to the superior silencing of MIAT_2 and MIAT_3, MIAT_1 was excluded from this series of experiments. The levels of apoptosis were measured with fluorescent microscopy after acridine orange staining 48 h, 72 h and 96 h after transfection. Importantly, the levels of apoptotic cells were increased at all time intervals after downregulation by all *MIAT*-specific siRNAs, especially 72 h post-nucleofection, with apoptotic cells comprising about 20% of the cell population (Figure 3.2a, b).

Furthermore, the influence of the silencing of *MIAT* on long-term survival was assessed subsequently. The long-term survival of SH-SY5Y cells, as measured by clonogenic assay, was decreased due to the downregulation of *MIAT.* Specifically, the findings show an overall significant decrease in the number of colonies for the two of the three *MIAT*-specific siRNAs assessed (Figure 3.2c) (34.3% for MIAT_2 and 45.8% for MIAT_3), suggesting that the survival-inhibitory effect of *MIAT* knockdown may take longer to appear.

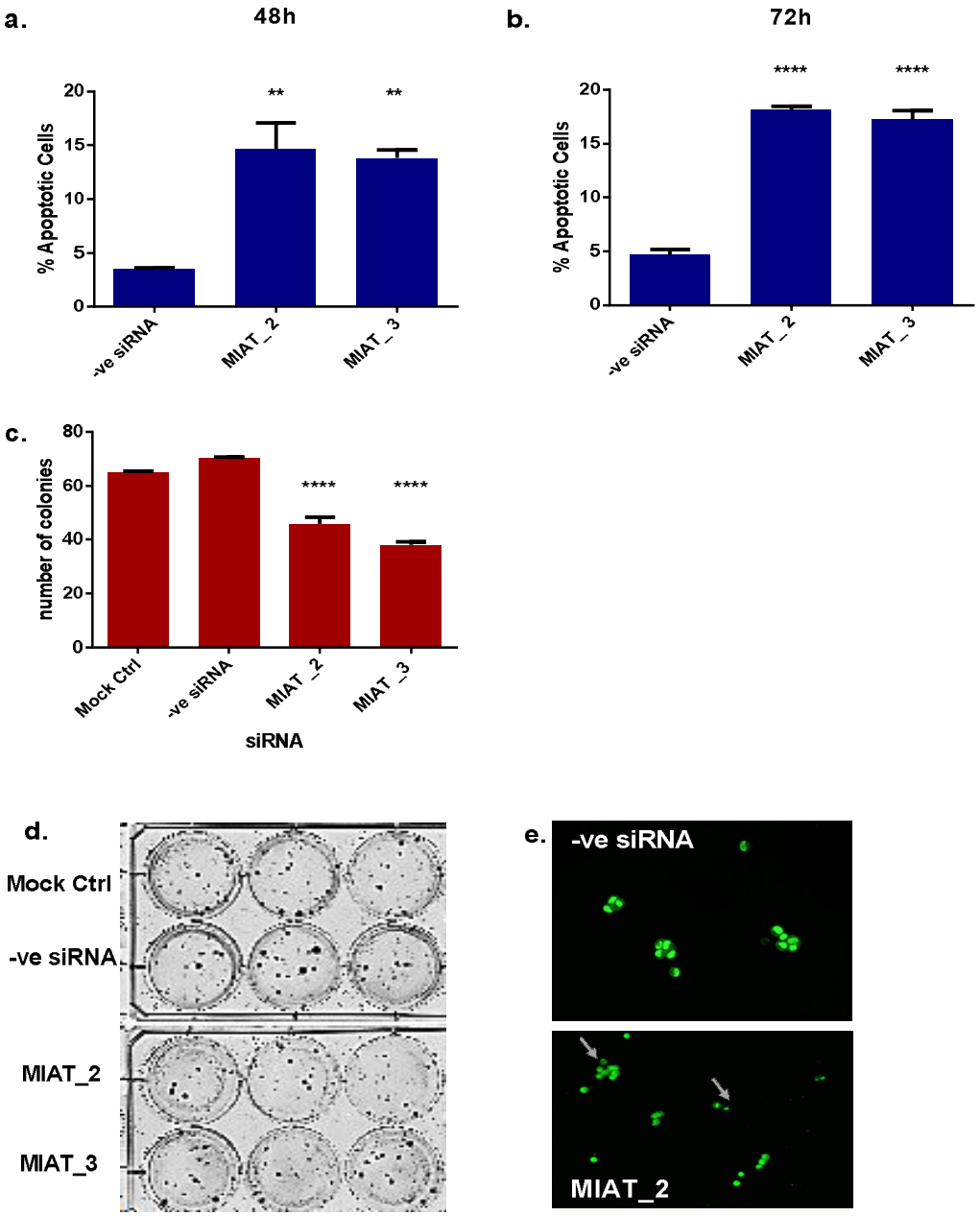

Figure 3.2. *MIAT*-specific down-regulation reduces the long-term survival and increases the levels of apoptosis of SH-SY5Y cells. SH-SY5Y cells were transfected with the negative siRNA or one of the two *MIAT*-specific siRNAs (MIAT_2/3) using nucleofection and were assessed 48 and 72 h post-nucleofection. The levels of apoptosis were significantly elevated, reaching a 3-fold increase (a, b); Cells were also seeded and incubated (37°C, 5% CO_2) for three weeks, and the colonies formed were stained with crystal violet (1% w/v) and counted. *MIAT* knockdown induced by *MIAT*-specific siRNAs led to a reduction of the number of colonies formed (c); representative illustration of a clonogenic assay (d); representative illustration of apoptotic cells 72 h post-nucleofection, stained with acridine orange and observed using fluorescent microscopy (e). Grey arrows indicate cells undergoing apoptosis; ** indicate a *p-value*<0.01; **** indicate a *p-value*<0.001, as measured by One-way ANOVA tests with multiple comparisons (MCT). Data are represented as mean +/- SEM, in n=3 experiments.

In order to provide further confirmation of the effect of *MIAT* downregulation on apoptosis and long term survival in SH-SY5Y neuroblastoma cells, a LNA GapmeR-mediated silencing approach was employed.

In fact, all of the used GapmeRs (namely 1_1, 2_1, 2_2) were capable of silencing *MIAT*, as evaluated with RT-qPCR (Figure 3.3a). In specific, the expression of *MIAT* was reduced by 65%, 60% and 55%, for 1_1, 2_1 and 2_2, respectively. In terms of long-term survival as assessed by colony forming assay, a decrease in the number of colonies was observed, which was significant for two of the three *MIAT*-specific GapmeRs, with 1_1 causing an average 20% decrease and 2_2 triggering an important 33% reduction in the number of colonies (Figure 3.3b). As far as basal apoptosis is concerned, as evaluated with acridine orange staining via fluorescent microscopy, the obtained results confirmed the siRNA results, suggesting that the downregulation of *MIAT* indeed induces a 2-fold increase of apoptotic cells for all of the three different GapmeRs at both assessed time points (48 h and 72 h) (Figure 3.3c, d). Although overall the effect of *MIAT* was confirmed with the use of GapmeRs as a means of down-regulation, the observed effect in SH-SY5Y was not as strong as the one observed when using the siRNA-mediated approach.

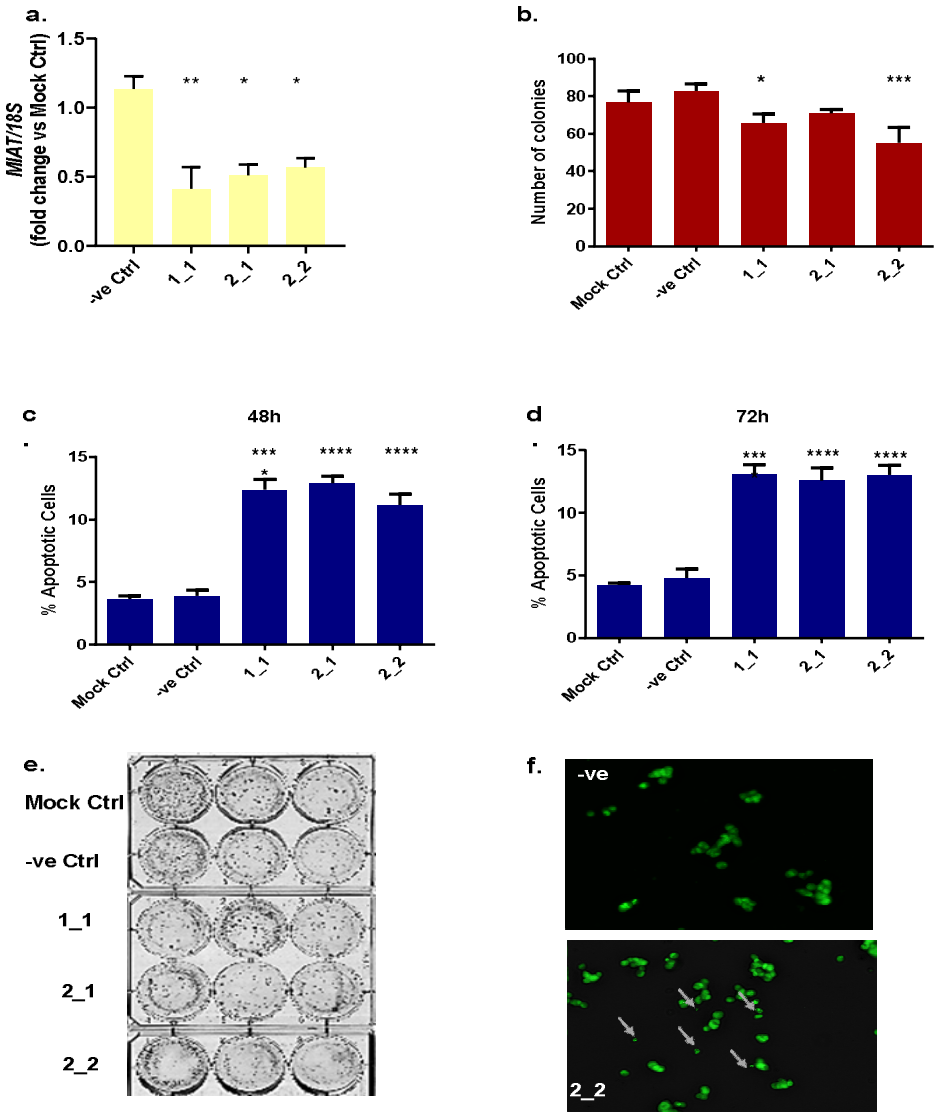

Figure 3.3. LNA GapmeR- mediated *MIAT*-specific down-regulation increases the levels of apoptosis of SH-SY5Y cells. SH-SY5Y cells were transfected with the -ve Ctrl GapmeR or one of the three *MIAT*-specific LNA GapmeRs using nucleofection and were assessed 48 and 72 h post-nucleofection. The relative expression of *MIAT* was significantly lowered for all the three GapmeRs, as measured by Real-Time PCR 48 h post-transfection (a); Cells were also seeded and incubated (37°C, 5% CO_2) for two weeks, and the colonies formed were stained with crystal violet (1% w/v) and counted. The number of colonies was significantly reduced upon 1_1- and 2_2- mediated *MIAT* knockdown, but the decrease was non-significant for 2_1 (b). *MIAT* knockdown induced by *MIAT*-specific LNA GapmeRs led to a significant increase of apoptosis levels, especially 72 h after nucleofection, reaching a 2-fold increase (c, d); representative illustration of a clonogenic assay (e); representative illustration of apoptotic cells 72 h post-nucleofection, stained with acridine orange and observed using fluorescent microscopy (f). Grey arrows indicate cells undergoing apoptosis; 1_1, 2_1, 2_2 *MIAT*-specific LNA GapmeRs. * indicates a *p-value*<0.05; ** indicate a *p-value*<0.01; ***/**** indicate a *p-value*<0.001, as measured by One-way ANOVA tests with multiple comparisons (MCT). Data are represented as mean +/- SEM, n= 3 experiments.

3.3.2. The effects of *MIAT* knockdown on the survival of 1321N1 glioblastoma cells

The effects of *MIAT* knockdown on the levels of apoptosis and cell survival observed in the neuroblastoma cells, together with previous literature that strongly associated *MIAT* with cell survival (Zhang et al., 2013; Zhang and Leung, 2014; Mei-Yee Kiang *et al.,* 2015), generated the question whether the same effects would be observed in GBM cell lines. For this purpose, 1321N1 astrocytoma/GBM, similarly to the protocols followed for SH-SY5Y cells, were transfected via nucleofection with one of three different siRNAs which target different sites of *MIAT*. The short-term survival was measured via trypan blue exclusion and flow cytometry. Again, all of the *MIAT*-specific siRNAs significantly silenced the expression of *MIAT* by 85%, 80% and 70% for MIAT_1, MIAT_2 and MIAT_3, respectively, as measured with RT-qPCR (Figure 3.4a). Nevertheless, although there was again a tendency of reduced-short term survival, especially at 72 h post-plating, this reduction was not drastic enough to be statistically significant for any of the three siRNAs, as measured by trypan blue 48 h post-plating (Figure 3.4b) and 72 h post-plating (Figure 3.4d), or as measured by flow cytometry 48 h post-plating (Figure 3.4c) and 72 h post-plating (Figure 3.4e).

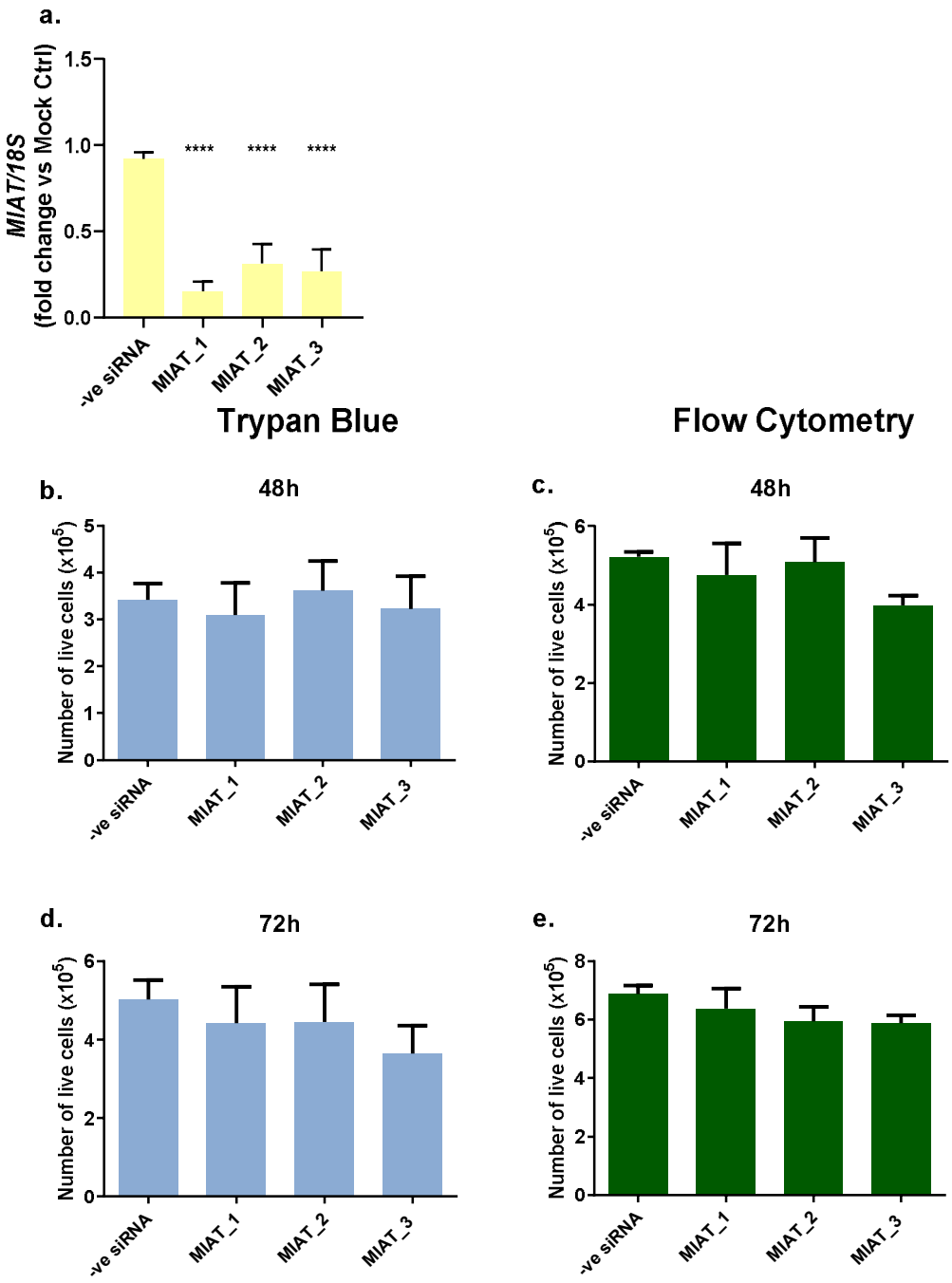

Figure 3.4. *MIAT*-specific siRNAs effectively down-regulate *MIAT* in 1321N1 cells. 1321N1 cells were transfected with the –ve siRNA or one of the three *MIAT*-specific siRNAs using nucleofection, incubated for 48 h, plated, incubated for another 48 and 72 h and assessed. The relative levels of *MIAT* expression were measured using Real-Time PCR 48 h post-transfection, and were found significantly lower for all siRNAs (a); however, *MIAT* down-regulation does not lead to a statistically significant change in the number of viable cells as assessed with trypan blue exclusion (b, d) and flow cytometry (c, e) after 48 or 72 h, respectively; **** indicate a *p-value*<0.001, as measured by One-way ANOVA tests with multiple comparisons (MCT). Data are represented as mean +/- SEM, n=4 experiments for MIAT_1, n=5 experiments for MIAT_2/3.

Following the same rationale and process followed for the SH-SY5Y cells, apoptosis-mediated cell death was the next feature to be assessed, using acridine orange staining. The acquired results have revealed an outstanding increase of apoptosis for all the three siRNAs at all both points (48 and 72 h), especially for MIAT_2. As was the case for SH-SY5Y, the strongest effects were acquired 72 h after transfection (Figure 3.5a, b). In fact, MIAT_2- and MIAT_3-mediated knockdown triggered apoptosis in about 23% of the total cell population at 72 h, corresponding to a ~3-fold increase.

The next question that arose was whether, similar to neuroblastoma cells, there is a reduction in the long-term survival of the GBM cells upon *MIAT* knockdown. To this end, and similar to the response of the SH-SY5Y neuroblastoma cells to *MIAT* down-regulation, the 1321N1 cells showed a similar response pattern as far as long-term survival is concerned. As observed in the colony forming assays, the number of colonies was significantly decreased for all three *MIAT*-specific siRNAs (Figure 3.5c) (18.5% for MIAT_1, 23.1% for MIAT_2 and 26.2% for MIAT_3, n=5 experiments).

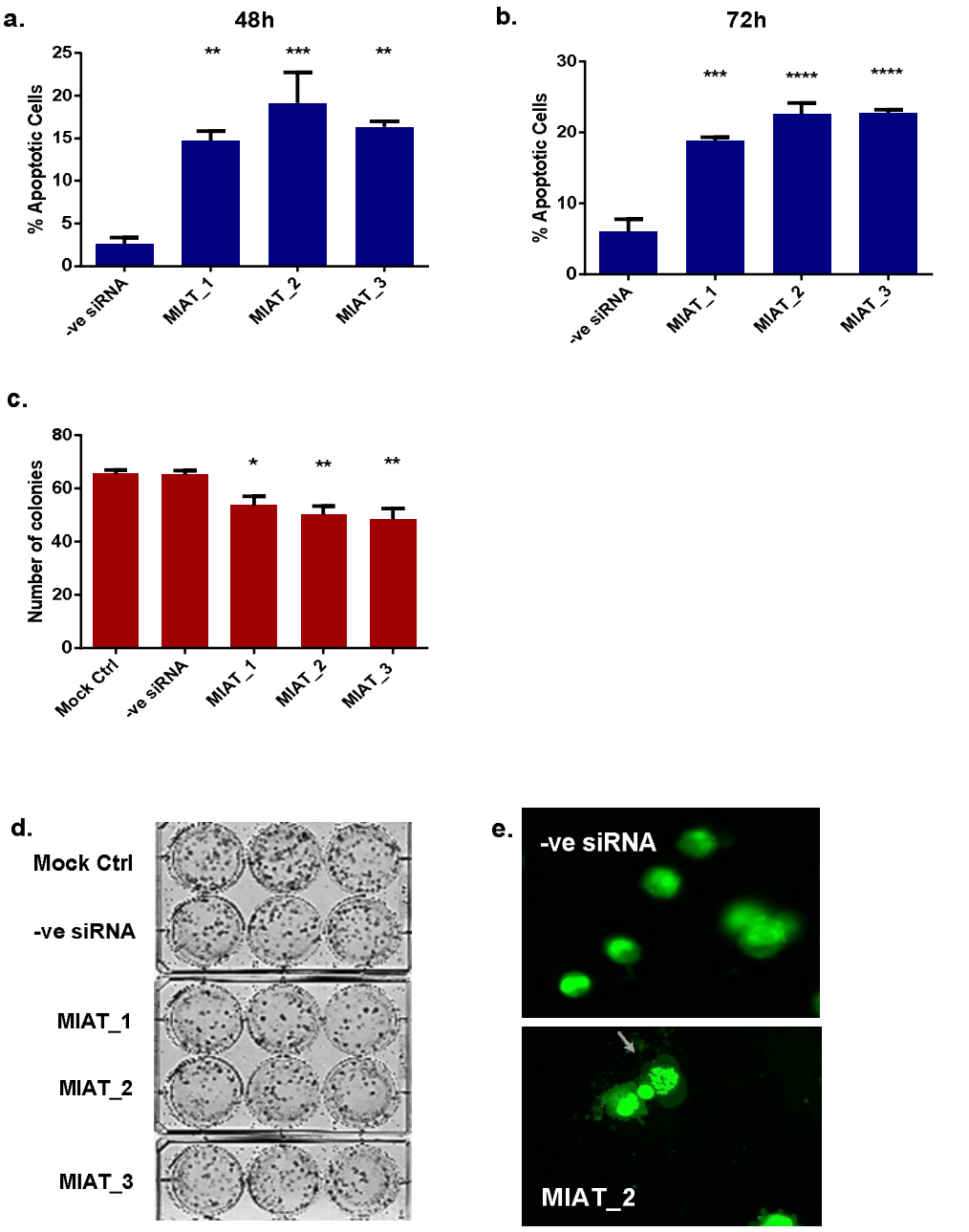

Figure 3.5. *MIAT*-specific down-regulation reduces the long-term survival and increases the levels of apoptosis of 1321N1 cells. 1321N1 cells were transfected with the negative siRNA or one of the three *MIAT*-specific siRNAs using nucleofection and were assessed 48 and 72 h post-nucleofection. The levels of apoptosis were significantly elevated, reaching a 3-fold increase (a, b); Cells were also seeded and incubated (37°C, 5% CO_2) for three weeks, and the colonies formed were stained with crystal violet (1% w/v) and counted. *MIAT* knockdown induced by *MIAT*-specific siRNAs led to a reduction of the number of colonies formed (c); representative illustration of a clonogenic assay (d); representative illustration of apoptotic cells 72 h post-nucleofection, stained with acridine orange and observed using fluorescent microscopy (e). Grey arrows indicate cells undergoing apoptosis; * indicates a *p-value*<0.05; ** indicate a *p-value*<0.01; ***/**** indicate a *p-value*<0.001, as measured by One-way ANOVA tests with multiple comparisons (MCT). Data are represented as mean +/- SEM, in n=5 experiments.

Following the confirmation of the effect of *MIAT* provided by GapmeRs in neuroblastoma cells, we next followed the same strategy for the glioblastoma cell lines. To this end, GapmeRs were employed to confirm the effect on long-term survival and apoptotic cell death. Similar to SH-SY5Y, in 1321N1 cells, all GapmeRs were capable of silencing the expression of *MIAT*, with two of them (1_1 and 2_2) reaching a ~85% effect, while 2_1 caused a 55 % decrease in expression (Figure 3.6a). In this case, all of the three GapmeRs were capable of reducing the colony numbers from ~25% for 1_1 and 2_1 to ~35% for 2_2 (Figure 3.6b). In addition, in terms of apoptosis, again all the three GapmeRs induced elevated (~2-fold) apoptosis levels after both 48 h and 72 h (Figure 3.6c, d).

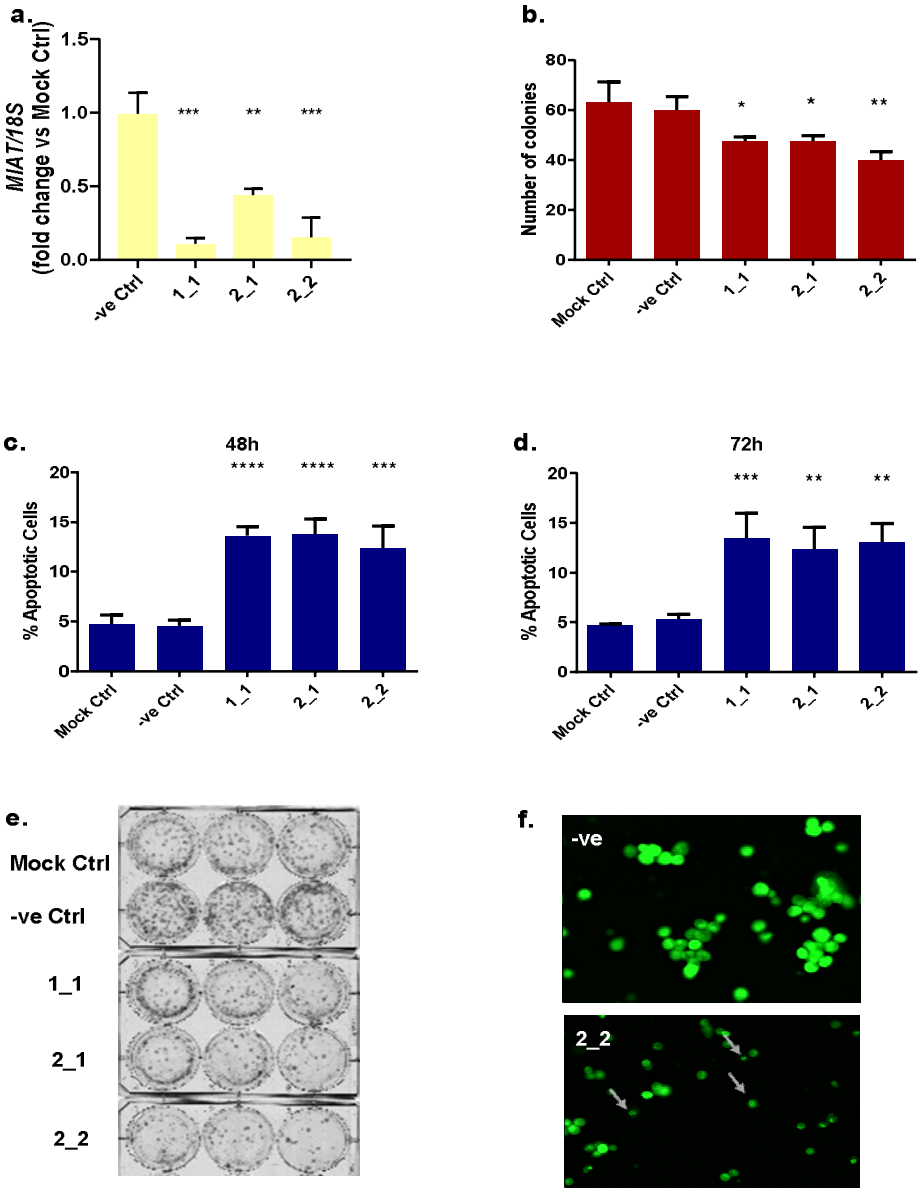

Figure 3.6. LNA GapmeR- mediated *MIAT*-specific downregulation increases the levels of apoptosis of 1321N1 cells. 1321N1 cells were transfected with the -ve Ctrl GapmeR or one of the three *MIAT*-specific LNA GapmeRs using nucleofection and were assessed 48 and 72 h post-nucleofection. The relative expression of *MIAT* was significantly lowered for all the three GapmeRs, as measured by Real-Time PCR 48 h post-transfection (a); Cells were also seeded and incubated (37°C, 5% CO_2) for two weeks, and the colonies formed were stained with crystal violet (1%w/v) and counted. The number of colonies was significantly reduced upon *MIAT* knockdown mediated by all GapmeRs (b). Also, *MIAT* knockdown induced by *MIAT*-specific LNA GapmeRs led to a significant increase of apoptosis levels, especially 72 h after nucleofection, reaching a 2-fold increase (c, d); representative illustration of a clonogenic assay (e); representative illustration of apoptotic cells 72 h post-nucleofection, stained with acridine orange and observed using fluorescent microscopy (f). Grey arrows indicate cells undergoing apoptosis; 1_1, 2_1, 2_2: *MIAT*-specific LNA GapmeRs. * indicates a *p-value*<0.05; ** indicate a *p-value*<0.01; ***/**** indicate a *p-value*<0.001, as measured by One-way ANOVA tests with multiple comparisons (MCT). Data are represented as mean +/- SEM, n= 3 experiments.

3.3.3. The effect of *MIAT* knockdown on the survival of T98G glioblastoma cells

Given the consistency in most of the observations between the two tested cell lines, the next step implicated the assessment of the role of *MIAT* in a third cell line, which was again a GBM cell line, T98G. In agreement with the previous observations, although the siRNA-mediated knockdown was efficient (75%, 65% and 80% down-regulation of *MIAT* for MIAT_1, MIAT_2 and MIAT_3, respectively) (Figure 3.7a) the T98G glioblastoma cells also failed to display significant changes in the number of viable cells upon *MIAT* knockdown short-term (Figure 3.7b-e), as assessed with vital dye exclusion and flow cytometry.

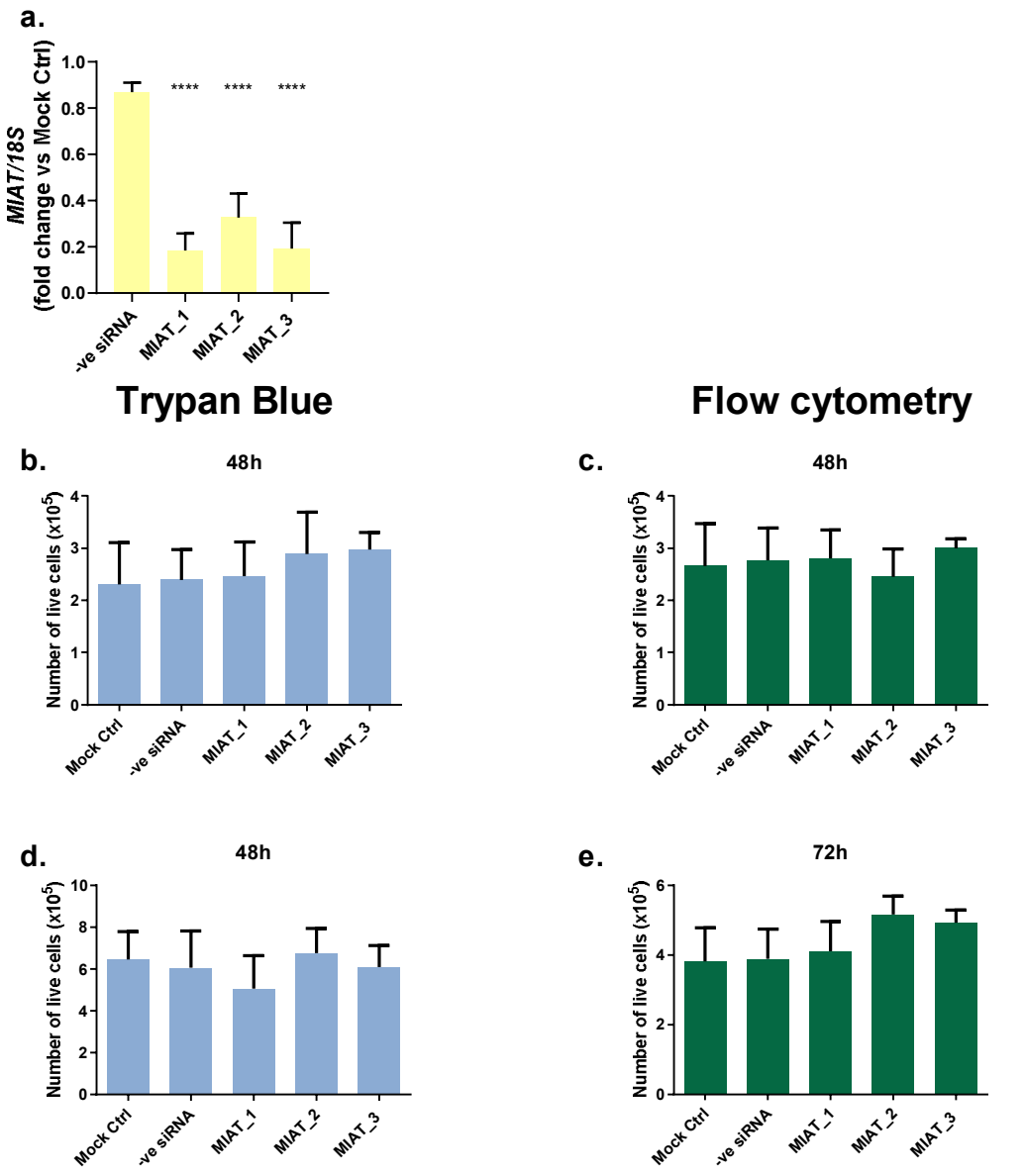

Figure 3.7. *MIAT*-specific down-regulation does not affect the short-term cell survival of T98G cells. T98G cells were transfected with the –ve siRNA or one of the three *MIAT*-specific siRNAs using nucleofection, incubated for 48 h, plated, incubated for another 48 and 72 h and assessed. The relative expression of *MIAT* was measured by Real-Time PCR 48 h post-transfection, and was significantly lower for all siRNAs (a); *MIAT* down-regulation does not lead to a statistically significant change in the number of viable cells as assessed with trypan blue exclusion (b, d) and flow cytometry (c, e) after 48 or 72 h, respectively **** indicate a *p-value*<0.001, as measured by One-way ANOVA tests with multiple comparisons (MCT). Data are represented as mean +/- SEM, n=4 experiments.

As far as the apoptosis levels -as assessed by acridine orange- are concerned, the results acquired for the T98G cell line are again in full agreement with previous observations. The results have revealed a significant increase of apoptosis for all the three siRNAs at both time points assessed (48 and 72 h). The magnitude of the effect was similar at both time points, ranging from ~11% to ~13% of apoptotic cells for siRNA-treated cells versus ~4% for the negative control, reaching, in this case, a ~2-fold increase (Figure 3.8a, b).

At the same time, the silencing of *MIAT* induced a substantial decrease in the colony number for all the three *MIAT*-specific siRNAs (Figures 3.8c), however, this decrease was statistically significant only for MIAT_1 and MIAT_3 (24.2% for MIAT_1, and 34.9% for MIAT_3, n=4 experiments), while the decrease in MIAT_2 (~19%) was not significant.

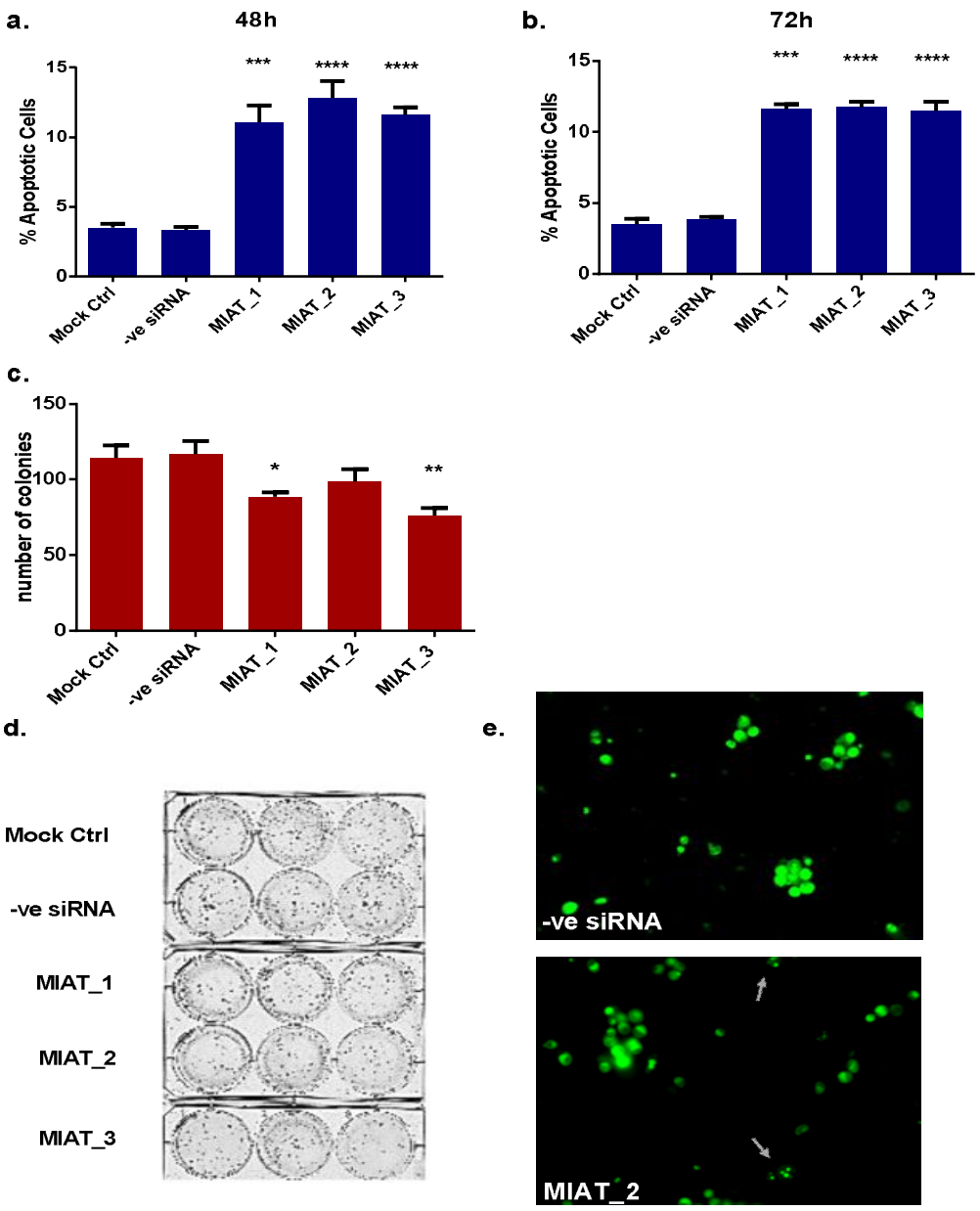

Figure 3.8. *MIAT*-specific down-regulation elevates the levels of apoptosis-mediated cell death and reduces long-term survival in T98G cells. T98G cells were transfected with the –ve siRNA or one of the three *MIAT*-specific siRNAs using nucleofection, incubated for 48 h, plated, incubated for another 48 and 72 h and assessed. The levels of apoptosis were statistically significantly increased for all siRNAs reaching a 2-fold increase, as assessed by acridine orange fluorescent microscopy at 48 (a) and 72 h (b). Cells were also seeded and incubated (37°C, 5% CO_2) for two weeks, and the colonies formed were stained with crystal violet (1% w/v) and counted. *MIAT*-specific down-regulation causes a statistically significant decrease in the number of colonies formed upon MIAT_1- and MIAT_3- mediated nucleofection, but not MIAT_2 (c); representative illustration of a clonogenic assay (d); representative illustration of apoptotic cells 48 h post-plating, stained with acridine orange and observed using fluorescent microscopy (e). Grey arrows indicate cells undergoing apoptosis; * indicates a *p-value*<0.05; ** indicate a *p-value*<0.01; ***/**** indicate a *p-value*<0.001, as measured by One-way ANOVA tests with multiple comparisons (MCT). Data are represented as mean +/- SEM, n=3 experiments.

In the case of T98G cells, the validation of the effect of *MIAT* downregulation on long-term survival and apoptosis was again performed using *MIAT*-specific GapmeRs. In this case, although all three GapmeRs significantly knocked down *MIAT* (60% for 1_1 and 80% for 2_1 and 2_2), the down-regulation was not as strong as it was for the aforementioned cell lines or the siRNA-mediated silencing (Figure 3.9a). As a direct consequence, possibly, the number of colonies was slightly decreased for all GapmeRs, but the decrease did not display statistical significance for any of them (Figure 3.9b). However, the knockdown of *MIAT* had a stronger influence on apoptosis, causing a significant elevation in the number of apoptotic cells compared to the negative control (2-fold) for all the GapmeRs used at both time points assessed (48 h and 72 h) (Figure 3.9c, d). Collectively, these data suggest that although the effect of *MIAT* down-regulation was overall confirmed in glioblastoma cells using a LNA GapmeR-mediated approach, the magnitude of the effect was somewhat smaller, suggesting a poorer performance of GapmeRs as compared to siRNAs.

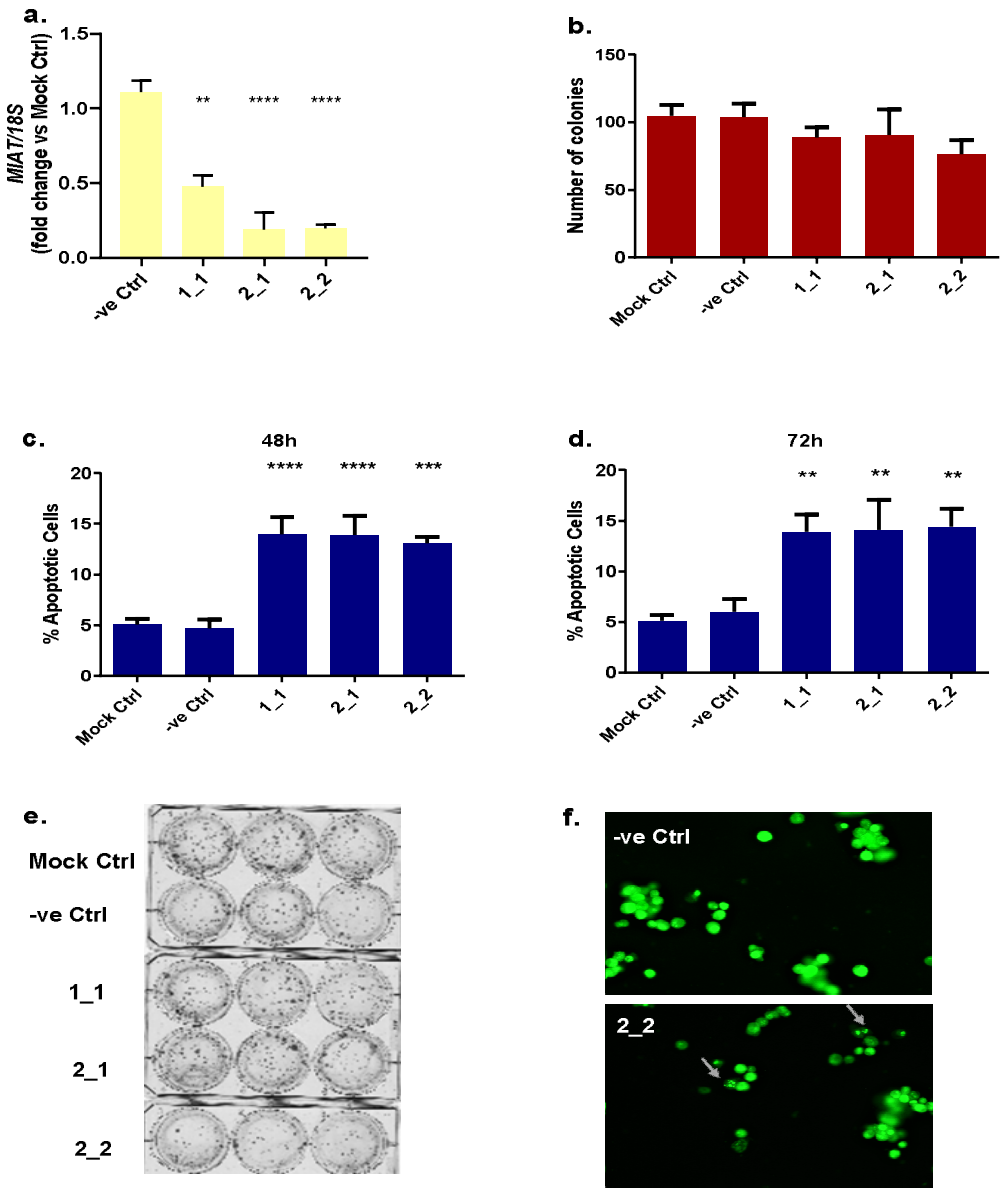

Figure 3.9. LNA GapmeR- mediated *MIAT*-specific downregulation increases the levels of apoptosis of T98G cells. T98G cells were transfected with the -ve Ctrl GapmeR or one of the three *MIAT*-specific LNA GapmeRs using nucleofection and were assessed 48 and 72 h post-nucleofection. The relative expression of *MIAT* was significantly lowered for all the three GapmeRs, as measured by Real-Time PCR 48 h post-transfection (a); Cells were also seeded and incubated (37°C, 5% CO_2) for two weeks, and the colonies formed were stained with crystal violet (1% w/v) and counted. The number of colonies was reduced upon *MIAT* knockdown mediated by all GapmeRs, but none of the changes was statistically significant (b). In addition, *MIAT* knockdown induced by *MIAT*-specific LNA GapmeRs led to a significant increase of apoptosis levels, especially 72 h after nucleofection, reaching a 2-fold increase (c, d); representative illustration of a clonogenic assay (e); representative illustration of apoptotic cells 72 h post-nucleofection, stained with acridine orange and observed using fluorescent microscopy (f). Grey arrows indicate cells undergoing apoptosis; 1_1, 2_1, 2_2: *MIAT*-specific LNA GapmeRs. * indicates a *p-value*<0.05; ** indicate a *p-value*<0.01; ***/**** indicate a *p-value*<0.001, as measured by One-way ANOVA tests with multiple comparisons (MCT). Data are represented as mean +/- SEM, n= 3 experiments.

3.3.4. The effect of siRNA-mediated *MIAT* knockdown on cell migration in neuroblastoma and glioblastoma cells

The observation of an altered morphology of the SH-SY5Y cells under the microscope following transfection, which revealed more sparsely distributed and truncated structures (Figure 3.10), led to the hypothesis that the migratory ability of the cells could be also affected, as an indirect consequence of the elevated apoptosis levels. To this end, this hypothesis was tested via the wound healing ("scratch") assay. The results confirmed that the migratory capability of the cells is reduced in response to the silencing of *MIAT* at both time points tested (24 and 48 h) for all the three *MIAT*-specific siRNAs. Specifically, there was significantly less gap closure, with the greatest effect being observed after 48 h for MIAT_1 (35% less gap closure), MIAT_2 (33% less gap closure) and MIAT_3 (28% less gap closure) (Figure 3.11).

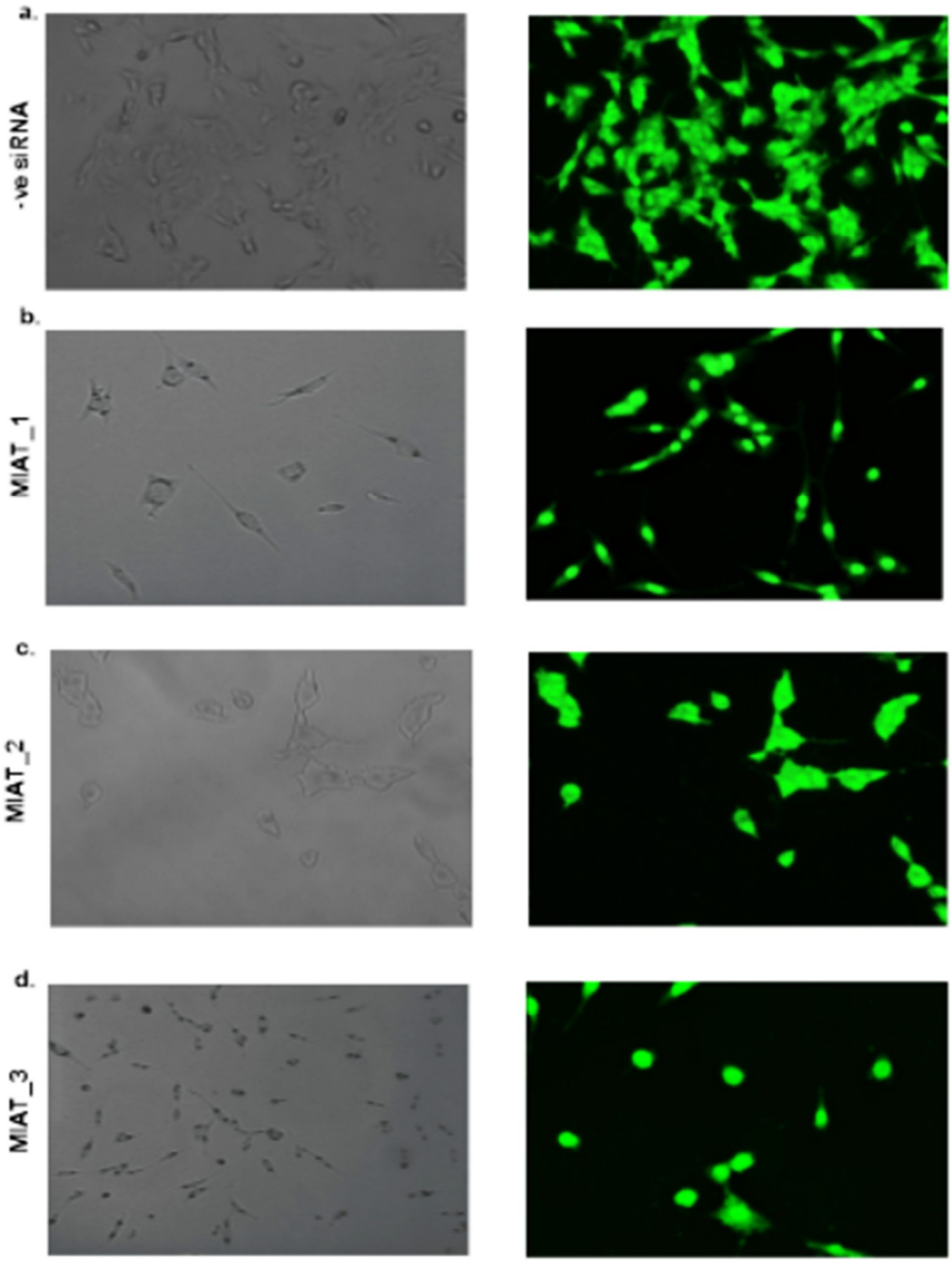

Figure 3.10. *MIAT*-specific knockdown alters the cellular morphology of SH-SY5Y cells. SH-SY5Y cells were transfected with the negative siRNA or one of the three *MIAT*-specific siRNAs using nucleofection, and were subsequently stained with acridine orange and observed using light (left panels) and fluorescent (right panels) microscopy. The morphology of the cells was changed after transfection. The cells displayed less elongated structures, as well as a more sparse spatial distribution pattern. Representative illustration of cells treated with the -ve siRNA (a) and the three *MIAT*-specific siRNAs (b-d). For b, d, the light and fluorescent images do not represent the same microscopic field.

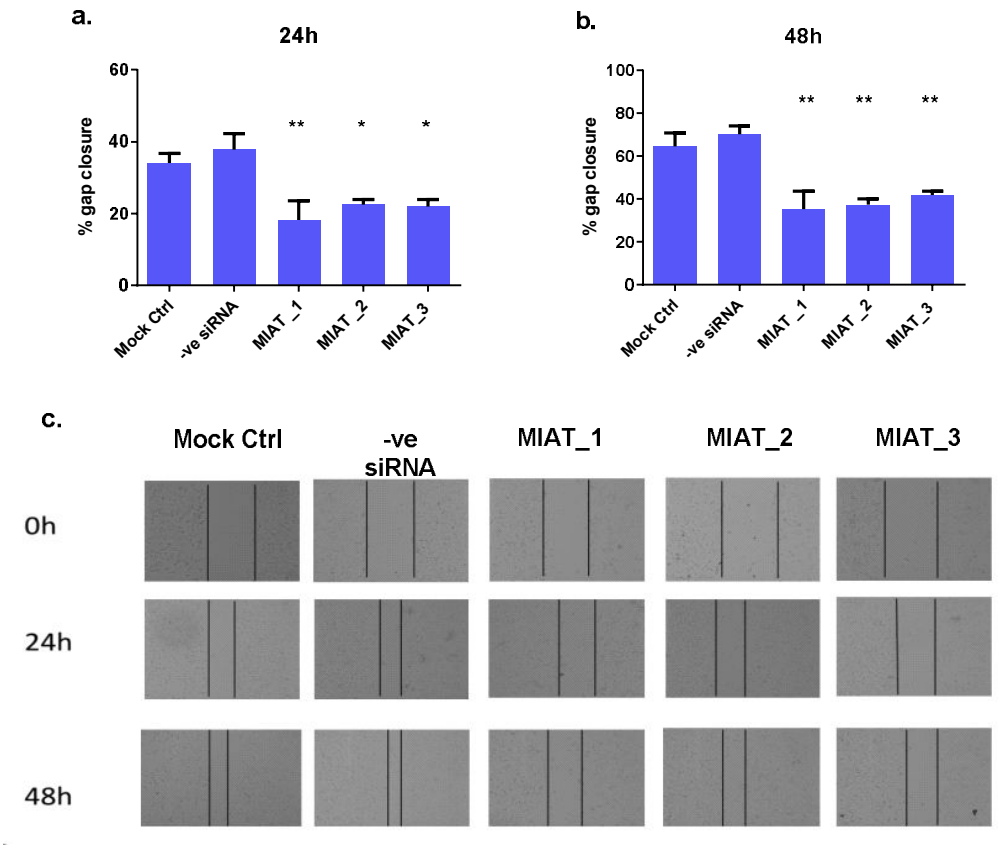

Figure 3.11. *MIAT*-specific down-regulation deteriorates the migrating ability of SH-SY5Y cells. SH-SY5Y cells were transfected with the -ve siRNA or one of the three *MIAT*-specific siRNAs using nucleofection, plated, and a linear scratch was introduced 48 h post-plating. The % gap closure of the scratch was measured after 24 and 48 h. The migrating ability of the cells is reduced for all three *MIAT*-specific siRNAs at both time points assessed, especially at 48 h (a); relative gap closure of *MIAT*-specific siRNAs versus the –ve siRNA (b); representative illustration of a wound healing ("scratch") assay (c); * indicates a *p-value*<0.05; ** indicate a *p-value*<0.01, as measured by One-way ANOVA tests with multiple comparisons (MCT). Data are represented as mean +/- SEM, in n=3 experiments.

Taken together, these data suggest that although the influence of *MIAT* down-regulation on the short-term survival of neuroblastoma cells is minimal, the long-term survival and migratory ability of the cells are significantly reduced, while a ~3-fold increase in apoptosis is observed.

Similar to the SH-SY5Y cells, an unexpected change in morphology was observed in the 1321N1 cells as well, giving a lead to assess the cells' migration ability using the wound healing assay. The results provided again confirmation that the ability of cells to migrate is radically reduced upon the silencing of *MIAT* at both 18h and 24h for all the three *MIAT*-specific siRNAs. Specifically, there was significantly less gap closure, with the greatest results being observed after 24h for MIAT_2 (~38% less gap closure) and MIAT_3 (~37% less gap closure) (Figure 3.12).

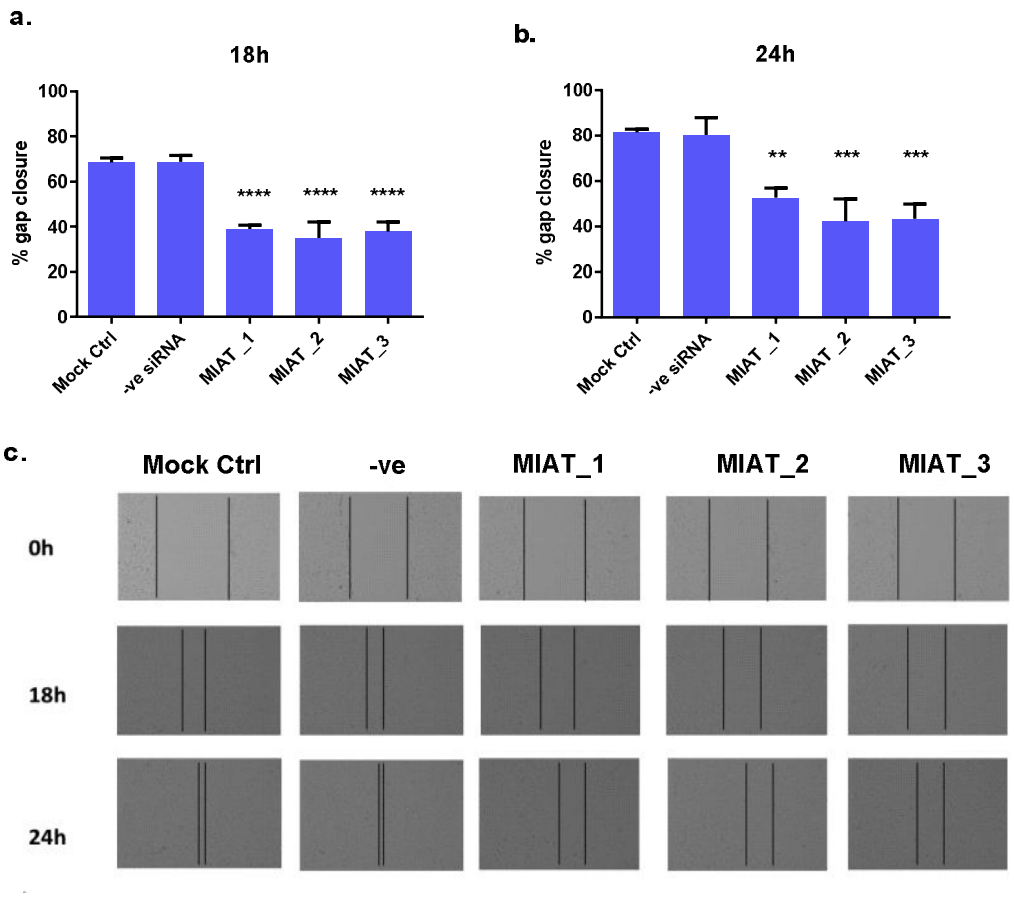

Figure 3.12. *MIAT*-specific down-regulation reduces the migratory ability of 1321N1. 1321N1 cells were transfected with the negative siRNA or one of the three *MIAT*-specific siRNAs using Nucleofection, plated, and a linear scratch was introduced 24 h post-plating. The % gap closure of the scratch was measured after 18 and 24h. The migrating ability of the cells is overall reduced for all three *MIAT*-specific siRNAs at both time points assessed, especially for MIAT_2 and MIAT_3 at 24 h (a); relative gap closure of *MIAT*-specific siRNAs versus the –ve siRNA (b); representative illustration of a wound healing ("scratch") assay (c); ** indicate a *p-value*<0.01; ***/**** indicate a *p-value*<0.001, as measured by One-way ANOVA tests with multiple comparisons (MCT). Data are represented as mean +/- SEM, n=3 experiments.

Finally, to be able to generalise the influence of *MIAT* down-regulation on cell migration, and following the same rationale we followed for the other two cell lines, the migratory activity of the T98G cells upon *MIAT* knockdown was assessed next. The wound healing assay results have shown that the ability of the cells to migrate is affected by the downregulation of *MIAT* in this case, as well. In detail, the invasive ability of T98G cells is decreased following the downregulation of *MIAT* by all three *MIAT*-specific siRNAs. This effect is again observed at both time points tested (18 and 24h). Specifically, the greatest results were observed after 18h for MIAT_2 (~38% less gap closure), reaching a magnitude greater than the one observed for SH-SY5Y cells, and equivalent to this of the 1321N1 cells (Figure 3.13).

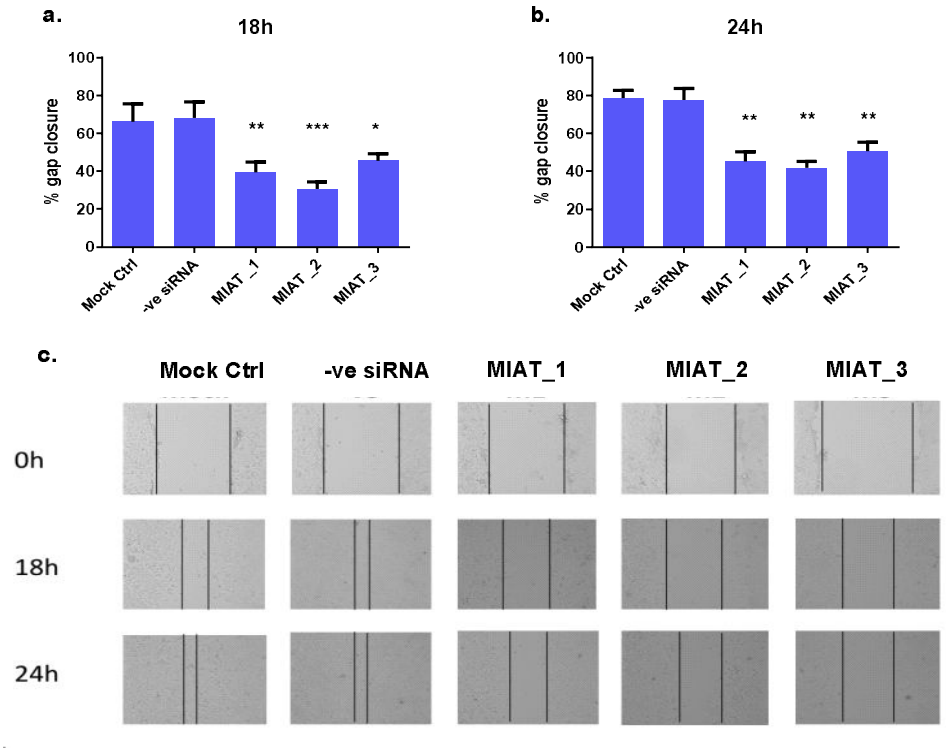

Figure 3.13. *MIAT*-specific down-regulation reduces the migrating ability of T98G. T98G cells were transfected with the negative siRNA or one of the three *MIAT*-specific siRNAs using nucleofection, plated, and a linear scratch was introduced 24 h post-plating. The % gap closure of the scratch was measured after 18 and 24 h. The migrating ability of the cells is tremendously reduced for all three *MIAT*-specific siRNAs at both time points assessed, especially for MIAT_2 (a); relative gap closure of *MIAT*-specific siRNAs versus the –ve siRNA (b); representative illustration of a wound healing ("scratch") assay (c);. * indicates a *p-value*<0.05; ** indicate a *p-value*<0.01; *** indicate a *p-value*<0.001, as measured by One-way ANOVA tests with multiple comparison tests (MCT). Data are represented as mean +/- SEM, n=3 experiments.

3.4. Discussion

MIAT has lately been the subject of intense research and a growing body of evidence is suggesting its role as an oncogenic lncRNA in multiple tumours. For example, it has been shown that *MIAT* is involved in CLL and DLBL (Diffuse Large B-Cell Lymphoma) (Sattari *et al.*, 2016), multiple types of breast cancer (Almnaseer and Mourtada-Maarabouni, 2018; Li *et al.*, 2018; Zhang *et al.*, 2019; Liu *et al.*, 2019), gastric cancer (Zhang *et al.*, 2013; Pop *et al.*, 2018), clear cell renal cell carcinoma (Qu *et al.*, 2018; Zhang *et al.*, 2019), osteosarcoma (Zhang *et al.*, 2019), lung cancer (Fu *et al*., 2018; Zhang *et al*., 2019), neuroendocrine prostate cancer (Crea *et al*., 2016), papillary thyroid cancer (Liu *et al.,* 2019) and intrahepatic cholangiocarcinoma (Zhou *et al.*, 2019), and it has been proved to be the most abundant lincRNA in NB, as well as a central expression modulator of both *MYCN* and *PHOX2B* (Rombaut *et al.*, 2019), two of the most critical genes for NB. Therefore, *MIAT* could become a tool of diagnostic, prognostic and even therapeutic value for these tumours.

In order to extrapolate the role of *MIAT* in NB and GBM, a series of functional assays were performed to evaluate the influence of its silencing on fundamental cell processes, such as basal cell survival and apoptosis, as well as cell migration. To this end, this chapter aimed at unravelling the role of *MIAT* in the regulation of these processes in neuroblastoma and glioblastoma. To perform this, a siRNA-mediated *MIAT* down-regulation approach was adopted followed by a GapmeR-mediated confirmation approach, using one neuroblastoma (SH-SY5Y) and two GBM (1321N1 and T98G) cell lines, which led to a variety of interesting observations. Although the silencing of *MIAT* did not affect the short-term survival, it caused a significant decrease in the long-term survival and the migratory ability of the cells, and substantially increased the levels of basal apoptosis, suggesting that *MIAT* is a new lncRNA player in cell fate decisions in neuroblastoma and glioblastoma. The GapmeR-mediated approach returned results similar to those of the siRNA-mediated approach; however, the effects observed with the GapmeRs were weaker and in some cases insignificant. In

general, both siRNAs and GapmeRs are considered to be very potent silencers of gene expression, although the concentrations required to obtain the same effect may differ (Grünweller *et al.*, 2003) depending on the cellular location of the lncRNA and its transcriptional landscape (Lennox and Behlke, 2016). In addition, although ASOs are considered to be more effective in knocking down nuclear lncRNAs compared to siRNA (Lennox and Behlke, 2016), this was not the case in this study, potentially due to the localisation of *MIAT* special subnuclear bodies. Given that the effects of ASOs tend to be rather short-lived, it can be speculated that higher concentration of GapmeRs is essential in order to prolong their effects so that they are better reflected in the observed phenotypes (Watts and Corey, 2012; MacLeod and Crooke, 2017).

Interestingly, these results have confirmed the oncogenic properties of *MIAT* in our systems, i.e. in neuroblastoma and GBM cells, as revealed by an overall tendency of *MIAT*-specific siRNA- and LNA GapmeR-mediated knockdown to cause reduced long-term cell viability and a significant increase of the apoptosis levels in all the tested cell lines. These effects are in full agreement with several previous studies investigating the role of *MIAT* in the regulation of cell survival. For instance, the *in vitro* silencing of *MIAT* leads to reduced cell viability and increased levels of basal apoptosis in endothelial cells, Müller glia and neurons upon hypoxic or oxidative stress, as well as *in vivo*, as studied in oxygen-induced retinopathy (OIR), optic nerve transection (ONT), Alzheimer's disease and diabetic retinopathy mouse and rat models, causing neurovascular dysfunctions ultimately leading to these neurodegenerative disorders (Jiang *et al.*, 2016). Furthermore, Shen *et al.* (2016) found that the down-regulation of *MIAT* leads to reduced survival of lens epithelial cells in cataract patients as a result of augmented ROS production. In a cancerous context, Sattari *et al*. (2016) discovered that siRNA-mediated suppression of *MIAT* expression led to increased apoptosis in a Diffuse Large B-Cell Lymphoma cell line. Recently, another recent study has also revealed augmented basal apoptosis levels in various breast cancer cell lines representing different types of breast tumours in response to *MIAT* down-regulation

(Almnaseer and Mourtada-Maarabouni, 2018), while another study has shown that overexpression of *MIAT* promotes tumour cell growth in ER-positive breast cancer cells (Li *et al.*, 2018). Moreover, in lung cancer cells the knockdown of *MIAT* results in increased apoptosis, as revealed by elevated levels of the pro-apoptotic Bax and cleaved Caspase 3, as well as decreased levels of the anti-apoptotic BCL-2 (Fu *et al.*, 2018), and the same effect is also present for colorectal cancer cells (Liu *et al.*, 2018) and gastric cancer cells (Li *et al.*, 2017). In line with this, another study has revealed that the silencing of *MIAT* expression increases apoptosis as measured by flow cytometry, and also reduces long-term survival, as measured by colony forming assays non-small cell lung cancer cells, in full agreement with our results (Wu *et al.,* 2020). At the same time, colony formation has been shown to be decreased in human papillary thyroid cancer cell lines (Wang *et al.*, 2019) and clear cell renal cell carcinoma (Qu *et al.*, 2018), while increased apoptosis is a phenomenon also observed in osteosarcoma (Zhang *et al.*, 2019) and ovarian cancer cell lines (Shao *et al.*, 2018).

Notably, the effect on long-term survival was not very pronounced in all cases, whereas apoptosis was significantly affected. Cancer is a complex disease in which there exist numerous pathway cross-talks. There is a variety of cell growth, proliferation and pro-survival pathways that could potentially be affected following *MIAT* downregulation to confer the observed phenotypes. For instance, the overlapping MAPK, TGF-β and EGFR pathways could be downregulated, and as a result, the long-term cell survival of neuroblastoma and GBM cells would be decreased. The PI3K/Akt pathway, as a part of the MAPK/ERK signalling cascade, could be suspected to exert a crucial role. In fact, all of these pathways have been established to be classical cancer-related pathways responsible for cell survival, growth and motility in several tumours (Babu and Tay, 2019). Furthermore, a recent study has shown that the down-regulation of another well-known lncRNA, *H19*, leads to the inactivation of the MAPK/ERK pathway by reducing the expression levels of p-MAPK and p-ERK1/2 in HCC (hepatocellular carcinoma) (Ding *et al.*, 2018), raising the

possibility that *MIAT* could exert the same effect. In fact, another study conducted by Yang *et al*. (2019) in melanoma cancer cells has revealed the intriguing finding that *MIAT* can also up-regulate the phosphorylation of PI3K and Akt, thereby activating the pathway (Yang *et al.*, 2019), providing extra evidence to speculate that the pathway, and let alone its down-regulation, could be heavily involved in response to *MIAT* knockdown in NB and GBM cells.

Another ambiguous candidate that could mediate the observed phenotypes upon *MIAT* silencing is c-Myc, a master transcription factor responsible for transcribing a multitude of genes, mainly associated with cell survival, growth and proliferation. Nevertheless, many studies have established that when deregulated, c-Myc favours apoptosis over survival. More specifically, it participates in both the mitochondrial apoptotic pathway, therefore promoting apoptosis either through the suppression of anti-apoptotic molecules, mainly of the BCL-2 family, or through promoting the expression of pro-apoptotic molecules, and the death receptor apoptotic pathway (Hoffman and Liebermann, 2008; McMahon, 2014). Therefore, it could be hypothesised that short-term after *MIAT* knockdown, c-Myc is either repressed or exerts its unconventional, pro-apoptotic role and, that on the long-term, it remains repressed by mechanisms involving *MIAT*, to further prevent neuroblastoma and GBM cells from growing. In line with this hypothesis, *MIAT* has been found to up-regulate the expression of *c-Myc* in melanoma cells via the up-regulated phosphorylation of PI3K and Akt (Yang *et al.*, 2019). It has also been discovered that in HCC cells *MIAT* up-regulation is capable of up-regulating c-Myc through the EPHA2 (Ephrin Type-A Receptor 2) axis, suggesting another potential mechanism that could be implicated in neuroblastoma and GBM cells, as well (Xiang *et al.*, 2019). Meanwhile, another study has shown that the inhibition of the expression of c-*Myc* triggered *MIAT*'s significant up-regulation in GBM. In specific, Omomyc (a ninety amino acid long polypeptide obtained by targeted mutations of *c-Myc* bHLHZip domain)-mediated suppression of c-Myc led to the elevated expression – among others- of *MIAT* in glioblastoma stem cells (GSCs), thus mediating an onco-suppressive phenotype (Galardi *et al.*, 2016). Finally, given the fact that *c-Myc* is also

actively epigenetically regulated through various mechanisms including histone modifications and DNA methylation (O'Hagan *et al.*, 2011) and that, to at least some extent, the action of lncRNAs involves chromatin remodelling (Clark and Blackshaw, 2014; Schmitz *et al*., 2016), a possible scenario would be that *MIAT* also epigenetically regulates the expression of *c-Myc*. Taken together, it is clear that both *c-Myc* and *MIAT* display high versatility in terms of gene function and roles, and are involved in complex, potentially overlapping molecular networks, with effects ranging among various tumour types. Although it is becoming profound that *MIAT* exerts a crucial role in regulating cell survival and apoptosis, the exact mechanisms of action remain to be unveiled, and the potential feedback loops with c-Myc still need to be clarified in neuroblastoma and GBM cells. Finally, because ROS above a certain threshold exert a pro-apoptotic role, thereby inducing apoptosis instead of promoting cell survival, and that c-Myc is a sensor of fluctuations in ROS levels (Galadari *et al*., 2017; Lin, 2019), an attractive scenario would be that there is a *MIAT*/c-Myc/ ROS axis that determines whether cell survival or apoptosis will be favoured in neuroblastoma and GBM cells.

Our functional studies also revealed that the down-regulation of *MIAT* was associated with the attenuation of the migratory ability of neuroblastoma and GBM cells, as shown by the significant reduction in gap closure in wound healing assays. Prior functional annotation has implied that *MIAT* is associated with EMT-related canonical pathways in hepatocellular carcinoma cells, including the TGF-β pathway, and further *MIAT* knockdown resulted in the increase in the mRNA level of the epithelial marker E-cadherin and in decreased expression of the mesenchymal marker N-cadherin and deteriorated migratory and invasive capacity of HCC cells (Zhang *et al.*, 2018). Moreover, *MIAT* downregulation caused similar effects (suppressed expression of vimentin, β-catenin, N-cadherin and SNAI1, induced expression of E-cadherin) in tongue squamous cell carcinoma cells, effects speculated to be mediated by the Wnt/β-catenin axis, given that DKK1 (Dickkopf WNT Signaling Pathway Inhibitor 1- an inhibitor of the pathway) effectively reversed the effects *MIAT* on the

expression of EMT markers and the numbers of invasive cells (Zhong *et al.*, 2019). At the molecular level, both mechanisms could be mediating the reduced migration phenotype in our systems as well. Furthermore, in full concordance with our results, a plethora of other studies have also implicated *MIAT* in cell migration. For instance*, MIAT* knockdown has been shown to reduce the migration of NSCLC cells (Zhang *et al.*, 2017), colorectal cancer cells (Liu *et al.,* 2018), clear cell renal cell carcinoma cells (Qu *et al.*, 2018) and breast cancer cells (Alipoor *et al.*, 2018). In addition, similar effects have been reported in HCC (Xiang *et al.*, 2019), gastric (Li *et al.*, 2017), pancreatic (Li *et al.*,2018), papillary thyroid carcinoma (Liu *et al.*, 2019), melanoma (Yang *et al.*, 2019) and osteosarcoma cell lines (Zhang *et al.*, 2019), with all of the cases showing a markedly decreased ability of the tumour cells to migrate upon *MIAT* silencing. All of these pieces of evidence strongly suggest that *MIAT*, apart from being a cell survival and apoptosis regulator, is also a very potent mediator of cell migration. Given that cell migration comprises one of the first steps towards tumour metastasis, *MIAT* downregulation could be a potent therapeutic approach towards the prevention of metastasis. Mechanistically, this could be achieved by disrupting some of the suggested *MIAT*-involving metastasis-related axes, such as the miR-150-5p/VEGF axis (Jiang *et al.*, 2016), the miR-141/DDX5 pathway as described in gastric cells (Sha *et al.*, 2018), the miR-132/Derlin-1 pathway as described in CRC cells (Liu *et al.*, 2018), or through the *MIAT*/MMP9 axis (Lai *et al.*, 2017).

In conclusion, the current chapter suggests that the downregulation of *MIAT,* siRNA- or GapmeR-mediated, reduces the long-term survival of neuroblastoma and GBM cells, while it promotes basal apoptosis, as well as deteriorates the cells' ability to migrate. These findings highlight the crucial role of *MIAT* in a variety of cancer-promoting processes in neuroblastoma and glioblastoma pathogenesis, verifying its observed role in other tumours. Nevertheless, further research is essential in order to establish that *MIAT* could potentially be used as a biomarker in neuroblastoma and GBM, like numerous other lncRNAs in a variety of tumours (Melissari and Grote, 2016; Wu *et al.*, 2016; Rao *et al.*, 2017) and open

new prognostic, predictive and even therapeutic avenues for patients suffering from these tumours.

3.5. Chapter Highlights

1. **siRNA-mediated *MIAT* silencing does not significantly influence the short-term survival of neuroblastoma and GBM cells.**

2. ***MIAT* knockdown mediated by siRNA significantly reduces the long-term survival in SH-SY5Y, and 1321N1 and T98G cells.**

3. **siRNA-mediated *MIAT* down-regulation causes a significant ~3-fold increase in the levels of basal apoptosis in NB and GBM cells**

4. **siRNA-mediated *MIAT* silencing markedly attenuates the migratory ability of SH-SY5Y, and 1321N1 and T98G cells.**

5. **GapmeR-mediated *MIAT* silencing confirms the effects of siRNA-mediated silencing in long-term survival and apoptosis. However, the effects, in this case, are not as strong, as compared to the siRNA-induced effects.**

Chapter 4: RNA sequencing reveals the potential molecular mechanisms underlying the action of *MIAT*

4.1. Introduction

Mounting pieces of evidence suggest that lncRNAs can regulate gene expression in diverse ways along every step of it, including post-transcriptional processes, and notably, this regulation can be exerted *in cis* and *in trans* (Kornienko *et al.*, 2013; Bergmann and Spector, 2014; Cheng *et al.*, 2016; Ding *et al.*, 2018). In this context, post-transcriptionally during alternative splicing, lncRNAs can regulate the process via sponging essential for proper splicing factors, as in the case of *MALAT1* (Geisler and Coller, 2013) and *MIAT. MIAT* has been found to act by sequestering SF1, QK1, SRSF1 (Tsuiji *et al.*, 2011; Cheng *et al.*, 2016) and Celf3 (Ishizuka *et al.*, 2014), to obstruct normal alternative splicing.

In addition to its fundamental role in regulating alternative splicing by sponging splicing factors that are essential for proper splicing, *MIAT* is also known to function as a miRNA sponge to regulate gene expression and cell fate decisions through diverse axes. In non-cancerous context, *MIAT* has been found to sponge miR-150 to promote cardiac hypertrophy in cardiomyocytes and mouse models (Zhu *et al.*, 2016), as well as to sponge miR-93 to up-regulate toll-like receptor 4 (TLR4) to promote the same condition (Li *et al.*, 2018). Moreover, in diabetes mellitus-induced microvascular dysfunction *MIAT* functioned as a ceRNA to form a feedback loop with vascular endothelial growth factor (VEGF) and miR-150-5p to regulate endothelial cell function (Yan *et al.*, 2015) and as a sponge for miR-181b to regulate atherosclerosis progression via the regulation of STAT3 (Zhong *et al.*, 2018). The same ceRNA activity has also been discovered in cancerous settings. For instance, *MIAT* knockdown enhanced the expression of miR-214 to down-regulate its targets EZH2 and β-catenin, leading to decreased cell proliferation and migration in HCC (Huang *et al.*, 2018). Besides, again in a HCC model, it was discovered that *MIAT* acts as a decoy for miR-22-3p to up-regulate the expression of Sirt1 and that upon *MIAT* silencing cellular senescence was promoted via the activation of the tumour suppressor pathways p53/p21 and p16/pRb (Zhao *et al.*, 2019). Together with these, it also sponges miR-155-5p in breast cancer cells to up-regulate DUSP7 (Dual Specificity Phosphatase 7), while its

knockdown increases apoptosis and eliminates EMT to ultimately decrease cell invasion (Luan *et al.*, 2017). Finally, *MIAT* also acts as a ceRNA to sponge miR-141 in an AGO2-dependent manner via targeting DDX5 (DEAD-Box Helicase) in gastric cancer, and its silencing led to cell cycle arrest, apoptosis and decreased migration and invasion (Sha *et al.*, 2018). Finally, *MIAT* sequesters miR-132 to de-repress its target gene Derlin-1, and its down-regulation ultimately leads to reduced cell proliferation, migration and invasion in CRC cells (Liu *et al*., 2018).

The lines of evidence presented in Chapter 3 support the oncogenic nature of *MIAT*, given that its down-regulation increases the levels of apoptotic cell death and eliminates the long-term survival and the migratory ability of neuroblastoma and glioma cells. However, the molecular mechanisms through which *MIAT* exerts its functions remained an enigma. In line with this, this chapter aims to unveil the underpinning molecular mechanisms of *MIAT*'s effects in neuroblastoma cells via a siRNA-mediated knockdown approach followed by RNA sequencing. Through sequencing of the whole transcriptome, the study investigates gene expression changes and key molecular pathways modulated in response to altered *MIAT* levels.

4.2. Materials and Methods

4.2.1. Cell culture

The experiments incorporated in this chapter were conducted using the human neuroblastoma SH-SY5Y cell line and the human astrocytoma/ glioblastoma 1321N1 cell line, cultured using the HyClone™ DMEM/F12 1:1 growth media, supplemented with 10% heat-inactivated fetal bovine serum, 2μM L-Glutamine, 1μM Sodium Pyruvate and 10mg/ml gentamicin solution, as well as the human glioblastoma T98G cell line, cultured in the aforementioned growth media, supplemented with an extra 10% FBS, 15% cell-conditioned growth media and 1% MEM non-essential amino acid solution, as described in section 2.1.

4.2.2. RNA sequencing and Pathway analysis

Global gene expression changes in response to *MIAT* knockdown were determined by sequencing the whole transcriptome, as detailed in section 2.10. Next-generation sequencing was conducted by the Earlham Institute. Quality controlled reads were aligned to Human Genome build (hg19) using Tophat, transcripts were assembled using Cufflinks (with GTF support) and the number of reads mapping to each feature counted and expressed as FPKM using the CuffNorm package. Differentially expressed mRNAs were condensed into gene networks representing biological and disease processes using iPathwayGuide (Advaita Bioinformatics, Ann Arbor, MI, USA). The differential expression was measured and compared between SH-SY5Y cells transfected with the –ve control siRNA and SH-SY5Y cells transfected with *MIAT*-specific siRNAs, and a cutoff threshold of 1.5-fold change (and an equivalent 0.6 Log_2 Fold Change) was applied. The Log_2 Fold Change (Log_2FC) is referred to as "–fold change" in this chapter.

4.2.3. Target validation: mRNA level

Real-time PCR (RT-qPCR) and RT^2 Profiler PCR Arrays

The validation of changes in expression in several genes of interest was performed on the mRNA level via RT-qPCR and RT^2 Profiler PCR Arrays.

Total RNA was extracted from cells using the Direct-zol™ RNA MiniPrep kit, according to the manufacturer's protocol and the quality was measured with NanoDrop and gel electrophoresis (as detailed in sections 2.4 and 2.4.1). RNA extracted from transfected cells was then reverse transcribed into cDNA using the Omniscript® RT kit, as described in section 2.5.1. Real-time PCR was subsequently performed for the synthesised cDNA. Specific primers were used against *c-Myc* and *Oct1 (POU2F1),* while 18S rRNA was used as a housekeeping gene (Table 4.1), as described in section 2.5.2.

Two different Arrays were used: the RT² Profiler™ PCR Array Human Cell Death PathwayFinder and the RT² Profiler™ PCR Array Human Apoptosis, each one containing in total 84 genes (one/well) and 12 quality and endogenous controls, as detailed in section 2.5.3.

Table 4.1. TaqMan® gene expression assays' details.

Method	Catalogue #/ ID	Target	Exon boundary	Assay location
TaqMan®	**Hs99999901_s1**	*18S*	1-1	604
	Hs00153408_m1	*c-Myc*	2-3	1325
	Hs01552829_m1	*Oct1 (POU2F1)*	8-9	1013

4.2.4. Target validation: protein level

The validation of changes in expression in several genes of interest was performed on the protein level via Western Blot, as detailed in sections 2.12.1 and 2.12.2. The proteins whose level was measured include Mcl1, Caspase 8, XIAP, BAD and BID, while β-actin was used as a housekeeping gene (Table 2.9).

4.2.5. Assessment of Reactive Oxygen Species (ROS) production

The production of ROS as part of the apoptotic response upon the down-regulation of *MIAT* in 1321N1 and T98G cells was measured by flow cytometry using the CellROX® Green Reagent. 1321N1 cells and T98G cells were nucleofected with either the Negative control siRNA or MIAT_2 and subsequently, the levels of ROS production were assessed after 48 h and 72 h, as detailed in section 2.11.1.

Alpha-phenyl-N-tert-butyl nitrone (PBN), a free radical scavenger was used to assess ROS levels in SH-SY5Y cells. After a series of optimisation experiments, it was shown that the most efficient scavenger was the administration of 600μM PBN in a sequential way (described in section 2.11.2).

4.2.6. Functional analysis: determination of cell survival, apoptosis and cell migration

In response to ROS scavenging, **cell survival** was assessed using the MTS assay (CellTiter 96® Aqueous One Solution Cell Proliferation Assay), as described in sections 2.6.3 and 2.11.2. **Cell death via apoptosis** was assessed after 8, 24 or 48 h with fluorescence microscopy after staining of the cells acridine orange (25μg/ml), as described in section 2.7.2

The **migratory ability** of the cells was assessed by the wound healing assay (detailed in section 2.9.). The gaps were measured using the EVOS FL Cell Imaging System at 0/24/48 h and the gap closure was calculated using the formula **[(Pre-migration)area-(Migration)area/(Pre-migration)area] x100** for 15 measurements per sample. Image analysis was performed using the ImageJ software.

4.2.7. Statistical analysis

Statistical analyses were performed using GraphPad Prism 6 (GraphPad Software). Data are presented as the mean ± SEM; the number of observations (n) refers to different transfected samples, each transfection being conducted on a separate culture of cells. Comparisons were made using an unpaired T-test or One-Way ANOVA with Bonferroni's multiple comparison test (MCT). Where multiple parameters were compared, Two-Way ANOVA with Sidak, Tukey or Dunnett multiple comparisons was used. Statistical significance was set at the 0.05 level. Differences were considered as statistically significant when the *p-value* was <0.05 (95% confidence intervals). The RT^2 Profiler PCR Array analysis was performed using QIAGEN's Data Analysis web portal (geneglobe.qiagen.com/gb/analyze/). The RNA sequencing results were analysed using the iPathway Guide by Advaita Bioinformatics (advaitabio.com).

4.3. Results

4.3.1. RNA Sequencing reveals ROS-mediated molecular and biological perturbations upon *MIAT* down-regulation in SH-SY5Y cells

In order to elucidate the molecular mechanisms through which *MIAT* exerts its biological effects, RNA sequencing was performed and the genes that exhibited the most pronounced expression changes in response to *MIAT* knockdown were identified. Global gene expression analysis revealed that the two *MIAT* knockdown experiments (MIAT_2 and MIAT_3) did not perform equally, with very pronounced effects of the MIAT_2 siRNA noted in comparison with almost non-existent effects of the MIAT_3 siRNA, due to the fact that MIAT_3 siRNA knockdown did not lead to the desired down-regulation levels of MIAT in these specific experiments (Figure 4.1a).

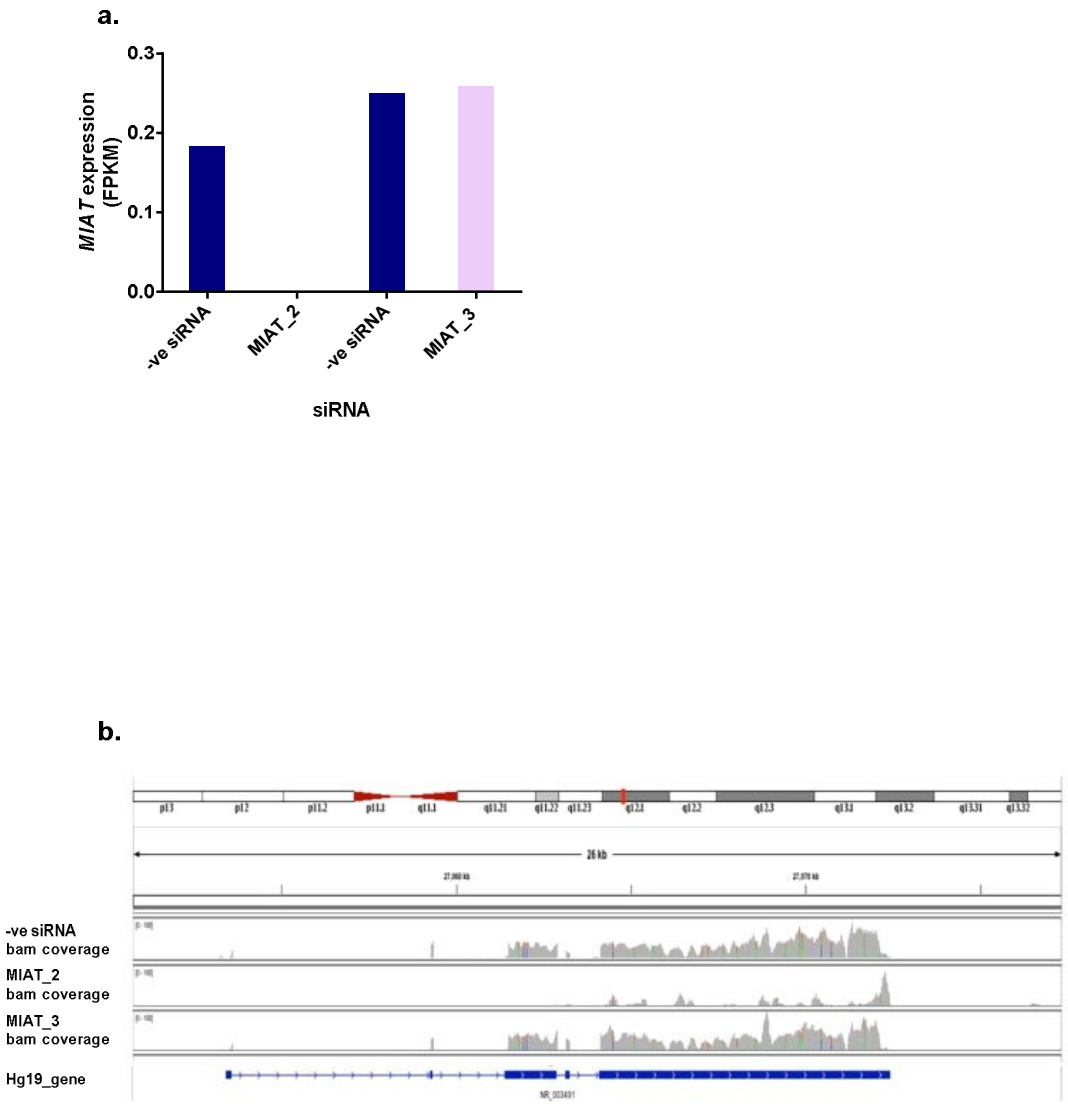

Figure 4.1. Expression values of *MIAT*. Data are expressed as Fragments Per Kilobase of transcript per Million mapped reads (FPKM) for the full-length *MIAT* transcript [NR_003491 (10193 bp)] (a); MIAT sequence coverage in the different samples (b); -ve: negative siRNA; browser view from RefSeq on the GRCh38.p13 primary assembly [Integrative Genomics Viewer (IGV)]

Given the superior effects of our MIAT_2 knockdown siRNA, we next investigated those genes that were deregulated by a factor of at least 1.5 fold ($log_2FC \geq 0.6$) between the control and MIAT_2 knockdown samples. 11085 differentially expressed genes were identified out of a total of 13412 genes with measured expression, of which the 10000 most variable in response to reduced *MIAT* levels are presented as a heatmap (Figure 4.2). These data were analyzed in the context of pathways obtained from the Kyoto

Encyclopedia of Genes and Genomes (KEGG) database (Release 81.0+/01-20, Jan 17), gene ontologies from the Gene Ontology Consortium database, and miRNAs from the miRBase (Release 21) and TARGETSCAN (Targetscan version: 7.1) databases.

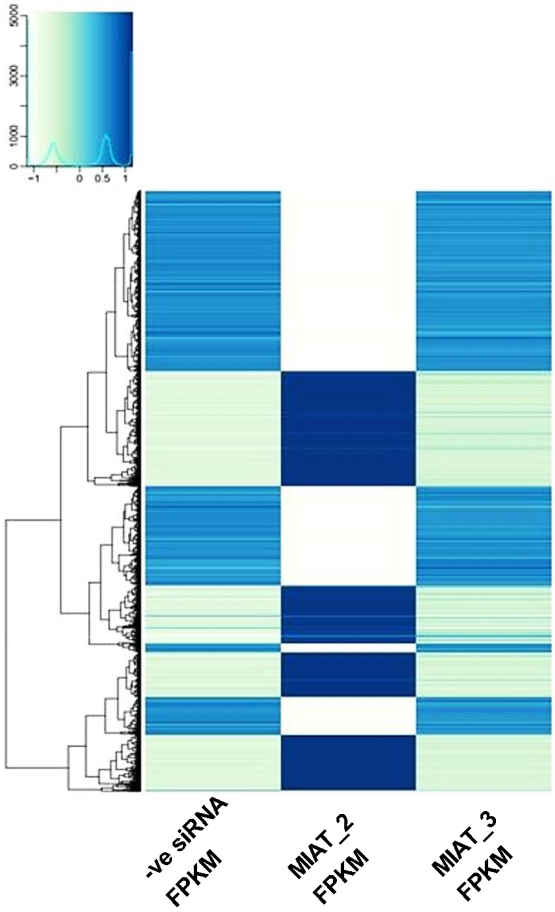

Figure 4.2. *MIAT* down-regulation induces extensive expressional perturbations. Heatmap of Log_2 normalised expression values for the 10000 most variable genes. Data are Log normalised read counts expressed as Fragments Per Kilobase of transcript per Million mapped reads (FPKM). Dark blue colouration represents higher expression, whilst light green colouration denotes lower expression for each given gene. Y-axis clustering identifies groups of genes with similar expression patterns. The key (top left) represents the density of data (y) against expression level (x); -ve: negative siRNA.

As an excess of 10000 genes was identified as being deregulated by at least 1.5 fold, we elected to condense the individual gene changes into common biological processes and pathways prior to interpretation. Pathway analysis revealed that several cellular processes were affected by the downregulation of *MIAT*. Among them, numerous cancer-related processes were significantly affected, including apoptosis-mediated cell death, oxidative stress, cell migration, angiogenesis and autophagy. These perturbations were also reflected in the corresponding molecular pathways. Eight pathways were found to be significantly impacted and of these, three were cancer-independent (Alcoholism, Vascular smooth muscle contraction and Ribosome), while five were cancer-related: MAPK signalling pathway, EGFR tyrosine kinase inhibitor resistance, TGF-beta signalling pathway, Phospholipase D signalling pathway and NOD-like receptor signalling pathway (Table 4.2). In these cell survival- and apoptosis-related pathways, a plethora of genes displayed aberrant expression (168, 63, 59, 88 and 103 differentially expressed genes, respectively). Figure 4.3 shows the expression of genes implicated in each of these five pathways. Figures 4.4a and 4.4b, c graphically represent the most deregulated pathways, and the most deregulated cancer-related pathway, respectively.

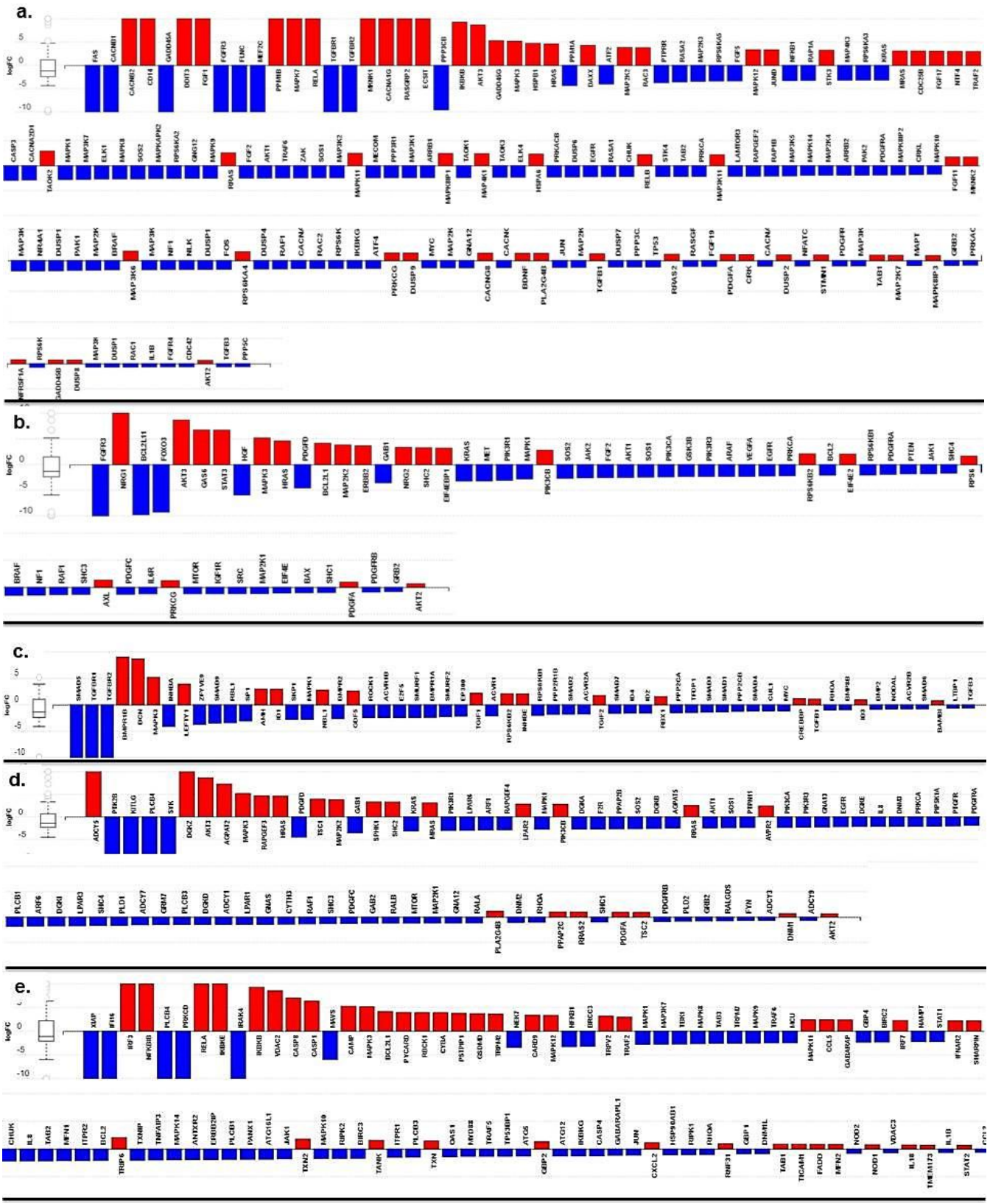

Figure 4.3. The expression of individual genes implicated in cancer-related pathways: MAPK signalling (a), EGFR tyrosine kinase inhibitor resistance (b), TGF-beta signalling (c), Phospholipase D signalling (d) and NOD-like receptor signalling (e), as determined by sequencing and analysis of the whole transcriptome. Red coloured bars correspond to up-regulated gene expression, while blue coloured bars correspond to down-regulated gene expression. Data are the difference in expression between cells nucleofected with the –ve siRNA and cells nucleofected with MIAT_2 expressed as a normalised log_2 fold change (log_2FC). A threshold of 0.05 for statistical significance (*p-value*) and a log_2 fold change of expression with an absolute value of at least 0.6 were applied.

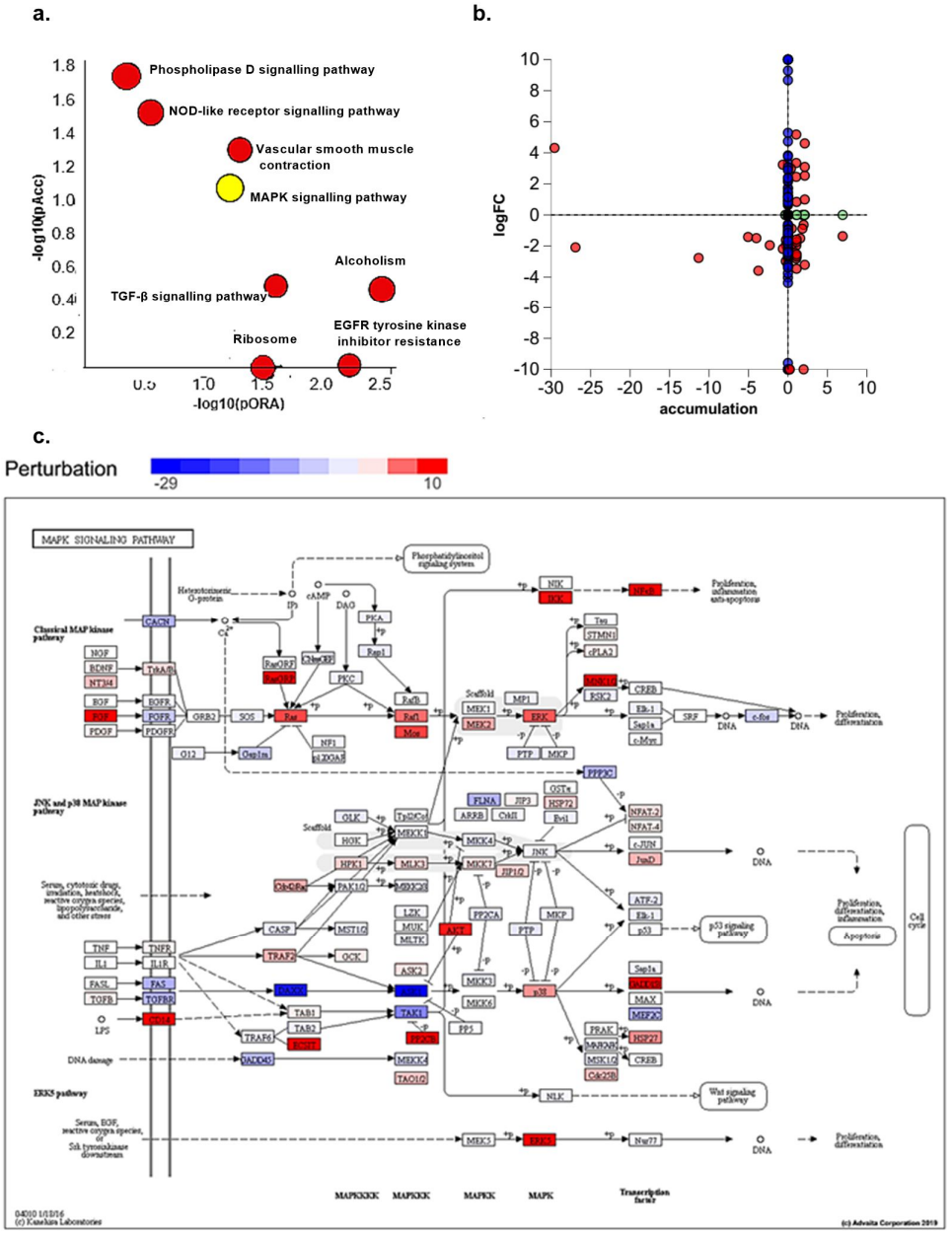

Figure 4.4. Top perturbed cancer-related pathway: MAPK signalling pathway (KEGG: 04010). Perturbation vs over-representation: MAPK signalling pathway (yellow circle) is shown, using negative log of the accumulation and over-representation p-values, along with the other most significant pathways (red circles). Pathways in red are significant, based on the combined uncorrected *p-values* (a). Measured expression vs accumulation of pathway genes: all the genes from this pathway are represented in terms of their measured fold change (y-axis) and accumulation (x-axis). Accumulation is the perturbation received by the gene from any upstream genes. Genes displayed in red had both accumulation and measured fold change. Genes in blue had only measured fold change. Genes in green had only accumulation. The remaining genes that were not measured and had no accumulation are shown in black. (b). Graphically, the pathway diagram is overlayed with the computed perturbation of each gene. The perturbation accounts both for the gene's measured fold change and for the accumulated perturbation propagated from any upstream genes (accumulation). The highest negative perturbation is shown in dark blue, while the highest positive perturbation in dark red. The legend describes the values on the gradient (c).

Table 4.2 Top differentially expressed pathways in response to *MIAT* down-regulation in SH-SY5Y cells and their biological relevance to cancer.

Pathway name	Upregulated Genes	Downregulated Genes	Cancer Hallmark	Oncogene/ TSG	(*p-value*)
MAPK signalling pathway	*DDIT3*		Sustaining Proliferative Signalling/ Resisting Cell Death/ Activating Invasion and Metastasis	Oncogene/TSG	0.032
		c-Myc	Evading Growth Suppressors	Oncogene/TSG	
		FAS	Resisting Cell Death	Oncogene	
		GADD45A	Evading Growth Suppressors/ Resisting Cell Death	Oncogene/TSG	
		DAXX	Resisting Cell Death	TSG	
EGFR tyrosine kinase inhibitor resistance	*NRG1*		Sustaining Proliferative Signalling	Oncogene	0.035
	HRAS		Evading Growth Suppressors	Oncogene	
	AKT3		Resisting Cell Death	Oncogene	
	STAT3		Sustaining Proliferative Signalling/ Resisting Cell Death/ Activating Invasion and Metastasis/ Inducing Angiogenesis	Oncogene	
TGF-beta signalling pathway	*DCN*		Inducing Angiogenesis/ Avoiding Immune Destruction	TSG	0.046
		SMAD5	Evading Growth Suppressors	TSG	
		TGFBR1/2	Evading Growth Suppressors	TSG	
Phospholipase D signalling pathway	*HRAS*		Evading Growth Suppressors	Oncogene	0.046
	MAPK3		Sustaining Proliferative Signalling	Oncogene	
		SYK	Evading Growth Suppressors/ Resisting Cell Death	Oncogene/TSG	
NOD-like receptor signalling pathway	*CASP1/8*		Resisting Cell Death	TSG	0.048
	IKBKB/E		Sustaining Proliferative Signalling/ Resisting Cell Death/ Activating Invasion and Metastasis	Oncogene	
	RELA		Sustaining Proliferative Signalling/ Resisting Cell Death/ Activating Invasion and Metastasis	Oncogene	
	VDAC2		Resisting Cell Death	TSG	
		XIAP	Resisting Cell Death	Oncogene	

In addition, 387 Gene Ontology (GO) terms were significantly enriched, including a variety of cancer-related processes, as well as multiple molecular functions (Table 4.3). Noteworthy, among the perturbed pathways and biological processes as revealed by the RNA sequencing, cell survival- and cell growth-associated pathways, such as the MAPK and EGFR pathways, as well as apoptosis-related pathways and processes (e.g. the NOD-like receptor signalling pathway, “Cell death in response to oxidative stress”, “Cellular response to oxidative stress” and “Regulation of oxidative stress-induced intrinsic apoptotic signalling pathway”) and migration/invasion-associated processes, such as “Tissue migration”, “Regulation of cell adhesion mediated by integrin” and “Regulation of cell migration”, were significantly deregulated. Importantly, the most perturbed biological process, “Cell death in response to oxidative stress”, displayed expressional perturbations in 58/59 involved genes, while another highly altered process, “Regulation of oxidative stress-induced intrinsic apoptotic signalling pathway”, had 25/26 genes perturbed. In addition, “Regulation of MAPK cascade” involved 393/446 perturbed genes, and at the same time “Regulation of cell migration” displayed changes in 411/480 genes involved in the process. Furthermore, in “angiogenesis” 250/285 genes involved had aberrant expression. Collectively, these results provide a confirmation of the effects of *MIAT* silencing on long-term survival, apoptosis and migration, as these were observed in the experimental series described in Chapter 3 since they show that multiple molecular pathways related to these phenotypes are perturbed.

Table 4.3. Top perturbed Gene Ontology (GO) terms in response to down-regulation in SH-SY5Y cells.

Biological Process	Upregulated Genes	Downregulated Genes	Cancer Hallmark	Oncogene/ TSG	Number of perturbed genes/ total genes in the pathway	(*p-value*)
ROS-induced cell death						
Cell death in response to oxidative stress	*MAPK7*	*HIF1A*	Sustaining Proliferative Signalling/ Resisting Cell Death/ Activating Invasion and Metastasis Sustaining Proliferative Signalling/ Inducing Angiogenesis/ Deregulating cellular energetics	Oncogene Oncogene	58/59	1.800e-4
Cellular response to oxidative stress	*ETS1* *RELA*		Resisting Cell Death/ Activating Invasion and Metastasis/ Inducing Angiogenesis Sustaining Proliferative Signalling/ Resisting Cell Death/ Activating Invasion and Metastasis	Oncogene Oncogene	155/173	0.008
Regulation of cellular response to oxidative stress		*FUT8* *MCL1*	Activating Invasion and Metastasis Resisting Cell Death	Oncogene Oncogene	46/49	0.021
Regulation of oxidative stress-induced intrinsic apoptotic signalling pathway		*XIAP* *BAG5*	Resisting Cell Death Resisting Cell Death	Oncogene Oncogene	25/26	0.046
Cell survival						
Regulation of MAPK cascade	*ADAM8* *FGF1*		Inducing Angiogenesis/ Activating Invasion and Metastasis Evading Growth Suppressors/ Inducing Angiogenesis	Oncogene Oncogene	393/446	8.400e-4

	HRAS	*FAS* *GADD45A*	Evading Growth Suppressors Resisting Cell Death Evading Growth Suppressors/ Resisting Cell Death	Oncogene Oncogene Oncogene/TSG		
Cell migration						
Tissue migration	*FGF1* *CDH13* *TGFBR1/2*		Evading Growth Suppressors/ Inducing Angiogenesis Sustaining Proliferative Signalling /Evading Growth Suppressors/ Resisting Cell Death/ Activating Invasion and Metastasis Evading Growth Suppressors	Oncogene TSG TSG	149/165	0.004
Regulation of cell adhesion mediated by integrin	*MUC1*	*SYK* *ITGAV*	Activating Invasion and Metastasis Evading Growth Suppressors/ Resisting Cell Death Sustaining Proliferative Signalling/ Activating Invasion and Metastasis	Oncogene Oncogene/TSG Oncogene	40/42	0.016
Regulation of cell migration	*ADAM8* *NRG1* *TERT* *LAMA4*		Inducing Angiogenesis/ Activating Invasion and Metastasis Sustaining Proliferative Signalling Enabling Replicative Immortality Inducing Angiogenesis/ Activating Invasion and Metastasis	Oncogene Oncogene Oncogene Oncogene	411/480	0.045

4.3.2. RNA Sequencing reveals perturbations of the non-coding elements upon *MIAT* down-regulation in SH-SY5Y cells

Given the importance of lncRNAs in cellular and molecular functions, perturbations of the non-coding genome were investigated next. The RNA sequencing analysis revealed that apart from the perturbations in protein-coding genes and pathways, numerous and significant changes in expression were observed in the non-coding repertoire, as well. In particular, 502 lncRNAs were found to be deregulated upon *MIAT* knockdown (Supplementary Table 1, Appendix II), belonging to various subcategories: 41% fell within the NAT subclass, while 20% were lincRNAs and 17% were pseudogenes, as shown in Figure 4.5. Markedly, most of the most highly deregulated ones have been associated with cancer (Figure 4.5, highlighted in green). Interestingly, the tumour suppressor *CASC2*, which was among the top deregulated lncRNAs, has already been associated with a wide variety of tumours, while *ZNFX1-AS1*, one of the most upregulated lncRNAs has been attributed a dual role, depending on the cancer type (Wang *et al.*, 2016; Shi *et al.*, 2019). Furthermore, the oncogenic *TP73-AS1*, implicated in numerous cancers, was ~6-fold upregulated, although at the same time the tumour suppressor *TP73* was also ~10-fold upregulated. *MIR22HG*, a well-studied tumour suppressive lncRNA in a variety of cancers, was also found to be deregulated in response to *MIAT* knockdown. Finally, of note is the fact that the expression of *HIF1A-AS2,* the NAT of *HIF1A*, a transcription factor that tightly regulates cellular responses in hypoxic conditions, was found to be ~4.5-fold increased, while the expression of *HIF1A* itself was decreased ~3-fold upon *MIAT* knockdown, suggesting a potential role of *MIAT* in the regulation of transcript/NAT pairs.

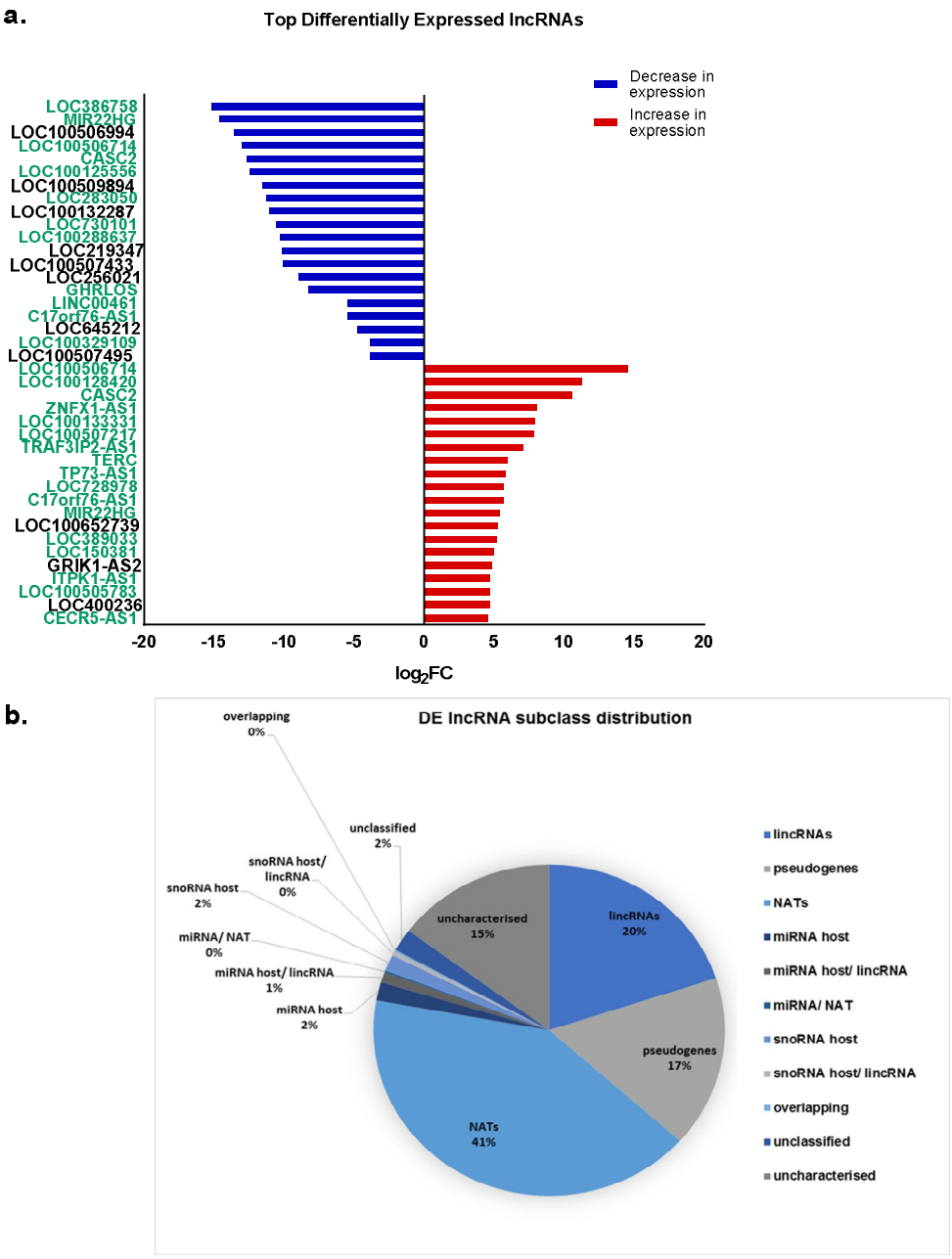

Figure 4.5. The effect of *MIAT* down-regulation on lncRNA expression of SH-SY5Y cells. The knockdown of *MIAT* induces alterations in the expression of several lncRNAs. The bar chart presents only the top perturbed genes in both directions (a). Red coloured bars correspond to up-regulated gene expression, while blue coloured bars correspond to down-regulated gene expression. Data are the difference in expression between cells nucleofected with the –ve siRNA and cells nucleofected with MIAT_2 expressed as a normalised $\log_2$ fold change ($\log_2$FC). A threshold of 0.05 for statistical significance (*p-value*) and a log fold change of expression with an absolute value of at least 0.6 were applied. The pie chart schematically presents the distribution of differentially expressed lncRNAs into different lncRNA subclasses (b); lncRNAs highlighted in green represent cancer-related lncRNAs; **DE**: differentially expressed; **NAT**: Natural Anti-sense Transcript; **lincRNA**: Long Intergenic RNA; **miRNA host**: microRNA host gene; **snoRNA host**: small nucleolar RNA host gene.

Furthermore, the expression of 263 miRNAs was predicted to be perturbed in response to *MIAT* down-regulation (Supplementary Table 2, Appendix II). Notably, miR-124, which is predicted to be the most deregulated miRNA, is a known tumour suppressor miRNA and targets important for tumour progression genes, such as *Smad5, Abl2* and the transcription factor Oct1. On the contrary, the oncomirs miR-27a/b, which are also predicted to be highly perturbed, target important anti-apoptotic molecules such as XIAP, as well as CDK6 and the *MIAT*-related splicing factor QK1.

4.3.3. RNA Sequencing reveals *MIAT* –mediated *in cis* regulation in SH-SY5Y cells and regulation of splice variant relative abundance

LncRNAs are potent regulators of gene expression both *in cis* and *in trans.* In line with this, after we established the effect of the down-regulation of *MIAT* on global gene expression, we were then prompted to explore this effect *in cis,* and, therefore, we sought expressional changes in genes located on the same chromosome as *MIAT* (chromosome 22). The analysis of the RNA sequencing results showed that an astonishing 334 neighbouring genes were differentially expressed in response to *MIAT* knockdown, including in the vast majority protein-coding genes (310), but also multiple lncRNAs (24), as depicted in Figure 4.6 (and Supplementary Table 3, Appendix II). Among them, the most upregulated (17-fold), PARVB- a focal adhesion protein, has been associated with tumour progression in colorectal cancer (Bravou *et al.*, 2015), but also with inhibition of tumourigenicity in breast cancer (Johnstone *et al.*, 2008). In addition, the miRNA biogenesis machinery component DGCR8 (DiGeorge Syndrome Critical Region gene 8), which has been attributed oncogenic properties, was up-regulated ~5-fold, a fact that could partially explain the perturbations in miRNAs. In line with the elevated levels of apoptosis induced due to *MIAT* knockdown, the pro-apoptotic BID and BIK were shown to be ~2-fold upregulated. Interestingly, *MIAT*

seems to be responsible for the simultaneous regulation of protein-coding/NAT pairs on chromosome 22, as in the case of *NUP50* (Nucleoporin 50) and *NUP50-DT* (*LOC100506714*), *PPARA* (Peroxisome Proliferator-Activated Receptor Alpha) and *MIRLET7BHG (linc-PPARA), CHKB* (Choline Kinase Beta) *and CHKB-AS1,* and *MIF* (Macrophage Migration Inhibitory Factor) and *MIF-AS1.*

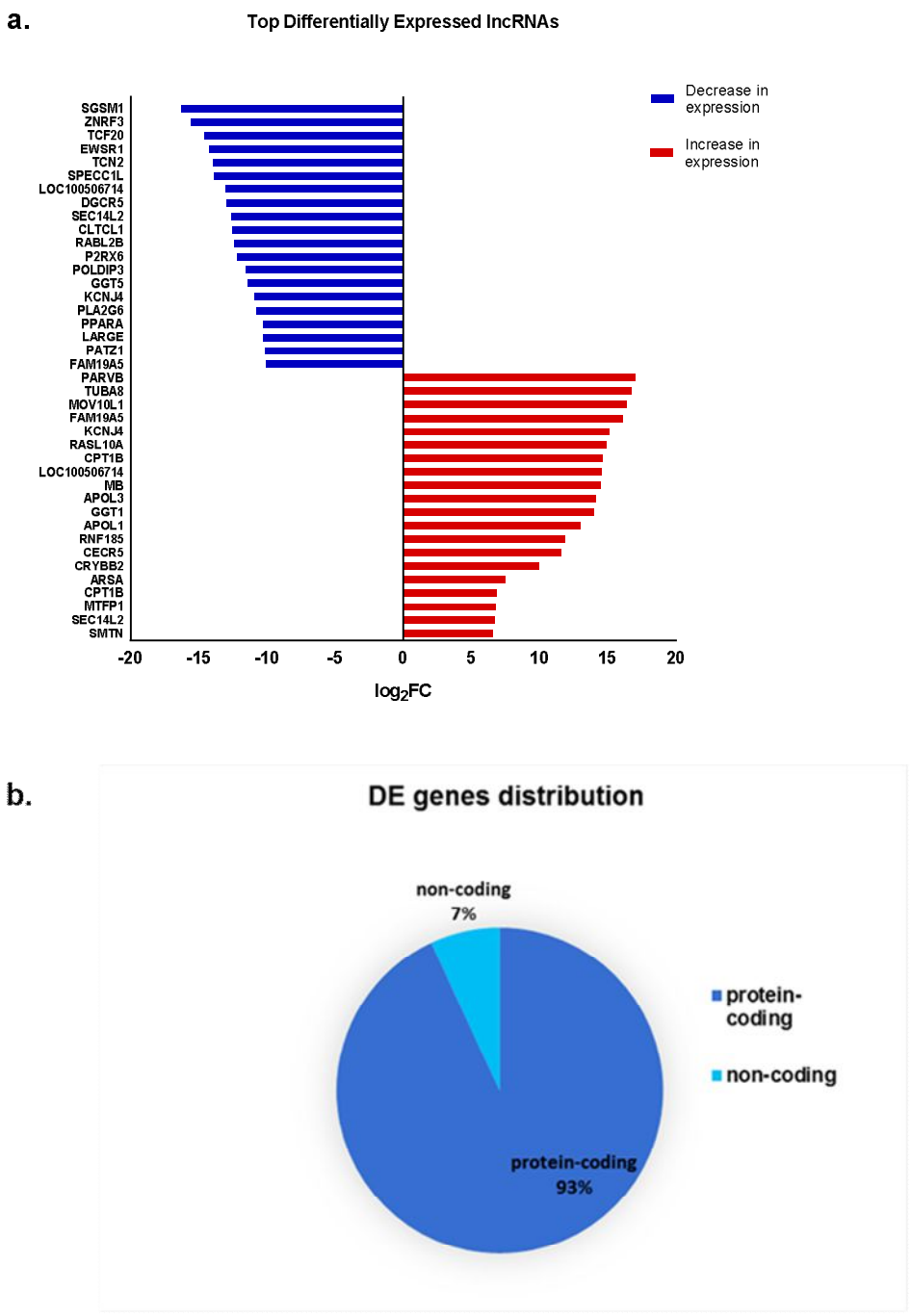

Figure 4.6. *MIAT* down-regulation acts in cis to induce perturbations in gene expression on chromosome 22. Top perturbed genes on chromosome 22 upon *MIAT* knockdown, including protein-coding genes and lncRNAs. Red coloured bars correspond to upregulated gene expression, while blue coloured bars correspond to downregulated gene expression. Data are the difference in expression between cells nucleofected with the –ve siRNA and cells nucleofected with MIAT_2 expressed as a normalised $\log_2$ fold change ($\log_2$FC). A threshold of 0.05 for statistical significance (*p-value*) and a $\log_2$ fold change of expression with an absolute value of at least 0.6 were applied (a); the pie chart schematically presents the distribution of differentially expressed genes into protein-coding and non-coding (b).

Multiple lines of evidence suggest that *MIAT* functions as a splicing factor sponge, thereby regulating alternative splicing (Tsuiji *et al.*, 2011; Ishizuka *et al.*, 2014; Cheng *et al.*, 2016). Therefore, we attempted to identify differentially expressed alternatively spliced genes associated with *MIAT* down-regulation. Among the genes on chromosome 22 whose expression was perturbed in response to *MIAT* knockdown, a great number (119) presented differential expression changes depending on the isoform of the gene assessed. This differential expression often followed both directions, with the expression of one isoform being up-regulated, whilst the expression of another isoform being down-regulated, suggesting that *MIAT* regulates the relative abundance of isoforms. This was in agreement with up to date literature and the established role of *MIAT* as a regulator of alternative splicing. Thus, we were prompted to assess whether this effect can be extrapolated on global gene expression, testing whether *MIAT* knockdown controls the abundance of splice variants. Based on the RNA sequencing results, it was discovered that this was the case, at least for a number of genes of interest for this study, including important protein-coding regulators of apoptosis (*BID, XIAP, CASP8*), cell survival *(MAPK7)* and response to oxidative stress (*HIF1A)*, as well as cancer-associated lncRNAs (*CASC2, MIR22HG),* and the lncRNA *LOC100506714*, located on chromosome 22, as presented in Figure 4.7. These differentially expressed alternatively spliced genes could potentially mediate aspects of the response to *MIAT* knockdown.

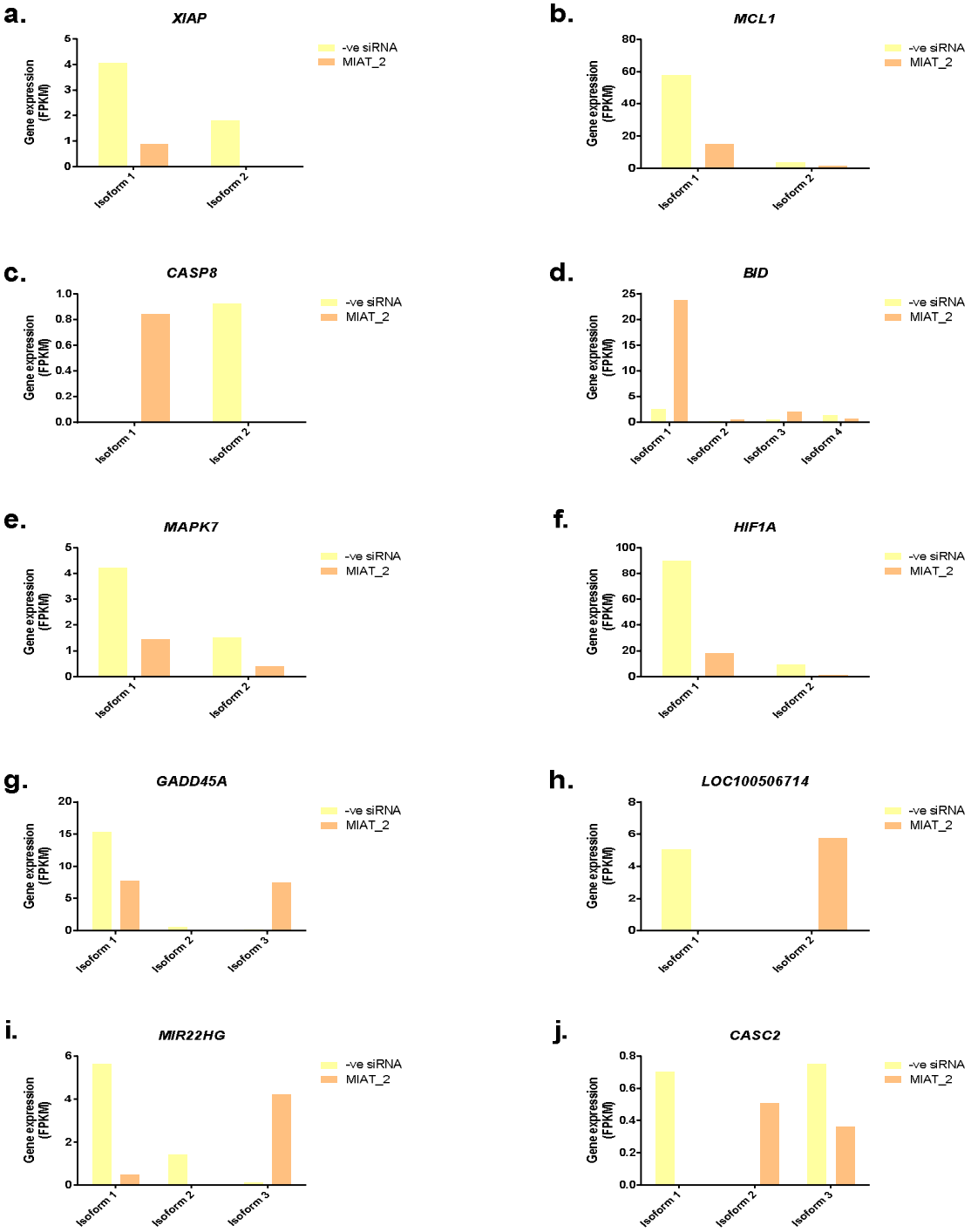

Figure 4.7. *MIAT* knockdown induces changes in the relative abundance of gene splice variants. *XIAP* (a); *MCL1* (b); *CASP8* (c); *BID* (d); *MAPK7* (e); *HIF1A* (f); *GADD45A* (g); *LOC100506714* (h); *MIR22HG* (i); *CASC2* (j). Isoform 1 represents the longest transcript. Data are Log_2 normalised read counts expressed as Fragments Per Kilobase of transcript per Million mapped reads (FPKM) and comparisons were made between cells nucleofected with the –ve siRNA and cells nucleofected with MIAT_2.

4.3.4. The effects of *MIAT* down-regulation on programmed cell death

Following the RNA sequencing results, which suggested that ROS-mediated apoptosis is induced upon *MIAT* knockdown, we decided to further validate the influence of *MIAT* on programmed cell death, including apoptosis, given the findings discussed in Chapter 3 suggesting that the down-regulation of *MIAT* induces a pronounced elevation in the levels of basal apoptosis. The validation was performed for a selection of genes on the mRNA level with the use of RT-qPCR and RT^2 Profiler PCR Arrays, including the RT² Profiler™ PCR Array Human Cell Death PathwayFinder and the RT² Profiler™ PCR Array Human Apoptosis, which assessed a panel of cell death- and apoptosis-related genes, respectively, as well as on the protein level with the use of western blotting.

4.3.4.1. The effects of *MIAT* down-regulation on the expression of genes associated with cell death

The RT² Profiler™ PCR Array Human Cell Death PathwayFinder assessed the differential expression of a panel of 84 genes associated with three different types of programmed cell death: apoptosis, necroptosis and autophagy, with a number of genes being associated with more than one type, given the abundance of programmed cell death networks. The analysis of the results revealed that among the 84 tested genes only two were upregulated upon *MIAT* knockdown, *CD40* (CD40 molecule, TNF receptor superfamily member 5) and *CD40LG* (CD40 Ligand), while 34 were down-regulated and 48 remained unaffected. The list of down-regulated genes included caspases (*CASP7/9*), apoptosis-related genes such as *BCL-2* and *BAX*, as well as autophagy-related genes (*ATG5/7*) and necroptosis-related genes (Supplementary Figure 1a, Appendix II). We then investigated whether this down-regulation of the genes coincided with the results acquired with the RNA sequencing. In fact, 16 of the 34 down-regulated genes were validated to be perturbed as assessed by both means, including *TP53, PIK3C3, IGF1R, GRB2, GADD45A, DFFA* (DNA Fragmentation Factor

Subunit Alpha), *CASP7/9, BMF* (BCL-2 Modifying Factor), *BCL-2, BAX* and *ABL1,* suggesting the important role of *MIAT* in the control of programmed cell death (Table 4.4 and Supplementary Figure 1b, Appendix II).

Table 4.4. Programmed cell death-associated differentially expressed genes in response to *MIAT* down-regulation.

Gene Symbol	Gene Name	Up-regulated/Down-regulated	Function
ABL1	ABL Proto-Oncogene 1, Non-Receptor Tyrosine Kinase.	Down-regulated	cell division, adhesion, differentiation, response to stress
APP	Amyloid Beta Precursor Protein	Down-regulated	apoptosis-inducing pathways (mediated by G(O) and JIP), oxidative stress
BAX	BCL-2 Associated X	Down-regulated	heterodimerises with BCL-2 , functions as an apoptotic activator
BCL-2	BCL-2 Apoptosis Regulator	Down-regulated	integral outer mitochondrial membrane protein blocking the apoptotic death
BMF	BCL-2 Modifying Factor	Down-regulated	binds BCL-2 proteins, and functions as an apoptotic activator
CASP7/9	Caspase 7/9	Down-regulated	execution-phase of cell apoptosis
DENND4A	DENN Domain Containing 4A	Down-regulated	interferon stimulated, c-Myc regulator
DFFA	DNA Fragmentation Factor Subunit Alpha	Down-regulated	substrate for caspase-3, triggers DNA fragmentation during apoptosis
GADD45A	Growth Arrest And DNA Damage Inducible Alpha	Down-regulated	responds to environmental stresses by mediating activation of the p38/JNK pathway
GRB2	Growth Factor Receptor Bound Protein 2	Down-regulated	EGFR/Ras pathway regulator
IGF1R	Insulin-Like Growth Factor 1 Receptor	Down-regulated	highly overexpressed in malignant tissues, functions as an anti-apoptotic agent
PIK3C3	Phosphatidylinositol 3-Kinase Catalytic Subunit Type 3	Down-regulated	involved in the initiation of autophagosomes
SNCA	Synuclein Alpha	Down-regulated	phospholipase D2 inhibitor
SYCP2	Synaptonemal Complex Protein 2	Down-regulated	cell division
TP53	Tumor Protein P53	Down-regulated	responds to diverse cellular stresses to regulate expression, thereby inducing cell cycle arrest, apoptosis, senescence, DNA repair, or changes in metabolism

In an attempt to establish apoptosis as the main route of programmed cell death that is affected by the down-regulation of *MIAT,* the RT² Profiler™ PCR Array Human Apoptosis was subsequently employed in order to assess a panel of 84 apoptosis-related genes, including genes related to both extrinsic and intrinsic apoptotic pathways and all apoptotic stages, from initiation to execution. The analysis of the results showed that unlike the other RT^2 profiler, the expression of most genes was perturbed, with only 4 being unaffected. At the same time, 49 genes were up-regulated, including caspases 8 and 10, *APAF1, BIK, TP73, CFLAR* (CASP8 And FADD Like Apoptosis Regulator) and *BAD*, while 31 were down-regulated, including several caspases (*CASP2/3/4/7), MCL1, FAS, FASLG, FADD, DIABLO, BIRC2/3/6* (Baculoviral IAP Repeat Containing 2/3/6) (Supplementary Figure 2a, Appendix II). To further validate these results, the differential gene expression was compared between the RNA sequencing results and the RT² Profiler results. Notably, this comparison brought to light 28 genes whose expression was perturbed in the same direction in both approaches (Table 4.5 and Supplementary Figure 2b, Appendix II). This list contains a variety of well-known apoptosis-associated genes, such as *APAF1, BAD, BCL2L11, BIK, TRADD, TRAF2/3, TP73, BIRC2/5/6, CASP2/3/4/6/7/8, FAS, MCL1* and *XIAP*.

Table 4.5. Apoptosis-associated differentially expressed genes in response to *MIAT* down-regulation.

Gene Symbol	Gene Name	Up-regulated/Down-regulated	Function
APAF1	Apoptotic Peptidase Activating Factor 1	Up-regulated	apoptosis initiator, component of the apoptosome
BAD	BCL-2 Associated Agonist Of Cell Death	Up-regulated	cell apoptosis regulator by forming heterodimers with BCL-xL and BCL-2
BAG1	BCL-2 Associated Athanogene 1	Up-regulated	BCL-2-associated athanogene, enhances the anti-apoptotic effects of BCL-2
BCL2L11	BCL-2 Like 11	Up-regulated	interacts with other members of the BCL-2 protein family, acting as an apoptotic activator
BIK	BCL-2 Interacting Killer	Up-regulated	pro-apoptotic activity, interaction with anti-apoptotic members of the BCL-2 family
BIRC5	Baculoviral IAP Repeat Containing 5	Up-regulated	member of the inhibitor of apoptosis (IAP) gene family, negative regulatory protein preventing apoptotic cell death
BIRC2/6	Baculoviral IAP Repeat Containing 2/6	Down-regulated	apoptosis inhibitor by means of binding to TRAF1 and TRAF2/ apoptosis inhibitor through facilitating the degradation of apoptotic proteins by ubiquitination
BNIP2	BCL-2 Interacting Protein 2	Down-regulated	interacts with the E1B 19 kDa protein, which protects cells from virally-induced cell death and the E1B 19 kDa-like sequences of BCL-2
BNIP3L	BCL-2 Interacting Protein 3 Like	Down-regulated	targets mitochondria and causes apoptotic changes, including loss of membrane potential and the release of cytochrome c
CASP6/8	Caspase 6/8	Up-regulated	downstream enzyme in the caspase activation cascade/ involved in apoptosis induced by Fas and various apoptotic stimuli
CASP2/3/4/7	Caspase 2/3/4/7	Down-regulated	functions in stress-induced cell death pathways, cell cycle maintenance, and suppression of tumorigenesis/ cleaves and activates caspases 6, 7, and 9/ cleaves and activates its own precursor protein and caspase 1 precursor/ cleaved by caspase 3 and 10, activated upon cell death stimuli and induces apoptosis
CIDEB	Cell Death Inducing DFFA Like Effector B	Down-regulated	apoptosis activator
DAPK1	Death Associated Protein Kinase 1	Down-regulated	tumour suppressor candidate
FAS	Fas Cell Surface Death Receptor	Down-regulated	apoptosis initiator upon ligand binding and NF-kappaB, MAPK3/ERK1, and MAPK8/JNK

			inducer
HRK	Harakiri, BCL-2 Interacting Protein	Up-regulated	localised in intracellular membranes, promotes apoptosis by interacting with the apoptotic inhibitors BCL-2 and BCL-X(L) via its BH3 domain
MCL1	MCL1 Apoptosis Regulator, BCL-2 Family Member	Down-regulated	BCL-2 family member, enhances cell survival by inhibiting apoptosis
NOD1	Nucleotide Binding Oligomerization Domain Containing 1	Up-regulated	induces apoptosis via its N-terminal caspase recruitment domain (CARD)
TNFRSF10B	TNF Receptor Superfamily Member 10b	Down-regulated	TNF-receptor superfamily member, containing an intracellular death domain. Can be activated by TNFSF10/TRAIL/APO-2L, and transduces an apoptosis signal
TP73	Tumor Protein P73	Up-regulated	participates in the apoptotic response to DNA damage
TRADD	TNFRSF1A Associated Via Death Domain	Up-regulated	interacts with TNFRSF1A/TNFR1 and mediates programmed cell death signalling and NF-κB activation. Binds TRAF2, reduces the recruitment of IAPs by TRAF2, suppressing TRAF2 -mediated apoptosis, interacts with TNFRSF6/FAS and adaptor protein FADD/MORT1, and is involved in the Fas-induced cell death pathway
TRAF2/3	TNF Receptor Associated Factor 2/3	Up-regulated	functions as a mediator of the anti-apoptotic signals from TNF receptors/ induces NF-κB activation and cell death initiated by LTβ ligation
XIAP	X-Linked Inhibitor Of Apoptosis	Down-regulated	functions through binding to TRAF1/2 and TRAF2, and inhibits at least two members of the caspase family of cell-death proteases, CASP3/7

In light of the fact that several genes with perturbed expression as revealed by RNA sequencing and the RT^2 are regulated by transcription factors with established roles in cancerous contexts, the down-regulation of two of them in response to *MIAT* knockdown was validated, given the fact that they regulate the expression of the perturbed genes. Therefore, the expression levels of *c-Myc* and *Oct1 (POU2F1*) were validated with RT-qPCR, as c-Myc mediates the transcription of *BNIP3L, TP53 and GADD45A*, and Oct1 the transcription of *ABL1, NFκB1, BCL2L2* and *GADD45A.* In line with this, the expression of both transcription factors was found to be significantly down-regulated (~50% and ~70%, for *c-Myc* and *Oct1*, respectively, in agreement with the RNA sequencing results, which reported a ~1.2- and ~6-fold decrease, for *c-Myc* and *Oct1*, respectively (Figure 4.8).

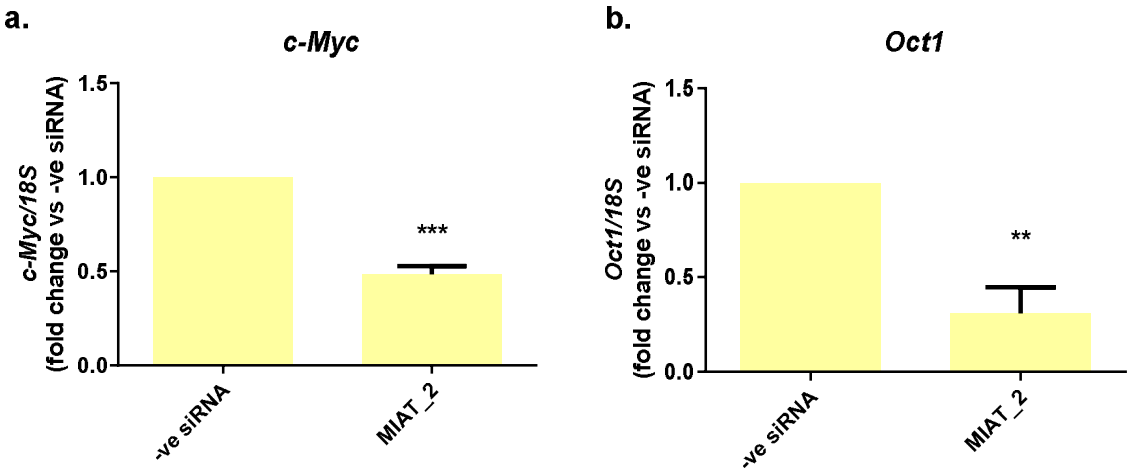

Figure 4.8. *MIAT* down-regulation triggers the down-regulation of the transcription factors *C-Myc* and *Oct1* (*POU2F1*) in SH-SY5Y cells. SH-SY5Y cells were transfected with the negative siRNA or MIAT_2 using nucleofection, incubated for 48 h and the relative expression of *MIAT* was measured by Real-Time PCR 48 h post-transfection. The samples chosen for the assessment of *C-Myc* and *Oct1* levels had a validated reduction in expression of at least 55%. Subsequently, the expression of c-Myc and Oct1 was measured and was found to be significantly lower for both c-Myc (~50%) (a) and Oct1 (~70%) (b); ** indicate a *p-value*<0.01;*** indicate *a p-value*<0.001, as measured by unpaired t-test, n=3 experiments. Data are represented as mean +/- SEM.

4.3.4.2. The effects of *MIAT* down-regulation on the protein levels of proteins involved in programmed cell death

Mature mRNA transcripts are subject to various post-transcriptional modifications and undergo multi-level control steps before they enter the process of translation (Corbett, 2018). Therefore, the fact that the mRNA levels of numerous genes were perturbed in response to *MIAT* knockdown does not guarantee that the same effect would be observed on the protein level. To this end, the next step encompassed in the study was to assess the changes of protein levels of a number of apoptosis-related genes, namely *CASP8, XIAP, BID, BAD* and *MCL1*, via western blotting.

Western Blot analysis revealed that the effects of the down-regulation of *MIAT,* despite being very pronounced for the aforementioned genes on the mRNA level, were indeed present on the protein level of these –mainly intrinsic apoptosis-related genes but, in a less pronounced fashion. In specific, the anti-apoptotic MCL1 and XIAP showed the most highlighted decrease in protein levels in accordance with the decrease on the mRNA level, which, although present for all three *MIAT*-specific siRNAs, was significant only for two of them (MIAT_2, MIAT_3), reaching a ~65% reduction for MIAT_2 and ~80% reduction for MIAT_3 for MCL1 (Figure 4.9a), and a ~65% decrease for MIAT_2 and a ~70% decrease for MIAT_3 for XIAP (Figure 4.9b). In contrast, although the pro-apoptotic BID, BAD and CASP8 did show an increase in levels in agreement with the observations on the mRNA level, this increase was not again equally pronounced. In fact, as far as BAD is concerned a statistically significant increase of ~50% was observed for MIAT_1 only (Figure 4.9c). As shown in Figure 4.9d, e, for BID and CASP8, although all the three *MIAT*-specific siRNAs caused an increase in the protein levels of both genes, this effect was only significant for MIAT_3 -treated cells (~40% and ~75% increase, respectively). Collectively, these data suggest

that *MIAT* plays a vital role in triggering the ROS-mediated apoptotic response of SH-SY5Y cells.

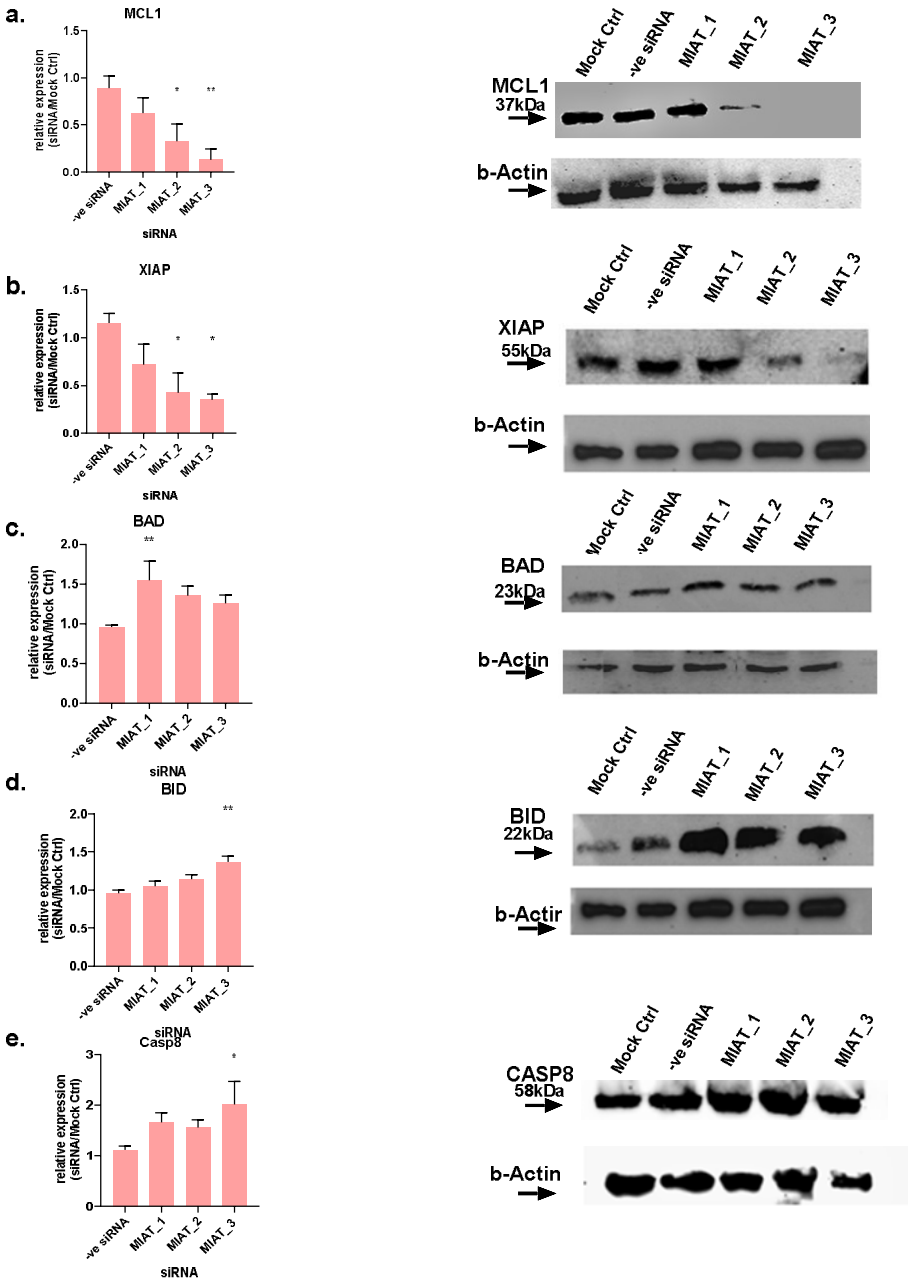

Figure 4.9. *MIAT* down-regulation induces changes on the levels of apoptosis-related proteins in SH-SY5Y cells. SH-SY5Y cells were transfected with the negative siRNA or one of the *MIAT*-specific siRNAs using nucleofection, incubated for 48 h and the protein levels were measured via Western Blot. The levels of MCL1 are significantly reduced for MIAT_2- (~65%) and MIAT_3- (~80%) treated cells (a), while the levels of XIAP are also significantly reduced for MIAT_2- (~65%) and MIAT_3- (~70%) treated cells (b). On the contrary, *MIAT* knockdown causes a statistically significant increase in the levels of BAD for MIAT_1- treated cells (~50%) (c), while for BID (~40%) (d) and CASP8 (~75%) (e) the increase is significant only for MIAT_3 -treated cells; representative images of Western Blots for MCL1, XIAP, BAD, BID and CASP8: right panels, a-e, respectively; data are presented as relative expression of *MIAT*-specific siRNA/ -ve Ctrl, following normalisation against the housekeeping gene β-Actin; * indicates a *p-value*<0.05; ** indicate a *p-value*<0.01, as measured by unpaired T-test, n=4 experiments. Data are represented as mean +/- SEM.

4.3.5. *MIAT* silencing induces fluctuations in ROS levels in neuroblastoma and glioma cells

On the grounds that the RNA sequencing revealed numerous ROS-associated processes to be perturbed upon *MIAT* knockdown, we further investigated whether there is an increase in ROS levels when down-regulating *MIAT*, and whether this perturbation is related to the increased apoptosis and decreased migration of neuroblastoma and GBM cells, as observed in Chapter 3. It was, therefore, tested whether MIAT_2- and MIAT_3- mediated knockdown of *MIAT* affects the production of ROS. ROS levels were assessed by flow cytometry using the CellROX® Green Reagent in all cell lines. However, due to the constant acquisition of very high levels of autofluorescence in SH-SY5Y cells, a different approach was adopted (described below).

4.3.5.1. *MIAT* knockdown augments ROS levels in glioma cells

To evaluate the levels of ROS in response to *MIAT*-specific knockdown, the astrocytoma/GBM 1321N1 cells and the GBM T98G cells were transfected with either the –ve siRNA or MIAT_2, were incubated for 48 and 72 h, and ROS production levels were assessed by flow cytometry. Notably, for 1321N1 cells, there was a significant elevation in ROS levels upon *MIAT* down-regulation. In particular, a ~100% increase was observed both 48 h and 72 h post-seeding (Figure 4.10a, b, respectively). The results obtained for T98G cells followed the same trend. There was a ~100% increase in the ROS levels of the cells in which *MIAT* was down-regulated, both 48 h (Figure 4.10c) and 72 h (Figure 4.10d) post-seeding; however, the increase was statistically significant only at 48 h.

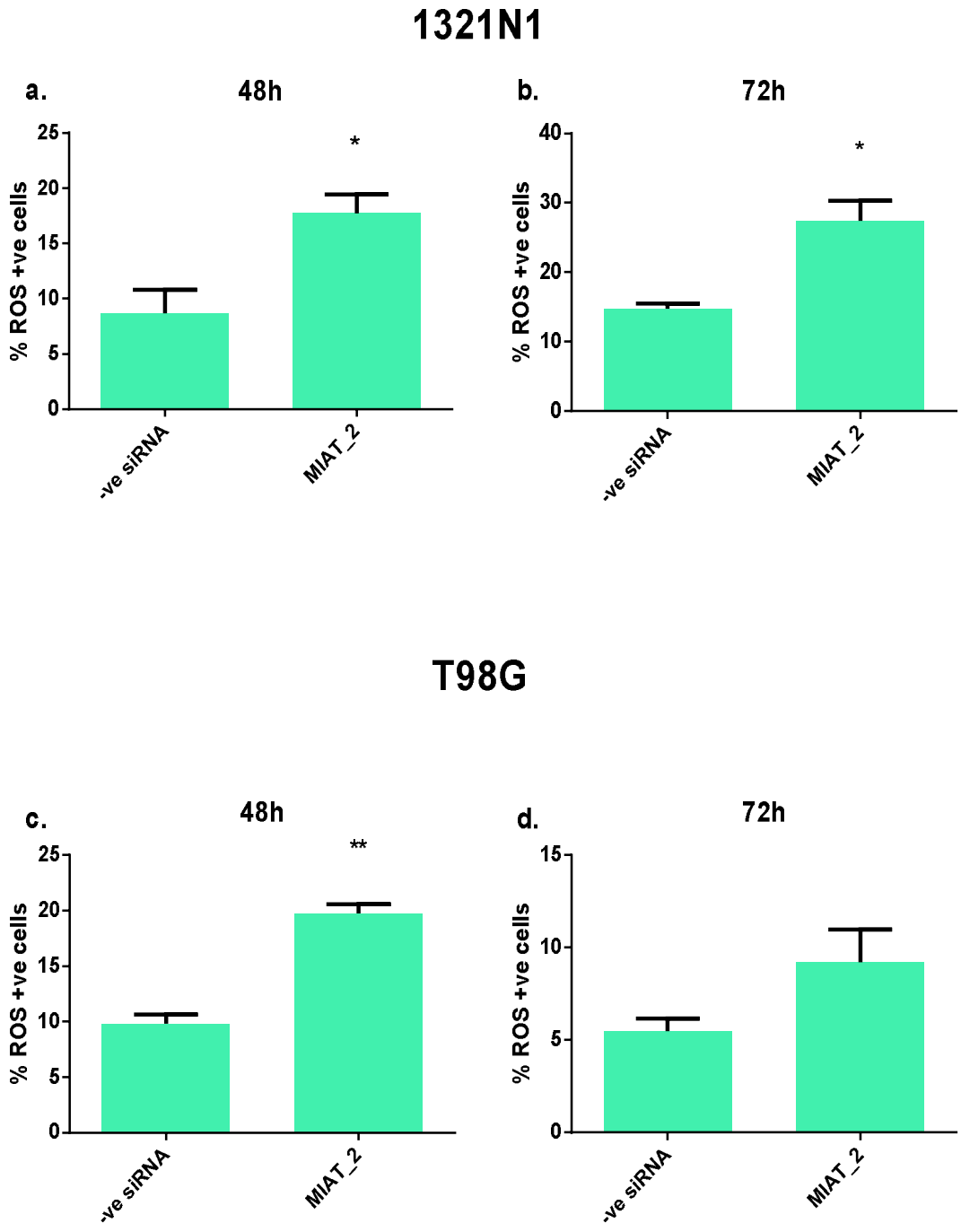

Figure 4.10. *MIAT*-specific down-regulation increases ROS levels in glioma cells. 1321N1 and T98G cells were transfected with the –ve siRNA or the *MIAT*-specific siRNA MIAT_2 using nucleofection, incubated for 48/72 h and assessed for ROS production by flow cytometry using the CellROX® Green Reagent. In 1321N1 cells, a statistically significant ~1-fold increase was observed both at 48 h (a) and at 72 h (b). In T98G cells, a statistically significant increase of ~1-fold was observed at 48 h (c), but the equivalent increase at 72 h was not statistically significant (d); * indicates a *p-value*<0.05; ** indicate a *p-value*<0.01, as measured by unpaired T-test, n=3 experiments. Data are represented as mean +/- SEM.

4.3.5.2. PBN rescues the *MIAT*-knockdown-mediated increase in apoptosis and the decrease in migration of neuroblastoma cells

In SH-SY5Y cells, the contribution of ROS production in basal apoptosis was evaluated through a ROS scavenging approach. To this end, Alpha-phenyl-N-tert-butyl nitrone (PBN), a widely used ROS scavenger, was employed. Based on existing literature (Miyajima and Kotake, 1995; Gao *et al.*, 2007; Deshmukh and Trivedi, 2013) and optimisation experiments (data not shown), 600μM PBN were added to the cells 1 hour prior to the addition of equal amount of the ROS inducer H_2O_2 It was revealed that PBN can restore the apoptosis levels in SH-SY5Y cells to levels similar to those of the untreated control cells (~2% at 8 h and 24 h), as assessed by acridine orange (Figure 4.11). Moreover, PBN was capable of partially restoring apoptosis caused by H_2O_2 at both time points (Figure 4.11).

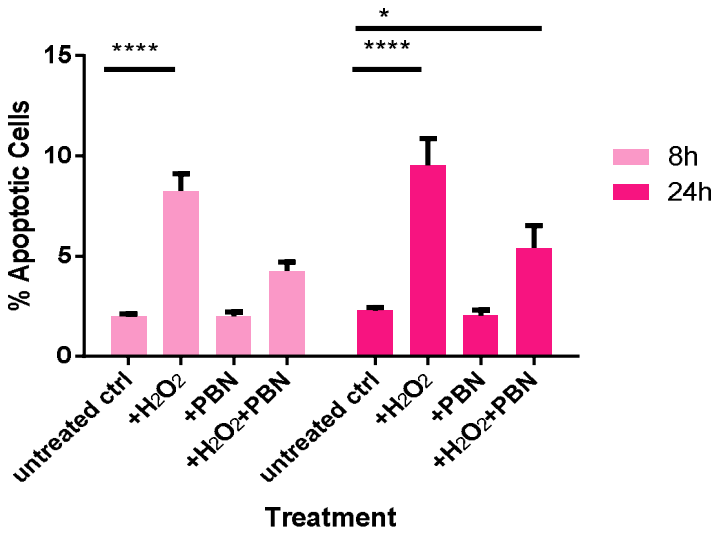

Figure 4.11. PBN rescues apoptosis caused by *MIAT*-specific knockdown in SH-SY5Y cells. The best rescue results were acquired when 600μM PBN were added to SH-SY5Y cells, the cells were incubated for 1h and then the ROS inducer H_2O_2 was added to the cells. PBN was capable of significantly reducing apoptosis levels in the cells, as assessed by acridine orange 8 and 24h after H_2O_2 addition (b); * indicates a *p-value*<0.05; **** indicate a *p-value*<0.001, as measured by Two-way ANOVA tests with multiple comparisons (MCT), n=3 experiments. Data are represented as mean +/- SEM.

Since the optimisation results revealed that the ROS scavenger PBN is capable of rescuing the elevated apoptosis levels in SH-SY5Y cells, it was hypothesised that the same effect would be obtained for MIAT_2/3-induced *MIAT* down-regulation, and in addition, that PBN would also be able to restore the migrating ability of SH-SY5Y cells, which was severely eliminated upon *MIAT* knockdown, as described in section 3.3.4. In order to test this hypothesis, SH-SY5Y cells were nucleofected with the –ve siRNA or one of the two MIAT-specific siRNAs (MIAT_2, MIAT_3), were re-plated after 48 h, and PBN was added 24 h post-replating. Apoptosis levels were tested after 24 and 48 h by acridine orange staining and the effect on cell migration was tested with the wound healing assay at 0, 24 and 48 h post-treatment.

Acridine orange staining not only confirmed that both MIAT_2- and MIAT_3-mediated knockdown increased the levels of apoptosis ~2-fold 48 h post-plating (as described in section 3.3.1), but also showed that a ~2-fold statistically significant increase in apoptosis levels is obtained 24h post-plating, while PBN alone did not have effects on basal apoptosis and migration (results not shown). Notably, it was revealed that, as hypothesised, the addition of PBN is capable of fully restoring the apoptosis levels caused as a result of *MIAT* down-regulation to levels similar to those of the control groups, i.e. from ~9% to ~2/3% for MIAT_2 and MIAT_3, respectively, at 24h (Figure 4.12a) and from ~10% to ~3/2% for MIAT_2 and MIAT_3, respectively, at 48 h (Figure 4.12b).

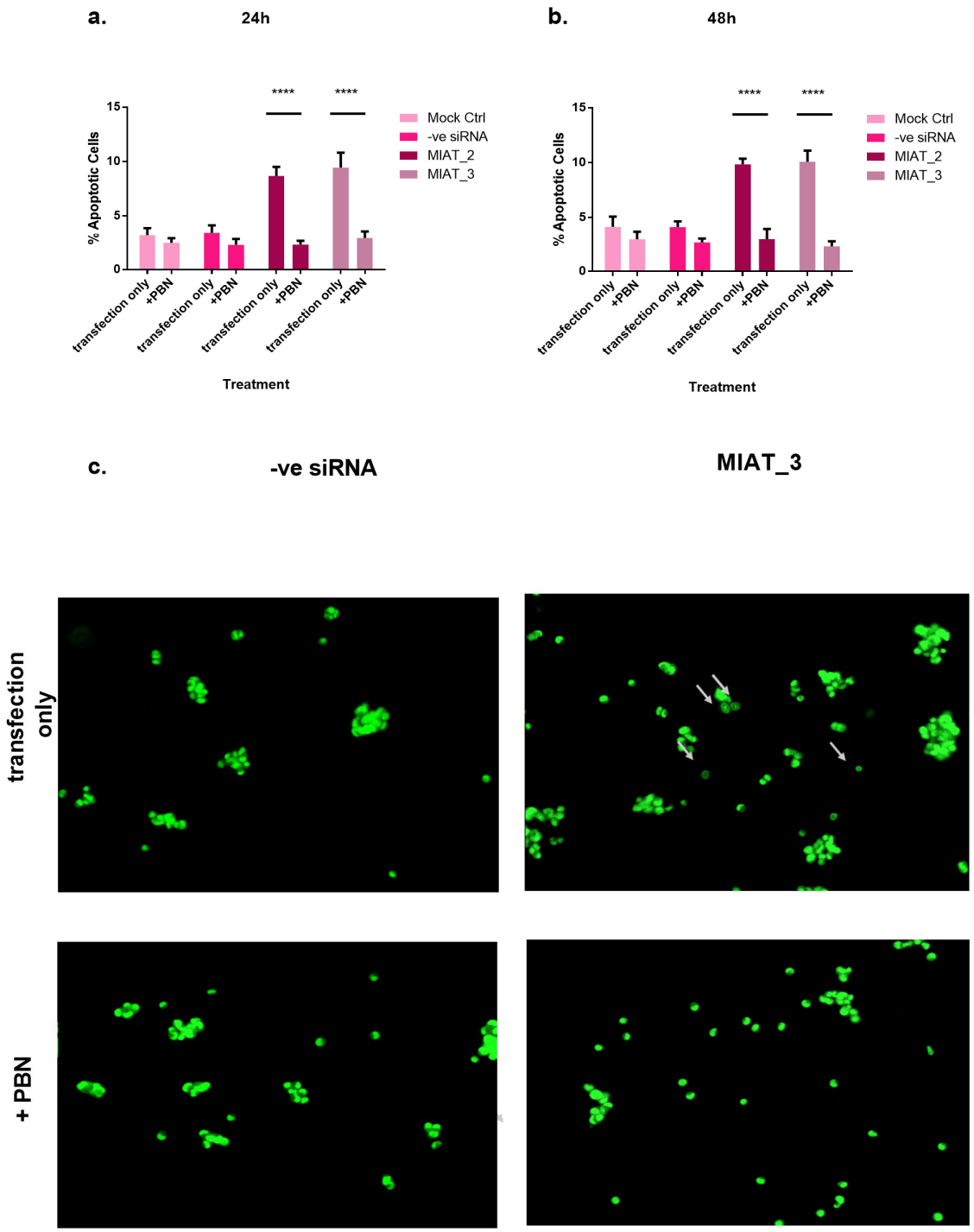

Figure 4.12. PBN scavenges *MIAT* knockdown-mediated apoptosis in SH-SY5Y cells. SH-SY5Y cells were nucleofected with the –ve siRNA or one of the two *MIAT*-specific siRNAs (MIAT_2, MIAT_3), were re-plated after 48 h, and PBN was added 24h post-plating. Apoptosis levels were tested after 24h and 48 h by acridine orange staining. PBN fully restored the apoptosis levels caused as a result of *MIAT* down-regulation to levels similar to those of the control groups for both MIAT_2 and MIAT_3 at 24h (a) and 48 h (b); representative illustration of apoptotic cells 48 h post-treatment, stained with acridine orange and observed using fluorescent microscopy (c). Grey arrows indicate cells undergoing apoptosis; **** indicate a p-value<0.001, as measured by Two-way ANOVA tests with multiple comparisons (MCT), n=3 experiments. Data are represented as mean +/- SEM.

Further to restoring basal apoptosis levels, the addition of PBN to SH-SY5Y cells was also able to reverse the effect of *MIAT* down-regulation on cell migration, i.e. PBN administration re-potentiated cells to migrate, in levels equivalent to those of the control groups. In specific, this experimental series, not only confirmed the fact that the knockdown of *MIAT* significantly inhibited the migratory ability of the cells ~30-35% (as described in section 3.3.4), but also revealed that the addition of PBN can reverse the inhibitory effects of *MIAT* silencing, as reflected in gap closure levels of wound healing assays. In detail, for MIAT_2-treated cells, the gap closure was augmented from 38% to 65% at 24h (Figure 4.13a) and from 53% to 78% at 48 h (Figure 4.14b), while for MIAT_3-treated cells the gap closure was increased from 37% to 64% at 24h (Figure 4.15a) and from 48% to 77% at 48 h (Figure 4.13b).

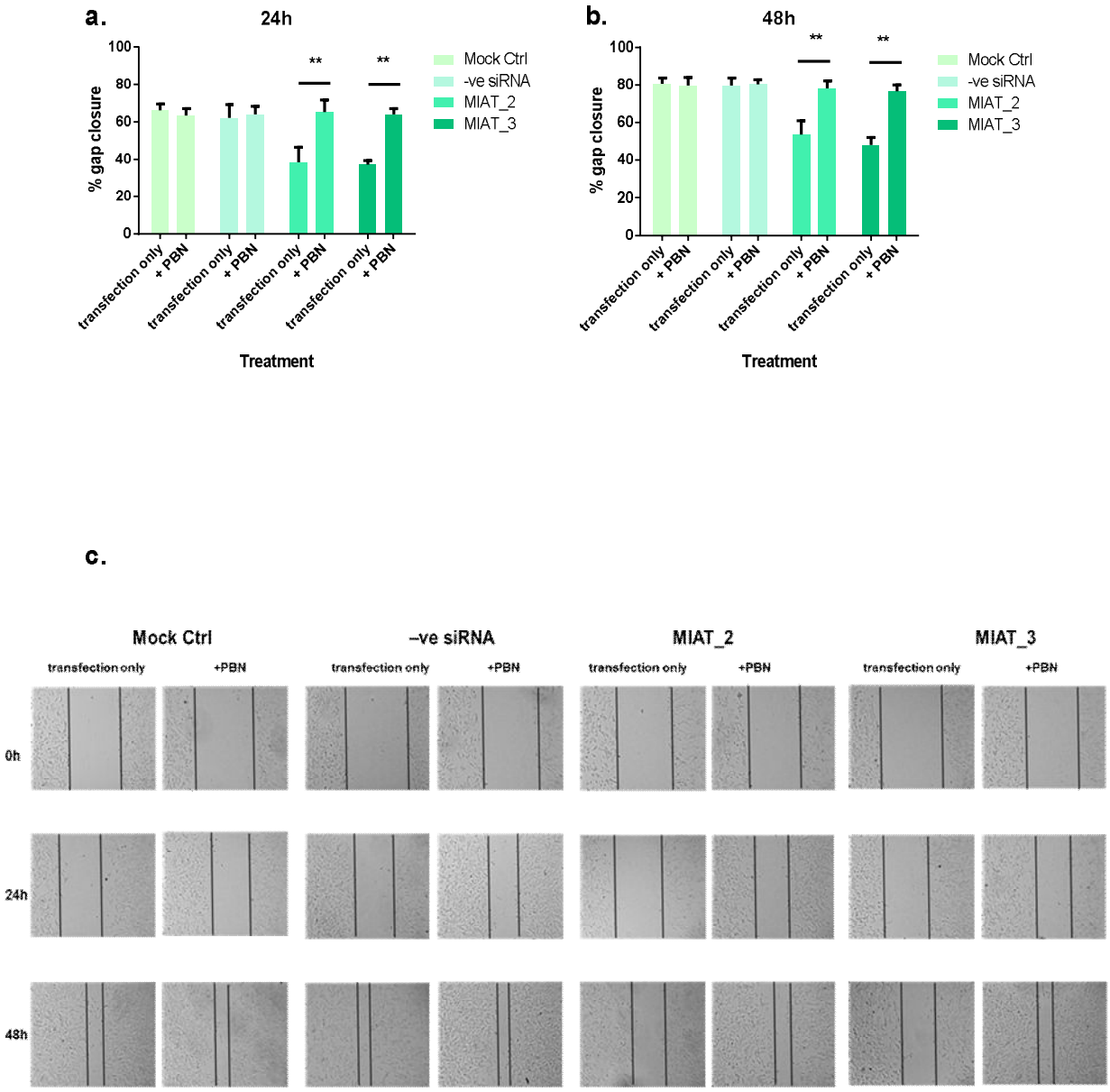

Figure 4.13. PBN scavenges *MIAT* knockdown-mediated inhibition of migration in SH-SY5Y cells. SH-SY5Y cells were transfected with the –ve siRNA or one of the two *MIAT*-specific siRNAs (MIAT_2, MIAT_3) using nucleofection, incubated for 48 h, re-plated, incubated for another 24h before the addition of 600μM PBN, and a linear scratch was introduced 24h post-treatment. The % gap closure of the scratch was measured after 24 and 48 h. PBN significantly increases the migratory ability of the cells. Both for MIAT_2- and MIAT_3-treated cells the gap closure is increased to the levels of the control groups at 24h (a) and 48 h (b), i.e. to~60% and 80%, respectively; representative illustration of a wound healing ("scratch") assay (c); ** indicate a *p-value*<0.01, as measured by Two-way ANOVA tests with multiple comparisons (MCT), n=3 experiments. Data are represented as mean +/- SEM.

4.4. Discussion

MIAT has been attributed an important role in alternative splicing by acting as a sponge to prevent splicing factors, such as SF1, QK1, SRSF1 (Tsuiji *et al.*, 2011; Cheng *et al.*, 2016) and Celf3 (Ishizuka *et al.*, 2014) from exerting their normal role. In addition, *MIAT* has been found to act as a miRNA sponge, as in the cases of miR-214 and miR-22-3p in HCC (Huang *et al.*, 2018; Zhao *et al.*, 2019), miR-155-5p in breast cancer (Luan *et al.*, 2017) and miR-141 in gastric cancer (Sha *et al.*, 2018). Nevertheless, the exact molecular mechanisms underpinning the action of *MIAT* and its involvement in the regulation of cell fate determination remain largely undiscovered. To this end, and in light of the evidence presented in Chapter 3 suggesting the involvement of *MIAT* in the regulation of cell survival, basal apoptosis and migration, the current chapter aimed at expanding the knowledge on the modes of action of *MIAT* in neuroblastoma cells, as well as at linking *MIAT* to the regulation of elevated apoptosis and reduced cell survival and migration of SH-SY5Y cells. The analysis of the RNA sequencing provided some interesting insights. The silencing of *MIAT* is capable of modulating cancer-related processes including ROS-mediated apoptosis, and as an indirect consequence, reducing the migratory ability of the cells. Moreover, fluctuation in the levels of *MIAT* can alter the lncRNA landscape, regulate gene expression *in cis* and affect alternative splicing. Following the RNA sequencing lead, aberrant expression of apoptosis-related genes was also herein confirmed, as was the fact that cell death induced by *MIAT* down-regulation could be attributed to elevated ROS levels.

The RNA sequencing demonstrated that a striking 11085 genes were differentially expressed, along with 5 cancer-related pathways. In light of the fact that our functional studies (described in Chapter 3) showed an overall tendency of *MIAT*-specific siRNA knockdown to cause reduced long-term cell viability and an impressive multi-fold increase of the apoptosis levels in all the tested cell lines, our attention was shifted towards survival- and apoptosis-related processes and pathways. As the RNA

sequencing suggests, a number of cell growth and pro-survival pathways are affected following *MIAT* down-regulation, for example, the overlapping MAPK, TGF-β, EGFR and Phospholipase D pathways, with a lot of crucial genes being perturbed in both directions (*HRAS* and *SMAD 5*, for example), making it extremely hard to decipher the direction in which the system is balancing.

ROS are responsible for activating signal transduction pathways, as well as early response TFs (Wei *et al.*, 2019). Notably, the MAPK/ERK pathway, including PI3K/AKT and NFκB, have been established to be initiated by changes in ROS levels, leading to different outcomes depending on cellular contexts (Babu and Tay, 2019; NavaneethaKrishnan *et al*., 2019). Another such example of complicated regulation is c-Myc, a transcription factor that transcribes several target genes, mainly associated with cell survival and proliferation. However, it has also been found that when deregulated, it participates in both the intrinsic apoptotic pathway, therefore promoting apoptosis via anti-apoptotic molecule suppression (e.g. BCL-2 family) and pro-apoptotic molecule induction, and the extrinsic apoptotic pathway (Hoffman and Liebermann, 2008; McMahon, 2014). Additionally, *c-Myc*, which was found to be down-regulated (as part of the perturbed MAPK signalling cascade) following *MIAT* knockdown in SH-SY5Y cells in our RNA sequencing, had been previously found to cause *MIAT*'s significant up-regulation when inhibited in GBMs (Galardi *et al.*, 2016). In a ROS-related context, high ROS levels induce the up-regulation of *c-Myc* favouring tumour progression; however, above a certain threshold, ROS-induced *c-Myc* expression favours apoptosis and cell death (Babu and Tay, 2019; Florean *et al.*, 2019; Lin, 2019). This suggests a high versatility of these genes' functions, as well as great network complexity, especially among different tumour types. Whether *MIAT* or its downregulation is somehow involved in these pathways leading to these phenotypes, or whether there is a regulatory loop between the two molecules in neuroblastoma cells remains to be elucidated.

Given that the most pronounced changes observed in response to *MIAT* knockdown included the elevation of apoptosis levels, it was essential to analyse the molecular changes underpinning this phenotype, as well. Following the lead of our RNA sequencing results, we performed a series of expression analyses to validate the suggested effects. As the sequencing reveals in one of the most pronounced deregulated pathways, the NOD-like receptor signalling pathway, there is a tremendous upregulation of the initiator *Caspase 8*, together with a significant downregulation of the anti-apoptotic *XIAP*. To validate that programmed cell death, and especially apoptosis, is indeed one of the most affected processes upon *MIAT* knockdown, as indicated by the RNA sequencing, we employed two RT² Profiler™ PCR Arrays, assessing cell death including apoptosis, necroptosis and autophagy, and apoptosis more in-depth. The former suggested that indeed all the assessed aspects of cell death were affected, and validated numerous genes whose expression was perturbed as assessed by the sequencing, including *TP53, PIK3C3, IGF1R, GRB2, GADD45A, DFFA, CASP7/9, BMF, BCL-2, BAX* and *ABL1.* The latter provided even more convincing evidence that the down-regulation of *MIAT* induces both intrinsic and extrinsic apoptosis. In this case, a striking 80/84 assessed genes were found to be perturbed, including *APAF1, BIK, TP73, CFLAR*, *BAD*, several caspases (*CASP2/3/4/7), MCL1, FAS, FASLG, FADD, DIABLO* and *BIRC2/3/6*. Of these, in 28 genes, including the well-known apoptosis-associated *APAF1, BAD, BCL2L11, BIK, TRADD, TRAF2/3, TP73, BIRC2/5/6, CASP2/3/4/6/7/8, FAS, MCL1* and *XIAP*, the expressional perturbation followed the same direction in both the RNA sequencing and the array, pinpointing their crucial role in the process.

Cell death, including apoptosis, may in many cases be caused by increased levels of ROS mediating JNK activation as a response to TNFα stimuli, as well as by regulating various elements of the intrinsic apoptotic pathway (Galadari *et al.*, 2017; Aggarwal *et al.*, 2019; Florean *et al.*, 2019). In line with this, there is a fundamental link between

ROS accumulation and the mitochondrial apoptotic pathway: increased ROS production, given that their primary site of generation is the mitochondrion, is capable of depolarising the mitochondrial membrane, leading to cytochrome C release, thus initiating the cascade. Apart from that, elevated ROS levels can directly trigger Caspase 8, as well as modulate Fas- and TRAIL-mediated (extrinsic) apoptosis (Galadari *et al.*, 2017; NavaneethaKrishnan *et al.*, 2019). Additionally, it has been observed that in the mitochondrial pathway ROS mediate the release of pro-apoptotic molecules such as AIF and Smac/DIABLO, in an APAF1-independent way, as well as to directly regulate BCL-2 family members, such as BCL-2, MCL1, BAX and BAD (Galadari *et al.*, 2017). Our data showing that upon *MIAT* knockdown ROS levels are increased and in turn increase the expression of pro-apoptotic molecules (e.g. TP73, BID, BAD, DIABLO and CASP8) and on the contrary, decrease the expression of anti-apoptotic ones (e.g. BCL-2, MCL1, BIRC2/6 and XIAP), are aligned with up to date literature and can propose this as a novel mechanism via which *MIAT* dictates how neuroblastoma cells respond to its silencing to ultimately undergo apoptosis. Finally, the fact that *MIAT* down-regulation also interferes with necroptosis and autophagy, in agreement with previous literature (Galadari *et al.*, 2017; Florean *et al.*, 2019), should not be neglected.

Strikingly, the down-regulation of *MIAT*, on top of the pathway and protein-coding gene perturbations, triggers the differential expression of more than 500 lncRNAs, suggesting the existence of a complex, probably abundant, network of lncRNAs that work synergistically or antagonistically to regulate the response of neuroblastoma cells to the silencing of *MIAT* and further to ROS production, in order for the equilibrium to lean towards apoptosis. Notably, apart from the fact that these perturbed lncRNAs were spread into most of the known different lncRNA subclasses (with NATs and lincRNAs dominating), the expression of a variety of them was co-modulated with their protein-coding transcripts. This was particularly important in the case of significant

genes with established roles in cancer. For instance, the oncogenic *TP73-AS1* (~6-fold up-regulated) was co-upregulated with its protein-coding gene *TP73* (~10-fold), although TP73 is a well-known tumour suppressor. The expression of *HIF1A-AS2,* the NAT of *HIF1A*, was found to be ~4.5-fold increased, while the expression of *HIF1A* itself was decreased ~3-fold upon *MIAT* knockdown. Finally, *MIRLET7BHG*, the lncRNA located on chromosome 22, hosting the well-known tumour suppressor miR-let7b (targeting the down-regulated *Fas* and *Oct1*) was ~4-fold up-regulated, while its coding transcript PPARA [which is also a redox sensor (Lavrovsky *et al.*, 2000)] was 10-fold down-regulated, suggesting that *MIAT* is responsible for elegantly, yet tightly, regulating the expression of transcript/NAT pairs. Taken together, this evidence highlights the importance of epigenetics, as described broadly to include miRNA- and lncRNA- mediated regulation (Kietzmann *et al.*, 2017), on top of genetics, in regulating the cell fate of neuroblastoma cells.

In order to add one more piece to the puzzle of how *MIAT* regulates gene expression, the regulation of *in cis* gene expression was investigated next, on the grounds that numerous lncRNAs are very potent *in cis* regulators (Cheng *et al.*, 2016). It was demonstrated that this is also the case for *MIAT*, at least in neuroblastoma cells, as more than 300 neighbouring genes, coding and non-coding, were differentially expressed in response to its knockdown, including up-regulation and down-regulation, while the magnitude of the effect reached a 17-fold factor (*PARVB*). Interestingly, the number of genes on chromosome 22 that underwent an increase in expression was double the number of those undergoing decrease in expression, possibly revealing a tendency of *MIAT* to suppress gene expression, which is in agreement with its traditional role as a decoy (Tsuiji *et al.*, 2011; Cheng *et al.*, 2016). Moreover, in line with the observation that the levels of intrinsic apoptosis as induced by *MIAT* knockdown are increased, the pro-apoptotic *BID* and *BIK* were shown to be ~2-fold upregulated. Furthermore, the ability of *MIAT* to simultaneously regulate protein-coding/NAT pairs,

as described above, is observed on chromosome 22 as well, as in the case of *NUP50*/*NUP50-DT*, *PPARA*/*MIRLET7BHG, CHKB/CHKB-AS1,* and *MIF*/*MIF-AS1.* Finally, since *MIAT* has been suggested to regulate alternative splicing through sponging basic splicing factors (Tsuiji *et al.*, 2011; Ishizuka *et al.*, 2014; Cheng *et al.*, 2016), it could be hypothesised that this is reflected on the relative abundance of *MIAT*-regulated targets. Our study confirmed this hypothesis, as the down-regulation of *MIAT* caused the differential distribution of same gene isoforms for numerous genes, including a selection of genes of interest, located not only on chromosome 22 but also spanning other chromosomes (*XIAP, MCL1, CASP8, BID, MAPK7, HIF1A, GADD45A, MIR22HG, CASC2).*

Interestingly, the analysis of the RNA sequencing data also revealed that numerous processes associated with oxidative stress-induced cell death, such as the regulation of cellular response to oxidative stress and the regulation of oxidative stress-induced intrinsic apoptotic signalling pathway, were remarkably perturbed in response to *MIAT* knockdown. Notably, these RNA sequencing results were confirmed by functional assays which revealed an increase in ROS levels in glioma cells, as well as the ability of PBN, a ROS scavenger, to reverse the *MIAT* knockdown-induced apoptosis and migration phenotypes. It has long been established that cancer cells are metabolically active and undergo severe oxidative stress, leading to the production of ROS (Pelicano *et al*., 2004). ROS have also long been speculated to be associated with diverse cellular responses of the cancer cell depending on the cellular background, ranging from a transient growth arrest and adaptation, increase in cellular proliferation, permanent growth arrest or senescence, apoptosis, and necrosis (Davies, 1999; Florean *et al.*, 2019). Recent findings suggest that an extensive list of lncRNAs, including *NEAT1, lincRNA-p21, UCA1, H19*, and *MALAT1*, are implicated in oxidative stress and the consequent hypoxia (Choudhry et al., 2014; Ding et al., 2018), as well as in ROS-mediated apoptosis (e.g. *SNHG15, NLUCAT1*) (Moreno Leon et al., 2019;

Saeinasab et al., 2019). In turn, a lot of other cellular processes are affected by oxidative stress, including angiogenesis, migration and metastasis, through different mechanisms (Dong et al., 2016). Therefore, it comes as no surprise that *MIAT* seems to be involved in oxidative stress regulation and its downstream effects, an effect that has also previously been reported in a cataract lenses study, where *MIAT*-specific knockdown enhanced the effects of H_2O_2-mediated oxidative stress to ultimately decrease cell proliferation and enhance apoptosis (Shen *et al.*, 2016).

Of note, a number of transcription factors implicated in these responses happen to be sensors of redox changes. For example, the notorious *c-Myc,* whose expression was downregulated upon *MIAT* knockdown, has been implicated in the production of ROS through oncogenic processes (Vafa *et al.*, 2002; Lin, 2019). In addition, the master regulator transcription factor of hypoxia, HIF1A, which regulates and is, at the same time, regulated by ROS (Rodic and Vincent, 2018; Ghanbari Movahed *et al.*, 2019; Lin, 2019), was found to be significantly downregulated (3-fold) upon *MIAT* down-regulation, suggesting that the knockdown of *MIAT* is involved in the regulation of the expression of HIF1A, potentially in a ROS-dependent manner, ultimately leading to the inhibition of cell survival and proliferation, and/or the increase of apoptosis. Finally, NRF2 (Nuclear Factor Erythroid 2-Related Factor 2), a master regulator of the oxidative stress response known for its role in the expression of the anti-oxidant machinery to promote oxidative stress-scavengers' expression, is also a redox sensor and was also down-regulated (~3-fold) in response to *MIAT* down-regulation, suggesting that the silencing of *MIAT* is also capable of attenuating the anti-oxidant response to promote ROS-mediated apoptosis in neuroblastoma cells.

On top of protein-coding players in the ROS-regulating network, there are accumulating lines of evidence that the non-coding genome vastly contributes to the regulation of ROS, and is, simultaneously, regulated by ROS. MicroRNA networks comprise a complicated variant in the regulation of oxidative stress (Lin, 2019). In response to the

down-regulation of *MIAT*, a plethora of miRNAs were predicted to be perturbed. Among them, a handful has already been implicated in ROS production and ROS-mediated cell responses. For instance, miR-15b-5p has been found to induce the production of ROS through the GSK3β axis (Xie *et al.*, 2019), which is also down-regulated and belongs to one of the most perturbed pathways upon *MIAT* knockdown (EGFR tyrosine kinase inhibitor resistance). MiR-21, a miRNA triggered by TGF-β, is also responsible for inhibiting the ROS scavenger SOD2 (Superoxide Dismutase 2) (Lin, 2019; Wei *et al.*, 2019) that was found to be ~2-fold down-regulated, as well. Furthermore, miR-30 has been associated with the response to radiation and oxidative stress (Wei *et al.*, 2019). Moreover, miR-200 is upregulated in response to elevated ROS and mediates apoptosis through inhibiting its target ZEB1 (~2-fold decreased expression) (Lin, 2019). Most intriguingly, miR-34a targets the master regulator TF NRF2 and consequently contributes to the attenuation of multiple components of the anti-oxidant machinery (Lin, 2019). On top of this, it targets the histone deacetylase SIRT1, which is in turn responsible for silencing c-Myc, but also directly targets c-Myc (O'Hagan *et al.*, 2011; Kong *et al.*, 2019). Therefore, although SIRT1 was ~4-fold down-regulated, c-Myc remained downregulated potentially due to the fact, at least partly, that EZH2, a significant component of the epigenetic silencing complex PRC, was up-regulated ~6-fold, given that the promoter of c-Myc is CpG island-rich and that ROS production bridges multiple components of the epigenetic machinery including DNA methylases (DNMTs) (O'Hagan *et al.*, 2011).

To link the aforementioned observations, it could be speculated that *MIAT* also exerts its effects through a ROS-induced SP (Specificity Protein) TF mechanism. Sps belong to the Sp/Krüppel-like factor (KLF) family of TFs and play important roles in healthy and pathological settings, including cancer (Hedrick *et al.*, 2016). It has also been established that elevated ROS levels result in decreased expression of Sps, primarily Sp1 (Lavrovsky *et al.*, 2000; Lee *et al.*, 2019; Upadhyaya, Liu and Dey, 2019). Among

the various family members, Sp1, Sp3 and Sp4 have gained attention, with Sp1 being the subject of thorough investigation (Safe *et al.*, 2018), and importantly all three members displayed at least a 3-fold decrease upon *MIAT* knockdown in our RNA sequencing, and in addition, numerous regulators of Sp1, including various miRNAs (Supplementary Table 4, Appendix II) and eighteen members of the ZBTB (zinc finger and BTB) family were significantly deregulated. Since the elevated activity of Sp1 has been associated with malignancy and tumour progression in various cancers including glioma (Guan *et al.*, 2012; Dong *et al.*, 2014; Safe *et al.*, 2018), it could be assumed that its down-regulation could prevent this effect. In fact, a reasonable mechanism would suggest that *MIAT* knockdown induces an increase in ROS production, which in turn induces a ROS-mediated epigenetic down-regulation of c-Myc, as described above (O'Hagan *et al.*, 2011), leading to the down-regulation of Sp1 via the regulation of miRNAs and ZBTB proteins. Interestingly, the downstream effectors of Sp1 include a variety of crucial cancer-related genes involved in survival, apoptosis and migration, such as c-MET (tyrosine-protein kinase Met), survivin, Fas, BCL-2, VEGFs and MMPs (matrix metallopeptidases), of which a variety are deregulated in our study (Supplementary Table 5, Appendix II).

In conclusion, this chapter attempts to elucidate how the downregulation of *MIAT* influences the global gene expression in neuroblastoma cells, to ultimately reduce the long-term survival and promote basal apoptosis, as well as to deteriorate the cells' ability to migrate, as demonstrated in Chapter 3. However, the study encompasses one important limitation: the acquired RNA sequencing results and their analysis are based on single replicates and not triplicates. To compensate for this, target validation was performed using multiple means, including RT² Profiler™ PCR Arrays, RT-qPCR, Western Blot and functional analyses to confirm ROS levels fluctuations.

Herein, we are suggesting that these effects are primarily ROS-mediated, as the knockdown of *MIAT* increases ROS levels in neuroblastoma cells, but can also be

ROS-independent. It is also essential to highlight the importance of the fact that the silencing of *MIAT* induces the down-regulation of important master regulator transcription factors, such as c-Myc, HIF1A, NRF2, Oct1 and Sp1, thus controlling the expression of a multitude of downstream targets involved in cell survival, apoptosis and migration, as well as ROS production, as well as to bring to onset the vast contribution of epigenetics, including miRNAs and lncRNAs, in these processes. The findings on *MIAT*'s modes of action in neuroblastoma cells presented in this chapter are multiple and diverse. Therefore, further research is essential to establish that *MIAT* could be used as a biomarker in neuroblastoma samples in the future, like numerous other lncRNAs for a variety of tumours (Melissari and Grote, 2016; Wu *et al.*, 2016; Rao *et al.*, 2017) and open new prognostic, predictive and even therapeutic avenues, especially as part of the "redox" therapy, to further elevate the apoptosis-promoting ROS levels. Finally, it is worth noting that across *MIAT* the area with the most differential expression between the control cells and those with silenced *MIAT* is localised at and includes the 3' UTR. It has been observed that the 3' UTR of ~1500 protein-coding human genes can be expressed in an independent way of the coding part of the same transcript, and about half such genes in mice show distinct expression patterns of the 3'UTRs comparing to the rest of the mRNA (Mercer *et al.*, 2011). In line with this, it has been suggested that 3' UTR-derived lncRNAs are also expressed independently of and convey differential signals from their associated mRNAs (Mattick, 2018). To this end, whether the 3'UTR of *MIAT* is, at least partly, responsible for the effect of *MIAT* on survival, apoptosis, migration and ROS production in neuroblastoma cells, or the expressional change involving it is an artefact, remains to be investigated.

4.5. Chapter Highlights

1. ***MIAT*** **silencing triggers the differential expression of 11085 protein-coding genes and eight pathways, including five cancer-related ones: the MAPK signalling pathway, EGFR tyrosine kinase inhibitor resistance, the TGF-beta signalling pathway, the Phospholipase D signalling pathway and the NOD-like receptor signalling pathway.**

2. ***MIAT*** **down-regulation was also associated with differential expression of genes involved in programmed cell death and especially intrinsic and extrinsic apoptosis. These changes were validated by RT² Profiler™ PCR Arrays.**

3. ***MIAT*** **down-regulation induces changes in the non-coding landscape, including 263 (predicted) miRNAs and 502 lncRNAs.**

4. ***MIAT*** **is capable of** ***in cis*** **gene regulation and control of the relative abundance of splicing variants.**

5. **RNA sequencing implicates** ***MIAT*** **down-regulation in oxidative stress-induced apoptosis in SH-SY5Y neuroblastoma cells. Functional assays further supported these findings in SH-SY5Y neuroblastoma cells, 1321N1 and T98G astrocytoma/GBM cells and suggest that down-regulation of** ***MIAT*** **is associated with ROS-mediated apoptosis.**

6. ***MIAT*** **silencing triggers complex pathway networks, which involve transcription factors, such as c-Myc, NRF2, HIF1A, Oct1 and Sp1, epigenetic changes, and are potentially regulated by the cellular levels of ROS.**

Chapter 5: Identification of novel lncRNAs involved in the regulation of the cell fate decision of neuroblastoma cells

5.1. Introduction

In light of the findings described in Chapters 3 and 4, suggesting that *MIAT* is a key lncRNA regulator of cell fate decisions, especially apoptotic cell death, the focus of the study shifted towards the identification of more lncRNAs that would potentially mediate these decisions.

LncRNAs are implicated in physiological cell processes, as well as in diseases, including cancer (Schmitz *et al*., 2016). In line with this, multiple oncogenic and tumour suppressor lncRNAs have been identified and studied in NB. Among the oncogenes, some are co-deregulated with typical chromosomal aberrations, as in the case of the overexpressed *ncRAN* in 17q gain neuroblastomas (Watters *et al.*, 2013; Pandey and Kanduri, 2015; Rombaut *et al.*, 2019). Others are co-amplified with *MYCN*, with *lncUSMycN* (Pandey and Kanduri, 2015; Zhao *et al.*, 2018), *lncNB1* (Liu *et al.*, 2019) and *MYCNOS* (Vadie *et al.*, 2015; O'Brien *et al.*, 2018) being three representative examples. The oncogenic lncRNA list includes lncRNA *CAI2,* whose overexpression is associated with high risk NBs (Barnhill *et al.*, 2014; Pandey and Kanduri, 2015), *T-UC 300A* (Domingo-Fernandez *et al.*, 2013; Pandey and Kanduri, 2015), the pro-proliferative and anti-apoptotic *LINC01105* (Tang *et al*., 2016; Ye *et al.*, 2019), *Xist* (Zhang *et al*., 2019), *MALAT1* (Bi *et al*., 2017) and *MIAT* (Bountali *et al*., 2019) (as presented in Chapters 3 and 4, as well). On the other hand, the tumour suppressor lncRNA list also includes numerous lncRNAs whose down-regulation contributes to NB progression. Such examples are *NDM29* in NBs with chromosome 11 loss (Nakagawara *et al.*, 2018; Zhao *et al.*, 2018), *FOXD3-AS1* (Zhao *et al.*, 2018), *MEG3* (Tang *et al.*, 2016; Chi *et al.*, 2019), *NBAT1* and *CASC15* on chromosome 6 (Russell *et al.*, 2015; Mondal *et al.*, 2018). The well-known *GAS5* (Mazar *et al.*, 2017) and *KCNQ1OT1* (Li *et al.*, 2019) also act as tumour suppressors in NB context. Many lncRNAs have been implicated in tumour-drug resistance (Smallegan and Rinn, 2019;

Zhao *et al.*, 2019) in different types of cancer. For instance, down-regulation of *GAS5* enhances the tumour resistance to doxrubicine in liver cancer (Wang *et al.*, 2019) and to trastuzumab in breast cancer (Li *et al.*, 2016), while lncRNA *MIR100HG* mediates cetuximab resistance in CRC and HNSCC (Lu *et al.*, 2017). Finally, autophagy is another process tightly regulated by lncRNAs (Bermúdez *et al.*, 2019), as in the case of *GAS5* promoting autophagy in CRC (Liu *et al.*, 2019) and lncRNA *SCAMP1* (Secretory Carrier Membrane Protein 1) regulating autophagy in paediatric renal cell carcinoma (Shao *et al.*, 2019). Notably, these two processes are often linked with each other (Wang *et al.*, 2019; Li *et al.*, 2019; Liu *et al.*, 2019). Thus, many approaches have been attempted to generate accurate lncRNA-based profiles and signatures, in order to classify patients robustly and provide the most suitable treatment (Sahu *et al.*, 2018; Gao *et al.*, 2019; Rombaut *et al.*, 2019; Yerukala Sathipati *et al.*, 2019), as well as predict the chances of recurrence (Utnes *et al.*, 2019).

Metformin is a synthetic biguanide (N', N' dimethylbiguanide) that has been used in the clinic as a golden standard treatment for type 2 diabetes (T2D) and has been identified as an effective anti-cancer drug (Sahra *et al.*, 2010). The target of metformin appears to be the mitochondria and in particular Complex I of the mitochondrial electron transport chain (ETC) (Vial *et al.*, 2019). The rationale of repurposing metformin as an anti-cancer drug lies in the fact that chronic augmented levels of plasma insulin may be a pro-tumourigenic factor, as insulin possesses mitogenic and pro-survival activity, and that tumour cells express high levels of the insulin receptor (Emami Riedmaier *et al.*, 2013). Further studies established that metformin acts through the activation of LKB1(liver kinase B1)/AMPK pathway to inhibit mTOR, the induction of (caspase-mediated) apoptosis and cell cycle arrest (Kourelis and Siegel, 2012; Kumar *et al.*, 2014; Gong *et al.*, 2016) and protein synthesis inhibition, which can occur via c-Myc/ N-Myc destabilisation (Wang *et al.*, 2014; Gong *et al.*, 2016). Metformin also promotes sensitisation of DNA damage response (DDR) (Menendez *et al.*, 2011) and

chemotherapeutic agents/ irradiation, and improvement of the response of chemotherapy-resistant CSCs (Li, 2011; Emami Riedmaier *et al.*, 2013; Mouhieddine *et al.*, 2015). Moreover, metformin prevents tumour initiation/ progression via inducing autophagy-mediated cell death (De Santi *et al.*, 2019) and suppressing the NF-κB signalling pathway (Podhorecka *et al.,* 2017; Nguyen *et al.*, 2019). Notably, metformin also mediates epigenetic modifications (Yu *et al.*, 2017) and, given that it vastly affects the tumour cell metabolism, it is natural to alter the metabolism-related (Sun *et al.*, 2018), as well as the broader, lncRNA landscape.

Cellular processes are controlled by a plethora of interacting molecular signalling pathways, comprised of and controlled by numerous protein- and non-protein-coding elements. Chemotherapeutic agents tend to alter the molecular landscape in cancerous cells, and therefore, their administration comprises a useful platform for the study of these changes, which will ultimately affect the fate of the cells, including their survival, proliferation, differentiation and death. In line with this, the fact that metformin targets multiple signalling pathways in cancer led us to the hypothesis that transcriptome analysis of neuroblastoma cells treated with metformin will allow the identification of lncRNAs that are potentially involved in the regulation of cell fate decision in these cells in response to the administration of the drug. To this end, the initial aim of this study, the findings of which are preliminary, was to identify novel lncRNAs that can potentially act as regulators of cell fate using RNA sequencing analysis of neuroblastoma cells after short- and long-term metformin treatment.

5.2. Materials and Methods

5.2.1. Cell culture and chronic exposure to metformin

The experiments incorporated in this chapter were conducted using the human neuroblastoma SH-SY5Y cell line, cultured using the HyClone™ DMEM/F12 1:1 growth

media, supplemented with 10% heat-inactivated fetal bovine serum, 2μM L-Glutamine, 1μM Sodium Pyruvate and 10mg/ml gentamicin solution, as described in section 2.1. In a subset of experiments for which the effects of continuous exposure to metformin was assessed, SH-SY5Y cells were cultured for two consecutive months in growth media supplemented with increasing concentrations of metformin, in the range of 1-20mM. In each round, SH-SY5Y cells were seeded in cell culture flasks and after 24h metformin was added (parental SH-SY5Y cells without metformin addition were also cultured to be used as control cells). The cells were then incubated (37°C, 5% CO_2) until reaching ~80% confluence. Afterwards, the detached dead cells were removed from the culture, whilst the viable attached ones were trypsinised and passaged so that the next round of increased metformin dose would follow.

5.2.4. Determination of cell survival

For the metformin cytotoxicity experiments (10-200μM and 0.25-100 mM) cells were seeded in 96-well plates (100μl/well), incubated for 24h and subsequently, treatment was added (drug diluted in growth media- 100μl/well) and cells were incubated for 48/72 h. **Cell survival** was assessed using MTS (CellTiter 96® Aqueous One Solution Cell Proliferation Assay) (detailed in section 2.6.3). The growth inhibitory effect of metformin was calculated according to the following equation: **% inhibition of cell growth = 100- [OD490 of treated sample / OD490 of untreated sample (control)] x 100**.

5.2.5. RNA sequencing and Pathway analysis

Global gene expression changes in response to metformin treatment were determined by sequencing the whole transcriptome, as detailed in section 2.10. Next-generation sequencing was conducted by the Earlham Institute. Quality controlled reads were

aligned to Human Genome build (hg19) using Tophat, transcripts were assembled using Cufflinks (with GTF support) and the number of reads mapping to each feature counted and expressed as FPKM using the CuffNorm package. Differentially expressed mRNAs were condensed into gene networks representing biological and disease processes using iPathwayGuide (Advaita Bioinformatics, Ann Arbor, MI, USA). The differential expression was measured in three different comparison sets: untreated SH-SY5Y cells versus SH-SY5Y treated with 20mM metformin (Data Set 1), untreated SH-SY5Y cells versus SH-SY5Y with continuous exposure to 3mM metformin (Data set 2) and SH-SY5Y cells treated with 20mM metformin versus SH-SY5Y with continuous exposure to 3mM metformin (Data set 3), and a cutoff threshold of 1.5-fold change (and an equivalent 0.6 Log_2 Fold Change) was applied. The Log_2 Fold Change (Log_2FC) is referred to as "–fold change" in this chapter. The RNA sequencing results were analysed using the iPathway Guide by Advaita Bioinformatics (advaitabio.com).

5.2.6. Statistical

Statistical analyses were performed using GraphPad Prism 6 (GraphPad Software). Data are presented as the mean ± SEM; the number of observations (n) refers to biological replicates, each replicate being conducted on a separate culture of cells. Comparisons were made using an unpaired T-test or One-Way ANOVA with Bonferroni's multiple comparison test (MCT).

5.3. Results

5.3.1. The role of metformin treatment in SH-SY5Y cells

Effects of metformin treatment on the survival of SH-SY5Y cells

To assess the cytotoxic effect of metformin, two series of dose-response optimisation experiments were performed, in which micromolar, as well as millimolar concentrations (10-1000μM and 2-50 mM), were tested at 48/72 h. Metformin was ineffective in killing cells at μM concentrations, while it was too toxic at very high doses (e.g. ~60% inhibition of cell growth at 48/72 h for 50mM and 100mM metformin) (Figure 5.1 and Supplementary Figure 1, Appendix III). The concentration of 20mM was selected for subsequent experiments, based on the optimisation experiments and prior literature (Costa *et al.*, 2014; Garbati *et al.*, 2017; Li *et al.*, 2019; Wu *et al.*, 2019).

In addition, to assess the effect of the prolonged exposure of the cells to metformin, MTS assays were employed to examine the cell viability after 48 and 72 h. As expected, only slight, statistically non-significant changes in cell viability were observed between non-treated and metformin-resistant SH-SY5Y cells after the administration of metformin (Figure 5.2).

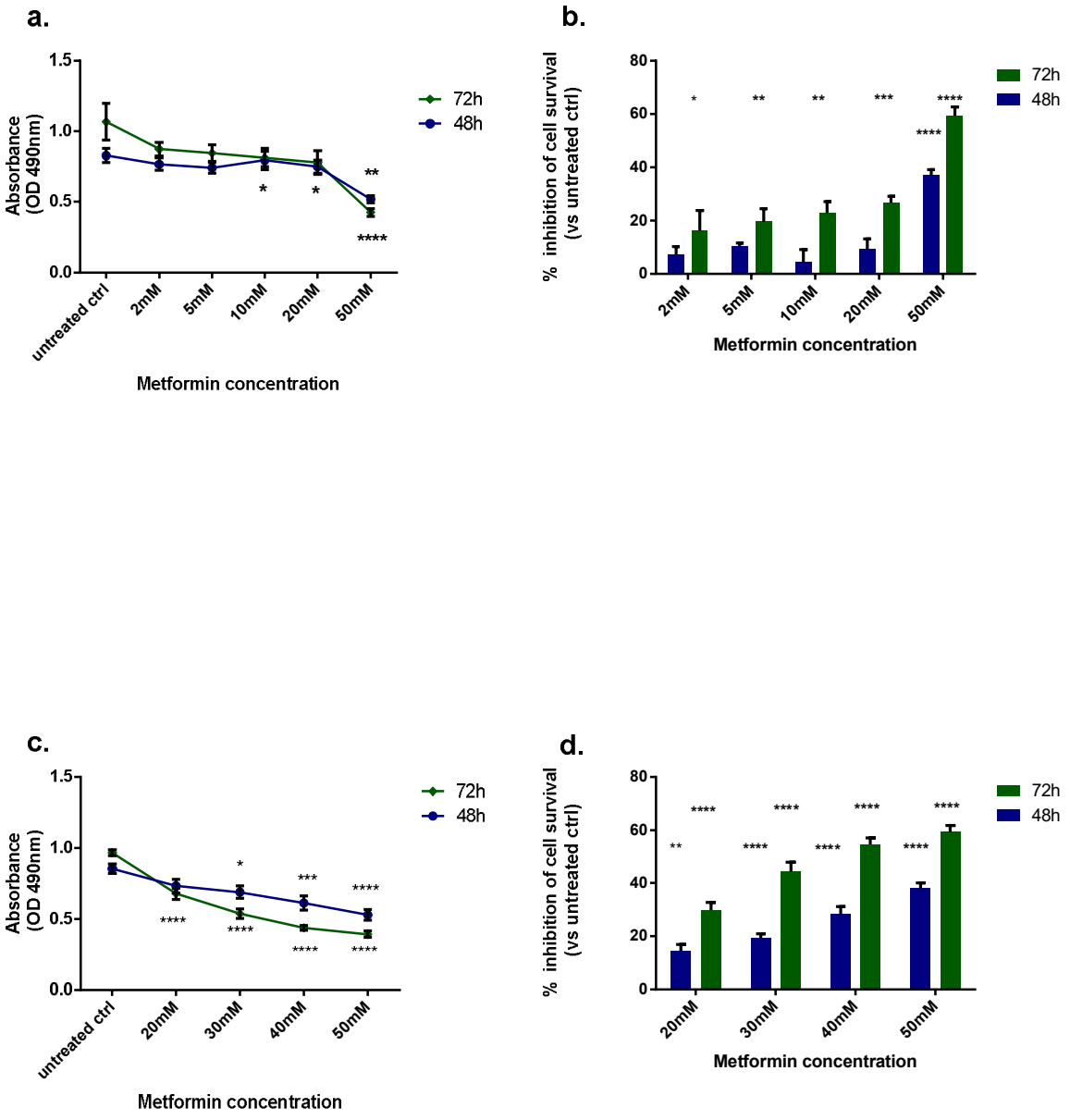

Figure 5.1. The effects of metformin on the cell survival of SH-SY5Y cells. Cells were seeded in 96-well plates (100µl/well), incubated for 24h and metformin (2-50mM-a, b- and 20-50mM- c, d) was subsequently added (diluted in growth media-100µl/well). Cell survival is reduced by the treatment with various concentrations of metformin comparing to cells growing in the absence of metformin, as measured by the MTS assay 48 h and 72 h post-treatment. The concentration of 20mM was selected for further experiments. Optical density (OD) at 490nm is represented in a, c, while % inhibition of cell survival is represented in b, d. * indicates a *p-value*<0.05, ** indicate a *p-value*<0.01; ***/**** indicate a *p-value*<0.001, compared to the untreated control for 48 and 72 h, respectively, as measured by Two-way ANOVA tests with multiple comparisons (MCT). Data are represented as mean +/- SEM, n=3.

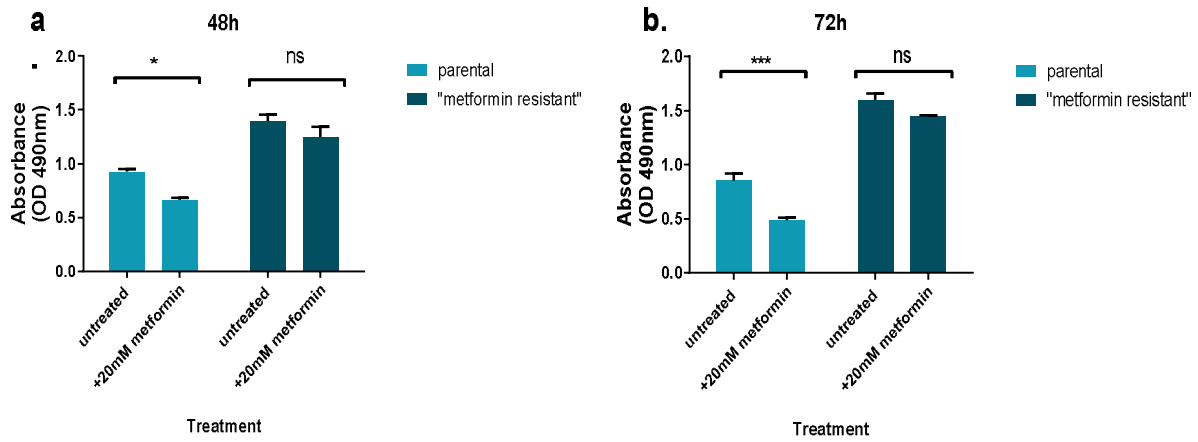

Figure 5.2. Continuous exposure to metformin generates "metformin resistant" SH-SY5Y cells. SH-SY5Y cells were cultured in the continuous presence of increasing concentration of metformin (1→20mM) for two months. In order to assess the cells for resistance to metformin, at the end of this period, cell viability was compared between parental cells without any treatment and cells with suspected resistance, without and after the addition of 20mM metformin, via MTS assay at 48 h and 72 h. As expected, metformin reduces cell viability in parental cells, but viability levels do not differ between untreated and treated with metformin cells in the "metformin resistant" group, both at 48 h (a) and 72 h (b), as measured by One-way ANOVA tests with multiple comparisons (MCT), n=4 replicates. Data are represented as mean +/- SEM.

Identification of novel lncRNAs involved in the response to metformin treatment

In light of the importance of the non-coding component of the human genome, the attention of this study was shifted towards the identification of novel lncRNAs that are potentially involved in the determination of cell fate. For the purposes of the current study, SH-SY5Y neuroblastoma cells were either cultured as a negative control (untreated) or were exposed to 20mM metformin for 48 h, followed by total RNA extraction and RNA sequencing (Data set 1).

The RNA sequencing analysis revealed that 5652 out of a total of 13481 were differentially expressed genes with measured expression. Among these changes, a plethora of perturbations affected the lncRNAome of the cells. Interestingly, 418 lncRNAs, which are novel in the context of neuroblastoma as they have not been

studied before in this tumour, were shown to be differentially expressed, belonging to different lncRNA subclasses. The ten most up-regulated lncRNAs were *LOC100652730, GHRLOS, LOC100130700, PCBP1-AS1, CBR3-AS1, CASC2, LOC730227, MIR22HG, LOC100288637* and *LOC100507557,* presenting a >10-fold increase in expression, while the ten most down-regulated included *TP73-AS1, PEG3-AS1, LOC100128420, LOC100288637, LOC100506714, LOC256021, LOC100509894, LOC283050, LOC730227* and *LOC151300* with a >8-fold decrease in expression. Of these, numerous have already been implicated in various types of cancer, confirming that the metformin treatment approach used has successfully provided relevant results. Such an example is the NAT of *TP73, TP73-AS1,* which was down-regulated by more than 8-fold in metformin-treated cells, and is a well-established driver of tumourigenesis in many malignancies (Gong *et al.*, 2020). Another such example is the 9-fold down-regulated *PEG3-AS1*, a paternally expressed transcript that has recently been associated with head and neck (Hsu *et al.*, 2016) and colorectal cancer (Zhang *et al.*, 2019). Besides, *LOC100288637* is a pseudogene whose expression was massively down-regulated upon treatment with metformin (11-fold) and has previously been associated with HER-2 positive breast cancer (Yang *et al.*, 2016) and ovarian cancer (Feng *et al.*, 2019). In the opposite direction*, PCBP1-AS1* (Poly(RC) Binding Protein 1 anti-sense 1), is a NAT that showed a ~14-fold increase in expression in metformin-treated cells and has been implicated in B-cell lymphoma (Dai *et al.*, 2015). Moreover, the well-studied onco-suppressor *CASC2,* which has been related with multiple tumours (Palmieri *et al.*, 2017), displayed a ~13-fold increase in expression, while the NAT *CBR3-AS1*, which has also been associated with a variety of tumours was 13-fold up-regulated, as well. Furthermore, *MIR22HG*, the thoroughly studied tumour suppressive lncRNA, host gene of the microRNAs miR-22-3p and miR-22-5p, showed a 12-fold up-regulation. Among the most deregulated lncRNAs, *LOC100507557, LOC100505695* and *LOC100506801* are still uncharacterised. Of the lncRNAs displaying perturbed expression, 43% belonged to the NAT category (e.g. *PCBP1-AS1,*

CBR3-AS1, LOC641364, LOC100509894, LOC283050, LOC100506714) rendering this class the most abundant, 22% were lincRNAs (such as *LOC730227, LOC151300, LOC256021, LOC100652730, LOC730227*) and 12% pseudogenes, while ~15% were uncharacterised genes, proposing a broad lncRNA interference in the molecular pathways affected by the action of metformin (Figure 5.3 and Supplementary Table 1, Appendix III).

In addition to lncRNA perturbations, numerous changes in the miRNA repertoire were brought to light, enhancing the hypothesis the novel lncRNAs may exert their functions via lncRNA-miRNA axes. The prediction of active miRNAs is based on enrichment of differentially downregulated target genes of the miRNAs (Friedman *et al.*, 2009), and, in general, miRNAs have an inhibitory effect on their targets. The RNA sequencing predicted an astonishing 304 miRNAs (Table 5.1) to be altered in response to the treatment with metformin, affecting the expression of downstream targets, with miR-101-3p bearing the most pronounced changes. Some representative targets of miR-101-3p include APC, a tumour suppressor key regulator of the Wnt signalling pathway, involved in processes including cell migration and adhesion, transcriptional activation, and apoptosis, c-Myb, a well-studied regulator of transcription, the apoptosis-related BCL2L11, and the chromatin remodelling regulator EZH2. In addition, the second most perturbed miRNA, miR-519d-3p, also targets a variety of important cancer-related genes, including the pro-apoptotic BID, and STAT3, a protein that mediates the expression of a variety of genes in response to cell stimuli, and thus plays a key role in many cellular processes such as cell growth and apoptosis.

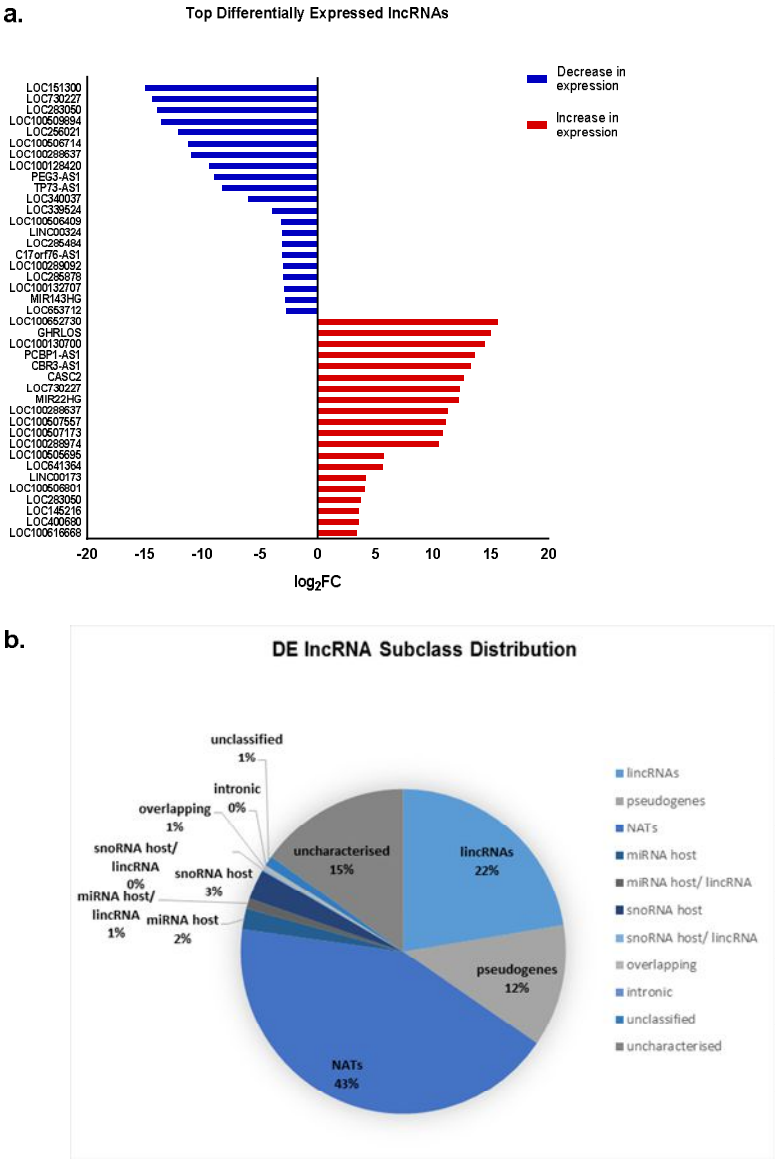

Figure 5.3. The effects of metformin on lncRNA expression. Exposure of SH-SY5Y cells to 20mM metformin for 48 h induces alterations in the expression of lncRNAs. The bar chart presents only the top perturbed genes in both directions (a). Red coloured bars correspond to upregulated gene expression, while blue coloured bars correspond to downregulated gene expression. Data are the difference in expression between untreated control cells and cells exposed to 20mM metformin, expressed as a normalised $\log_2$ fold change ($\log_2$FC). A threshold of 0.05 for statistical significance (*p-value*) and a log fold change of expression with an absolute value of at least 0.6 were applied. The pie chart schematically presents the distribution of differentially expressed lncRNAs into different lncRNA subclasses (b). **DE**: differentially expressed; **NAT**: Natural Anti-sense Transcript; **lincRNA**: Long Intergenic RNA; **miRNA host**: microRNA host gene; **snoRNA host**: small nucleolar RNA host gene.

Table 5.1. Top predicted perturbed miRNAs in metformin-treated SH-SY5Y cells.

miRNA name	Number of perturbed targets/ total genes	Number of targets/ total genes	*p-value*
hsa-miR-101-3p	313 / 426	703 / 1156	6.821e-12
hsa-miR-519d-3p	303 / 428	689 / 1182	2.411e-11
hsa-miR-526b-3p	303 / 428	689 / 1181	2.827e-11
hsa-miR-106b-5p	303 / 428	689 / 1180	3.314e-11
hsa-miR-20a-5p	303 / 428	689 / 1180	3.314e-11
hsa-miR-17-5p	303 / 428	689 / 1180	3.314e-11
hsa-miR-93-5p	303 / 428	689 / 1180	3.314e-11
hsa-miR-20b-5p	303 / 428	689 / 1180	3.314e-11
hsa-miR-106a-5p	303 / 428	689 / 1180	3.314e-11
hsa-miR-29c-3p	301 / 405	652 / 1051	3.609e-11

Protein-coding gene alterations and pathway perturbations

Apart from changes in the expression of lncRNAs, a variety of protein-coding genes and pathway perturbations were observed in response to metformin treatment, which could potentially be correlated with the novel identified lncRNAs. The top upregulated protein-coding genes include *ACP5* (acid phosphatase 5), *SLC23A3* (solute carrier family 23 member 3), *GPNMB* (Glycoprotein Nmb) and a plethora more, while the top downregulated ones include *RSPH4A* (Radial Spoke Head Protein 4 Homolog A), *CMPK2* (Cytidine/Uridine Monophosphate Kinase 2) and *LDB2* (LIM Domain Binding 2) (Figure 5.4a). In addition, significant alterations in cancer-related protein-coding genes were observed, with a great number of them being either up-regulated or down-regulated (Figure 5.4b). For instance, the master regulators of transcription, primarily c-Myc, but also c-Myb, both displayed a multi-fold decrease in expression levels, especially c-Myb (~15-fold). The Wnt signalling-associated *APC* also showed a 13-fold decrease in expression, while the DDR-associated *BRCC3* (BRCA1/BRCA2-Containing Complex Subunit 3) and *XRCC3* (X-Ray Repair Cross Complementing 3) were also down-regulated by 4- and 3-fold, respectively. On the other hand, multiple pro-apoptotic components of the apoptotic machinery were up-regulated, including *BBC3* (BCL-2 Binding Component 3) (~13-fold), *Fas* (3-fold) and *CASP8* (4-fold), while *GADD45A*, a crucial component of the DDR also showed a nearly 5-fold increase in expression.

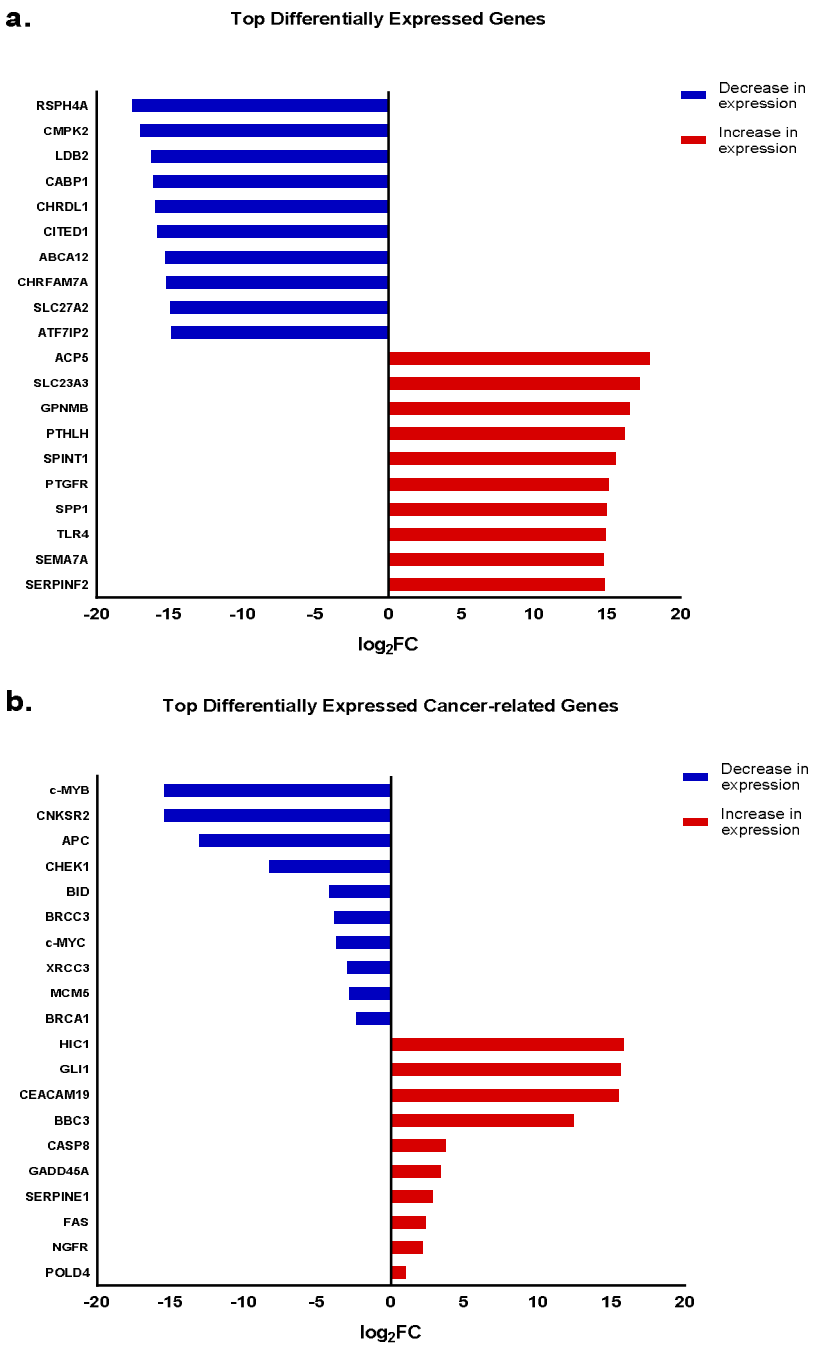

Figure 5.4. The effect of metformin on protein-coding gene expression. Exposure of SH-SY5Y cells to 20mM metformin for 48 h induces alterations in the expression of protein-coding genes (a), including a variety of genes involved in cancer-related processes, including cell survival, apoptosis, cell cycle progression and DNA repair (b). The graphs present only some representative top perturbed genes. Red coloured bars correspond to upregulated gene expression, while blue coloured bars correspond to downregulated gene expression. Data are the difference in expression between untreated control cells and cells exposed to 20mM metformin, expressed as a normalised $\log_2$ fold change ($\log_2$FC). A threshold of 0.05 for statistical significance (*p-value*) and a log fold change of expression with an absolute value of at least 0.6 were applied.

In addition to revealing single gene expression perturbations, the RNA sequencing analysis also unveiled perturbations on the molecular pathway level and revealed moderations in Gene Ontology terms and diseases, in which the newly identified lncRNAs presented above could exert a role. In particular, 28 pathways were found to be significantly impacted (Table 5.2 and Supplementary Table 2, Appendix III), including numerous cancer-related ones. Intriguingly, some of the already annotated cancer-related pathways that have previously been found to be involved in the response to metformin have been confirmed, such as cell cycle, apoptosis and cytokine/chemokine interactions. Notably, some understudied or even novel ones have been brought to onset, including DNA replication and DNA repair processes (e.g. mismatch repair, base excision repair and homologous recombination), and Hippo (Table 5.3, Figure 5.5. and Supplementary Table 2, Appendix III). Furthermore, 1813 Gene Ontology (GO) terms, with the most perturbed ones shown in Table 5.4, were found to be significantly enriched. Interestingly, some of the most deregulated lncRNAs mentioned in the previous section are part of these processes. For instance, *TP73-AS1* mediates p53 signalling and apoptotic responses (Xiao *et al.*, 2018; Yao *et al.*, 2018), as well as cell cycle (Xiuyun *et al.*, 2018), *PCBP1-AS1* has been implicated in cell cycle regulation (Peng *et al.*, 2017) and Fanconi anaemia DNA repair (Velimezi *et al.*, 2018), while *MIR22HG* has also been implicated to regulate cell cycle (Vidyasekar *et al.*, 2015).

Table 5.2. Top perturbed molecular pathways in metformin-treated SH-SY5Y cells.

Pathway name	*p-value*
Neuroactive ligand-receptor interaction	1.896e-6
Complement and coagulation cascades	6.917e-4
HTLV-I infection	0.005
Olfactory transduction	0.008
Glycine, serine and threonine metabolism	0.010

Table 5.3. Top cancer-related perturbed molecular pathways in metformin-treated SH-SY5Y cells.

Pathway name	Key DEGs	*p-value*
DNA replication	*MCM5/7, POLE2*	1.088e-9
Cytokine-cytokine receptor interaction	*BMPR1B,CTF1, TNFSF18/19, PDGFC*	1.041e-6
Cell cycle	*CHEK1, MYC*	5.928e-6
Mismatch Repair	*EXO1, RFC2/4, LIG1*	2.230e-5
Homologous recombination	*BRCC3, XRCC3, RAD54L*	1.518e-4
p53 signalling pathway	*CHEK1, BID*	4.947e-4
Basal cell carcinoma	*APC, FZD3, LEF1*	0.004
Fanconi Anaemia pathway	*BRCA1, FANCI, HES1, BRIP1*	0.009
Base Excision repair	*UNG, POLE2*	0.023
Hippo signalling pathway	*APC, BMPR1B, LEF1, FZD3, TEAD2*	0.024
Apoptosis	*BCL2L11, BID*	0.035
Colorectal cancer	*APC, BCL2L11, LEF1*	0.04

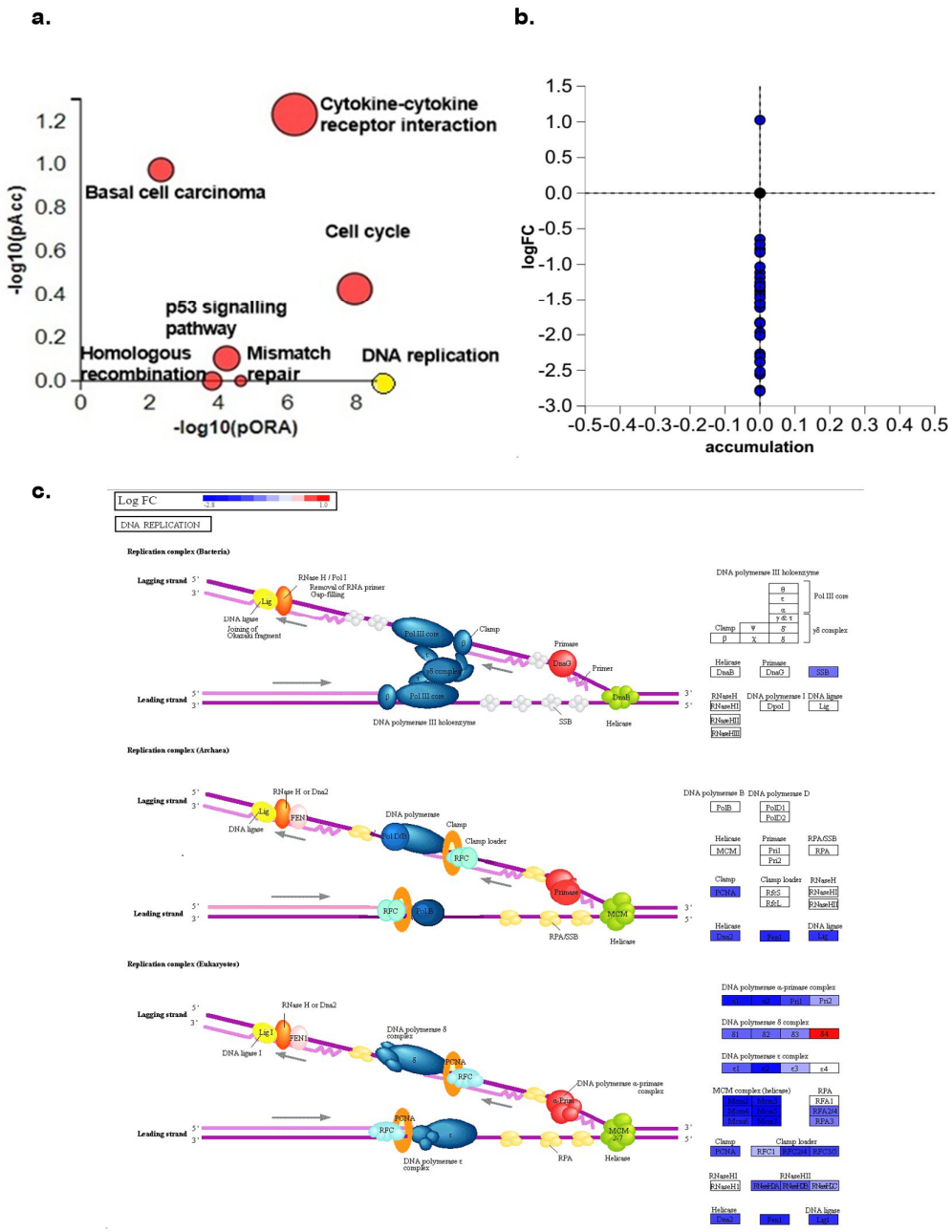

Figure 5.5. Top perturbed cancer-related pathway: DNA replication (KEGG: 03030). Perturbation vs over-representation: DNA replication (yellow circle) is shown, using the negative log of the accumulation and over-representation p-values, along with the other most significant pathways (red circles). Pathways in red are significant, based on the combined uncorrected *p-values* (a). Measured expression vs accumulation of pathway genes: all the genes from this pathway are represented in terms of their measured fold change (y-axis) and accumulation (x-axis). Accumulation is the perturbation received by the gene from any upstream genes. Genes in blue had only measured fold change. The remaining genes that were not measured and had no accumulation are shown in black (b). Graphically, the pathway diagram is overlayed with the computed perturbation of each gene. The perturbation accounts both for the gene's measured fold change and for the accumulated perturbation propagated from any upstream genes (accumulation). The highest negative perturbation is shown in dark blue, while the highest positive perturbation in dark red. The legend describes the values on the gradient (c).

Table 5.4. Top perturbed Gene Ontology (GO) terms in metformin-treated SH-SY5Y cells.

	Pathway name	Number of perturbed genes/ total genes in the pathway	*p-value*
Biological Processes	**Multicellular organismal process**	1999 / 4365	1.100e-12
	Multicellular organism development	1586 / 3418	1.200e-11
	Cell proliferation	658 / 1318	7.300e-11
	System development	1410 / 3026	8.200e-11
	Cellular response to stimulus	2121 / 4697	1.400e-10
Molecular functions	**Receptor ligand activity**	110 / 165	3.900e-11
	Signalling receptor activity	243 / 437	8.000e-10
	Receptor regulator activity	115 / 181	1.300e-9
	Transmembrane signalling receptor activity	206 / 371	1.900e-8
	Transmembrane receptor activity	214 / 389	2.700e-8

5.3.2. Continuous exposure to metformin alters the molecular landscape of SH-SY5Y cells

Identification of novel lncRNAs involved in the response to continuous exposure to metformin

Given that low risk NB patients often benefit from spontaneous regression, during which cells become differentiated again (Nakagawara *et al.*, 2018), inducing NB cell differentiation comprises an attractive strategy. This is usually achieved via the administration of all-trans-retinoic acid (ATRA), however, alternative approaches have proved to be effective *in vitro*, such as the use of N-acetylaspartate (NAA) (Mazzoccoli *et al.*, 2016). Moreover, metformin promotes neuronal differentiation via ROS production (Binlateh *et al.*, 2019). Taking everything into account, and after the microscopic observation that long-term exposure of SH-SY5Y cells to metformin leads to a neuron-like morphology very similar to the one observed by Costa *et al.,* (2014) and Mazzoccoli *et al.,* (2016), it was speculated that continuous exposure to metformin could cause moderations in the molecular and cellular landscape of the cells, and therefore we would be able to identify novel lncRNAs involved in cell fate decision, potentially including cell differentiation as such an aspect. To this end, total RNA was extracted from parental SH-SY5Y cells (untreated control) and SH-SY5Y cells with continuous exposure to metformin and, therefore, acquired resistance to it (that was achieved after weeks of continuous exposure to increasing concentrations of metformin) (Figure 5.2), followed by RNA sequencing.

In this experiment 7855 differentially expressed genes were identified out of a total of 13741 genes with measured expression. In line with the primary aim of this chapter to identify novel lncRNAs mediating cell fate decisions associated with chronic exposure to metformin, lncRNA perturbations were analysed next. The analysis of the RNA sequencing shed light to a great number of lncRNA perturbations of the cells. Notably, 482 lncRNAs showed differential expression between the two compared groups,

belonging to different lncRNA subcategories. The revealed changes followed both directions, with the top ten up-regulated lncRNAs being *GHRLOS, LOC100133331, CASC2, LOC729678, LOC100288974, LOC100288637, LOC100507173, LOC100505695, LOC643401* and *LOC100507557* (>5-fold increase), whilst in the opposite direction, the most down-regulated lncRNAs were *LINC00478, LOC653712, LINC00304, LOC392232, LINC00176, LOC100288637, LOC256021, LOC100125556, LOC648987* and *LOC151300* (>4-fold decrease). Among them, various lncRNAs have already been linked with cancer. Astonishingly, the NAT *GHRLOS* (Ghrelin opposite strand/antisense RNA), a lncRNA participating in rather complicated cancerous contexts, which has finally been attributed clinical significance in cancer (Soleyman-Jahi *et al.*, 2019), was found to be ~15-fold up-regulated. The tumour suppressor *CASC2*, similar to brief exposure to metformin, showed again a massive 12-fold increase in expression, while *LOC643401* (also known as *PURPL*-p53 upregulated regulator of p53 levels), a modulator of basal p53 levels, also displayed a 5-fold up-regulation. *MIR7-3HG*, an autophagy-related, c-Myc-dependent modulator of cell proliferation (Capizzi *et al.*, 2017), displayed a 4-fold increase, as well. The continuous exposure to metformin also induced a decrease in the expression of multiple other important lncRNAs. Importantly, *LOC151300*, a lincRNA that has been linked to colon cancer and its metastases (Lan *et al.*, 2012), showed the most pronounced decrease in expression (15-fold) in response to continuous metformin exposure. Furthermore, *LINC00176*, a lincRNA implicated in ovarian (Dai et al., 2019), hepatocellular (Tran et al., 2018) and oesophageal (Fan and Liu, 2016) cancer, was 9-fold down-regulated. In addition, *LINC00304* (5-fold decrease) and *LINC00478* (4-fold decrease), have also been previously associated with cancer. Besides the lncRNAs already implicated in other tumours, some of the most deregulated ones remain uncharacterised, such as *LOC100133331, LOC100505695, LOC100507557* and *LOC648987* (as well as the up-regulated *LOC100133161, LOC284080* and *LOC284865*, which complete the list of the top twenty-in each direction- deregulated

lncRNAs). Similarly to data set 1, the largest category was NATs (~39%), including *GHRLOS, LOC285965, LOC100287559*, and *LOC100144603*, followed by lincRNAs (23%) (e.g. *LOC729678, LOC100507173, LINC00176, LOC151300, LOC256021)* and pseudogenes (15%), like *LOC100125556, LOC100288637, LOC100288974* and *LOC100288637*. Albeit, ~16% of the identified lncRNAs were newly-discovered, uncharacterised genes. Collectively, these results suggest that the lncRNAome holds a crucial role in the mechanisms and pathways determining the fate of neuroblastoma cells in response to long-term exposure to metformin (Figure 5.6 and Supplementary Table 3, Appendix III).

Based on the biological scenario in which lncRNAs and miRNAs regulate gene expression through common axes, on top of the identification of novel lncRNAs, the RNA sequencing analysis predicted 321 miRNAs (Table 5.5) to be altered as a result of resistance to metformin after continuous exposure, affecting the expression of downstream targets, with miR-30c-5p showing the greatest changes. Some representative targets of miR-30c-5p include MECP2 (Methyl-CpG Binding Protein 2), a protein capable of binding specifically to methylated DNA repressing transcription from methylated gene promoters, BCOR (BCL6 Corepressor), a potential influencer of apoptosis, and NRP1 (neuropilin 1), which is part of several different signalling pathways that control cell survival, migration, and attraction. Other than the miR-30 family of miRNAs, of which several members were perturbed, miR-183-5p was also predicted to be highly perturbed. MiR-183-5p targets and regulates the expression of apoptosis-related genes, such as *XIAP*, as well as genes related to DNA repair processes, such as *BRCA1*, and the p53 inhibitor *MDM4*.

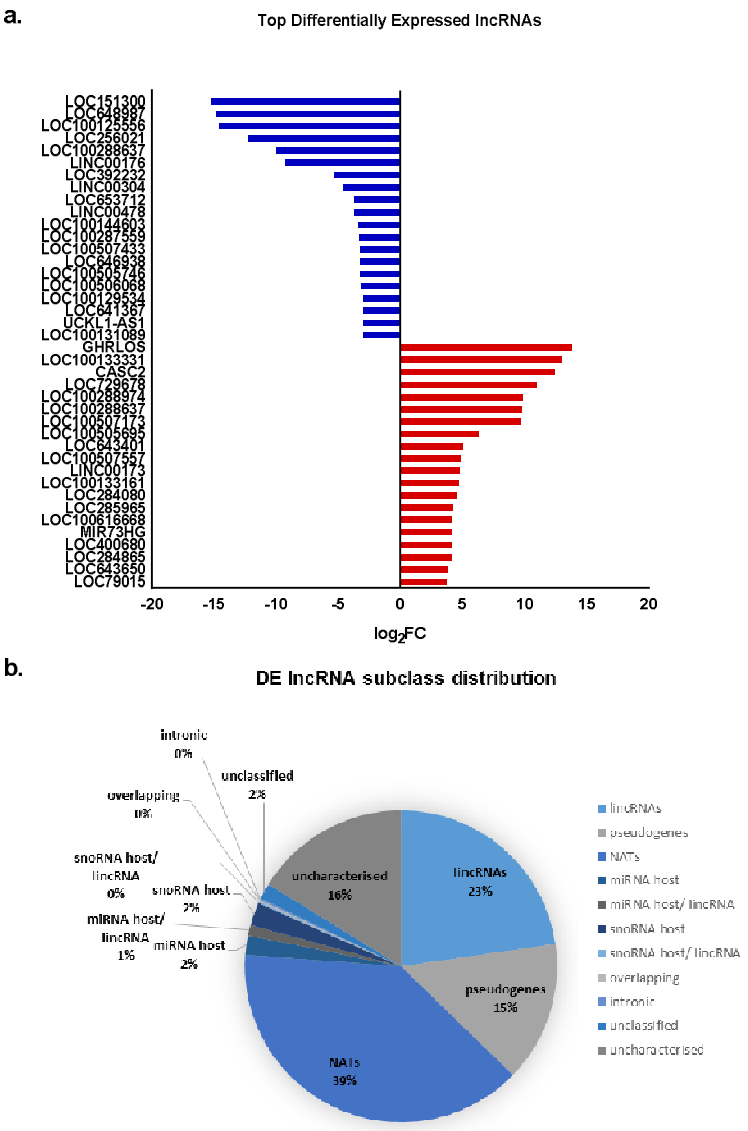

Figure 5.6. The effects of continuous exposure to metformin on lncRNA expression. Continuous exposure of SH-SY5Y cells to 3mM metformin induces alterations in the expression of lncRNAs. The bar chart presents only the top perturbed genes in both directions (a). Red coloured bars correspond to upregulated gene expression, while blue coloured bars correspond to downregulated gene expression. Data are the difference in expression between untreated control cells and cells with acquired resistance to 3mM metformin, expressed as a normalised $\log_2$ fold change ($\log_2$FC). A threshold of 0.05 for statistical significance (*p-value*) and a log fold change of expression with an absolute value of at least 0.6 were applied. The pie chart schematically presents the distribution of differentially expressed lncRNAs into different lncRNA subclasses (b). DE: differentially expressed; **NAT**: Natural Anti-sense Transcript; **lincRNA**: Long Intergenic RNA; **miRNA host**: microRNA host gene; **snoRNA host**: small nucleolar RNA host gene.

Table 5.5. Top predicted perturbed miRNAs in SH-SY5Y cells with continuous exposure to metformin.

miRNA name	Number of perturbed targets/ total genes	Number of targets/ total genes	*p-value*
hsa-miR-30c-5p	526 / 688	868 / 1311	1.078e-16
hsa-miR-30a-5p	526 / 688	868 / 1311	1.078e-16
hsa-miR-30d-5p	526 / 688	868 / 1311	1.078e-16
hsa-miR-30b-5p	526 / 688	868 / 1311	1.078e-16
hsa-miR-30e-5p	526 / 688	868 / 1311	1.078e-16
hsa-miR-183-5p	410 / 529	644 / 970	7.397e-16
hsa-miR-101-3p	514 / 641	829 / 1169	1.133e-14
hsa-miR-302c-3p	491 / 625	777 / 1123	2.093e-14
hsa-miR-124-3p	728 / 999	1257 / 1932	5.905e-14
hsa-miR-9-5p	475 / 631	770 / 1166	3.393e-13

Protein-coding gene alterations and pathway perturbations

In our effort to identify novel deregulated lncRNAs involved in cell fate determination we also identified highly perturbed protein-coding genes and pathways, which could potentially be associated with our novel lncRNAs. Therefore, in addition to the perturbations in expression observed for the non-coding elements of the genome, some of the top differentially expressed protein-coding genes include the up-regulated *ACP5, NPNT* (Nephronectin), whilst *ZNF771* (Zinc Finger Protein 771), *MAP2* (Microtubule Associated Protein 2) and *CDH7* (Cadherin 7) were among the top down-regulated ones. Similar to data set 1, multiple cancer-related genes were deregulated in both directions, including *MMP1* (Matrix Metallopeptidase 1), *ITGB4* (Integrin Subunit Beta 4) and *RASA4* (RAS P21 Protein Activator 4), which were all up-regulated, and *CNKSR2* (Connector Enhancer Of Kinase Suppressor Of Ras 2), *DOK3* (Docking Protein 3) and *FAM86B1* (Family With Sequence Similarity 86 Member B1), which displayed decreased expression (Figure 5.7).

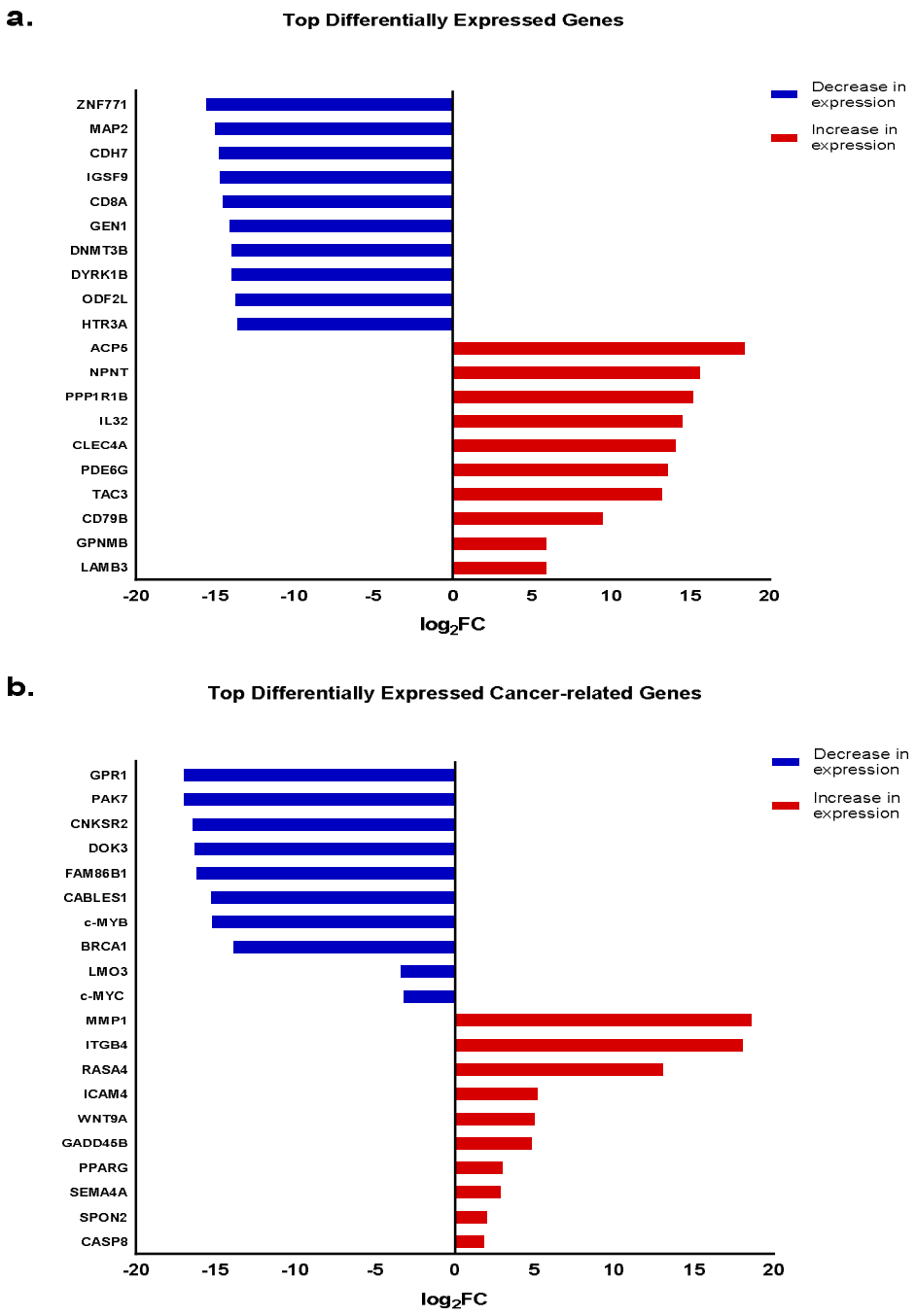

Figure 5.7. The effect of continuous exposure to metformin on protein-coding gene expression. Continuous exposure of SH-SY5Y cells to 3mM metformin induces alterations in the expression of protein-coding genes (a), including a variety of genes involved in cancer-related processes, such as cell survival and growth, apoptosis and DNA repair (b). The graphs present only some representative top perturbed genes. Red coloured bars correspond to upregulated gene expression, while blue coloured bars correspond to downregulated gene expression. Data are the difference in expression between untreated control cells and cells with continuous exposure to 3mM metformin, expressed as a normalised $\log_2$ fold change ($\log_2$FC). A threshold of 0.05 for statistical significance (*p-value*) and a log fold change of expression with an absolute value of at least 0.6 were applied.

Apart from revealing single gene expression perturbations, the RNA sequencing analysis also unveiled perturbations on the molecular pathway level, as well as alterations in Gene Ontology terms and diseases, which could possibly involve some of the identified lncRNAs. Specifically, 31 pathways were found to be significantly impacted (Table 5.6. and Supplementary Table 4, Appendix III), including numerous cancer-related ones. Intriguingly, similarly to data set 1, some of them that have been previously studied and found to be involved in the mechanism of action of metformin have been confirmed, such as cell cycle, p53-induced apoptosis and cytokine/chemokine interactions. Notably, some understudied or even novel ones have been revealed, including DNA replication and DNA repair processes (e.g. mismatch repair, base excision repair and homologous recombination) (Table 5.7, Figure 5.8. and Supplementary Table 4, Appendix III). Also, 1437 Gene Ontology (GO) terms including biological processes and molecular functions, with the most perturbed ones shown in Table 5.9, were found to be significantly enriched. Interestingly, some of the key perturbed lncRNAs in response to continuous exposure to metformin are also key players in these processes, suggesting they could potentially mediate the cell fate decisions in neuroblastoma cells. For example, *CASC2* is a Wnt signalling (Wang *et al.*, 2017) and apoptosis (Wang *et al.*, 2015; Fan *et al.*, 2018) regulator, *LOC643401* is involved in p53 signalling regulation (Li *et al.*, 2017) and DNA repair (Rashi-Elkeles *et al.*, 2011), whilst *LINC00176* is an established cell cycle (Tran *et al.*, 2018) and apoptosis (Dai *et al.*, 2019) regulator.

Table 5.6. Top perturbed molecular pathways in SH-SY5Y cells with continuous exposure to metformin.

Pathway name	*p-value*
Lysosome	0.001
Antigen processing and presentation	0.002
Protein digestion and absorption	0.003
HTLV-I infection	0.004
Pertussis	0.004

Table 5.7. Top cancer-related perturbed molecular pathways in SH-SY5Y cells with continuous exposure to metformin.

Pathway name	Key DEGs	*p-value*
Cytokine-cytokine receptor interaction	*BMPR1B, CSF2, IL15RA*	1.809e-6
DNA replication	*POLE2/3, POLA1*	2.998e-4
Cell cycle	*CHEK1, E2F5, GADD45B*	4.963e-4
Mismatch Repair	*EXO1, RFC4*	0.004
Base Excision Repair	*UNG, POLE2*	0.008
p53 signalling pathway	*CHEK1, GADD45B, MDM4*	0.013
Fanconi Anemia pathway	*BRCA1*	0.014
Chemokine signalling pathway	*GNGT1, CXCL8, CCL20, RELA*	0.016
Homologous recombination	*BRCA1*	0.02
ECM-receptor interaction	*ITGB4, LAMB3*	0.022
Wnt signalling pathway	*MAPK10, PRICKLE1, VANGL1*	0.043

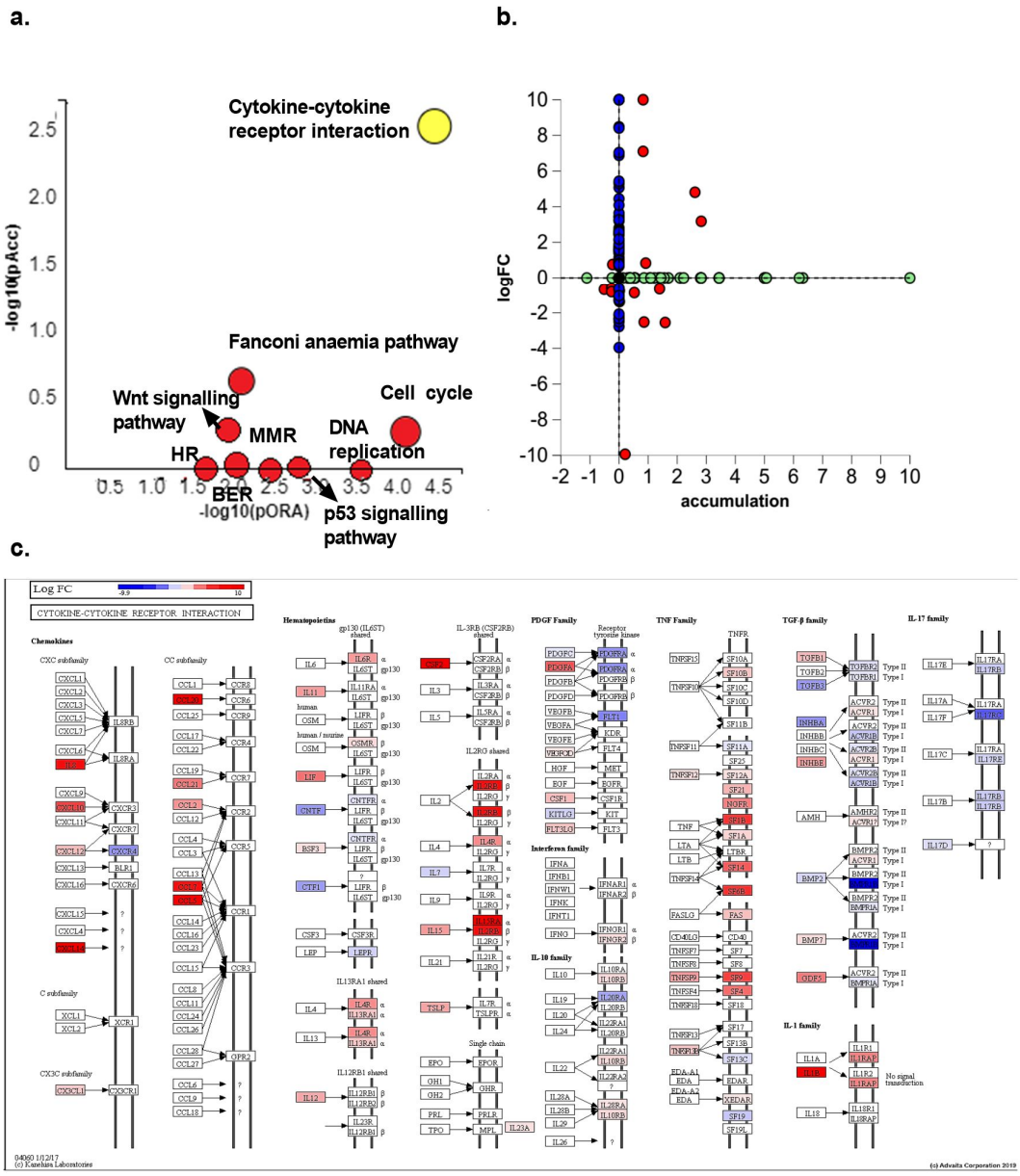

Figure 5.8. Top perturbed cancer-related pathway: Cytokine-cytokine receptor interaction (KEGG: 04060). Perturbation vs over-representation: Cytokine-cytokine receptor interaction (yellow circle) is shown, using negative log of the accumulation and over-representation p-values, along with the other most significant pathways (red circles). Pathways in red are significant, based on the combined uncorrected *p-values* (a). Measured expression vs accumulation of pathway genes: all the genes from this pathway are represented in terms of their measured fold change (y-axis) and accumulation (x-axis). Accumulation is the perturbation received by the gene from any upstream genes. Genes displayed in red had both accumulation and measured fold change. Genes in blue had only measured fold change. Genes in green had only accumulation. The remaining genes that were not measured and had no accumulation are shown in black. (b). Graphically, the pathway diagram is overlayed with the computed perturbation of each gene. The perturbation accounts both for the gene's measured fold change and for the accumulated perturbation propagated from any upstream genes (accumulation). The highest negative perturbation is shown in dark blue, while the highest positive perturbation in dark red. The legend describes the values on the gradient (c); **MMR**: Mismatch repair; **HR**: homologous recombination; **BER**: Base excision repair

Table 5.8. Top perturbed Gene Ontology (GO) terms in SH-SY5Y cells with continuous exposure to metformin.

	Pathway name	Number of perturbed genes/ total genes in the pathway	*p-value*
Biological Processes	**positive regulation of multicellular organismal process**	634 / 933	2.700e-13
	inflammatory response	257 / 355	5.500e-10
	defense response	535 / 802	2.000e-9
	regulation of multicellular organismal process	1110 / 1764	9.600e-9
	positive regulation of developmental process	537 / 811	9.600e-9
Molecular functions	**helicase activity**	105 / 140	5.700e-6
	cytokine activity	64 / 80	1.100e-5
	DNA binding	1179 / 1926	1.300e-5
	double-stranded DNA binding	371 / 573	5.000e-5
	deoxyribonuclease activity	48 / 59	6.300e-5

5.3.3. Metformin treatment and continuous exposure to metformin share molecular perturbations

In an attempt to further explore which aberrations in the lncRNA repertoire and the novel molecular pathway changes they are involved in are persistent in neuroblastoma cells, as a result from either short term exposure (48 h) to metformin or more chronic exposure potentially leading to resistance to metformin, shared alterations between the two experiments (Data set 1 and Data set 2) were pinpointed. This was performed primarily at lncRNA level, as well as at a cancer-related pathway level. Importantly, a significant number of lncRNAs (269), more than half of the perturbed lncRNAs in each individual condition, were perturbed in common in both data sets. Among them, a number were consistently very highly up- (e.g. *GHRLOS, LOC100130700, CASC2, MIR22HG, LOC100288637, LOC100507173, LOC100288974, LOC641364,* and the uncharacterised *LOC100505695, LOC100507557* and *LOC100506801*) or down-regulated (e.g. *LOC100132707, LOC100289092, C17orf76-AS1, LOC285484, LOC100506409, LOC340037, LOC100288637, LOC100506714, LOC256021*, *LOC151300,* and the uncharacterised *LOC100506136, LOC143666* and *LOC100507346*), suggesting their crucial role in mediating the cell fate decisions, as well as in transitioning between the simple short-term exposure and continuous, chronic exposure effects. For instance, *LOC151300* was consistently ~15-fold down-regulated, and given its association with components of the Wnt signalling pathway (Puiggros *et al*., 2013), it can be speculated that this pathway is a key mediator via which metformin exerts its effects. In the opposite direction, the expression of *GHRLOS* was constantly 15-fold increased. Similar to *LOC151300*, the link of *GHRLOS* and its transcript *Ghrelin* with components of the Wnt pathway (Seim *et al*., 2010), points towards the importance of the pathway in responses to metformin. Moreover, the well-known *CASC2,* which is established to promote apoptotic responses, was 12-13-fold up-regulated in both conditions, supporting the hypothesis that metformin induces

apoptosis, and potentially, that longer exposure to metformin enhances the levels of apoptosis. The shared perturbed lncRNAs also included some well-studied cancer-related ones, such as *MIR22HG, LINC00173*, *GAS5, MALAT1* and *linc-NeD125* (Figure 5.9b-c and Supplementary Table 1: lilac highlights, Appendix III). Noteworthily, the subclass distribution of the shared differentially expressed lncRNAs followed the distribution of the individual data sets, i.e. the majority belonged to the NAT subcategory (38%), followed by lincRNAs and pseudogenes.

In addition, of note is the fact that 8 perturbed cancer-related pathways were shared between the two data sets, including DNA repair mechanisms, cell cycle regulation, DNA replication and apoptosis-related pathways, suggesting their importance in the mechanistic action of metformin, regardless of the duration of exposure (Figure 5.9a).

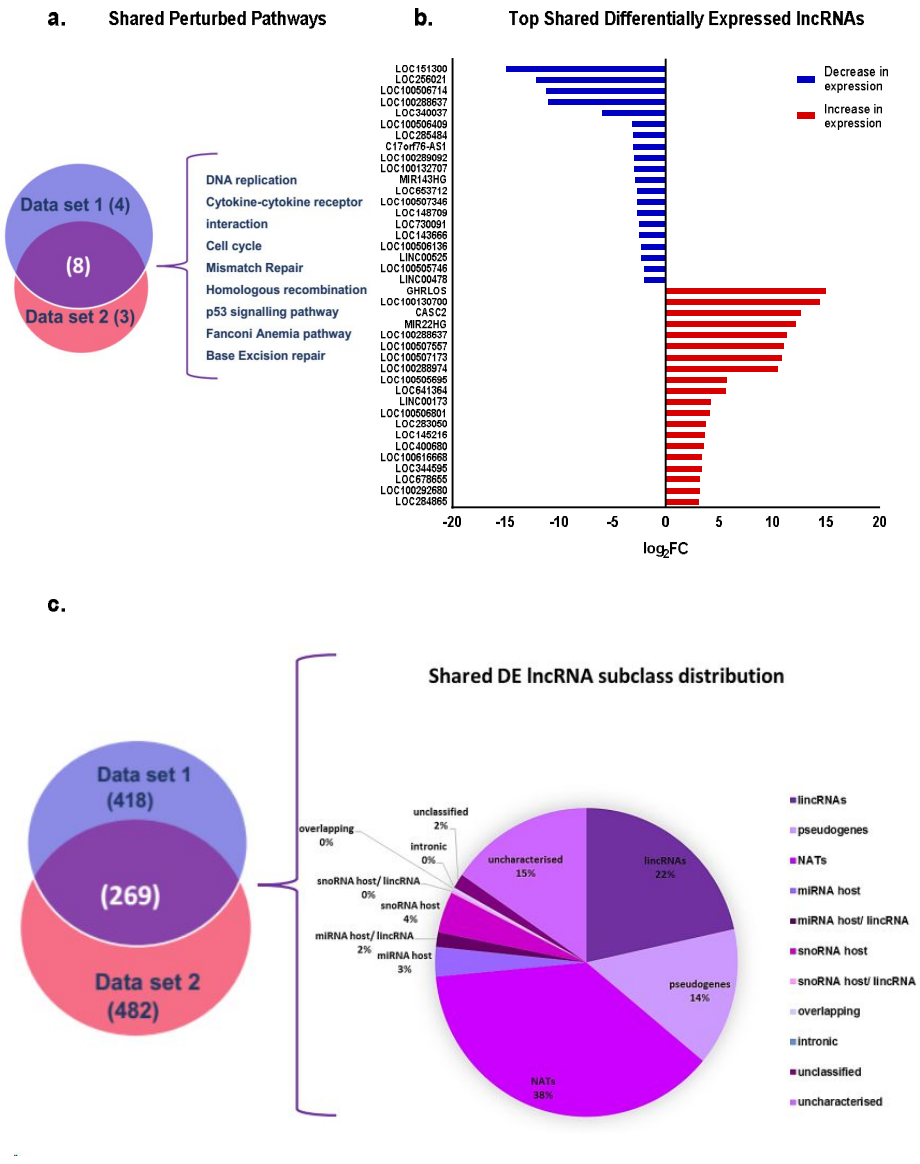

Figure 5.9. The shared effects of metformin treatment and continuous exposure to metformin. Both short term exposure to 20mM metformin and continuous exposure of SH-SY5Y cells to 3mM metformin induce shared alterations in the molecular landscape. This is observed at the pathway level, summarised in the Venn diagram (a), and at the lncRNA level. The bar chart presents only the top perturbed lncRNAs in both directions (b). Red coloured bars correspond to upregulated gene expression, while blue coloured bars correspond to downregulated gene expression. Data are the difference in expression between untreated control cells and cells exposed to 20mM metformin, expressed as a normalised $\log_2$ fold change ($\log_2$FC). A threshold of 0.05 for statistical significance (*p-value*) and a log fold change of expression with an absolute value of at least 0.6 were applied. The pie chart schematically presents the distribution of shared differentially expressed lncRNAs into different lncRNA subclasses (c). **DE**: differentially expressed; **NAT**: Natural Anti-sense Transcript; **lincRNA**: Long Intergenic RNA; **miRNA host:** microRNA host gene; **snoRNA host**: small nucleolar RNA host gene.

5.3.4. The molecular differences between the response to metformin and continuous exposure to metformin

In order to explore whether, despite the shared changes on the molecular level, there are novel lncRNAs whose expression is highly perturbed and could possibly be drivers of cell fate determination leading to the switch of cells to behave differently after long-term exposure to metformin, a comparison between the RNA sequencing profile of the two conditions (i.e. cells exposed to 20mM metformin for 48 h versus cells with continuous exposure to metformin) was generated (Data set 3).

The RNA sequencing analysis revealed that the lncRNA landscape was again massively changed. In this case, the magnitude of the effect was similar to the one described in the previous sections, with 468 lncRNAs being significantly up-regulated or down-regulated. The top ten up-regulated lncRNAs were *LOC283050, LOC730227, LOC100509894, LOC100506714, LOC100133331, LOC729678, LOC100128420, TP73-AS1, LINC00176* and *C17orf76-AS1* (>5-fold increase), and in the opposite direction, the top down-regulated ones were *LOC115110, LINC00327, LOC400940, LOC392232, LOC641364, LINC00304, LOC100507557, PCBP1-AS1, LOC100125556* and *LOC100652730* (>3-fold increase). Some of them have already been attributed a cancer-related identity. *LOC283050*, a novel lncRNA, was the lncRNA with the most pronounced increase in expression (14-fold) in cells with continuous exposure to metformin, suggesting it may be a key driver of cell fate decisions leading to acquired metformin resistance. *LOC730227,* another relatively new lncRNA, also displayed a more than 13-fold increase in expression levels, and given its association with the response to radiation via ATM and p53 (Narayanan *et al.*, 2017), it may also be a key player. In addition, the well-investigated *TP73-AS1* was 8-fold up-regulated as a result of continuous exposure to metformin, and given the role of its transcript *TP73* in cellular responses to stress, it may as well be a driver

of metformin resistance. On the other hand, another novel lncRNA, *LOC100652730 (LINC00659),* was the most down-regulated (16-fold) and has been associated with the PI3K pathway (Tsai *et al.*, 2018), suggesting a potential involvement in driving metformin resistance. *PCBP1-AS1*, 14-fold down-regulated after continuous exposure to metformin, is an autophagy-associated NAT (Luan *et al.*, 2019) whose massive decrease in expression could also serve as a driver of cell fate decision events ultimately leading to metformin resistance, given the role of autophagy in drug response. Curiously, some of the most deregulated lncRNAs comprise totally novel, uncharacterised genes, for instance, *LOC100133331, LOC400940* and *LOC100507557.* Furthermore, amongst the lncRNAs with pronounced differential expression, a number have been previously linked to various cancers, including *MIR497HG, FLVCR1-AS1, CRYM-AS1, H19* and *LINC00092*. The subclass distribution following the same pattern; NATs were the most abundant category (40%), followed by lincRNAs (24%) and pseudogenes (15%), while a generous 16% of the lncRNAs were uncharacterised (Figure 5.10 and Supplementary Table 5, Appendix III).

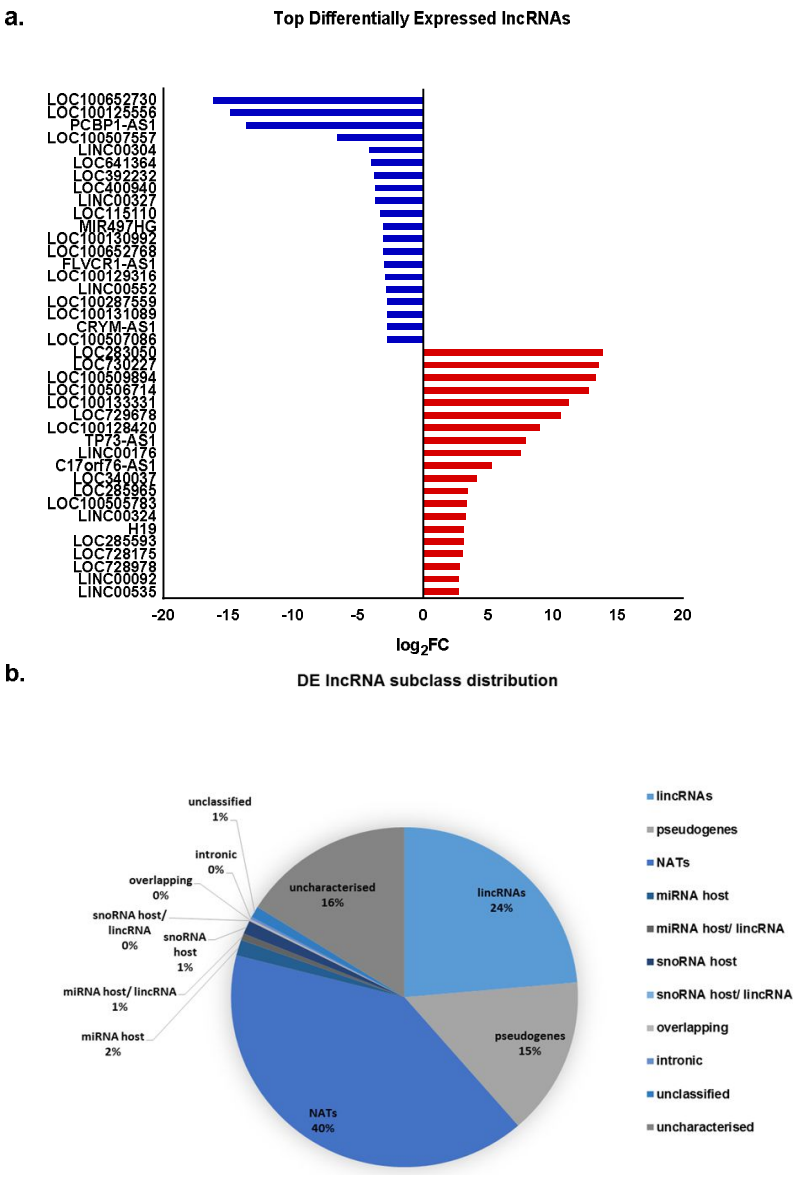

Figure 5.10. The effect of metformin-treated SH-SY5Y cells versus SH-SY5Y cells with continuous exposure to metformin on lncRNA expression Short-term metformin exposure and continuous exposure of SH-SY5Y cells to 3mM metformin induces different alterations in the expression of lncRNAs. The bar chart presents only the top perturbed genes in both directions (a). Red coloured bars correspond to upregulated gene expression, while blue coloured bars correspond to downregulated gene expression. Data are the difference in expression between cells treated with 20mM metformin for 48 h and cells with acquired resistance to 3mM metformin, expressed as a normalised $\log_2$ fold change ($\log_2$FC). A threshold of 0.05 for statistical significance (*p-value*) and a log fold change of expression with an absolute value of at least 0.6 were applied. The pie chart schematically presents the distribution of differentially expressed lncRNAs into different lncRNA subclasses (b). DE: differentially expressed; NAT: Natural Anti-sense Transcript; lincRNA: Long Intergenic RNA; miRNA host: microRNA host gene; snoRNA host: small nucleolar RNA host gene.

Interestingly, the analysis of the comparison generated some useful findings regarding the driver changes that convert SH-SY5Y cells from metformin-responding to potentially metformin resistant. As far as pathways are concerned, 64 were significantly impacted, including multiple cancer-related ones, some of which were not present in any of the comparisons described in sections 5.3.1. and 5.3.2., such as the NF-κB signalling pathway, the TNF signalling pathway and proteoglycans in cancer (Table 5.9 and Supplementary Table 6a, Appendix III). Besides, 1615 Gene Ontology terms were found to be significantly deregulated (Supplementary Table 6b, Appendix III). Taken together, these changes signify that the key drivers of metformin resistance as compared to responsiveness to metformin treatment include not only lncRNA elements, but also protein-coding ones.

Table 5.9. Top perturbed molecular pathways (including cancer-related) in metformin-treated SH-SY5Y cells versus SH-SY5Y cells with continuous exposure to metformin.

Pathway name	*p-value*
NF-kappa B signalling pathway	1.951e-5
TNF signalling pathway	5.358e-5
Steroid biosynthesis	5.742e-5
Chemokine signalling pathway	6.808e-5
HTLV-I infection	8.278e-5
Cytokine-cytokine receptor interaction	8.368e-5
Kaposi's sarcoma-associated herpesvirus infection	8.746e-5
Terpenoid backbone biosynthesis	1.228e-4
Antigen processing and presentation	3.310e-4
Systemic lupus erythematosus	4.165e-4

5.4. Discussion

LncRNAs have lately been established as important modulators of cell fate determination, including cell survival, apoptosis and migration (Wapinski and Chang, 2011; Dhamija and Diederichs, 2016; Melissari and Grote, 2016), as well as drug resistance in various tumours interfering with diverse mechanisms of acquired resistance (Smallegan and Rinn, 2019; Zhao *et al.*, 2019). Given the very low survival rates of high risk neuroblastoma patients, as well as the lack not only of understanding of the mechanisms that confer the aggressiveness of the tumour in these patients but also of druggable therapeutic targets, there is an urge to meet these needs. To this end, this chapter aimed to identify novel lncRNAs, which are potentially capable of mediating cell fate decisions in SH-SY5Y neuroblastoma cells by measuring and evaluating the perturbations in their expression in response to metformin, a biguanide traditionally administered orally for the treatment of type 2 diabetes that has been widely repurposed over the last decade for the treatment of various cancer types with promising results, and has been shown to affect multiple signalling pathways involved in cancer (Janjetovic et al., 2011; Li et al., 2019).

The first line strategy to identify lncRNAs responsible for cell fate decisions driving the acute effects of short-term exposure to metformin was to treat NB cells with metformin for 48 h. Apart from this, on the grounds that chronic exposure of NB cells to metformin, leading, potentially, to acquired resistance to it, could result in permanent senescent cell growth arrest, as a result of excessive autophagy that targets vital metabolic cancer cell components, and therefore, activating such a senescence programme in tumour cells could be an attractive therapeutic strategy (Menendez *et al.*, 2011), such an approach was adopted. In particular, the discovery of novel lncRNAs and their role in cells with continuous exposure to metformin was investigated next. The molecular and pathway alterations between untreated cells and cells with

acquired resistance to metformin were also explored, and further, the short-term-treated group was compared with the long-term-treated one to discover fundamental similarities and differences in lncRNA expression, in order to identify novel mediators of fate determination driving the switch of the “metformin-responsive” phenotype to the “metformin-resistant”.

The analysis of RNA sequencing results showed that numerous alterations were caused in the non-coding landscape. Hundreds of lncRNAs displayed differential expression upon metformin treatment, including *TP73-AS1, LOC100288637, CBR3-AS1* and *MIR22HG*, which were also distributed into different lncRNA subclasses, predominantly NATs. The oncogenic *TP73-AS1*, which was one of the most down-regulated lncRNAs (8-fold) has been implicated in numerous cancers, (Chu *et al.*, 2019). *TP73-AS1* has been established as a promoter of cell proliferation and invasion and metastasis (Wang *et al.*, 2018; Yao *et al.*, 2018), and given that the mechanisms of action of metformin include the regulation of these processes (Kourelis and Siegel, 2012; Emami Riedmaier *et al.*, 2013), it could, therefore, be speculated that *TP73-AS1* is part of the mechanism by which metformin eliminates these processes in neuroblastoma. Another highly down-regulated lncRNA (11-fold), *LOC100288637,* has so far been implicated in gynaecological tumours only (Yang *et al.*, 2016; Huang *et al.*, 2019), but not in NB, suggesting it may play a yet to be discovered mechanistic role in cell fate decisions in response to metformin. *CBR3-AS1* is a thoroughly studied oncogenic lncRNA, implicated in a plethora of cancers such as prostate (Fang *et al.*, 2016), osteosarcoma (Luo *et al.*, 2019) and breast (Faramarzi *et al.*, 2018) cancer, that was surprisingly 13-fold up-regulated in response to metformin treatment. Due to its involvement in the regulation of cell cycle (Li *et al.,* 2014), as well as in the Notch signalling pathway (Wang *et al.*, 2018), it could be assumed that *CBR3-AS1* exerts its role in the response to metformin via this –understudied in terms of metformin mechanisms of action- pathway, as well as via a non-canonical regulation of the cell

cycle. Moreover, *MIR22HG*, a tumour suppressor lncRNA, was vastly up-regulated (12-fold) in cells treated with metformin. *MIR22HG* has very recently been reported to attenuate cell proliferation and migration via negatively regulating the Wnt pathway in GBM (Han *et al.*, 2019) and cholangiocarcinoma (Hu *et al.*, 2019). Notably, although regulating the Wnt signalling pathway is not the main mechanism of action for metformin, metformin has been found to deregulate this pathway in neural crest cells (Banerjee *et al.,* 2016) and pancreatic cancer cells (Yue *et al.*, 2014). Taken together, these suggest that *MIR22HG* could participate in a Wnt-dependent mode of action of metformin in neuroblastoma. Despite the fact that the aforementioned lncRNAs have already been implicated in multiple cancers, they have not been associated with neuroblastoma before. Importantly, the list of the most deregulated lncRNAs in metformin-treated cells contains a number of lncRNAs that are completely novel and remain uncharacterised (e.g. *LOC100507557, LOC100505695*) or for which very limited studies have been conducted, including in some cases studies related to cancer, for instance, *LOC100130700* (Dai *et al.*, 2015)*, PEG3-AS1* (Hsu *et al.*, 2016; Zhang *et al.*, 2019)*,* suggesting the existence of novel key players, potentially involved in pathways that have not been previously associated with cell fate determination in response to metformin in neuroblastoma cells.

In the attempt to incorporate the novel lncRNAs found to be perturbed in response to metformin in a cancer-related molecular pathway context, we also assessed which pathways were perturbed, in order to isolate the cell fate-related ones in which these lncRNAs could be implicated. Our approach has not only confirmed already studied pathways in which our novel lncRNAs could fit as mediators but has also identified a number of novel potential mechanisms by which cell fate decisions could be mediated in response to metformin. It has now been well established that metformin suppresses tumour cell growth through the mTOR pathway, induces p53-related apoptosis, causes cell cycle arrest and interferes with tumour-related inflammation (Kourelis and Siegel,

2012; Emami Riedmaier *et al.*, 2013), all of which were confirmed to be perturbed in our system. Analysis of the results has revealed that there is a significant change in the cell cycle pathway, p53 signalling pathway and cytokine-cytokine receptor interactions when untreated SH-SY5Y cells were compared to cells treated with 20mM of metformin for 48 h. Intriguingly, apart from the pathways that have already been implicated in metformin's mechanisms of action, numerous understudied or even novel cancer-related pathways were found to be significantly perturbed. Notably, DNA replication was the most downregulated pathway (among cancer-related and non-related pathways) in response to metformin, a finding which is in agreement with the study by Ma *et al.*, 2014, in which metformin in combination with tamoxifen inhibited DNA replication in ER-positive breast carcinoma, as well as with the study by Kim *et al.* (2017), in which metformin downregulated the DNA replication machinery in colorectal cancer cells. In addition to DNA replication, the analysis of the RNA sequencing result unveiled massive and significant changes in pathways involved in the DNA damage response, including mismatch repair (MMR), homologous recombination (HR) and base excision repair (BER), all of which were downregulated. The same effect has previously been reported in lung cancer cells, where metformin downregulated ERCC1 (Excision Repair Cross Complementing 1) to sensitise them to paclitaxel (Tseng *et al.*, 2013). Metformin has also previously been found to sensitise tumour cells against further damage via the activation of ATM, an upstream sensor of double strand breaks and, therefore, a regulator of HR (Menendez *et al.*, 2011). At the same time of the current study, a meta-analysis report confirmed that DNA replication and DDR are among the top perturbed pathways in response to metformin as assessed in multiple cell lines, not containing neuroblastomas, though (Schulten and Bakhashab, 2019). Besides, Hippo, another cancer-related pathway emerged as significantly perturbed. Although the link between Hippo and metabolic stress and metformin is still not fully elucidated, there is evidence that links the beneficial effect of metformin to Hippo via YAP/TAZ (Yes-associated Protein/ Tafazzin) upregulation in glioma cells (Yuan *et al.*,

2018), similar to our results. In agreement with these studies, our sequencing results showed perturbations in expression of key genes, including *MDM4, PCNA*, the *MCM* family, *CHEK1/2, ERCC1, XRCC3, BRCA1* and *BID.*

Importantly, some master regulators of gene expression were significantly perturbed, mainly proteins of the MYC family, such as c-*Myb* and, primarily*, c-Myc*, which are responsible for the regulation of cell cycle, DNA damage, cell survival and apoptosis (Kumar *et al.*, 2014). In this case, in the SH-SY5Y system, the MYC family equilibrium leaned towards the pro-apoptotic side in response to metformin. As the decrease in expression of both *c-Myb* and *c-Myc* seemed to promote a tumour suppressive response, it can be speculated that these transcription factors kept their traditional oncogenic identity. Although in neuroblastomas *MYCN* amplification is traditionally vastly responsible for poor outcome, in *MYCN* non-amplified tumours-and consequently cell lines, such as SH-SY5Y, *c-Myc* is responsible for aggressiveness (Wang *et al.*, 2014). In our case, the decrease in the levels of c-Myc could be attributed, at least partly, to the massive increase of *MIR22HG* in response to metformin, as this lncRNA has been shown to negatively regulate c-Myc in breast cancer (Zurlo *et al.*, 2019). In addition, *c-Myb*, a basal transcription factor, has been implicated in cell proliferation, differentiation and apoptosis, and its overexpression in multiple cancers has led to its classification as a proto-oncogene, like *c-Myc* (Liu *et al.*, 2018; Fry and Inoue, 2019). Interestingly, and in line with our results, BRCA1 is a c-Myb target (Mitra, 2018), and given the abundance of their targets, some of the newly identified lncRNAs described above could be targeted by either transcription factor or vice versa. Consequently, given their central role as master tumour-promoting transcription factors, their reduced expression in response to metformin confirms the beneficial, anti-tumour survival role of metformin in this context.

The continuous exposure of NB cells to metformin gradually led to the reduced responsiveness of the cells to the drug, an effect which was –at least partly- mediated

by novel lncRNAs. In particular, there was again a massive, significant change in the expression of hundreds of lncRNAs (482), including NATs, lincRNAs, pseudogenes and a lot of novel, uncharacterised ones. The most deregulated lncRNAs include *GHRLOS, CASC2, LOC643401 (PURPL)* and *LINC00176*. Importantly, the most upregulated lncRNA, *GHRLOS*, has recently been implicated in colorectal cancer (Wu *et al.*, 2017). *GHRLOS* is the NAT of *Ghrelin*, which is a hormone responsible-among others- for energy homeostasis and pancreatic glucose-stimulated insulin secretion (Seim *et al.*, 2010). Since metformin is capable of modulating the levels of glucose and insulin (Kourelis and Siegel, 2012; Vial *et al.,* 2019), it could be assumed that *GHRLOS* modulating the levels of Ghrelin could be a new link through which chronic exposure to metformin exerts its role in neuroblastoma cells. Furthermore, *CASC2,* a tumour suppressor lncRNA known for its ability to attenuate tumour cell growth, proliferation, migration and invasion in multiple cancers (Wang *et al.*, 2015; Li *et al.*, 2019; Sun *et al.*, 2019; Xing *et al.*, 2019), was among the most upregulated lncRNAs, suggesting its vital role in metformin-mediated effects in terms of inhibiting tumour progression, including the inhibition of cell growth and invasion. *LOC643401,* another highly up-regulated lncRNA as a result of continuous exposure to metformin, is a recently discovered suppressor of the basal levels of p53, thereby leading to tumourigenesis (Ashouri *et al.*, 2016; Li *et al.*, 2017). Therefore, its up-regulation could be a driver of metformin resistance, as apoptosis and DDR may be eliminated as a result of chronic exposure. In the opposite direction, one of the most downregulated lncRNAs, *LINC00176*, which was ~9-fold downregulated and is also a c-Myc target, has been involved in multiple cancers, including ovarian (Dai *et al*., 2019), hepatocellular (Tran *et al.*, 2018), clear cell renal carcinoma (Wang *et al.*, 2019) and oesophageal (Fan and Liu, 2016), and has been shown to be involved in cell survival and proliferation (Wang *et al.*, 2019), as well as in cell cycle (Tran *et al.*, 2018) and apoptosis (Dai *et al.,*2019; Niehus *et al.*, 2019). Therefore, perturbations in these processes leading to metformin resistance could be the result of the tremendous down-regulation of *LINC00176*. Interestingly,

although these lncRNAs have been implicated in a variety of tumours, a link with neuroblastoma has not been generated yet. Notably, the most perturbed lncRNAs included novel lncRNAs, often yet to be characterised (*LOC100133331*-13-fold upregulated, *LOC100505695*- 6-fold up-regulated, *LOC648987*-15-fold down-regulated), or lncRNAs that are newly discovered with very limited research already conducted for them. A typical such example is *LOC151300 (LINC00608)*, which was recently discovered as part of non-coding signatures with prognostic value in HNSCC (Yang *et al.*, 2019; Ghafouri-Fard *et al.*, 2020), but whose mechanisms of action remain to be elucidated. Taken together, these findings suggest that these lncRNAs could be used as biomarkers of metformin resistance in neuroblastoma.

Intriguingly, the two comparisons shed light to multiple shared changes, both in the pathway level, and the lncRNA level in the context of neuroblastoma. Surprisingly, 8 of the most deregulated cancer-related pathways were shared in the two data sets, including DNA repair and DDR pathways. This is a strong indication-supported by other studies (Schulten and Bakhashab, 2019)- that these pathways are key players in the response of SH-SY5Y cells to metformin, regardless of the duration of exposure and the potential acquired resistance, and from a therapeutic prism, they could be druggable in combination with metformin for the treatment of neuroblastoma. More importantly, the fact that the deregulation in the expression of 269 lncRNAs was shared in the two tested conditions, pinpoints the importance of the lncRNAome in neuroblastoma and the mechanisms of action of metformin. For instance, *GHRLOS, CASC2* and *LOC151300* were massively deregulated in both conditions, stressing the central role of them per se, and their related processes, such as apoptosis, in this system, and opening the opportunity for them to be exploited therapeutically as part of combination therapy together with metformin. Importantly, the distribution of shared lncRNAs followed this of each data set separately: NATs were the most abundant

subclass, followed by lincRNAs, stressing the evolutionary preference for overlapping genes (Ning *et al.*, 2017).

Nevertheless, as expected, extended exposure to the drug also attributed some changes on the molecular level, allowing the identification of new lncRNAs that regulate cell fate aspects accompanying this extended exposure. As far as lncRNAs are concerned, 468 were significantly perturbed. Among the most up-regulated, *LOC283050* (14-fold) is a so far under-studied NAT. However, its coding transcript *ZMIZ1* (Zinc Finger MIZ-Type Containing 1) has been attributed oncogenic properties (Rogers *et al.*, 2013), and therefore this pair could be a candidate contributor to the metformin responsiveness switch. Additionally, *LOC730227* (13-fold up-regulated) is a novel lncRNA that could also mediate this switch. Curiously, *TP73-AS1*, which was down-regulated in response to short-term metformin exposure, was massively (8-fold) up-regulated in response to continuous exposure. Owing to the fact that TP73 mediates cellular responses to stress, a very simplistic potential scenario could be that the up-regulation of its NAT induces the elimination of TP73, which in turn silences DDR components, rendering metformin incapable of exploiting them. On the other hand, the most down-regulated lncRNA *LOC100652730* (16-fold), is a novel lncRNA, whose modes of action mediating the resistance to metformin need to be investigated. Another dramatically down-regulated lncRNA, *PCBP1-AS1* (14-fold) has already been considered as a biomarker in recurrent neuroblastoma (Utnes *et al.*, 2019), implying it could also be used as a predictive marker for potential metformin resistance in these patients. In conclusion, all of these lncRNAs are putative drivers of metformin resistance in neuroblastoma and could be utilised as biomarkers of predictive value.

Surprisingly, despite the link of metformin with inflammation via the NF-κB pathway (Kourelis and Siegel, 2012; Rizos and Elisaf, 2013), the pathway only emerged- and with the highest effect-when comparing the short-term exposure with resistance, and not in the comparisons between untreated and treated cells. Moreover, the apoptosis-

related TNF signalling pathway was the second most affected. Both of them were upregulated, suggesting a stronger effect of metformin in terms of apoptosis induction, and, therefore, a more efficient anti-tumour effect. Finally, the chemokine and cytokine pathways were upregulated. Collectively, these results should be interpreted with caution, as the cancer inflammation networks are extremely complex and there is a fine line between tumour-eliminating and tumour-promoting inflammation (Hanahan and Weinberg, 2011). In addition, it is possible that the aforementioned lncRNAs could be associated with these processes, a scenario that needs further investigation.

Taking everything into account, although the RNA sequencing has revealed numerous mechanistic relationships and, primarily, has provided very useful insights of novel, key lncRNA mediators of the cell fate determination linked to metformin and of how neuroblastoma cells potentially acquire resistance to metformin after prolonged exposure to it, this study has only scratched the surface of these complicated effects. In fact, due to their preliminary nature, the findings presented herein need to be interpreted with caution, and require further investigation. Nevertheless, despite the limitation of the RNA sequencing results being extracted by a single replicate (as analysed in section 4.4), this study provides confirmation that pathways already established to be perturbed in other systems (e.g. cell cycle, DNA replication, apoptosis) are indeed altered in our system, the SH-SY5Y neuroblastoma cells, and also reveals new modes of action of metformin, including DDR and the Hippo pathway. Among the key novel lncRNAs, some are well-studied genes in other tumours; however, herein we have established a strong link to neuroblastoma. Other highly deregulated lncRNAs, such as *LOC100507557, LOC100505695* and *LOC648987* remain uncharacterised, and therefore, their characterisation would facilitate the attribution of a specific, evidence-based role in mediating cell fate decisions in metformin responses, as well as their connection with the observed perturbed molecular pathways. However, metformin is a multifaceted drug, participating in a

plethora of signalling pathways and exerting a diversity of tumour-eliminating functions, such as inhibiting tumour cell growth and promoting programmed cell death. Thus, identifying the key lncRNAs mediating all these effects remains a difficult task that needs further investigation. Further research is also needed to establish the link between the newly identified lncRNAs that present with highly deregulated expression and the perturbed pathways so that the exact mechanisms of action of these lncRNAs are elucidated and they gain contextual importance in neuroblastoma.

5.5. Chapter Highlights

1. **RNA sequencing has identified 418 perturbed novel lncRNAs, including *TP73-AS1, LOC100288637, CBR3-AS1* and *MIR22HG,* in response to treatment with 20mM metformin in SH-SY5Y neuroblastoma cells.**

2. **482 lncRNAs, including *GHRLOS, CASC2, LOC643401 (PURPL), LOC648987* and *LINC00176* were identified to be altered after continuous exposure of SH-SY5Y cells to metformin.**

3. **Treatment with and prolonged exposure to metformin share expression perturbations in 269 lncRNAs, including *GHRLOS, CASC2* and *LOC151300*.**

4. **Besides changes in the lncRNA repertoire, the RNA sequencing demonstrated novel cancer-associated perturbations in cell fate-related processes and molecular pathways, such as DNA replication and DDR, in SH-SY5Y cells exposed to metformin short-and long-term, some of which maintain their deregulation in both experimental conditions.**

5. **Long term exposure to metformin causes modulations in the expression levels of 468 lncRNAs, for instance, *LOC2830509000, LOC730227, TP73-AS1*, *LOC100652730* and *PCBP1-AS1*, when compared to short-term treatment. Such lncRNAs could be considered as resistance drivers and could be exploited as biomarkers of metformin resistance in neuroblastoma.**

Chapter 6: Investigation into the role of *LINC00176* and *LOC648987* in the cell fate determination of neuroblastoma cells

6.1. Introduction

The evidence presented in Chapter 5 revealed that a multitude of lncRNAs are also capable of mediating the neuroblastoma cells' response to metformin and the switching process via which they become resistant to it after continuous exposure. Among the lncRNAs whose expression was massively (more than 5-fold) perturbed after continuous metformin exposure, a variety has been implicated in cell fate determination, including cell survival, apoptosis and invasion. *CASC2*, a well-studied onco-suppressor lncRNA highly up-regulated in response to continuous metformin exposure*,* is involved in Wnt signalling to eliminate tumour growth in glioma (Wang *et al.*, 2017) and HCC (Li *et al.*, 2019), and is also an apoptosis, cell survival and invasion regulator in HCC cells (Fan *et al.*, 2018; Sun *et al.*, 2019), glioma cells (Wang *et al.*, 2015) and pancreatic cancer cells (Xu, *et al.,* 2020). *LOC643401*, also known as *PURPL*, a highly up-regulated lncRNA*,* is involved in p53 signalling regulation as p53 suppressor, and therefore, in p53-related responses, such as cell proliferation and apoptosis in CRC (Li *et al.*, 2017) and liver cancer (Fu *et al.*, 2019), while its overexpression is also a potential biomarker in gastric cancer (Moridi *et al.*, 2019). The two most down-regulated (15-fold) lncRNAs in SH-SY5Y cells with continuous exposure to metformin*, LOC151300* and *LOC648987,* are both novel lncRNAs that remain largely understudied. Nevertheless, *LOC151300* has been reported to be differentially expressed between primary colon carcinoma and its lymphatic and hepatic metastases (Lan *et al.*, 2012). *LINC00176* is another highly down-regulated (9-fold) lncRNA, which in contrast to *LOC151300* and *LOC648987* has been given more scientific attention and has been associated with cancer (Fan and Liu, 2016; Tran *et al.*, 2018; Dai *et al.,* 2019).

In an attempt to further explore the role of novel lncRNAs characterised in Chapter 5, two of the most downregulated lncRNAs, *LINC00176* and *LOC648987,* were chosen for further functional analysis. *LINC00176* is a lincRNA that spans ~5kb on

chromosome 20 and has previously been implicated in a diversity of cancers. Not only has it been verified as a biomarker lncRNA in clear cell renal carcinoma (Wang *et al.*, 2019), HCC (Zhang *et al.*, 2015; Gong *et al.*, 2020) and oesophageal cancer (Fan and Liu, 2016), as well as a candidate biomarker in pancreatic cancer (Liu *et al.*, 2019), but also it has been attributed a role in tumour cell growth (Zhu *et al.*, 2016) and cancer cell fate determination. For instance, it has been demonstrated that *LINC00176* can regulate cell proliferation, cell cycle and necroptosis and apoptosis-mediated cell death in HCC cells (Tran *et al.*, 2018), and apoptosis, invasion and EMT in ovarian cells (Dai *et al.,* 2019). Finally, it has also been shown to act as a miRNA sponge in HCC (Zhang *et al.*, 2015; Tran *et al.*, 2018) and to be involved in oxaliplatin resistance in the chemotherapy of colorectal cancer (Sun *et al.,* 2019). On the other hand, *LOC648987* is a 52kb, still uncharacterised, non-coding locus across chromosome 5, which has been demonstrated to be differentially methylated in patients with lung adenocarcinoma (Daugaard *et al.*, 2016). Nevertheless, a splice variant of *LOC648987,* named *MPRL* (miRNA processing–related lncRNA), was found to regulate mitochondrial fission, cisplatin sensitivity and apoptosis through miR–483-5p in tongue squamous cell carcinoma (TSCC) (Tian *et al.*, 2019).

Despite the findings described above, the influence of *LINC00176* and *LOC648987* on neuroblastoma cell fate determination, including survival, apoptosis and migration, currently remains largely unknown. Based on the findings of Chapter 5, it would be expected that the knockdown of *LINC00176* and *LOC648987* would lead to radical changes in terms of cell fate decisions, given that both survival- and apoptosis-related pathways were deregulated in response to metformin, and that the expression of both of these genes was dramatically reduced. Therefore, the aim of this chapter was to investigate whether *LINC00176* and *LOC648987* regulate these processes in SH-SY5Y neuroblastoma cells, both under basal conditions and after challenging the cells with metformin.

6.2. Materials and Methods

6.2.1. Cell culture

The experiments incorporated in this chapter were conducted using the human neuroblastoma SH-SY5Y cell line, cultured using the HyClone™ DMEM/F12 1:1 growth media, supplemented with 10% heat-inactivated fetal bovine serum, 2μM L-Glutamine, 1μM Sodium Pyruvate and 10mg/ml gentamicin solution, as described in section 2.1.

6.2.2. LNA GapmeR –mediated knockdown

LNA GapmeRs were used in this series of experiments to knockdown *LINC00176* and *LOC648987*. The GapmeRs that were used (200nM) included the Negative control A Antisense LNA GapmeR, three custom-designed GapmeRs (namely LINC_1, LINC_2, LINC_3) targeting different sites of *LINC00176* and three custom-designed GapmeRs (namely LOC_1, LOC_2, LOC_3) targeting different sites of *LOC648987* (Table 6.1), as described in section 2.3.3.

Table 6.1. *LINC00176*- and *LOC648987*-specific LNA GapmeRs details.

Method	Cat #/ ID	Name/ Symbol	Target	Sequence (5'→3')
LNA GapmeRs	**LG00000002**	-ve	N/A	N/A
	LG00200609	LINC_1	*LINC00176*	GGATAAATCAGGAGAC
	LG00200610	LINC_2	*LINC00176*	GGTCTTGGATTAACTT
	LG00200611	LINC_3	*LINC00176*	TGTGATTAAATGCTGT
	LG00200628	LOC_1	*LOC648987*	GAGAACCTCCGGAATA
	LG00200629	LOC_2	*LOC648987*	AGCGACGCGAAACAAG
	LG00200630	LOC_3	*LOC648987*	GCATTGGAGTGGTAGT

6.2.3. Real-time PCR (RT-qPCR)

Total RNA was extracted from cells using the Direct-zol™ RNA MiniPrep kit, according to the manufacturer's protocol and the quality was measured with NanoDrop (as detailed in sections 2.4. and 2.4.1.).

RNA extracted from transfected cells was then reverse transcribed into cDNA using the Omniscript® RT kit, as described in section 2.5.1. Real-time PCR was subsequently

performed for the synthesised cDNA. Specific primers were used against *LINC00176* and *LOC648987,* while 18S rRNA was used as a housekeeping gene (Table 6.2), as described in section 2.5.2.

Table 6.2. TaqMan® gene expression assays' details.

Method	Catalogue #/ ID	Target	Exon boundary	Assay location
TaqMan®	**Hs99999901_s1**	*18S*	1-1	604
	Hs00988121_s1	*LINC00176*	1-1	378
	Hs00987326_s1	*LOC648987*	1-1	2304

6.2.4. Functional analysis: determination of cell survival, apoptosis and cell migration

For the lncRNA knockdown experiments, after transfection, cells were harvested by trypsinisation and after 48 h were re-plated for 48/72 h. **Cell survival** was assessed using trypan blue solution vital dye staining (explained in section 2.6.1.) and MTS assay using the CellTiter 96® Aqueous One Solution Cell Proliferation Assay (as described in section 2.6.3.). For the experiments testing whether *LINC00176* and *LOC648987* down-regulation sensitises SH-SY5Y cells to metformin (sections 6.3.1.4 and 6.3.2.4, respectively) cells were treated with 20mM metformin at 24h after plating and were then incubated for an extra 48/72 h.

The long term survival of the cells was assessed with the clonogenic assay. GapmeR-transfected cells were incubated for three weeks, were stained with 1% w/v crystal violet and counted, as presented in section 2.8. For the experiments testing whether *LINC00176* and *LOC648987* down-regulation sensitises SH-SY5Y cells to metformin, cells were seeded, 20mM metformin was added at 24h post-seeding and after 48 h the metformin-containing growth medium was replaced by fresh cell-conditioned growth medium.

In order to evaluate the effect of the knockdown of *LINC00176* and *LOC648987* on the levels of **cell death** in SH-SY5Y cells, dual staining was performed using the FITC-Annexin V Apoptosis Detection Kit with 7-AAD, and, in addition to flow cytometry, apoptosis was determined with fluorescence microscopy after staining of the cells with acridine orange (25μg/ml), at specific time intervals after re-plating (48 and 72 h), as described in sections 2.7.1 and 2.7.2., respectively. For the experiments testing whether *LINC00176* and *LOC648987* down-regulation sensitises SH-SY5Y cells to metformin, the assessment was performed 48 h after the addition of metformin.

The **migratory ability** of the cells was assessed by the wound healing assay (detailed in section 2.9.). The gaps were measured using the EVOS FL Cell Imaging System at 0/24/48 h and the gap closure was calculated using the formula **[(Pre-migration)area-(Migration)area/(Pre-migration)area] x100** for 15 measurements per sample. Image analysis was performed using the ImageJ software.

6.2.5. Statistical analysis

Statistical analyses were performed using GraphPad Prism 6 (GraphPad Software). Data are presented as the mean ± SEM; the number of observations (n) refers to different transfected samples, each transfection being conducted on a separate culture of cells. Comparisons were made using an unpaired T-test or One-Way ANOVA with Bonferroni's multiple comparison test (MCT). Where multiple parameters were compared, Two-Way ANOVA with Sidak, Tukey or Dunnett multiple comparisons was used. Statistical significance was set at the 0.05 level. Differences were considered as statistically significant when the *p-value* was <0.05 (95% confidence intervals).

6.3. Results

Following the analysis of lncRNA perturbations in all data sets as revealed by RNA sequencing (Chapter 5), two highly perturbed lncRNAs were chosen to further examine their role in cell fate determination of SH-SY5Y cells: *LINC00176* (-9.23 log_2FC) and *LOC648987* (-14.85 log_2FC). To this end, the two lncRNAs were silenced using 3 different LNA GapmeRs for each one. The effectiveness of down-regulation was measured with RT-qPCR. The effect of the lncRNAs was explored in terms of cell survival, apoptotic cell death and cell migration.

6.3.1. The role of *LINC00176* in the cell fate determination of SH-SY5Y cells

6.3.1.1. The effects of *LINC00176* down-regulation on the survival of SH-SY5Y cells

To examine the effect of the down-regulation of *LINC00176* on cell survival, SH-SY5Y cells were nucleofected, incubated for 48 h, re-plated and incubated for another 48/72 h. Cell survival was measured with trypan blue dye exclusion and MTS assay (short-term), and via clonogenic assay (long-term). All the *LINC00176*-specific GapmeRs effectively knocked down *LINC00176* (Figure 6.1a), eliminating its expression by 75%, 85% and 90% for LOC_1, LOC_2 and LOC_3, respectively. Nevertheless, the knockdown did not result in significant changes in the cell viability at 48/72 h, as assessed by trypan blue (Figure 5.10b, d) and MTS assay (Figure 6.1c, e). In addition, the long term survival was not affected significantly by the down-regulation of *LINC00176* either, although the number of colonies was very slightly reduced for LINC_1 and LINC_2 as assessed by colony forming assay, and ~22% reduced for LINC_3 (Figure 6.1f).

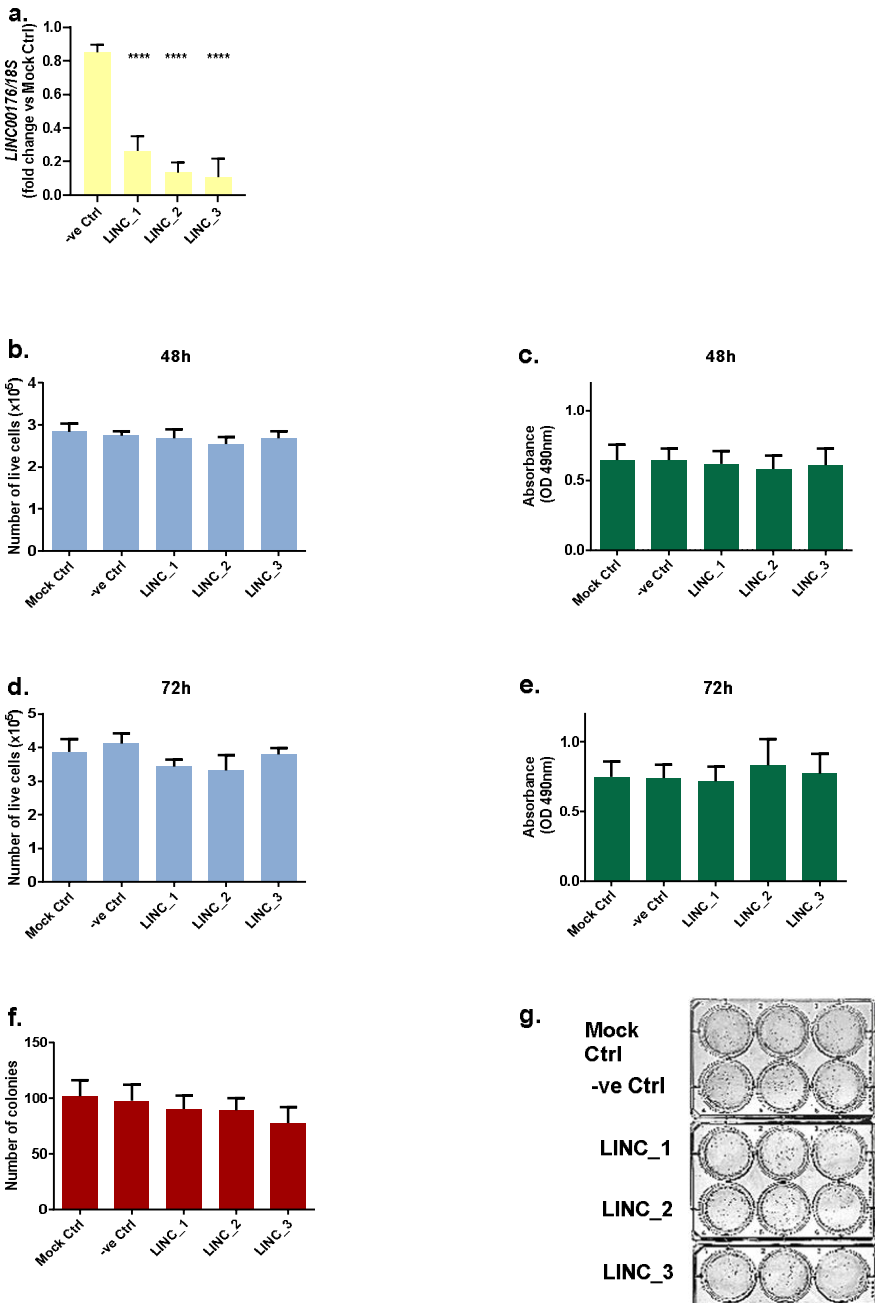

Figure 6.1. *LINC00176*-specific down-regulation does not affect the cell survival of SH-SY5Y cells. SH-SY5Y cells were transfected with the negative GapmeR or one of the three *LINC00176*-specific GapmeRs using nucleofection, incubated for 48 h, re-plated, incubated for another 48/72 h and assessed. The relative expression of *LINC00176* was measured by Real-Time PCR 48 h post-transfection(a); *LINC00176*-specific downregulation does not lead to a statistically significant change in the number of viable cells as assessed with trypan blue exclusion (b, d) and MTS assay (c, e) after 48 h or 72 h, respectively. Cells were also seeded and incubated (37°C, 5% CO_2) for three weeks, and the colonies formed were stained with crystal violet (1%w/v) and counted. *LINC00176*-specific downregulation causes a slight decrease in the number of colonies formed, without statistical significance (f); representative illustration of a clonogenic assay (g); **** indicate a *p-value*<0.001, as measured by One-way ANOVA tests with multiple comparisons (MCT). Data are represented as mean +/- SEM (n=3).

6.3.1.2. The effects of *LINC00176* down-regulation on basal apoptosis level in SH-SY5Y cells

In addition to assessing the effect of *LINC00176* down-regulation on short- and long-term survival, the potential effect on cell death, especially apoptosis, was tested next. In order to do so, SH-SY5Y cells were nucleofected, incubated for 48 h, re-plated and incubated for another 48/72 h. Apoptosis levels were assessed with Flow Cytometry using Annexin V/7-AAD dual staining, as well as with the use of fluorescent microscopy after acridine orange staining. Annexin V staining did not reveal any significant changes in the percentages of total apoptotic cells when comparing the negative control with *LINC00176*-downregulated cells after 48 h (Figure 6.2a). In comparison, assessment with acridine orange showed a significant, near 1-fold increase in apoptosis levels for all *LINC00176*-specific GapmeRs at 48 h (Figure 6.2b). Finally, there were no significant changes in apoptosis levels at 72 h, as assessed by both means (data not shown).

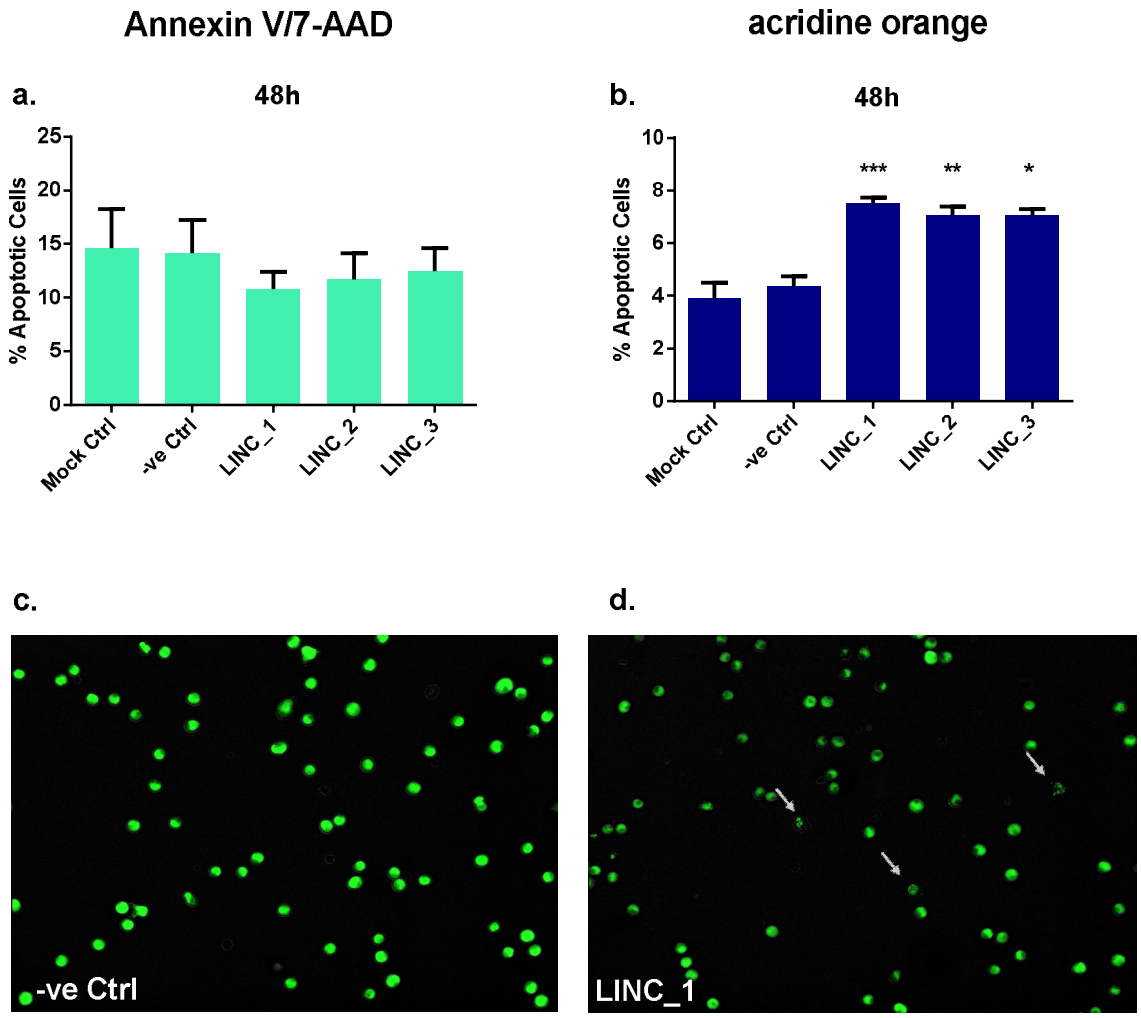

Figure 6.2. The effect of *LINC00176*-specific down-regulation on apoptosis-mediated cell death of SH-SY5Y cells. SH-SY5Y cells were transfected with the negative GapmeR or one of the three *LINC00176*-specific GapmeRs using nucleofection, incubated for 48 h, re-plated, incubated for another 48/72 h and assessed. The levels of apoptosis are overall not affected by *LINC00176* down-regulation as assessed by Flow Cytometry using dual staining Annexin V/7-AAD after 48 h (a); however, there is a statistically significant increase in apoptosis levels for all GapmeRs, as assessed by acridine orange fluorescent microscopy, especially for LINC_1 after 48 h (b); representative illustration of apoptotic cells 48 h post-re-plating, stained with acridine orange and observed using fluorescent microscopy (c, d). Grey arrows indicate cells undergoing apoptosis; * indicates a *p-value*<0.05; ** indicate a *p-value*<0.01; *** indicate a *p-value*<0.001, as measured by One-way ANOVA tests with multiple comparisons (MCT). Data are represented as mean +/- SEM (n=3).

6.3.1.3. The effect of *LINC00176* down-regulation on the migratory ability of SH-SY5Y cells

In line with the indications of the potential interference of *LINC00176* knockdown in the increase of levels of apoptosis, the effect of *LINC00176* knockdown on the cells' potential to migrate was examined next via wound healing assays. SH-SY5Y cells were incubated for 48 h, re-plated, and a linear scratch was introduced 48 h post-re-plating. The % gap closure of the scratch was measured after 24 and 48 h. Notably, the down-regulation of *LINC00176* reduced the migratory capacity of the cells nucleofected with all the three *LINC00176*-specific GapmeRs by ~15% after 24h (Figure 6.3a,), and primarily, by ~25% after 48 h (Figure 6.3cb), but the reduction was significant only at 24 h.

Collectively, these data suggest that, even though the down-regulation of *LINC00176* did not cause dramatic changes in the survival rate short- or long-term, or in the apoptosis levels as assessed by Flow Cytometry, it did, however, slightly decrease the long-term survival, increase apoptosis as assessed by acridine orange, especially as assessed at 48 h post-re-plating, and importantly reduce the ability of cells to migrate.

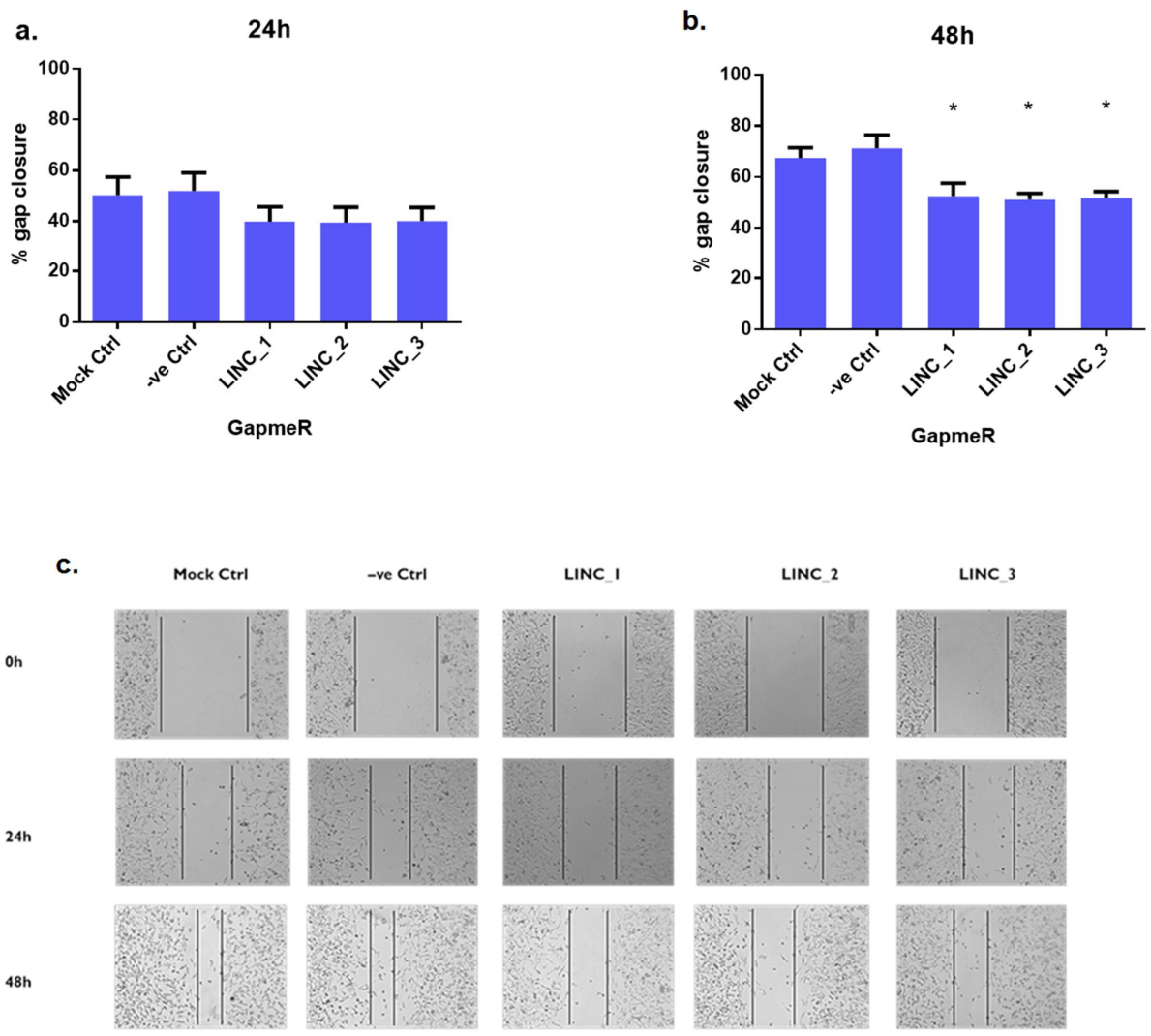

Figure 6.3. *LINC00176*-specific down-regulation reduces the migrating ability of SH-SY5Y cells. SH-SY5Y cells were transfected with the negative GapmeR or one of the three *LINC00176*-specific GapmeRs using nucleofection, incubated for 48 h, re-plated, and a linear scratch was introduced 48 h post-re-plating. The % gap closure of the scratch was measured after 24 and 48 h. The migrating ability of the cells is overall reduced for all three *LINC00176*-specific GapmeRs at both time points assessed, especially at 48 h. % Gap closure values and relative gap closure of *LINC00176*-specific GapmeRs versus the –ve Ctrl at 24h (a) and 48 h (b); representative illustration of a wound healing ("scratch") assay (c); * indicates a *p-value*<0.05, as measured by One-way ANOVA tests with multiple comparisons (MCT). Data are represented as mean +/- SEM, n=3.

6.3.1.4. The effect of *LINC00176* down-regulation on the survival of SH-SY5Y cells after treatment with metformin

Given the fact that *LINC00176* was selected for further assessment because of its high deregulation in response to metformin, after assessing the effects of its down-regulation on the determination of cell fate of SH-SY5Y cells, the next stage was to assess whether this down-regulation could act synergistically or antagonistically with the exposure to metformin. In line with this hypothesis, it was then assessed if the down-regulation of *LINC00176* sensitises, or on the contrary, desensitises SH-SY5Y cells to metformin, and whether, therefore, it improves or deteriorates the cytotoxic effect of metformin, as well as its effect on cell apoptosis.

The short-term cell survival of SH-SY5Y cells was assessed with MTS assay. In terms of cell survival, although metformin seemed to significantly reduce cell viability at 48 h only for the control groups and LINC_1-treated cells, as assessed by MTS assay (Figure 6.4a), it significantly reduced cell survival at 72 h for all experimental groups, apart from LINC_2-treated cells, as assessed by MTS (Figure 6.4c). On the contrary, pre-treatment of cells with *LINC00176*-specific Gapmers seemed to attenuate the percentage of cell viability loss as compared to treated cells, with this attenuation, however, being significant only for LINC_2, both at 48 h and 72 h (~18% and 19% less viability loss, respectively) (Figures 6.4b, d), suggesting a rather non-significant effect of *LINC00176* on the action of metformin in cell survival terms.

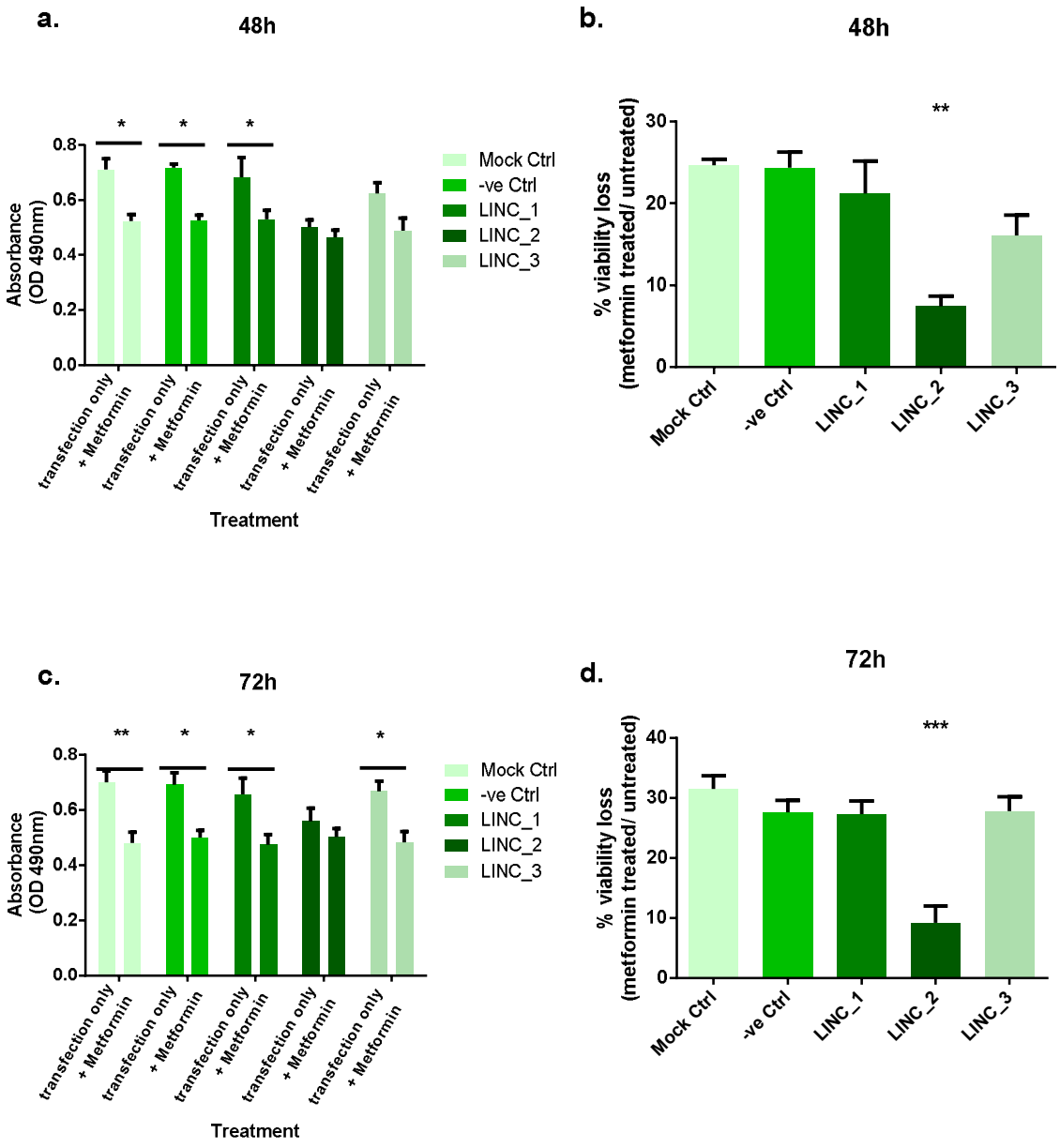

Figure 6.4. The effect of *LINC00176*-specific down-regulation on the survival of SH-SY5Y cells after treatment with metformin. After transfection, cells were harvested by trypsinisation, re-plated after 48 h, treated with 20mM metformin at 24h after re-plating, and incubated for an extra 48/72 h to be assessed for cell survival. Metformin reduces the number of live cells in a statistically significant fashion only for control groups and LINC_1, as measured by MTS assay (a), but % viability loss was significantly reduced only for LINC_2 (b), at 48 h. Metformin significantly reduces cell viability for all groups other than LINC_2 at 72 h (c), with % loss of viability being significantly reduced for LINC_2 (d); * indicates a *p-value*<0.05; ** indicate a *p-value*<0.01; *** indicate a *p-value*<0.001, as measured by One- and Two-way ANOVA tests with multiple comparisons (MCT) in n=4 experiments. Data are represented as mean +/- SEM.

Moreover, the effect on apoptosis levels was evaluated with Flow Cytometry and fluorescent microscopy, as above. Metformin increases cell apoptosis significantly ~10% for the negative control and LINC_2 only at 48 h, as assessed with Annexin V/7-AAD staining measured with Flow Cytometry (Figure 6.5a). In contrast to Annexin V staining, acridine orange staining revealed that metformin significantly increases basal apoptosis in all experimental groups at 48 h (Figure 6.5b). In particular, there was a ~1.5-fold increase in apoptosis levels for the control groups, but only a slighter increase (<1-fold) for *LINC00176*-specific GapmeR-treated cells, without any significant differences among the groups.

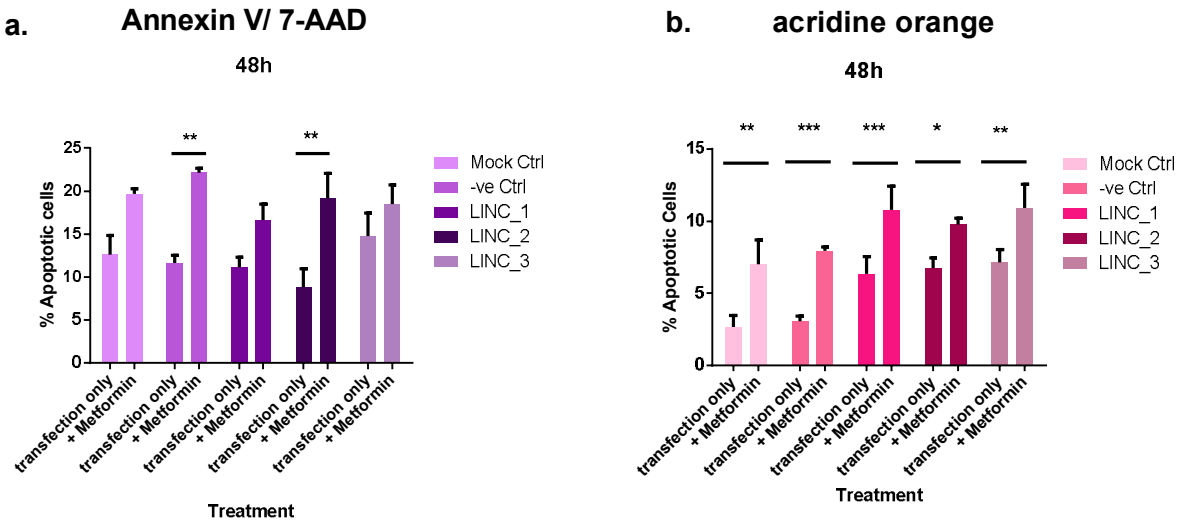

Figure 6.5. The effect of *LINC00176*-specific down-regulation on apoptosis levels of SH-SY5Y after treatment with metformin. After transfection, cells were harvested by trypsinisation, re-plated after 48 h, treated with 20mM metformin at 24h after re-plating, and incubated for an extra 48 h to be assessed for cell apoptosis. Metformin increased the levels of apoptosis with statistical significance only for the –ve Ctrl and LINC_2, as measured by Flow Cytometry with dual Annexin V/7-AAD staining at 48 h (a). However, this increase was significant for all experimental groups, as measured by acridine orange staining at 48 h (b). Nevertheless, the increase occurred regardless of *LINC00176*-specific down-regulation, and, therefore *LINC00176* specific down-regulation did not contribute a statistically significant enhancing or protective effect on the action of metformin; * indicates a *p-value*<0.05; ** indicate a *p-value*<0.01; *** indicate a *p-value*<0.001, as measured by Two-Way Anova tests with multiple comparisons (MCT). Data are represented as mean +/- SEM, n=3.

Taken together, these results suggest a neutral role for *LINC00176* when used in combination with metformin treatment, since its down-regulation does not change the effect of metformin in terms of cell survival and apoptosis.

6.3.2. The role of *LOC648987* in the cell fate determination of SH-SY5Y cells

6.3.2.1. The effects of *LOC648987* down-regulation on the survival of SH-SY5Y cells

Similarly to the rationale behind the experiments checking the effect of *LINC00176* down-regulation, to examine the effect of the down-regulation of *LOC648987* on cell survival, SH-SY5Y cells were nucleofected, incubated for 48 h, re-plated and incubated for another 48/72 h. Cell survival was measured with trypan blue dye exclusion and MTS assay (short-term), and via clonogenic assay (long-term). All the *LOC648987*-specific GapmeRs effectively knocked down *LOC648987*, with LOC_1 causing a 60% reduction in expression, while LOC_2 and LOC_3 caused a 70% and a 80 % reduction, respectively (Figure 6.6a). Nonetheless, the knockdown was not accompanied by significant changes in the cell viability at 48/72 h, as assessed by trypan blue (Figure 6.6b, d) and MTS assay (Figure 6.6c, e). Furthermore, the long term survival was not affected significantly by the down-regulation of *LOC648987* either, although the number of colonies formed was slightly reduced as assessed by colony forming assay for LOC_3 (Figure 6.6f,).

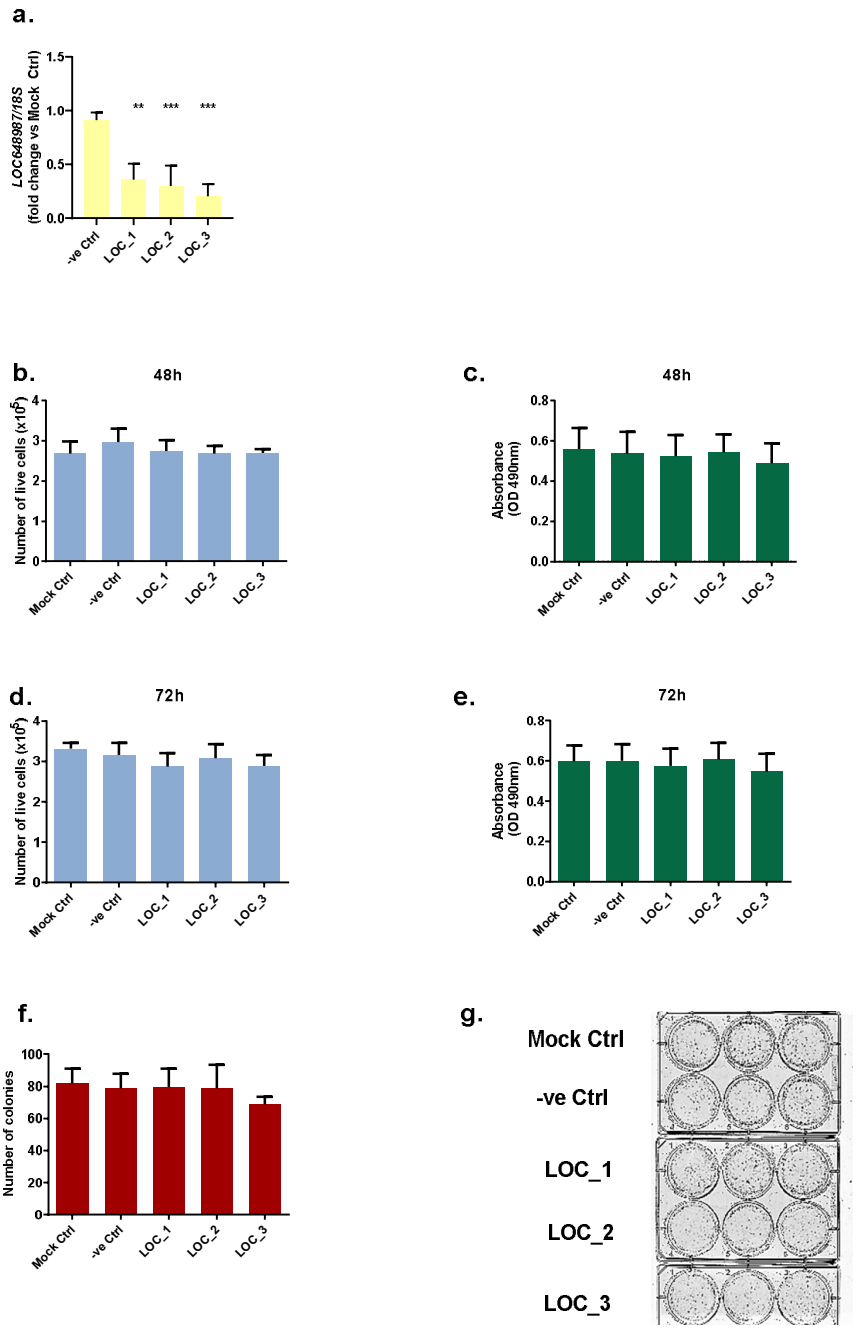

Figure 6.6. *LOC648987*-specific down-regulation does not affect the cell survival of SH-SY5Y cells. SH-SY5Y cells were transfected with the negative GapmeR or one of the three *LOC648987*-specific GapmeRs using nucleofection, incubated for 48 h, re-plated, incubated for another 48/72 h and assessed. The relative expression of *LOC648987* was measured by Real-Time PCR 48 h post-transfection, and was lower for all GapmeRs (a); Overall, *LOC648987*-specific down-regulation does not lead to a statistically significant change in the number of viable cells as assessed with trypan blue exclusion (b, d) and MTS assay (c, e) after 48 h or 72 h, respectively. Cells were also seeded and incubated (37°C, 5% CO_2) for three weeks, and the colonies formed were stained with crystal violet (1%w/v) and counted. *LINC00176*-specific down-regulation causes a slight decrease in the number of colonies formed, without statistical significance (f); representative illustration of a clonogenic assay (g); ** indicate a *p-value*<0.01; *** indicate a *p-value*<0.001, as measured by One-way ANOVA tests with multiple comparisons (MCT). Data are represented as mean +/- SEM, n=4.

6.3.2.2. The effects of *LOC648987* down-regulation on basal apoptosis level in SH-SY5Y cells

The next step incorporated in our investigation on top of assessing the effect of *LOC648987* down-regulation on short- and long-term survival, was to examine the potential effect on apoptosis-mediated cell death. SH-SY5Y cells were nucleofected, incubated for 48 h, re-plated and incubated for another 48/72 h. Apoptosis levels were assessed with Flow Cytometry using Annexin V/7-AAD dual staining, as well as with the use of fluorescent microscopy after acridine orange staining. Flow Cytometry did not reveal any significant changes in the percentages of apoptotic cells when comparing the negative control with *LOC648987* down-regulated cells after 48 and 72 h (Figure 6.7a, c). In comparison, assessment with acridine orange showed a significant, near 1-fold increase in apoptosis levels for LOC_2 and LOC_3 at 48 h (Figure 6.7b), and for all *LOC648987*-specific GapmeRs at 72 h (Figure 6.7d).

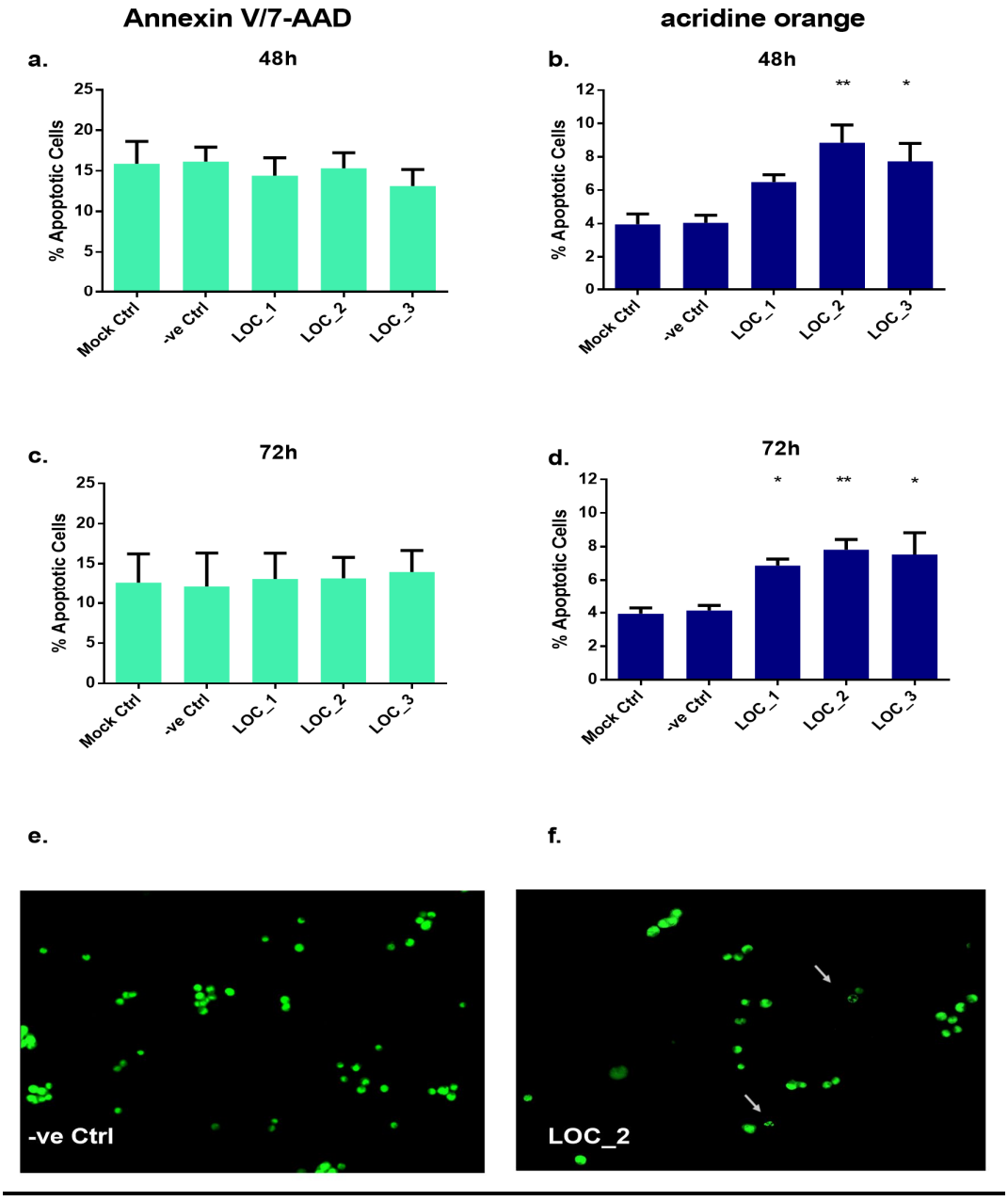

Figure 6.7. The effect of *LOC648987*-specific down-regulation on basal apoptosis rate in SH-SY5Y cells. SH-SY5Y cells were transfected with the negative GapmeR or one of the three *LOC648987*-specific GapmeRs using nucleofection, incubated for 48 h, re-plated, incubated for another 48/72 h and assessed. The levels of apoptosis are overall not affected by *LOC648987* down-regulation as assessed by Flow Cytometry using dual staining Annexin V/7-AAD after 48 h (a); however, there is a statistically significant increase in apoptosis levels as assessed by Acridine orange fluorescent microscopy, for LOC_2 and LOC_3 after 48 h (b). There was no significant effect on apoptosis levels after 72 h, as assessed by Flow Cytometry (c), however, acridine orange fluorescent microscopy showed a small but statistically significant increase for all GapmeRs at 72 h (d); representative illustration of apoptotic cells 48 h post-re-plating, stained with acridine orange and observed using fluorescent microscopy (e, f). Grey arrows indicate cells undergoing apoptosis; * indicates a *p-value*<0.05; ** indicate a *p-value*<0.01, as measured by One-way ANOVA (a, b) and Two-Way Anova (c, d) tests with multiple comparisons (MCT). Data are represented as mean +/- SEM, n=4.

6.3.2.3. The effect of *LOC648987* down-regulation on the migratory ability of SH-SY5Y cells

In line with the indications of the potential interference of *LOC648987* knockdown in the increase of levels of apoptosis, the effect of *LOC648987* knockdown on the cells' potential to migrate was examined next with scratch assays. SH-SY5Y cells were incubated for 48 h, re-plated, and a linear scratch was introduced 48 h post-re-plating. The % gap closure of the scratch was measured after 24 and 48 h. Of note, the down-regulation of *LOC648987* significantly reduced the ability of the cells to migrate for all the three *LOC648987*-specific GapmeRs by nearly 15% after 24h (Figure 6.8a), and primarily, by ~30% after 48 h (Figure 6.8b).

Collectively, these observations imply that, although the down-regulation of *LOC648987* did not cause dramatic changes in the survival rate short- or long-term, it enhanced apoptosis, and as a direct consequence, it also significantly impeded the migration of neuroblastoma cells.

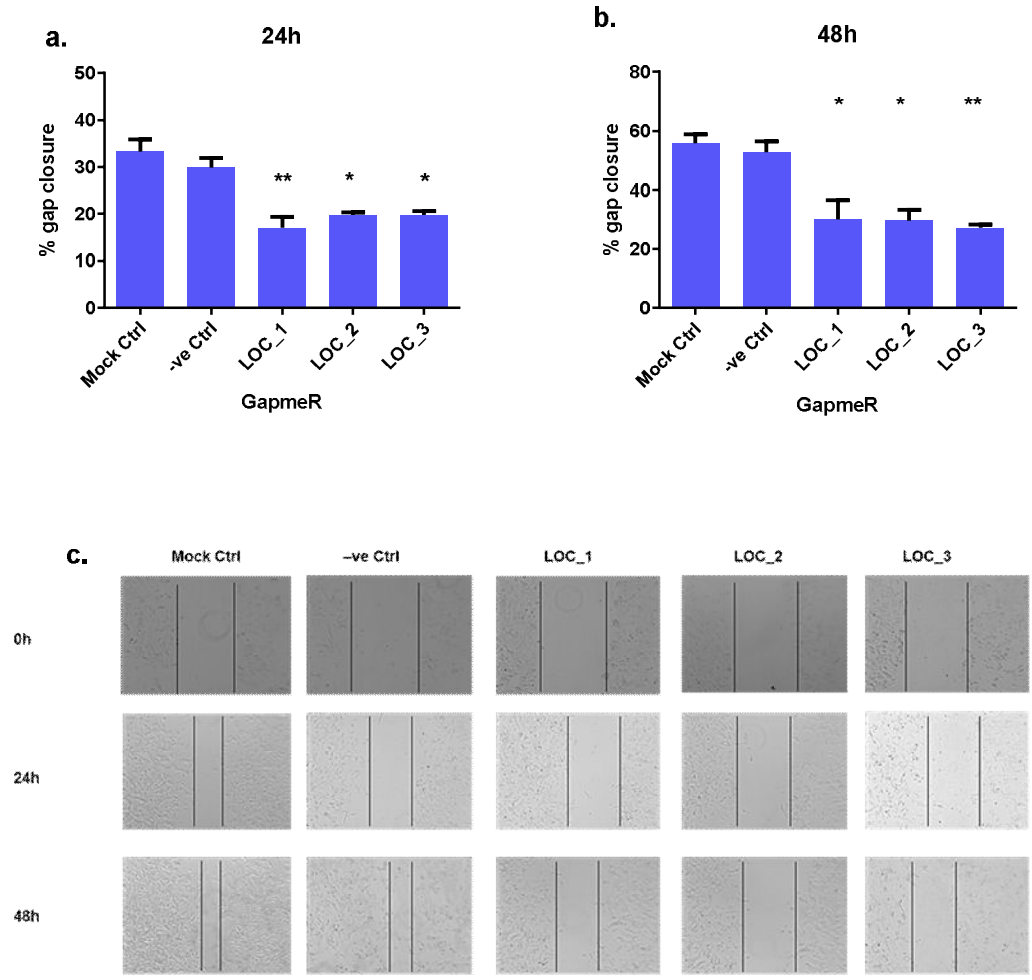

Figure 6.8. *LOC648987*-specific down-regulation reduces the migrating ability of SH-SY5Y cells. SH-SY5Y cells were transfected with the negative GapmeR or one of the three *LOC648987*-specific GapmeRs using nucleofection, incubated for 48 h, re-plated, and a linear scratch was introduced 48 h post-re-plating. The % gap closure of the scratch was measured after 24 and 48 h. The migrating ability of the cells is overall reduced for all three *LOC648987*-specific GapmeRs at both time points assessed, especially at 48 h. % Gap closure values and relative gap closure of *LOC648987*-specific GapmeRs versus the –ve Ctrl at 24h (a respectively) and 48 h (b); representative illustration of a wound healing ("scratch") assay (c); * indicates a *p-value*<0.05; ** indicate a *p-value*<0.01, as measured by One-way ANOVA tests with multiple comparisons (MCT). Data are represented as mean +/- SEM, n=3.

6.3.2.4. The effect of *LOC648987* down-regulation on the survival of SH-SY5Y cells after metformin treatment

On the grounds that, similarly to *LINC00176, LOC648987* was selected for further assessment because of its highly altered expression in response to metformin treatment, after assessing the effects of its down-regulation on the determination of cell fate of SH-SY5Y cells, the next stage was to assess whether this down-regulation could have a combinatory effect together with the exposure to metformin. Therefore it was then assessed if the down-regulation of *LOC648987* affects SH-SY5Y cells' response to metformin.

The short-term cell survival was assessed with MTS assay. In terms of cell survival, although metformin seemed to non-significantly reduce cell viability at 48 h, as assessed MTS assay (Figure 6.9a), it did significantly reduce cell survival at 72 h, as assessed by MTS (Figure 6.9b). However, the percentages of cell viability loss were similar for *LOC648987*-specific GapmeR-treated cells and the control cells both at 48 h (~15-20%) (Figure 6.9b) and 72 h (~30-35%) (Figure 6.9d), implying that the knockdown of *LOC648987* does not influence the effect of metformin on short-term survival of neuroblastoma cells.

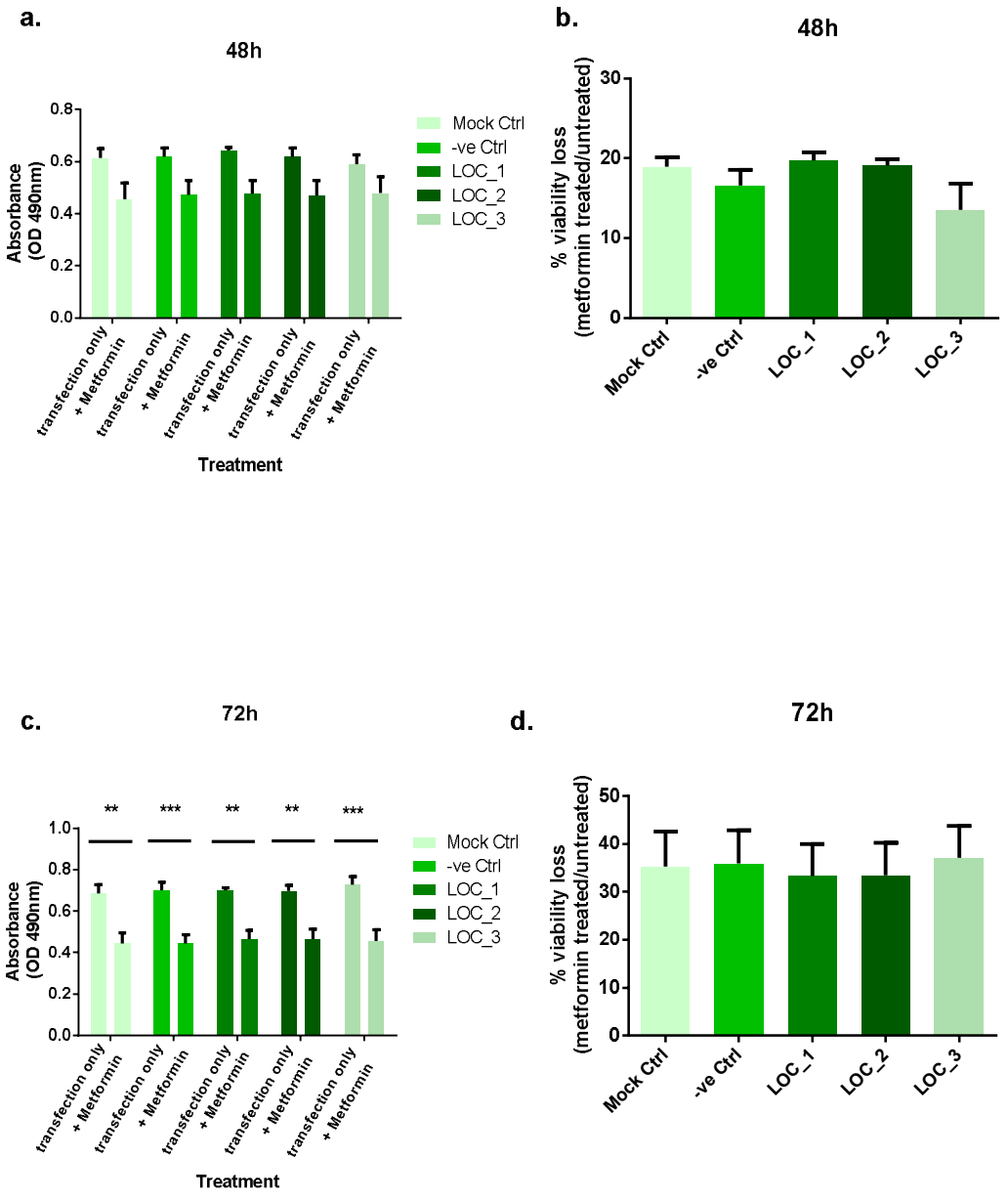

Figure 6.9. The effect of *LOC648987*-specific down-regulation on the survival of SH-SY5Y cells after treatment with metformin. After transfection, cells were harvested by trypsinisation, re-plated after 48 h, treated with 20mM metformin at 24h after re-plating, and incubated for an extra 48/72 h to be assessed for cell survival. Metformin reduces the number of live cells in a statistically non-significant fashion, as measured by MTS assay at 48 h (a), with % viability loss also being non-significantly altered (b). However, there is a statistically significant decrease in cell viability at 72 h, as assessed by MTS assay (c), but with % loss of viability being non-significantly moderated (d); ** indicate a *p-value*<0.01; *** indicate a *p-value*<0.001, as measured by One- and Two-way ANOVA tests with multiple comparisons (MCT) in n=4 experiments. Data are represented as mean +/- SEM.

The effect on apoptosis levels was measured with Flow Cytometry and fluorescent microscopy. In terms of apoptosis levels, metformin increases basal apoptosis significantly only for the negative control and LOC_2 by ~8% in both cases at 48 h, as assessed by Annexin V staining with Flow Cytometry (Figure 6.10a). Albeit, metformin increases the levels of apoptosis significantly for all experimental groups at 48 h, as assessed with acridine orange staining by ~2-fold for the control groups and by ~1-fold for *LOC648987* KD cells (Figure 6.10b). Nonetheless, silencing of *LOC648987* did not lead to statistically significant additive or protective effects in combination with metformin, as far as apoptosis is concerned.

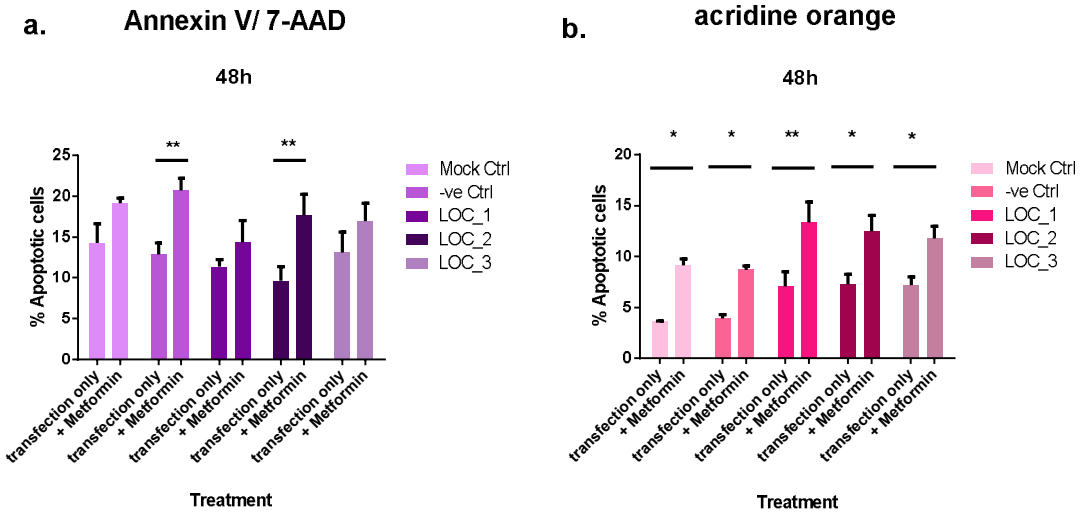

Figure 6.10. The effect of *LOC648987*-specific down-regulation on apoptosis levels of SH-SY5Y after treatment with metformin. After transfection, cells were harvested by trypsinisation, re-plated after 48 h, treated with 20mM metformin at 24h after re-plating, and incubated for an extra 48 h to be assessed for cell apoptosis. Metformin increased the levels of apoptosis with statistical significance only for the –ve Ctrl and LOC_2, as measured by Flow Cytometry with dual Annexin V/7-AAD staining at 48 h (a). This increase was, however, significant for all experimental groups, as measured by acridine orange staining at 48 h (b). However, the increase occurred regardless of *LOC648987*-specific down-regulation, and, therefore *LOC648987* specific down-regulation did not have a statistically significant additive or protective effect on the action of metformin; * indicates a *p-value*<0.05; ** indicate a *p-value*<0.01, as measured by Two-Way Anova tests with multiple comparisons (MCT). Data are represented as mean +/- SEM, n=3.

Collectively, these results propose that the knockdown of *LOC648987* does not have an effect, promoting or inhibitory, in terms of cell survival and apoptosis when combined with metformin treatment.

6.4. Discussion

The studies and analyses performed in Chapter 5 principally aimed at identifying novel lncRNAs whose deregulation is tightly connected to the regulation of cell fate in SH-SY5Y neuroblastoma cells. Given that high-risk neuroblastoma patients still face very poor prognosis and that the reliable and robust biomarkers that can be used for diagnosis and prediction are very limited (Nakagawara *et al*., 2018; Tolbert and Matthay, 2018), there is an urgent need for the discovery of such biomarkers. Apart from protein-coding genes, lncRNAs comprise perfect candidates due to their diverse role in cellular processes in healthy and cancerous cells (Costa, 2005; Chandra Gupta and Nandan Tripathi, 2017). Therefore, the identification of novel lncRNAs that can be exploited for diagnostic, predictive and prognostic purposes towards more reliable patient stratification, as well as therapeutically, is of paramount importance for neuroblastoma.

Among the novel in neuroblastoma lncRNAs with the most pronounced perturbation in expression in response to continuous exposure to metformin, *LINC00176* and *LOC648987* were selected to further explore their role in cell fate decisions by performing various functional analyses. *LINC00176* spans ~5kb on chromosome 20, is composed of 7 exons and has previously been implicated in cancer. *LOC648987* is a 52kb, uncharacterised, non-coding locus across chromosome 5, comprised of 6 exons. The functional analyses have revealed that neither of the two lncRNAs can cause significant changes in the survival of SH-SY5Y cells, short- or long-term. On the contrary, both lncRNAs augmented the levels of apoptosis and, in line with the increased apoptotic levels, the knockdown of both lncRNAs resulted in the reduced

ability of SH-SY5Y cells to migrate, as assessed by wound healing assay, suggesting a potential role of both lncRNAs in apoptosis and invasion regulation.

LINC00176 has already been assessed as a biomarker for clear cell renal carcinoma (Wang *et al.*, 2019), HCC (Zhang *et al.*, 2015; Gong *et al.*, 2020), oesophageal cancer (Fan and Liu, 2016), and pancreatic cancer (Liu *et al.*, 2019). Also, in a CRISPR-Cas9 screening conducted by Zhu *et al.* (2016), *LINC00176* was identified among 51 lncRNAs that can positively or negatively regulate human cancer cell growth. In fact, this regulation was partly mediated by the "regulation of gene expression" and "regulation of transcription", giving the first hint that *LINC00176* could potentially mediate the regulation of cell fate (Zhu *et al.*, 2016). To this end, we assessed the effect of *LINC00176* knockdown on short-and long-term survival of neuroblastoma cells. Our study showed that, although there is a tendency of reduced survival upon *LINC00176* down-regulation, especially long-term, there is not a significant impairment of cell survival in NB cells. This is not in agreement with two previous studies demonstrating that the knockdown of *LINC00176* leads to impaired tumour growth in HCC (Tran *et al.*, 2018) and ovarian cancer (Dai *et al.,* 2019), as evaluated, however by the cells' ability to proliferate rather than survive. Nevertheless, our study demonstrates that silencing *LINC00176* leads to increased apoptosis-mediated cell death as assessed by acridine orange staining, as well as the deteriorated ability of NB cells to migrate as a direct consequence of increased apoptosis, which is in full agreement with the study conducted by Dai and colleagues (Dai *et al.,* 2019). However, given that Annexin V staining failed to demonstrate the same results as acridine orange staining, the apoptosis-related findings should be cautiously interpreted. In addition, Tran *et al.* (2018) also reported increased cell death upon *LINC00176* silencing, although in their case it was necroptosis-mediated rather than apoptosis.

When combining the knockdown of *LINC00176* with the treatment with metformin, the observed effect tended to be rather neutral, as the down-regulation of *LINC00176*

neither enhanced nor deteriorated significantly the cytotoxic effect of metformin. This is supported by the fact that although one of the *LINC00176*-specific GapmeRs led to significantly less viability loss comparing to control cells, implying there might be a protective effect, in general, the effects both on cell survival and apoptosis were non-significant. This is at odds with similar studies assessing combinations of lncRNA manipulations or chemotherapeutic drugs with metformin. For instance, Costa *et al.* (2014), found that *NDM29* overexpression, contributed a synergistic effect on metformin, as assessed in NB cells. On the contrary, metformin has been shown to be protective against therapeutic interventions, as, for example, in the case where it has been demonstrated that it reduces cisplatin-induced apoptosis in glioma, leukaemia, fibrosarcoma, and importantly, SH-SY5Y neuroblastoma cells (Janjetovic *et al.*, 2011).

LOC648987, an uncharacterised lncRNA, was found to be the second most down-regulated lncRNA in neuroblastoma cells with continuous exposure to metformin. Similar to *LINC00176*, the silencing of *LOC648987*, although it induced a slight reduction in cell survival short- and long-term, did not cause a dramatic, significant effect. Albeit, it doubled the levels of basal apoptosis in SH-SY5Y cells, as evaluated by acridine orange staining, and this increase in apoptosis was accompanied by a significant reduction in cell migration. As was the case for *LINC00176*, the apoptosis results are not backed by the Annexin V staining results, a fact that should be brought to attention when interpreting the effects of *LOC648987* down-regulation on apoptotic cell death. Although no functional studies have been conducted on *LOC648987 per se* in the past, a study performed on a variant of *LOC648987* by Tian et al. (2019), *MPRL*, has also demonstrated the ability of *MPRL* to interfere with apoptosis in tongue squamous cell carcinoma (TSCC); however, in that case, the shRNA-mediated knockdown approach led to the attenuation of apoptosis (Tian *et al.*, 2019). Similar to the approach adopted for *LINC00176*, we also suspected that *LOC648987* would interfere with the effect of metformin. Nevertheless, similar to *LINC00176*, silencing

LOC648987 does not significantly affect the cell viability loss or the apoptosis levels conferred by metformin. Of note, this absence of significant effects is not in agreement with the significant cisplatin-sensitising effect of *MPRL* knockdown that has been observed in TSCC cells (Tian *et al.*, 2019).

Despite their moderate effect on the cell fate determination, especially cell survival, *LINC00176* and *LOC648987* have, as discussed above, both displayed very pronounced alterations in expression when treated with metformin, and, therefore, a more significant correlation between their down-regulation and the exposure to metformin would be suspected. However, this was not the case for our system, SH-SY5Y cells. Curiously enough, although cell survival was not significantly affected, the effect on apoptosis, at least as assessed by acridine orange staining, and consequently cell migration, was very pronounced for both lncRNAs. This could be attributed, at least to some extent, to the dual nature of c-Myc. A plethora of studies has established that *c-Myc*, despite being a traditional oncogene, can also promote apoptosis over survival depending on the cellular context and the availability of factors controlling its own transcription (Matsumura *et al.,* 2003; Pelengaris and Khan, 2003). In fact, it can promote apoptosis via various mechanisms affecting the intrinsic and extrinsic apoptotic pathways, (Hoffman and Liebermann, 2008; McMahon, 2014) and key players such as the BCL-2 family members and p53 (Pelengaris and Khan, 2003). Given the fact that the expression of *LINC00176* is c-Myc-dependent (Tran *et al.*, 2018), it may be speculated that the complex functional effects of *LINC00176* in cell fate determination of neuroblastoma cells are a reflection of the complex networks and behaviours of c-Myc.

Notably, the study encompasses some limitations. Although the evaluation of the effect of *LINC00176* and *LOC648987* silencing provided some interesting insights in terms of apoptosis, it has to be noted that the increase was only detected as assessed with acridine orange, but not as assessed with Annexin V/7-AAD staining. This test is

based on the changes in the cell membrane caused by apoptotic processes. The loss of cell membrane asymmetry is an early step in apoptosis. In viable cells, the membrane phospholipid phosphatidylserine (PS) is located at the inner leaflet of the plasma membrane; however, during apoptosis, it is externalised and exposed at the cell surface. Annexin V is a Ca2+- dependent phospholipid-binding protein with high affinity to PS. Since annexin V is not able to penetrate the phospholipid bilayer, vital cells cannot be stained (Bundscherer *et al.*, 2013). A variety of factors could potentially influence the detection of apoptosis by this method. For instance, the trypsinisation method used (standardised trypsin/EDTA trypsinisation) may not have been the best solution, as enzymatic trypsinisation does not comprise the best method of harvesting cells in all cases (Bundscherer *et al.*, 2013). Another factor that could influence the outcome is the timing of the assessment (Schuffner *et al.*, 2002). It is likely that the time of assessment (48 h post-re-plating) was too early and the externalisation of PS had not occurred yet**.** PS externalisation also depends on the bioavailability of calcium, temperature (Bundscherer *et al.*, 2013; Stewart *et al.*, 2018), levels of ATP and cholesterol (Young *et al.*, 2019), as well as differential flippase (the enzyme responsible for the translocation of PS) activity (Vallabhapurapu *et al.*, 2015), either one of which could potentially have been sub-optimal, leading to misleading results. In order to overcome this problem, the use of alternative methods to assess apoptosis, such as DNA fragmentation assessment by TUNEL assay, PARP (Poly (ADP-ribose) polymerase) cleavage assessment or, importantly, Caspase determination would provide a solution (Elmore, 2007). Especially for the last case, either colorimetric/ fluorimetric assays or antibody-based assays would potentially be a reliable alternative. On top of this, this discrepancy could be the result of the limited sensitivity of the used flow cytometer in distinguishing subtle changes, as observed in other cases of laboratory practice in our laboratory (personal communication). Finally, the lack of significant effects, especially in the case of *LOC648987*, could be attributed to the efficiency of the GapmeR-mediated knockdown of the gene. As discussed in section

3.4, in the SH-SY5Y cell system, the use of LNA GapmeRs has proved to be less efficient comparing to the use of siRNAs, although both manage to down-regulate their targets. Consequently, conducting the same experiments using siRNA-mediated knockdown may generate clearer and more pronounced results.

In this set of experiments only limited aspects of cell fate regulation were assessed, and as a result, investigating other aspects such as the effect on cell proliferation and cell cycle, or -further to migration- invasion and metastasis, may generate more useful information to determine the role of these two lncRNAs in the regulation of cell fate. Moreover, the weaker than the anticipated effect on some aspects of cell fate, as well as on the combinatory effect with metformin, in response to the lncRNAs knockdown, could be salvaged by adopting a siRNA-mediated silencing approach. In addition, investigating a reverse order of “treatments” may provide more insights on how the two lncRNAs mediate the regulation of cellular fate. Whether exposure to metformin prior to down-regulation of the two lncRNAs enhances their action remains to be investigated and could uncover other roles of the lncRNAs. Finally, due to *LINC00176* being a c-Myc target, it may worth investigating the expression status of *c-Myc* for the potential existence of feedback loops and further effects, given the diverse role of c-Myc.

The discovery of *LINC00176* and *LOC648987* as novel, exploitable lncRNAs is a matter of utmost importance for neuroblastoma, yet remaining a laborious ‘needle in a haystack’ task. This study provided evidence that both lncRNAs can potentially have oncogenic properties mainly affecting apoptosis and cell migration. Further research on other aspects of cell fate, such as cell proliferation and cell cycle, is essential, for *LINC00176* and *LOC648987* to be considered as biomarker candidates and druggable targets in neuroblastoma.

6.5. Chapter Highlights

1. ***LINC00176*** **and** ***LOC648987*** **are among the most down-regulated lncRNAs in response to continuous exposure to metformin.**

2. **GapmeR-mediated knockdown of** ***LINC00176*** **and** ***LOC648987*** **does not significantly affect cell survival in SH-SY5Y cells.**

3. **GapmeR-mediated down-regulation of** ***LINC00176*** **and** ***LOC648987*** **increases significantly the levels of apoptosis, and simultaneously, reduces the migratory ability of SH-SY5Y cells.**

4. **Down-regulation of** ***LINC00176*** **attenuates the effect of metformin on the short-term survival of SH-SY5Y cells non-significantly.**

5. ***LOC648987*****-specific silencing does not influence the effect of metformin on the survival of SH-SY5Y cells.**

Chapter 7: General Discussion and Concluding remarks

Neuroblastoma is the most common extracranial solid paediatric tumour, accounting for 15% of cancer-related deaths in children (Hwang *et al.*, 2019; Yoda *et al.*, 2019). However, neuroblastomas are highly heterogeneous tumours, presenting diverse characteristics and variable response to treatment even within the same risk group, rendering patient stratification very challenging. In addition, the mutational spectrum is very broad with only few recurrent mutations, suggesting that the diversity in behaviour may also be a reflection of epigenetic alterations, potentially including changes in the lncRNA repertoire (Hwang *et al.*, 2019). High-risk patients still suffer from poor prognosis (Matthay *et al.*, 2016; Nakagawara *et al.*, 2018), high relapse rate and high mortality after recurrence (Hurtado *et al.*, 2019).

Similarly, although GBM comprises one of the most common brain tumours in adults accounting for almost half of all malignant brain tumours, it remains the most mortal and morbid one, with current treatments being inefficient in conferring a better prognosis (Marlow *et al.*, 2017; Stepp and Stummer, 2018). GBMs are highly resistant to conventional radiotherapy and chemotherapy, and owing to their infiltrative growth nature, their complete surgical resection is a major challenge in controlling the tumours, ultimately resulting in high rates of local recurrence, which comprises the primary cause of mortality (Sampetrean and Saya, 2018; Wang *et al.*, 2019). Moreover, they are genetically heterogeneous and relatively less antigenic as compared to other tumours, rendering immunotherapy, a promising therapeutic approach, as well as anti-angiogenesis therapy, less effective (Arrieta *et al.*, 2018; Stepp and Stummer, 2018). Therefore, due to the lack of not only incomplete patient stratification but also efficient treatments for both nervous system cancers, it is of paramount importance to discover robust and significant biomarkers of the cancers and to explore new therapeutic avenues in order to discover novel, potent treatments to improve the prognosis and survival of neuroblastoma and GBM patients.

The advent of new, powerful technologies, such as Next Generation Sequencing, has

enabled the discovery of new key players in gene expression regulation, whose contribution had previously been ignored. LncRNAs fall within this category; however, these >200nt long transcripts have been now brought from the backstage to the onset of gene regulation. The paradigm has eventually shifted to an RNA-dominating world, and important roles have been attributed to non-coding molecules. In line with this, lncRNAs have been thoroughly studied in the context of cancer and have been associated with virtually all hallmarks of cancer (Gutschner and Diederichs, 2012; Rao *et al.*, 2017). It is also established that lncRNAs can act as oncogenes, tumour suppressors, as well as drivers of metastasis (Cao, 2014; Chandra Gupta and Nandan Tripathi, 2017). Although the implication of lncRNAs in carcinogenesis and cancer progression has been established for a variety of well-known lncRNAs, such as *HOTAIR, H19, GAS5* and *MALAT1*, there is still a profound gap in our understanding of the exact mechanisms for most of them. Still, lncRNAs are excellent candidates as biomarkers to achieve a more precise and reliable patient stratification, as well as promising therapeutic targets (Gutschner and Diederichs, 2012).

In this regard, the sub-nuclear lncRNA *MIAT* is of particular interest given the fact that there are piling lines of evidence implicating it in various tumours, including GBM but not neuroblastoma. However, the knowledge of its functional role and the molecular mechanisms associated with tumour progression in these cancers remains lagging. Together with this, the discovery of novel lncRNAs that could be potent players in cell fate decisions in these cancers is also an unmet need, especially for neuroblastoma. To this end, to address these questions and needs, this work focuses on the role of lncRNAs in neuroblastoma and GBM.

7.1. The role of *MIAT* in neuroblastoma and glioblastoma

7.1.1. Effects of *MIAT* silencing on cell fate determination

MIAT gene is located on chromosome 22q12.1. Its ~10kb long transcript is localised in special sub-nuclear bodies, non-overlapping with other known sub-nuclear entities, across the nucleoplasm in a spotted, actively maintained pattern (Sone *et al.*, 2007; Cheng *et al.*, 2016). *MIAT* is primarily expressed in some fetal brain cells and the adult brain/CNS (Tsuiji *et al.*, 2011; Jiang *et al.*, 2016; Sha *et al.*, 2018). It is a mRNA-like lincRNA, that is invariably retained in the nucleus (Sone *et al.*, 2007; Tsuiji *et al.*, 2011) and whose main role is to act as a molecular sponge for splicing factors (primarily SF1, QK1, SRSF1 and Celf3) to restrain proper alternative splicing, potentially via UACUAAC repeat sequence on *MIAT* (Tsuiji *et al.*, 2011; Ishizuka *et al.*, 2014; Cheng *et al.*, 2016; Sattari *et al.*, 2016). Along with its role in regulating physiological processes in healthy cells, it has been established that *MIAT* is involved in the aetiology of heart conditions (Ishii *et al.*, 2006; Boon *et al.*, 2016; Liao *et al.*, 2016), vasculature-related disorders, eye diseases (Jiang *et al.*, 2016; Shen *et al.*, 2016), a variety of CNS disorders including brain disorders (Fenoglio *et al.*, 2013; Barry *et al.*, 2014; Liao *et al.*, 2016) and, as anticipated, cancer.

The expression of *MIAT* is increased in a diversity of cancers, contributing to poor prognosis, as in the case of diffuse large B-cell lymphoma (Sattari *et al.*, 2016), clear cell renal cell carcinoma (Qu *et al.*, 2018; Zhang *et al.*, 2019), breast cancer (Almnaseer and Mourtada-Maarabouni, 2018; Zhang *et al.*, 2019; Liu *et al.*, 2019) and others. This not only suggests that *MIAT* may be used as a biomarker in several types of tumours, following the example of GBM in which *MIAT* is part of a molecular signature of the disease (Zhang *et al.*, 2013), but also that it holds oncogenic properties, at least in the majority of tumours.

The functional analyses carried out in Chapter 3 have confirmed some aspects of the tumour-promoting nature of *MIAT* for the first time in neuroblastoma and GBM cells.

LncRNAs are involved in the regulation of cell survival, apoptosis (Wapinski and Chang, 2011; Melissari and Grote, 2016) and migration (Dhamija and Diederichs, 2016), and *MIAT* followed this rule. Silencing *MIAT* with the use of *MIAT*-specific siRNAs resulted in elevated levels of basal apoptosis, with the increase reaching 2-3-fold in both neuroblastoma and GBM cells. In addition to the pronounced changes in basal apoptosis levels, the down-regulation of *MIAT* resulted in the reduced long-term survival of the cells, suggesting the possibility that the knockdown of *MIAT* may be involved in in the regulation of the survival of these cells as well. Together with the elimination of long-term survival and the elevated levels of basal apoptosis, an important attenuation of the migratory ability of the cells was also observed in response to *MIAT* down-regulation, reaching on average ~30% and ~35% less migration for neuroblastoma and GBM cells, respectively. The same effects were observed when using locked ASOs (GapmeRs) to achieve the down-regulation of *MIAT* both in neuroblastoma and glioblastoma cells, although the obtained magnitude of the effect was slightly lower compared to siRNA-mediated silencing.

Similar effects in concordance with the results herein described have already been reported in the literature for multiple conditions, including neurovascular dysfunctions and neurodegenerative disorders, such as oxygen-induced retinopathy (OIR), optic nerve transection (ONT), Alzheimer's disease and diabetic retinopathy (Jiang *et al.*, 2016), as well as cataract, where Shen *et al.* (2016) also reported that *MIAT* exerts its effects in cataract patients cells via augmented ROS production. Essentially, there are also accumulating studies demonstrating similar effects in a variety of cancerous contexts. The study conducted by Sattari *et al*. (2016) demonstrating the oncogenic role of *MIAT* and its involvement in apoptosis in a Diffuse Large B-Cell Lymphoma cell line opened Pandora's box for further studies in other tumours. For example, *MIAT* fluctuations have been studied different types of breast cancer cells, demonstrating the oncogenic properties of *MIAT* (Almnaseer and Mourtada-Maarabouni, 2018; Li *et al.*,

2018), while the implications of *MIAT*'s role have also been intensively studied in lung cancer cells, also suggesting its role as a promoter of the tumour in terms of enhanced survival and migration/invasion and inhibited apoptosis, especially the mitochondrial pathway (Fu *et al.*, 2018; Wu *et al.*, 2020; Zeng *et al.*, 2020). The same effects have also been reported in other cancer cells, including gastric cancer cells (Li *et al.*, 2017), colorectal cancer cells (Liu *et al.*, 2018), clear cell renal cell carcinoma cells (Qu *et al.*, 2018), ovarian cancer cell lines (Shao *et al.*, 2018) and most recently, papillary thyroid cancer cell lines (Wang *et al.*, 2019) and osteosarcoma cells (Zhang *et al.*, 2019), altogether suggesting a rather universally crucial role of *MIAT* in the regulation of cell fate decisions.

7.1.2. Effects of *MIAT* silencing on gene expression

Given the magnitude of the *MIAT*-regulated effects described in Chapter 3, it was hypothesised that *MIAT* would be involved in molecular pathways and networks of great significance in cancer settings, and, therefore, that its fluctuations would heavily impact significant players linked with carcinogenesis and cancer progression. To this end, RNA sequencing approach was adopted in order to investigate the molecular mechanisms underpinning the effects observed upon the knockdown of *MIAT*.

As presented in Chapter 4, the results of the RNA sequencing were highly enlightening in terms of molecular modifications associated with *MIAT* levels. In terms of apoptosis, cell survival and cell migration, numerous pathways and processes were affected, including the MAPK, EGFR, TGF-β, Phospholipase D and NOD-like receptor signalling pathways, as well as multiple of their overlapping brunches. The EGFR and MAPK pathways have been broadly implicated in both tumours, as their mutations are indicators of poor prognosis and tumour aggressiveness in neuroblastoma (Eleveld *et al.*, 2018; Takeuchi *et al.*, 2018) and comprise very frequent events also contributing tumourigenic outcomes in GBM (Anand *et al.*, 2011; Li *et al.*, 2014; Saadeh *et al.,*

2018). Furthermore, the TGF-β pathway and its related proteins have been established to undergo expressional changes both in neuroblastoma (Mestdagh *et al.*, 2010; Lynch *et al.*, 2012) and GBM (Wang *et al.*, 2016; Guo *et al.*, 2018; Zhou *et al.*, 2018), while the phospholipase D NOD-like receptor signalling pathways are also deregulated in both tumours, as part of the complex networks formed by all the aforementioned signalling pathways. Notably, a variety of biological processes associated with apoptosis as a response to oxidative stress, for instance, cell death in response to oxidative stress, cellular response to oxidative stress, regulation of cellular response to oxidative stress and regulation of oxidative stress-induced intrinsic apoptotic signalling pathway, as well as cell migration, for example, tissue migration, regulation of cell adhesion mediated by integrin and regulation of cell migration, were among the most deregulated processes upon *MIAT* knockdown.

Moreover, it is noteworthy that the silencing of *MIAT,* on top of changing the molecular landscape on a pathway and on a miRNA level, also led to a massive perturbation of the lncRNAome, with hundreds of lncRNAs being deregulated, which could also contribute to the final phenotype of neuroblastoma cells. Among them, *CASC2* (Palmieri *et al.*, 2017)*, ZNFX1-AS1* (Wang *et al.*, 2016; Shi *et al.*, 2019), *TP73-AS1* (Gong *et al.*, 2020), *MIR22HG* (Han *et al.*, 2019) and *HIF1A-AS2* (Pop *et al.*, 2018)*,* which have all been implicated in several tumours, were highly perturbed. The RNA sequencing analysis also predicted changes in expression of multiple miRNAs in response to *MIAT* knockdown, including miR-124, the miR-27 and miR-181 families, and miR-34, all of which are known mediators of key cancer-related processes (De Antonellis *et al.*, 2014; Ding *et al.*, 2017; Xiao *et al.*, 2018; Zhong *et al.*, 2018).

Moreover, the RNA sequencing revealed that *MIAT,* together with regulating gene expression in trans*,* also regulates gene expression *in cis*, with numerous important genes-protein-coding and non-coding- located on chromosome 22 being up- or down-regulated, including the pro-apoptotic *BID* and *BIK*, as well as the invasion-related

PARVB, and *DGCR8,* a miRNA biogenesis machinery component (~5-fold up-regulated). In fact, the expression of *DGCR8* has already been shown to be regulated by *MIAT* in Wilm's tumour. LncRNAs display broad mechanistic diversity to exert their function and in this regard, they can function both *in cis* and *in trans* (Kornienko *et al.*, 2013; Slack and Chinnaiyan, 2019). A plethora of well-studied, significant lncRNAs have been established to act in both ways, including *DHFR* (Wilusz *et al*., 2009) and *CISTR-ACT* (*cis*- and *trans*- chromosomal interaction) lncRNA (Maass *et al*., 2014), *ANRIL* (Boon *et al*., 2016) and *NEAT1* (Almnaseer and Mourtada-Maarabouni, 2016), and, consequently, the fact that *MIAT* seems to fall in this category highlights its crucial role in gene expression regulation.

Intriguingly, upon *MIAT* down-regulation the relative isoform abundance of numerous mRNAs was vastly affected, not only confirming the role of *MIAT* as an alternative splicing regulator (Tsuiji *et al.*, 2011; Ishizuka *et al.*, 2014; Cheng *et al.*, 2016) but also potentially defining the molecular picture of the cells and determining their fate. Of note, a multitude is key mediators of the processes perturbed upon *MIAT* knockdown, for instance, *BID, XIAP, CASP8* in apoptosis, *MAPK7* in cell survival and *HIF1A* in response to oxidative stress, while others comprise cancer-associated lncRNAs (*CASC2, MIR22HG, LOC100506714*). LncRNAs have been recognised as essential players both in transcriptional and post-transcriptional regulation of gene expression including mRNA maturation and translation (Kornienko *et al.*, 2013; Slack and Chinnaiyan, 2019). Therefore, it comes as no surprise that *MIAT*, like other lncRNAs, is part of complex transcriptional and post-transcriptional networks and feedback loops, exerting a fundamental role.

7.1.3. The role of *MIAT* in apoptosis and ROS-mediated responses

Although cell survival/ growth pathways seemed to be affected by the knockdown of *MIAT*, the most pronounced effect was observed in the levels of basal apoptosis, which

were massively elevated, thereby shifting our attention to the mechanisms and key players mediating this phenotype. In line with this, the RNA sequencing revealed that among all perturbed biological processes, including the ROS-related ones mentioned above, “cell death in response to oxidative stress” was the most deregulated process, with an impressive 58/59 involved genes displaying altered expression. This prompted us to further investigate the role of ROS in the in response to *MIAT* silencing and their interplay with apoptosis. Therefore, some of the mechanisms and key players mediating this phenotype were further validated.

Consequently, besides the RNA sequencing, RT² Profiler™ PCR arrays and Western Blotting were employed for target validation and revealed that programmed cell death, and primarily apoptosis, are highly deregulated in response to *MIAT* silencing. In fact, both the extrinsic and, mainly the intrinsic, apoptotic pathways exhibited tremendous changes in the expression of fundamental components. According to the RT² Profiler™ PCR arrays’ results, numerous factors essential for apoptosis displayed perturbed expression, including the up-regulation of *APAF1, BAD, BCL2L11, BIK, TRADD, TRAF2/3, TP73* and *CASP8* and the down-regulation of *FAS, MCL1* and *XIAP*.

Notably, according to the RNA sequencing results, these excessive apoptosis levels are attributed, at least to an important extent, to the elevation of ROS levels in neuroblastoma cells upon *MIAT* knockdown, a hint that was further supported and confirmed by experimental data that indeed showed augmented ROS levels in response to *MIAT* silencing in neuroblastoma (and GBM) cells. It has been established that numerous non-coding RNAs, including lncRNAs and miRNAs, are regulated by ROS and/or, inversely, can regulate ROS levels in a cell (Kietzmann *et al.*, 2017; Wei *et al.*, 2019). Interestingly, this interplay involves some of the perturbed pathways and processes that emerged in the RNA sequencing, as in the case of *H19* regulating ROS levels via activating the MAPK/ERK pathway in hepatocellular carcinoma (Ding *et al.*, 2018), and *SNHG15* promoting CRC through a ROS/AIF mechanism (Saeinasab *et al.*,

2019). In addition, it is noteworthy that, in concordance with our findings, *MIAT*-specific knockdown has been found to enhance the effects of H_2O_2-mediated oxidative stress to reduce cell proliferation and enhance apoptosis in cataract lenses (Shen *et al.*, 2016). Finally, a recent study revealed an oncogenic role for *MIAT* in Wilms' tumour through ROS-mediated regulation of DGCR8 (Zhao *et al.*, 2019). There is also increasing evidence that apart from apoptosis, ROS also mediate necroptosis-mediated cell death, as well as autophagy (Galadari *et al.*, 2017; Florean *et al.*, 2019). In this context, numerous autophagy-related genes were perturbed, like ATGs, suggesting there may be ROS-mediated autophagy, as well, in response to *MIAT* silencing in our system.

7.1.4. The multidimensional mechanisms of *MIAT* function

Taking all these factors into account, the current study suggests a variety of mechanisms, ROS-dependent and ROS-independent, via which *MIAT* could potentially exert its role and mediate the observed phenotypes. Nevertheless, in order to do so, it is first essential to recap the nature of a key player in the regulation of cell fate determination, *c-Myc,* which this study suggests that is affected by *MIAT* down-regulation, given that its expression was confirmed to be reduced both by the RNA sequencing and RT-qPCR. C-Myc is a master regulator transcription factor, which is known to promote cell proliferation, survival and growth, thereby acting as an oncogene, but at the same time, it is simultaneously a potent regulator of apoptosis (Hoffman and Liebermann, 2008; McMahon, 2014). Importantly, the expression of *c-Myc* is also dependent on the cellular levels of ROS, as it acts as a redox sensor, and in line with this, high ROS levels trigger *c-Myc* up-regulation to favour tumour progression. Nevertheless, above a certain threshold, *c-Myc* expression as induced by elevated ROS levels favours apoptosis (Babu and Tay, 2019; Florean *et al.*, 2019; Lin, 2019). In line with these, a plethora of lncRNAs have so far been associated with oxidative stress and ROS production (Giannakakis *et al.*, 2015; De Paepe *et al*., 2018),

and yet another multitude of lncRNAs has been shown to be involved in regulatory loops of c-Myc (Iaccarino, 2017; Slack and Chinnaiyan, 2019), including *MIAT* (Galardi *et al.*, 2016; Xiang *et al.*, 2019).

As hypothesised and confirmed by the RNA sequencing, silencing *MIAT* induces perturbations in numerous survival-related pathways (MAPK, TGF-β, EGFR and Phospholipase D pathways) established to contribute to cancer, with the most important being the down-regulation of the MAPK cascade, including the PI3K/Akt pathway. There is a growing body of evidence that proposes the involvement of lncRNAs in regulating the pathway (reviewed by Benetatos *et al.*, 2017). Importantly, a recent study in melanoma cancer cells reported that *MIAT* is a regulator of the phosphorylation of PI3K and Akt, thereby activating the pathway (Yang *et al.*, 2019), introducing the possibility that this could be the case in neuroblastoma cells as well. Besides, the PI3K/Akt pathway can also be triggered by disturbed ROS levels (Babu and Tay, 2019) (Figure 7.1).

According to the RNA sequencing results, as well as our target validation experiments, a variety of oxidative stress- and apoptosis-related genes were perturbed in response to *MIAT* down-regulation. Therefore, we are herein suggesting two possible core mechanisms. As far apoptosis is concerned, the knockdown of *MIAT* could decrease the expression of NRF2 (2-fold down-regulated in our dataset), a master regulator of the redox machinery (Hybertson and Gao, 2014; Kitamura and Motohashi, 2018), which would, in turn, decrease the availability of anti-oxidant proteins and ROS scavengers including GSH (glutathione)-a well-known cell death mediator (Lv *et al.*, 2019) [GCLC (Glutamate-Cysteine Ligase Catalytic Subunit)/GCLM (Glutamate-Cysteine Ligase Modifier Subunit): the first rate-limiting enzyme of glutathione synthesis, both down-regulated), resulting in increased accumulation of ROS in the mitochondria. This would consequently lead to increased MOMP, release of Cyt-c and would trigger the mitochondrial apoptosis cascade. In addition, *MIAT* knockdown could

induce both the extrinsic and intrinsic pathways independent of ROS production, as components of both were found to have aberrant expression. For instance, in the former case, Fas and Caspase 8 were down- and up-regulated, respectively, while in the latter case, a diversity of pro-apoptotic players were up-regulated (e.g. *BID, BIK, BAD, APAF1* and *NOXA*) and at the same time, insidious anti-apoptotic factors were down-regulated, including IAPs- and mainly *XIAP, BAX, MCL1* and *BCL-2*. Of note, other types of PCD were affected by the silencing of *MIAT*, including autophagy, as revealed by the aberrant, both directions expression of ATGs, and necroptosis (Figure 7.1).

The other significant core mechanism suggested evolves around the predominant role of c-Myc. Interestingly, apart from the down-regulated c-Myc, the RNA sequencing also demonstrated the up-regulation of *EZH2* and *HIF1A-AS2*, and the down-regulation of *SIRT1*, *EPHA2*, *HIF1A*, Sp transcription factors and their upstream *ZBTB* family members, as well as the perturbations of Sp downstream targets. Therefore, in this scenario, it is possible that the down-regulation of *MIAT* would lead to augmented ROS levels, which in turn could cause the deregulation of elements of the epigenetic machinery, such as the down-regulation of *SIRT1* and the up-regulation of *EZH2* (O'Hagan *et al.*, 2011), two elements conferring opposite outcomes in transcription, to ultimately knockdown c-Myc. In addition, *MIAT* could directly regulate *SIRT1* (Zhao *et al.*, 2019) or *c-Myc* itself. Silencing *MIAT* could also lead to the down-regulation of c-Myc via up-regulating miR-520d to reduce the expression of *EPHA2* (Wang *et al.*, 2014; Xiang *et al.*, 2019). From this point on, it could be assumed that reduced expression of c-Myc leads to eliminated expression of Sp transcription factors, especially Sp1/3/4, via the regulation of a diversity of miRNAs and ZBTB proteins. Interestingly, the decrease in Sp expression could be also c-Myc independent and obtained due to high ROS levels (Lavrovsky *et al.*, 2000; Lee *et al.*, 2019; Upadhyaya *et al.*, 2019). Consequently, decreased Sp expression would cause aberrant

expression of downstream targets associated with survival, apoptosis and migration, such as down-regulation of *c-MET, Fas, BCL-2, MMPs* and *VEGFA/C* (all verified in our RNA sequencing). Curiously, down-regulated VEGFs could also be the result of reduced expression of *HIF1A*, driven either by increased ROS levels or by the increased activity of its NAT *HIF1A-AS2*, ultimately leading to a possible reduction of angiogenesis. Another noteworthy loop/ balance is the one of *MIAT*-induced ROS/ c-Myc/ GSH, as it is established that all players in this axis regulate the expression and bioavailability of each other (Biroccio *et al.*, 2004; Benassi *et al.*, 2006; Torres *et al.*, 2009; Weldy *et al.*, 2012; Lv *et al.*, 2019). Finally, *MIAT* knockdown-induced PI3K/Akt down-regulation could be intermingled in both core pathways, as it could not only promote apoptosis by de-repressing BAD (Manning and Cantley, 2007) but also down-regulate c-Myc (Yang *et al.*, 2019) (Figure 7.1).

A third, probably equally important mechanism, includes *MIAT*/ miRNA/ protein-coding gene axes. Apart from acting as a ceRNA for splicing factors, *MIAT* is also an established miRNA sponge (Fakhr-Eldeen *et al*., 2019). To this end, we are proposing that *MIAT* could be sponging a variety or miRNAs with known roles in cancer progression that were predicted to be perturbed in the RNA sequencing, including miR-34a, miR-124, miR-27a/b and others. Of particular interest, the knockdown of *MIAT* could increase miR-34a to downregulate the expression of *MYCN* (Wei et al., 2008) and its targets *MDM2* and *FAK* (Focal Adhesion Kinase) (both slightly down-regulated in our dataset). The same effect could also be independent of miR-34a, as *MIAT* has also been elucidated to be the most abundant lincRNA in neuroblastoma, as well as a *MYCN* modulator (Rombaut *et al*., 2019). Besides, increased miR-34a could decrease the expression of Oct1, which in this study was down-regulated as demonstrated by RNA sequencing and RT-qPCR, and its downstream targets (e.g. *ABL1, BCL2L, NFκB* and *GADD45A*-all confirmed to be down-regulated) and be responsible for the increased levels of TP73, which could also be regulated by its NAT *TP73-AS1.* In

addition, *TP73-AS1* is also targeted by miR-124 (Xiao *et al.*, 2018), and so is Oct1. Interestingly, 263 miRNAs were predicted to be deregulated, including the aforementioned ones. Deregulation of such a scale could be attributed to the increased expression of DGCR8 (~5-fold up-regulated in the RNA sequencing), a component of the miRNA processing machinery, which has also been demonstrated to be linked to *MIAT* in Wilm's tumour (Zhao *et al.*, 2019). Collectively, these perturbations, together with the c-Myc-related mechanisms, could ultimately lead to decreased cell survival, increased apoptosis and attenuated cell migration (Figure 7.1).

Taking everything into account, the current study has verified *MIAT* as an oncogenic lncRNA in neuroblastoma and GBM, as its knockdown led to the significant reduction of long-term survival, the pronounced elevation of basal apoptosis levels and, in turn, an important attenuation of cell migration in both tumour cells. The Bioinformatics approach adopted together with the target validation using RT² Profiler™ PCR Arrays and functional assays to quantify ROS levels, have revealed that these phenotypes, and especially apoptosis, were ROS-mediated, at least to some extent, and based on the RNA sequencing analysis, several potential mechanisms via which *MIAT* exerts its effects are herein suggested.

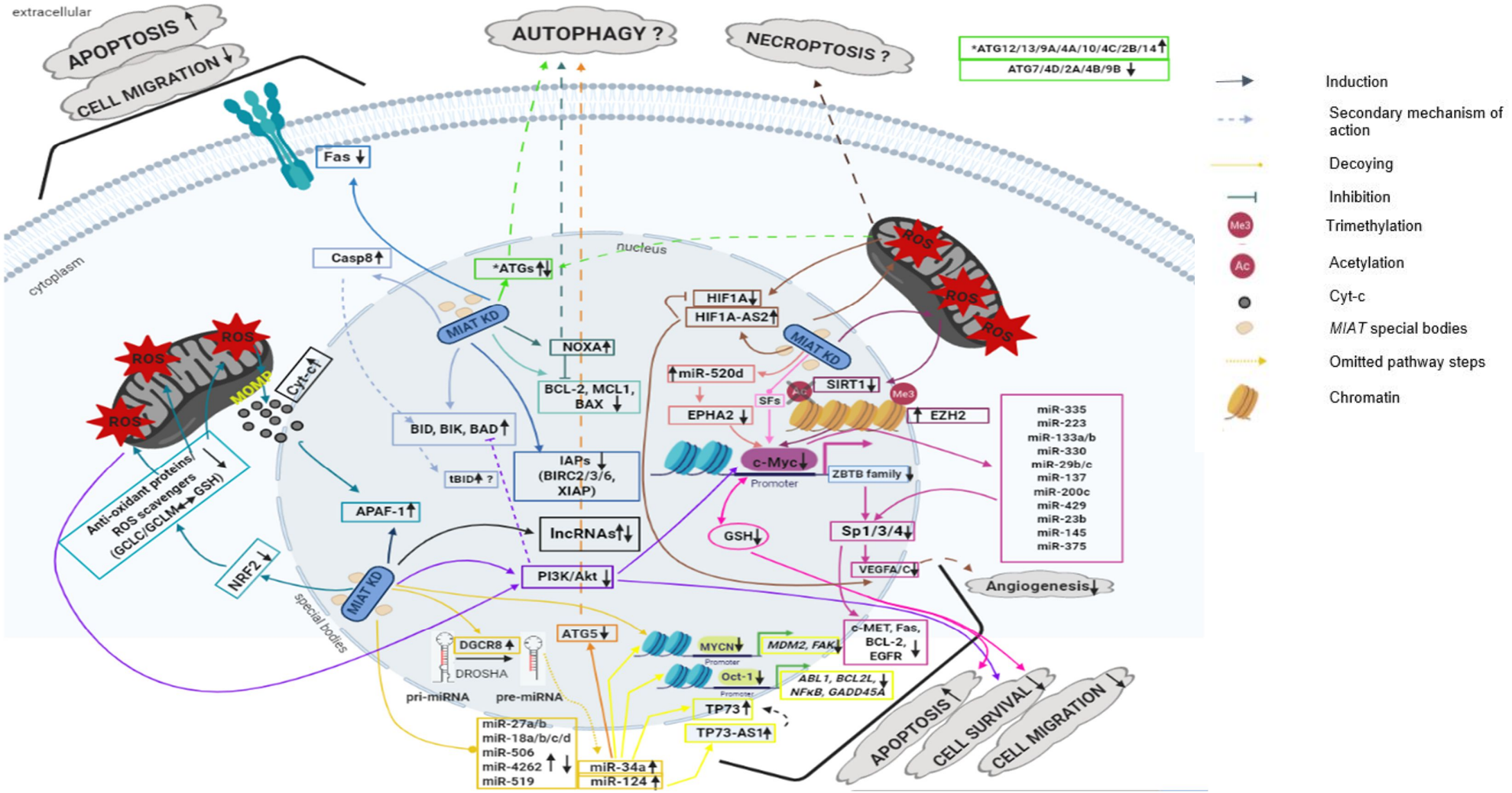

Figure 7.1. Schematic representation of the suggested molecular mechanisms underpinning the response to MIAT down-regulation. The silencing of MIAT potentially leads to increased apoptosis, reduced cell survival, migration and angiogenesis, and deregulated autophagy and necroptosis, via multiple molecular pathways in ROS-dependent and independent ways. MIAT knockdown augments ROS levels via down-regulating NRF2, and causes their accumulation in mitochondria, while it also down-regulates c-Myc and Oct-1, affecting their downstream targets, as well as the MAPK/PI3K/Akt pathway, and changes the expression of multiple lncRNAs and miRNAs, both via decoying them and via up-regulating DGCR8. Apoptosis-related genes and mechanisms are presented in blue shades, c-Myc-related ones in pink shades, PI3K/Akt-related ones in purple, miRNA-related ones in yellow shades and angiogenesis-related ones in brown. Subcellular organelles are not designed in scale; figure created using biorender.com.

7.2. Novel lncRNAs as cell fate regulators in neuroblastoma

A plethora of lncRNAs has been reported to act either as oncogenes, tumour suppressors or to display dual roles depending on the cancerous context in a variety of tumours, including neuroblastoma (Pandey and Kanduri, 2015; Slack and Chinnaiyan, 2019), and can be of prognostic and predictive value for neuroblastoma patients. The list of such lncRNAs that are associated with neuroblastoma is steadily growing (Batagov *et al.*, 2013), and several approaches have been attempted to generate accurate lncRNA-based profiles and signatures, in order to classify patients robustly and provide the most suitable treatment (Sahu *et al.*, 2018; Gao *et al.*, 2019; Rombaut *et al.*, 2019; Yerukala Sathipati *et al.*, 2019). Nevertheless, accurate patient stratification, as well as efficient therapeutic approaches for high risk patients, remain an unmet need (Nakagawara *et al.*, 2018), urging the discovery of biomarkers and novel therapeutic approaches.

Metformin is an old anti-diabetic treatment deriving from the plant *Galega officinalis* (French lilac) (Emami Riedmaier *et al.*, 2013; Vial *et al.*, 2019). In contemporary medicine, metformin is a synthetic biguanide (N', N' dimethylbiguanide), and has been used in the clinic as a golden standard treatment for type 2 diabetes (T2D) (Sahra *et al.*, 2010). Metformin is a multifaceted chemotherapeutic drug that acts on multiple levels and mechanisms [reviewed in depth by Kourelis and Siegel (2012) and Daugan *et al.* (2016)]. On the grounds that metformin interferes with such a great diversity of cellular processes and molecular pathways and in so many levels, treatment with metformin, both short-term and prolonged, comprises a useful platform to explore the possibility of novel lncRNAs potentially regulating cell fate decisions in neuroblastoma cells. To this end, an RNA sequencing approach was adopted to identify such lncRNAs. The analysis of the RNA sequencing results, as presented in Chapter 5, revealed some preliminary, yet interesting, insights towards this direction.

First, short-term treatment of neuroblastoma SH-SY5Y cells with metformin modified the expression of 418 lncRNAs, while prolonged exposure to metformin led to expressional changes in 482 lncRNAs, distributed virtually into all lncRNAs subtypes, with NATs being the most abundant. In the former group, several lncRNAs displaying high expressional aberrations have been characterised either as oncogenes (e.g. *TP73-AS1, LOC100288637, CBR3-AS1)* or as tumour suppressors (e.g. *MIR22HG),* and, intriguingly, have been implicated in diverse cancer-related processes that are affected by the action of metformin, for instance, *TP73-AS1* in cell proliferation and metastasis (Wang *et al.*, 2018; Yao *et al.*, 2018), *CBR3-AS1* in cell cycle regulation (Li *et al.,* 2014) and Notch signalling (Wang *et al.*, 2018) and *MIR22HG* in cell proliferation and migration (Han *et al.*, 2019), confirming that our approach of using metformin was suitable. Nevertheless, to the best of our knowledge, this is the first report implicating them in the cell fate determination of neuroblastoma cells. Substantially, the most deregulated lncRNAs include *LOC100507557* and *LOC100505695*, which are completely novel and uncharacterised, and others like *LOC100130700, PEG3-AS1* and *LOC100288637,* with very limited, relatively recent research on them. *LOC100130700* has been found to be recurrently deleted in primary mediastinal B-Cell lymphoma (Dai *et al.*, 2015), while *PEG3-AS1* exhibits differential expression in cell carcinoma of the head and neck and is part of an eight-long non-coding RNA signature for colorectal cancer (Hsu *et al.*, 2016; Zhang *et al.*, 2019). Finally, *LOC100288637* has been positively correlated with HER-2 expression in HER-2-enriched subtype breast cancer and up-regulated in ovarian cancer tissues (Yang *et al.*, 2016; Feng *et al.*, 2019).

Similarly, in the latter group of cells exposed to metformin long-term, multiple highly deregulated lncRNAs have a tumour-promoting identity, for instance, *LOC643401 (PURPL)* and *LINC00176,* while others have a tumour-suppressive one [*e.g. GHRLOS* (Zhu *et al.*, 2016; Wu *et al.*, 2017; Soleyman-Jahi *et al.*, 2019), *CASC2*], and are, again, involved in tumour formation-related processes that can be affected by

metformin, such as apoptosis [*PURPL* (Ashouri *et al.*, 2016; Li *et al.*, 2017), *LINC00176*: (Dai *et al.,*2019; Niehus *et al.*, 2019)], cell survival and proliferation [*CASC2* (Wang *et al.*, 2015; Li *et al.*, 2019; Sun *et al.*, 2019; Xing *et al.*, 2019), *LINC00176* (Wang *et al.*, 2019)], cell cycle [*LINC00176* (Tran *et al.*, 2018)] and cell migration and invasion [*CASC2* (Wang *et al.*, 2015; Li *et al.*, 2019; Sun *et al.*, 2019; Xing *et al.*, 2019)]. Noteworthy, although these lncRNAs are well-studied, this is the first study attempting to establish a link with neuroblastoma. In addition, it should not be neglected that *LOC100133331*, *LOC100505695 and LOC648987,* which were among the discovered lncRNAs in this group are yet to be characterised and attributed a specific role, whilst *LOC151300 (LINC00608)* has just recently discovered but without mechanistic details about its role. In particular, *LOC151300* is part of a prognostic signature for Head and Neck Squamous Cell Carcinoma (Yang *et al.*, 2019; Ghafouri-Fard *et al.*, 2020).

Secondly, in Chapter 5 we also identified a series of lncRNAs (269) whose expression was perturbed in both conditions, short- and long-term exposure to metformin, suggesting their critical role in mediating metformin-triggered responses, yet their rather neutral role in regulating the cell fate decisions in neuroblastoma cells. Such lncRNAs include the up-regulated *GHRLOS, LOC100130700, CASC2, MIR22HG, LOC100288637, LOC100507557, LOC100507173, LOC100288974, LOC100505695* and *LOC641364* and the down-regulated *LOC100132707, LOC100289092, C17orf76-AS1, LOC285484, LOC100506409, LOC340037, LOC100288637, LOC100506714, LOC256021* and *LOC151300*. Among them, *GHRLOS, CASC2* and *LOC151300* maintained their high expressional deregulation across different experimental conditions further highlighting the central role not only of them per se, but also of the molecular processes they are part of, including cell survival and apoptosis, in neuroblastoma cells. On the contrary, when comparing short- and long-term exposure to metformin *LOC283050, LOC730227, TP73-AS1*, *LOC100652730* and *PCBP1-AS1,*

displayed differential expression, opening the possibility they could be used as biomarkers of neuroblastoma cells' resistance to metformin resulting from prolonged exposure to the drug.

Thirdly, in our approach to identify novel lncRNAs driving cell fate determination, whether this was cell survival, proliferation, apoptosis, migration, differentiation or drug resistance, we also identified molecular pathways with significant perturbations, in the context of which the newly discovered lncRNAs could be incorporated. In line with this, our study confirmed the perturbation of multiple established metformin-related pathways in which these novel lncRNAs could exert a crucial role to determine the final outcome in terms of cell fate, such as the mTOR survival pathway, the p53-related apoptosis pathway, cell cycle arrest pathways and cytokine-cytokine receptor interactions (Kourelis and Siegel, 2012; Emami Riedmaier *et al.*, 2013) and numerous understudied processes and pathways, such as DNA replication (Ma *et al.*, 2014; Kim *et al.*, 2017) that displayed the most pronounced change, and the Hippo pathway (Yuan *et al.*, 2018). In addition, novel cancer-related pathways in the context of metformin action were revealed to be affected, for example, multiple DDR-related processes such as MMR, BER and HR, which were found to be significantly perturbed (Schulten and Bakhashab, 2019). Finally, given the substantial emerging role of miRNAs in cancer (Lekka and Hall, 2018) and the growing body of evidence of lncRNAs acting as miRNA sponges (Wang and Chang, 2011; Tay *et al.*, 2014), we also explored the deregulation of the miRNA repertoire. As anticipated, hundreds of miRNAs were predicted to have perturbed expression and, importantly some of them are known participants of lncRNA/miRNA/mRNA axes, as in the case of *CASC2*/miR-24/MUC6 (Xu *et al.,* 2020), *CASC2*/miR-183/Wnt-β-catenin (Sun *et al.*, 2019), *MIR22HG*/miR-22/ p21-p53 pathway (Vidyasekar *et al.*, 2015) and *MIR22HG*/miR-22/ADSL (adenylosuccinate lyase)-c-Myc (Zurlo *et al.*, 2019). Nonetheless, it should be taken into account that these results comprise only preliminary indications of how

lncRNAs are involved in cell fate decisions in neuroblastoma cells, and further research is required to validate and accredit them.

7.2.1. *LINC00176* and *LOC648987* in neuroblastoma cell fate determination

Among the perturbed lncRNAs described in Chapter 5, which were highly deregulated in neuroblastoma cells exposed to metformin long-term, several were suspected to be potential regulators of cell fate decisions. To this end, Chapter 6 investigated the role of two such lncRNAs, the down-regulated *LINC00176* (9-fold) and *LOC648987* (15-fold), via a series of functional analyses. *LINC00176* is a c-Myc-related lncRNA that has previously been associated with a variety of cancers, either as a biomarker [clear cell renal carcinoma (Wang *et al.*, 2019), HCC (Zhang *et al.*, 2015; Gong *et al.*, 2020), oesophageal cancer (Fan and Liu, 2016) and pancreatic cancer (Liu *et al.*, 2019)] or as an oncogenic regulator of multiple aspects of cell fate in multiple tumours [HCC cells (Zhang *et al.*, 2015; Tran *et al.*, 2018), ovarian cancer cells (Dai *et al.,* 2019) and colorectal cancer (Sun *et al.,* 2019)]. On the other hand, *LOC648987* is an uncharacterised lncRNA, which, however, has been found to display differential methylation patterns in patients with lung adenocarcinoma (Daugaard *et al.*, 2016) and whose isoform *MPRL* has been implicated in cisplatin sensitivity and apoptosis in tongue squamous cell carcinoma (Tian *et al.*, 2019). Taking the known evidence into account, we were prompted to explore the role of these two lncRNAs in cell fate determination of neuroblastoma cells, including cell survival, apoptosis, migration and combination effect with metformin treatment following a GapmeR-mediated gene silencing approach.

The functional analyses confirmed the oncogenic properties of *LINC00176*, as it was demonstrated that silencing *LINC00176* leads to increased levels of basal apoptosis, accompanied by an attenuated migratory ability of neuroblastoma cells as a direct

consequence of increased apoptosis, in full concordance with the study conducted by Dai *et al*. (2019) and in partial agreement with Tran and colleagues (2018), who also showed that *LINC00176* silencing leads to increased necroptosis-mediated cell death. However, the study failed to establish significant changes in short-and long-term survival in neuroblastoma cells in response to *LINC00176* knockdown, as the aforementioned studies did, although there was a tendency for decreased long-term survival.

Finally, whether the down-regulation of *LINC00176* would confer an additive or, on the contrary, an inhibitory effect on the action of metformin, since, on top of a diversity of other roles that have been attributed to lncRNAs as far as the regulation of cell decisions is concerned, lncRNAs have been implicated in the regulation of drug response and resistance in multiple tumours (Deng *et al.*, 2016; Majidinia and Yousefi, 2016; Bester *et al.*, 2018; Corrà *et al.*, 2018; Bermúdez *et al.*, 2019; Smallegan and Rinn, 2019; Zhao *et al.*, 2019). Contrary to our anticipations given the massive down-regulation of the lncRNA in cells with extended exposure to metformin as revealed by the RNA sequencing, *LINC00176* tended not to confer a significant effect on the action of metformin, at least as far as cell survival and apoptosis are concerned, as indicated by the fact that its knockdown led to non-significantly different viability loss and apoptosis comparing to control cells.

Similar to *LINC00176,* knockdown of *LOC648987*, induced only a slight, statistically non-significant reduction of short- and long-term cell survival, however, it led to doubled levels of basal apoptosis in SH-SY5Y cells a significant reduction in cell migration. Even though *LOC648987* is an uncharacterised lncRNA with no functional studies on it so far, the only study performed on its variant *MPRL* (miRNA processing–related lncRNA) has also reported the ability of *MPRL* to interfere with apoptosis in tongue squamous cell carcinoma cells, but in the opposite direction, with its knockdown mediating the attenuation of apoptosis (Tian *et al.*, 2019). However, this would not be

the first case of different isoforms of the same gene causing opposite effects, as this has been the case for *HIF1A* and *HIF2A* (Florczyk *et al.*, 2011), p38 variants (Pramanik *et al.*, 2003) and Wilm's Tumour isoforms (Menke *et al.*, 1996). Following the approach adopted for *LINC00176*, we also assessed the possibility that *LOC648987* could modify the effect of metformin. Nevertheless, contrary to our expectations, the silencing *LOC648987* does not significantly affect the cell viability loss or the levels of apoptosis conferred by metformin in neuroblastoma cells.

Both *LINC00176* and *LOC648987* were chosen on the grounds that they displayed a massive decrease in expression in metformin-treated neuroblastoma cells, a fact that led to the hypothesis they may act as regulators of cell fate decisions. Albeit, they both minimally affected cell survival, but on the contrary, they caused an increase in basal apoptosis and decreased the cells' migratory ability. Notably, the increased levels of apoptosis-mediated cell death were only detected with acridine orange staining, failing to be demonstrated by Annexin V staining, a fact that should be taken into account when interpreting these results, In this regard, it could be speculated that these effects are the outcome of the dual identity of c-Myc (Matsumura, Tanaka and Kanakura, 2003; Pelengaris and Khan, 2003; Hoffman and Liebermann, 2008; McMahon, 2014), which, apart from its traditional role as an oncogene, also promotes apoptosis, depending on the context, and was as well down-regulated. It is possible that short-term after the knockdown of the lncRNAs, c-Myc is either repressed or exerts its pro-apoptotic role and, that on the long-term, it remains repressed to inhibit, even slightly the survival and growth of the cells. This could be relevant especially for *LINC00176*, which is a c-Myc-regulated lncRNA (Tran *et al.*, 2018). In addition, concerning the down-regulation of the lncRNAs as a single intervention and in combination with metformin, one should not neglect the fact that the outcome in terms of cell survival, apoptosis and migration is the merge of numerous, complex and compensatory signalling pathways, and therefore, although the deregulation of certain lncRNAs *per se*

may seem staggering, their effect can be neutralised as a result of complicated cellular and molecular procedures.

Overall, this study suggests that numerous protein-coding and non-coding RNA components are involved in the determination of cell fate in neuroblastoma cells. Having metformin treatment as a platform, we have identified novel- at least in the context of neuroblastoma- lncRNAs, which could be drivers of cell fate decisions and be used as biomarkers of resistance to metformin. These novel lncRNAs could also be integrated into some of the established metformin action-related mechanisms confirmed herein, or in the newly-discovered molecular mechanisms, including DNA replication and DDR pathways. In addition, these lncRNAs could act as parts of lncRNA/miRNA/mRNA axes mediating these decisions. Two such lncRNAs, *LINC00176* and *LOC648987,* were reported to be significantly associated with apoptosis and cell migration to promote neuroblastoma.

7.3. Concluding Remarks and Future Perspectives

The present study comprises an attempt to investigate the role of lncRNAs in two cancers, neuroblastoma and GBM. Despite its multiple and novel findings, this study is far from being exhaustive. Further research concerning *MIAT* is essential and should entail studies investigating which parts of *MIAT*'s sequence are responsible for the observed effects and whether the 3'UTR has got a special role, as well as studies elucidating key molecules that mediate its action, such as co-lncRNAs or proteins interacting with it, potentially transcribed from chromosome 22. It would also be interesting to assess which-if any- of the suggested mechanisms can be established as modes of action of *MIAT*. Additionally, future work could involve the validation of the effects on other pathways, in addition to apoptosis. For instance, the MAPK/PI3K/Akt pathway is a druggable target, and, therefore, modulating the levels of *MIAT* using gene silencing techniques or mimics (Gutschner and Diederichs, 2012; Salehi *et al.*, 2017) could be a novel way to target the pathway. Similarly, whether *LINC00176* and

LOC648987 affect other aspects of cell fate, such as cell proliferation or differentiation, should also be investigated. The latter could be very useful, as differentiation therapy comprises a promising therapeutic approach for neuroblastoma (Nakagawara *et al.*, 2018).

A plethora of lncRNAs have been thoroughly studied, such as *GAS5, TERRA*, *HOTAIR, ANRIL* and *MALAT1*, and are being tested as potential tumour biomarkers (Gutschner and Diederichs, 2012), highlighting their importance in tumour diagnosis, prediction and prognosis. In line with this, there is accumulating evidence of lncRNAs implicated in neuroblastoma (Pandey and Kanduri, 2015) and GBM (Pop *et al.*, 2018), including *MIAT*. Since almost all of the hallmarks of cancer can be seen through a lncRNA glass [as reviewed by Gutschner and Diederichs (2012) and Kunej *et al.* (2014)], therapeutic approaches for cancer are now including lncRNA-based treatment as a potential solution. Nevertheless, there is still a growing demand for new biomarkers and therapeutic targets for NB and GBM. However, to exploit *MIAT* and other novel lncRNAs therapeutically in these cancers, it is of paramount significance to first unveil the underlying mechanisms of their action in order to ultimately aid neuroblastoma and GBM patients.

References

Adan, A. et al. (2017) 'Flow cytometry: basic principles and applications', Critical Reviews in Biotechnology. doi: 10.3109/07388551.2015.1128876.

Aggarwal, V., Tuli, H. S., Varol, A., Thakral, F., Yerer, M. B., Sak, K., Varol, M., Jain, A., Khan, M. A. and Sethi, G. (2019) 'Role of reactive oxygen species in cancer progression: Molecular mechanisms and recent advancements', Biomolecules. doi: 10.3390/biom9110735.

Ahmed, A. A. et al. (2017) 'Neuroblastoma in children: Update on clinicopathologic and genetic prognostic factors', Pediatric Hematology and Oncology. doi: 10.1080/08880018.2017.1330375.

Alipoor, F. J., Asadi, M. H. and Torkzadeh-Mahani, M. (2018) 'Miat lncRNA is overexpressed in breast cancer and its inhibition triggers senescence and G1 arrest in MCF7 cell line', Journal of Cellular Biochemistry. Wiley Online Library. doi: 10.1002/jcb.26678.

Almnaseer, Z. A. and Mourtada-Maarabouni, M. (2016) 'NEAT1, a long non-coding RNA, controls cell survival and is up-regulated in breast cancer', European Journal of Cancer. doi: 10.1016/s0959-8049(16)61263-7.

Almnaseer, Z. A. and Mourtada-Maarabouni, M. (2018) 'Long non-coding RNA MIAT regulates apoptosis and the apoptotic response to chemotherapeutic agents in breast cancer cell lines', Bioscience Reports. Available at: http://www.bioscirep.org/content/early/2018/06/18/BSR20180704.abstract.

Amaral, P. P. and Mattick, J. S. (2008) 'Noncoding RNA in development', Mammalian Genome, pp. 454–492. doi: 10.1007/s00335-008-9136-7.

Anand, M., Van Meter, T. E. and Fillmore, H. L. (2011) 'Epidermal growth factor induces matrix metalloproteinase-1 (MMP-1) expression and invasion in glioma cell lines via the MAPK pathway', Journal of Neuro-Oncology. doi: 10.1007/s11060-011-0549-x.

André-Grégoire, G. and Gavard, J. (2017) 'Spitting out the demons: Extracellular vesicles in glioblastoma', Cell Adhesion and Migration. doi: 10.1080/19336918.2016.1247145.

Applebaum, M. A., Vaksman, Z., Lee, S. M., Hungate, E. A., Henderson, T. O., London, W. B., Pinto, N., Volchenboum, S. L., Park, J. R., Naranjo, A., Hero, B., Pearson, A. D., Stranger, B. E., Cohn, S. L. and Diskin, S. J. (2017) 'Neuroblastoma survivors are at increased risk for second malignancies: A report from the International Neuroblastoma Risk Group Project', European Journal of Cancer. doi:

10.1016/j.ejca.2016.11.022.

Arora, G. and Bandopadhyaya, G. (2018) ‘Paradigm shift in theranostics of neuroendocrine tumors: conceptual horizons of nanotechnology in nuclear medicine’, Annals of Nuclear Medicine. doi: 10.1007/s12149-018-1235-2.

Arrieta, V. A. Cacho-Díaz, B., Zhao, J., Rabadan, R., Chen, L. and Sonabend, Adam M. (2018) ‘The possibility of cancer immune editing in gliomas. A critical review’, OncoImmunology. doi: 10.1080/2162402X.2018.1445458.

Ashouri, A., Sayin, V. I., Van den Eynden, J., Singh, S. X., Papagiannakopoulos, T. and Larsson, E. (2016) ‘Pan-cancer transcriptomic analysis associates long non-coding RNAs with key mutational driver events’, Nature communications. doi: 10.1038/ncomms13197.

Aveic, S. Corallo, D., Porcù, E., Pantile, M., Boso, D., Zanon, C., Viola, G., Sidarovich, V., Mariotto, E., Quattrone, A., Basso, G. and Tonini, Gian Paolo (2018) ‘TP-0903 inhibits neuroblastoma cell growth and enhances the sensitivity to conventional chemotherapy’, European Journal of Pharmacology. doi: 10.1016/j.ejphar.2017.11.016.

Azam, Z., Quillien, V., Wang, G. and To, S. S. T. (2019) ‘The potential diagnostic and prognostic role of extracellular vesicles in glioma: current status and future perspectives’, Acta Oncologica. doi: 10.1080/0284186X.2018.1551621.

Azzalin, C. M., Reichenbach, P., Khoriauli, L., Giulotto, E. and Lingner, J. (2007) ‘Telomeric repeat containing RNA and RNA surveillance factors at mammalian chromosome ends.’, Science (New York, N.Y.), 318(5851), pp. 798–801. doi: 10.1126/science.1147182.

Babu, K. R. and Tay, Y. (2019) ‘The Yin-Yang regulation of reactive oxygen species and microRNAs in cancer’, International Journal of Molecular Sciences. doi: 10.3390/ijms20215335.

Banerjee, P., Dutta, S. and Pal, R. (2016) ‘Dysregulation of Wnt-Signaling and a Candidate Set of miRNAs Underlie the Effect of Metformin on Neural Crest Cell Development’, Stem Cells. doi: 10.1002/stem.2245.

Banfai, B., Jia, H., Khatun, J., Wood, E., Risk, B., Gundling, W. E., Kundaje, A., Gunawardena, H. P., Yu, Y., Xie, L., Krajewski, K., Strahl, B. D., Chen, X., Bickel, P., Giddings, M. C., Brown, J. B. and Lipovich, L. (2012) ‘Long noncoding RNAs are rarely translated in two human cell lines’, Genome Research, 22(9), pp. 1646–1657. doi: 10.1101/gr.134767.111.

Barnhill, L. M., Williams, R. T., Cohen, O., Kim, Y., Batova, A., Mielke, J. A., Messer, K., Pu, M., Bao, L., Yu, A. L. and Diccianni, M. B. (2014) 'High expression of CAI2, a9p21-embedded long noncoding RNA, contributes to advanced-stage neuroblastoma', Cancer Research. doi: 10.1158/0008-5472.CAN-13-3447.

Barry, G., Briggs, J. A., Vanichkina, D. P., Poth, E. M., Beveridge, N. J., Ratnu, V. S. Batagov, A. O., Yarmishyn, A., Jenjaroenpun, P., Tan, J. Z., Nishida, Y. and Kurochkin, I. V. (2013) 'Role of genomic architecture in the expression dynamics of long noncoding RNAs during differentiation of human neuroblastoma cells.' BMC systems biology, 7(Suppl 3), p. S11. doi: 10.1186/1752-0509-7-S3-S11.

Belcaid, Z., Phallen, J. A., Zeng J., See, A. P., Mathios, D., Gottschalk, C., Nicholas, S., Kellett, M., Ruzevick, J., Jackson, C., Albesiano, E., Durham, N. M., Ye, X., Tran, P. T., Tyler, B., Wong, J. W., Brem, H., Pardoll, D. M., Drake, C. G. and Lim, M. (2014) 'Focal radiation therapy combined with 4-1BB activation and CTLA-4 blockade yields long-term survival and a protective antigen-specific memory response in a murine glioma model', PLoS ONE. doi: 10.1371/journal.pone.0101764.

Benassi, B., Fanciulli, M., Fiorentino, F., Porrello, A., Chiorino, G., Loda, M., Zupi, G. and Biroccio, A. (2006) 'c-Myc phosphorylation is required for cellular response to oxidative stress', Molecular Cell. doi: 10.1016/j.molcel.2006.01.009

Benetatos, L., Voulgaris, E. and Vartholomatos, G. (2017) 'The crosstalk between long non-coding RNAs and PI3K in cancer', Medical Oncology. doi: 10.1007/s12032-017-0897-2.

Bergmann, J. H. and Spector, D. L. (2014) 'Long non-coding RNAs: Modulators of nuclear structure and function', Current Opinion in Cell Biology. doi: 10.1016/j.ceb.2013.08.005.

Bermúdez, M., Aguilar-Medina, M., Lizárraga-Verdugo, E., Avendaño-Félix, M., Silva-Benítez, E., López-Camarillo, C. and Ramos-Payán, R. (2019) 'LncRNAs as Regulators of Autophagy and Drug Resistance in Colorectal Cancer', Frontiers in Oncology. doi: 10.3389/fonc.2019.01008.

Bernstein, B. E., Birney, E., Dunham, I., Green, E. D., Gunter, C. and Snyder, M. (2012) 'An integrated encyclopedia of DNA elements in the human genome', Nature, 489(7414), pp. 57–74. doi: 10.1038/nature11247.

Bernstein, E. and Allis, C. D. (2005) 'RNA meets chromatin', Genes and Development, pp. 1635–1655. doi: 10.1101/gad.1324305.

Bester, A. C., Lee, J. D., Chavez, A., Lee, Y. R., Nachmani, D., Vora, S., Victor, J., Sauvageau, M., Monteleone, E., Rinn, J. L., Provero, P., Church, G. M., Clohessy, J. G. and Pandolfi, P. P. (2018) 'An Integrated Genome-wide CRISPRa Approach to Functionalize lncRNAs in Drug Resistance', Cell. doi: 10.1016/j.cell.2018.03.052.

Bevilacqua, V., Gioia, U., Di Carlo, V., Tortorelli, A. F., Colombo, T., Bozzoni, I., Laneve, P. and Caffarelli, E. (2015) 'Identification of linc-NeD125, a novel long non coding RNA that hosts miR-125b-1 and negatively controls proliferation of human neuroblastoma cells.', RNA biology, 12(12), pp. 1323–1337. doi: 10.1080/15476286.2015.1096488.

Bi, S., Wang, C., Li, Y., Zhang, W., Zhang, J., Lv, Z. and Wang, J. (2017) 'LncRNA-MALAT1-mediated Axl promotes cell invasion and migration in human neuroblastoma', Tumor Biology. doi: 10.1177/1010428317699796.

Binlateh, T., Tanasawet, S., Rattanaporn, O., Sukketsiri, W., and Hutamekalin, P. (2019). 'Metformin Promotes Neuronal Differentiation via Crosstalk between Cdk5 and Sox6 in Neuroblastoma Cells', Evidence-Based Complementary and Alternative Medicine. https://doi.org/10.1155/2019/1765182

Biroccio, A. (2006) 'c-Myc phosphorylation is required for cellular response to oxidative stress', Molecular Cell. doi: 10.1016/j.molcel.2006.01.009.

Biroccio, A., Benassi, B., Fiorentino, F., and Zupi, G. (2004). 'Glutathione depletion induced by c-Myc downregulation triggers apoptosis on treatment with alkylating agents', Neoplasia. https://doi.org/10.1593/neo.3370

Blackshaw, S., Harpavat, S., Trimarchi, J., Cai, L., Huang, H., Kuo, W. P., Weber, G., Lee, K., Fraioli, R. E., Cho, S. H., Yung, R., Asch, E., Ohno-Machado, L., Wong, W. H. and Cepko, C. L. (2004). 'Genomic analysis of mouse retinal development', PLoS Biology, 2(9). https://doi.org/10.1371/journal.pbio.0020247

Bono, H., Kasukawa, T., Furuno, M., Hayashizaki, Y., and Okazaki, Y. (2003). 'FANTOM-DB: database of functional annotation of RIKEN mouse cDNA clones', Seikagaku, The Journal of Japanese Biochemical Society. https://doi.org/10.1093/nar/30.1.116

Boon, R. A., Ja, N., Holdt, L., and Dimmeler, S. (2016). 'Long Noncoding RNAs from Clinical Genetics to Therapeutic Targets', Journal of the American College of Cardiology, 67(10), 1214–1226. https://doi.org/10.1016/j.jacc.2015.12.051

Borriello, L., Seeger, R. C., Asgharzadeh, S., and DeClerck, Y. A. (2016). 'More than the genes, the tumor microenvironment in neuroblastoma', Cancer Letters. https://doi.org/10.1016/j.canlet.2015.11.017

Bountali, A., Tonge, D. P., and Mourtada-Maarabouni, M. (2019). 'RNA sequencing reveals a key role for the long non-coding RNA MIAT in regulating neuroblastoma and glioblastoma cell fate', International Journal of Biological Macromolecules, 130, 878–891. https://doi.org/https://doi.org/10.1016/j.ijbiomac.2019.03.005

Boussiotis, V. A., and Charest, A. (2018). 'Immunotherapies for malignant glioma', Oncogene. https://doi.org/10.1038/s41388-017-0024-z

Bracken, A. P. and Helin, K. (2009). 'Polycomb group proteins: navigators of lineage pathways led astray in cancer', Nature Reviews. Cancer, 9(11), 773–784. https://doi.org/10.1038/nrc2736

Bravou, V., Antonacopoulou, A., Papanikolaou, S., Nikou, S., Lilis, I., Giannopoulou, E., and Kalofonos, H. P. (2015). 'Focal Adhesion Proteins α- And β-Parvin are Overexpressed in Human Colorectal Cancer and Correlate with Tumor Progression', Cancer Investigation. https://doi.org/10.3109/07357907.2015.1047508

Brown, C. E., Alizadeh, D., Starr, R., Weng, L., Wagner, J. R., Naranjo, A., Ostberg, J. R., Blanchard, M. S., Kilpatrick, J., Simpson, J., Kurien, A., Priceman, S. J., Wang, X., Harshbarger, T. L., D'Apuzzo, M., Ressler, J. A., Jensen, M. C., Barish, M. E., Chen, M., Portnow, J., Forman, S. J. and Badie, B. (2016). 'Regression of glioblastoma after chimeric antigen receptor T-cell therapy', New England Journal of Medicine. https://doi.org/10.1056/NEJMoa1610497

Bundscherer, A., Malsy, M., Lange, R., Hofmann, P., Metterlein, T., Graf, B. M., and Gruber, M. (2013). 'Cell harvesting method influences results of apoptosis analysis by annexin v staining'. Anticancer Research.

Byvaltsev, V. A. et al. (2019) 'Acridine orange: A review of novel applications for surgical cancer imaging and therapy', Frontiers in Oncology. doi: 10.3389/fonc.2019.00925.

Cabili, M., Trapnell, C., Goff, L., Koziol, M., Tazon-Vega, B., Regev, A., and Rinn, J. L. (2011). 'Integrative annotation of human large intergenic noncoding RNAs reveals global properties and specific subclasses', Genes and Development, 25(18), 1915–1927. https://doi.org/10.1101/gad.17446611

Campbell, K. J., and Tait, S. W. G. (2018). 'Targeting BCL-2 regulated apoptosis in cancer', Open Biology. https://doi.org/10.1098/rsob.180002

Campisi, L., Cummings, R. J., and Blander, J. M. (2014). 'Death-defining immune responses after apoptosis', American Journal of Transplantation. https://doi.org/10.1111/ajt.12736

Cao, J. (2014). 'The functional role of long non-coding RNAs and epigenetics', Biological Procedures Online, 16, 11. https://doi.org/10.1186/1480-9222-16-11

Capdevila, C., Rodríguez Vázquez, L., and Martí, J. (2017). 'Glioblastoma Multiforme and Adult Neurogenesis in the Ventricular-Subventricular Zone: A Review', Journal of Cellular Physiology. https://doi.org/10.1002/jcp.25502

Capizzi, M., Strappazzon, F., Cianfanelli, V., Papaleo, E., and Cecconi, F. (2017). 'MIR7–3HG, a MYC-dependent modulator of cell proliferation, inhibits autophagy by a regulatory loop involving AMBRA1', Autophagy. https://doi.org/10.1080/15548627.2016.1269989

Carrieri, C., Cimatti, L., Biagioli, M., Beugnet, A., Zucchelli, S., Fedele, S., Pesce, E., Ferrer, I., Collavin, L., Santoro, C., Forrest, A. R. R., Carninci, P., Biffo, S.S. and Elia Gustincich, S. (2012). 'Long non-coding antisense RNA controls Uchl1 translation through an embedded SINEB2 repeat', Nature, 491(7424), 454–457. https://doi.org/10.1038/nature11508

Chandra Gupta, S., and Nandan Tripathi, Y. (2017).' Potential of long non-coding RNAs in cancer patients: From biomarkers to therapeutic targets', International Journal of Cancer. https://doi.org/10.1002/ijc.30546

Chen, G., Cao, Y., Zhang, L., Ma, H., Shen, C., and Zhao, J. (2017). 'Analysis of long non-coding RNA expression profiles identifies novel lncRNA biomarkers in the tumorigenesis and malignant progression of gliomas', Oncotarget. https://doi.org/10.18632/oncotarget.18832

Chen, L. L., and Carmichael, G. G. (2010). 'Decoding the function of nuclear long non-coding RNAs', Current Opinion in Cell Biology. https://doi.org/10.1016/j.ceb.2010.03.003

Chen, M., Chen, J., and Zhang, D. (2015). 'Exploring the secrets of long noncoding RNAs', International Journal of Molecular Sciences. https://doi.org/10.3390/ijms16035467

Chen, W., Wang, D., Du, X., He, Y., Chen, S., Shao, Q., He, Y., Ma, C., Huang, B., Chen, A., Zhao, P., Qu, X. and Li, X. (2015). 'Glioma cells escaped from cytotoxicity of temozolomide and vincristine by communicating with human astrocytes. Medical Oncology. https://doi.org/10.1007/s12032-015-0487-0

Chen, Y. H., Zeng, W. J., Wen, Z. P., Cheng, Q., and Chen, X. P. (2018). 'Underexplored epigenetic modulators: role in glioma chemotherapy', European Journal of Pharmacology. https://doi.org/10.1016/j.ejphar.2018.05.047

Chen, Z., and Hambardzumyan, D. (2018). 'Immune microenvironment in glioblastoma subtypes'. Frontiers in Immunology. https://doi.org/10.3389/fimmu.2018.01004

Cheng, L., Ming, H., Zhu, M., and Wen, B. (2016). 'Long noncoding RNAs as Organizers of Nuclear Architecture', Science China Life Sciences. https://doi.org/10.1007/s11427-016-5012-y

Chi, R., Chen, X., Liu, M., Zhang, H., Li, F., Fan, X., Wang, W. and Lu, H. (2019). 'Role of SNHG7-miR-653-5p-STAT2 feedback loop in regulating neuroblastoma progression'. Journal of Cellular Physiology. https://doi.org/10.1002/jcp.28017

Chi, Wang, Wang, Yu, and Yang. (2019). 'Long Non-Coding RNA in the Pathogenesis of Cancers', Cells. https://doi.org/10.3390/cells8091015

Chu, F., Xue, L., and Miao, H. (2019). 'Long noncoding RNA TP73-AS1 in human cancers.' Clinica Chimica Acta. https://doi.org/https://doi.org/10.1016/j.cca.2019.09.024

Chu, L., Yu, L., Liu, J., Song, S., Yang, H., Han, F., Liu, F. and Hu, Y. (2019). 'Long intergenic non-coding LINC00657 regulates tumorigenesis of glioblastoma by acting as a molecular sponge of miR-190a-3p', Aging. https://doi.org/10.18632/aging.101845

Clark, B. S., and Blackshaw, S. (2014). 'Long non-coding RNA-dependent transcriptional regulation in neuronal development and disease', Frontiers in Genetics. https://doi.org/10.3389/fgene.2014.00164

Collet, S., Valable, S., Constans, J. M., Lechapt-Zalcman, E., Roussel, S., Delcroix, N., Abbas, A., Ibazizene, M., Bernaudin, M., Barré, L., Derlon, J. M. and Guillamo, J. S. (2015). [18F]-fluoro-l-thymidine PET and advanced MRI for preoperative grading of gliomas. NeuroImage: Clinical. https://doi.org/10.1016/j.nicl.2015.05.012

Corbett, A. H. (2018). 'Post-transcriptional regulation of gene expression and human disease', Current Opinion in Cell Biology. https://doi.org/10.1016/j.ceb.2018.02.011

Corrà, F., Agnoletto, C., Minotti, L., Baldassari, F., and Volinia, S. (2018). 'The network of non-coding RNAs in cancer drug resistance', Frontiers in Oncology. https://doi.org/10.3389/fonc.2018.00327

Costa, D., Gigoni, A., Würth, R., Cancedda, R., Florio, T., and Pagano, A. (2014). 'Metformin inhibition of neuroblastoma cell proliferation is differently modulated by cell differentiation induced by retinoic acid or overexpression of NDM29 non-coding RNA', Cancer Cell International, 14, 59. https://doi.org/10.1186/1475-2867-14-59

Costa, F. F. (2005). 'Non-coding RNAs: New players in eukaryotic biology', Gene. https://doi.org/10.1016/j.gene.2005.06.019

Crea, F., Venalainen, E., Ci, X., Cheng, H., Pikor, L., Parolia, A., Xue, H., Nur Saidy, N. R., Lin, D., Lam, W., Collins, C. and Wang, Y (2016) 'The role of epigenetics and long noncoding RNA MIAT in neuroendocrine prostate cancer', Epigenomics. doi: 10.2217/epi.16.6.

Cremer, T., and Cremer, M. (2010). 'Chromosome territories', Cold Spring Harbor Perspectives in Biology. https://doi.org/10.1101/cshperspect.a003889

da Cunha, M. L. V., and Maldaun, M. V. C. (2019). 'Metastasis from glioblastoma multiforme: A meta-analysis', Revista Da Associacao Medica Brasileira. https://doi.org/10.1590/1806-9282.65.3.424

da Fonseca, R. R., Kosiol, C., Vinař, T., Siepel, A., and Nielsen, R. (2010). 'Positive selection on apoptosis related genes', FEBS Letters. https://doi.org/10.1016/j.febslet.2009.12.022

Dai, H., Ehrentraut, S., Nagel, S., Eberth, S., Pommerenke, C., Dirks, W. G., Geffers, R., Kalavalapalli, S., Kaufmann, M., Meyer, C., Faehnrich, S., Chen, S., Drexler, H. G. and MacLeod, R. A. F. (2015). 'Genomic landscape of primary mediastinal B-cell lymphoma cell lines', PLoS ONE. https://doi.org/10.1371/journal.pone.0139663

Dai, L., Niu, J., and Feng, Y. (2019). 'Knockdown of long non-coding RNA LINC00176 suppresses ovarian cancer progression by BCL3-mediated down-regulation of ceruloplasmin', Journal of Cellular and Molecular Medicine. https://doi.org/10.1111/jcmm.14701

Daugaard, I., Dominguez, D., Kjeldsen, T. E., Kristensen, L. S., Hager, H., Wojdacz, T. K., and Hansen, L. L. (2016). 'Identification and validation of candidate epigenetic

biomarkers in lung adenocarcinoma', Scientific Reports. https://doi.org/10.1038/srep35807

Daugan, M., Dufaÿ Wojcicki, A., d'Hayer, B., and Boudy, V. (2016). 'Metformin: An anti-diabetic drug to fight cancer', Pharmacological Research. https://doi.org/10.1016/j.phrs.2016.10.006

Davies, K. (1999). 'The Broad Spectrum of Responses to Oxidants in Proliferating Cells: A New Paradigm for Oxidative Stress', IUBMB Life, 48(1), 41–47. https://doi.org/10.1080/713803463

De Antonellis, P., Carotenuto, M., Vandenbussche, J., De Vita, G., Ferrucci, V., Medaglia, C., Boffa, I., Galiero, A., Di Somma, S., Magliulo, D., Aiese, N., Alonzi, A., Spano, D., Liguori, L., Chiarolla, C., Verrico, A., Schulte, J. H., Mestdagh, P., Vandesompele, J. and
De Paepe, B., Lefever, S., and Mestdagh, P. (2018). 'How long noncoding RNAs enforce their will on mitochondrial activity: regulation of mitochondrial respiration, reactive oxygen species production, apoptosis, and metabolic reprogramming in cancer', Current Genetics. https://doi.org/10.1007/s00294-017-0744-1

De Santi, M., Baldelli, G., Diotallevi, A., Galluzzi, L., Schiavano, G. F., and Brandi, G. (2019). 'Metformin prevents cell tumorigenesis through autophagy-related cell death', Scientific Reports. https://doi.org/10.1038/s41598-018-37247-6

Dedoni, S., Olianas, M. C., and Onali, P. (2010). 'Interferon β induces apoptosis in human SH-SY5Y neuroblastoma cells through activation of JAK-STAT signaling and down-regulation of PI3K/Akt pathway', Journal of Neurochemistry, 115(6), 1421–1433. https://doi.org/10.1111/j.1471-4159.2010.07046.x

Deng, H., Zhang, J., Shi, J. J., Guo, Z. D., He, C. R., Ding, L., Tang, J. H. and Hou, Y. (2016). 'Role of long non-coding RNA in tumor drug resistance', Tumor Biology. https://doi.org/10.1007/s13277-016-5125-8

Deshmukh, R., and Trivedi, V. (2013). 'Methemoglobin exposure produces toxicological effects in macrophages due to multiple ROS spike induced apoptosis', Toxicology in Vitro. https://doi.org/10.1016/j.tiv.2012.09.016

Dhamija, S., and Diederichs, S. (2016). 'From junk to master regulators of invasion: LncRNA functions in migration, EMT and metastasis', International Journal of Cancer. https://doi.org/10.1002/ijc.30039

Diederichs, S., Bartsch, L., Berkmann, J. C., Fröse, K., Heitmann, J., Hoppe, C., Iggena, D., Jazmati, D., Karschnia, P., Linsenmeier, M., Maulhardt, T., Möhrmann, L., Morstein, J., Paffenholz, S. V., Röpenack, P., Rückert, T., Sandig, L., Schell, M., Steinmann, A., Voss, G., Wasmuth, J., Weinberger, M. E. and Wullenkord, R. (2016). 'The dark matter of the cancer genome : aberrations in regulatory elements, untranslated regions, splice sites, non-coding RNA and synonymous mutations', EMBO Molecular Medicine, 8(5), 1–16. https://doi.org/10.15252/emmm.201506055

Ding, K., Liao, Y., Gong, D., Zhao, X., and Ji, W. (2018). 'Effect of long non-coding RNA H19 on oxidative stress and chemotherapy resistance of CD133+ cancer stem cells via the MAPK/ERK signaling pathway in hepatocellular carcinoma', Biochemical and Biophysical Research Communications. https://doi.org/10.1016/j.bbrc.2018.05.143

Ding, L., Ni, J., Yang, F., Huang, L., Deng, H., Wu, Y., Ding, X. and Tang, J. (2017). 'Promising therapeutic role of miR-27b in tumor', Tumor Biology. https://doi.org/10.1177/1010428317691657

Dinger, M., Amaral, P., and Mercer, T. (2008). 'Long noncoding RNAs in mouse embryonic stem cell pluripotency and differentiation', Genome Research, 1433–1445. https://doi.org/10.1101/gr.078378.108.7

Domingo-Fernandez, R., Watters, K., Piskareva, O., Stallings, R. L., and Bray, I. (2013). 'The role of genetic and epigenetic alterations in neuroblastoma disease pathogenesis', Pediatric Surgery International. https://doi.org/10.1007/s00383-012-3239-7

Dong, Q., Cai, N., Tao, T., Zhang, R., Yan, W., Li, R., Zhang, J., Luo, H. S., Yan
Eleveld, T. F., Schild, L., Koster, J., Zwijnenburg, D. A., Alles, L. K., Ebus, M. E., Volckmann, R., Tijtgat, G. A., van Sluis, P., Versteeg, R. and Molenaar, J. J. (2018). 'RaS–MAPK pathway-driven tumor progression is associated with loss of CIC and other genomic aberrations in neuroblastoma', Cancer Research. https://doi.org/10.1158/0008-5472.CAN-18-1045
Emami Riedmaier, A., Fisel, P., Nies, A. T., Schaeffeler, E., and Schwab, M. (2013). 'Metformin and cancer: From the old medicine cabinet to pharmacological pitfalls and prospects', Trends in Pharmacological Sciences. https://doi.org/10.1016/j.tips.2012.11.005

ENCODE Project Consortium, T. E. P. (2004).' The ENCODE (ENCyclopedia Of DNA Elements) Project', Science, 306(5696), 636–640. https://doi.org/10.1126/science.1105136

Engreitz, J. M., Haines, J. E., Perez, E. M., Munson, G., Chen, J., Kane, M., McDonel, P. E., Guttman, M. and Lander, E. S. (2016). 'Local regulation of gene expression by lncRNA promoters, transcription and splicing', Nature. https://doi.org/10.1038/nature20149

Esquenazi, Y., Lo, V. P., and Lee, K. (2017). 'Critical Care Management of Cerebral Edema in Brain Tumors', Journal of Intensive Care Medicine. https://doi.org/10.1177/0885066615619618

Fadul, C. E., Fisher, J. L., Gui, J., Hampton, T. H., Côté, A. L., and Ernstoff, M. S. (2011). 'Immune modulation effects of concomitant temozolomide and radiation therapy on peripheral blood mononuclear cells in patients with glioblastoma multiforme', Neuro-Oncology. https://doi.org/10.1093/neuonc/noq204

Fakhr-Eldeen, A., Toraih, E. A., and Fawzy, M. S. (2019). 'Long non-coding RNAs MALAT1, MIAT and ANRIL gene expression profiles in beta-thalassemia patients: a cross-sectional analysis', Hematology (Amsterdam, Netherlands). https://doi.org/10.1080/16078454.2019.1570616

Fan, J. C., Zeng, F., Le, Y. G., and Xin, L. (2018). 'LncRNA CASC2 inhibited the viability and induced the apoptosis of hepatocellular carcinoma cells through regulating miR-24-3p', Journal of Cellular Biochemistry. https://doi.org/10.1002/jcb.26479

Fan, Q., and Liu, B. (2016). 'Identification of a RNA-Seq based 8-long non-coding RNA signature predicting survival in esophageal cancer', Medical Science Monitor. https://doi.org/10.12659/MSM.902615

Fang, Y., and Fullwood, M. J. (2016). 'Roles, Functions, and Mechanisms of Long Non-coding RNAs in Cancer', Genomics, Proteomics and Bioinformatics. https://doi.org/10.1016/j.gpb.2015.09.006

Fang, Z., Xu, C., Li, Y., Cai, X., Ren, S., Liu, H., Wang, Y., Wang, F., Chen, R., Qu, M., Wang, Y., Zhu, Y., Zhang, W., Shi, X., Yao, J., Gao, X., Hou, J., Xu, C. and Sun, Y. (2016). 'A feed-forward regulatory loop between androgen receptor and PlncRNA-1 promotes prostate cancer progression', Cancer Letters. https://doi.org/10.1016/j.canlet.2016.01.033

Faramarzi, S., Dianatpour, A., Geranpayeh, L., Mirfakhraie, R., Shams, R., Seifi-Alan, M., Oskooei, V. K. and Ghafouri-Fard, S. (2018). 'Expression analysis of CBR3-AS1 and androgen receptor genes in breast cancer', Meta Gene. https://doi.org/10.1016/j.mgene.2018.05.004

Feng, H., Gu, Z. Y., Li, Q., Liu, Q. H., Yang, X. Y., and Zhang, J. J. (2019). 'Identification of significant genes with poor prognosis in ovarian cancer via bioinformatical analysis', Journal of Ovarian Research. https://doi.org/10.1186/s13048-019-0508-2

Fenoglio, C., Ridolfi, E., Galimberti, D., and Scarpini, E. (2013). 'An emerging role for long non-coding RNA dysregulation in neurological disorders', International Journal of Molecular Sciences. https://doi.org/10.3390/ijms141020427

Ferrer, V. P., Moura Neto, V., and Mentlein, R. (2018). 'Glioma infiltration and extracellular matrix: key players and modulators', GLIA. https://doi.org/10.1002/glia.23309

Firme, M. R., and Marra, M. A. (2014). 'The molecular landscape of pediatric brain tumors in the next-generation sequencing era', Current Neurology and Neuroscience Reports. https://doi.org/10.1007/s11910-014-0474-4

Florczyk, U., Czauderna, S., Stachurska, A., Tertil, M., Nowak, W., Kozakowska, M., Poellinger, L., Jozkowicz, A., Loboda, A. and Dulak, J. (2011). 'Opposite effects of HIF-1α and HIF-2α on the regulation of IL-8 expression in endothelial cells', Free Radical Biology and Medicine. https://doi.org/10.1016/j.freeradbiomed.2011.08.023

Florean, C., Song, S., Dicato, M., and Diederich, M. (2019). 'Redox biology of regulated cell death in cancer: A focus on necroptosis and ferroptosis', Free Radical Biology and Medicine. https://doi.org/10.1016/j.freeradbiomed.2019.01.008

Fontebasso, A. M., Liu, X. Y., Sturm, D., and Jabado, N. (2013). 'Chromatin remodeling defects in pediatric and young adult glioblastoma: A tale of a variant histone 3 tail', Brain Pathology (Vol. 23, pp. 210–216). https://doi.org/10.1111/bpa.12023

Franken, N. A. P., Rodermond, H. M., Stap, J., Haveman, J., and van Bree, C. (2006). 'Clonogenic assay of cells in vitro', Nature Protocols. https://doi.org/10.1038/nprot.2006.339

Friedman, R. C., Farh, K. K. H., Burge, C. B., and Bartel, D. P. (2009). 'Most mammalian mRNAs are conserved targets of microRNAs', Genome Research. https://doi.org/10.1101/gr.082701.108

Fry, E. A., and Inoue, K. (2019). 'c-MYB and DMTF1 in Cancer', Cancer Investigation. https://doi.org/10.1080/07357907.2018.1550090

Fu, X., Wang, Y., Wu, G., Zhang, W., Xu, S., and Wang, W. (2019). 'Long noncoding RNA PURPL promotes cell proliferation in liver cancer by regulating p53', Molecular Medicine Reports. https://doi.org/10.3892/mmr.2019.10159

Fu, Y., Li, C., Luo, Y., Li, L., Liu, J., and Gui, R. (2018). 'Silencing of long non-coding RNA MIAT sensitizes lung cancer cells to gefitinib by epigenetically regulating miR-34a', Frontiers in Pharmacology. https://doi.org/10.3389/fphar.2018.00082

Fulda, S. (2009). 'Tumor resistance to apoptosis', International Journal of Cancer. https://doi.org/10.1002/ijc.24064

Furlan, G., Gutierrez Hernandez, N., Huret, C., Galupa, R., van Bemmel, J. G., Romito, A., Heard, E., Morey, C. and Rougeulle, C. (2018). 'The Ftx Noncoding Locus Controls X Chromosome Inactivation Independently of Its RNA Products', Molecular Cell. https://doi.org/10.1016/j.molcel.2018.03.024

Galadari, S., Rahman, A., Pallichankandy, S., and Thayyullathil, F. (2017).' Reactive oxygen species and cancer paradox: To promote or to suppress?', Free Radical Biology and Medicine. https://doi.org/10.1016/j.freeradbiomed.2017.01.004

Galardi, S., Savino, M., Scagnoli, F., Pellegatta, S., Pisati, F., Zambelli, F., Illi, B., Annibali, D., Beji, S., Orecchini, E., Alberelli, M. A., Apicella, C., Fontanella, R. A., Michienzi, A., Finocchiaro, G., Farace, M. G., Pavesi, G., Ciafrè, S. and Anna Nasi, S. (2016). 'Resetting cancer stem cell regulatory nodes upon MYC inhibition', EMBO Reports. https://doi.org/10.15252/embr.201541489

Gao, K., Li, G., Qu, Y., Wang, M., Cui, B., Ji, M., Shi, B. and Hou, P. (2016). 'TERT promoter mutations and long telomere length predict poor survival and radiotherapy resistance in gliomas', Oncotarget. https://doi.org/10.18632/oncotarget.6007

Gao, L., Lin, P., Chen, P., Gao, R. Z., Yang, H., He, Y., Chen, J. B., Luo, Y. G., Xu, Q. Q., Liang, S. W., Gu, J. H., Huang, Z. G., Dang, Y. W. and Chen, G. (2019). 'A novel risk signature that combines 10 long noncoding RNAs to predict neuroblastoma prognosis', Journal of Cellular Physiology. https://doi.org/10.1002/jcp.29277

Gao, X., Kim, H. K., Chung, J. M., and Chung, K. (2007). 'Reactive oxygen species (ROS) are involved in enhancement of NMDA-receptor phosphorylation in animal models of pain', Pain. https://doi.org/10.1016/j.pain.2007.01.011

Gao, Y. F., Wang, Z.-B., Zhu, T., Mao, C.-X., Mao, X.-Y., Li, L. J.-Y., Yin, J. Y., Zhou, H. H. and Liu, Z.-Q. (2016). 'A critical overview of long non-coding RNA in glioma etiology 2016: an update', Tumor Biology, 37(11), 14403–14413.

Garbati, P., Ravera, S., Scarfì, S., Salis, A., Rosano, C., Poggi, A., Damonte, G., Millo, E. and Balestrino, M. (2017). 'Effects on Energy Metabolism of Two Guanidine Molecules, (Boc)2-Creatine and Metformin', Journal of Cellular Biochemistry. https://doi.org/10.1002/jcb.25914

Geisler, S., and Coller, J. (2013). 'RNA in unexpected places: long non-coding RNA functions in diverse cellular contexts', Nature Reviews. Molecular Cell Biology, 14(11), 699–712. https://doi.org/10.1038/nrm3679

Gevaert, K. (2014) 'Early targets of miR-34a in neuroblastoma', Molecular and Cellular Proteomics. doi: 10.1074/mcp.M113.035808.

Ghafouri-Fard, S., Mohammad-Rahimi, H., Jazaeri, M., and Taheri, M. (2020). 'Expression and function of long non-coding RNAs in head and neck squamous cell carcinoma', Experimental and Molecular Pathology. https://doi.org/10.1016/j.yexmp.2019.104353

Ghanbari Movahed, Z., Rastegari-Pouyani, M., Mohammadi, M. H., and Mansouri, K. (2019). 'Cancer cells change their glucose metabolism to overcome increased ROS: One step from cancer cell to cancer stem cell?', Biomedicine and Pharmacotherapy. https://doi.org/10.1016/j.biopha.2019.108690

Giannakakis, A., Zhang, J., Jenjaroenpun, P., Nama, S., Zainolabidin, N., Aau, M. Y., Yarmishyn, A. A., Vaz, C., Ivshina, A. V., Grinchuk, O. V., Voorhoeve, M., Vardy, L. A., Sampath, P., Kuznetsov, V. A., Kurochkin, I. V. and Guccione, E. (2015). 'Contrasting expression patterns of coding and noncoding parts of the human genome upon oxidative stress', Scientific Reports. https://doi.org/10.1038/srep09737

Gong, C.-Y., Tang, R., Liu, K.-X., Xiang, G., and Zhang, H.-H. (2020). 'Long non-coding RNA TP73-AS1 in cancers', Clinica Chimica Acta, 503, 151–156. https://doi.org/10.1016/j.cca.2019.12.025

Gong, D., Feng, P.-C., Ke, X.-F., Kuang, H.-L., Pan, L.-L., Ye, Q., and Wu, J.-B. (2020). 'Silencing Long Non-coding RNA LINC01224 Inhibits Hepatocellular Carcinoma Progression via MicroRNA-330-5p-Induced Inhibition of CHEK1', Molecular Therapy - Nucleic Acids. https://doi.org/10.1016/j.omtn.2019.10.007

Gong, J., Kelekar, G., Shen, J., Shen, J., Kaur, S., and Mita, M. (2016). 'The expanding role of metformin in cancer: an update on antitumor mechanisms and clinical development', Targeted Oncology. https://doi.org/10.1007/s11523-016-0423-z

Goodenberger, M. L., and Jenkins, R. B. (2012). 'Genetics of adult glioma. Cancer Genetics', https://doi.org/10.1016/j.cancergen.2012.10.009

Grünweller, A., Wyszko, E., Bieber, B., Jahnel, R., Erdmann, V. A., and Kurreck, J. (2003). ,Comparison of different antisense strategies in mammalian cells using locked nucleic acids, 2′-O-methyl RNA, phosphorothioates and small interfering RNA', Nucleic Acids Research. https://doi.org/10.1093/nar/gkg409

Guan, H., Cai, J., Zhang, N., Wu, J., Yuan, J., Li, J., and Li, M. (2012). 'Sp1 is upregulated in human glioma, promotes MMP-2-mediated cell invasion and predicts poor clinical outcome', International Journal of Cancer. https://doi.org/10.1002/ijc.26049

Guo, H., Wu, L., Yang, Q., Ye, M., and Zhu, X. (2015). 'Functional linc-POU3F3 is overexpressed and contributes to tumorigenesis in glioma', Gene, 554(1), 114–119. https://doi.org/10.1016/j.gene.2014.10.038

Guo, S. K., Shen, M. F., Yao, H. W., and Liu, Y. S. (2018). 'Enhanced expression of TGFBI promotes the proliferation and migration of glioma cells', Cellular Physiology and Biochemistry. https://doi.org/10.1159/000493293

Gupta, A., and Dwivedi, T. (2017). 'A simplified overview of World Health Organization classification update of central nervous system tumors 2016', Journal of Neurosciences in Rural Practice. https://doi.org/10.4103/jnrp.jnrp_168_17

Gutschner, T., and Diederichs, S. (2012). 'The hallmarks of cancer: a long non-coding RNA point of view', RNA Biology, 9(6), 703–719. https://doi.org/10.4161/rna.20481

Guttman, M., Amit, I., Garber, M., French, C., Lin, M. F., Feldser, D., Huarte, M., Zuk, O., Carey, B. W., Cassady, J. P., Cabili, M. N., Jaenisch, R., Mikkelsen, T. S., Jacks, T., Hacohen, N., Bernstein, B. E., Kellis, M., Regev, A., Rinn, J. L. and Lander, E. S. (2009). 'Chromatin signature reveals over a thousand highly conserved large non-coding RNAs in mammals', Nature, 458(7235), 223–227. https://doi.org/10.1038/nature07672

Hadjidaniel, M. D., Muthugounder, S., Hung, L. T., Sheard, M. A., Shirinbak, S., Chan, R. Y., Nakata, R., Borriello, L., Malvar, J., Kennedy, R. J., Iwakura, H., Akamizu, T., Sposto, R., Shimada, H., DeClerck, Y. A. and Asgharzadeh, S. (2017). 'Tumor-

associated macrophages promote neuroblastoma via STAT3 phosphorylation and up-regulation of c-MYC', Oncotarget. https://doi.org/10.18632/oncotarget.21066

Han, L., Zhang, K., Shi, Z., Zhang, J., Zhu, J., Zhu, S., Zhang, A., Jia, Z., Wang, G., Yu, S., Pu, P., Dong, L. and Kang, C. (2012). 'LncRNA profile of glioblastoma reveals the potential role of lncRNAs in contributing to glioblastoma pathogenesis', International Journal of Oncology. https://doi.org/10.3892/ijo.2012.1413

Han, M., Wang, S., Fritah, S., Wang, X., Zhou, W., Yang, N., Ni, S., Huang, B., Chen, A., Li, G., Miletic, H., Thorsen, F., Bjerkvig, R., Li, X. and Wang, J. (2019). 'Interfering with long non-coding RNA MIR22HG processing inhibits glioblastoma progression through suppression of Wnt/β-catenin signalling', Brain. https://doi.org/10.1093/brain/awz406

Hanahan, D., and Weinberg, R. A. (2011). 'Hallmarks of cancer: The next generation', Cell. https://doi.org/10.1016/j.cell.2011.02.013

Hao, S., Wang, L., Zhao, K., Zhu, X., and Ye, F. (2019). 'Rs1894720 polymorphism in MIAT increased susceptibility to age-related hearing loss by modulating the activation of miR-29b/SIRT1/PGC-1α signaling', Journal of Cellular Biochemistry. https://doi.org/10.1002/jcb.27773

Hara, J. (2012). 'Development of treatment strategies for advanced neuroblastoma', International Journal of Clinical Oncology. https://doi.org/10.1007/s10147-012-0417-5

Hargrave, D. (2009). 'Paediatric high and low grade glioma: the impact of tumour biology on current and future therapy', British Journal of Neurosurgery, 23(4), 351–363. https://doi.org/10.1080/02688690903158809

Hassan, M., Watari, H., Abualmaaty, A., Ohba, Y., and Sakuragi, N. (2014). 'Apoptosis and molecular targeting therapy in cancer', BioMed Research International. https://doi.org/10.1155/2014/150845

Hedrick, E., Cheng, Y., Jin, U.-H., Kim, K., and Safe, S. (2016). 'Specificity protein (Sp) transcription factors Sp1, Sp3 and Sp4 are non-oncogene addiction genes in cancer cells', Oncotarget. https://doi.org/10.18632/oncotarget.7925

Hegarty, S. V., Togher, K. L., O'Leary, E., Solger, F., Sullivan, A. M., and O'Keeffe, G. W. (2017). 'Romidepsin induces caspase-dependent cell death in human neuroblastoma cells', Neuroscience Letters. https://doi.org/10.1016/j.neulet.2017.05.025

Hempel, J. M., Schittenhelm, J., Bisdas, S., Brendle, C., Bender, B., Bier, G., Skardelly, M., Tabatabai, G., Castaneda Vega, S., Ernemann, U. and Klose, U. (2018). 'In vivo assessment of tumor heterogeneity in WHO 2016 glioma grades using diffusion kurtosis imaging: Diagnostic performance and improvement of feasibility in routine clinical practice', Journal of Neuroradiology. https://doi.org/10.1016/j.neurad.2017.07.005

Hirose, T., and Nakagawa, S. (2012). 'Paraspeckles: Possible nuclear hubs by the RNA for the RNA', Biomolecular Concepts. https://doi.org/10.1515/bmc-2012-0017

Hoffman, B., and Liebermann, D. a. (2008). 'Apoptotic signaling by c-MYC', Oncogene, 27(50), 6462–6472. https://doi.org/10.1038/onc.2008.312

Hsu, C. M., Lin, P. M., Lin, H. C., Lai, C. C., Yang, C. H., Lin, S. F., and Yang, M. Y. (2016). 'Altered expression of imprinted genes in squamous cell carcinoma of the head and neck', Anticancer Research.

Hu, L., Lv, Q.-L., Chen, S.-H., Sun, B., Qu, Q., Cheng, L., Guo, Y., Zhou, H. H. and Fan, L. (2016). 'Up-Regulation of Long Non-Coding RNA AB073614 Predicts a Poor Prognosis in Patients with Glioma', International Journal of Environmental Research and Public Health, 13(4), 433. https://doi.org/10.3390/ijerph13040433

Hu, X., Tan, Z., Yang, Y., and Yang, P. (2019). 'Long non-coding RNA MIR22HG inhibits cell proliferation and migration in cholangiocarcinoma by negatively regulating the Wnt/β-catenin signaling pathway', Journal of Gene Medicine, 21(5).

Hua, H., Zhang, X., Mu, H., Meng, Q., Jiang, Y., Wang, Y., Lu, X., Wang, A., Liu, S., Zhang, Y., Wan, Z. and Sun, K. (2018). 'RVG29-modified docetaxel-loaded nanoparticles for brain-targeted glioma therapy', International Journal of Pharmaceutics. https://doi.org/10.1016/j.ijpharm.2018.03.028

Huang, M., and Weiss, W. A. (2013). 'Neuroblastoma and MYCN'. Cold Spring Harbor Perspectives in Medicine. https://doi.org/10.1101/cshperspect.a014415

Huang, Q. Y., Liu, G. F., Qian, X. L., Tang, L. B., Huang, Q. Y., and Xiong, L. X. (2019). 'Long non-coding RNA: Dual effects on breast cancer metastasis and clinical applications', Cancers. https://doi.org/10.3390/cancers11111802

Huang, X., Gao, Y., Qin, J., and Lu, S. (2018). 'lncRNA MIAT promotes proliferation and invasion of HCC cells via sponging miR-214', American Journal of Physiology - Gastrointestinal and Liver Physiology. https://doi.org/10.1152/ajpgi.00242.2017

Huarte, M. (2015). ‘The emerging role of lncRNAs in cancer’, Nature Medicine. https://doi.org/10.1038/nm.3981

Huarte, M., Guttman, M., Feldser, D., Garber, M., Koziol, M. J., Kenzelmann-Broz, D., Khalil, A. M., Zuk, O., Amit, I., Rabani, M., Attardi, L. D., Regev, A., Lander, E. S., Jacks, T. and Rinn, J. L. (2010). ‘A large intergenic noncoding RNA induced by p53 mediates global gene repression in the p53 response’, Cell, 142(3), 409–419. https://doi.org/10.1016/j.cell.2010.06.040

Hung, T. and Chang, H. Y. (2011). ‘Long noncoding RNA in genome regulation: prospects and mechanisms’, RNA Biol, 7(5), 582–585. https://doi.org/10.4161/rna.7.5.13216

Hung, T., Wang, Y., Lin, M. F., Koegel, A. K., Kotake, Y., Grant, G. D., Horlings, H. M., Shah, N., Umbricht, C., Wang, P., Wang, Y., Kong, B., Langerød, A., Børresen-Dale, A., Kim, S. K., van de Vijver, M., Sukumar, S., Whitfield, M. L., Kellis, M., Xiong, Y., Wong, D.J. and Chang, H. Y. (2011). ‘Extensive and coordinated transcription of noncoding RNAs within cell-cycle promoters’, Nature Genetics, 43(7), 621–629. https://doi.org/10.1038/ng.848

Hurtado, M. O., Wolbert, J., Fisher, J., Flutter, B., Stafford, S., Barton, J., Jain, N., Barone, G., Majani, Y. and Anderson, J. (2019). ‘Tumour-infiltrating lymphocytes expanded from pediatric neuroblastoma display heterogeneity of phenotype and function’, PLoS ONE. https://doi.org/10.1371/journal.pone.0216373

Hwang, W. L., Wolfson, R. L., Niemierko, A., Marcus, K. J., Dubois, S. G., and Haas-Kogan, D. (2019). ‘Clinical Impact of Tumor Mutational Burden in Neuroblastoma’, Journal of the National Cancer Institute. https://doi.org/10.1093/jnci/djy157

Hybertson, B. M., and Gao, B. (2014). ‘Role of the Nrf2 signaling system in health and disease’. Clinical Genetics. https://doi.org/10.1111/cge.12474

Iaccarino, I. (2017). ‘LncRNAs and MYC: An intricate relationship’, International Journal of Molecular Sciences. https://doi.org/10.3390/ijms18071497

Ingolia, N. T., Lareau, L. F., and Weissman, J. S. (2011). ‘Ribosome profiling of mouse embryonic stem cells reveals the complexity and dynamics of mammalian proteomes’, Cell, 147(4), 789–802. https://doi.org/10.1016/j.cell.2011.10.002

Ishii, N., Ozaki, K., Sato, H., Mizuno, H., Susumu, S., Takahashi, A., Miyamoto, Y., Ikegawa, S., Kamatani, N., Hori, M., Satoshi S., Nakamura, Y. and Tanaka, T. (2006). 'Identification of a novel non-coding RNA, MIAT, that confers risk of myocardial infarction', Journal of Human Genetics, 51(12), 1087–1099. https://doi.org/10.1007/s10038-006-0070-9

Ishizuka, A., Hasegawa, Y., Ishida, K., Yanaka, K., and Nakagawa, S. (2014). 'Formation of nuclear bodies by the lncRNA Gomafu-associating proteins Celf3 and SF1', Genes to Cells. https://doi.org/10.1111/gtc.12169

Iyer, M., Niknafs, Y., Malik, R., Singhal, U., Sahu, A., Hosono, Y., Barrette, T., Prensner, J., Evans, J., Zhao, S., Poliakov, A., Cao, X., Dhanasekaran, S., Wu, Y., Robinson, D., Beer, D., Feng, F., Iyer, H. and Chinnaiyan, A. (2015). 'The landscape of long noncoding RNAs in the human transcriptome', Nature Genetics, 47(3), 199–208. https://doi.org/10.1038/ng.3192

Janjetovic, K., Vucicevic, L., Misirkic, M., Vilimanovich, U., Tovilovic, G., Zogovic, N., Nikolic, Z., Jovanovic, S., Bumbasirevic, V., Trajkovic, V. and Harhaji-Trajkovic, L. (2011). 'Metformin reduces cisplatin-mediated apoptotic death of cancer cells through AMPK-independent activation of Akt', European Journal of Pharmacology. https://doi.org/10.1016/j.ejphar.2010.11.005

Jiang, Q., Shan, K., Qun-Wang, X., Zhou, R.-M., Yang, H., Liu, C., Li, Y., and Yao, J., (2016). 'Long non-coding RNA-MIAT promotes neurovascular remodeling in the eye and brain.' Oncotarget, 7(31). doi: 10.18632/oncotarget.10434.

Jiang, Y. Z., Liu, Y. R., Xu, X. E., Jin, X., Hu, X., Yu, K. Da, and Shao, Z. M. (2016). 'Transcriptome Analysis of Triple-Negative Breast Cancer Reveals an Integrated mRNA-lncRNA Signature with Predictive and Prognostic Value', Cancer Research. https://doi.org/10.1158/0008-5472.CAN-15-3284

Johnstone, C. N., Mongroo, P. S., Rich, A. S., Schupp, M., Bowser, M. J., deLemos, A. S., Tobias, J. W., Liu, Y., Hannigan, G. E. and Rustgi, A. K. (2008). 'Parvin- Inhibits Breast Cancer Tumorigenicity and Promotes CDK9-Mediated Peroxisome Proliferator-Activated Receptor Gamma 1 Phosphorylation'. Molecular and Cellular Biology. https://doi.org/10.1128/mcb.01617-06

Jones, C., and Baker, S. J. (2014). 'Unique genetic and epigenetic mechanisms driving paediatric diffuse high-grade glioma', Nature Reviews Cancer. https://doi.org/10.1038/nrc3811

Jonkman, J. E. N., Cathcart, J. A., Xu, F., Bartolini, M. E., Amon, J. E., Stevens, K. M., and Colarusso, P. (2014). 'An introduction to the wound healing assay using live-cell microscopy', Cell Adhesion and Migration. https://doi.org/10.4161/cam.36224

Kamijo, T., and Nakagawara, A. (2012). 'Molecular and genetic bases of neuroblastoma', International Journal of Clinical Oncology. https://doi.org/10.1007/s10147-012-0415-7

Khalil, A. M., Guttman, M., Huarte, M., Garber, M., Raj, A., Rivea Morales, D., Thomas, K., Presser, A., Bernstein, B. E., van Oudenaarden, A., Regev, A., Lander, E. S. and Rinn, J. L. (2009). 'Many human large intergenic noncoding RNAs associate with chromatin-modifying complexes and affect gene expression', Proceedings of the National Academy of Sciences of the United States of America, 106(28), 11667–11672. https://doi.org/10.1073/pnas.0904715106

Kietzmann, T., Petry, A., Shvetsova, A., Gerhold, J. M., and Görlach, A. (2017). 'The epigenetic landscape related to reactive oxygen species formation in the cardiovascular system', British Journal of Pharmacology. https://doi.org/10.1111/bph.13792

Kim, S. H., Kim, S. C., and Ku, J. L. (2017). 'Metformin increases chemo-sensitivity via gene downregulation encoding DNA replication proteins in 5-Fu resistant colorectal cancer cells', Oncotarget. https://doi.org/10.18632/oncotarget.17798

Kim, Y., and Jang, H. H. (2019). 'The Role of Peroxiredoxin Family in Cancer Signaling', Journal of Cancer Prevention. https://doi.org/10.15430/jcp.2019.24.2.65

Kitagawa, M., Kitagawa, K., Kotake, Y., Niida, H., and Ohhata, T. (2013). 'Cell cycle regulation by long non-coding RNAs', Cellular and Molecular Life Sciences : CMLS, 70(24), 4785–4794. https://doi.org/10.1007/s00018-013-1423-0

Kitamura, H., and Motohashi, H. (2018). 'NRF2 addiction in cancer cells', Cancer Science. https://doi.org/10.1111/cas.13537

Kloc, M., Wilk, K., Vargas, D., Shirato, Y., Bilinski, S., and Etkin, L. D. (2005). 'Potential structural role of non-coding and coding RNAs in the organization of the cytoskeleton at

the vegetal cortex of Xenopus oocytes', Development (Cambridge, England), 132(15), 3445–3457. https://doi.org/10.1242/dev.01919

Kmiecik, J., Poli, A., Brons, N. H. C., Waha, A., Eide, G. E., Enger, P. Ø., Zimmer, J. and Chekenya, M. (2013). 'Elevated CD3+ and CD8+ tumour-infiltrating immune cells correlate with prolonged survival in glioblastoma patients despite integrated immunosuppressive mechanisms in the tumor microenvironment and at the systemic level', Journal of Neuroimmunology. https://doi.org/10.1016/j.jneuroim.2013.08.013

Kondo, T. (2017). 'Molecular mechanisms involved in gliomagenesis', Brain Tumor Pathology. https://doi.org/10.1007/s10014-017-0278-8

Kong, X., Liu, C. xiao, Wang, G. dong, Yang, H., Yao, X. ming, Hua, Q., and Lv, K. (2019). 'LncRNA LEGLTBC Functions as a ceRNA to Antagonize the Effects of miR-34a on the Downregulation of SIRT1 in Glucolipotoxicity-Induced INS-1 Beta Cell Oxidative Stress and Apoptosis', Oxidative Medicine and Cellular Longevity. https://doi.org/10.1155/2019/4010764

Kornienko, A. E., Guenzl, P. M., Barlow, D. P., and Pauler, F. M. (2013). 'Gene regulation by the act of long non-coding RNA transcription', BMC Biology, 11(1), 59. https://doi.org/10.1186/1741-7007-11-59

Kotake, Y., Nakagawa, T., Kitagawa, K., Suzuki, S., Liu, N., Kitagawa, M., and Xiong, Y. (2011). 'Long non-coding RNA ANRIL is required for the PRC2 recruitment to and silencing of p15 (INK4B) tumor suppressor gene', Oncogene, 30(16), 1956–1962. https://doi.org/10.1038/onc.2010.568

Kourelis, T. V., and Siegel, R. D. (2012). 'Metformin and cancer: New applications for an old drug', Medical Oncology. https://doi.org/10.1007/s12032-011-9846-7

Kumar, A, Al-Sammarraie, N., DiPette, D. J., and Singh, U. S. (2014). 'Metformin impairs Rho GTPase signaling to induce apoptosis in neuroblastoma cells and inhibits growth of tumors in the xenograft mouse model of neuroblastoma', Oncotarget, 5(1949-2553 (Electronic)), 11709–11722. https://doi.org/10.18632/oncotarget.2606

Kumar, Ambrish, Al-Sammarraie, N., DiPette, D. J., and Singh, U. S. (2014). 'Metformin impairs Rho GTPase signaling to induce apoptosis in neuroblastoma cells and inhibits growth of tumors in the xenograft mouse model of neuroblastoma', Oncotarget. https://doi.org/10.18632/oncotarget.2606

Kunej, T., Obsteter, J., Pogacar, Z., Horvat, S., and Calin, G. A. (2014). 'The decalog of long non-coding RNA involvement in cancer diagnosis and monitoring', Critical

Reviews in Clinical Laboratory Sciences. https://doi.org/10.3109/10408363.2014.944299

La Fougère, C., Suchorska, B., Bartenstein, P., Kreth, F. W., and Tonn, J. C. (2011). 'Molecular imaging of gliomas with PET: Opportunities and limitations', Neuro-Oncology. https://doi.org/10.1093/neuonc/nor054

Lai, I. L., Yang, C. A., Lin, P. C., Chan, W. L., Lee, Y. T., Yen, J. C., and Chang, J. G. (2017). 'Long noncoding RNA MIAT promotes non-small cell lung cancer proliferation and metastasis through MMP9 activation', Oncotarget. https://doi.org/10.18632/oncotarget.21465

Lan, H., Jin, K., Xie, B., Han, N., Cui, B., Cao, F., and Teng, L. (2012). 'Heterogeneity between primary colon carcinoma and paired lymphatic and hepatic metastases', Molecular Medicine Reports. https://doi.org/10.3892/mmr.2012.1051

Laurent, G. S., Savva, Y. A., and Kapranov, P. (2012). 'Dark matter RNA: An intelligent scaffold for the dynamic regulation of the nuclear information landscape', Frontiers in Genetics, 3(APR). https://doi.org/10.3389/fgene.2012.00057

Lavrovsky, Y., Chatterjee, B., Clark, R. A., and Roy, A. K. (2000). 'Role of redox-regulated transcription factors in inflammation, ageing and age-related diseases', Experimental Gerontology. https://doi.org/10.1016/S0531-5565(00)00118-2

Lazorthes, S., Vallot, C., Briois, S., Aguirrebengoa, M., Thuret, J.-Y., St Laurent, G., Rougeulle, C., Kapranov, P., Mann, C., Trouche, D. and Nicolas, E. (2015). 'A vlincRNA participates in senescence maintenance by relieving H2AZ-mediated repression at the INK4 locus', Nature Communications, 6, 5971. https://doi.org/10.1038/ncomms6971

Lee, Y. J., Kim, W. Il, Kim, S. Y., Cho, S. W., Nam, H. S., Lee, S. H., and Cho, M. K. (2019). 'Flavonoid morin inhibits proliferation and induces apoptosis of melanoma cells by regulating reactive oxygen species, Sp1 and Mcl-1', Archives of Pharmacal Research. https://doi.org/10.1007/s12272-019-01158-5

Lekka, E., and Hall, J. (2018). 'Noncoding RNAs in disease', FEBS Letters. https://doi.org/10.1002/1873-3468.13182

Lennartsson, A., and Ekwall, K. (2009). 'Histone modification patterns and epigenetic codes', Biochimica et Biophysica Acta - General Subjects. https://doi.org/10.1016/j.bbagen.2008.12.006

Lennox, K. A., and Behlke, M. A. (2016). 'Cellular localization of long non-coding RNAs affects silencing by RNAi more than by antisense oligonucleotides', Nucleic Acids Research, 44(2), 863–877. https://doi.org/10.1093/nar/gkv1206

Lewis, G. D., Rivera, A. L., Tremont-Lukats, I. W., Ballester-Fuentes, L. Y., Zhang, Y. J., and Teh, B. S. (2017). 'GBM skin metastasis: a case report and review of the literature', CNS Oncology. https://doi.org/10.2217/cns-2016-0042

Li, C., Yang, L., and Lin, C. (2014). 'Long noncoding RNAs in prostate cancer: mechanisms and applications', Molecular and Cellular Oncology. https://doi.org/10.4161/23723548.2014.963469

Li, Dan, Wang, X., Mei, H., Fang, E., Ye, L., Song, H., Yang, Feng
Li, Donghui. (2011). 'Metformin as an antitumor agent in cancer prevention and treatment', Journal of Diabetes. https://doi.org/10.1111/j.1753-0407.2011.00119.x

Li, H., Huang, K., Zheng, L. and Tong, Q. (2018). 'Long noncoding RNA pancEts-1 promotes neuroblastoma progression through hnRNPK-mediated β-catenin stabilization', Cancer Research. https://doi.org/10.1158/0008-5472.CAN-17-2295

Li, J., An, G., Zhang, M., and Ma, Q. (2016). 'Long non-coding RNA TUG1 acts as a miR-26a sponge in human glioma cells', Biochemical and Biophysical Research Communications, 477(4), 743–748. https://doi.org/10.1016/j.bbrc.2016.06.129

Li, M. M., Liu, X. H., Zhao, Y. C., Ma, X. Y., Zhou, Y. C., Zhao, Y. X., and Liu, X. Y. (2019). 'Long noncoding RNA KCNQ1OT1 promotes apoptosis in neuroblastoma cells by regulating miR-296-5p/Bax axis', FEBS Journal. https://doi.org/10.1111/febs.15047

Li, P., Tong, L., Song, Y., Sun, J., Shi, J., Wu, Z., and Wang, Z. (2019). 'Long noncoding RNA H19 participates in metformin-mediated inhibition of gastric cancer cell invasion', Journal of Cellular Physiology. https://doi.org/10.1002/jcp.27269

Li, Q. Y., Yang, K., Liu, F. G., Sun, X. G., Chen, L., Xiu, H., and Liu, X. S. (2019). 'Long noncoding RNA CASC2c inhibited cell proliferation in hepatocellular carcinoma by inactivated ERK1/2 and Wnt/β-catenin signaling pathway', Clinical and Translational Oncology. https://doi.org/10.1007/s12094-019-02223-7

Li, R., Qian, J., Wang, Y. Y., Zhang, J. X., and You, Y. P. (2014). 'Long Noncoding RNA Profiles Reveal Three Molecular Subtypes in Glioma. CNS Neuroscience and Therapeutics', https://doi.org/10.1111/cns.12220

Li, T. F., Liu, J., and Fu, S. J. (2018). 'The interaction of long non-coding RNA MIAT and miR-133 play a role in the proliferation and metastasis of pancreatic carcinoma', Biomedicine and Pharmacotherapy. https://doi.org/10.1016/j.biopha.2018.05.043

Li, Wentong, Zhai, L., Wang, H., Liu, C., Zhang, J., Chen, W., and Wei, Q. (2016). 'Downregulation of LncRNA GAS5 causes trastuzumab resistance in breast cancer', Oncotarget. https://doi.org/10.18632/oncotarget.8413

Li, Wusheng, Li, K., Zhao, L., and Zou, H. (2014). 'Bioinformatics analysis reveals disturbance mechanism of MAPK signaling pathway and cell cycle in Glioblastoma multiforme', Gene. https://doi.org/10.1016/j.gene.2014.06.042

Li, X. L., Subramanian, M., Jones, M. F., Chaudhary, R., Singh, D. K., Zong, X., Gryder, B., Sindri, S., Mo, M., Schetter, A., Wen, X., Parvathaneni, S., Kazandjian, D., Jenkins, L. M., Tang, W., Elloumi, F., Martindale, J. L., Huarte, M., Zhu, Y., Robles, A. I., Frier, S. M., Rigo, F., Cam, M., Ambs, S., Sharma, S., Harris, C. C., Dasso, M., Prasanth, K. V. and Lal, A. (2017). 'Long Noncoding RNA PURPL Suppresses Basal p53 Levels and Promotes Tumorigenicity in Colorectal Cancer', Cell Reports. https://doi.org/10.1016/j.celrep.2017.08.041

Li, X., Zhou, Y., Yang, L., Ma, Y., Peng, X., Yang, S., and Liu, J. (2019). 'LncRNA NEAT1 promotes autophagy via regulating miR-204/ATG3 and enhanced cell resistance to sorafenib in hepatocellular carcinoma', Journal of Cellular Physiology. https://doi.org/10.1002/jcp.29230

Li, X.M., Shen, Y., Cheng, H., Yuan, J., Zhang, Y. Y. and Yan, B. (2016). 'Long non-coding RNA-MIAT promotes neurovascular remodeling in the eye and brain', Oncotarget, 7(31). https://doi.org/10.18632/oncotarget.10434

Li, Yanfeng, Wang, K., Wei, Y., Yao, Q., Zhang, Q., Qu, H., and Zhu, G. (2017). 'lncRNA-MIAT regulates cell biological behaviors in gastric cancer through a mechanism involving the miR-29a-3p/HDAC4 axis', Oncology Reports. https://doi.org/10.3892/or.2017.6020

Li, Yuehua, Jiang, B., Wu, X., Huang, Q., Chen, W., Zhu, H., and Huang, G. (2018). 'Long non-coding RNA MIAT is estrogen-responsive and promotes estrogen-induced proliferation in ER-positive breast cancer cells', Biochemical and Biophysical Research Communications. https://doi.org/10.1016/j.bbrc.2018.05.146

Li, Yunwei, Wang, J., Sun, L., and Zhu, S. (2018). 'LncRNA myocardial infarction-associated transcript (MIAT) contributed to cardiac hypertrophy by regulating TLR4 via miR-93', European Journal of Pharmacology. https://doi.org/10.1016/j.ejphar.2017.11.031

Li, Z., Shen, J., Chan, M. T., and Wu, W. K. (2016). 'TUG1: a pivotal oncogenic long non-coding RNA of human cancers', Cell Proliferation, 49(4), 471–475. https://doi.org/10.1111/cpr.12269

Liao, J., He, Q., Li, M., Chen, Y., Liu, Y., and Wang, J. (2016). 'LncRNA MIAT: Myocardial infarction associated and more', Gene. https://doi.org/10.1016/j.gene.2015.12.032

Lin, D., Lam, W., Collins, C. and Wang, Y. (2016). 'The role of epigenetics and long noncoding RNA MIAT in neuroendocrine prostate cancer'. Epigenomics. https://doi.org/10.2217/epi.16.6

Lin, Y. H. (2019). 'MicroRNA networks modulate oxidative stress in cancer', International Journal of Molecular Sciences. https://doi.org/10.3390/ijms20184497

Ling, H., Vincent, K., Pichler, M., Fodde, R., Berindan-Neagoe, I., Slack, F. J., and Calin, G. A. (2015). 'Junk DNA and the long non-coding RNA twist in cancer genetics', Oncogene, 34, 5003–5011. https://doi.org/10.1038/onc.2014.456

Liu, H., Li, J., Koirala, P., Ding, X., Chen, B., Wang, Y., Wang, Z., Wang, C., Zhang, X. and Mo, Y. Y. (2016). 'Long non-coding RNAs as prognostic markers in human breast cancer', Oncotarget. https://doi.org/10.18632/oncotarget.7828

Liu, L., Wang, H. J., Meng, T., Lei, C., Yang, X. H., Wang, Q. S., and Zhu, J. F. (2019). 'lncRNA GAS5 Inhibits Cell Migration and Invasion and Promotes Autophagy by Targeting miR-222-3p via the GAS5/PTEN-Signaling Pathway in CRC', Molecular Therapy - Nucleic Acids. https://doi.org/10.1016/j.omtn.2019.06.009

Liu, P. Y., Tee, A. E., Milazzo, G., Hannan, K. M., Maag, J., Mondal, S., Atmadibrata, B., Bartonicek, N., Peng, H., Ho, N., Mayoh, C., Ciaccio, R., Sun, Y., Henderson, M. J., Gao, J., Everaert, C., Hulme, A. J., Wong, M., Lan, Q., Cheung, B. B., Shi, L., Wang, J. Y., Simon, T., Fischer, M., Zhang, X. D., Marshall, G. M., Norris, M. D., Haber, M., Vandesompele, J., Li, J., Mestdagh, P., Hannan, R. D., Dinger, M. E., Perini, G. and Liu, T. (2019). 'The long noncoding RNA lncNB1 promotes tumorigenesis by interacting with ribosomal protein RPL35', Nature Communications. https://doi.org/10.1038/s41467-019-12971-3

Liu, Q., Sun, S., Yu, W., Jiang, J., Zhuo, F., Qiu, G. and Jiang, X. (2015). 'Altered expression of long non-coding RNAs during genotoxic stress-induced cell death in human glioma cells', Journal of Neuro-Oncology, 122(2), 283–292. https://doi.org/10.1007/s11060-015-1718-0

Liu, W., Wang, Z., Wang, C., and Ai, Z. (2019). 'Long non-coding RNA MIAT promotes papillary thyroid cancer progression through upregulating LASP1', Cancer Cell International. https://doi.org/10.1186/s12935-019-0913-z

Liu, X., Xu, Y., Han, L., and Yi, Y. (2018). 'Reassessing the potential of MYB-targeted anti-cancer therapy', Journal of Cancer. https://doi.org/10.7150/jca.23992

Liu, Yawen, Feng, W., Liu, W., Kong, X., Li, L., He, J., and Xu, M. (2019). 'Circulating lncRNA ABHD11-AS1 serves as a biomarker for early pancreatic cancer diagnosis', Journal of Cancer. https://doi.org/10.7150/jca.32052

Liu, Yunfei, Wang, J., Dong, L., Xia, L., Zhu, H., Li, Z., and Yu, X. (2019). 'Long noncoding RNA HCP5 regulates pancreatic cancer gemcitabine (GEM) resistance by sponging Hsa-miR-214-3p to target HDGF', OncoTargets and Therapy. https://doi.org/10.2147/OTT.S222703

Lo, P., Zhang, Y., Wolfson, B., Gernapudi, R., Yao, Y., Duru, N., and Zhou, Q. (2016). ''Dysregulation of the BRCA1/long non-coding RNA NEAT1 signaling axis contributes to breast tumorigenesis', Oncotarget. https://doi.org/10.18632/oncotarget.11364

Louis, D. N., Perry, A., Reifenberger, G., von Deimling, A., Figarella-Branger, D., Cavenee, W. K., Ohgaki, H., Wiestler, O. D., Kleihues, P. and Ellison, D. W. (2016). 'The 2016 World Health Organization Classification of Tumors of the Central Nervous System: a summary', Acta Neuropathologica. ttps://doi.org/10.1007/s00401-016-1545-1

Lu, Y., Zhao, X., Liu, Q., Li, C., Graves-Deal, R., Cao, Z., Singh, B., Franklin, J. L., Wang, J., Hu, H., Wei, T., Yang, M., Yeatman, T. J., Lee, E., Saito-Diaz, K., Hinger, S., Patton, J. G., Chung, C. H., Emmrich, S., Klusmann, J. H., Fan, D. and Coffey, R. J. (2017). 'LncRNA MIR100HG-derived miR-100 and miR-125b mediate cetuximab resistance via Wnt/β-catenin signaling', Nature Medicine. https://doi.org/10.1038/nm.4424

Luan, F., Chen, W., Chen, M., Yan, J., Chen, H., Yu, H. and Mo, L. (2019). 'An autophagy-related long non-coding RNA signature for glioma', FEBS Open Bio. https://doi.org/10.1002/2211-5463.12601

Luan, T., Zhang, X., Wang, S., Song, Y., Zhou, S., Lin, J., and Wang, L. (2017). 'Long non-coding RNA MIAT promotes breast cancer progression and functions as ceRNA to regulate DUSP7 expression by sponging miR-155-5p', Oncotarget. https://doi.org/10.18632/oncotarget.19190

Luan, W., Zhang, Y., You, Y., Wang, Y. and Liu, N. (2014). 'An axis involving SNAI1, microRNA-128 and SP1 modulates glioma progression', PLoS ONE. https://doi.org/10.1371/journal.pone.0098651

Luksch, R., Castellani, M. R., Collini, P., De Bernardi, B., Conte, M., Gambini, C., Gandola, L., Garaventa, A., Biasoni, D., Podda, M., Sementa, A. R., Gatta, G. and Tonini, G. P. (2016). 'Neuroblastoma (Peripheral neuroblastic tumours)', Critical Reviews in Oncology/Hematology, 107, 163–181. https://doi.org/10.1016/j.critrevonc.2016.10.001

Lundin, K. E. et al. (2013) 'Biological Activity and Biotechnological Aspects of Locked Nucleic Acids', in Advances in Genetics. doi: 10.1016/B978-0-12-407676-1.00002-0

Luo, Z., Xiao, L., Li, J., Dong, B., Wang, C., and Qi, P. (2019). 'Integrative analysis reveals driver long non-coding RNAs in osteosarcoma', Medicine (United States). https://doi.org/10.1097/MD.0000000000014302

Lv, H., Zhen, C., Liu, J., Yang, P., Hu, L., and Shang, P. (2019). 'Unraveling the Potential Role of Glutathione in Multiple Forms of Cell Death in Cancer Therapy', Oxidative Medicine and Cellular Longevity. https://doi.org/10.1155/2019/3150145

Lv, Q. L., Chen, S. H., Zhang, X., Sun, B., Hu, L., Qu, Q., and Zhou, H. H. (2017). 'Upregulation of long noncoding RNA zinc finger antisense 1 enhances epithelial-mesenchymal transition in vitro and predicts poor prognosis in glioma', Tumor Biology. https://doi.org/10.1177/1010428317695022

Lynch, J., Fay, J., Meehan, M., Bryan, K., Watters, K. M., Murphy, D. M., and Stallings, R. L. (2012). 'MiRNA-335 suppresses neuroblastoma cell invasiveness by direct targeting of multiple genes from the non-canonical TGF-β signalling pathway', Carcinogenesis. https://doi.org/10.1093/carcin/bgs114

Ma, J., Guo, Y., Chen, S., Zhong, C., Xue, Y., Zhang, Y., Lai, X., Wei, Y., Yu, S., Zhang, J. and Liu, W. (2014). 'Metformin enhances tamoxifen-mediated tumor growth inhibition in ER-positive breast carcinoma', BMC Cancer. https://doi.org/10.1186/1471-2407-14-172

Maass, P. G., Luft, F. C., and Bähring, S. (2014). 'Long non-coding RNA in health and disease', Journal of Molecular Medicine. https://doi.org/10.1007/s00109-014-1131-8

MacLeod, A. R., and Crooke, S. T. (2017). 'RNA Therapeutics in Oncology: Advances, Challenges, and Future Directions', Journal of Clinical Pharmacology. https://doi.org/10.1002/jcph.957

Mahmoudi, S, Henriksson, S., Farnebo, L., Roberg, K., and Farnebo, M. (2011). 'WRAP53 promotes cancer cell survival and is a potential target for cancer therapy', Cell Death and Disease, 2(1), e114. https://doi.org/10.1038/cddis.2010.90

Mahmoudi, S., Henriksson, S., Corcoran, M., Méndez-Vidal, C., Wiman, K. G., and Farnebo, M. (2009). 'Wrap53, a Natural p53 Antisense Transcript required for p53 Induction upon DNA Damage', Molecular Cell, 33(4), 462–471. https://doi.org/10.1016/j.molcel.2009.01.028

Majidinia, M., and Yousefi, B. (2016). 'Long non-coding RNAs in cancer drug resistance development', DNA Repair. https://doi.org/10.1016/j.dnarep.2016.06.003

Manning, B. D., and Cantley, L. C. (2007). 'AKT/PKB Signaling: Navigating Downstream', Cell. https://doi.org/10.1016/j.cell.2007.06.009

Mao, Y. S., Zhang, B., and Spector, D. L. (2011). 'Biogenesis and function of nuclear bodies', Trends in Genetics. https://doi.org/10.1016/j.tig.2011.05.006

Marín-Rubio, J. L., Vela-Martín, L., Fernández-Piqueras, J., and Villa-Morales, M. (2019). 'FADD in Cancer: Mechanisms of Altered Expression and Function, and Clinical Implications', Cancers. https://doi.org/10.3390/cancers11101462

Marlow, M. M., Shah, S. S., Véliz, E. A., Ivan, M. E., and Graham, R. M. (2017). 'Treatment of adult and pediatric high-grade gliomas with Withaferin A: antitumor mechanisms and future perspectives', Journal of Natural Medicines. https://doi.org/10.1007/s11418-016-1020-2

Marques, A. C., Hughes, J., Graham, B., Kowalczyk, M. S., Higgs, D. R., and Ponting, C. P. (2013). 'Chromatin signatures at transcriptional start sites separate two equally populated yet distinct classes of intergenic long noncoding RNAs', Genome Biology, 14(11), R131. https://doi.org/10.1186/gb-2013-14-11-r131

Martianov, I., Ramadass, A., Serra Barros, A., Chow, N., and Akoulitchev, A. (2007). 'Repression of the human dihydrofolate reductase gene by a non-coding interfering transcript', Nature, 445(February), 666–670. https://doi.org/10.1038/nature05519

Marvel, D., and Gabrilovich, D. I. (2015). 'Myeloid-derived suppressor cells in the tumor microenvironment: Expect the unexpected', Journal of Clinical Investigation. https://doi.org/10.1172/JCI80005

Matsumura, I., Tanaka, H., and Kanakura, Y. (2003). 'E2F1 and c-Myc in cell growth and death', Cell Cycle (Georgetown, Tex.). https://doi.org/10.4161/cc.2.4.428

Matthay, K. K., Maris, J. M., Schleiermacher, G., Nakagawara, A., Mackall, C. L., Diller, L., and Weiss, W. A. (2016). 'Neuroblastoma', Nature Reviews Disease Primers, 2(1), 16078. https://doi.org/10.1038/nrdp.2016.78

Mattick, J. S. (2018). 'The state of long non-coding RNA biology', Non-Coding RNA. https://doi.org/10.3390/ncrna4030017

Mattick, J. S., and Makunin, I. V. (2005). 'Small regulatory RNAs in mammals', Human Molecular Genetics. https://doi.org/10.1093/hmg/ddi101

Maxwell, R., Luksik, A. S., Garzon-Muvdi, T., and Lim, M. (2017). 'The Potential of Cellular- and Viral-Based Immunotherapies for Malignant Glioma–Dendritic Cell Vaccines, Adoptive Cell Transfer, and Oncolytic Viruses', Current Neurology and Neuroscience Reports. https://doi.org/10.1007/s11910-017-0754-x

Mazar, J., Rosado, A., Shelley, J., Marchica, J., and Westmoreland, T. J. (2017). 'The long non-coding RNA GAS5 differentially regulates cell cycle arrest and apoptosis through activation of BRCA1 and p53 in human neuroblastoma', Oncotarget. https://doi.org/10.18632/oncotarget.14244

Mazzoccoli, C., Ruggieri, V., Tataranni, T., Agriesti, F., Laurenzana, I., Fratello, A., Capitanio, N. and Piccoli, C. (2016). ''N-acetylaspartate (NAA) induces neuronal differentiation of SH-SY5Y neuroblastoma cell line and sensitizes it to chemotherapeutic agents', European Journal of Cancer, 61, S81–S82. https://doi.org/10.1016/S0959-8049(16)61284-4

McMahon, S. B. (2014). 'MYC and the control of apoptosis', Cold Spring Harbor Perspectives in Medicine, 4(7). https://doi.org/10.1101/cshperspect.a014407

McNeil, E. M., Ritchie, A. M., and Melton, D. W. (2013). 'The toxicity of nitrofuran compounds on melanoma and neuroblastoma cells is enhanced by Olaparib and

ameliorated by melanin pigment', DNA Repair, 12(11), 1000–1006. https://doi.org/10.1016/j.dnarep.2013.08.017

Mei-Yee Kiang, K., Zhang, X. Q., and Leung, G. K. K. (2015). 'Long non-coding RNAs: The key players in glioma pathogenesis', Cancers. https://doi.org/10.3390/cancers7030843

Melissari, M.-T., and Grote, P. (2016). 'Roles for long non-coding RNAs in physiology and disease', Pflügers Archiv : European Journal of Physiology, 468(6), 945–958. https://doi.org/10.1007/s00424-016-1804-y

Méndez, O., Zavadil, J., Esencay, M., Lukyanov, Y., Santovasi, D., Wang, S. C., Newcomb, E. W. and Zagzag, D. (2010). 'Knock down of HIF-1α in glioma cells reduces migration in vitro and invasion in vivo and impairs their ability to form tumor spheres', Molecular Cancer. https://doi.org/10.1186/1476-4598-9-133

Menendez, J. A., Cufí, S., Oliveras-Ferraros, C., Martin-Castillo, B., Joven, J., Vellon, L., and Vazquez-Martin, A. (2011). 'Metformin and the ATM DNA damage response (DDR): Accelerating the onset of stress-induced senescence to boost protection against cancer', Aging. https://doi.org/10.18632/aging.100407

Menke, A. L., Riteco, N., Van Ham, R. C. A., De Bruyne, C., Rauscher, F. J., Van Der Eb, A. J., and Jochemsen, A. G. (1996). 'Wilms' Tumor 1 splice variants have opposite effects on the tumorigenicity of adenovirus-transformed baby-rat kidney cells', Oncogene.

Mercer, T R, Dinger, M. E., and Mattick, J. S. (2009). 'Long non-coding RNAs: insights into functions', Nature Reviews. Genetics, 10, 155–159. https://doi.org/10.1038/nrg2521

Mercer, Tim R, Dinger, M. E., Sunkin, S. M., Mehler, M. F., and Mattick, J. S. (2008). 'Specific expression of long noncoding RNAs in the mouse brain', Proceedings of the National Academy of Sciences of the United States of America, 105(2), 716–721. https://doi.org/10.1073/pnas.0706729105

Mercer, Tim R., Wilhelm, D., Dinger, M. E., Soldà, G., Korbie, D. J., Glazov, E. A., Truong, V., Schwenke, M., Simons, C., Matthaei, K. I., Saint, R., Koopman, P. and Mattick, J. S. (2011). 'Expression of distinct RNAs from 3′ untranslated regions', Nucleic Acids Research, 39(6), 2393–2403. https://doi.org/10.1093/nar/gkq1158

Mestdagh, P., Boström, A. K., Impens, F., Fredlund, E., Van Peer, G., De Antonellis, P., von Stedingk, K., Ghesquière, B., Schulte, S., Dews, M., Thomas-Tikhonenko, A.,

Schulte, J. H., Zollo, M., Schramm, A., Gevaert, K., Axelson, H., Speleman, F. and Vandesompele, J. (2010). 'The miR-17-92 MicroRNA Cluster Regulates Multiple Components of the TGF-β Pathway in Neuroblastoma', Molecular Cell. https://doi.org/10.1016/j.molcel.2010.11.038

Micheau, O., Shirley, S., and Dufour, F. (2013). 'Death receptors as targets in cancer', British Journal of Pharmacology. https://doi.org/10.1111/bph.12238

Mitra, P. (2018). 'Transcription regulation of MYB: a potential and novel therapeutic target in cancer', Annals of Translational Medicine. https://doi.org/10.21037/atm.2018.09.62

Miyajima, T., and Kotake, Y. (1995). 'Spin Trapping Agent, Phenyl N-tertbutyl Nitrone (PBN) Inhibits Induction of Nitric Oxide Synthase in Endotoxin-Induced Shock in Mice', Biochemical and Biophysical Research Communications. https://doi.org/10.1006/bbrc.1995.2440

Mohammadi, F., Soltani, A., Ghahremanloo, A., Javid, H., and Hashemy, S. I. (2019). 'The thioredoxin system and cancer therapy: a review', Cancer Chemotherapy and Pharmacology. https://doi.org/10.1007/s00280-019-03912-4

Mohanty, V., Gökmen-Polar, Y., Badve, S., and Janga, S. C. (2015). 'Role of lncRNAs in health and disease-size and shape matter', Briefings in Functional Genomics, 14(2), 115–129. https://doi.org/10.1093/bfgp/elu034

Mondal, T., and Kanduri, C. (2019). 'LncRNAs join hands together to regulate neuroblastoma progression', Molecular and Cellular Oncology. https://doi.org/10.1080/23723556.2018.1553697

Mondal, T., Juvvuna, P. K., Kirkeby, A., Mitra, S., Kosalai, S. T., Traxler, L., Hertwig, F., Wernig-Zorc, S., Miranda, C., Deland, L., Volland, R., Bartenhagen, C., Bartsch, D., Bandaru, S., Engesser, A., Subhash, S., Martinsson, T., Carén, H., Akyürek, L. M., Kurian, L., Kanduri, M., Huarte, M., Kogner, P., Fischer, M. and Kanduri, C. (2018). 'Sense-Antisense lncRNA Pair Encoded by Locus 6p22.3 Determines Neuroblastoma Susceptibility via the USP36-CHD7-SOX9 Regulatory Axis', Cancer Cell. https://doi.org/10.1016/j.ccell.2018.01.020

Moran, V. A., Perera, R. J., and Khalil, A. M. (2012). 'Emerging functional and mechanistic paradigms of mammalian long non-coding RNAs', Nucleic Acids Research. https://doi.org/10.1093/nar/gks296

Moridi, H., Karimi, J., Tavilani, H., Khodadadi, I., and Emami Razavi, A. N. (2019). 'Overexpression of PURPL and downregulation of NONHSAT062994 as potential biomarkers in gastric cancer', Life Sciences. https://doi.org/10.1016/j.lfs.2019.116904

Mouhieddine, T. H., Nokkari, A., Itani, M. M., Chamaa, F., Bahmad, H., Monzer, A., El-Merahbi, R., Daoud, G., Eid, A., Kobeissy, F. H. and Abou-Kheir, W. (2015). 'Metformin and ara-a effectively suppress brain cancer by targeting cancer stem/progenitor cells', Frontiers in Neuroscience. https://doi.org/10.3389/fnins.2015.00442

Mourtada-Maarabouni, M., Pickard, M., Hedge, V., Farzaneh, F., and Williams, G. (2009). 'GAS5, a non-protein-coding RNA, controls apoptosis and is downregulated in breast cancer', Oncogene, 28373, 195–208. https://doi.org/10.1038/onc.2008.373

Mullassery, D., and Losty, P. (2016). 'Neuroblastoma', Paediatrics and Child Health, 26(2), 68–72. https://doi.org/https://doi.org/10.1016/j.paed.2015.11.005

Mullassery, D., Farrelly, P., and Losty, P. D. (2014). 'Does aggressive surgical resection improve survival in advanced stage 3 and 4 neuroblastoma? A systematic review and meta-analysis', In Pediatric Hematology and Oncology. https://doi.org/10.3109/08880018.2014.947009

Munoz, F. M., Gao, R., Tian, Y., Henstenburg, B. A., Barrett, J. E., and Hu, H. (2017). 'Neuronal P2X7 receptor-induced reactive oxygen species production contributes to nociceptive behavior in mice', Scientific Reports. https://doi.org/10.1038/s41598-017-03813-7

Murray, P. J., Allen, J. E., Biswas, S. K., Fisher, E. A., Gilroy, D. W., Goerdt, S., Gordon, S., Hamilton, J. A., Ivashkiv, L. B., Lawrence, T., Locati, M., Mantovani, A., Martinez, F. O., Mege, J. L., Mosser, D. M., Natoli, G., Saeij, J. P., Schultze, J. L., Shirey, K. A., Sica, A., Suttles, J., Udalova, I., VanGinderachter, J. A., Vogel, S. N. and Wynn, T. A. (2014). 'Macrophage Activation and Polarization: Nomenclature and Experimental Guidelines', Immunity. https://doi.org/10.1016/j.immuni.2014.06.008

Nakagawara, A., Li, Y., Izumi, H., Muramori, K., Inada, H., and Nishi, M. (2018). 'Neuroblastoma', Japanese Journal of Clinical Oncology, 48(3), 214–241.

Narayanan, I. V., Paulsen, M. T., Bedi, K., Berg, N., Ljungman, E. A., Francia, S., Veloso, A., Magnuson, B., Di Fagagna, F. D. A., Wilson, T. E. and Ljungman, M. (2017). 'Transcriptional and post-transcriptional regulation of the ionizing radiation response by ATM and p53', Scientific Reports. https://doi.org/10.1038/srep43598

NavaneethaKrishnan, S., Rosales, J. L., and Lee, K. Y. (2019). 'ROS-Mediated Cancer Cell Killing through Dietary Phytochemicals'. Oxidative Medicine and Cellular Longevity. https://doi.org/10.1155/2019/9051542

Nayler, S. P., Nones, K., Hu, J., Bredy, T. W., Nakagawa, S., Rigo, F., Taft, R. J., Cairns, M. J., Blackshaw, S., Wolvetang, E. J. and Mattick, J. S. (2014) 'The long non-coding RNA Gomafu is acutely regulated in response to neuronal activation and involved in schizophrenia-associated alternative splicing', Molecular Psychiatry. doi: 10.1038/mp.2013.45.

Nguyen, T. T., Ung, T. T., Li, S., Lian, S., Xia, Y., Park, S. Y., and Do Jung, Y. (2019). 'Metformin inhibits lithocholic acid-induced interleukin 8 upregulation in colorectal cancer cells by suppressing ROS production and NF-kB activity', Scientific Reports. https://doi.org/10.1038/s41598-019-38778-2

Niehus, S. E., Allister, A. B., Hoffmann, A., Wiehlmann, L., Tamura, T., and Tran, D. D. H. (2019). 'Myc/Max dependent intronic long antisense noncoding RNA, EVA1A-AS, suppresses the expression of Myc/Max dependent anti-proliferating gene EVA1A in a U2 dependent manner', Scientific Reports. https://doi.org/10.1038/s41598-019-53944-2

Nihashi, T., Dahabreh, I. J., and Terasawa, T. (2013). 'Diagnostic accuracy of PET for recurrent glioma diagnosis: A meta-analysis', American Journal of Neuroradiology. https://doi.org/10.3174/ajnr.A3324

Nikaki, A., Angelidis, G., Efthimiadou, R., Tsougos, I., Valotassiou, V., Fountas, K., Prasopoulos, V. and Georgoulias, P. (2017). '18F-fluorothymidine PET imaging in gliomas: an update', Annals of Nuclear Medicine. https://doi.org/10.1007/s12149-017-1183-2

Ning, Q., Li, Y., Wang, Z., Zhou, S., Sun, H., and Yu, G. (2017). 'The Evolution and Expression Pattern of Human Overlapping lncRNA and Protein-coding Gene Pairs', Scientific Reports. https://doi.org/10.1038/srep42775

Nishizawa, M., Komai, T., Katou, Y., Shirahige, K., Ito, T., and Toh-E, A. (2008). 'Nutrient-regulated antisense and intragenic RNAs modulate a signal transduction pathway in yeast', PLoS Biology, 6(12), 2817–2830. https://doi.org/10.1371/journal.pbio.0060326

O'Brien, E. M., Selfe, J. L., Martins, A. S., Walters, Z. S., and Shipley, J. M. (2018). 'The long non-coding RNA MYCNOS-01 regulates MYCN protein levels and affects

growth of MYCN-amplified rhabdomyosarcoma and neuroblastoma cells', BMC Cancer. https://doi.org/10.1186/s12885-018-4129-8

O'Hagan, H. M., Wang, W., Sen, S., DeStefano Shields, C., Lee, S. S., Zhang, Y. W., Clements, E. G., Cai, Y., Van Neste, L., Easwaran, H., Casero, R.A., Sears, C. L. and Baylin, S. B. (2011). 'Oxidative Damage Targets Complexes Containing DNA Methyltransferases, SIRT1, and Polycomb Members to Promoter CpG Islands', Cancer Cell. https://doi.org/10.1016/j.ccr.2011.09.012

Olson, J. J., Nayak, L., Ormond, D. R., Wen, P. Y., Kalkanis, S. N., and Ryken, T. C. (2014). 'The role of targeted therapies in the management of progressive glioblastoma: A systematic review and evidence-based clinical practice guideline', Journal of Neuro-Oncology. https://doi.org/10.1007/s11060-013-1339-4

Paff, M., Alexandru-Abrams, D., Hsu, F. P. K., and Bota, D. A. (2014). 'The evolution of the EGFRvIII (rindopepimut) immunotherapy for glioblastoma multiforme patients', Human Vaccines and Immunotherapeutics. https://doi.org/10.4161/21645515.2014.983002

Palmieri, G., Paliogiannis, P., Sini, M. C., Manca, A., Palomba, G., Doneddu, V., Tanda, F., Pascale, M.R. and Cossu, A. (2017). 'Long non-coding RNA CASC2 in human cancer', Critical Reviews in Oncology / Hematology, 111, 31–38. https://doi.org/10.1016/j.critrevonc.2017.01.003

Pandey, G. K., and Kanduri, C. (2015). 'Long noncoding RNAs and neuroblastoma', Oncotarget, 6(21), 18265.

Pandey, G. K., Mitra, S., Subhash, S., Hertwig, F., Kanduri, M., Mishra, K., Fransson, S., Ganeshram, A., Mondal, T., Bandaru, S., Östensson, M., Akyürek, L. M., Abrahamsson, J., Pfeifer, S., Larsson, E., Shi, L., Peng, Z., Fischer, M., Martinsson, T., Hedborg, F., Kogner, P. and Kanduri, C. (2014). 'The Risk-Associated Long Noncoding RNA NBAT-1 Controls Neuroblastoma Progression by Regulating Cell Proliferation and Neuronal Differentiation', Cancer Cell. https://doi.org/10.1016/j.ccell.2014.09.014

Pang, K. C., Frith, M. C., and Mattick, J. S. (2006). 'Rapid evolution of noncoding RNAs: lack of conservation does not mean lack of function', Trends in Genetics. https://doi.org/10.1016/j.tig.2005.10.003

Pelengaris, S., and Khan, M. (2003). 'The many faces of c-MYC', Archives of Biochemistry and Biophysics. https://doi.org/10.1016/S0003-9861(03)00294-7

Pelicano, H., Carney, D., and Huang, P. (2004). 'ROS stress in cancer cells and therapeutic implications', Drug Resistance Updates. https://doi.org/10.1016/j.drup.2004.01.004

Peng, F., Wang, R., Zhang, Y., Zhao, Z., Zhou, W., Chang, Z., and Gu, Y. (2017). 'Differential expression analysis at the individual level reveals a lncRNA prognostic signature for lung adenocarcinoma', Molecular Cancer. https://doi.org/10.1186/s12943-017-0666-z

Perng, P., and Lim, M. (2015). 'Immunosuppressive mechanisms of malignant gliomas: Parallels at non-CNS sites', Frontiers in Oncology. https://doi.org/10.3389/fonc.2015.00153

Pistritto, G., Trisciuoglio, D., Ceci, C., Alessia Garufi, and D'Orazi, G. (2016). 'Apoptosis as anticancer mechanism: Function and dysfunction of its modulators and targeted therapeutic strategies', Aging. https://doi.org/10.18632/aging.100934

Podhorecka, M., Ibanez, B., and Dmoszyńska, A. (2017). 'Metformin - it's potential anti-cancer and anti-ageing effects', Postepy Higieny I Medycyny Doswiadczalnej (Online). https://doi.org/10.5604/01.3001.0010.3801

Ponting, C. P., Oliver, P. L., and Reik, W. (2009). 'Evolution and Functions of Long Noncoding RNAs', Cell. https://doi.org/10.1016/j.cell.2009.02.006

Pop, S., Enciu, A. M., Necula, L. G., and Tanase, C. (2018). 'Long non-coding RNAs in brain tumours: Focus on recent epigenetic findings in glioma', Journal of Cellular and Molecular Medicine. https://doi.org/10.1111/jcmm.13781

Prados, M. D., Byron, S. A., Tran, N. L., Phillips, J. J., Molinaro, A. M., Ligon, K. L., Wen, P. Y., Kuhn, J. G., Mellinghoff, I. K., De Groot, J. F., Colman, H., Cloughesy, T. F., Chang, S. M., Ryken, T. C., Tembe, W. D., Kiefer, J. A., Berens, M. E., Craig, D. W., Carpten, J. D. and Trent, J. M. (2015). 'Toward precision medicine in glioblastoma: The promise and the challenges', Neuro-Oncology. https://doi.org/10.1093/neuonc/nov031

Pramanik, R., Qi, X., Borowicz, S., Choubey, D., Schultz, R. M., Han, J., and Chen, G. (2003). 'p38 Isoforms have opposite effects on AP-1-dependent transcription through regulation of c-Jun: The determinant role of the isoforms in the p38 MAPK signal specificity', Journal of Biological Chemistry. https://doi.org/10.1074/jbc.M207732200

Puiggros, A., Puigdecanet, E., Salido, M., Ferrer, A., Abella, E., Gimeno, E., Nonell, L., Herranz, M. J., Galván, A. B., Rodríguez-Rivera, M., Melero, C., Pairet, S., Bellosillo,

B., Serrano, S., Florensa, L., Solé, F. and Espinet, B. (2013). 'Genomic arrays in chronic lymphocytic leukemia routine clinical practice: Are we ready to substitute conventional cytogenetics and fluorescence in situ hybridization techniques?', Leukemia and Lymphoma. https://doi.org/10.3109/10428194.2012.731598

Qu, Y., Xiao, H., Xiao, W., Xiong, Z., Hu, W., Gao, Y., and Yang, H. (2018). 'Upregulation of MIAT Regulates LOXL2 Expression by Competitively Binding MiR-29c in Clear Cell Renal Cell Carcinoma', Cellular Physiology and Biochemistry : International Journal of Experimental Cellular Physiology, Biochemistry, and Pharmacology. https://doi.org/10.1159/000491974

Qureshi, I. A., and Mehler, M. F. (2012). 'Emerging roles of non-coding RNAs in brain evolution, development, plasticity and disease', Nature Reviews. Neuroscience, 13(8), 528–541. https://doi.org/10.1038/nrn3234

Qureshi, I. A., Mattick, J. S., and Mehler, M. F. (2010). 'Long non-coding RNAs in nervous system function and disease', Brain Research. https://doi.org/10.1016/j.brainres.2010.03.110

Rackham, O., Shearwood, A.-M. J., Mercer, T. R., Davies, S. M. K., Mattick, J. S., and Filipovska, A. (2011). 'Long noncoding RNAs are generated from the mitochondrial genome and regulated by nuclear-encoded proteins', RNA (New York, N.Y.). https://doi.org/10.1261/rna.029405.111

Radogna, F., Dicato, M., and Diederich, M. (2015). 'Cancer-type-specific crosstalk between autophagy, necroptosis and apoptosis as a pharmacological target', Biochemical Pharmacology. https://doi.org/10.1016/j.bcp.2014.12.018

Ramos, A. D., Attenello, F. J., and Lim, D. A. (2016). 'Uncovering the roles of long noncoding RNAs in neural development and glioma progression', Neuroscience Letters. https://doi.org/10.1016/j.neulet.2015.12.025

Rao, A. K. D. M., Rajkumar, T., and Mani, S. (2017). 'Perspectives of long non-coding RNAs in cancer', Molecular Biology Reports. https://doi.org/10.1007/s11033-017-4103-6

Rao, S. Q., Hu, H. L., Ye, N., Shen, Y., and Xu, Q. (2014). 'Genetic variants in long non-coding RNA MIAT contribute to risk of paranoid schizophrenia in a Chinese Han population' Schizophrenia Research. https://doi.org/10.1016/j.schres.2015.04.032

Rashi-Elkeles, S., Elkon, R., Shavit, S., Lerenthal, Y., Linhart, C., Kupershtein, A., Amariglio, N., Rechavi, G., Shamir, R. and Shilo, Y. (2011). 'Transcriptional modulation

induced by ionizing radiation: P53 remains a central player', Molecular Oncology. https://doi.org/10.1016/j.molonc.2011.06.004

Ratner, N., Brodeur, G. M., Dale, R. C., and Schor, N. F. (2016). 'The "neuro" of neuroblastoma: Neuroblastoma as a neurodevelopmental disorder', Annals of Neurology. https://doi.org/10.1002/ana.24659

Reardon, D. A., and Mitchell, D. A. (2017). 'The development of dendritic cell vaccine-based immunotherapies for glioblastoma', Seminars in Immunopathology. https://doi.org/10.1007/s00281-016-0616-7

Reon, B. J., Anaya, J., Zhang, Y., Mandell, J., Purow, B., Abounader, R., and Dutta, A. (2016). 'Expression of lncRNAs in Low-Grade Gliomas and Glioblastoma Multiforme: An In Silico Analysis', PLoS Medicine. https://doi.org/10.1371/journal.pmed.1002192

Rijal, N. (2015). 'Acridine Orange Staining: Principle, Procedure, Results and Applications', Microbeonline.

Rizos, C. V., and Elisaf, M. S. (2013). 'Metformin and cancer', European Journal of Pharmacology. https://doi.org/10.1016/j.ejphar.2013.02.038

Rodic, S., and Vincent, M. D. (2018). 'Reactive oxygen species (ROS) are a key determinant of cancer's metabolic phenotype', International Journal of Cancer. https://doi.org/10.1002/ijc.31069

Rogers, L. M., Riordan, J. D., Swick, B. L., Meyerholz, D. K., and Dupuy, A. J. (2013). 'Ectopic expression of Zmiz1 induces cutaneous squamous cell malignancies in a mouse model of cancer', Journal of Investigative Dermatology. https://doi.org/10.1038/jid.2013.77

Rombaut, D., Chiu, H. S., Decaesteker, B., Everaert, C., Yigit, N., Peltier, A., Janoueix, I., Bartenhagen, C., Fischer, M., Roberts, S., D'Haene, N., De Preter, K., Speleman, F., Denecker, G., Sumazin, P., Vandesompele, J., Lefever, S. and Mestdagh, P. (2019). 'Integrative analysis identifies lincRNAs up- and downstream of neuroblastoma driver genes', Scientific Reports. https://doi.org/10.1038/s41598-019-42107-y

Romero-Barrios, N., Legascue, M. F., Benhamed, M., Ariel, F., and Crespi, M. (2018). 'Splicing regulation by long noncoding RNAs', Nucleic Acids Research. https://doi.org/10.1093/nar/gky095

Russell, M. R., Penikis, A., Oldridge, D. A., Alvarez-Dominguez, J. R., McDaniel, L., Diamond, M., Padovan, O., Raman, P., Li, Y., Wei, J. S., Zhang, S., Gnanchandran, J., Seeger, R., Asgharzadeh, S., Khan, J., Diskin, S. J., Maris, J. M. and Cole, K. A.

(2015). ‘CASC15-S is a tumor suppressor lncRNA at the 6p22 neuroblastoma susceptibility locus’, Cancer Research. https://doi.org/10.1158/0008-5472.CAN-14-3613

Ryall, S., Tabori, U., and Hawkins, C. (2017). ‘A comprehensive review of paediatric low-grade diffuse glioma: pathology, molecular genetics and treatment’, Brain Tumor Pathology. https://doi.org/10.1007/s10014-017-0282-z

Saadeh, F. S., Mahfouz, R., and Assi, H. I. (2018). ‘Egfr as a clinical marker in glioblastomas and other gliomas’, International Journal of Biological Markers. https://doi.org/10.5301/ijbm.5000301

Saeinasab, M., Bahrami, A. R., González, J., Marchese, F. P., Martinez, D., Mowla, S. J., Matin, M. M. and Huarte, M. (2019). ‘SNHG15 is a bifunctional MYC-regulated noncoding locus encoding a lncRNA that promotes cell proliferation, invasion and drug resistance in colorectal cancer by interacting with AIF’, Journal of Experimental and Clinical Cancer Research. https://doi.org/10.1186/s13046-019-1169-0

Safe, S., Abbruzzese, J., Abdelrahim, M., and Hedrick, E. (2018). ‘Specificity protein transcription factors and cancer: Opportunities for drug development’, Cancer Prevention Research. https://doi.org/10.1158/1940-6207.CAPR-17-0407

Sahra, I. Ben, Marchand-Brustel, Y. Le, Tanti, J. F., and Bost, F. (2010). ‘Metformin in cancer therapy: A new perspective for an old antidiabetic drug?’, Molecular Cancer Therapeutics. https://doi.org/10.1158/1535-7163.MCT-09-1186

Sahu, D., Ho, S.-Y., Juan, H.-F., and Huang, H.-C. (2018). ‘High-risk, expression-based Prognostic Long Noncoding RNA Signature in Neuroblastoma’, JNCI Cancer Spectrum. https://doi.org/10.1093/jncics/pky015

Sahu, D., Hsu, C. L., Lin, C. C., Yang, T. W., Hsu, W. M., Ho, S. Y., and Huang, H. C. (2016). ‘Co-expression analysis identifies long noncoding RNA SNHG1 as a novel predictor for event-free survival in neuroblastoma’, Oncotarget. https://doi.org/10.18632/oncotarget.11158

Saito, R., and Tominaga, T. (2017). ‘Convection-enhanced delivery of therapeutics for malignant gliomas’, Neurologia Medico-Chirurgica. https://doi.org/10.2176/nmc.ra.2016-0071

Salehi, S., Taheri, M. N., Azarpira, N., Zare, A., and Behzad-Behbahani, A. (2017). ‘State of the art technologies to explore long non-coding RNAs in cancer’, Journal of Cellular and Molecular Medicine. https://doi.org/10.1111/jcmm.13238

Sampetrean, O., and Saya, H. (2018). 'Modeling phenotypes of malignant gliomas. Cancer Science', https://doi.org/10.1111/cas.13351

Sattari, A., Siddiqui, H., Moshiri, F., Ngankeu, A., Nakamura, T., Kipps, T. J., and Croce, C. M. (2016). 'Upregulation of long noncoding RNA MIAT in aggressive form of chronic lymphocytic leukemias', Oncotarget. https://doi.org/10.18632/oncotarget.11099

Schmitz, S. U., Grote, P., and Herrmann, B. G. (2016). 'Mechanisms of long noncoding RNA function in development and disease', Cellular and Molecular Life Sciences. https://doi.org/10.1007/s00018-016-2174-5

Schuffner, A., Morshedi, M., Vaamonde, D., Duran, E. H., and Oehninger, S. (2002). 'Effect of different incubation conditions on phosphatidylserine externalization and motion parameters of purified fractions of highly motile human spermatozoa', Journal of Andrology. https://doi.org/10.1002/j.1939-4640.2002.tb02615.x

Schulten, H. J., and Bakhashab, S. (2019). 'Meta-analysis of microarray expression studies on metformin in cancer cell lines', International Journal of Molecular Sciences. https://doi.org/10.3390/ijms20133173

Seim, I., Amorim, L., Walpole, C., Carter, S., Chopin, L. K., and Herington, A. C. (2010). 'Ghrelin gene-related peptides: Multifunctional endocrine/autocrine modulators in health and disease'. In Clinical and Experimental Pharmacology and Physiology. https://doi.org/10.1111/j.1440-1681.2009.05241.x

Sha, M., Lin, M., Wang, J., Ye, J., Xu, J., Xu, N., and Huang, J. (2018). 'Long non-coding RNA MIAT promotes gastric cancer growth and metastasis through regulation of miR-141/DDX5 pathway', Journal of Experimental and Clinical Cancer Research. https://doi.org/10.1186/s13046-018-0725-3

Shankar, G. M., Kirtane, A. R., Miller, J. J., Mazdiyasni, H., Rogner, J., Tai, T., Williams, E. A., Higuchi, F., Juratli, T. A., Tateishi, K., Koerner, M. V.A., Tummala, S. S., Fink, A. L., Penson, T., Schmidt, S. P., Wojtkiewicz, G. R., Baig, A., Francis, J. M., Rinne, M. L., Batten, J. M., Batchelor, T. T., Brastianos, P. K., Curry, W. T., Barker, F. G., Jordan, J. T., Iafrate, A. J., Chi, A. S, Lennerz, J. K., Meyerson, M., Langer, R., Wakimoto, H., Traverso, G. and Cahill, D. P. (2018). 'Genotype-targeted local therapy of glioma', Proceedings of the National Academy of Sciences of the United States of America. https://doi.org/10.1073/pnas.1805751115

Shao, Q., Wang, Q., and Wang, J. (2019). 'LncRNA SCAMP1 regulates ZEB1/JUN and autophagy to promote pediatric renal cell carcinoma under oxidative stress via

miR-429', Biomedicine and Pharmacotherapy. https://doi.org/10.1016/j.biopha.2019.109460

Shao, S., Tian, J., Zhang, H., and Wang, S. (2018). 'LncRNA myocardial infarction-associated transcript promotes cell proliferation and inhibits cell apoptosis by targeting miR-330-5p in epithelial ovarian cancer cells', Biomedicine and Pharmacotherapy, 14(6), 1263–1270.

Sheik Mohamed, J., Gaughwin, P. M., Lim, B., Robson, P., and Lipovich, L. (2010). 'Conserved long noncoding RNAs transcriptionally regulated by Oct4 and Nanog modulate pluripotency in mouse embryonic stem cells', RNA (New York, N.Y.), 16(2), 324–337. https://doi.org/10.1261/rna.1441510

Shen, Y., Dong, L. F., Zhou, R. M., Yao, J., Song, Y. C., Yang, H., Jiang, Q. and Yan, B. (2016). 'Role of long non-coding RNA MIAT in proliferation, apoptosis and migration of lens epithelial cells: A clinical and in vitro study', Journal of Cellular and Molecular Medicine, 20(3), 537–548. https://doi.org/10.1111/jcmm.12755

Shi, J., Dong, B., Cao, J., Mao, Y., Guan, W., Peng, Y., and Wang, S. (2017). 'Long non-coding RNA in glioma: Signaling pathways', Oncotarget. https://doi.org/10.18632/oncotarget.15175

Shi, L., Hong, X., Ba, L., He, X., Xiong, Y., Ding, Q., Yang, S. and Peng, G. (2019). 'Long non-coding RNA ZNFX1-AS1 promotes the tumor progression and metastasis of colorectal cancer by acting as a competing endogenous RNA of miR-144 to regulate EZH2 expression', Cell Death and Disease. https://doi.org/10.1038/s41419-019-1332-8

Shohet, J., and Foster, J. (2017). 'Neuroblastoma', The BMJ, 357. https://doi.org/10.1136/bmj j1836

Shortt, J., Ott, C. J., Johnstone, R. W., and Bradner, J. E. (2017). 'A chemical probe toolbox for dissecting the cancer epigenome', Nature Reviews Cancer. https://doi.org/10.1038/nrc.2016.148

Silva, G. Á. F., Nunes, R. A. L., Morale, M. G., Boccardo, E., Aguayo, F., and Termini, L. (2018). 'Oxidative stress: therapeutic approaches for cervical cancer treatment', Clinics (Sao Paulo, Brazil). https://doi.org/10.6061/clinics/2018/e548s

Singhal, S. S., Nagaprashantha, L., Singhal, P., Singhal, S., Singhal, J., Awasthi, S., and Horne, D. (2017). 'RLIP76 Inhibition: A Promising Developmental Therapy for Neuroblastoma', Pharmaceutical Research. https://doi.org/10.1007/s11095-017-2154-y

Slack, F. J., and Chinnaiyan, A. M. (2019). 'The Role of Non-coding RNAs in Oncology', Cell. https://doi.org/10.1016/j.cell.2019.10.017

Smallegan, M. J., and Rinn, J. L. (2019). 'Linking long noncoding RNA to drug resistance', Proceedings of the National Academy of Sciences of the United States of America. https://doi.org/10.1073/pnas.1915690116

Soleyman-Jahi, S., Sadeghi, F., Pastaki Khoshbin, A., Khani, L., Roosta, V., and Zendehdel, K. (2019). 'Attribution of Ghrelin to Cancer; Attempts to Unravel an Apparent Controversy', Frontiers in Oncology. https://doi.org/10.3389/fonc.2019.01014

Sone, M., Hayashi, T., Tarui, H., Agata, K., Takeichi, M., and Nakagawa, S. (2007). 'The mRNA-like noncoding RNA Gomafu constitutes a novel nuclear domain in a subset of neurons', Journal of Cell Science, 120(Pt 15), 2498–2506. https://doi.org/10.1242/jcs.009357

Spitale, R. C., Tsai, M. C., and Chang, H. Y. (2011). 'RNA templating the epigenome: Long noncoding RNAs as molecular scaffolds', Epigenetics, 6(5), 539–543. https://doi.org/10.4161/epi.6.5.15221

Stepp, H., and Stummer, W. (2018). '5-ALA in the management of malignant glioma', Lasers in Surgery and Medicine. https://doi.org/10.1002/lsm.22933

Stevens, M., and Oltean, S. (2019). 'Modulation of the Apoptosis Gene Bcl-x Function Through Alternative Splicing', Frontiers in Genetics. https://doi.org/10.3389/fgene.2019.00804

Stewart, S. E., Ashkenazi, A., Williamson, A., Rubinsztein, D. C., and Moreau, K. (2018). 'Transbilayer phospholipid movement facilitates the translocation of annexin across membranes', Journal of Cell Science. https://doi.org/10.1242/jcs.217034

Sturm, D., Bender, S., Jones, D. T. W., Lichter, P., Grill, J., Becher, O., Hawkins, C., Majewski, J., Jones, C., Costello, J. F., Iavarone, A., Aldape, K., Brennan, C. W., Jabado, N. and Pfister, S. M. (2014). 'Paediatric and adult glioblastoma: multiform (epi)genomic culprits emerge', Nature Reviews. Cancer, 14(2), 92–107. https://doi.org/10.1038/nrc3655

Sun, F., Liang, W., and Qian, J. (2019). 'The identification of CRNDE, H19, UCA1 and HOTAIR as the key lncRNAs involved in oxaliplatin or irinotecan resistance in the chemotherapy of colorectal cancer based on integrative bioinformatics analysis', Molecular Medicine Reports. https://doi.org/10.3892/mmr.2019.10588

Sun, H., Huang, Z., Sheng, W., and Xu, M. D. (2018). 'Emerging roles of long non-coding RNAs in tumor metabolism', Journal of Hematology and Oncology. https://doi.org/10.1186/s13045-018-0648-7

Sun, J., Liu, L., Zou, H., and Yu, W. (2019). 'The long non-coding RNA casc2 suppresses cell viability, migration, and invasion in hepatocellular carcinoma cells by directly downregulating mir-183.', Yonsei Medical Journal. https://doi.org/10.3349/ymj.2019.60.10.905

Sun, Y., Atmadibrata, B., Yu, D., Wong, M., Liu, B., Ho, N. and Liu, T. (2017). 'Upregulation of LYAR induces neuroblastoma cell proliferation and survival', Cell Death and Differentiation. https://doi.org/10.1038/cdd.2017.98

Takeuchi, Y., Tanaka, T., Higashi, M., Fumino, S., Iehara, T., Hosoi, H., Sakai, T. and Tajiri, T. (2018). 'In vivo effects of short- and long-term MAPK pathway inhibition against neuroblastoma', Journal of Pediatric Surgery. https://doi.org/10.1016/j.jpedsurg.2018.08.026

Tang, W., Dong, K., Li, K., Dong, R., and Zheng, S. (2016). 'MEG3, HCN3 and linc01105 influence the proliferation and apoptosis of neuroblastoma cells via the HIF-1α and p53 pathways', Scientific Reports. https://doi.org/10.1038/srep36268

Tay, Y., Rinn, J., and Pandolfi, P. P. (2014). 'The multilayered complexity of ceRNA crosstalk and competition', Nature. https://doi.org/10.1038/nature12986

Thompson, and Sontheimer. (2019). 'Acetylcholine Receptor Activation as a Modulator of Glioblastoma Invasion', Cells. https://doi.org/10.3390/cells8101203

Tian, T., Lv, X., Pan, G., Lu, Y., Chen, W., He, W., Lei, X., Zhang, H., Liu, M., Sun, S., Ou, Z., Lin, X., Cai, L., He, L., Tu, Z., Wang, X., Tannous, B. A., Ferrone, S., Li, J. and Fan, S. (2019). 'Long noncoding RNA MPRL promotes mitochondrial fission and cisplatin chemosensitivity via disruption of Pre-miRNA processing', Clinical Cancer Research. https://doi.org/10.1158/1078-0432.CCR-18-2739

Tolbert, V. P., and Matthay, K. K. (2018). 'Neuroblastoma: clinical and biological approach to risk stratification and treatment', Cell and Tissue Research. https://doi.org/10.1007/s00441-018-2821-2

Torres, L., Sandoval, J., Penella, E., Zaragozá, R., García, C., Rodríguez, J. L., Viña, J. R. and García-Trevijano, E. R. (2009). 'In vivo GSH depletion induces c-Myc expression by modulation of chromatin protein complexes', Free Radical Biology and Medicine. https://doi.org/10.1016/j.freeradbiomed.2009.03.005

Tran, D. D. H., Kessler, C., Niehus, S. E., Mahnkopf, M., Koch, A., and Tamura, T. (2018). 'Myc target gene, long intergenic noncoding RNA, Linc00176 in hepatocellular carcinoma regulates cell cycle and cell survival by titrating tumor suppressor microRNAs', Oncogene. https://doi.org/10.1038/onc.2017.312

Tripathi, V., Ellis, J. D., Shen, Z., Song, D. Y., Pan, Q., Watt, A. T., Freier, S. M., Bennett, C. F., Sharma, A., Bubulya, P. A., Blencowe, B. J., Prasanth, S. G. and Prasanth, K. V. (2010). 'The nuclear-retained noncoding RNA MALAT1 regulates alternative splicing by modulating SR splicing factor phosphorylation', Molecular Cell, 39(6), 925–938. https://doi.org/10.1016/j.molcel.2010.08.011

Tsai, K. W., Lo, Y. H., Liu, H., Yeh, C. Y., Chen, Y. Z., Hsu, C. W. and Wang, J. H. (2018). 'Linc00659, a long noncoding RNA, acts as novel oncogene in regulating cancer cell growth in colorectal cancer', Molecular Cancer. https://doi.org/10.1186/s12943-018-0821-1

Tsai, M.-C., Manor, O., Wan, Y., Mosammaparast, N., Wang, J. K., Lan, F., Shi, Y., Segal, E. and Chang, H. Y. (2010). 'Long noncoding RNA as modular scaffold of histone modification complexes', Science (New York, N.Y.), 329(5992), 689–693. https://doi.org/10.1126/science.1192002

Tseng, S. C., Huang, Y. C., Chen, H. J., Chiu, H. C., Huang, Y. J., Wo, T. Y. and Lin, Y. W. (2013). 'Metformin-mediated downregulation of p38 mitogen-activated protein kinase-dependent excision repair cross-complementing 1 decreases DNA repair capacity and sensitizes human lung cancer cells to paclitaxel', Biochemical Pharmacology. https://doi.org/10.1016/j.bcp.2012.12.001

Tsuiji, H., Yoshimoto, R., Hasegawa, Y., Furuno, M., Yoshida, M., and Nakagawa, S. (2011). 'Competition between a noncoding exon and introns: Gomafu contains tandem UACUAAC repeats and associates with splicing factor-1', Genes to Cells, 16(5), 479–490. https://doi.org/10.1111/j.1365-2443.2011.01502.x

Tummers, B., and Green, D. R. (2017). 'Caspase-8: regulating life and death', Immunological Reviews. https://doi.org/10.1111/imr.12541

Upadhyaya, B., Liu, Y., and Dey, M. (2019). 'Phenethyl isothiocyanate exposure promotes oxidative stress and suppresses sp1 transcription factor in cancer stem cells', International Journal of Molecular Sciences. https://doi.org/10.3390/ijms20051027

Utnes, P., Løkke, C., Flægstad, T., and Einvik, C. (2019). 'Clinically Relevant Biomarker Discovery in High-Risk Recurrent Neuroblastoma', Cancer Informatics. https://doi.org/10.1177/1176935119832910

Vadie, N., Saayman, S., Lenox, A., Ackley, A., Clemson, M., Burdach, J., Hart, J., Vogt, P. K. and Morris, K. V. (2015). 'MYCNOS functions as an antisense RNA regulating MYCN', RNA Biology. https://doi.org/10.1080/15476286.2015.1063773

Vafa, O., Wade, M., Kern, S., Beeche, M., Pandita, T. K., Hampton, G. M., and Wahl, G. M. (2002). 'c-Myc can induce DNA damage, increase reactive oxygen species, and mitigate p53 function: A mechanism for oncogene-induced genetic instability', Molecular Cell, 9(5), 1031–1044. https://doi.org/10.1016/S1097-2765(02)00520-8

Vallabhapurapu, S. D., Blanco, V. M., Sulaiman, M. K., Vallabhapurapu, S. L., Chu, Z., Franco, R. S., and Qi, X. (2015). 'Variation in human cancer cell external phosphatidylserine is regulated by flippase activity and intracellular calcium', Oncotarget. https://doi.org/10.18632/oncotarget.6045

van Heesch, S., van Iterson, M., Jacobi, J., Boymans, S., Essers, P. B., de Bruijn, E., Hao, W., MacInnes, A. W., Cuppen, E. and Simonis, M. (2014). 'Extensive localization of long noncoding RNAs to the cytosol and mono- and polyribosomal complexes', Genome Biology, 15(1), R6. https://doi.org/10.1186/gb-2014-15-1-r6

Vasilikos, L., Spilgies, L. M., Knop, J., and Wong, W. W. L. (2017). 'Regulating the balance between necroptosis, apoptosis and inflammation by inhibitors of apoptosis proteins', Immunology and Cell Biology. https://doi.org/10.1038/icb.2016.118

Velimezi, G., Robinson-Garcia, L., Muñoz-Martínez, F., Wiegant, W. W., Ferreira Da Silva, J., Owusu, M., Moder, M., Wiedner, M., Rosenthal, S.B., Fisch, K. M., Moffat, J., Menche, J., Van Attikum, H., Jackson, S. P. and Loizou, J. I. (2018). 'Map of synthetic rescue interactions for the Fanconi anemia DNA repair pathway identifies USP48', Nature Communications. https://doi.org/10.1038/s41467-018-04649-z

Vial, G., Detaille, D., and Guigas, B. (2019). 'Role of mitochondria in the mechanism(s) of action of metformin', Frontiers in Endocrinology. https://doi.org/10.3389/fendo.2019.00294

Vidyasekar, P., Shyamsunder, P., Arun, R., Santhakumar, R., Kapadia, N. K., Kumar, R., and Verma, R. S. (2015). 'Genome-wide expression profiling of cancer cell lines cultured in microgravity reveals significant dysregulation of cell cycle and MicroRNA gene networks', PLoS ONE. https://doi.org/10.1371/journal.pone.0135958

Wang, C., Ke, S., Li, M., Lin, C., Liu, X., and Pan, Q. (2019). 'Downregulation of LncRNA GAS5 promotes liver cancer proliferation and drug resistance by decreasing PTEN expression', Molecular Genetics and Genomics. https://doi.org/10.1007/s00438-019-01620-5

Wang, D., Wang, C., Wang, L., and Chen, Y. (2019). 'A comprehensive review in improving delivery of small-molecule chemotherapeutic agents overcoming the blood-brain/brain tumor barriers for glioblastoma treatment', Drug Delivery. https://doi.org/10.1080/10717544.2019.1616235

Wang, Ji, Xie, S., Yang, J., Xiong, H., Jia, Y., Zhou, Y., and Zhou, J. (2019). 'The long noncoding RNA H19 promotes tamoxifen resistance in breast cancer via autophagy', Journal of Hematology and Oncology. https://doi.org/10.1186/s13045-019-0747-0

Wang, Jiguang, Cazzato, E., Ladewig, E., Frattini, V., Rosenbloom, D. I. S., Zairis, S., Abate, F., Liu, Z., Elliott, O., Shin, Y. J., Lee, J. K., Lee, I. H., Park, W. Y., Eoli, M., Blumberg, A. J., Lasorella, A., Nam, D. H., Finocchiaro, G., Iavarone, A. and Rabadan, R. (2016). 'Clonal evolution of glioblastoma under therapy', Nature Genetics. https://doi.org/10.1038/ng.3590

Wang, Jing, Wang, Z., Yao, W., Dong, K., Zheng, S., and Li, K. (2019). 'The Association between lncRNA LINC01296 and the Clinical Characteristics in Neuroblastoma', Journal of Pediatric Surgery. https://doi.org/10.1016/j.jpedsurg.2019.08.032

Wang, K. C., and Chang, H. Y. (2011). 'Molecular Mechanisms of Long Noncoding RNAs', Molecular Cell. https://doi.org/10.1016/j.molcel.2011.08.018

Wang, K. C., Yang, Y. W., Liu, B., Sanyal, A., Corces-Zimmerman, R., Chen, Y., Lajoie, B. R., Protacio, A., Flynn, R. A., Gupta, R. A., Wysocka, J., Lei, M., Dekker, J., Helms, J. A. and Chang, H. Y. (2011). 'A long noncoding RNA maintains active chromatin to coordinate homeotic gene expression', Nature, 472(7341), 120–124. https://doi.org/10.1038/nature09819

Wang, M. J., Liu, S., Liu, Y., and Zheng, D. (2007). 'Actinomycin D enhances TRAIL-induced caspase-dependent and -independent apoptosis in SH-SY5Y neuroblastoma cells', Neuroscience Research, 59(1), 40–46. https://doi.org/10.1016/j.neures.2007.05.010

Wang, P., Liu, Y. hui, Yao, Y. long, Li, Z., Li, Z. qing, Ma, J., and Xue, Y. (2015). 'Long non-coding RNA CASC2 suppresses malignancy in human gliomas by miR-21', Cellular Signalling, 27(2), 275–282. https://doi.org/10.1016/j.cellsig.2014.11.011

Wang, Renjie, Zhao, L., Ji, L., Bai, L., and Wen, Q. (2019). 'Myocardial infarction associated transcript (MIAT) promotes papillary thyroid cancer progression via sponging miR-212', Biomedicine and Pharmacotherapy. https://doi.org/10.1016/j.biopha.2019.109298

Wang, Ronglin, Li, Y., Zhu, G., Tian, B., Zeng, W., Yang, Y., and Li, Z. (2017). 'Long noncoding RNA CASC2 predicts the prognosis of glioma patients and functions as a suppressor for gliomas by suppressing Wnt/β-catenin signaling pathway', Neuropsychiatric Disease and Treatment, 13, 1805–1813. https://doi.org/10.2147/NDT.S137171

Wang, S. S., Hsiao, R., Limpar, M. M., Lomahan, S., Tran, T. A., Maloney, N. J. and Tang, X. X. (2014). 'Destabilization of MYC/MYCN by the mitochondrial inhibitors, metaiodobenzylguanidine, metformin and phenformin', International Journal of Molecular Medicine. https://doi.org/10.3892/ijmm.2013.1545

Wang, T., Ma, S., Qi, X., Tang, X., Cui, D., Wang, Z., and Zhai, B. (2016). 'Long noncoding RNA ZNFX1-AS1 suppresses growth of hepatocellular carcinoma cells by regulating the methylation of miR-9', OncoTargets and Therapy. https://doi.org/10.2147/OTT.S103329

Wang, W., Song, J., Zhang, W., Tang, Y., Luo, R., Ran, L., and Song, F. (2019). 'Identification of Long Non-Coding RNA Signatures for Specific Disease-Free Prognosis in Clear Cell Renal Carcinoma', IEEE Access. https://doi.org/10.1109/access.2019.2929588

Wang, Xiangting, Arai, S., Song, X., Reichart, D., Du, K., Pascual, G., Tempst, P., Rosenfeld, M. G., Glass, C. K. and Kurokawa, R. (2008). 'Induced ncRNAs allosterically modify RNA-binding proteins in cis to inhibit transcription', Nature, 454(7200), 126–130. https://doi.org/10.1038/nature06992

Wang, Xiaolong, Yan, Y., Zhang, C., Wei, W., Ai, X., Pang, Y., and Bian, Y. (2018). 'Upregulation of lncRNA PlncRNA-1 indicates the poor prognosis and promotes glioma progression by activation of Notch signal pathway', Biomedicine and Pharmacotherapy. https://doi.org/10.1016/j.biopha.2018.03.150

Wang, Xiaoqian, Yang, B., She, Y., and Ye, Y. (2018). 'The lncRNA TP73-AS1 promotes ovarian cancer cell proliferation and metastasis via modulation of MMP2 and MMP9', Journal of Cellular Biochemistry. https://doi.org/10.1002/jcb.27158

Wang, Y., Xu, Z., Jiang, J., Xu, C., Kang, J., Xiao, L., Wu, M., Xiong, J., Guo, X. and Liu, H. (2013).' Endogenous miRNA Sponge lincRNA-RoR Regulates Oct4, Nanog, and Sox2 in Human Embryonic Stem Cell Self-Renewal', Developmental Cell. https://doi.org/10.1016/j.devcel.2013.03.002

Wapinski, O., and Chang, H. Y. (2011). 'Long noncoding RNAs and human disease', Trends in Cell Biology. https://doi.org/10.1016/j.tcb.2011.04.001

Watters, K. M., Bryan, K., Foley, N. H., Meehan, M., and Stallings, R. L. (2013). 'Expressional alterations in functional ultra-conserved non-coding RNAs in response to all-trans retinoic acid-induced differentiation in neuroblastoma cells', BMC Cancer, 13, 184. https://doi.org/10.1186/1471-2407-13-184

Watts, J., and Corey, D. (2012). 'Gene silencing by siRNAs and antisense oligonucleotides in the laboratory and the clinic', The Journal of Pathology. https://doi.org/10.1002/path.2993.Gene

Wei, J. S., Song, Y. K., Durinck, S., Chen, Q. R., Cheuk, A. T. C., Tsang, P., Zhang, Q., Thiele, C. J., Slack, A., Shohet, J. and Khan, J. (2008). 'The MYCN oncogene is a direct target of miR-34a', Oncogene. https://doi.org/10.1038/onc.2008.154

Wei, J., Wang, B., Wang, H., Meng, L., Zhao, Q., Li, X., Xin, Y. and Jiang, X. (2019). 'Radiation-induced normal tissue damage: oxidative stress and epigenetic mechanisms', Oxidative Medicine and Cellular Longevity. https://doi.org/10.1155/2019/3010342

Weldy, C. S., Luttrell, I. P., White, C. C., Morgan-Stevenson, V., Bammler, T. K., Beyer, R. P., Afsharinejad, Z., Kim, F., Chitaley, K. and Kavanagh, T. J. (2012). 'Glutathione (GSH) and the GSH synthesis gene Gclm modulate vascular reactivity in mice', Free Radical Biology and Medicine. https://doi.org/10.1016/j.freeradbiomed.2012.07.006

Weller, M., Wick, W., Aldape, K., Brada, M., Berger, M., Pfister, S. M., Nishikawa, R., Rosenthal, M., Wen, P. Y., Stupp, R. and Reifenberger, G. (2015). 'Glioma'. Nature Reviews Disease Primers, (July), 15017. https://doi.org/10.1038/nrdp.2015.17

Weng, W. C., Lin, K. H., Wu, P. Y., Ho, Y. H., Liu, Y. L., Wang, B. J., and Lee, H. (2017). 'VEGF expression correlates with neuronal differentiation and predicts a favorable prognosis in patients with neuroblastoma', Scientific Reports. https://doi.org/10.1038/s41598-017-11637-8

Wesseling, P., and Capper, D. (2018). 'WHO 2016 Classification of gliomas', Neuropathology and Applied Neurobiology. https://doi.org/10.1111/nan.12432

Westphal, M., and Lamszus, K. (2015). 'Circulating biomarkers for gliomas', Nature Reviews Neurology. https://doi.org/10.1038/nrneurol.2015.171

White, E., and DiPaola, R. S. (2009). 'The double-edged sword of autophagy modulation in cancer', Clinical Cancer Research. https://doi.org/10.1158/1078-0432.CCR-07-5023

Wiendl, H., Mitsdoerffer, M., Hofmeister, V., Wischhusen, J., Bornemann, A., Meyermann, R., Weiss, E. H. Melms, A. and Weller, M. (2002). 'A Functional Role of HLA-G Expression in Human Gliomas: An Alternative Strategy of Immune Escape', The Journal of Immunology. https://doi.org/10.4049/jimmunol.168.9.4772

Wiestler, B., Capper, D., Holland-Letz, T., Korshunov, A., Von Deimling, A., Pfister, S. M., Platten, M., Weller, M. and Wick, W. (2013). 'ATRX loss refines the classification of anaplastic gliomas and identifies a subgroup of IDH mutant astrocytic tumours with better prognosis', Acta Neuropathologica. https://doi.org/10.1007/s00401-013-1156-z

Wilusz, J. E., Sunwoo, H., and Spector, D. L. (2009). 'Long noncoding RNAs: functional surprises from the RNA world', Genes and Development. https://doi.org/10.1101/gad.1800909

Wright, J. H. (1910). 'Neurocytoma or neuroblastoma, a kind of tumor not generally recognized', Journal of Experimental Medicine. https://doi.org/10.1084/jem.12.4.556

Wu, L., Liu, C., and Zhang, Z. (2020). 'Knockdown of lncRNA MIAT inhibits proliferation and cisplatin resistance in non-small cell lung cancer cells by increasing miR-184 expression', Oncology Letters, 19(1), 533–541.

Wu, R., Su, Y., Wu, H., Dai, Y., Zhao, M., and Lu, Q. (2016). 'Characters, functions and clinical perspectives of long non-coding RNAs', Molecular Genetics and Genomics. https://doi.org/10.1007/s00438-016-1179-y

Wu, S., Liu. J., Wang, X., Li, M., Chen, Z., and Tang, Y. (2017). 'Aberrant expression of the long non-coding RNA GHRLOS and its prognostic significance in patients with colorectal cancer', Journal of Cancer. https://doi.org/10.7150/jca.21304

Wu, Y., Zheng, Q., Li, Y., Wang, G., Gao, S., Zhang, X. and Wang, B. (2019). 'Metformin targets a YAP1-TEAD4 complex via AMPKα to regulate CCNE1/2 in bladder cancer cells', Journal of Experimental and Clinical Cancer Research. https://doi.org/10.1186/s13046-019-1346-1

Xiang, Y., Huang, Y., Sun, H., Pan, Y., Wu, M., and Zhang, J. (2019). 'Deregulation of miR-520d-3p promotes hepatocellular carcinoma development via lncRNA MIAT regulation and EPHA2 signaling activation', Biomedicine and Pharmacotherapy. https://doi.org/10.1016/j.biopha.2018.11.014

Xiao, S., Wang, R., Wu, X., Liu, W., and Ma, S. (2018). 'The Long Noncoding RNA TP73-AS1 Interacted with miR-124 to Modulate Glioma Growth by Targeting Inhibitor

of Apoptosis-Stimulating Protein of p53', DNA and Cell Biology. https://doi.org/10.1089/dna.2017.3941

Xie, N., Qi, J., Li, S., Deng, J., Chen, Y., and Lian, Y. (2019). 'Upregulated lncRNA small nucleolar RNA host gene 1 promotes 1-methyl-4-phenylpyridinium ion-induced cytotoxicity and reactive oxygen species production through miR-15b-5p/GSK3β axis in human dopaminergic SH-SY5Y cells', Journal of Cellular Biochemistry. https://doi.org/10.1002/jcb.27865

Xing, H. B., Qiu, H. M., Li, Y., Dong, P. F., and Zhu, X. M. (2019). 'Long noncoding RNA CASC2 alleviates the growth, migration and invasion of oral squamous cell carcinoma via downregulating CDK1', European Review for Medical and Pharmacological Sciences. https://doi.org/10.26355/eurrev_201906_18060

Xiuyun, L. I., Wang, X., Li, M. A. O., Zhao, S., and Haidong, W. E. I. (2018). 'LncRNA TP73-AS1 predicts poor prognosis and promotes cell proliferation in ovarian cancer via cell cycle and apoptosis regulation', Molecular Medicine Reports. https://doi.org/10.3892/mmr.2018.8951

Xu, D.-F., Wang, L.-S., and Zhou, J.-H. (2020). 'Long non-coding RNA CASC2 suppresses pancreatic cancer cell growth and progression by regulating the miR-24/MUC6 axis', International Journal of Oncology, 56(2), 494–507.

Xu, Q. Q., Liang, S. W., Gu, J. H., Huang, Z. G., Dang, Y. W. and Chen, G. (2019). 'A novel risk signature that combines 10 long noncoding RNAs to predict neuroblastoma prognosis', Journal of Cellular Physiology. https://doi.org/10.1002/jcp.29277

Yan, B., Yao, J., Liu, J. Y., Li, X. M., Wang, X. Q., Li, Y. J., Tao, Z. F., Song, Y. C. and Chen Q. (2015). 'LncRNA-MIAT regulates microvascular dysfunction by functioning as a competing endogenous RNA', Circulation Research, 116(7), 1143–1156. https://doi.org/10.1161/CIRCRESAHA.116.305510

Yan, Y., Zhao, J., Cao, C., Jia, Z., Zhou, N., Han, S. and Cui, H. (2014). 'Tetramethylpyrazine promotes SH-SY5Y cell differentiation into neurons through epigenetic regulation of Topoisomerase II', Neuroscience, 278, 179–193. https://doi.org/10.1016/j.neuroscience.2014.08.010

Yang, B., Shen, J., Xu, L., Chen, Y., Che, X., Qu, X., and Li, Z. (2019). 'Genome-Wide Identification of a Novel Eight-lncRNA Signature to Improve Prognostic Prediction in Head and Neck Squamous Cell Carcinoma', Frontiers in Oncology. https://doi.org/10.3389/fonc.2019.00898

Yang, F., Lyu, S., Dong, S., Liu, Y., Zhang, X., and Wang, O. (2016). 'Expression profile analysis of long noncoding RNA in HER-2-enriched subtype breast cancer by next-generation sequencing and bioinformatics', OncoTargets and Therapy. https://doi.org/10.2147/OTT.S97664

Yang, G., Lu, X., and Yuan, L. (2014). 'LncRNA: A link between RNA and cancer', Biochimica et Biophysica Acta - Gene Regulatory Mechanisms, 1839(11), 1097–1109. https://doi.org/10.1016/j.bbagrm.2014.08.012

Yang, T. W., Sahu, D., Chang, Y. W., Hsu, C. L., Hsieh, C. H., Huang, H. C., and Juan, H. F. (2019). ,RNA-Binding Proteomics Reveals MATR3 Interacting with lncRNA SNHG1 to Enhance Neuroblastoma Progression', Journal of Proteome Research. https://doi.org/10.1021/acs.jproteome.8b00693

Yang, Y., Zhang, Z., Wu, Z., Lin, W., and Yu, M. (2019). 'Downregulation of the expression of the lncRNA MIAT inhibits melanoma migration and invasion through the PI3K/AKT signaling pathway', Cancer Biomarkers. https://doi.org/10.3233/CBM-181869

Yao, H., Brick, K., Evrard, Y., Xiao, T., Camerini-Otero, R. D., and Felsenfeld, G. (2010). 'Mediation of CTCF transcriptional insulation by DEAD-box RNA-binding protein p68 and steroid receptor RNA activator SRA', Genes and Development, 24(22), 2543–2555. https://doi.org/10.1101/gad.1967810

Yao, J., Xu, F., Zhang, D., Yi, W., Chen, X., Chen, G., and Zhou, E. (2018). 'TP73-AS1 promotes breast cancer cell proliferation through miR-200a-mediated TFAM inhibition', Journal of Cellular Biochemistry. https://doi.org/10.1002/jcb.26231

Yao, R. W., Wang, Y., and Chen, L. L. (2019). 'Cellular functions of long noncoding RNAs', Nature Cell Biology. https://doi.org/10.1038/s41556-019-0311-8

Yarmishyn, A. A., Batagov, A. O., Tan, J. Z., Sundaram, G. M., Sampath, P., Kuznetsov, V. A., and Kurochkin, I. V. (2014). 'HOXD-AS1 is a novel lncRNA encoded in HOXD cluster and a marker of neuroblastoma progression revealed via integrative analysis of noncoding transcriptome', BMC Genomics, 15(Suppl 9), S7. https://doi.org/10.1186/1471-2164-15-S9-S7

Yavuz, B., Zeki, J., Coburn, J. M., Ikegaki, N., Levitin, D., Kaplan, D. L., and Chiu, B. (2018). 'In vitro and in vivo evaluation of etoposide - silk wafers for neuroblastoma treatment', Journal of Controlled Release. https://doi.org/10.1016/j.jconrel.2018.07.002

Ye, M., Ma, J., Liu, B., Liu, X., Ma, D., and Dong, K. (2019). 'Linc01105 acts as an oncogene in the development of neuroblastoma', Oncology Reports. https://doi.org/10.3892/or.2019.7257

Yen, C.-Y., Huang, H.-W., Shu, C.-W., Hou, M.-F., Yuan, S.-S. F., Wang, H.-R., Chang, Y. T., Farooqi, A. A., Tang, J. Y. and Chang, H.-W. (2016). 'DNA methylation, histone acetylation and methylation of epigenetic modifications as a therapeutic approach for cancers', Cancer Letters, 373(2), 185–192. https://doi.org/10.1016/j.canlet.2016.01.036

Yerukala Sathipati, S., Sahu, D., Huang, H. C., Lin, Y., and Ho, S. Y. (2019). 'Identification and characterization of the lncRNA signature associated with overall survival in patients with neuroblastoma', Scientific Reports. https://doi.org/10.1038/s41598-019-41553-y

Yoda, H., Inoue, T., Shinozaki, Y., Lin, J., Watanabe, T., Koshikawa, N., Takatori, A. and Nagase, H. (2019). 'Direct targeting of MYCN gene amplification by site-specific DNA alkylation in neuroblastoma'. Cancer Research. https://doi.org/10.1158/0008-5472.CAN-18-1198

Yoshimoto, R., Mayeda, A., Yoshida, M., and Nakagawa, S. (2016). 'MALAT1 long non-coding RNA in cancer', Biochimica et Biophysica Acta - Gene Regulatory Mechanisms, 1859(1), 192–199. https://doi.org/10.1016/j.bbagrm.2015.09.012

Young, M. M., Bui, V., Chen, C., and Wang, H. G. (2019). 'FTY720 induces non-canonical phosphatidylserine externalization and cell death in acute myeloid leukemia', Cell Death and Disease. https://doi.org/10.1038/s41419-019-2080-5

Youssef, G., Gillett, C., Agbaje, O., Crompton, T., and Montano, X. (2014). 'Phosphorylation of NTRK1 at Y674/Y675 induced by TP53-dependent repression of PTPN6 expression: A potential novel prognostic marker for breast cancer', Modern Pathology. https://doi.org/10.1038/modpathol.2013.129

Yu, X., Mao, W., Zhai, Y., Tong, C., Liu, M., Ma, L. and Li, S. (2017). 'Anti-tumor activity of metformin: from metabolic and epigenetic perspectives', Oncotarget. https://doi.org/10.1103/PhysRevD.72.045006

Yu, Y., Chen, F., Yang, Y., Jin, Y., Shi, J., Han, S., Chu, P., Lu, J., Tai, J., Wang, S., Yang, W., Wang, H., Guo, Y. and Ni, X. (2019). 'LncRNA SNHG16 is associated with proliferation and poor prognosis of pediatric neuroblastoma', International Journal of Oncology. https://doi.org/10.3892/ijo.2019.4813

Yuan, X., Wei, W., Bao, Q., Chen, H., Jin, P., and Jiang, W. (2018). ‘’Metformin inhibits glioma cells stemness and epithelial-mesenchymal transition via regulating YAP activity’, Biomedicine and Pharmacotherapy. https://doi.org/10.1016/j.biopha.2018.03.031

Yue, W., Yang, C. S., DiPaola, R. S., and Tan, X. L. (2014). ‘Repurposing of metformin and aspirin by targeting AMPK-mTOR and inflammation for pancreatic cancer prevention and treatment’, Cancer Prevention Research. https://doi.org/10.1158/1940-6207.CAPR-13-0337

Zeng, F., Yu, N., Han, Y., and Ainiwaer, J. (2020). ‘The long non-coding RNA MIAT/miR-139-5p/MMP2 axis regulates cell migration and invasion in non-small-cell lung cancer’, Journal of Biosciences. https://doi.org/10.1007/s12038-020-0019-8

Zhang et al. (2016). ‘LncRNAs and cancer (Review)’, ONCOLOGY LETTERS, 12, 1233–1239.

Zhang, C., Xie, L., Liang, H., and Cui, Y. (2019). ‘LncRNA MIAT facilitates osteosarcoma progression by regulating mir-128-3p/VEGFC axis’, IUBMB Life. https://doi.org/10.1002/iub.2001

Zhang, H. Y., Zheng, F. S., Yang, W., and Lu, J. Bin. (2017). ‘The long non-coding RNA MIAT regulates zinc finger E-box binding homeobox 1 expression by sponging miR-150 and promoting cell invasion in non-small-cell lung cancer’, Gene, 633, 61–65. https://doi.org/10.1016/j.gene.2017.08.009

Zhang, Jian, Fan, D., Jian, Z., Chen, G. G., and Lai, P. B. S. (2015). ‘Cancer-specific long noncoding RNAs show differential expression patterns and competing endogenous RNA potential in hepatocellular carcinoma’, PLoS ONE. https://doi.org/10.1371/journal.pone.0141042

Zhang, Jiao, Li, W. Y., Yang, Y., Yan, L. Z., Zhang, S. Y., He, J., and Wang, J. X. (2019). ‘LncRNA XIST facilitates cell growth, migration and invasion via modulating H3 histone methylation of DKK1 in neuroblastoma’, Cell Cycle. https://doi.org/10.1080/15384101.2019.1632134

Zhang, L., Chen, S., Wang, B., Su, Y., Li, S., Liu, G., and Zhang, X. (2019). ‘An eight-long noncoding RNA expression signature for colorectal cancer patients’ prognosis’, Journal of Cellular Biochemistry, 120(19), 5636–5643. https://doi.org/10.1002/jcb.27847

Zhang, N., Liu, F. L., Ma, T. S., Zeng, Z. D., and Zhang, J. J. (2019). 'LncRNA SNHG1 contributes to tumorigenesis and mechanism by targeting MIR-338-3p to regulate PLK4 in human neuroblastoma', European Review for Medical and Pharmacological Sciences. https://doi.org/10.26355/eurrev_201910_19296

Zhang, X. Q., Kiang, K. M. Y., Wang, Y. C., Pu, J. K. S., Ho, A., Cheng, S. Y. and Leung, G. K. K. (2015). IDH1 mutation-associated long non-coding RNA expression profile changes in glioma. Journal of Neuro-Oncology, 125(2), 253–263. https://doi.org/10.1007/s11060-015-1916-9

Zhang, X. Q., Sun, S., Lam, K. F., Kiang, K. M. Y., Pu, J. K. S., Ho, A. S. W., and Leung, G. K. K. (2013). 'A long non-coding RNA signature in glioblastoma multiforme predicts survival', Neurobiology of Disease. https://doi.org/10.1016/j.nbd.2013.05.011

Zhang, X., Sun, S., Pu, J. K. S., Tsang, A. C. O., Lee, D., Man, V. O. Y., Lui, W. M., Wong, S. T. S. and Leung, G. K. K. (2012). 'Long non-coding RNA expression profiles predict clinical phenotypes in glioma', Neurobiology of Disease. https://doi.org/10.1016/j.nbd.2012.06.004

Zhang, X.-Q., and Leung, G. K.-K. (2014). ,Long non-coding RNAs in glioma: Functional roles and clinical perspectives', Neurochemistry International, 77C, 78–85. https://doi.org/10.1016/j.neuint.2014.05.008

Zhang, X.-Q., Sun, S., Lam, K.-F., Kiang, K. M.-Y., Pu, J. K.-S., Ho, A. S.-W., and Leung, G. K.-K. (2013). 'A long non-coding RNA signature in glioblastoma multiforme predicts survival', Neurobiology of Disease, 58, 123–131. https://doi.org/10.1016/j.nbd.2013.05.011

Zhang, Z., Wang, S., and Liu, W. (2018). 'EMT-related long non-coding RNA in hepatocellular carcinoma: A study with TCGA database', Biochemical and Biophysical Research Communications. https://doi.org/10.1016/j.bbrc.2018.07.075

Zhao, L., Hu, K., Cao, J., Wang, P., Li, J., Zeng, K., He, X., Tu, P. F., Tong, T. and Han, L. (2019). 'lncRNA miat functions as a ceRNA to upregulate sirt1 by sponging miR-22-3p in HCC cellular senescence', Aging. https://doi.org/10.18632/aging.102240

Zhao, M., Zhu, N., Hao, F., Song, Y., Wang, Z., Ni, Y., and Ding, L. (2019). 'The Regulatory Role of Non-coding RNAs on Programmed Cell Death Four in Inflammation and Cancer', Frontiers in Oncology. https://doi.org/10.3389/fonc.2019.00919

Zhao, W., Shan, B., He, D., Cheng, Y., Li, B., Zhang, C., and Duan, C. (2019). 'Recent Progress in Characterizing Long Noncoding RNAs in Cancer Drug Resistance', J Cancer, 10(26), 6693–6702. https://doi.org/doi:10.7150/jca.30877

Zhao, Xiang, Li, D., Huang, D., Song, H., Mei, H., Fang, E., and Tong, Q. (2018). 'Risk-Associated Long Noncoding RNA FOXD3-AS1 Inhibits Neuroblastoma Progression by Repressing PARP1-Mediated Activation of CTCF', Molecular Therapy. https://doi.org/10.1016/j.ymthe.2017.12.017

Zhao, XS, Tao, N., Zhang, C., Gong, C., and Dong, C. (2019). 'Long noncoding RNA MIAT acts as an oncogene in Wilms' tumor through regulation of DGCR8', European Review for Medical and Pharmacological Sciences, 23, 10257–10263. https://doi.org/10.26355/eurrev_201912_19663

Zhaoxia Liu, Hai Wang, Hongwei Cai, Ye Hong, Yan Li, Dongming Su, and Z. F. (2018). 'Long non-coding RNA MIAT promotes growth and metastasis of colorectal cancer cells through regulation of miR-132/Derlin-1 pathway', Cancer Cell International, Vol.18.

Zhen, L., Yun-hui, L., Hong-yu, D., Jun, M., and Yi-long, Y. (2016). 'Long noncoding RNA NEAT1 promotes glioma pathogenesis by regulating miR-449b-5p/c-Met axis', Tumor Biology, 37(1), 673–683. https://doi.org/10.1007/s13277-015-3843-y

Zhong, W., Xu, Z., Wen, S., Xie, T., Wang, F., Wang, Q., and Chen, J. (2019). 'Long non-coding RNA myocardial infarction associated transcript promotes epithelial-mesenchymal transition and is an independent risk factor for poor prognosis of tongue squamous cell carcinoma', Journal of Oral Pathology and Medicine. https://doi.org/10.1111/jop.12892

Zhong, X., Ma, X., Zhang, L., Li, Y., Li, Y., and He, R. (2018). 'MIAT promotes proliferation and hinders apoptosis by modulating miR-181b/STAT3 axis in ox-LDL-induced atherosclerosis cell models', Biomedicine and Pharmacotherapy. https://doi.org/10.1016/j.biopha.2017.11.052

Zhou, D., Gao, B., Yang, Q., Kong, Y., and Wang, W. (2019). 'Integrative Analysis of ceRNA Network Reveals Functional lncRNAs in Intrahepatic Cholangiocarcinoma', BioMed Research International, 2019. https://doi.org/10.1155/2019/2601271

Zhou, H., Sun, L., and Wan, F. (2019). 'Molecular mechanisms of TUG1 in the proliferation, apoptosis, migration and invasion of cancer cells (Review)', Oncology Letters. https://doi.org/10.3892/ol.2019.10848

Zhou, L., Tang, H., Wang, F., Chen, L., Shanshan, O. U., Tong, W. U. and Guo, K. (2018). 'Bioinformatics analyses of significant genes, related pathways and candidate prognostic biomarkers in glioblastoma', Molecular Medicine Reports. https://doi.org/10.3892/mmr.2018.9411

Zhou, X., Zhang, W., Jin, M., Chen, J., Xu, W., and Kong, X. (2017). 'lncRNA MIAT functions as a competing endogenous RNA to upregulate DAPK2 by sponging miR-22-3p in diabetic cardiomyopathy', Cell Death and Disease. https://doi.org/10.1038/cddis.2017.321

Zhou, Y., Cheunsuchon, P., Nakayama, Y., Lawlor, M. W., Zhong, Y., Rice, K., Zhang, L., Zhang, X., Gordon, F. E., Lidov, H. G. W., Bronson, R. T. and Klibanski, A. (2010). 'Activation of paternally expressed genes and perinatal death caused by deletion of the Gtl2 gene', Development (Cambridge, England), 137(16), 2643–2652. https://doi.org/10.1242/dev.045724

Zhu, S., Li, W., Liu, J., Chen, C. H., Liao, Q., Xu, P., Xu, H., Xiao, T., Cao, Z., Peng, J., Yuan, P., Brown, M., Liu, X. S. and Wei, W. (2016). 'Genome-scale deletion screening of human long non-coding RNAs using a paired-guide RNA CRISPR-Cas9 library', Nature Biotechnology. https://doi.org/10.1038/nbt.3715

Zhu, X. H., Yuan, Y. X., Rao, S. L., and Wang, P. (2016). 'LncRNA MIAT enhances cardiac hypertrophy partly through sponging miR-150', European Review for Medical and Pharmacological Sciences.

Zhu, X., Tian, X., Yu, C., Shen, C., Yan, T., Hong, J. and Chen, H. (2016). 'A long non-coding RNA signature to improve prognosis prediction of gastric cancer'. Molecular Cancer. https://doi.org/10.1186/s12943-016-0544-0

Zimmermann, M. and Meyer, N. (2011) 'Annexin V/7-AAD staining in keratinocytes.', Methods in molecular biology (Clifton, N.J.). doi: 10.1007/978-1-61779-108-6_8.

Zurlo, G., Liu, X., Takada, M., Fan, C., Simon, J. M., Ptacek, T. S. Rodriguez, J., von Kriegsheim, A., Liu, J., Locasale, J. W., Robinson, A., Zhang, J., Holler, J. M., Kim, B., Zikánová, M., Bierau, J., Xie, L., Chen, X., Li, M., Perou, C. M. and Zhang, Q. (2019). 'Prolyl hydroxylase substrate adenylosuccinate lyase is an oncogenic driver in triple negative breast cancer', Nature Communications. https://doi.org/10.1038/s41467-019-13168-4

.

APPENDICES

Appendix I

List of relevant publications

Filipp Frank, Nadieh Kavousi, Katerina Bountali, Mirna Mourtada-Maarabouni, Eric A. Ortlund (2020) The lncRNA Growth Arrest Specific 5 regulates cell survival via distinct structural modules with independent functions. Cell Reports, in press.

Bountali, A., Tonge, D. P. and Mourtada-Maarabouni, M. (2020) 'Identification of novel lncRNAs involved in cell fate decisions of neuroblastoma cells', manuscript in preparation.

Bountali, K., Mourtada-Maarabouni, M. and Tonge, D. (2018) 'PO-349 Identification of differentially expressed lncRNAs in metformin resistant SH-SY5Y neuroblastoma cells', *ESMO Open*, 3(Suppl 2), p. A365 LP-A366. Available at: http://esmoopen.bmj.com/content/3/Suppl_2/A365.2.abstract.

Bountali A. and Mourtada-Maarabouni M. Unravelling the role of novel uncharacterised long non-coding RNAs in the control of cell fate [1399]. In: NCRI; 5-8 November 2017; Liverpool, UK. *British Journal of Cancer (BJC).* Abstract number: 1399. Available from: http://abstracts.ncri.org.uk/abstract/unravelling-the-role-ofnovel-uncharacterised-long-non-coding-rnas-in-the-control-of-cell-fate/

Appendix II

Supplementary Table 1. Top differentially expressed lncRNAs upon *MIAT* down-regulation.

lncRNA	cytogenetic location	log_2 fold change	subclass
LOC100506714	chr22:45529638-45559662	14,57	NAT
LOC100128420	chrX:135721701-135724588	11,31	lincRNA
CASC2	chr10:119806331-119969665	10,56	unclassified
ZNFX1-AS1	chr20:47862438-47905795	8,12	NAT
LOC100133331	chr5:180750506-180755196	7,95	uncharacterised
LOC100507217	chr15:93426072-93441977	7,86	lincRNA
TRAF3IP2-AS1	chr6:111804674-111927477	7,07	NAT
TERC	chr3:169482397-169482848	5,99	unclassified
TP73-AS1	chr1:3569128-3663937	5,84	NAT
LOC728978	chr10:72972291-73062635	5,72	NAT
C17orf76-AS1	chr17:16342300-16395480	5,69	NAT
MIR22HG	chr17:1614797-1619566	5,42	miRNA host
LOC100652739	chr6:150139893-150244214	5,31	NAT
LOC389033	chr2:130680434-130691890	5,18	pseudogene
LOC150381	chr22:46446338-46454402	5,04	NAT
GRIK1-AS2	chr21:30909253-31312282	4,87	NAT
ITPK1-AS1	chr14:93403258-93582263	4,74	NAT
LOC100505783	chr20:42839599-42854667	4,74	NAT
LOC400236	chr14:89622515-90085494	4,71	NAT
CECR5-AS1	chr22:17618409-17646335	4,62	NAT
LOC100288778	chr12:87983-91263	4,58	pseudogene
HIF1A-AS2	chr14:62162118-62215807	4,47	NAT
LOC729678	chr5:180256953-180262726	4,30	lincRNA
LOC645638	chr17:58160926-58165828	4,25	pseudogene
LOC399715	chr10:6319649-6377937	4,23	lincRNA
MIR22HG	chr17:1614797-1619566	-3,53	miRNA
LOC283761	chr15:90048160-90067265	-3,61	lincRNA
BDNF-AS1	chr11:27528398-27743605	-3,62	NAT
ADAMTS9-AS2	chr3:64501330-64997143	-3,68	NAT
SNHG4	chr5:138609440-138667366	-3,80	snoRNA host
LOC100507495	chr20:1290554-1373816	-3,83	NAT
LOC100329109	chr2:206980296-206981296	-3,86	pseudogene
LOC645212	chr15:44826702-44829121	-4,80	NAT
C17orf76-AS1	chr17:16342300-16395480	-5,46	snoRNA host/ NAT
LINC00461	chr5:87836596-87980620	-5,46	lincRNA
GHRLOS	chr3:10327433-10335133	-8,27	NAT
LOC256021	chr12:92378751-92539673	-8,97	lincRNA
LOC100507433	chr19:38039850-38105079	-10,09	NAT
LOC219347	chr10:81805988-81852307	-10,17	NAT

LOC100288637	chr15:30938317-31065209	-10,29	pseudogene
LOC730101	chr6:52529198-52533951	-10,56	uncharacterised
LOC100132287	chr5:180750506-180755196	-11,03	uncharacterised
LOC283050	chr10:80703082-80827205	-11,30	NAT
LOC100509894	chr13:46626982-46679211	-11,56	NAT
LOC100125556	chr3:125635443-125655887	-12,47	pseudogene
CASC2	chr10:119806331-119969665	-12,71	unclassified
LOC100506714	chr22:45529638-45559662	-13,04	NAT
LOC100506994	chr3:61547242-62304622	-13,58	NAT
MIR22HG	chr17:1614797-1619566	-14,66	miRNA
LOC386758	chr19:56905044-56910544	-15,22	NAT

Supplementary Table 2. Top identified miRNAs upon *MIAT* knockdown in SH-SY5Y cells.

miRNA name	Number of perturbed targets/ total genes	Number of targets/ total genes	*p-value*
hsa-miR-124-3p	1291 / 1580	1462 / 1881	3.067e-19
hsa-miR-27a-3p	793 / 962	889 / 1138	1.439e-14
hsa-miR-27b-3p	793 / 962	889 / 1138	1.439e-14
hsa-miR-506-3p	821 / 975	914 / 1140	1.825e-14
hsa-miR-181a-5p	877 / 984	969 / 1131	2.465e-14
hsa-miR-181c-5p	877 / 984	969 / 1131	2.465e-14
hsa-miR-181b-5p	877 / 984	969 / 1131	2.465e-14
hsa-miR-181d-5p	877 / 984	969 / 1131	2.465e-14
hsa-miR-4262	877 / 984	969 / 1131	2.465e-14
hsa-miR-519d-3p	817 / 976	917 / 1152	3.512e-14

Supplementary Table 3. Top differentially expressed genes on chromosome 22 (including protein-coding and lncRNAs) upon *MIAT* down-regulation.

gene	cytogenetic location	log_2 fold change	protein-coding vs non-coding
PARVB	chr22:44395090-44565112	17,00	protein-coding
TUBA8	chr22:18593452-18614498	16,76	protein-coding
MOV10L1	chr22:50528434-50600116	16,36	protein-coding
FAM19A5	chr22:48885287-49147744	16,11	protein-coding
KCNJ4	chr22:38822332-38851203	15,14	protein-coding
RASL10A	chr22:29708921-29711748	14,86	protein-coding
CPT1B	chr22:51007289-51021428	14,60	protein-coding
LOC100506714	chr22:45529638-45559662	14,57	non-coding
MB	chr22:36002810-36019401	14,44	protein-coding
APOL3	chr22:36536370-36562225	14,09	protein-coding
GGT1	chr22:24979717-25024972	14,02	protein-coding
APOL1	chr22:36649116-36663577	13,00	protein-coding
RNF185	chr22:31556137-31603005	11,88	protein-coding
CECR5	chr22:17618409-17646335	11,56	protein-coding
CRYBB2	chr22:25211660-25231869	10,00	protein-coding
ARSA	chr22:51061181-51066601	7,50	protein-coding
CPT1B	chr22:51007289-51021428	6,85	protein-coding
MTFP1	chr22:30821610-30825041	6,75	protein-coding
SEC14L2	chr22:30792929-30821291	6,74	protein-coding
SMTN	chr22:31477281-31500610	6,58	protein-coding
C1QTNF6	chr22:37576205-37584330	6,44	protein-coding
TOM1	chr22:35695267-35743987	6,34	protein-coding
TSPO	chr22:43547519-43559248	6,32	protein-coding
CRYBB3	chr22:25595824-25603324	6,28	protein-coding
KLHL22	chr22:20795805-20850170	6,18	protein-coding
FOXRED2	chr22:36883232-36903148	-9,08	protein-coding
AIFM3	chr22:21319417-21335649	-9,74	protein-coding
TNRC6B	chr22:40440820-40731812	-9,97	protein-coding
ADM2	chr22:50919984-50924866	-10,00	protein-coding
TUBA8	chr22:18593452-18614498	-10,00	protein-coding
FAM19A5	chr22:48885287-49147744	-10,02	protein-coding
PATZ1	chr22:31721789-31742249	-10,17	protein-coding
LARGE	chr22:33669061-34316416	-10,27	protein-coding
PPARA	chr22:46546498-46639653	-10,30	protein-coding
PLA2G6	chr22:38507501-38577836	-10,80	protein-coding
KCNJ4	chr22:38822332-38851203	-10,97	protein-coding
GGT5	chr22:24615621-24641110	-11,40	protein-coding
POLDIP3	chr22:42979726-43010962	-11,56	protein-coding
P2RX6	chr22:21369441-21382302	-12,20	protein-coding
RABL2B	chr22:51195513-51238065	-12,39	protein-coding
CLTCL1	chr22:19166986-19279239	-12,55	protein-coding
SEC14L2	chr22:30792929-30821291	-12,60	protein-coding
DGCR5	chr22:18958010-18982142	-12,98	protein-coding
LOC100506714	chr22:45529638-45559662	-13,04	non-coding

SPECC1L	chr22:24666789-24813708	-13,89	protein-coding
TCN2	chr22:31003069-31023047	-13,96	protein-coding
EWSR1	chr22:29663997-29696515	-14,22	protein-coding
TCF20	chr22:42556018-42611445	-14,58	protein-coding
ZNRF3	chr22:29279754-29453476	-15,55	protein-coding
SGSM1	chr22:25202135-25322813	-16,27	protein-coding

Supplementary Table 4. Significantly deregulated miRNAs inhibiting Sp1 upon *MIAT* knockdown.

miRNA	*p-value*
miR-137	1,51E-08
miR-200c	1,96E-08
miR-429	1,96E-08
miR-23b	6,76E-06
miR-145	2,98E-05
miR-29b	4,90E-04
miR-29c	4,90E-04
miR-330	1,41E-02
miR-133b	1,88E-02
miR-133a	5,35E-02
miR-223	1,07E-01
miR-335	0.003
miR-375	0.036

Supplementary Table 5. Sp (Specificity protein) TF- regulated genes with significant (*p-value* <0.05) differential expression upon *MIAT* knockdown.

Sp1 target	Up-regulated/ Down-regulated	Pathway/ Process
FAS	Down-regulated	Apoptosis
Bcl-2	Down-regulated	Apoptosis
BIRC5	Up-regulated	Survival/ Proliferation
EGFR	Down-regulated	Membrane signalling
FGFR3	Down-regulated	Membrane signalling
cMET	Down-regulated	Membrane signalling
VEGFA	Down-regulated	Migration/ invasion/metastasis
VEGFB	Up-regulated	Migration/ invasion/metastasis
MMP9	Up-regulated	Migration/ invasion/metastasis

a.

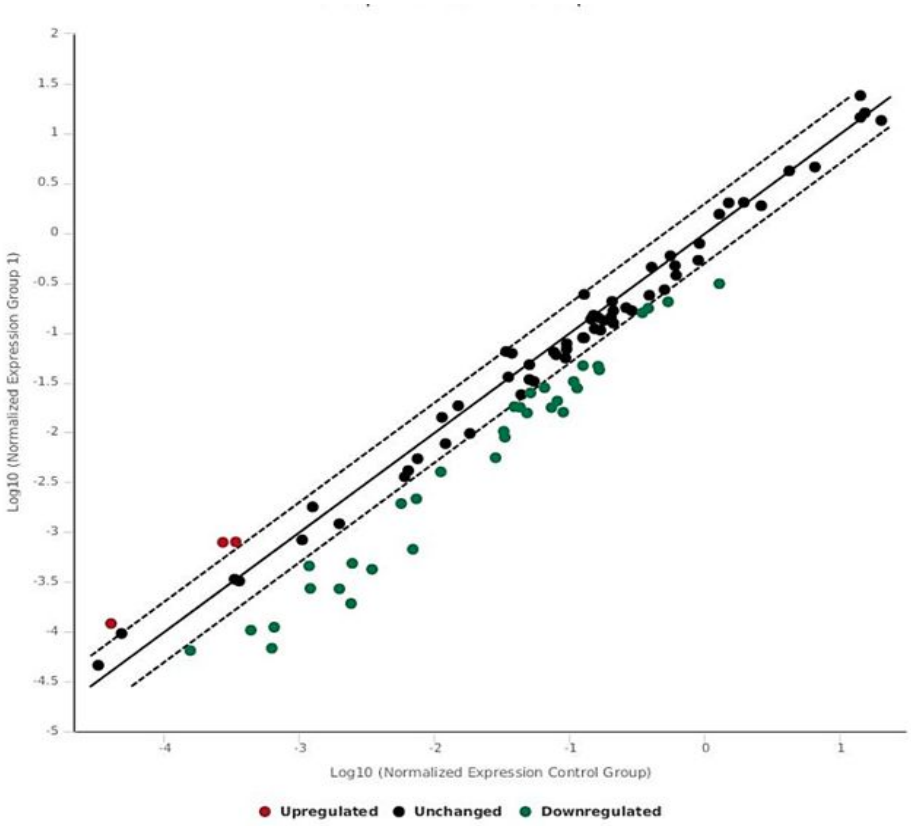
Log10 (Normalized Expression Group 1)
Log10 (Normalized Expression Control Group)
Upregulated
Unchanged
Downregulated

b.

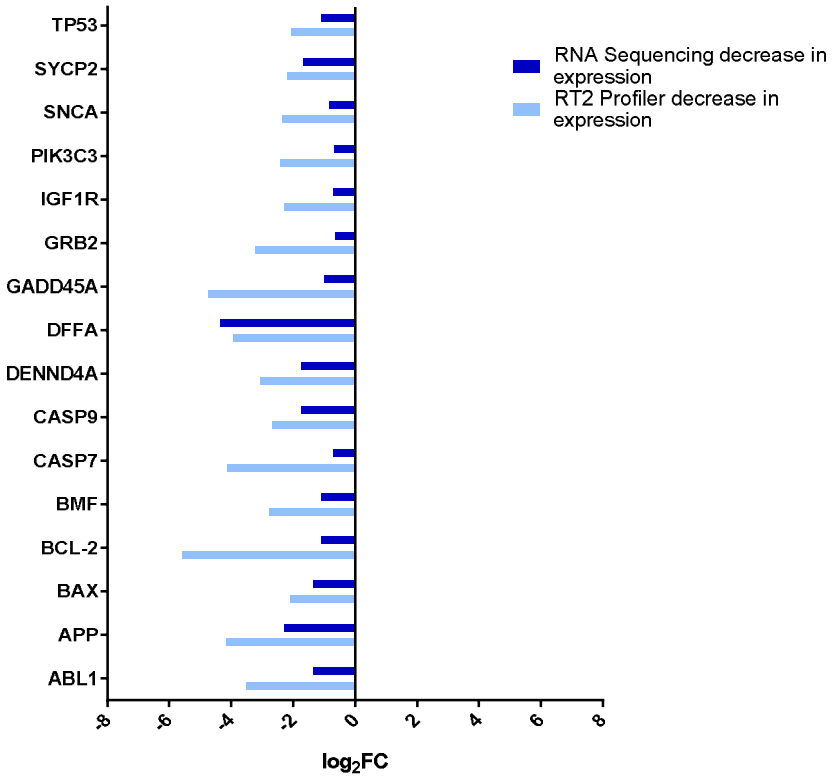
TP53
SYCP2
SNCA
PIK3C3
IGF1R
GRB2
GADD45A
DFFA
DENND4A
CASP9
CASP7
BMF
BCL-2
BAX
APP
ABL1
RNA Sequencing decrease in expression
RT2 Profiler decrease in expression
log2FC

Supplementary Figure 1. *MIAT* down-regulation affects a plethora of programmed cell death-related genes. The scatter plot compares the normalised expression of every gene on the array between cells treated with –ve siRNA and MIAT_2 by plotting them against one another. The central line indicates unchanged gene expression. The dotted lines indicate the selected fold regulation threshold. Red points represent genes with up-regulated expression, while green points represent genes with down-regulated expression. Average Ct value was normalised to a set of 5 own internal housekeeping genes at a cut-off of 38 (a). The graph presents perturbed genes validated both by RNA sequencing and the RT² Profiler™ PCR Array Human Cell Death PathwayFinder. Blue shaded bars correspond to down-regulated gene expression (b). Data are expressed as a normalised log_2 fold change (log_2FC). A threshold of 0.05 for statistical significance (p-value) and a log fold change of expression with an absolute value of at least 0.6 were applied; the analysis of the results was performed using a web-based PCR Array Data Analysis tool (dataanalysis.sabiosciences.com/pcr/arrayanalysis.php). **TP53**: Tumor Protein P53; **SYCP2**: Synaptonemal Complex Protein 2; **SNCA**: Synuclein Alpha; **PIK3C3**: Phosphatidylinositol 3-Kinase Catalytic Subunit Type 3; **IGF1R**: Insulin-Like Growth Factor 1 Receptor; **GRB2**: Growth Factor Receptor Bound Protein 2; **GADD45A**: Growth Arrest And DNA Damage Inducible Alpha; **DFFA**: DNA Fragmentation Factor Subunit Alpha; **DENND4A**: DENN Domain Containing 4A; **CASP7/9**: Caspase 7/9; **BMF**: BCL-2 Modifying Factor; **BCL-2**: BCL-2 Apoptosis Regulator; **BAX**: BCL2 Associated X, Apoptosis Regulator; **APP**: Amyloid Beta Precursor Protein; **ABL1**: ABL Proto-Oncogene 1, Non-Receptor Tyrosine Kinase.

a.

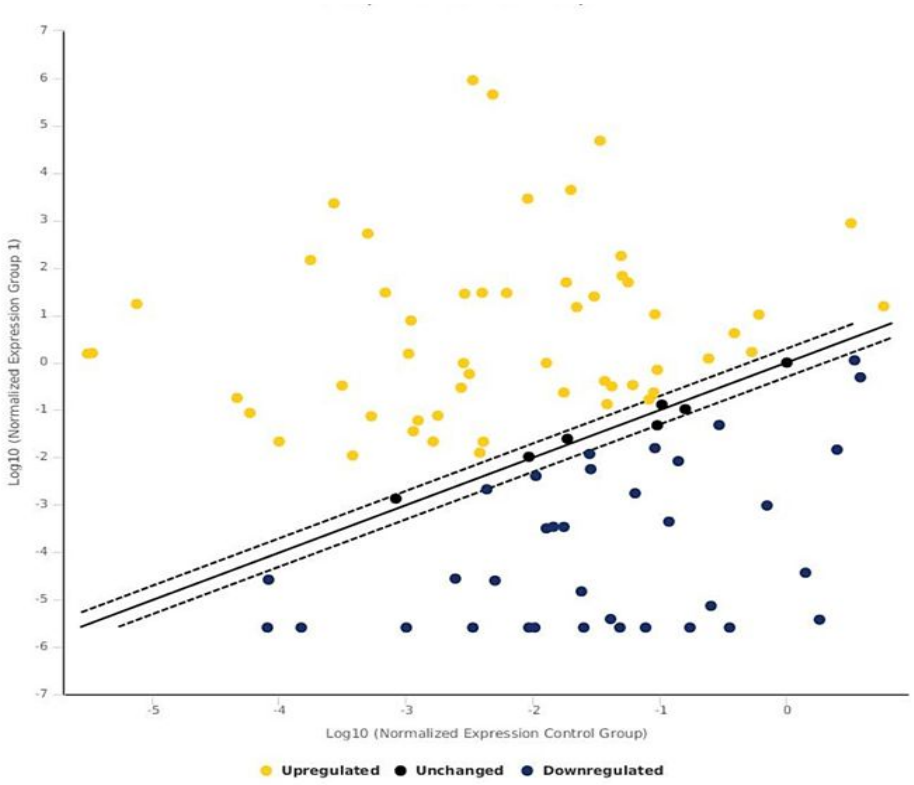
Log10 (Normalized Expression Group 1)
Log10 (Normalized Expression Control Group)
Upregulated
Unchanged
Downregulated

b.

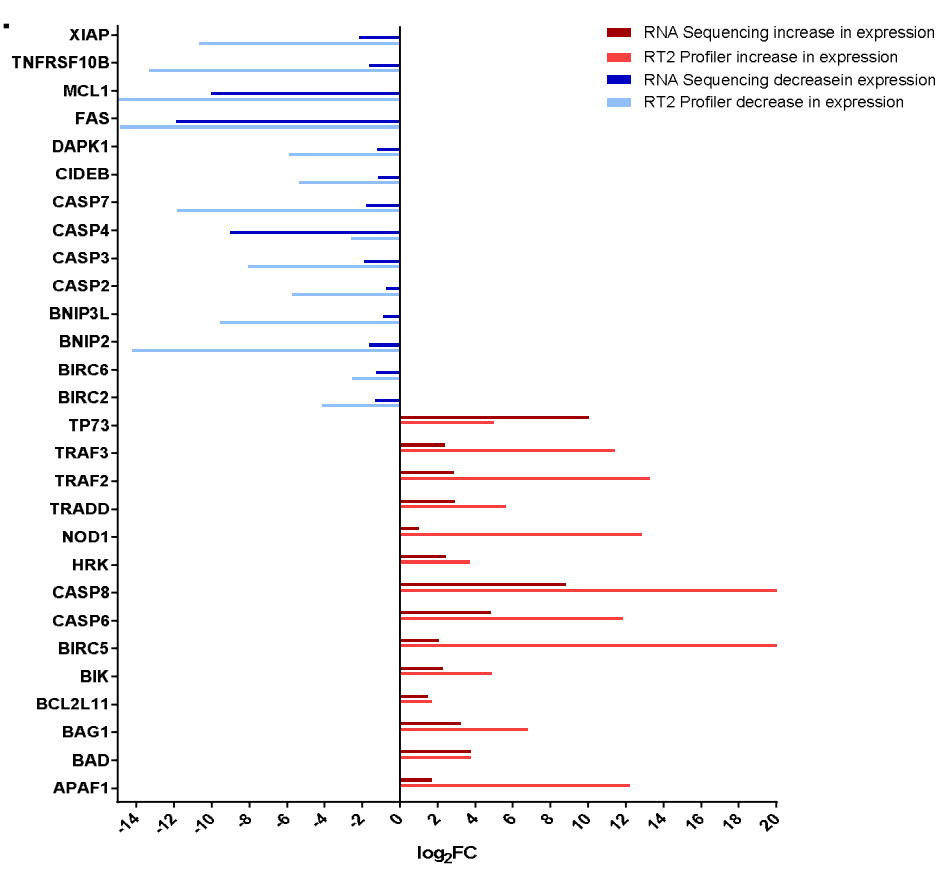
XIAP
TNFRSF10B
MCL1
FAS
DAPK1
CIDEB
CASP7
CASP4
CASP3
CASP2
BNIP3L
BNIP2
BIRC6
BIRC2
TP73
TRAF3
TRAF2
TRADD
NOD1
HRK
CASP8
CASP6
BIRC5
BIK
BCL2L11
BAG1
BAD
APAF1
RNA Sequencing increase in expression
RT2 Profiler increase in expression
RNA Sequencing decreasein expression
RT2 Profiler decrease in expression
log2FC

Supplementary Figure 2. *MIAT* down-regulation affects multiple apoptosis-associated genes. The scatter plot compares the normalised expression of every gene on the array between cells treated with –ve siRNA and MIAT_2 by plotting them against one another. The central line indicates unchanged gene expression. The dotted lines indicate the selected fold regulation threshold. Yellow points represent genes with up-regulated expression, while blue points represent genes with down-regulated expression. Average Ct value was normalised to a set of 5 own internal housekeeping genes at a cut-off of 40 (a). The graph presents perturbed genes validated both by RNA sequencing and the RT² Profiler™ PCR Array Human Cell Death PathwayFinder. Red shaded bars correspond to up-regulated gene expression, while blue shaded bars correspond to down-regulated gene expression (b). Data are expressed as a normalised $\log_2$ fold change ($\log_2$FC). A threshold of 0.05 for statistical significance (p-value) and a log fold change of expression with an absolute value of at least 0.6 were applied; the analysis of the results was performed using a web-based PCR Array Data Analysis tool (dataanalysis.sabiosciences.com/pcr/arrayanalysis.php). **XIAP**: X-Linked Inhibitor Of Apoptosis; **TNFRSF10B**: TNF Receptor Superfamily Member 10b; **MCL1**: MCL1 Apoptosis Regulator, BCL-2 Family Member; **FAS**: Fas Cell Surface Death Receptor; **DAPK1**: Death Associated Protein Kinase 1; **CIDEB**: Cell Death Inducing DFFA Like Effector B; **BNIP3L**: BCL2 Interacting Protein 3 Like; **BNIP2**: BCL-2 Interacting Protein 2; **TP73**: Tumor Protein P73; **TRAF2/3**: TNF Receptor Associated Factor 2/3; **TRADD**: TNFRSF1A Associated Via Death Domain; **NOD1**: Nucleotide Binding Oligomerization Domain Containing 1; **HRK**: Harakiri, BCL2 Interacting Protein; **CASP2/3/4/6/7/8**: Caspase 2/3/4/6/7/8; **BIRC2/5/6**: Baculoviral IAP Repeat Containing 2/5/6; **BIK**: BCL2 Interacting Killer; **BCL2L11**: BCL-2 Like 11; **BAG1**: BCL2 Associated Athanogene 1; **BAD**: BCL2 Associated Agonist Of Cell Death; **APAF1**: Apoptotic Peptidase Activating Factor 1.

Appendix III

Supplementary Table 1. Top differentially expressed lncRNAs in metformin-treated SH-SY5Y cells. Rows highlighted in lilac represent lncRNAs which are also differentially expressed in SH-SY5Y cells with continuous exposure to metformin.

lncRNA	location	log_2 fold change	subclass
LOC100652730	chr20:61405472-61408208	15,66	lincRNA
GHRLOS	chr3:10327433-10335133	14,97	NAT
LOC100130700	chr16:34739458-34740840	14,45	pseudogene
PCBP1-AS1	chr2:70187223-70314147	13,57	NAT
CBR3-AS1	chr21:37504064-37528606	13,27	NAT
CASC2	chr10:119806331-119969665	12,63	unclassified
LOC730227	chr1:203267885-203274453	12,33	lincRNA
MIR22HG	chr17:1614797-1619566	12,21	miRNA host
LOC100288637	chr15:30938317-31065209	11,32	pseudogene
LOC100507557	chr6:145946439-146285233	11,1	uncharacterised
LOC100507173	chr6:27661813-27678001	10,87	lincRNA
LOC100288974	chr10:81664653-81691557	10,49	pseudogene
LOC100505695	chr2:171627603-171634757	5,72	uncharacterised
LOC641364	chr4:138948576-139163503	5,64	NAT
LINC00173	chr12:116971226-116974318	4,22	lincRNA
LOC100506801	chr1:21543739-21672034	4,1	uncharacterised
LOC283050	chr10:80703082-80827205	3,73	NAT
LOC145216	chr14:104314057-104324386	3,62	lincRNA
LOC400680	chr19:21666516-21686040	3,52	lincRNA
LOC100616668	chr13:41363546-41495910	3,38	pseudogene
LOC344595	chr3:106959538-107045811	3,36	lincRNA
LOC678655	chr12:6548166-6560884	3,19	NAT
LOC100292680	chr12:1609656-1613590	3,15	lincRNA
LOC284865	chr22:20186252-20192441	3,09	uncharacterised
LOC644242	chr1:120140324-120141914	3,03	lincRNA
LOC730091	chr3:156465131-156534851	-2,54	lincRNA
LOC100134259	chr2:47055002-47086145	-2,58	lincRNA
LOC148709	chr1:202830881-202844369	-2,63	pseudogene
LOC100507346	chr9:98205263-98279247	-2,7	uncharacterised
LOC653712	chr3:128580350-128590384	-2,7	pseudogene
MIR143HG	chr5:148786439-148812399	-2,85	miRNA host
LOC100132707	chr7:154720226-154794682	-2,92	NAT
LOC285878	chr7:54610018-54639419	-2,99	overlapping
LOC100289092	chr16:28889808-28936532	-3	NAT
C17orf76-AS1	chr17:16342300-16395480	-3,09	snoRNA host
LOC285484	chr4:6202459-6235663	-3,09	lincRNA
LINC00324	chr17:8123947-8127361	-3,13	lincRNA
LOC100506409	chr6:10980992-11079377	-3,18	NAT

LOC339524	chr1:87595447-87634886	-3,96	lincRNA
LOC340037	chr5:176853686-176883287	-6,01	NAT
TP73-AS1	chr1:3569128-3663937	-8,35	NAT
PEG3-AS1	chr19:57285922-57352097	-9	NAT
LOC100128420	chrX:135721701-135724588	-9,4	lincRNA
LOC100288637	chr15:30938317-31065209	-11,01	pseudogene
LOC100506714	chr22:45529638-45559662	-11,21	NAT
LOC256021	chr12:92378751-92539673	-12,13	lincRNA
LOC100509894	chr13:46626982-46679211	-13,55	NAT
LOC283050	chr10:80703082-80827205	-13,94	NAT
LOC730227	chr1:203267885-203274453	-14,39	lincRNA
LOC151300	chr2:219841005-219842644	-15	lincRNA

Supplementary Table 2. Perturbed molecular pathways (including cancer-related) in metformin-treated cells. ipathwayguide.advaitabio.com/report/27441/contrast/33417/pathways/7438).

Pathway name	*p-value*
DNA replication	1.088e-9
Cytokine-cytokine receptor interaction	1.041e-6
Neuroactive ligand-receptor interaction	1.896e-6
Cell cycle	5.928e-6
Mismatch repair	2.230e-5
Homologous recombination	1.518e-4
p53 signalling pathway	4.947e-4
Complement and coagulation cascades	6.917e-4
Basal cell carcinoma	0.004
HTLV-I infection	0.005
Olfactory transduction	0.008
Fanconi anaemia pathway	0.009
Glycine, serine and threonine metabolism	0.010
Malaria	0.015
Protein digestion and absorption	0.016
Type I diabetes mellitus	0.017
Staphylococcus aureus infection	0.017
Antifolate resistance	0.019
Systemic lupus erythematosus	0.022
Base excision repair	0.023
Hippo signalling pathway	0.024
Intestinal immune network for IgA production	0.034
Apoptosis - multiple species	0.035

Pathogenic Escherichia coli infection	**0.035**
Pyrimidine metabolism	**0.038**
Colorectal cancer	**0.040**
Ovarian steroidogenesis	**0.042**
Oocyte meiosis	**0.043**

Supplementary Table 3. Top differentially expressed lncRNAs in SH-SY5Y cells with continuous exposure to metformin.

lncRNA	cytogenetic location	log_2 fold change	subclass
GHRLOS	chr3:10327433-10335133	13,82	NAT
LOC100133331	chr5:180750506-180755196	13	uncharacterised
LOC729678	chr5:180256953-180262726	10,96	lincRNA
LOC100288974	chr10:81664653-81691557	9,83	pseudogene
CASC2	chr10:119806331-119969665	12,44	unclassified
LOC100288637	chr15:30938317-31065209	9,81	pseudogene
LOC100507173	chr6:27661813-27678001	9,69	lincRNA
LOC100505695	chr2:171627603-171634757	6,3	uncharacterised
LOC643401	chr5:27472398-27496508	5,04	lincRNA
LOC100507557	chr6:145946439-146285233	4,9	uncharacterised
LINC00173	chr12:116971226-116974318	4,77	lincRNA
LOC100133161	chr11:126986-131920	4,67	uncharacterised
LOC284080	chr17:48127712-48133103	4,59	uncharacterised
LOC285965	chr7:143078359-143220540	4,24	NAT
LOC100616668	chr13:41363546-41495910	4,12	pseudogene
MIR7-3HG	chr19:4769116-4772568	4,1	miRNA host/ lincRNA
LOC400680	chr19:21666516-21686040	4,1	lincRNA
LOC284865	chr22:20186252-20192441	4,1	uncharacterised
MIR7-3HG	chr19:4769116-4772568	4,09	lincRNA
LOC643650	chr10:47096453-47151400	3,8	lincRNA
LOC79015	chr20:43285091-43300380	3,74	lincRNA
LOC389641	chr8:23082733-23088439	3,71	uncharacterised
LOC100129617	chr16:81478774-81745367	3,63	uncharacterised
LOC285593	chr5:173006645-173012075	3,63	uncharacterised
LOC678655	chr12:6548166-6560884	3,31	NAT
LOC100506810	chr1:234859788-234867390	-2,05	lincRNA
LINC00319	chr21:44869903-44873771	-2,06	lincRNA
C17orf76-AS1	chr17:16342300-16395480	-2,06	snoRNA host
LOC729987	chr1:98676266-98738214	-2,09	lincRNA
LOC729080	chr5:141275190-141276260	-2,11	pseudogene
LOC283731	chr15:74418713-74421619	-2,14	uncharacterised
LOC100128361	chr9:95059639-95432547	-2,15	uncharacterised

LOC100130093	chr1:227916239-227968932	-2,15	uncharacterised
LOC100170939	chr5:69423288-69586004	-2,18	pseudogene
LOC100133091	chr7:76178657-76257299	-2,18	uncharacterised
LOC100506136	chr7:96250968-96293650	-2,19	uncharacterised
LINC00163	chr21:46409778-46414001	-2,2	lincRNA
LOC100379224	chr19:44598481-44617336	-2,21	uncharacterised
LOC729799	chr11:43902356-43942494	-2,22	pseudogene
LOC401127	chr4:39481874-39483523	-2,24	pseudogene
MAGI2-AS3	chr7:77646373-79100524	-2,26	NAT
MORC2-AS1	chr22:31318294-31364187	-2,28	NAT
LOC100128881	chr16:89773540-89883065	-2,3	NAT
LINC00461	chr5:87836596-87980620	-2,34	lincRNA
MIR143HG	chr5:148786439-148812399	-2,34	miRNA host
MIR137HG	chr1:98453555-98515249	-2,35	miRNA host
LOC90784	chr2:86247338-86250991	-2,37	uncharacterised
LOC283663	chr15:57592562-57599967	-2,39	lincRNA
LOC100499177	chr4:83814604-83841284	-2,4	NAT
LOC100128292	chr10:79686569-79689583	-2,42	NAT
CRYM-AS1	chr16:21269838-21329912	-2,44	NAT
LOC153684	chr5:43042235-43045370	-2,52	uncharacterised
LINC00208	chr8:11434043-11438850	-2,53	lincRNA
LOC100132215	chr2:62900985-63275656	-2,54	uncharacterised
LOC729683	chr17:61777697-61780045	-2,55	uncharacterised
LOC100505912	chr4:22328989-22341289	-2,56	uncharacterised
LOC100130992	chr10:22541000-22547477	-2,58	uncharacterised
MIR17HG	chr13:92000073-92006829	-2,6	miRNA host/ lincRNA
MIR17HG	chr13:92000073-92006829	-2,6	miRNA host
LOC100128191	chr12:98906750-98944157	-2,61	NAT
LINC00277	chr15:69116302-69564544	-2,63	lincRNA
LOC144571	chr12:9217772-9268558	-2,66	NAT
LOC149134	chr1:246952918-246954788	-2,75	lincRNA
LOC100506123	chr2:98081675-98091049	-2,76	uncharacterised
LOC157627	chr8:9757573-9760839	-2,82	lincRNA
LOC400940	chr2:6122109-6128364	-2,89	uncharacterised
LOC100129961	chr2:135596185-135676176	-2,9	NAT
LOC100131089	chr15:40331511-40359710	-2,97	NAT
UCKL1-AS1	chr20:62571181-62601218	-2,98	NAT
LOC641367	chr19:21906842-21950430	-3	pseudogene
LOC100129534	chr1:2252695-2322993	-3,01	pseudogene
LOC100506068	chr19:47150868-47220384	-3,12	NAT
LOC100505746	chr21:46305867-46349595	-3,22	NAT
LOC646938	chr15:79044378-79045734	-3,23	pseudogene
LOC100507433	chr19:38039850-38105079	-3,26	NAT
LOC100287559	chr15:73043707-73090540	-3,33	NAT
LOC100144603	chr22:51021454-51022355	-3,4	NAT

LINC00478	chr21:17442841-17982094	-3,64	lincRNA
LOC653712	chr3:128580350-128590384	-3,71	pseudogene
LINC00304	chr16:89225627-89230083	-4,59	lincRNA
LOC392232	chr8:73117533-73163869	-5,31	pseudogene
LINC00176	chr20:62665696-62671315	-9,23	lincRNA
LOC100288637	chr15:30938317-31065209	-9,96	pseudogene
LOC256021	chr12:92378751-92539673	-12,29	lincRNA
LOC100125556	chr3:125635443-125655887	-14,52	pseudogene
LOC648987	chr5:43014830-43018913	-14,85	uncharacterised
LOC151300	chr2:219841005-219842644	-15,24	lincRNA

Supplementary Table 4. Perturbed molecular pathways (including cancer-related) in SH-SY5Y cells with continuous exposure to metformin. (ipathwayguide.advaitabio.com/report/27030/contrast/32882/pathways/6400).

Pathway name	*p-value*
Cytokine-cytokine receptor interaction	1.809e-6
DNA replication	2.998e-4
Cell cycle	4.963e-4
Lysosome	0.001
Antigen processing and presentation	0.002
Protein digestion and absorption	0.003
HTLV-I infection	0.004
Mismatch repair	0.004
Pertussis	0.004
Base excision repair	0.008
Systemic lupus erythematosus	0.009
Type I diabetes mellitus	0.012
p53 signalling pathway	0.013
Malaria	0.013
Fanconi anaemia pathway	0.014
Chemokine signalling pathway	0.016
Bacterial invasion of epithelial cells	0.017
Osteoclast differentiation	0.019
Homologous recombination	0.020
Other types of O-glycan biosynthesis	0.020
ECM-receptor interaction	0.022
Legionellosis	0.025
Herpes simplex infection	0.026

Neuroactive ligand-receptor interaction	**0.028**
Cocaine addiction	**0.036**
Hypertrophic cardiomyopathy (HCM)	**0.038**
Oocyte meiosis	**0.039**
Complement and coagulation cascades	**0.040**
Wnt signalling pathway	**0.043**
Purine metabolism	**0.048**
Maturity onset diabetes of the young	**0.048**

Supplementary Table 5. Differentially expressed lncRNAs in metformin-treated SH-SY5Y cells versus SH-SY5Y cells with continuous exposure to metformin.

lncRNA	cytogenetic location	log_2 fold change	subclass
LOC283050	chr10:80703082-80827205	13,82	NAT
LOC730227	chr1:203267885-203274453	13,5	lincRNA
LOC100509894	chr13:46626982-46679211	13,3	NAT
LOC100506714	chr22:45529638-45559662	12,75	NAT
LOC100133331	chr5:180750506-180755196	11,22	uncharacterised
LOC729678	chr5:180256953-180262726	10,64	lincRNA
LOC100128420	chrX:135721701-135724588	8,99	lincRNA
TP73-AS1	chr1:3569128-3663937	7,9	NAT
LINC00176	chr20:62665696-62671315	7,52	lincRNA
C17orf76-AS1	chr17:16342300-16395480	5,3	snoRNA host
LOC340037	chr5:176853686-176883287	4,1	NAT
LOC285965	chr7:143078359-143220540	3,48	NAT
LOC100505783	chr20:42839599-42854667	3,36	NAT
LINC00324	chr17:8123947-8127361	3,26	lincRNA
H19	chr11:2016405-2019065	3,19	lincRNA
LOC285593	chr5:173006645-173012075	3,11	uncharacterised
LOC728175	chr4:185262183-185275130	3,01	lincRNA
LOC728978	chr10:72972291-73062635	2,85	NAT
LINC00092	chr9:98782013-98784037	2,77	lincRNA
LINC00535	chr8:94358694-94712661	2,72	lincRNA
LOC256021	chr12:92378751-92539673	2,69	lincRNA
LOC100133957	chrX:47511190-47519776	2,66	NAT
LOC100129617	chr16:81478774-81745367	2,64	uncharacterised
LOC100133161	chr11:126986-131920	2,63	lincRNA
LOC100131347	chr17:37213271-37307902	2,6	pseudogene
LOC100507433	chr19:38039850-38105079	-2,6	NAT
LOC145216	chr14:104314057-104324386	-2,62	lincRNA
MIAT	chr22:27053445-27072440	-2,65	lincRNA
LINC00461	chr5:87836596-87980620	-2,68	lincRNA
ZRANB2-AS2	chr1:71547006-71703406	-2,73	NAT
LOC100507086	chr3:196769430-197030621	-2,73	NAT
CRYM-AS1	chr16:21269838-21329912	-2,74	NAT
LOC100131089	chr15:40331511-40359710	-2,8	NAT
LOC100287559	chr15:73043707-73090540	-2,8	NAT
LINC00552	chr13:114451483-114454062	-2,85	lincRNA
LOC100129316	chr9:93825575-93837414	-2,95	uncharacterised
FLVCR1-AS1	chr1:213029945-213031480	-2,97	NAT
LOC100652768	chr11:117049938-117075508	-3,06	uncharacterised
LOC100130992	chr10:22541000-22547477	-3,07	uncharacterised
MIR497HG	chr17:6915735-6922973	-3,09	miRNA host
LOC115110	chr1:2481358-2484284	-3,3	NAT
LINC00327	chr13:24043650-24061603	-3,72	lincRNA
LOC400940	chr2:6122109-6128364	-3,73	uncharacterised

LOC392232	chr8:73117533-73163869	-3,79	pseudogene
LOC641364	chr4:138948576-139163503	-3,97	NAT
LINC00304	chr16:89225627-89230083	-4,11	lincRNA
LOC100507557	chr6:145946439-146285233	-6,56	uncharacterised
PCBP1-AS1	chr2:70187223-70314147	-13,61	NAT
LOC100125556	chr3:125635443-125655887	-14,86	pseudogene
LOC100652730	chr20:61405472-61408208	-16,16	lincRNA

Supplementary Table 6a. Top perturbed molecular pathways (including cancer-related) in metformin-treated SH-SY5Y cells SH-SY5Y cells with continuous exposure to metformin (https://ipathwayguide.advaitabio.com/report/40623/contrast/49745).

Pathway name	*p-value*
NF-kappa B signalling pathway	**1.951e-5**
TNF signalling pathway	**5.358e-5**
Steroid biosynthesis	**5.742e-5**
Chemokine signalling pathway	**6.808e-5**
HTLV-I infection	**8.278e-5**
Cytokine-cytokine receptor interaction	**8.368e-5**
Kaposi's sarcoma-associated herpesvirus infection	**8.746e-5**
Terpenoid backbone biosynthesis	**1.228e-4**
Antigen processing and presentation	**3.310e-4**
Systemic lupus erythematosus	**4.165e-4**
IL-17 signalling pathway	**4.402e-4**
NOD-like receptor signalling pathway	**7.143e-4**
Proteoglycans in cancer	**8.660e-4**
Chagas disease (American trypanosomiasis)	**9.639e-4**
MicroRNAs in cancer	**0.001**
Staphylococcus aureus infection	**0.001**
Rheumatoid arthritis	**0.001**

Renin secretion	**0.001**
AGE-RAGE signalling pathway in diabetic complications	**0.002**
Complement and coagulation cascades	**0.002**
Transcriptional misregulation in cancer	**0.003**
Pathways in cancer	**0.003**
Apelin signalling pathway	**0.006**
Circadian entrainment	**0.006**
Osteoclast differentiation	**0.007**
Herpes simplex infection	**0.007**
Wnt signalling pathway	**0.008**
Ferroptosis	**0.010**
Metabolic pathways *	**0.012**
Signalling pathways regulating pluripotency of stem cells	**0.014**
Axon guidance	**0.015**
MAPK signalling pathway	**0.015**
Protein digestion and absorption	**0.016**
cGMP-PKG signalling pathway	**0.018**
PI3K-Akt signalling pathway	**0.019**
Malaria	**0.022**
B cell receptor signalling pathway	**0.022**
Hematopoietic cell lineage	**0.022**
Phagosome	**0.022**
Colorectal cancer	**0.022**
Biosynthesis of amino acids	**0.024**
Thyroid hormone synthesis	**0.025**

Circadian rhythm	**0.026**
Pertussis	**0.027**
African trypanosomiasis	**0.029**
Small cell lung cancer	**0.029**
Bladder cancer	**0.033**
Focal adhesion	**0.033**
Apoptosis - multiple species	**0.034**
Glycosaminoglycan biosynthesis - keratan sulfate	**0.035**
Mineral absorption	**0.036**
Epstein-Barr virus infection	**0.037**
Viral carcinogenesis	**0.038**
Legionellosis	**0.038**
Hypertrophic cardiomyopathy (HCM)	**0.041**
Cholinergic synapse	**0.042**
Cytosolic DNA-sensing pathway	**0.043**
Regulation of actin cytoskeleton	**0.044**
Cell adhesion molecules (CAMs)	**0.044**
Salivary secretion	**0.045**
Alcoholism	**0.045**
Dilated cardiomyopathy (DCM)	**0.046**
Prostate cancer	**0.046**
Arrhythmogenic right ventricular cardiomyopathy (ARVC)	**0.048**

Supplementary Table 6b. Top perturbed Gene Ontology (GO) terms metformin-treated SH-SY5Y cells versus SH-SY5Y cells with acquired resistance to metformin.

	Pathway name	Number of perturbed genes/ total genes in the pathway	*p-value*
Biological Processes	Response to external stimulus	118 / 2076	1.400e-15
	Inflammatory response	54 / 674	9.600e-13
	Signalling	239 / 6194	5.700e-12
	Regulation of response to stimulus	168 / 3857	9.400e-12
	Response to stimulus	296 / 8338	1.800e-11
Molecular functions	Protein binding	354 / 11021	9.900e-8
	Receptor binding	70 / 1454	2.700e-6
	Collagen binding	9 / 63	5.300e-5
	Receptor regulator activity	28 / 464	9.300e-5
	Receptor ligand activity	26 / 437	2.100e-4

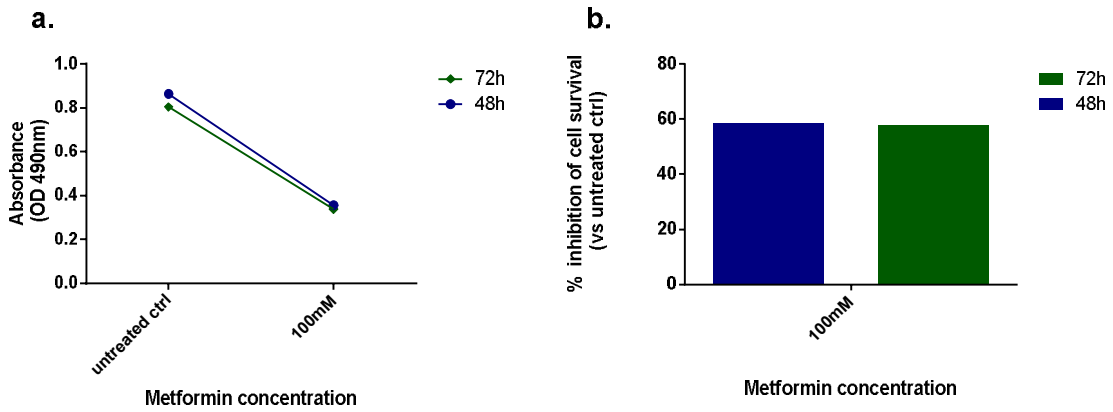

Supplementary Figure 1. The effects of metformin on the cell survival of SH-SY5Y cells. Cells were seeded in 96-well plates (100µl/well), incubated for 24h and 100mM metformin were subsequently added (diluted in growth media-100µl/well). Cell survival is reduced by the treatment with 100mM metformin comparing to cells growing in the absence of metformin, as measured by the MTS assay 48 h and 72 h post-treatment. The concentration of 100mM was too toxic for the cells. Optical density (OD) at 490nm is represented in a, while % inhibition of cell survival is represented in b. Data are represented as mean, in n=1 experiment.